NASA TM-84653

NASA Technical Memorandum 84653

AVSCOM Technical Memorandum 83-B-1

NASA-TM-84653 19840009950

FOR REFERENCE

NOT TO BE TAKEN FROM THIS ROOM

EXPERIMENTAL BLADE VORTEX INTERACTION NOISE CHARACTERISTICS OF A UTILITY HELICOPTER AT 1/4 SCALE

David A. Conner and Danny R. Hoad

LIBRARY COPY

FEB 10 1984

LANGLEY RESEARCH CENTER
LIBRARY, NASA
HAMPTON, VIRGINIA

January 1984

NASA
National Aeronautics and Space Administration

Langley Research Center
Hampton, Virginia 23665

U.S. ARMY AVSCOM

SUMMARY

An experimental investigation of the blade-vortex interaction impulsive noise characteristics of an advanced main rotor system for the UH-1 helicopter has been conducted. Models of both the advanced main rotor system and the standard or "baseline" UH-1 main rotor system were tested at one-quarter scale in the Langley 4- by 7-Meter (V/STOL) Tunnel using the General Rotor Model System (GRMS). Tests were conducted over a range of descent angles which bracketed the blade-vortex interaction phenomenon for a range of simulated forward speeds. The tunnel was operated in the open-throat configuration with acoustic treatment to improve the semi-anechoic characteristics of the test chamber. This investigation provided detailed acoustical data for these two rotor systems operating at similar flight conditions. These data are presented without analysis or discussion.

N84-18018#

INTRODUCTION

Helicopter rotor noise is typically separated into categories, such as rotational noise, broadband turbulence interaction noise, and impulsive noise. When present, impulsive noise is usually the most objectionable for the community (refs. 1, 2, & 3) and represents a significant problem for reducing ground detectability of military helicopters. Impulsive noise can occur during high-speed flight as a result of the relatively high advancing blade tip Mach numbers or during partial power descents as a result of the interaction of a blade with a vortex generated by a prior blade passage.

Advanced composite technology has permitted application of planform variation, high twist, and advanced airfoils on existing and new rotor systems (refs. 4 & 5). Such a rotor has been proposed for the UH-1 to take advantage of the new freedom in blade design primarily to improve the aerodynamic performance of the UH-1 in hover and forward flight. The design methodology indicated a substantial aerodynamic performance benefit was possible. An aerodynamic performance analysis of the results of a model rotor test (ref. 6) verified that the advanced rotor system (ARS) provided an improvement in rotor system efficiency of 10 percent in hover and as much as a 17 percent reduction in required torque in forward flight when compared with the "baseline" or standard rotor system (SRS). Acoustic analysis of the in-plane high-speed impulsive noise (ref. 7) demonstrated that a 7 to 8 dB reduction in noise generation is available by using the ARS on the UH-1 helicopter. The data presented herein were collected to evaluate the effect of the advanced rotor design on the blade-vortex interaction (BVI) impulsive noise.

SYMBOLS AND ABBREVIATIONS

Symbols

A_1	first harmonic of lateral cyclic blade pitch, deg
a_0	rotor coning angle, fixed at 2.75°
a_{1S}	first harmonic of longitudinal flapping, deg
B_1	first harmonic of longitudinal cyclic blade pitch, deg
b_{1S}	first harmonic of lateral flapping, deg
C_Q	rotor torque coefficient, $\frac{\text{ROTOR TORQUE}}{\rho\pi R^3(\Omega R)^2}$
C_T	rotor thrust coefficient, $\frac{\text{ROTOR THRUST}}{\rho\pi R^2(\Omega R)^2}$
C	standard rotor system blade chord, 0.1334 m
D	rotor drag, Newtons
L	rotor lift, Newtons
R	rotor radius, 1.829 m
V_T	rotor blade-tip speed, knots
V_∞	free-stream velocity, knots
x,y,z	coordinates for microphone locations in tunnel, m
α	angle of attack of rotor shaft, deg
α_{TPP}	rotor tip-path-plane angle of attack, referenced to tunnel geometric centerline, deg
γ	rotor descent angle, $\tan^{-1}$ (D/L)
θ_C	rotor collective control angle, deg
μ	advance ratio, V_∞/V_T
ρ	local free-stream density, kg/m^3
Ω	rotor angular rotational velocity, rad/sec

Abbreviations

ARS	advanced rotor system
BVI	blade-vortex interaction
GRMS	general rotor model system
rpm	revolutions per minute
SP	sound pressure, dynes/cm^2
SPL	sound pressure level, dB (re. 0.0002 dynes/cm^2)
SRS	standard rotor system

HELICOPTER MODEL AND TEST FACILITY

Helicopter Model

The General Rotor Model System (GRMS) mounted in the 4- by 7-Meter (V/STOL) Tunnel was used for this investigation (ref. 8). The fuselage was a one-quarter scale model of the UH-1 helicopter mounted to the GRMS (see fig. 1) with a balance to provide independent fuselage load data. A sketch of the model is provided in figure 2 and shows the two rotor systems tested.

Both main rotor systems used for this investigation were mounted to a geometrically scaled version of the UH-1 helicopter hub. One rotor system was geometrically and dynamically scaled to the current UH-1 helicopter rotor configuration and is referred to herein as the SRS. These blades were made of a fiberglass/kevlar composite having a graphite/epoxy composite structural torque box. The aerodynamic contours were formed by means of an external fiberglass/epoxy shell with a nomex honeycomb core in the trailing edge. The other rotor system had a modified blade planform and was constructed with dynamic characteristics as close as possible to the SRS and is herein referred to as the ARS. These advanced rotor blades were wider in root chord compared to the standard rotor blades with a 3 to 1 taper ratio beginning at the 50-percent radius. Advanced rotorcraft airfoils (ref. 9) were used with thickness ratios ranging from 12-percent inboard to 8-percent at the tip. Construction was similar to that of the standard rotor blades with the exception of a styrofoam/balsa trailing edge core. A sketch of the two different rotor blade designs tested is shown in figure 3 while their dimensional characteristics are presented in table 1.

The rotor had a teetering hub with cyclic and collective pitch on the blades controlled by a swash plate driven by remotely controlled actuators.

Rotor teetering measurements were made at the teetering axis. The rotor was driven by a 67-KW electric motor through a transmission. The entire system (rotor, transmission, and motor) was mounted on a six-component strain-gage balance within the model to measure rotor forces and moments. Performance data from this balance were used to obtain the necessary aerodynamic conditions for this test including lift coefficient and simulated descent angle.

Wind-Tunnel Facility

The model investigation was conducted in the NASA Langley 4- by 7-Meter (V/STOL) Tunnel configured in the optional open-throat configuration. The dimensions of the rectangular jet entrance to the test chamber are 4.42 m high by 6.63 m wide. The ceiling height in the open-throat configuration was approximately 7.50 m above the test chamber floor. The model was supported in the wind-tunnel test section by a three-joint sting which allows model pitch and yaw control to plus or minus 45° about a fixed point on the model. The three-joint sting was mounted on a model support system which allowed height control as well as limited additional pitch and yaw control.

In order to improve the semi-anechoic characteristics of the test chamber, acoustic treatment was installed on the test section floor and ceiling. This acoustic treatment, which is partially visible in figure 4 and indicated in figure 5, consisted of fiberglass-filled aluminum panels and open-cell polyurethane foam. The 12.7 cm thick aluminum panels were installed on the floor directly under the model for a semi-rigid floor to facilitate periodic maintenance and modifications to the model rotor system. The 10.2 cm thick foam was installed on the floor directly up-stream of the aluminum panels and overhead on the surface of the raised ceiling. An evaluation of the effectiveness of this acoustic treatment is reported in reference 10.

Instrumentation

The acoustic transducers used for this investigation were 1.27 cm diameter condenser microphones fitted with standard nose cones. Eight microphones were positioned in the flow around the model. A rear-quarter-view photograph of the model installed in the tunnel with acoustical treatment is presented in figure 4 and shows the relative locations of six of the microphones. A sketch showing more detail of the relative position of all components in the test chamber (microphones, model, ceiling, entrance lip, treatment, etc.) is provided in figure 5.

Data from four of the eight microphones are presented in this paper. The locations of these four microphones relative to the rotor hub with the model at $\alpha = 0°$ are presented in table II. Microphone 2, considered to be in the near-field, was mounted close to the fuselage under the rotor disk in a location shown to be relatively sensitive to BVI blade slap (refs. 11 and 12). Microphones 6, 7, and 8, considered to be in the far-field, were mounted upstream of the model as far as possible from the rotor, yet still in the free-field environment of the facility, at about 30° below the rotor tip-path-plane. The directivity of the BVI blade slap has been shown experimentally (ref. 13) and theoretically (ref. 14) to be a maximum in the direction of microphones 6, 7, and 8. Signals from each microphone were fed through an amplifier attenuator and into a 14-channel frequency-modulated (FM) tape recorder operating at 76.2 cm/sec tape speed. Blade azimuth and time-code were also recorded.

OPERATING PROCEDURES AND DATA REDUCTION

BVI impulsive noise has been shown to occur at partial-power descending flight. It was, therefore, necessary to determine the flight conditions (tunnel velocity and simulated descent angle) critical to BVI generation for each rotor system. At each tunnel velocity, with rotor operating at 1296 RPM, the simulated descent angle (computed from data obtained on the rotor balance only) was varied from a climb condition with no observable BVI through maximum BVI to a high descent angle where BVI was not observed. The rotor lift coefficient (defined as the rotor lift nondimensionalized by the product of rotor disk area, hover tip speed squared, and local free-stream density) was maintained as close as possible to 0.00315 during the first half of the investigation. During the latter half of the investigation the rotor lift coefficient was increased to 0.00365 in order to simulate the recent increases in gross weight of U.S. Army UH-1 helicopters.

The procedure used to establish each flight condition was to set a constant tunnel velocity equal to the desired flight speed, thus setting the advance ratio (μ). This was followed by adjusting the collective and cyclic controls to obtain the proper lift coefficient and zero teetering angle. While maintaining the desired lift coefficient and zero teetering, the model angle of attack was varied to encompass the range of simulated descent angles desired. With the rotor system at the desired condition, 30 seconds of information from the microphones were recorded on an FM tape recorder. Corresponding model and tunnel information were recorded simultaneously on the tunnel computer data acquisition system. Full aerodynamic performance characteristics corresponding to the acoustic data presented in this paper are listed in tables III and IV. Before and after the rotor tests, background noise

measurements were made at each speed tested with the blades off and the rotor hub turning at 1296 rpm.

Data Reduction, Correction, and Presentation

Corrections for jet-boundary and blockage effects were handled on-line to insure proper helicopter operating conditions and were computed in greater detail off-line for complete aerodynamic performance data reduction. The method used to correct the data is described in reference 15.

Before and after the tests, "pink noise" and "white noise" signals were recorded to verify that the complete system (excluding the microphones) had a flat frequency response over the range of interest (30 to 8000 Hz). All microphones were calibrated with a 124 dB piston phone at 250 Hz before and after each series of runs.

The acoustic data were analyzed for one-third-octave and narrowband sound pressure levels (SPL). The analyses used are described in references 16 and 17. The one-third-octave and narrowband spectra were obtained from a 2-second (43 rotor revolutions) digital record of each test condition. Each acoustic record was band-pass filtered at 30 to 10000 Hz and digitized at a rate of 1024 samples per rotor revolution in order to facilitate use of a fast Fourier transform technique (ref. 17). For the one-third-octave-band analysis, each record was divided into 40 blocks, each block corresponding to 1 rotor revolution (0.046 sec), thus providing 80 degrees of freedom for the confidence limits in the spectral estimate of the sound pressure level based upon the chi square random variable. Each record was triggered at the instant in time when the instrumented blade passed over the tail of the fuselage. The narrowband spectra were obtained by discrete Fourier transform of the 40 blocks in each record corresponding to 40 rotor revolutions. At the 80 percent confidence limits, the sound pressure estimates are accurate to within ±15 percent of the

true value at each frequency based on the chi square random variable. The resolution in the frequency calculations of this analysis was one-half the blade passage frequency or approximately 21.7 Hz.

In each figure, one-third-octave spectra are presented for each microphone for various descent angles, all at constant tunnel velocities. Background noise one-third-octave spectra (blades off and hub turning) are provided for similar tunnel velocities. Sample pressure-time histories and narrowband spectra are included for each microphone. Two of each are presented for each one-third-octave plot--one with light or no discernable blade slap and one with the most intense blade slap. These data are presented in the following order without analysis:

	Figure
Tunnel Velocity ≈ 50 knots	
A. Standard rotor system, C_T = .0032, V_∞ = 50.2 knots	6
1. One-third Octave, Microphone No. 2	(a)
2. Pressure-time Histories, Microphone No. 2	(b)
3. Narrowband Analysis, Microphone No. 2	(c)
4. One-third Octave, Microphone No. 6	(d)
5. Pressure-time Histories, Microphone No. 6	(e)
6. Narrowband Analysis, Microphone No. 6	(f)
7. One-third Octave, Microphone No. 7	(g)
8. Pressure-time Histories, Microphone No. 7	(h)
9. Narrowband Analysis, Microphone No. 7	(i)
10. One-Third Octave, Microphone No. 8	(j)
11. Pressure-time Histories, Microphone No. 8	(k)
12. Narrowband Analysis, Microphone No. 8	(l)
B. Advanced Rotor System, C_T = .0031, V_∞ = 50.2 knots	7
1. One-third Octave, Microphone No. 2	(a)
2. Pressure-time Histories, Microphone No. 2	(b)
3. Narrowband Analysis, Microphone No. 2	(c)
4. One-third Octave, Microphone No. 6	(d)
5. Pressure-time Histories, Microphone No. 6	(e)
6. Narrowband Analysis, Microphone No. 6	(f)
7. One-third Octave, Microphone No. 7	(g)
8. Pressure-time Histories, Microphone No. 7	(h)
9. Narrowband Analysis, Microphone No. 7	(i)
10. One-third Octave, Microphone No. 8	(j)
11. Pressure-time Histories, Microphone No. 8	(k)
12. Narrowband Analysis, Microphone No. 8	(l)

Figure

C. Standard Rotor System, C_T = .0036, V_∞ = 49.8 knots 8

1. One-third Octave, Microphone No. 2 . . . . . (a)
2. Pressure-time Histories, Microphone No. 2 . . . . . (b)
3. Narrowband Analysis, Microphone No. 2 . . . . . (c)
4. One-third Octave, Microphone No. 6 . . . . . (d)
5. Pressure-time Histories, Microphone No. 6 . . . . . (e)
6. Narrowband Analysis, Microphone No. 6 . . . . . (f)
7. One-third Octave, Microphone No. 7 . . . . . (g)
8. Pressure-time Histories, Microphone No. 7 . . . . . (h)
9. Narrowband Analysis, Microphone No. 7 . . . . . (i)
10. One-third Octave, Microphone No. 8 . . . . . (j)
11. Pressure-time Histories, Microphone No. 8 . . . . . (k)
12. Narrowband Analysis, Microphone No. 8 . . . . . (l)

D. Advanced Rotor System, C_T = .0036, V_∞ = 49.9 knots 9

1. One-third Octave, Microphone No. 2 . . . . . (a)
2. Pressure-time Histories, Microphone No. 2 . . . . . (b)
3. Narrowband Analysis, Microphone No. 2 . . . . . (c)
4. One-third Octave, Microphone No. 6 . . . . . (d)
5. Pressure-time Histories, Microphone No. 6 . . . . . (e)
6. Narrowband Analysis, Microphone No. 6 . . . . . (f)
7. One-third Octave, Microphone No. 7 . . . . . (g)
8. Pressure-time Histories, Microphone No. 7 . . . . . (h)
9. Narrowband Analysis, Microphone No. 7 . . . . . (i)
10. One-third Octave, Microphone No. 8 . . . . . (j)
11. Pressure-time Histories, Microphone No. 8 . . . . . (k)
12. Narrowband Analysis, Microphone No. 8 . . . . . (l)

Tunnel Velocity ≈ 55 knots

A. Standard Rotor System, C_T = .0032, V_∞ = 55.3 knots 10

1. One-third Octave, Microphone No. 2 . . . . . (a)
2. Pressure-time Histories, Microphone No. 2 . . . . . (b)
3. Narrowband Analysis, Microphone No. 2 . . . . . (c)
4. One-third Octave, Microphone No. 6 . . . . . (d)
5. Pressure-time Histories, Microphone No. 6 . . . . . (e)
6. Narrowband Analysis, Microphone No. 6 . . . . . (f)
7. One-third Octave, Microphone No. 7 . . . . . (g)
8. Pressure-time Histories, Microphone No. 7 . . . . . (h)
9. Narrowband Analysis, Microphone No. 7 . . . . . (i)
10. One-third Octave, Microphone No. 8 . . . . . (j)
11. Pressure-time Histories, Microphone No. 8 . . . . . (k)
12. Narrowband Analysis, Microphone No. 8 . . . . . (l)

Figure

B. Advanced Rotor System, C_T = .0031, V_∞ = 55.6 knots 11

1. One-third Octave, Microphone No. 2 . . . . . (a)
2. Pressure-time Histories, Microphone No. 2 . . . . . (b)
3. Narrowband Analysis, Microphone No. 2 . . . . . (c)
4. One-third Octave, Microphone No. 6 . . . . . (d)
5. Pressure-time Histories, Microphone No. 6 . . . . . (e)
6. Narrowband Analysis, Microphone No. 6 . . . . . (f)
7. One-third Octave, Microphone No. 7 . . . . . (g)
8. Pressure-time Histories, Microphone No. 7 . . . . . (h)
9. Narrowband Analysis, Microphone No. 7 . . . . . (i)
10. One-third Octave, Microphone No. 8 . . . . . (j)
11. Pressure-time Histories, Microphone No. 8 . . . . . (k)
12. Narrowband Analysis, Microphone No. 8 . . . . . (l)

C. Standard Rotor System, C_T = .0036, V_∞ = 55.6 knots 12

1. One-third Octave, Microphone No. 2 . . . . . (a)
2. Pressure-time Histories, Microphone No. 2 . . . . . (b)
3. Narrowband Analysis, Microphone No. 2 . . . . . (c)
4. One-third Octave, Microphone No. 6 . . . . . (d)
5. Pressure-time Histories, Microphone No. 6 . . . . . (e)
6. Narrowband Analysis, Microphone No. 6 . . . . . (f)
7. One-third Octave, Microphone No. 7 . . . . . (g)
8. Pressure-time Histories, Microphone No. 7 . . . . . (h)
9. Narrowband Analysis, Microphone No. 7 . . . . . (i)
10. One-third Octave, Microphone No. 8 . . . . . (j)
11. Pressure-time Histories, Microphone No. 8 . . . . . (k)
12. Narrowband Analysis, Microphone No. 8 . . . . . (l)

D. Advanced Rotor System, C_T = .0036, V_∞ = 55.5 knots 13

1. One-third Octave, Microphone No. 2 . . . . . (a)
2. Pressure-time Histories, Microphone No. 2 . . . . . (b)
3. Narrowband Analysis, Microphone No. 2 . . . . . (c)
4. One-third Octave, Microphone No. 6 . . . . . (d)
5. Pressure-time Histories, Microphone No. 6 . . . . . (e)
6. Narrowband Analysis, Microphone No. 6 . . . . . (f)
7. One-third Octave, Microphone No. 7 . . . . . (g)
8. Pressure-time Histories, Microphone No. 7 . . . . . (h)
9. Narrowband Analysis, Microphone No. 7 . . . . . (i)
10. One-third Octave, Microphone No. 8 . . . . . (j)
11. Pressure-time Histories, Microphone No. 8 . . . . . (k)
12. Narrowband Analysis, Microphone No. 8 . . . . . (l)

Figure

Tunnel Velocity ≈ 60 knots

A. Standard Rotor System, C_T = .0032, V_∞ = 60.2 knots 14

1. One-third Octave, Microphone No. 2 . . . . . (a)
2. Pressure-time Histories, Microphone No. 2 . . . . . (b)
3. Narrowband Analysis, Microphone No. 2 . . . . . (c)
4. One-third Octave, Microphone No. 6 . . . . . (d)
5. Pressure-time Histories, Microphone No. 6 . . . . . (e)
6. Narrowband Analysis, Microphone No. 6 . . . . . (f)
7. One-third Octave, Microphone No. 7 . . . . . (g)
8. Pressure-time Histories, Microphone No. 7 . . . . . (h)
9. Narrowband Analysis, Microphone No. 7 . . . . . (i)
10. One-third Octave, Microphone No. 8 . . . . . (j)
11. Pressure-time Histories, Microphone No. 8 . . . . . (k)
12. Narrowband Analysis, Microphone No. 8 . . . . . (l)

B. Advanced Rotor System, C_T = .0031, V_∞ = 60.3 knots 15

1. One-third Octave, Microphone No. 2 . . . . . (a)
2. Pressure-time Histories, Microphone No. 2 . . . . . (b)
3. Narrowband Analysis, Microphone No. 2 . . . . . (c)
4. One-third Octave, Microphone No. 6 . . . . . (d)
5. Pressure-time Histories, Microphone No. 6 . . . . . (e)
6. Narrowband Analysis, Microphone No. 6 . . . . . (f)
7. One-third Octave, Microphone No. 7 . . . . . (g)
8. Pressure-time Histories, Microphone No. 7 . . . . . (h)
9. Narrowband Analysis, Microphone No. 7 . . . . . (i)
10. One-third Octave, Microphone No. 8 . . . . . (j)
11. Pressure-time Histories, Microphone No. 8 . . . . . (k)
12. Narrowband Analysis, Microphone No. 8 . . . . . (l)

C. Standard Rotor System, C_T = .0036, V_∞ = 59.9 knots 16

1. One-third Octave, Microphone No. 2 . . . . . (a)
2. Pressure-time Histories, Microphone No. 2 . . . . . (b)
3. Narrowband Analysis, Microphone No. 2 . . . . . (c)
4. One-third Octave, Microphone No. 6 . . . . . (d)
5. Pressure-time Histories, Microphone No. 6 . . . . . (e)
6. Narrowband Analysis, Microphone No. 6 . . . . . (f)
7. One-third Octave, Microphone No. 7 . . . . . (g)
8. Pressure-time Histories, Microphone No. 7 . . . . . (h)
9. Narrowband Analysis, Microphone No. 7 . . . . . (i)
10. One-third Octave, Microphone No. 8 . . . . . (j)
11. Pressure-time Histories, Microphone No. 8 . . . . . (k)
12. Narrowband Analysis, Microphone No. 8 . . . . . (l)

Figure

D. Advanced Rotor System, C_T, = .0036, V_∞ = 60.8 knots 17

1. One-third Octave, Microphone No. 2 . . . . . (a)
2. Pressure-time Histories, Microphone No. 2 . . . . . (b)
3. Narrowband Analysis, Microphone No. 2 . . . . . (c)
4. One-third Octave, Microphone No. 6 . . . . . (d)
5. Pressure-time Histories, Microphone No. 6 . . . . . (e)
6. Narrowband Analysis, Microphone No. 6 . . . . . (f)
7. One-third Octave, Microphone No. 7 . . . . . (g)
8. Pressure-time Histories, Microphone No. 7 . . . . . (h)
9. Narrowband Analysis, Microphone No. 7 . . . . . (i)
10. One-third Octave, Microphone No. 8 . . . . . (j)
11. Pressure-time Histories, Microphone No. 8 . . . . . (k)
12. Narrowband Analysis, Microphone No. 8 . . . . . (l)

Tunnel Velocity ≈ 65 knots

A. Standard Rotor System, C_T = .0032, V_∞ = 65.2 knots 18

1. One-third Octave, Microphone No. 2 . . . . . (a)
2. Pressure-time Histories, Microphone No. 2 . . . . . (b)
3. Narrowband Analysis, Microphone No. 2 . . . . . (c)
4. One-third Octave, Microphone No. 6 . . . . . (d)
5. Pressure-time Histories, Microphone No. 6 . . . . . (e)
6. Narrowband Analysis, Microphone No. 6 . . . . . (f)
7. One-third Octave, Microphone No. 7 . . . . . (g)
8. Pressure-time Histories, Microphone No. 7 . . . . . (h)
9. Narrowband Analysis, Microphone No. 7 . . . . . (i)
10. One-third Octave, Microphone No. 8 . . . . . (j)
11. Pressure-time Histories, Microphone No. 8 . . . . . (k)
12. Narrowband Analysis, Microphone No. 8 . . . . . (l)

B. Advanced Rotor System, C_T = .0031, V_∞ = 65.4 knots 19

1. One-third Octave, Microphone No. 2 . . . . . (a)
2. Pressure-time Histories, Microphone No. 2 . . . . . (b)
3. Narrowband Analysis, Microphone No. 2 . . . . . (c)
4. One-third Octave, Microphone No. 6 . . . . . (d)
5. Pressure-time Histories, Microphone No. 6 . . . . . (e)
6. Narrowband Analysis, Microphone No. 6 . . . . . (f)
7. One-third Octave, Microphone No. 7 . . . . . (g)
8. Pressure-time Histories, Microphone No. 7 . . . . . (h)
9. Narrowband Analysis, Microphone No. 7 . . . . . (i)
10. One-third Octave, Microphone No. 8 . . . . . (j)
11. Pressure-time Histories, Microphone No. 8 . . . . . (k)
12. Narrowband Analysis, Microphone No. 8 . . . . . (l)

Figure

C. Standard Rotor System, C_T = .0036, V_∞ = 65.0 knots 20

1. One-third Octave, Microphone No. 2 . . . . . (a)
2. Pressure-time Histories, Microphone No. 2 . . . . . (b)
3. Narrowband Analysis, Microphone No. 2 . . . . . (c)
4. One-third Octave, Microphone No. 6 . . . . . (d)
5. Pressure-time Histories, Microphone No. 6 . . . . . (e)
6. Narrowband Analysis, Microphone No. 6 . . . . . (f)
7. One-third Octave, Microphone No. 7 . . . . . (g)
8. Pressure-time Histories, Microphone No. 7 . . . . . (h)
9. Narrowband Analysis, Microphone No. 7 . . . . . (i)
10. One-third Octave, Microphone No. 8 . . . . . (j)
11. Pressure-time Histories, Microphone No. 8 . . . . . (k)
12. Narrowband Analysis, Microphone No. 8 . . . . . (l)

D. Advanced Rotor System, C_T = .0036, V_∞ = 65.2 knots 21

1. One-third Octave, Microphone No. 2 . . . . . (a)
2. Pressure-time Histories, Microphone No. 2 . . . . . (b)
3. Narrowband Analysis, Microphone No. 2 . . . . . (c)
4. One-third Octave, Microphone No. 6 . . . . . (d)
5. Pressure-time Histories, Microphone No. 6 . . . . . (e)
6. Narrowband Analysis, Microphone No. 6 . . . . . (f)
7. One-third Octave, Microphone No. 7 . . . . . (g)
8. Pressure-time Histories, Microphone No. 7 . . . . . (h)
9. Narrowband Analysis, Microphone No. 7 . . . . . (i)
10. One-third Octave, Microphone No. 8 . . . . . (j)
11. Pressure-time Histories, Microphone No. 8 . . . . . (k)
12. Narrowband Analysis, Microphone No. 8 . . . . . (l)

Tunnel Velocity ≈ 70 knots

A. Standard Rotor System, C_T = .0032, V_∞ = 70.2 knots 22

1. One-third Octave, Microphone No. 2 . . . . . (a)
2. Pressure-time Histories, Microphone No. 2 . . . . . (b)
3. Narrowband Analysis, Microphone No. 2 . . . . . (c)
4. One-third Octave, Microphone No. 6 . . . . . (d)
5. Pressure-time Histories, Microphone No. 6 . . . . . (e)
6. Narrowband Analysis, Microphone No. 6 . . . . . (f)
7. One-third Octave, Microphone No. 7 . . . . . (g)
8. Pressure-time Histories, Microphone No. 7 . . . . . (h)
9. Narrowband Analysis, Microphone No. 7 . . . . . (i)
10. One-third Octave, Microphone No. 8 . . . . . (j)
11. Pressure-time Histories, Microphone No. 8 . . . . . (k)
12. Narrowband Analysis, Microphone No. 8 . . . . . (l)

Figure

B. Advanced Rotor System, C_T = .0031, V_∞ = 70.3 knots 23

1. One-third Octave, Microphone No. 2 . . . . . (a)
2. Pressure-time Histories, Microphone No. 2 . . . . . (b)
3. Narrowband Analysis, Microphone No. 2 . . . . . (c)
4. One-third Octave, Microphone No. 6 . . . . . (d)
5. Pressure-time Histories, Microphone No. 6 . . . . . (e)
6. Narrowband Analysis, Microphone No. 6 . . . . . (f)
7. One-third Octave, Microphone No. 7 . . . . . (g)
8. Pressure-time Histories, Microphone No. 7 . . . . . (h)
9. Narrowband Analysis, Microphone No. 7 . . . . . (i)
10. One-third Octave, Microphone No. 8 . . . . . (j)
11. Pressure-time Histories, Microphone No. 8 . . . . . (k)
12. Narrowband Analysis, Microphone No. 8 . . . . . (l)

C. Standard Rotor System, C_T = .0036, V_∞ = 70.4 knots 24

1. One-third Octave, Microphone No. 2 . . . . . (a)
2. Pressure-time Histories, Microphone No. 2 . . . . . (b)
3. Narrowband Analysis, Microphone No. 2 . . . . . (c)
4. One-third Octave, Microphone No. 6 . . . . . (d)
5. Pressure-time Histories, Microphone No. 6 . . . . . (e)
6. Narrowband Analysis, Microphone No. 6 . . . . . (f)
7. One-third Octave, Microphone No. 7 . . . . . (g)
8. Pressure-time Histories, Microphone No. 7 . . . . . (h)
9. Narrowband Analysis, Microphone No. 7 . . . . . (i)

D. Advanced Rotor System, C_T = .0036, V_∞ = 70.6 knots 25

1. One-third Octave, Microphone No. 2 . . . . . (a)
2. Pressure-time Histories, Microphone No. 2 . . . . . (b)
3. Narrowband Analysis, Microphone No. 2 . . . . . (c)
4. One-third Octave, Microphone No. 6 . . . . . (d)
5. Pressure-time Histories, Microphone No. 6 . . . . . (e)
6. Narrowband Analysis, Microphone No. 6 . . . . . (f)
7. One-third Octave, Microphone No. 7 . . . . . (g)
8. Pressure-time Histories, Microphone No. 7 . . . . . (h)
9. Narrowband Analysis, Microphone No. 7 . . . . . (i)
10. One-third Octave, Microphone No. 8 . . . . . (j)
11. Pressure-time Histories, Microphone No. 8 . . . . . (k)
12. Narrowband Analysis, Microphone No. 8 . . . . . (l)

Figure

Tunnel Velocity ≈ 75 knots

A. Standard Rotor System, C_T = .0032, V_∞ = 75.0 knots 26

1. One-third Octave, Microphone No. 2 . . . . . (a)
2. Pressure-time Histories, Microphone No. 2 . . . . . (b)
3. Narrowband Analysis, Microphone No. 2 . . . . . (c)
4. One-third Octave, Microphone No. 6 . . . . . (d)
5. Pressure-time Histories, Microphone No. 6 . . . . . (e)
6. Narrowband Analysis, Microphone No. 6 . . . . . (f)
7. One-third Octave, Microphone No. 7 . . . . . (g)
8. Pressure-time Histories, Microphone No. 7 . . . . . (h)
9. Narrowband Analysis, Microphone No. 7 . . . . . (i)
10. One-third Octave, Microphone No. 8 . . . . . (j)
11. Pressure-time Histories, Microphone No. 8 . . . . . (k)
12. Narrowband Analysis, Microphone No. 8 . . . . . (l)

B. Standard Rotor System, C_T = .0036, V_∞ = 74.8 knots 27

1. One-third Octave, Microphone No. 2 . . . . . (a)
2. Pressure-time Histories, Microphone No. 2 . . . . . (b)
3. Narrowband Analysis, Microphone No. 2 . . . . . (c)
4. One-third Octave, Microphone No. 6 . . . . . (d)
5. Pressure-time Histories, Microphone No. 6 . . . . . (e)
6. Narrowband Analysis, Microphone No. 6 . . . . . (f)
7. One-third Octave, Microphone No. 7 . . . . . (g)
8. Pressure-time Histories, Microphone No. 7 . . . . . (h)
9. Narrowband Analysis, Microphone No. 7 . . . . . (i)
10. One-third Octave, Microphone No. 8 . . . . . (j)
11. Pressure-time Histories, Microphone No. 8 . . . . . (k)
12. Narrowband Analysis, Microphone No. 8 . . . . . (l)

C. Advanced Rotor System, C_T = .0036, V_∞ = 75.0 knots 28

1. One-third Octave, Microphone No. 2 . . . . . (a)
2. Pressure-time Histories, Microphone No. 2 . . . . . (b)
3. Narrowband Analysis, Microphone No. 2 . . . . . (c)
4. One-third Octave, Microphone No. 6 . . . . . (d)
5. Pressure-time Histories, Microphone No. 6 . . . . . (e)
6. Narrowband Analysis, Microphone No. 6 . . . . . (f)
7. One-third Octave, Microphone No. 7 . . . . . (g)
8. Pressure-time Histories, Microphone No. 7 . . . . . (h)
9. Narrowband Analysis, Microphone No. 7 . . . . . (i)
10. One-third Octave, Microphone No. 8 . . . . . (j)
11. Pressure-time Histories, Microphone No. 8 . . . . . (k)
12. Narrowband Analysis, Microphone No. 8 . . . . . (l)

Figure

Tunnel Velocity ≈ 80 knots

A. Standard Rotor System, C_T = .0032, V_∞ = 80.2 knots 29

1. One-third Octave, Microphone No. 2 . . . . . (a)
2. Pressure-time Histories, Microphone No. 2 . . . . . (b)
3. Narrowband Analysis, Microphone No. 2 . . . . . (c)
4. One-third Octave, Microphone No. 6 . . . . . (d)
5. Pressure-time Histories, Microphone No. 6 . . . . . (e)
6. Narrowband Analysis, Microphone No. 6 . . . . . (f)
7. One-third Octave, Microphone No. 7 . . . . . (g)
8. Pressure-time Histories, Microphone No. 7 . . . . . (h)
9. Narrowband Analysis, Microphone No. 7 . . . . . (i)
10. One-third Octave, Microphone No. 8 . . . . . (j)
11. Pressure-time Histories, Microphone No. 8 . . . . . (k)
12. Narrowband Analysis, Microphone No. 8 . . . . . (l)

B. Advanced Rotor System, C_T = .0031, V_∞ = 80.4 knots 30

1. One-third Octave, Microphone No. 2 . . . . . (a)
2. Pressure-time Histories, Microphone No. 2 . . . . . (b)
3. Narrowband Analysis, Microphone No. 2 . . . . . (c)
4. One-third Octave, Microphone No. 6 . . . . . (d)
5. Pressure-time Histories, Microphone No. 6 . . . . . (e)
6. Narrowband Analysis, Microphone No. 6 . . . . . (f)
7. One-third Octave, Microphone No. 7 . . . . . (g)
8. Pressure-time Histories, Microphone No. 7 . . . . . (h)
9. Narrowband Analysis, Microphone No. 7 . . . . . (i)
10. One-third Octave, Microphone No. 8 . . . . . (j)
11. Pressure-time Histories, Microphone No. 8 . . . . . (k)
12. Narrowband Analysis, Microphone No. 8 . . . . . (l)

C. Advanced Rotor System, C_T = .0036, V_∞ = 80.3 knots 31

1. One-third Octave, Microphone No. 2 . . . . . (a)
2. Narrowband Analysis, Microphone No. 2 . . . . . (b)
3. One-third Octave, Microphone No. 6 . . . . . (c)
4. Narrowband Analysis, Microphone No. 6 . . . . . (d)
5. One-third Octave, Microphone No. 7 . . . . . (e)
6. Narrowband Analysis, Microphone No. 7 . . . . . (f)
7. One-third Octave, Microphone No. 8 . . . . . (g)
8. Narrowband Analysis, Microphone No. 8 . . . . . (h)

Figure

Tunnel Velocity ≈ 90 knots

A. Standard Rotor System, C_T = .0032, V_∞ = 90.1 knots 32

1. One-third Octave, Microphone No. 2 . . . . . (a)
2. Pressure-time Histories, Microphone No. 2 . . . . . (b)
3. Narrowband Analysis, Microphone No. 2 . . . . . (c)
4. One-third Octave, Microphone No. 6 . . . . . (d)
5. Pressure-time Histories, Microphone No. 6 . . . . . (e)
6. Narrowband Analysis, Microphone No. 6 . . . . . (f)
7. One-third Octave, Microphone No. 7 . . . . . (g)
8. Pressure-time Histories, Microphone No. 7 . . . . . (h)
9. Narrowband Analysis, Microphone No. 7 . . . . . (i)
10. One-third Octave, Microphone No. 8 . . . . . (j)
11. Pressure-time Histories, Microphone No. 8 . . . . . (k)
12. Narrowband Analysis, Microphone No. 8 . . . . . (l)

B. Advanced Rotor System, C_T = .0031, V_∞ = 90.4 knots 33

1. One-third Octave, Microphone No. 2 . . . . . (a)
2. Pressure-time Histories, Microphone No. 2 . . . . . (b)
3. Narrowband Analysis, Microphone No. 2 . . . . . (c)
4. One-third Octave, Microphone No. 6 . . . . . (d)
5. Pressure-time Histories, Microphone No. 6 . . . . . (e)
6. Narrowband Analysis, Microphone No. 6 . . . . . (f)
7. One-third Octave, Microphone No. 7 . . . . . (g)
8. Pressure-time Histories, Microphone No. 7 . . . . . (h)
9. Narrowband Analysis, Microphone No. 7 . . . . . (i)
10. One-third Octave, Microphone No. 8 . . . . . (j)
11. Pressure-time Histories, Microphone No. 8 . . . . . (k)
12. Narrowband Analysis, Microphone No. 8 . . . . . (l)

C. Standard Rotor System, C_T = .0036, V_∞ = 90.3 knots 34

1. One-third Octave, Microphone No. 2 . . . . . (a)
2. Pressure-time Histories, Microphone No. 2 . . . . . (b)
3. Narrowband Analysis, Microphone No. 2 . . . . . (c)
4. One-third Octave, Microphone No. 6 . . . . . (d)
5. Pressure-time Histories, Microphone No. 6 . . . . . (e)
6. Narrowband Analysis, Microphone No. 6 . . . . . (f)
7. One-third Octave, Microphone No. 7 . . . . . (g)
8. Pressure-time Histories, Microphone No. 7 . . . . . (h)
9. Narrowband Analysis, Microphone No. 7 . . . . . (i)
10. One-third Octave, Microphone No. 8 . . . . . (j)
11. Pressure-time Histories, Microphone No. 8 . . . . . (k)
12. Narrowband Analysis, Microphone No. 8 . . . . . (l)

Figure

D. Advanced Rotor System, C_T = .0036, V_∞ = 90.3 knots 35

1. One-third Octave, Microphone No.2 . . . . . (a)
2. Narrowband Analysis, Microphone No. 2 . . . . . (b)
3. One-third Octave, Microphone No. 6 . . . . . (c)
4. Narrowband Analysis, Microphone No. 6 . . . . . (d)
5. One-third Octave, Microphone No. 7 . . . . . (e)
6. Narrowband Analysis, Microphone No. 7 . . . . . (f)
7. One-third Octave, Microphone No. 8 . . . . . (g)
8. Narrowband Analysis, Microphone No. 8 . . . . . (h)

Background noise data indicate that the helicopter noise measured on microphones 2, 6, and 7 are well above background levels for most tunnel velocities tested. The exceptions are at the higher tunnel velocities for the higher frequencies only, where the background noise does contaminate the measured helicopter noise. Also, microphone 2 background noise contains a pure tone at about 1000 Hz while microphone 6 background noise contains a pure tone at about 5000 Hz. The helicopter noise measured at microphone 8 is heavily contaminated with background noise at all tunnel velocities for the higher frequencies and for all frequencies at the higher tunnel velocities. The reader should be careful in interpreting the generated helicopter noise for these cases and consider the effect of the background noise levels.

REFERENCES

1. Lowson, M. V.; and Ollerhead, J. B.: Studies of Helicopter Rotor Noise. USSAAVLABS Tech. Rep. 68-60, U.S. Army Aviation Labs., 1969.

2. Langenbucher, V.: Noise Phenomena With Helicopter Rotors and Possibilities of Noise Reduction. ESA-TT-244, European Space Agency, 1976.

3. Powell, C. A.; and McCurdy, D. A.: Effects of Repetition Rate and Impulsiveness of Simulated Helicopter Rotor Noise on Annoyance. NASA TP-1969, 1982.

4. Bingham, G. J.: The Aerodynamic Influence of Rotor Blade Airfoils, Twist, Taper, and Solidity on Hover and Forward Flight Performance. Preprint No. 81-49, Proceedings of the 37th Annual Forum of the American Helicopter Society, May, 1981.

5. Boxwell, D. A.; and Schmitz, F. H.: In-Flight Acoustic Comparison of the 540 and K747 Main Rotors for the AH-15 Helicopter. Appendix for the U.S. Army Aviation Engineering Flight Activity Report, Project 77-38, October 1979.

6. Berry, J. D.: Performance Testing of a Main Rotor System for a Utility Helicopter at 1/4 Scale. NASA TM 83274, 1982.

7. Hoad, D. R.; and Conner, D. A.: Acoustic Performance Evaluation of an Advanced UH-1 Helicopter Main Rotor System. Preprint No. 81-58, Proceedings of the 37th Annual Forum of the American Helicopter Society, May 1981.

8. Wilson, J. C.: A General Rotor Model System for Wind-Tunnel Investigations. Journal of Aircraft, 14, (7), 1977, pp. 639-643.

9. Bingham, G. J.; Noonan, K. W.; and Jones, K. W.: Two-Dimensional Aerodynamic Characteristics of Three Rotorcraft Airfoils at Mach Numbers from 0.35 to 0.90. NASA TP-2000, 1982.

10. Theobald, M. A.: Evaluation of the Acoustic Measurement Capability of the NASA Langley V/STOL Wind Tunnel Open Test Section with Acoustically Absorbent Ceiling and Floor Treatments. NASA CR 165796. (BBN Rep. No. 3820.) May 1978.

11. Cox, C. R.: Helicopter Rotor Aerodynamic and Aeroacoustic Environments. AIAA Preprint No. 77-1338, October 1977.

12. Hoad, D. R.; and Green, G. C.: Helicopter Noise Research at the Langley V/STOL Tunnel. NASA CP-2052, Pt. I, 1978, pp. 181-204.

13. Schmitz, F. H.; and Boxwell, D. A.: In-Flight Far-Field Measurement of Helicopter Impulsiveness Noise. Preprint No. 1062, Proceedings of the 32nd Annual National V/STOL Forum, AHS, May 1975.

14. Widnall, S.: Helicopter Noise Due to Blade-Vortex Interaction. Journal of the Acoustical Society of America, 50, Pt. 2, July 1971, pp. 354-365.

15. Heyson, H. H.: Use of Superposition in Digital Computers to Obtain Wind-Tunnel Interference Factors foir Arbitrary Configurations, With Particular Reference to V/STOL Models. NASA TR R-302, 1969.

16. Brown, T. J.; Brown, C. G.; and Hardin, J. C.: Program for the Analysis of Time Series. NASA TM X-2988, 1974.

17. Singleton, R. C.: On Computing the Fast Fourier Transform. Association for Computing Machinery Communications, (10), 1967, pp. 647-654.

Table I. Rotor Characteristics

Number of Blades	2
Airfoil Section	
Standard Blade	NACA 0012
Advanced Blade	RC12(B)3, RC10(B)3, RC08(B)3
Radius, m	1.829
Blade Chord	
Standard Blade, m	0.1334
Advanced Blade	Variable
Twist	
Standard Blade, deg.	-10.9
Advanced Blade, deg.	-14.0
Planform Solidity	
Standard Blade	0.04642
Advanced Blade	0.04863
Root Cutout, m	0.1554

Table II. Microphone Locations Relative To Rotor Hub With Model at an Angle of Attack of 0°

Microphone Location	x, m	y, m	z, m
2	-0.475	0.675	-0.760
6	-3.429	1.156	-1.727
7	-3.429	-0.051	-1.724
8	-3.429	-1.334	-1.727

TABLE III - STANDARD ROTOR OPERATING CONDITIONS

Run	Point	V_∞, knots	α, deg	μ	a_{1_S}, deg	b_{1_S}, deg	A_1, deg	B_1, deg	θ_C, deg	α_{TPP}, deg	C_Q	C_T	γ, deg
154	2015	50.9	0.42	0.11	-0.37	-1.45	-3.11	2.16	6.02	-4.84	.00014	.0032	-4.07
154	2016	49.7	1.43	0.10	-0.43	-1.43	-3.11	2.16	5.83	-3.90	.00013	.0032	-3.17
154	2017	49.9	2.48	0.10	-0.45	-1.40	-3.11	2.16	5.65	-2.87	.00012	.0032	-2.17
154	2018	49.7	3.39	0.10	-0.43	-1.46	-3.19	2.05	5.44	-1.93	.00011	.0031	-1.20
154	2019	49.6	4.36	0.10	-0.44	-1.44	-3.24	2.06	5.31	-0.97	.00011	.0031	-0.29
154	2022	50.0	7.40	0.10	-0.41	-1.51	-3.26	1.81	4.75	2.10	.00009	.0031	2.78
154	2024	50.2	9.36	0.10	-0.43	-1.45	-3.19	1.70	4.41	4.04	.00008	.0032	4.70
154	2027	50.5	11.28	0.10	-0.40	-1.45	-3.10	1.50	4.03	6.00	.00007	.0032	6.72
155	2028	55.1	11.27	0.11	-0.32	-1.35	-2.86	1.52	3.79	6.06	.00006	.0031	6.89
155	2031	55.3	8.28	0.11	-0.31	-1.35	-2.92	1.71	4.38	3.07	.00008	.0031	3.90
155	2033	55.3	6.28	0.12	-0.22	-1.38	-2.95	1.76	4.75	1.17	.00009	.0031	1.99
155	2035	55.5	4.26	0.12	-0.27	-1.36	-2.93	2.01	5.18	-0.90	.00011	.0031	-0.09
155	2037	55.4	2.32	0.12	-0.24	-1.37	-2.91	2.04	5.56	-2.81	.00012	.0031	-1.94
155	2039	55.3	0.43	0.11	-0.27	-1.37	-2.92	2.19	5.90	-4.74	.00013	.0031	-3.87
158	2055	60.6	0.33	0.13	-0.27	-1.28	-2.72	2.42	6.12	-4.84	.00014	.0032	-3.93
158	2056	60.3	1.33	0.12	-0.28	-1.39	-2.91	2.41	5.91	-3.84	.00013	.0032	-2.95
158	2057	60.1	2.38	0.12	-0.27	-1.32	-2.81	2.32	5.60	-2.78	.00012	.0032	-1.88
158	2059	60.0	4.33	0.12	-0.30	-1.38	-2.91	2.35	5.25	-0.87	.00011	.0032	-0.04
158	2061	60.1	6.22	0.12	-0.33	-1.37	-2.91	2.17	4.81	0.99	.00009	.0032	1.83
158	2065	59.9	10.27	0.12	-0.28	-1.41	-2.90	1.74	4.07	5.11	.00006	.0033	5.90
159	2066	65.2	0.33	0.13	-0.30	-1.40	-2.89	2.66	6.05	-4.85	.00013	.0032	-3.88
159	2067	65.6	1.33	0.14	-0.23	-1.32	-2.74	2.58	5.83	-3.80	.00013	.0032	-2.85
159	2068	65.5	2.29	0.14	-0.27	-1.42	-2.81	2.47	5.63	-2.86	.00012	.0032	-1.83
159	2070	64.8	4.26	0.13	-0.32	-1.32	-2.73	2.34	5.11	-0.95	.00010	.0032	0.00
159	2072	64.9	6.33	0.13	-0.17	-1.46	-2.83	1.97	4.70	1.28	.00009	.0032	2.22
159	2076	65.0	10.21	0.13	-0.36	-1.36	-2.64	1.80	3.85	4.97	.00006	.0032	5.94
160	2077	70.5	0.31	0.15	-0.31	-1.38	-2.61	2.67	6.08	-4.87	.00013	.0032	-3.72
160	2078	70.3	1.19	0.15	-0.26	-1.41	-2.64	2.56	5.84	-3.94	.00012	.0032	-2.79
160	2081	70.2	4.22	0.15	-0.29	-1.39	-2.62	2.35	5.11	-0.95	.00010	.0032	0.21
160	2083	70.2	6.20	0.15	-0.30	-1.33	-2.54	2.22	4.64	1.02	.00009	.0032	2.09
160	2085	70.2	8.14	0.15	-0.31	-1.35	-2.51	1.97	4.19	2.95	.00007	.0032	4.08
160	2087	69.8	10.09	0.14	-0.33	-1.40	-2.54	1.80	3.78	4.89	.00005	.0032	6.02

TABLE III - CONTINUED

Run	Point	V_∞, knots	α, deg	μ	a_{1_S}, deg	b_{1_S}, deg	A_1, deg	B_1, deg	θ_c, deg	α_{TPP}, deg	C_Q	C_T	γ, deg
161	2088	75.4	0.25	0.16	-0.32	-1.34	-2.52	2.94	6.18	-4.96	.00013	.0032	-3.81
161	2089	74.8	1.18	0.15	-0.30	-1.34	-2.54	2.88	5.93	-4.01	.00013	.0032	-2.92
162	2098	74.7	4.23	0.15	-0.09	-1.22	-2.36	2.27	5.08	-0.75	.00010	.0032	0.56
162	2100	75.1	6.06	0.16	-0.08	-1.21	-2.35	2.04	4.53	1.08	.00008	.0032	2.39
162	2102	75.1	8.16	0.16	-0.13	-1.12	-2.22	1.89	4.02	3.13	.00007	.0032	4.41
162	2103	75.1	9.06	0.15	0.01	-1.21	-2.32	1.65	3.78	4.18	.00006	.0032	5.49
163	2104	80.2	9.11	0.17	-0.10	-1.17	-2.23	1.94	3.74	4.11	.00006	.0032	5.51
163	2106	80.0	7.16	0.17	-0.07	-1.16	-2.25	2.11	4.23	2.19	.00007	.0032	3.56
163	2108	79.8	5.05	0.17	-0.05	-1.21	-2.28	2.31	4.78	0.11	.00009	.0032	1.52
163	2109	80.1	4.14	0.17	-0.04	-1.24	-2.35	2.48	5.06	-0.80	.00010	.0032	0.62
163	2110	80.6	3.15	0.17	-0.02	-1.18	-2.29	2.55	5.31	-1.78	.00011	.0032	-0.33
163	2112	80.7	1.14	0.17	-0.07	-1.20	-2.26	2.70	5.86	-3.83	.00013	.0032	-2.34
163	2113	79.9	0.15	0.16	-0.06	-1.16	-2.23	2.80	6.13	-4.82	.00013	.0032	-3.39
164	2114	90.1	0.23	0.19	-0.11	-1.23	-2.17	3.24	6.35	-4.77	.00014	.0032	-3.07
164	2115	90.1	1.18	0.19	-0.05	-1.26	-2.25	3.11	6.07	-3.77	.00013	.0032	-2.10
164	2116	90.1	2.08	0.19	0.02	-1.21	-2.18	2.95	5.74	-2.80	.00012	.0032	-1.14
164	2117	90.3	3.07	0.19	-0.11	-1.18	-2.11	2.93	5.44	-1.93	.00011	.0032	-0.25
164	2120	90.1	6.03	0.19	-0.01	-1.24	-2.16	2.45	4.50	1.13	.00008	.0032	2.73
164	2122	89.9	8.00	0.19	-0.04	-1.17	-2.09	2.31	3.90	3.06	.00006	.0032	4.65
165	2126	50.6	8.28	0.10	0.00	-1.21	-3.02	1.38	4.50	3.39	.00009	.0032	4.00
165	2127	50.4	7.27	0.10	-0.06	-1.14	-2.96	1.51	4.70	2.31	.00009	.0032	2.93
165	2130	50.4	4.52	0.10	-0.03	-1.20	-3.11	1.73	5.19	-0.41	.00011	.0032	0.16
165	2133	50.9	1.39	0.11	-0.01	-1.20	-3.04	1.88	5.71	-3.53	.00013	.0032	-2.90
179	2247	50.2	0.49	0.10	0.00	-1.10	-2.92	2.08	6.73	-4.43	.00016	.0036	-3.78
179	2248	50.0	2.46	0.10	-0.04	-1.00	-3.10	2.16	6.37	-2.50	.00015	.0036	-1.91
179	2249	49.6	4.39	0.10	0.07	-1.19	-3.31	1.87	6.00	-0.44	.00013	.0036	0.17
179	2250	49.8	6.45	0.10	0.03	-1.25	-3.34	1.76	5.67	1.58	.00012	.0037	2.15
179	2251	49.5	8.39	0.10	0.00	-1.19	-3.26	1.65	5.26	3.49	.00011	.0036	4.04
179	2253	49.5	12.43	0.10	-0.02	-1.18	-3.22	1.31	4.54	7.51	.00008	.0037	8.11
180	2255	55.5	12.25	0.11	-0.01	-1.09	-2.93	1.52	4.24	7.34	.00007	.0036	7.98
180	2258	55.8	6.34	0.12	-0.03	-1.15	-3.03	2.07	5.47	1.40	.00011	.0036	2.00
180	2259	55.7	4.33	0.12	-0.04	-1.12	-2.98	2.23	5.86	-0.63	.00013	.0036	-0.02
180	2260	55.5	2.46	0.12	0.03	-1.10	-2.97	2.34	6.30	-2.43	.00014	.0037	-1.84

TABLE III - CONCLUDED

Run	Point	V_∞, knots	α, deg	μ	a_{1_S}, deg	b_{1_S}, deg	A_1, deg	B_1, deg	θ_C, deg	α_{TPP}, deg	C_Q	C_T	γ, deg
181	2261	60.4	0.34	0.12	0.03	-1.11	-2.96	2.69	6.70	-4.54	.00016	.0037	-3.93
181	2262	60.2	2.26	0.12	0.05	-1.15	-2.96	2.51	6.29	-2.60	.00014	.0037	-2.00
181	2264	59.7	6.42	0.12	0.02	-1.09	-2.87	2.17	5.29	1.53	.00011	.0037	2.16
181	2267	59.4	12.25	0.12	-0.02	-1.17	-2.88	1.64	4.07	7.34	.00006	.0037	8.03
182	2272	64.8	0.37	0.13	0.06	0.05	-1.15	2.16	6.50	-4.58	.00015	.0036	-3.22
182	2273	65.1	2.36	0.14	0.05	-1.18	-2.62	2.38	6.08	-2.50	.00014	.0036	-1.50
182	2275	65.3	4.27	0.14	-0.03	-1.11	-2.63	2.30	5.61	-0.67	.00012	.0036	0.34
182	2276	65.1	6.26	0.13	-0.02	-1.16	-2.64	2.10	5.13	1.33	.00010	.0036	2.35
182	2277	64.9	8.14	0.13	-0.10	-1.19	-2.75	2.01	4.68	3.14	.00009	.0036	4.15
182	2278	64.8	10.31	0.13	0.00	-1.10	-2.49	1.67	4.17	5.41	.00007	.0036	6.48
183	2279	70.3	10.38	0.14	0.01	-1.12	-2.39	1.75	3.99	5.50	.00006	.0036	6.71
183	2280	70.5	8.14	0.15	0.02	-1.20	-2.47	1.97	4.53	3.27	.00008	.0036	4.43
183	2281	70.1	6.15	0.15	-0.02	-1.20	-2.48	2.17	5.00	1.22	.00010	.0036	2.42
183	2282	70.2	4.14	0.15	-0.09	-1.19	-2.49	2.41	5.55	-0.86	.00011	.0036	0.35
183	2283	70.4	2.34	0.15	-0.04	-1.18	-2.40	2.55	6.03	-2.61	.00013	.0036	-1.38
183	2284	70.6	0.27	0.15	-0.16	-1.20	-2.34	2.76	6.51	-4.79	.00015	.0036	-3.50
184	2285	74.6	0.31	0.15	-0.06	-1.17	-2.22	2.69	6.51	-4.66	.00015	.0036	-3.22
184	2286	75.3	2.17	0.16	-0.05	-1.08	-2.10	2.61	6.08	-2.79	.00013	.0036	-1.36
184	2288	74.7	6.25	0.15	0.02	-1.05	-2.09	2.01	4.89	1.37	.00009	.0035	2.83
184	2289	74.4	8.11	0.15	-0.03	-1.09	-2.18	2.02	4.46	3.18	.00007	.0036	4.52
184	2290	75.1	10.17	0.15	-0.09	-1.15	-2.23	1.91	3.94	5.18	.00006	.0036	6.52
185	2291	80.4	10.23	0.17	-0.05	-1.14	-2.14	2.07	3.89	5.28	.00005	.0036	6.69
185	2293	80.5	6.23	0.17	-0.05	-1.21	-2.13	2.24	4.90	1.28	.00009	.0036	2.86
185	2294	81.2	4.12	0.17	0.00	-1.16	-2.12	2.53	5.50	-0.78	.00011	.0035	0.78
185	2296	81.1	0.30	0.17	-0.01	-1.17	-2.10	3.08	6.71	-4.62	.00015	.0036	-3.16
186	2297	90.9	0.37	0.19	0.00	-1.17	-1.96	3.38	6.86	-4.53	.00016	.0036	-2.83
186	2298	90.2	2.12	0.19	-0.07	-1.12	-1.95	3.24	6.28	-2.86	.00014	.0036	-1.20
186	2299	90.3	4.15	0.19	-0.15	-1.13	-2.11	3.12	5.53	-0.90	.00011	.0035	0.71
186	2300	90.0	6.12	0.19	-0.02	-1.21	-2.02	2.72	4.95	1.21	.00009	.0036	2.74
186	2302	89.9	10.18	0.19	0.03	-1.09	-1.99	2.26	3.72	5.31	.00005	.0036	6.95

TABLE IV - ADVANCED ROTOR OPERATING CONDITIONS

Run	Point	V_∞, knots	α, deg	μ	a_{1_S}, deg	b_{1_S}, deg	A_1, deg	B_1, deg	θ_C, deg	α_{TPP}, deg	C_Q	C_T	γ, deg
193	2425	49.6	0.45	0.10	-0.13	-1.24	-3.33	2.14	7.86	-4.58	.00011	.0031	-4.14
193	2427	50.2	2.49	0.10	-0.16	-1.28	-3.39	2.09	7.48	-2.57	.00010	.0031	-2.31
193	2428	50.3	3.48	0.10	-0.24	-1.26	-3.39	2.09	7.29	-1.66	.00009	.0031	-1.36
193	2433	49.9	8.35	0.10	-0.21	-1.27	-3.49	1.78	6.41	3.25	.00007	.0031	3.48
193	2434	50.7	9.25	0.10	-0.07	-1.25	-3.45	1.56	6.22	4.28	.00006	.0031	4.60
193	2436	50.2	11.23	0.10	-0.06	-1.15	-3.32	1.33	5.86	6.27	.00005	.0031	6.68
193	2437	50.3	11.99	0.10	-0.07	-1.15	-3.32	1.33	5.74	7.01	.00004	.0031	7.40
194	2438	60.7	12.18	0.12	-0.13	-1.29	-3.15	1.57	5.36	7.17	.00003	.0031	7.85
194	2442	60.4	8.21	0.13	-0.11	-1.20	-3.11	1.79	6.16	3.19	.00005	.0031	3.81
194	2444	60.4	6.06	0.13	-0.06	-1.19	-3.12	1.96	6.60	1.09	.00007	.0031	1.59
194	2446	60.4	4.32	0.13	-0.15	-1.28	-3.20	2.27	7.05	-0.72	.00008	.0031	-0.33
194	2448	60.2	2.20	0.12	0.02	-1.29	-3.20	2.27	7.52	-2.68	.00010	.0031	-2.38
194	2449	60.0	1.36	0.12	-0.02	-1.30	-3.20	2.27	7.64	-3.55	.00010	.0031	-3.18
194	2450	60.3	0.29	0.12	0.00	-1.25	-3.10	2.41	7.91	-4.61	.00011	.0031	-4.35
195	2451	70.3	0.26	0.15	-0.05	-1.24	-2.88	2.73	7.99	-4.70	.00011	.0031	-4.17
195	2452	70.2	1.27	0.14	-0.13	-1.24	-2.88	2.73	7.76	-3.76	.00010	.0031	-3.20
195	2455	70.5	4.20	0.15	-0.17	-1.31	-3.00	2.55	7.08	-0.87	.00008	.0031	-0.32
195	2456	70.0	5.24	0.14	-0.28	-1.30	-3.01	2.55	6.84	0.07	.00007	.0031	0.57
195	2458	70.5	7.16	0.15	-0.29	-1.24	-2.85	2.25	6.27	1.96	.00006	.0030	2.56
195	2461	70.3	10.14	0.14	-0.13	-1.22	-2.83	1.81	5.54	5.10	.00003	.0031	5.66
196	2462	80.1	10.17	0.17	-0.24	-1.26	-2.67	2.20	5.47	5.04	.00003	.0031	5.75
196	2464	80.4	8.04	0.17	-0.09	-1.23	-2.67	2.20	5.96	3.05	.00004	.0031	3.66
196	2467	80.7	5.15	0.17	-0.12	-1.16	-2.64	2.61	6.82	0.13	.00007	.0031	0.54
196	2468	80.5	4.11	0.17	-0.02	-1.16	-2.64	2.62	7.10	-0.82	.00008	.0031	-0.48
196	2471	80.4	1.27	0.17	0.10	-1.27	-2.79	2.79	7.90	-3.53	.00010	.0031	-3.32
196	2472	80.5	0.27	0.17	-0.03	-1.20	-2.64	3.02	8.20	-4.67	.00011	.0031	-4.50
197	2473	90.4	0.23	0.19	-0.09	-1.20	-2.51	3.41	8.44	-4.76	.00011	.0031	-4.39
197	2474	90.4	-0.84	0.19	0.10	-1.14	-2.52	3.41	8.78	-5.66	.00012	.0032	-5.40
197	2475	90.3	1.10	0.19	-0.03	-1.14	-2.45	3.29	8.18	-3.85	.00011	.0031	-3.58
197	2476	90.4	2.18	0.19	-0.04	-1.19	-2.52	3.15	7.84	-2.77	.00009	.0031	-2.47
197	2479	90.1	4.19	0.19	-0.24	-1.24	-2.58	3.07	7.29	-0.95	.00008	.0031	-0.60

TABLE IV - CONTINUED

Run	Point	V_∞, knots	α, deg	μ	a_{1_S}, deg	b_{1_S}, deg	A_1, deg	B_1, deg	θ_c, deg	α_{TPP}, deg	C_Q	C_T	γ, deg
197	2480	90.5	5.12	0.19	-0.35	-1.26	-2.57	3.06	7.04	-0.13	.00007	.0031	0.24
197	2481	90.4	6.09	0.19	-0.26	-1.30	-2.59	2.80	6.70	0.94	.00006	.0031	1.38
197	2483	90.2	8.04	0.19	-0.19	-1.17	-2.41	2.58	6.08	2.94	.00004	.0031	3.41
197	2484	90.5	9.11	0.19	-0.10	-1.24	-2.46	2.32	5.62	4.11	.00003	.0031	4.59
199	2557	55.6	0.88	0.12	-0.11	-1.20	-2.94	2.13	7.88	-4.14	.00011	.0031	-2.41
199	2560	55.6	3.89	0.12	-0.13	-1.23	-3.04	1.98	7.28	-1.14	.00009	.0031	0.23
199	2562	55.6	5.84	0.12	0.11	-1.11	-2.96	1.53	6.86	1.04	.00008	.0031	2.41
199	2564	55.6	7.79	0.12	-0.23	-1.26	-3.07	1.69	6.50	2.66	.00007	.0031	3.89
199	2567	55.8	10.80	0.12	-0.09	-1.22	-2.98	1.30	5.89	5.81	.00005	.0032	6.88
200	2572	65.9	0.65	0.14	0.14	-1.04	-2.74	2.45	7.96	-4.13	.00011	.0032	-3.64
200	2574	65.1	2.69	0.13	0.21	-1.07	-2.83	2.13	7.56	-2.02	.00010	.0032	-1.48
200	2575	65.5	3.69	0.14	0.20	-0.99	-2.73	2.06	7.30	-1.04	.00009	.0031	-0.36
200	2576	65.3	4.66	0.13	0.08	-0.96	-2.73	2.06	7.10	-0.20	.00008	.0031	0.64
200	2578	65.0	6.60	0.13	0.21	-1.02	-2.76	1.69	6.57	1.88	.00007	.0031	2.97
200	2581	65.6	9.58	0.14	0.02	-1.03	-2.76	1.68	5.96	4.69	.00005	.0032	5.94
200	2582	65.4	10.54	0.13	0.18	-1.06	-2.77	1.41	5.69	5.81	.00004	.0032	7.21
201	2583	75.6	10.36	0.16	0.13	-0.97	-2.39	1.63	5.40	5.56	.00003	.0031	7.36
201	2588	75.4	5.48	0.16	0.29	-0.87	-2.36	2.00	6.75	0.82	.00007	.0032	2.40
201	2590	75.7	3.49	0.16	0.31	-0.88	-2.35	2.12	7.26	-1.14	.00009	.0032	0.40
201	2591	75.7	2.49	0.16	0.22	-0.96	-2.42	2.36	7.59	-2.22	.00010	.0032	-0.78
201	2592	75.2	5.02	0.16	0.03	-1.07	-2.56	2.31	6.94	0.12	.00008	.0031	1.55
211	2636	49.9	0.67	0.10	-0.33	-1.38	-3.82	2.89	8.70	-4.57	.00014	.0036	-4.57
211	2638	49.8	4.53	0.10	-0.28	-1.33	-3.85	2.57	7.91	-0.67	.00011	.0036	-0.62
211	2640	50.1	8.32	0.10	-0.22	-1.26	-3.82	2.27	7.22	3.18	.00009	.0036	3.28
211	2642	49.6	12.27	0.10	-0.27	-1.43	-3.97	1.94	6.49	7.11	.00006	.0036	7.42
212	2645	55.8	0.42	0.12	-0.19	-1.23	-3.50	2.96	8.74	-4.70	.00014	.0036	-4.45
212	2647	55.8	4.40	0.12	-0.30	-1.29	-3.61	2.79	7.85	-0.81	.00011	.0036	-0.62
212	2649	55.2	8.27	0.11	-0.17	-1.23	-3.60	2.31	7.01	3.18	.00008	.0036	3.48
212	2651	55.0	12.16	0.11	-0.18	-1.32	-3.63	1.97	6.29	7.09	.00005	.0037	7.49
213	2652	60.5	12.28	0.12	-0.12	-1.27	-3.49	2.15	6.07	7.25	.00004	.0037	7.73
213	2654	60.8	8.27	0.13	-0.21	-1.25	-3.51	2.58	6.98	3.14	.00007	.0037	3.45

TABLE IV - CONCLUDED

Run	Point	V_∞, knots	α, deg	μ	a_{1_S}, deg	b_{1_S}, deg	A_1, deg	B_1, deg	θ_c, deg	α_{TPP}, deg	C_Q	C_T	γ, deg
213	2658	61.1	2.29	0.13	-0.13	-1.14	-3.28	2.92	8.26	-2.77	.00012	.0036	-2.54
213	2659	60.7	0.44	0.13	0.01	-1.21	-3.32	2.95	8.67	-4.47	.00013	.0036	-4.29
214	2662	65.2	0.36	0.13	-0.11	-1.22	-3.20	3.27	8.73	-4.67	.00013	.0036	-4.32
214	2663	65.3	2.22	0.14	-0.23	-1.11	-3.20	3.27	8.38	-2.94	.00012	.0036	-2.70
214	2666	65.1	6.19	0.13	-0.03	-1.30	-3.38	2.62	7.30	1.24	.00008	.0036	0.98
214	2667	65.1	8.27	0.13	-0.13	-1.20	-3.25	2.54	6.87	3.21	.00007	.0036	2.94
215	2670	70.1	8.21	0.15	-0.15	-1.14	-3.07	2.70	6.75	3.14	.00006	.0036	2.89
215	2673	71.0	2.32	0.15	-0.09	-1.24	-3.25	3.25	8.34	-2.69	.00012	.0036	-3.13
215	2674	70.6	0.23	0.15	-0.06	-1.19	-3.15	3.41	8.85	-4.76	.00014	.0036	-5.22
216	2677	74.5	0.33	0.15	-0.22	-1.13	-3.00	3.83	8.98	-4.82	.00014	.0036	-4.36
216	2678	75.0	4.20	0.16	-0.43	-1.24	-3.14	3.63	7.89	-1.15	.00010	.0035	-0.55
216	2679	74.7	4.22	0.15	-0.14	-1.17	-3.03	3.33	7.86	-0.86	.00010	.0036	-0.02
216	2681	75.3	6.20	0.16	-0.04	-1.18	-2.97	2.91	7.18	1.23	.00007	.0035	2.10
216	2682	75.6	8.10	0.16	-0.08	-1.20	-3.02	2.83	6.77	3.09	.00006	.0036	3.91
217	2619	80.7	2.21	0.17	0.08	-1.09	-2.75	3.32	8.46	-2.65	.00012	.0036	-1.82
217	2620	80.3	4.20	0.17	0.15	-1.01	-2.59	2.81	7.70	-0.60	.00009	.0036	0.70
217	2623	79.9	10.11	0.16	0.12	-1.10	-2.80	2.49	6.08	5.30	.00003	.0036	7.04
217	2624	80.4	-1.76	0.17	-0.02	-1.13	-2.93	4.04	9.65	-6.71	.00016	.0036	-5.35
218	2628	90.6	0.15	0.19	-0.20	-1.41	-3.16	4.77	9.61	-4.94	.00015	.0037	-4.31
219	2632	90.6	2.37	0.19	0.03	-1.11	-2.77	4.15	8.77	-2.52	.00012	.0037	-1.82
219	2633	90.1	4.20	0.19	0.03	-1.10	-2.76	3.85	8.13	-0.68	.00010	.0037	0.14
219	2634	90.1	6.15	0.19	0.13	-1.07	-2.67	3.48	7.42	1.35	.00007	.0036	2.29
219	2636	90.0	10.09	0.19	-0.11	-1.22	-2.76	3.29	6.25	5.07	.00003	.0037	6.24

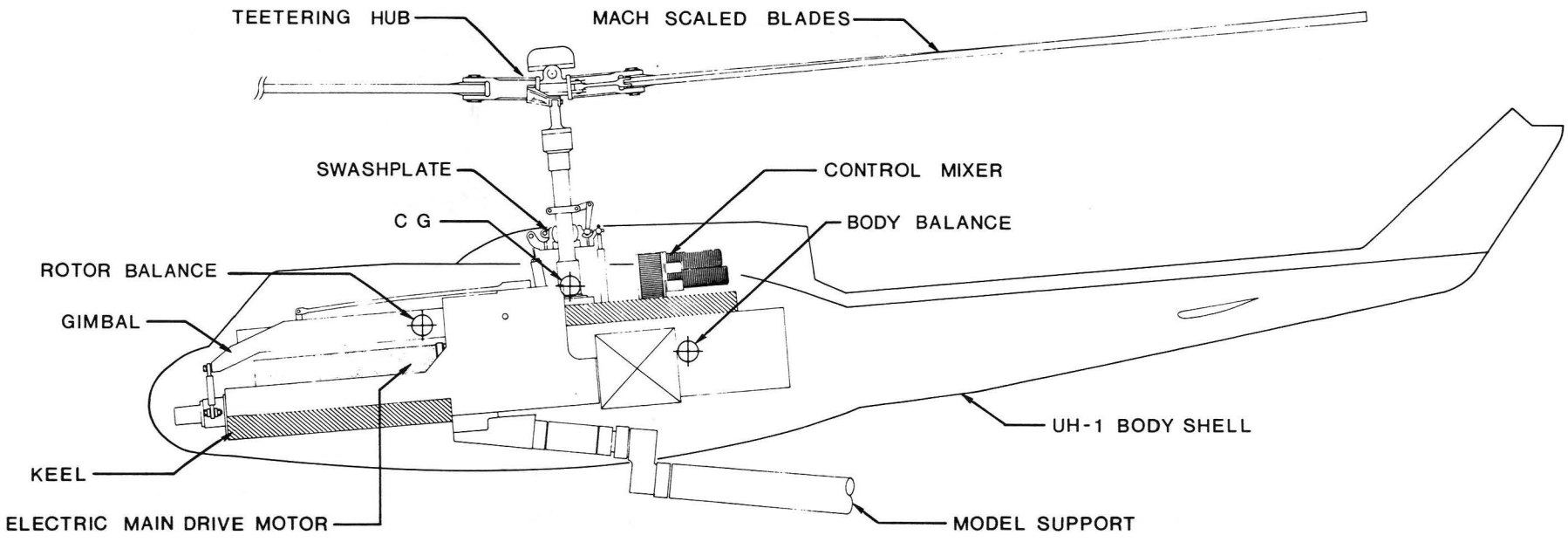

Figure 1. - Sketch of UH-1 fuselage installation on GRMS.

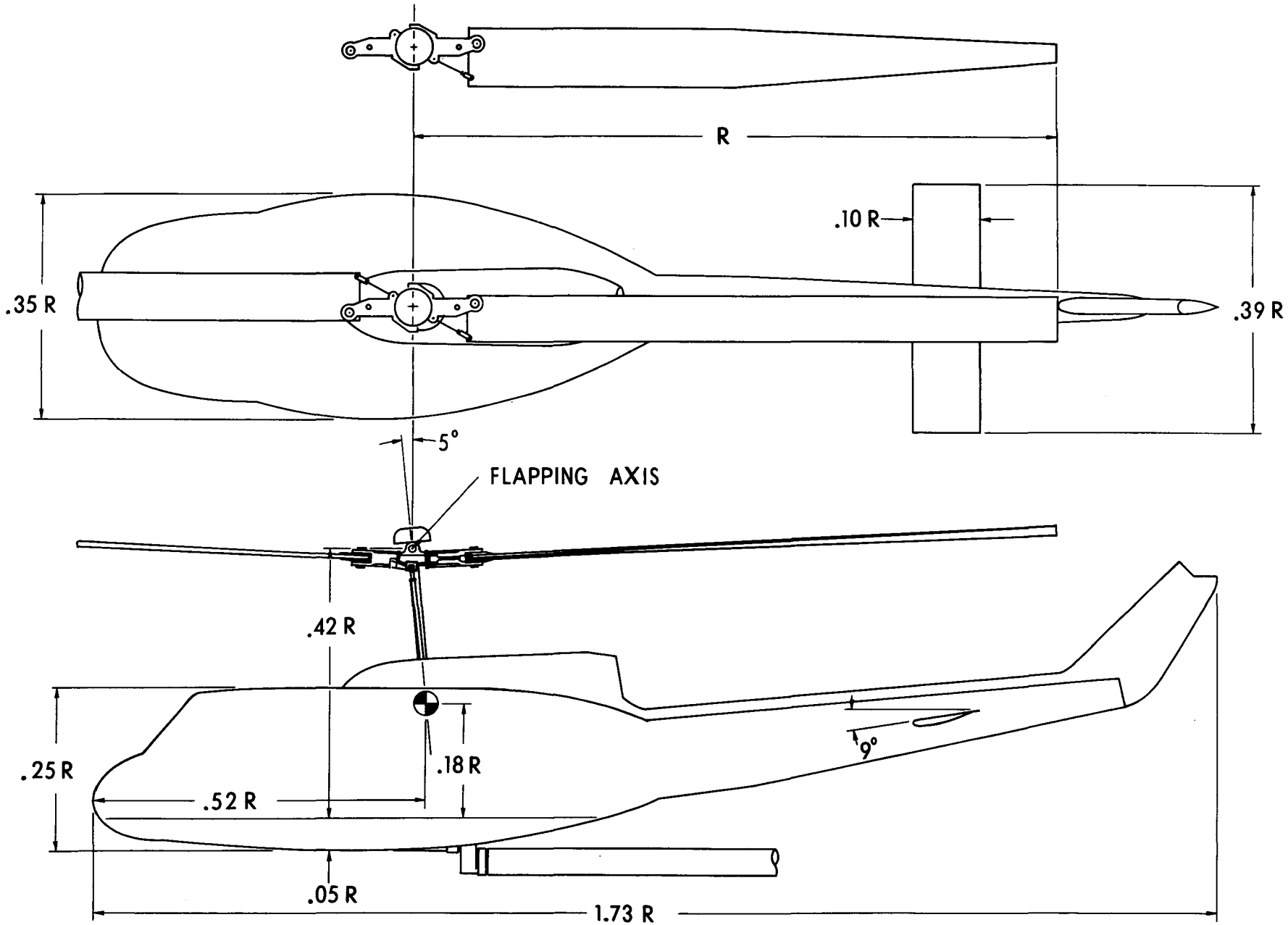

Figure 2. - Sketch of UH-1 helicopter model tested.

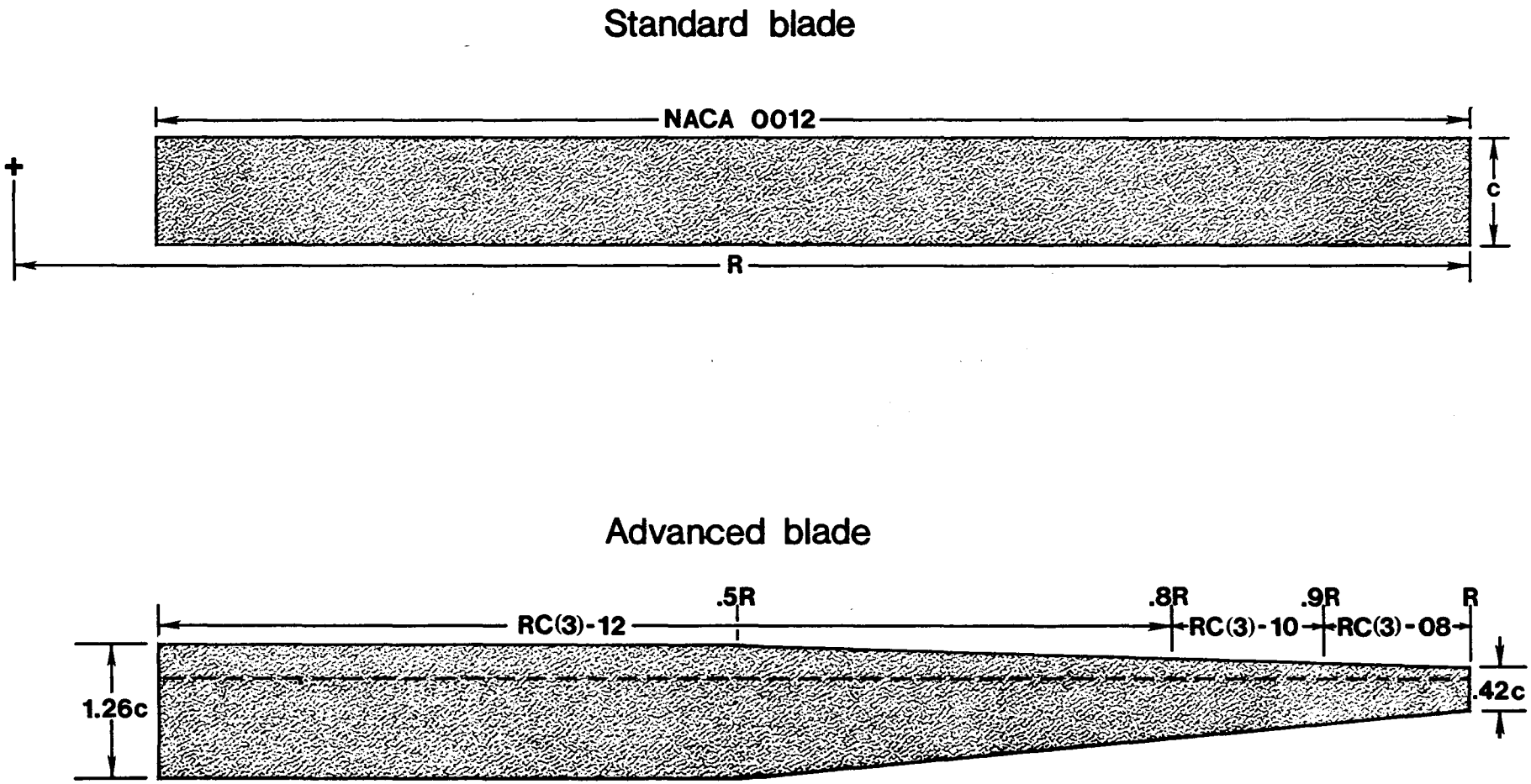

Figure 3. - Geometric comparison of the standard and advanced rotor blades.

Figure 4. - Rear-quarter view of UH-1 helicopter model in tunnel with acoustic treatment and microphones installed.

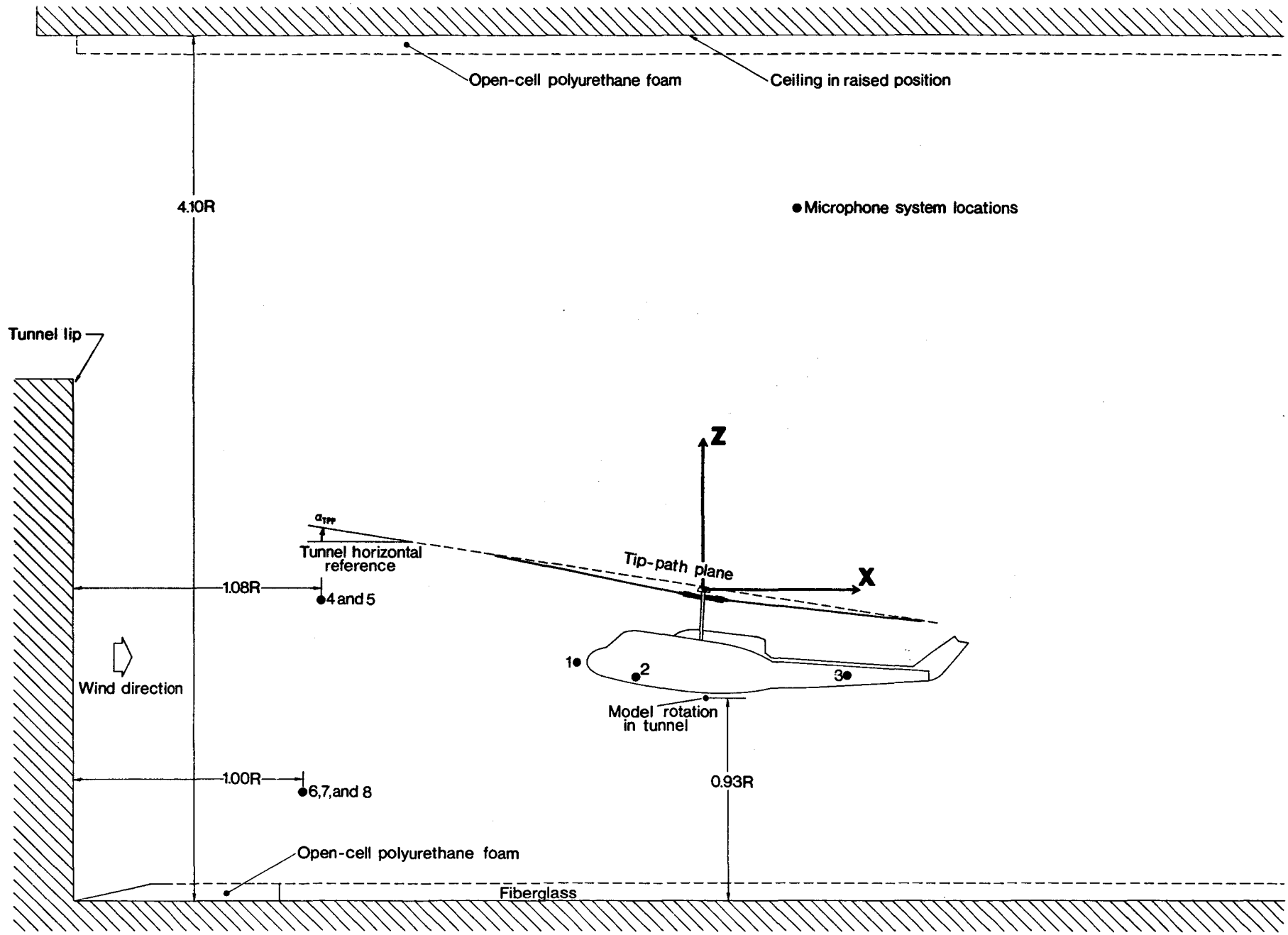

(a) side view

Figure 5. - Relative position of components in acoustic test of UH-1 helicopter model.

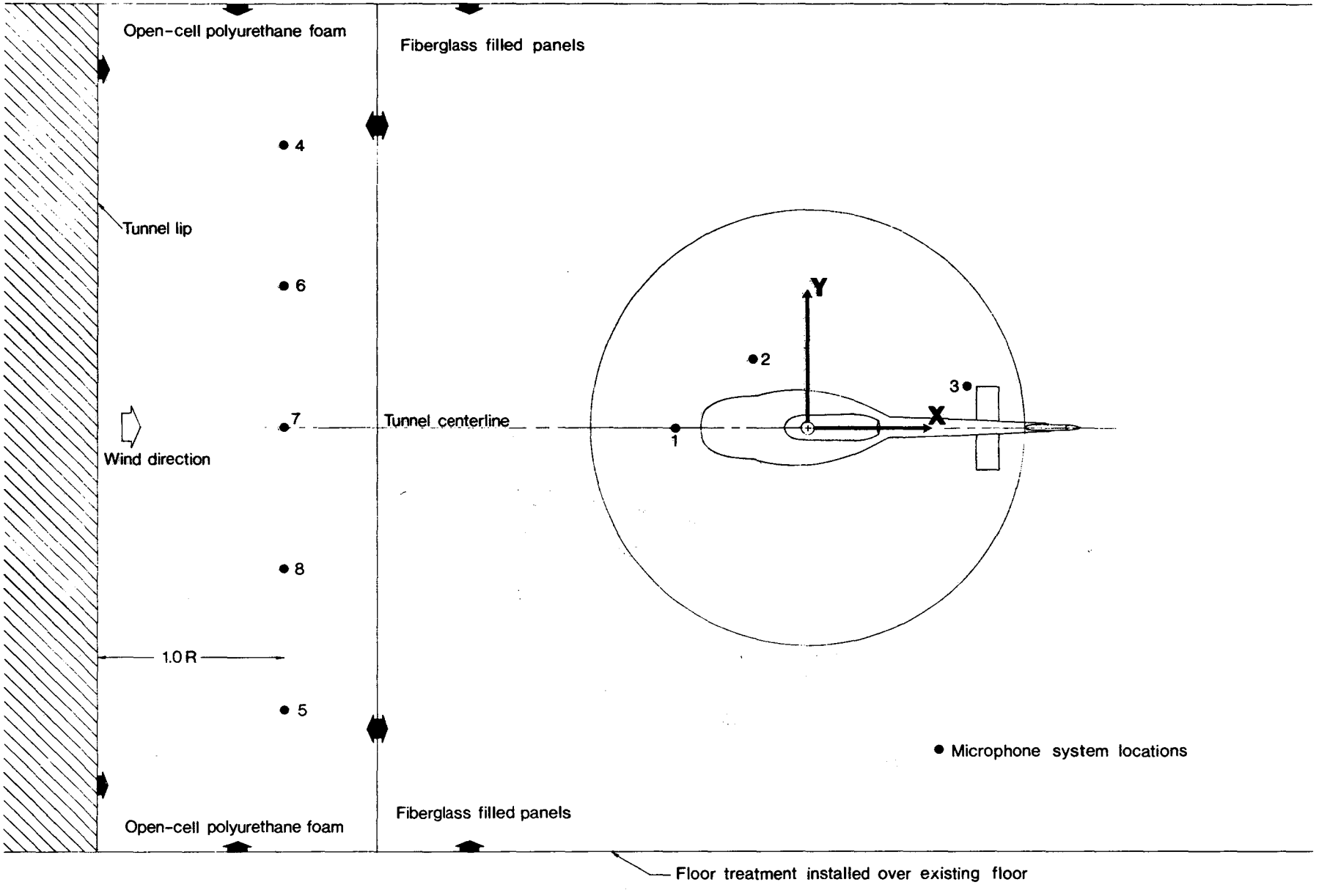

(b) top view

Figure 5. - Concluded.

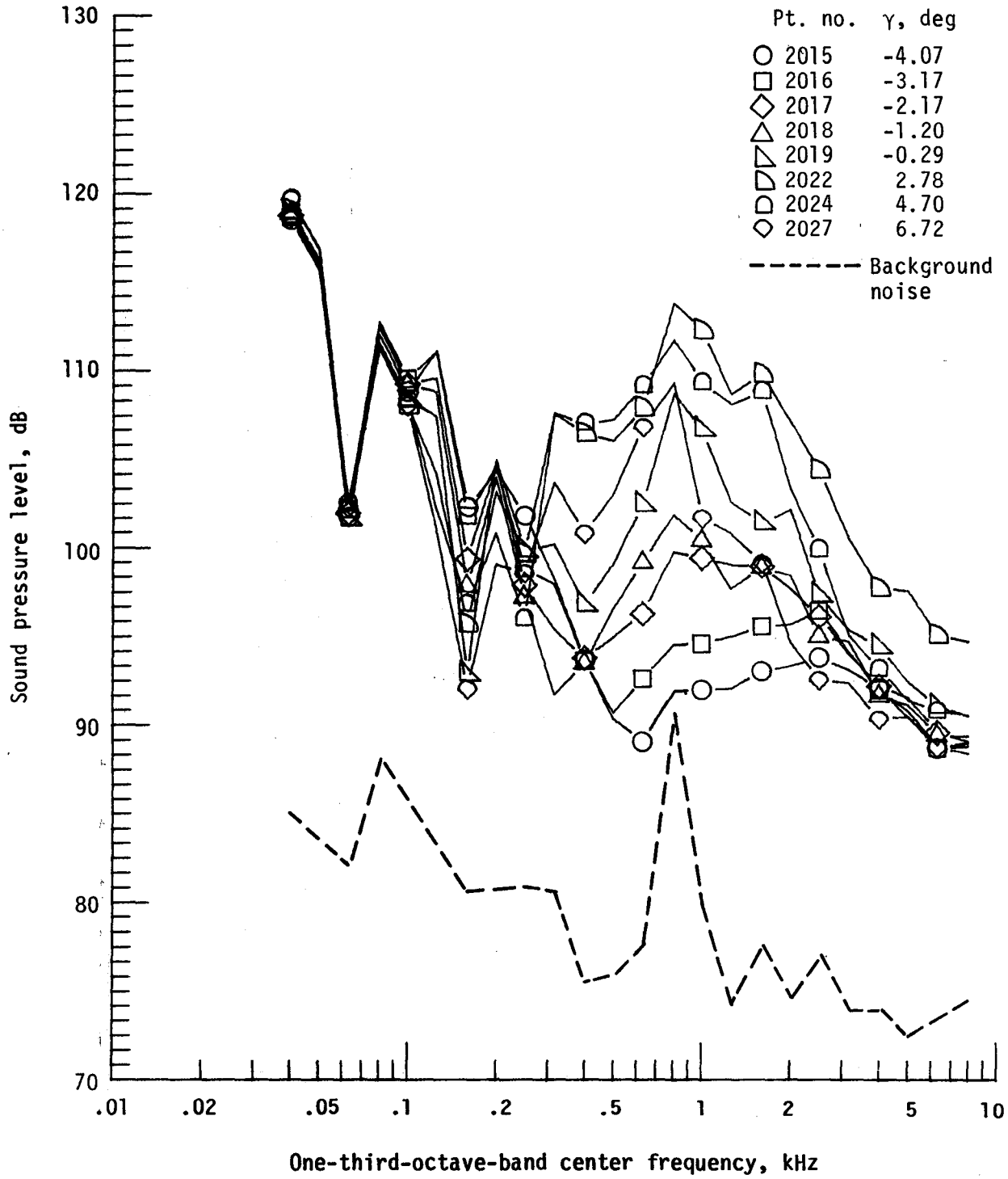

(a) One-third-octave spectra, run 154; microphone 2.

Figure 6. - Effect of descent angle variation on noise generated by helicopter model with standard rotor system. V_∞ = 50.2 knots, C_T = .0032.

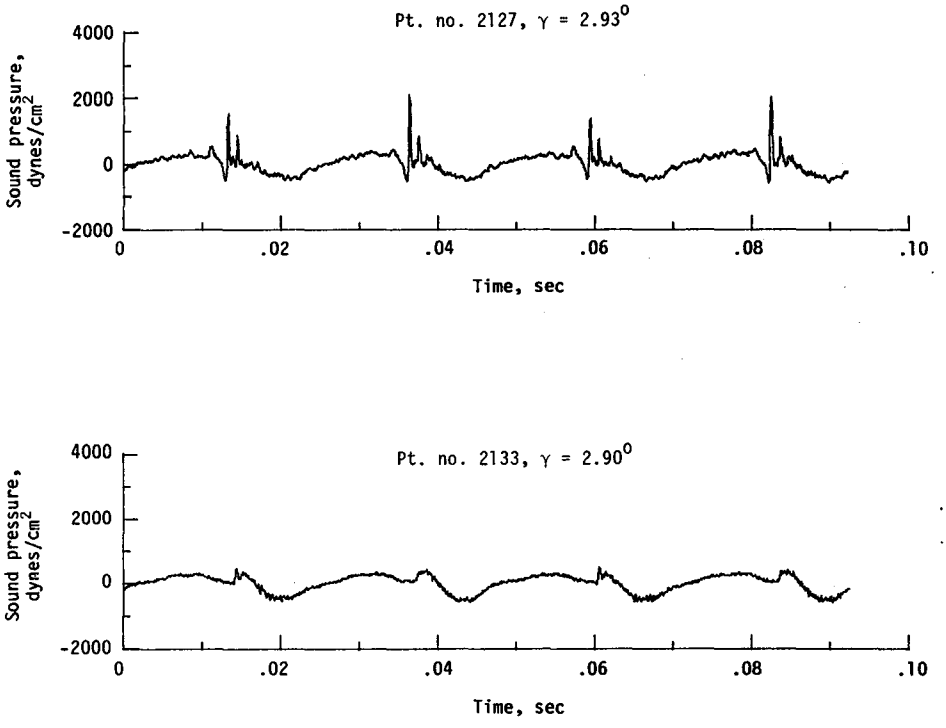

(b) Pressure-time histories, run 165; microphone 2.

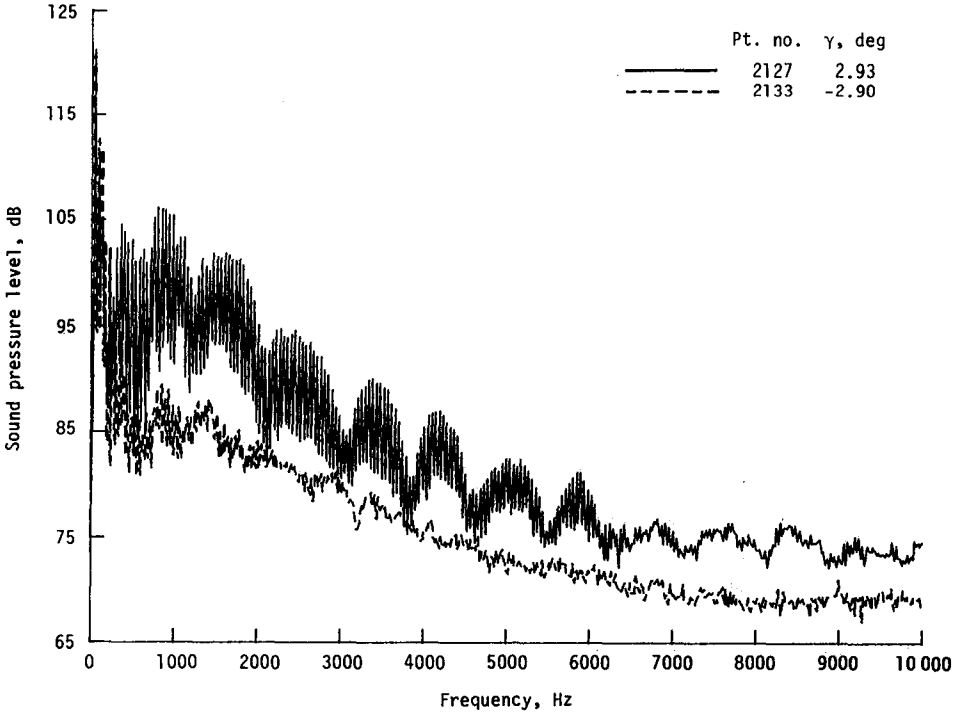

(c) Narrowband analysis, run 165; microphone 2.

Figure 6. - Continued.

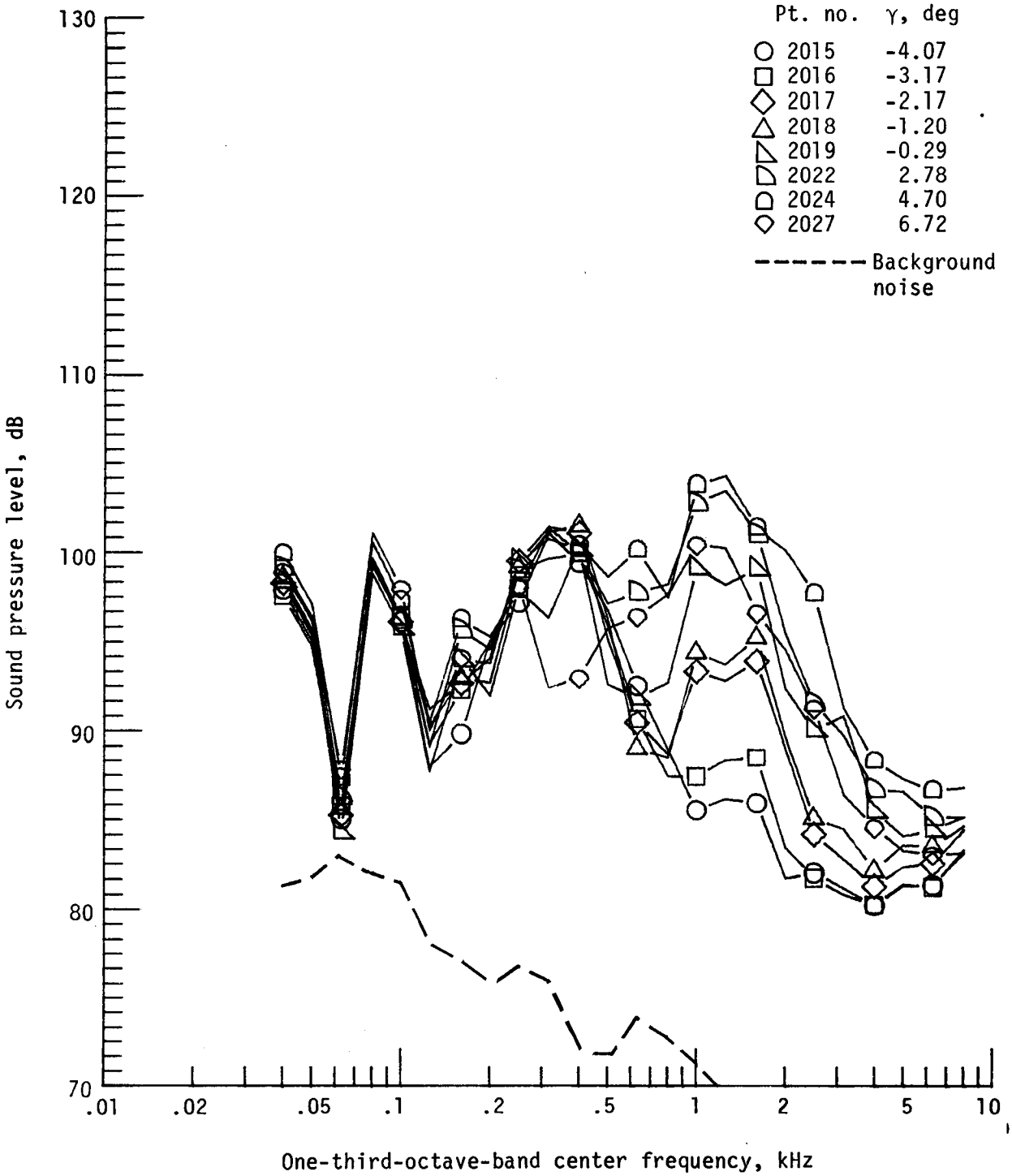

(d) One-third-octave spectra, run 154; microphone 6.

Figure 6. - Continued.

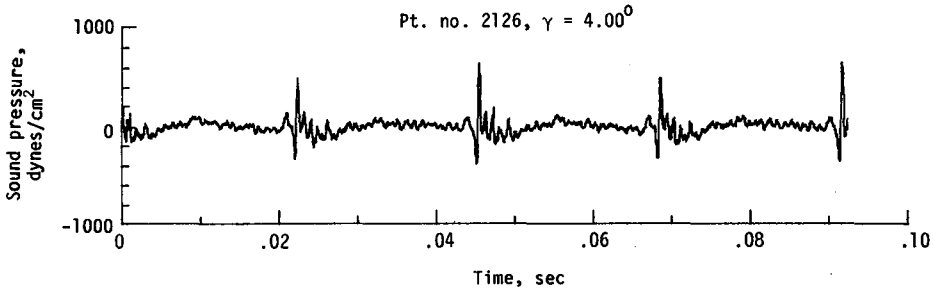

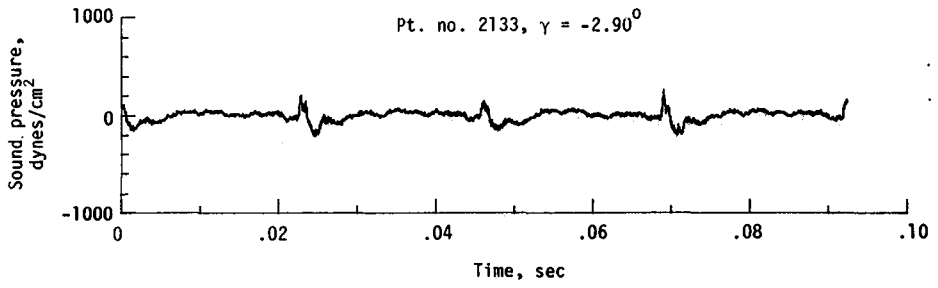

(e) Pressure-time histories, run 165; microphone 6.

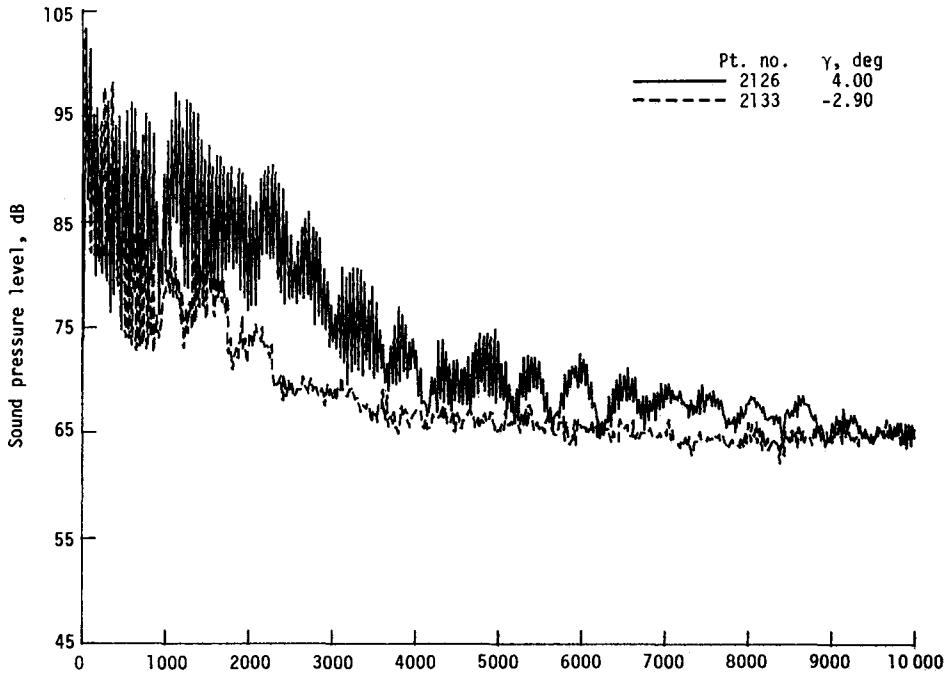

(f) Narrowband analysis, run 165; microphone 6.

Figure 6. - Continued.

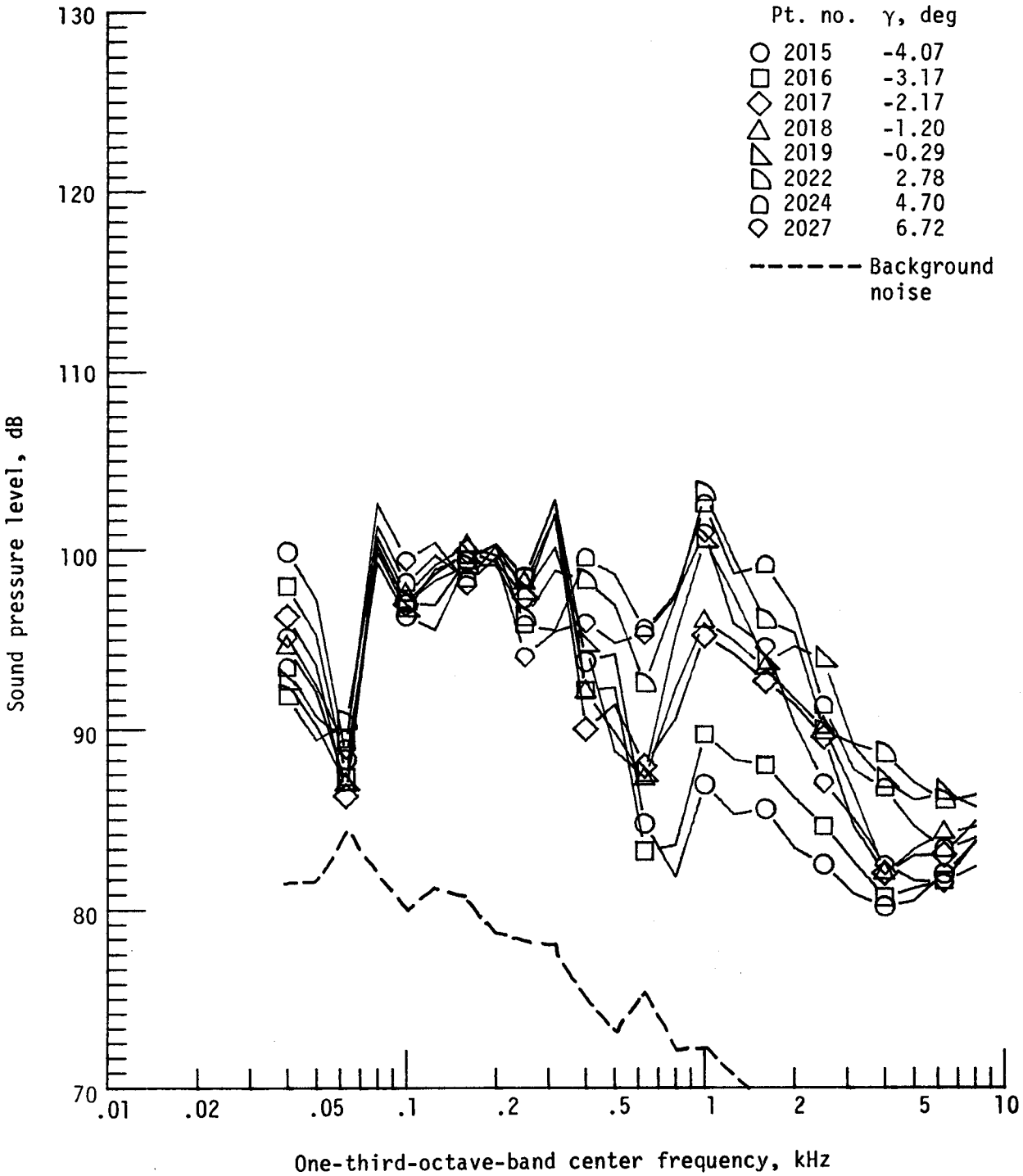

(g) One-third-octave spectra, run 154; microphone 7.

Figure 6. - Continued.

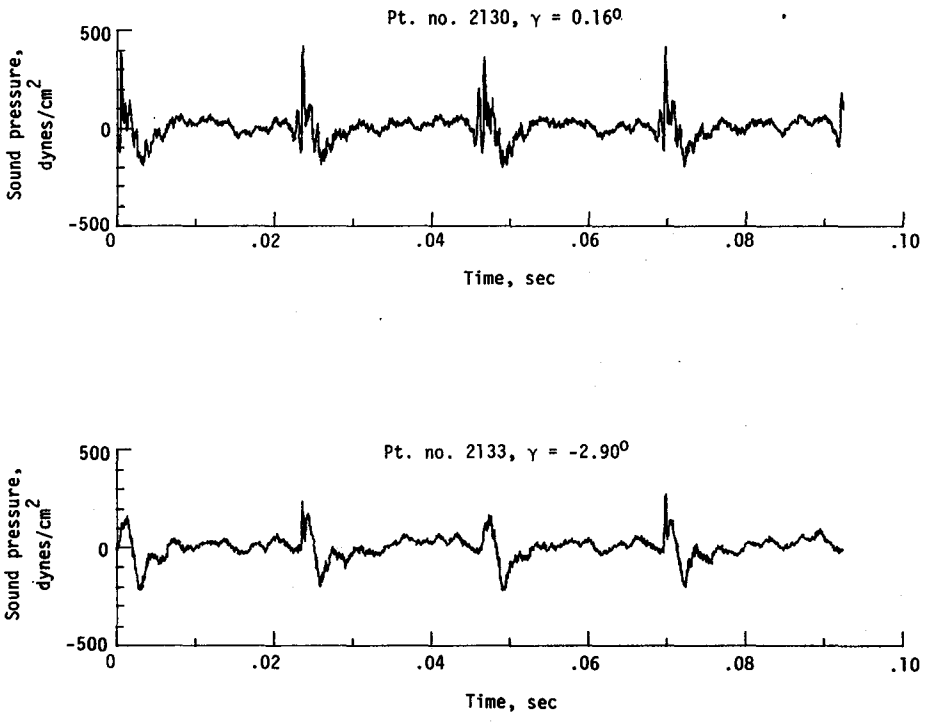

(h) Pressure-time histories, run 165; microphone 7.

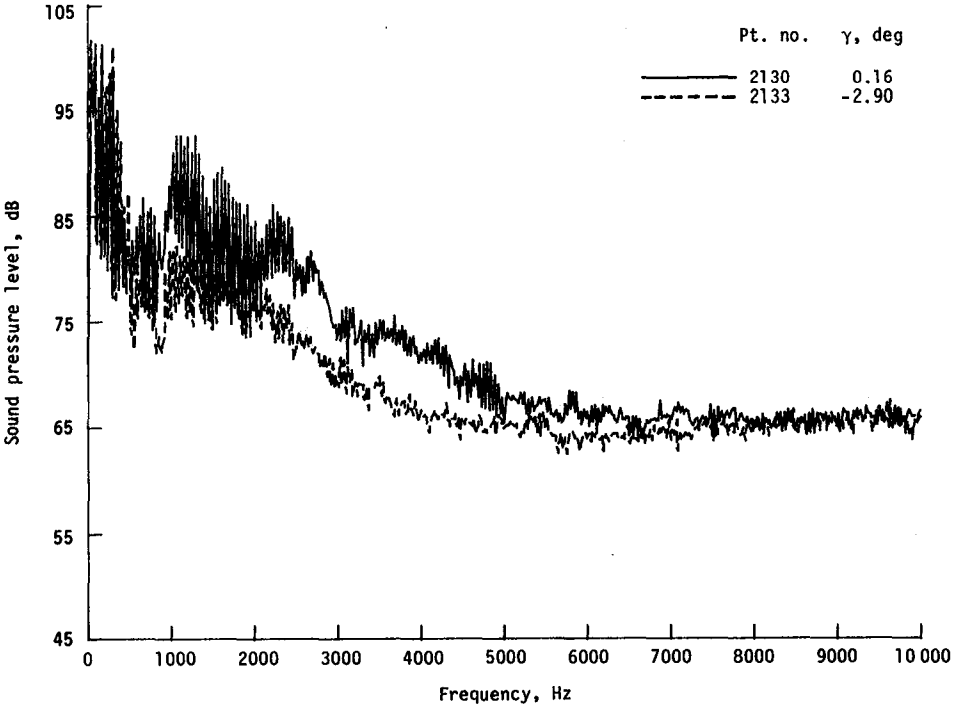

(i) Narrowband analysis, run 165; microphone 7.

Figure 6. - Continued.

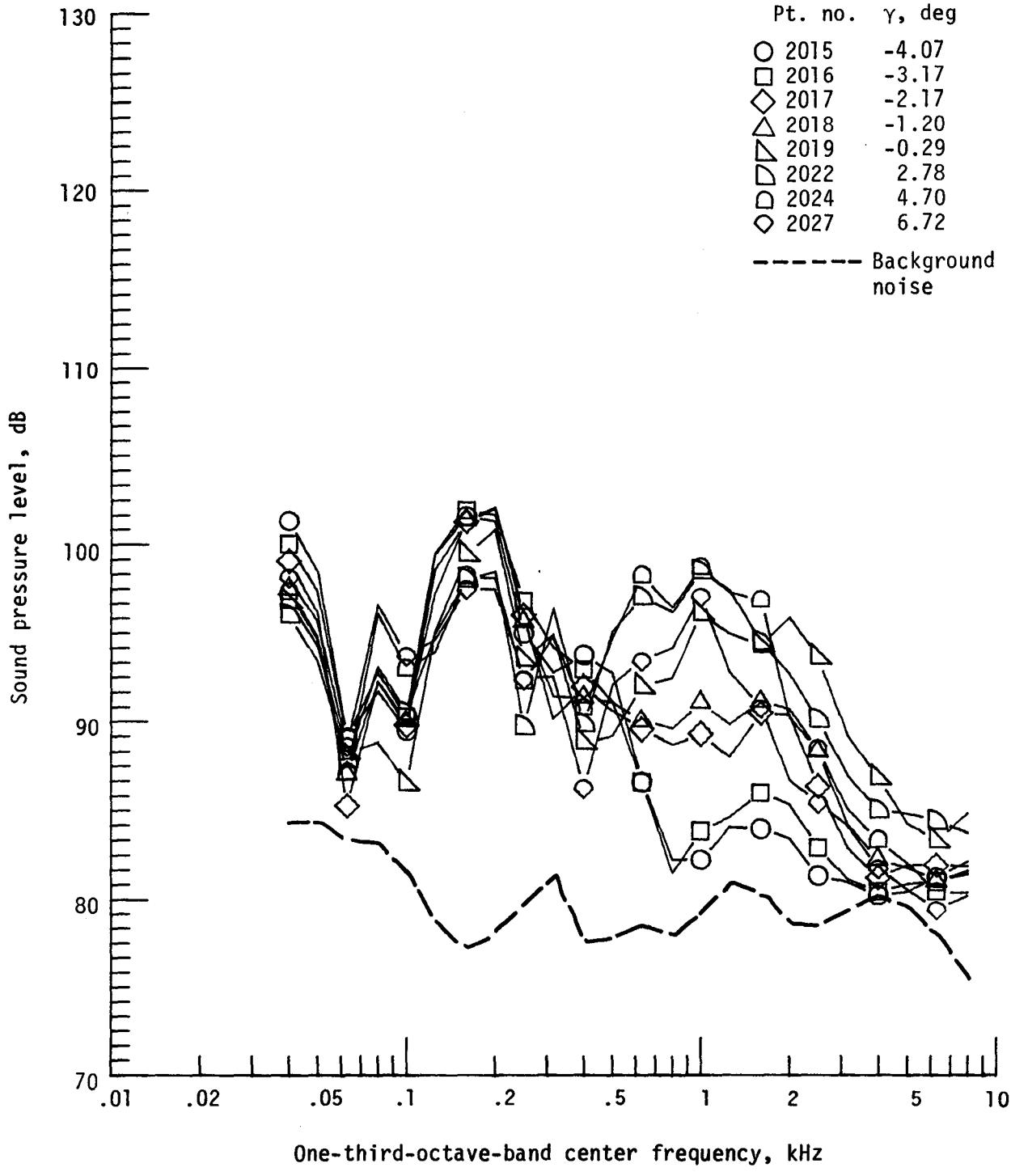

(j) One-third-octave spectra,run 154; microphone 8.

Figure 6. - Continued.

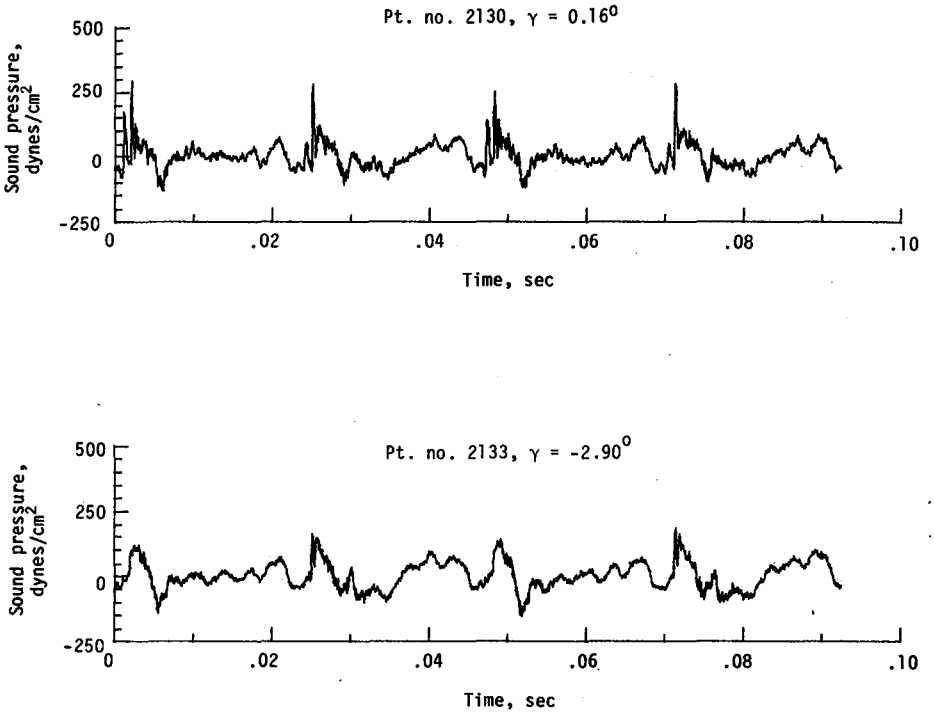

(k) Pressure-time histories, run 165; microphone 8.

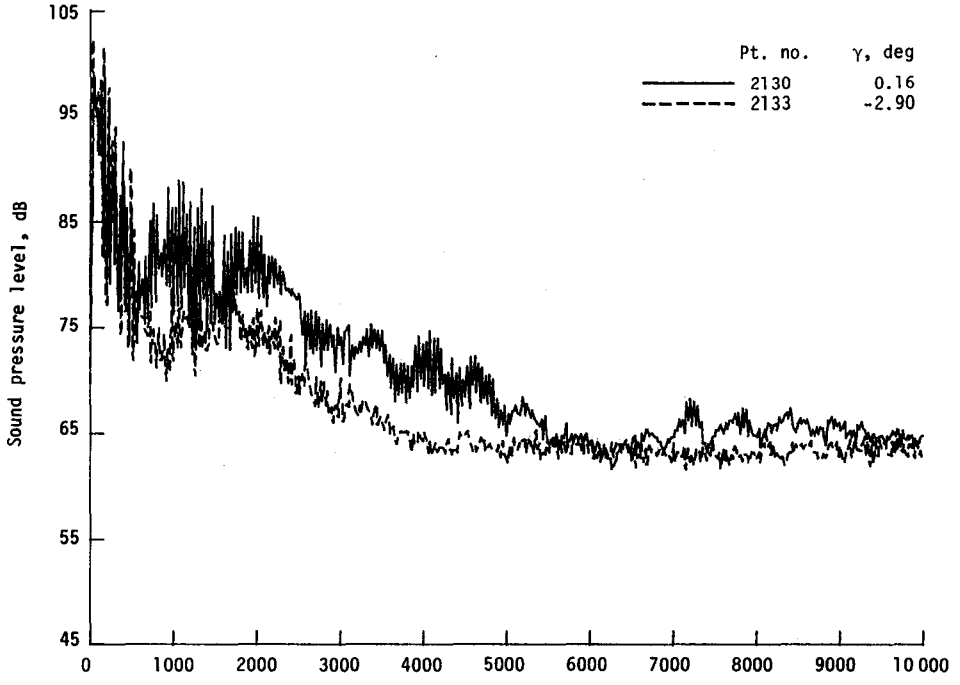

(l) Narrowband analysis, run 165; microphone 8.

Figure 6. - Concluded.

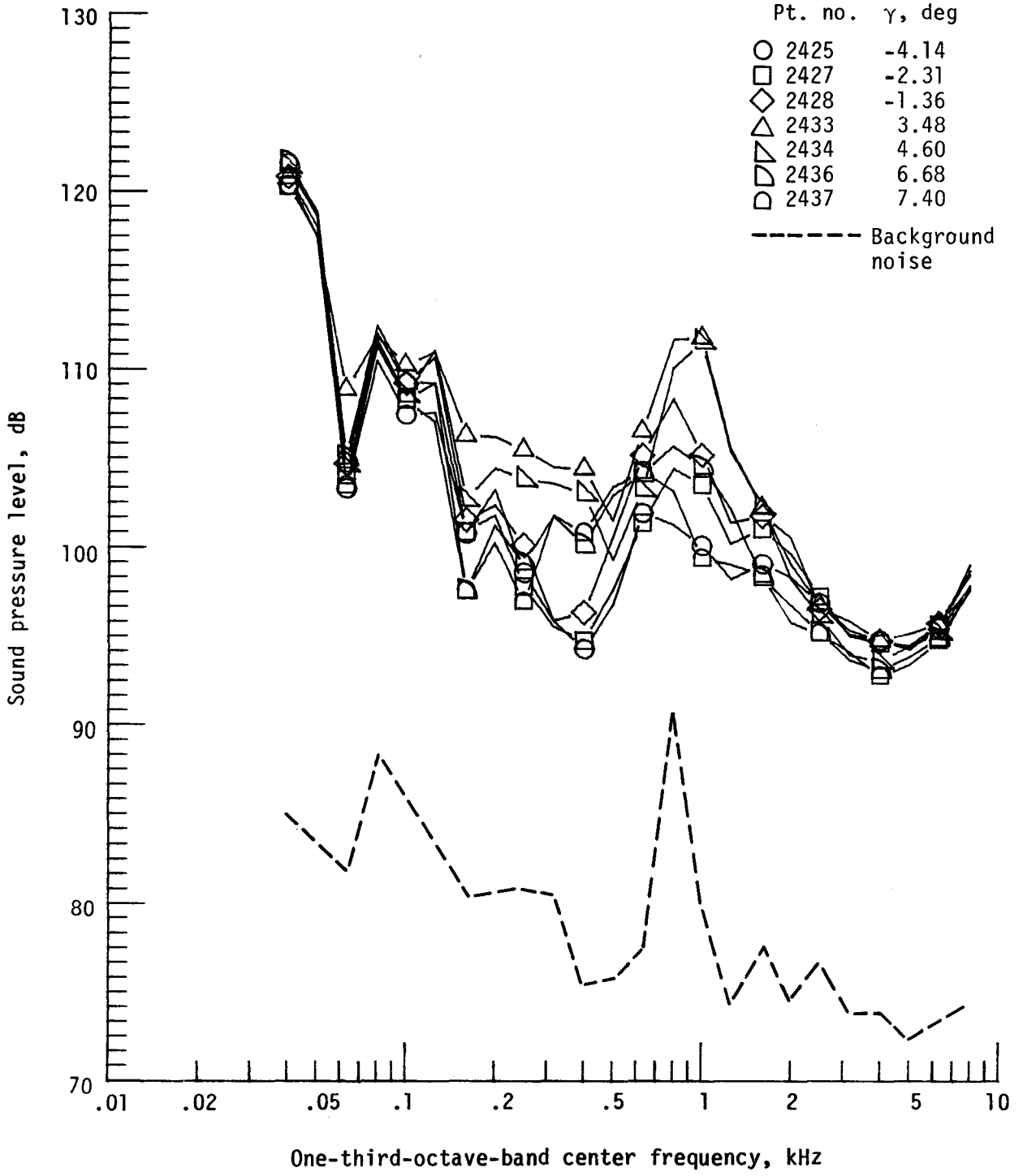

(a) One-third-octave spectra, microphone 2.

Figure 7. - Effect of descent angle variation on noise generated by helicopter model with advanced rotor system; run 193. V_∞ = 50.2 knots, C_T = .0031.

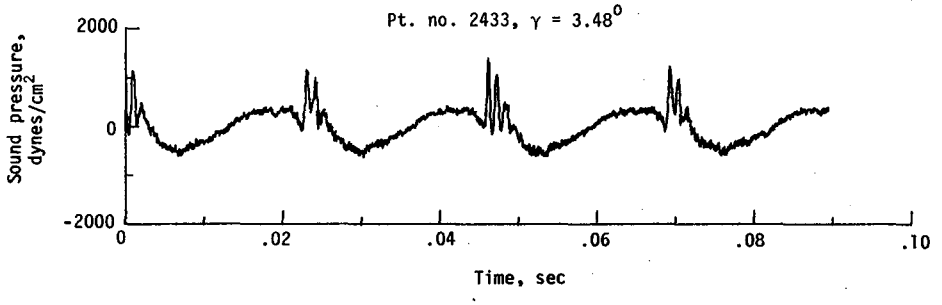

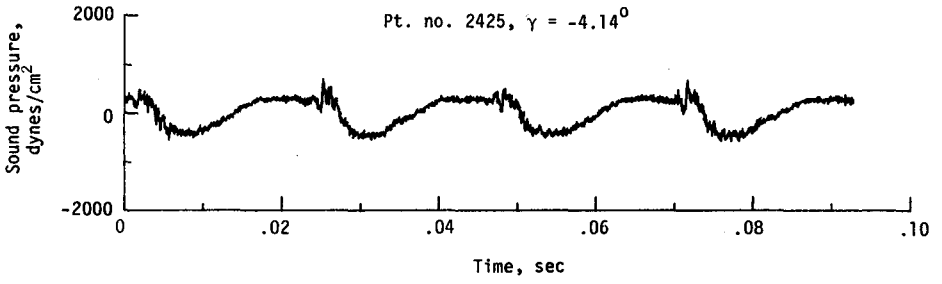

(b) Pressure-time histories; microphone 2.

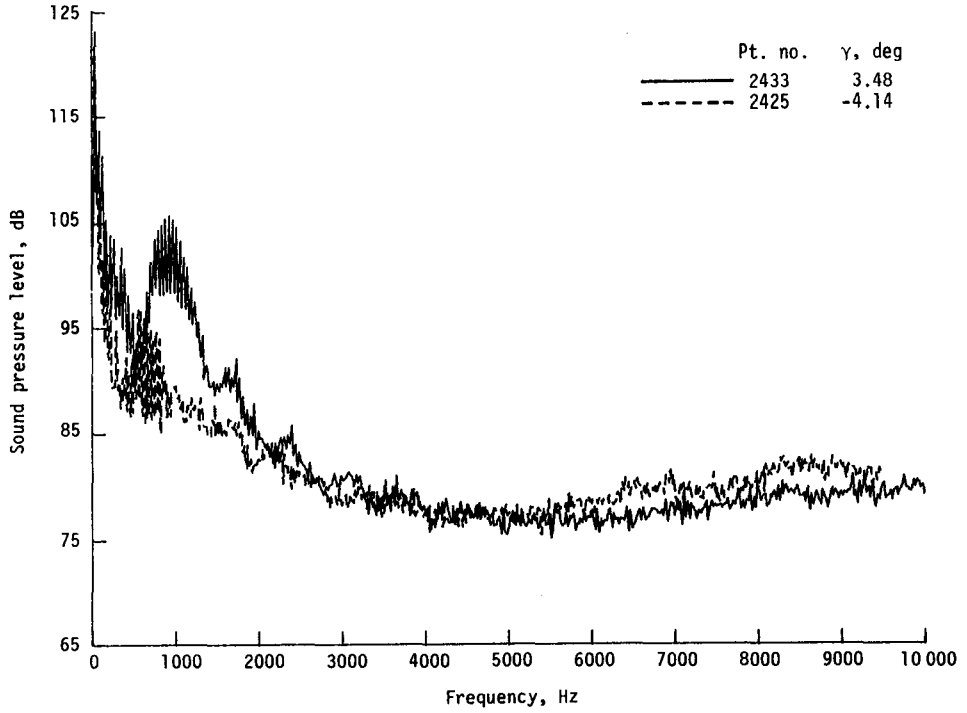

(c) Narrowband analysis; microphone 2.

Figure 7. - Continued.

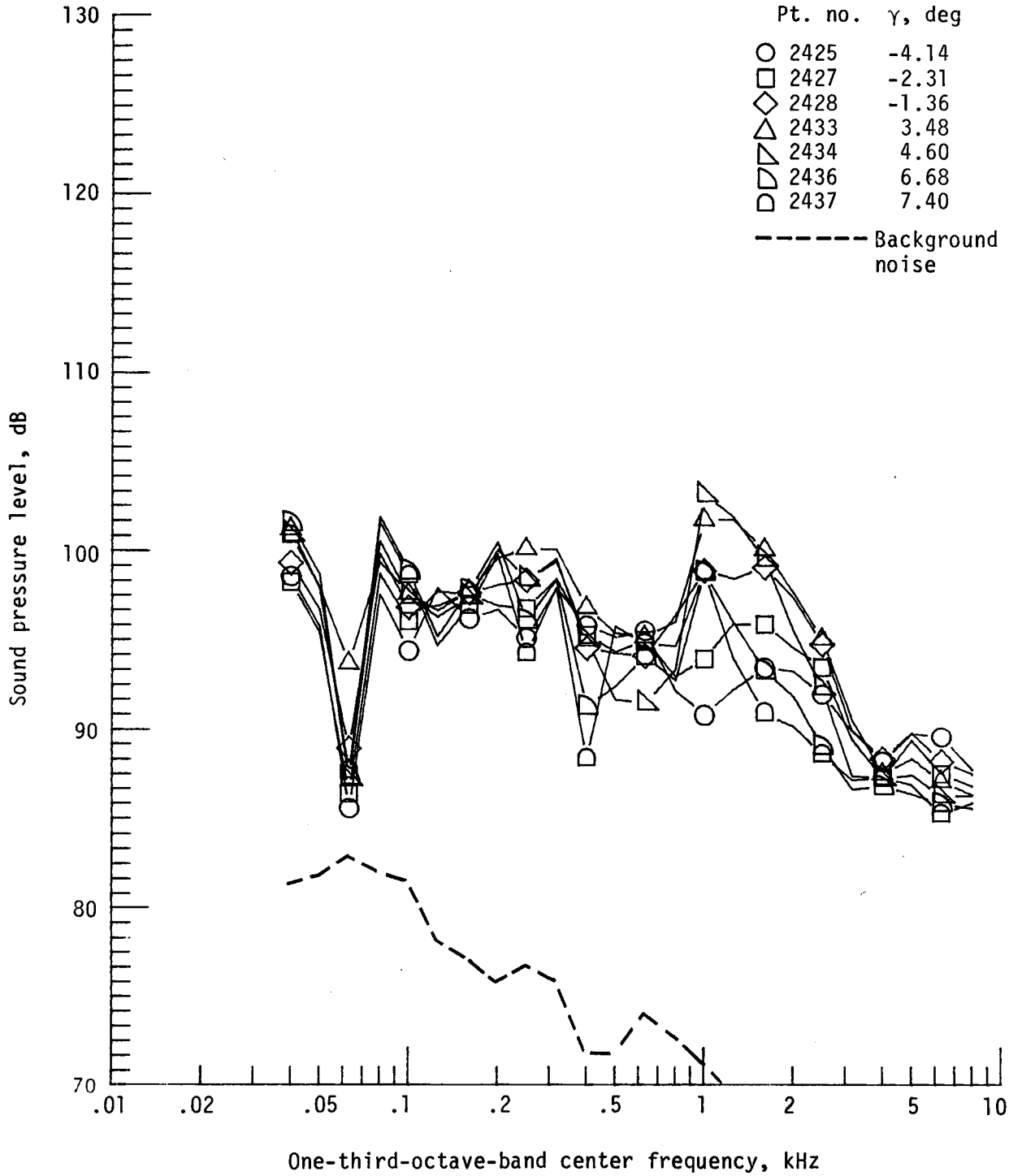

(d) One-third-octave spectra, microphone 6.

Figure 7. - Continued.

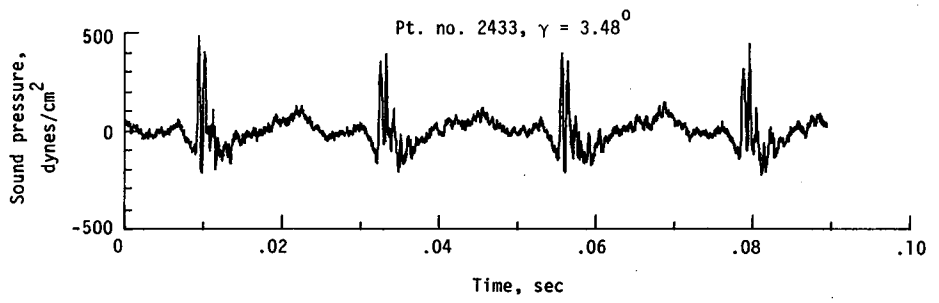

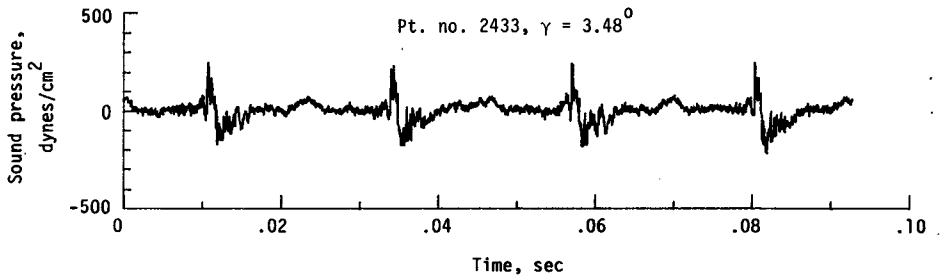

(e) Pressure-time histories; microphone 6.

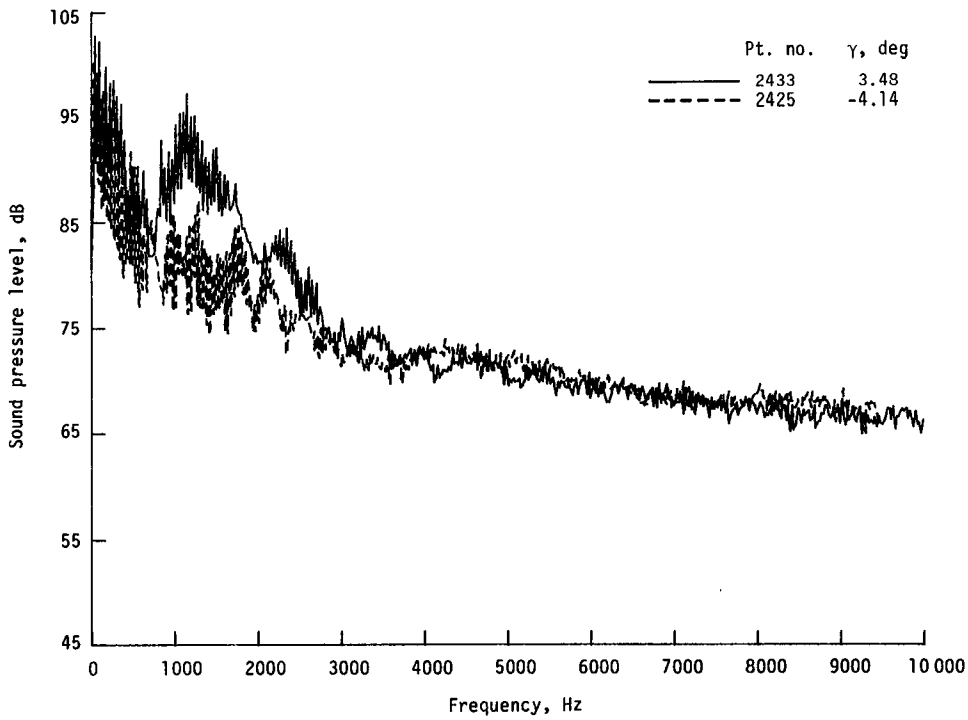

(f) Narrowband analysis; microphone 6.

Figure 7. - Continued.

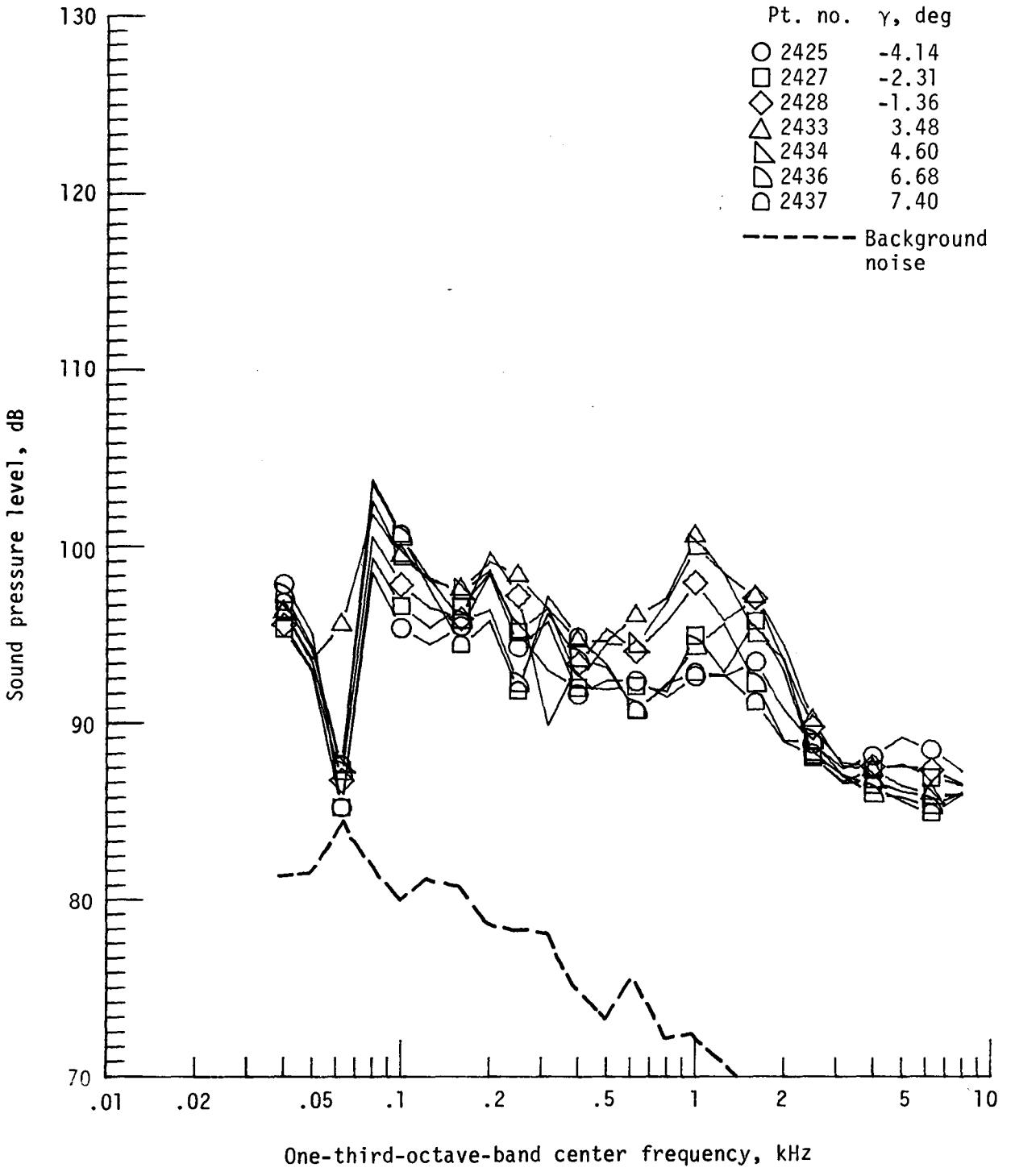

(g) One-third-octave spectra, microphone 7.

Figure 7. - Continued.

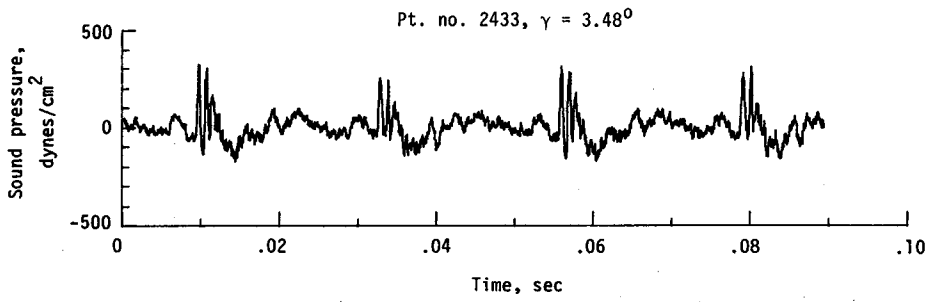

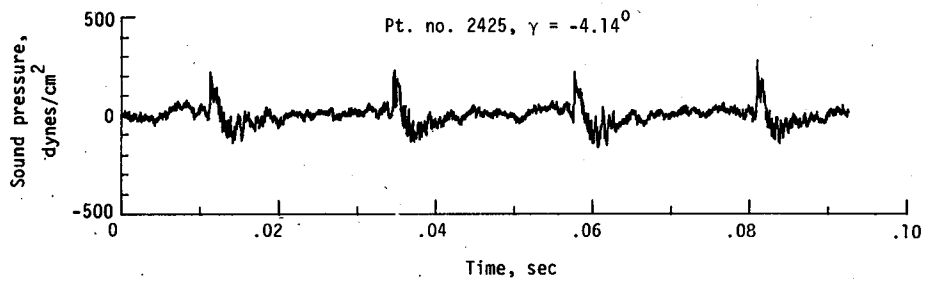

(h) Pressure-time histories; microphone 7.

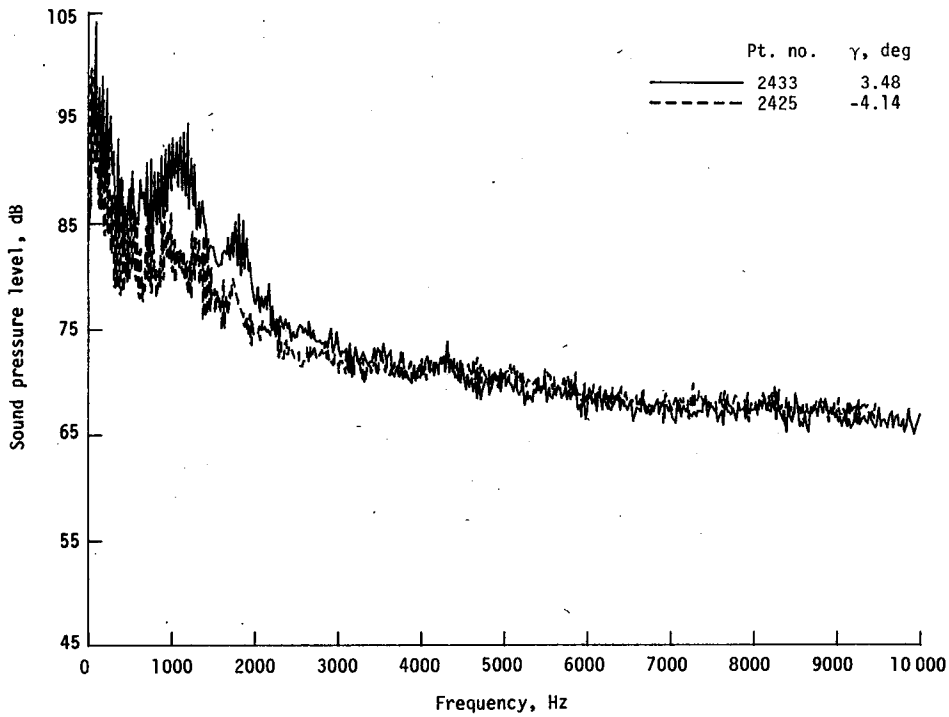

(i) Narrowband analysis; microphone 7.

Figure 7. - Continued.

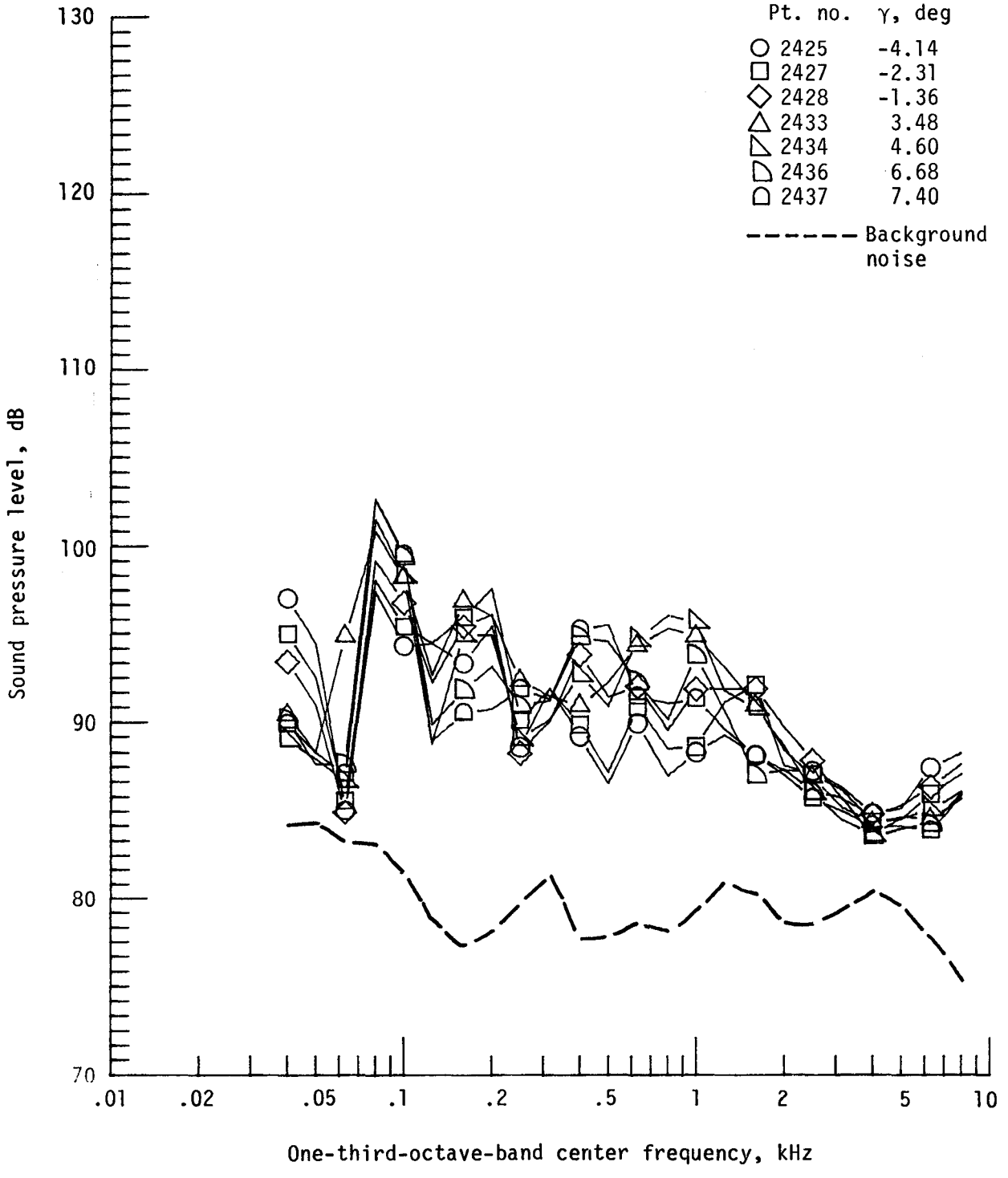

(j) One-third-octave spectra, microphone 8.

Figure 7. - Continued.

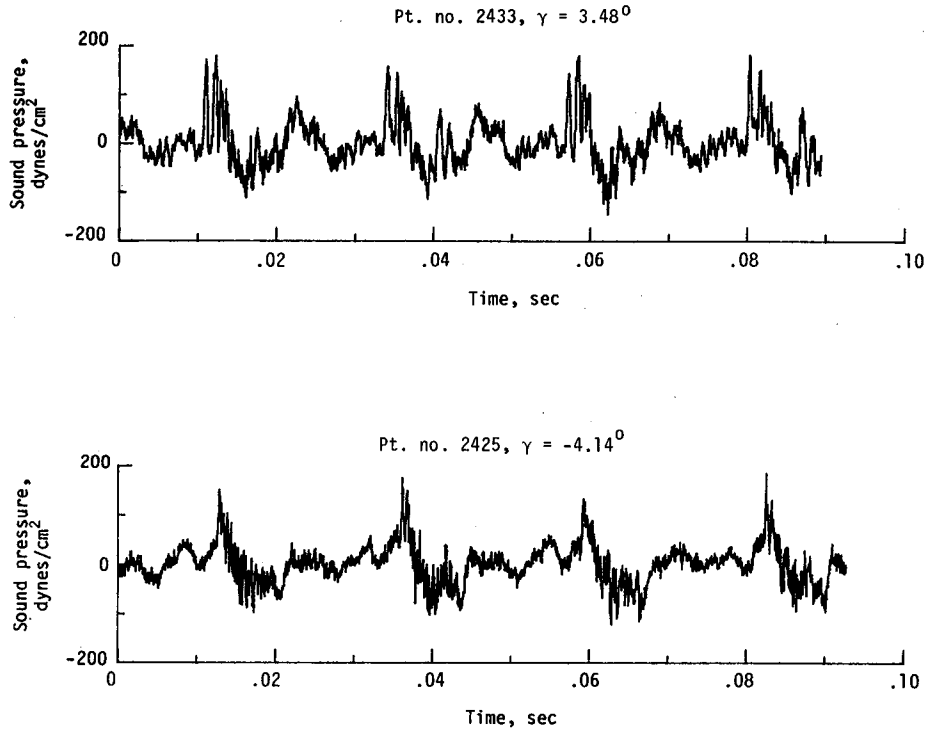

(k) Pressure-time histories; microphone 8.

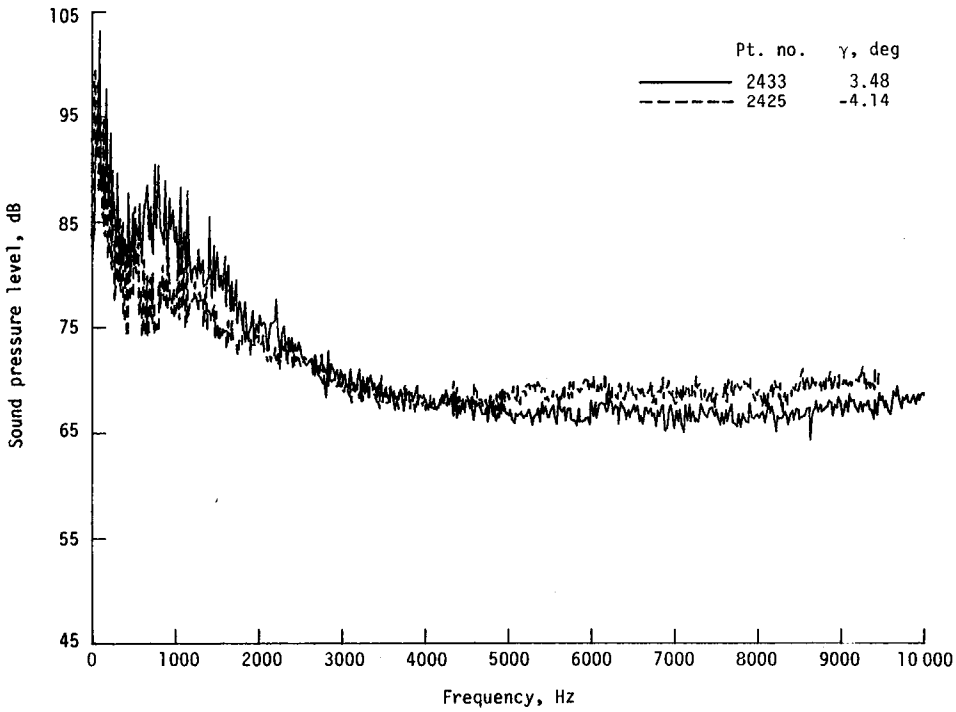

(l) Narrowband analysis; microphone 8.

Figure 7. - Concluded.

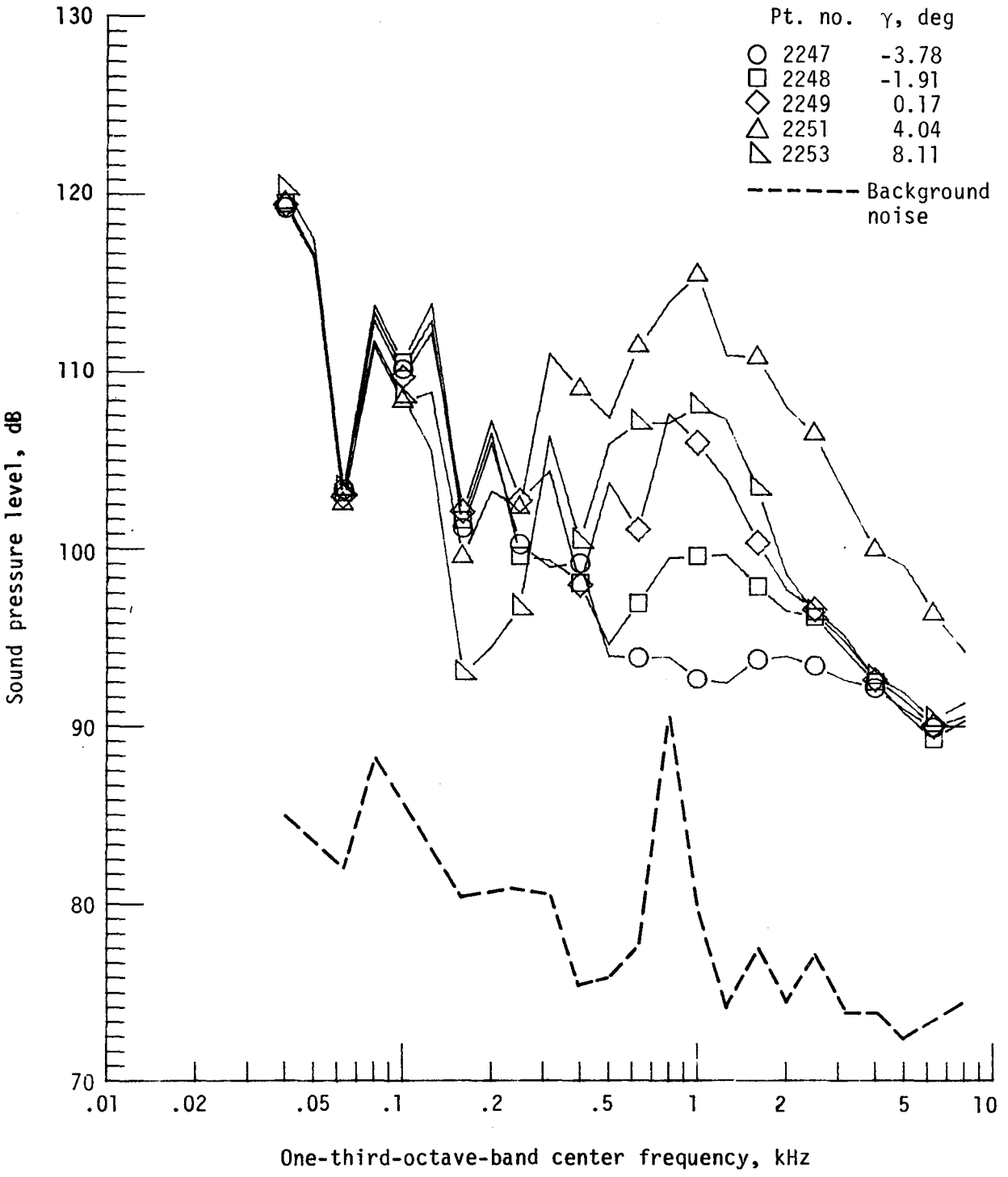

(a) One-third-octave spectra, microphone 2.

Figure 8. - Effect of descent angle variation on noise generated by helicopter model with standard rotor system. run 179. V_∞ = 49.8 knots, C_T = .0036.

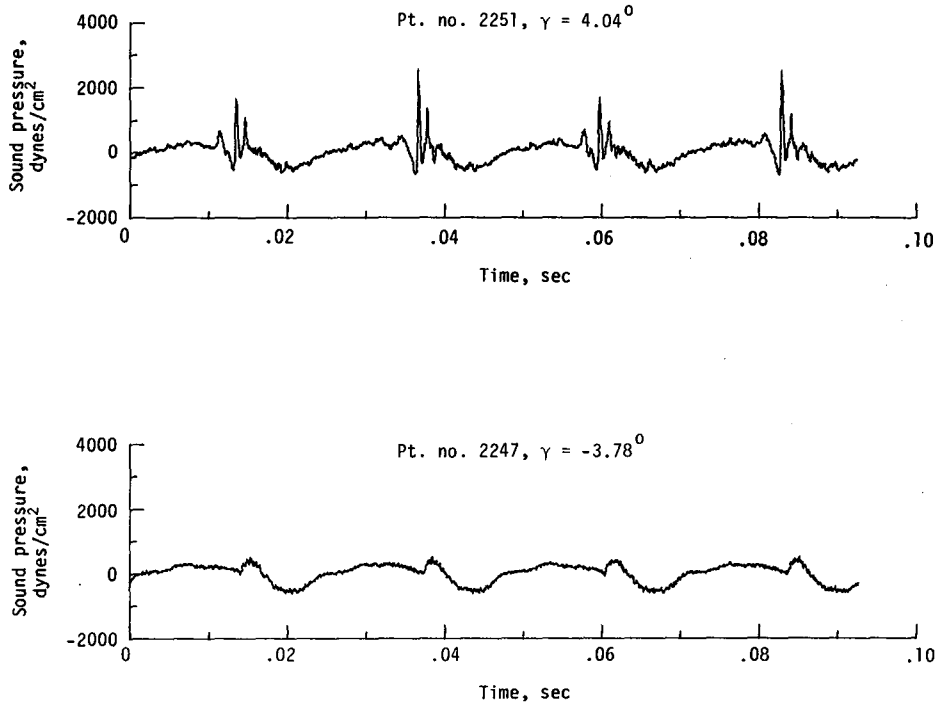

(b) Pressure-time histories; microphone 2.

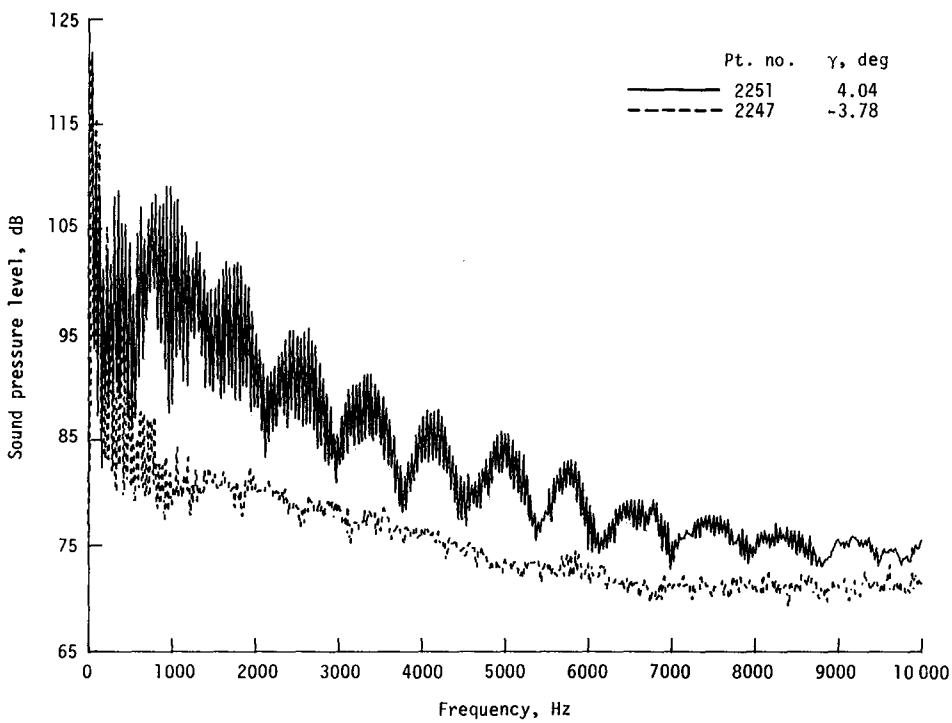

(c) Narrowband analysis; microphone 2.

Figure 8. - Continued.

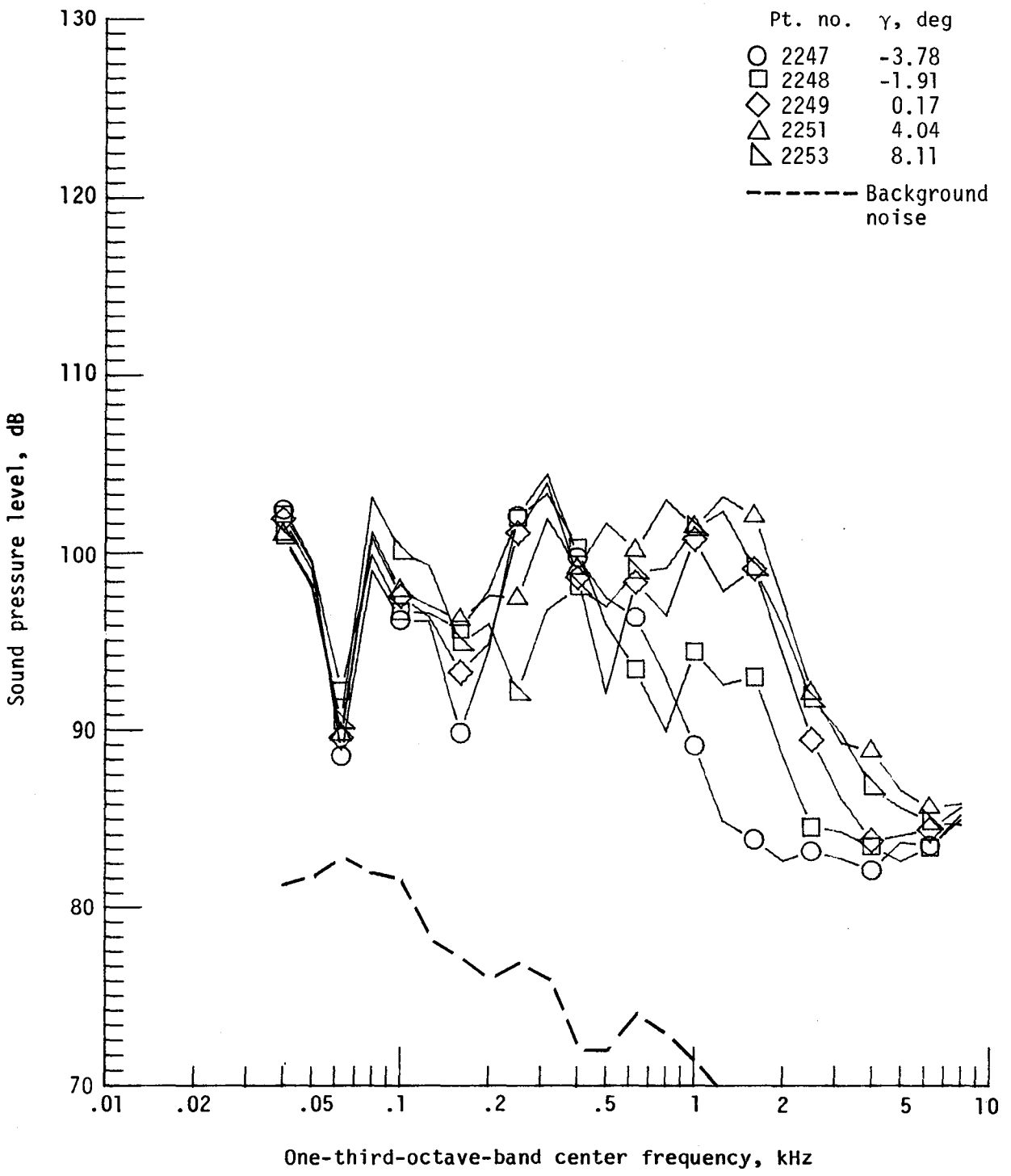

(d) One-third-octave spectra, microphone 6.

Figure 8. - Continued.

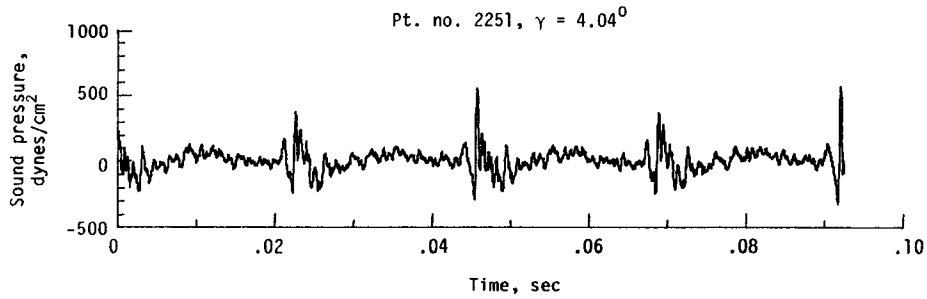

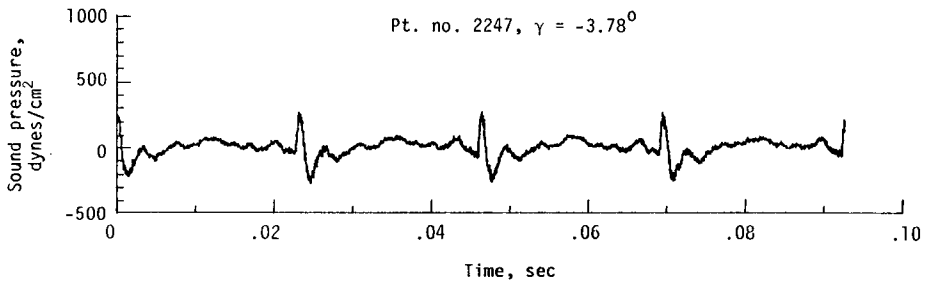

(e) Pressure-time histories; microphone 6.

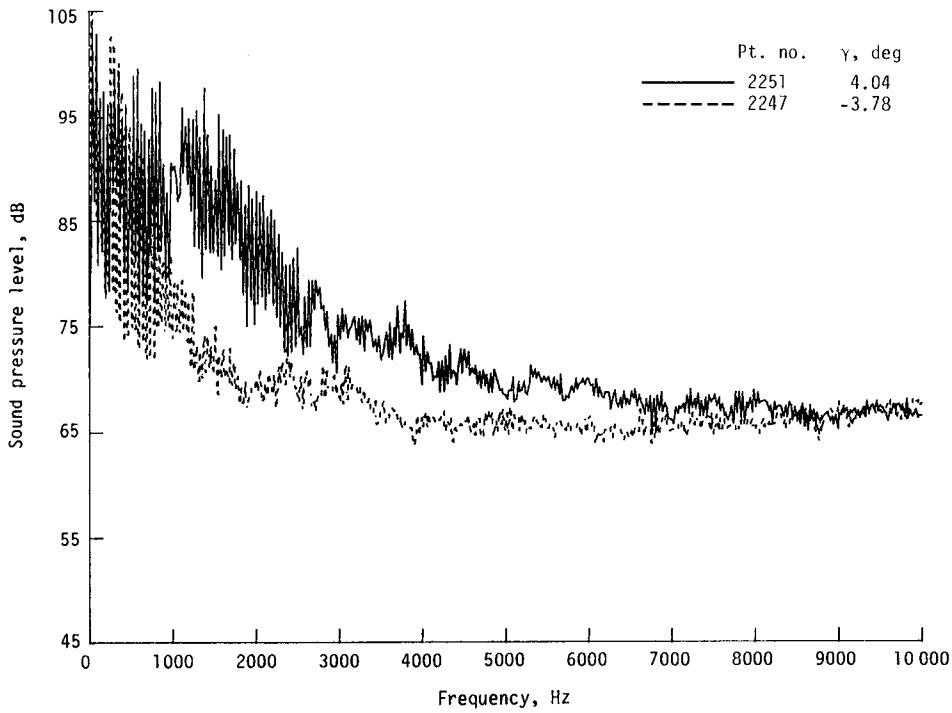

(f) Narrowband analysis; microphone 6.

Figure 8. - Continued.

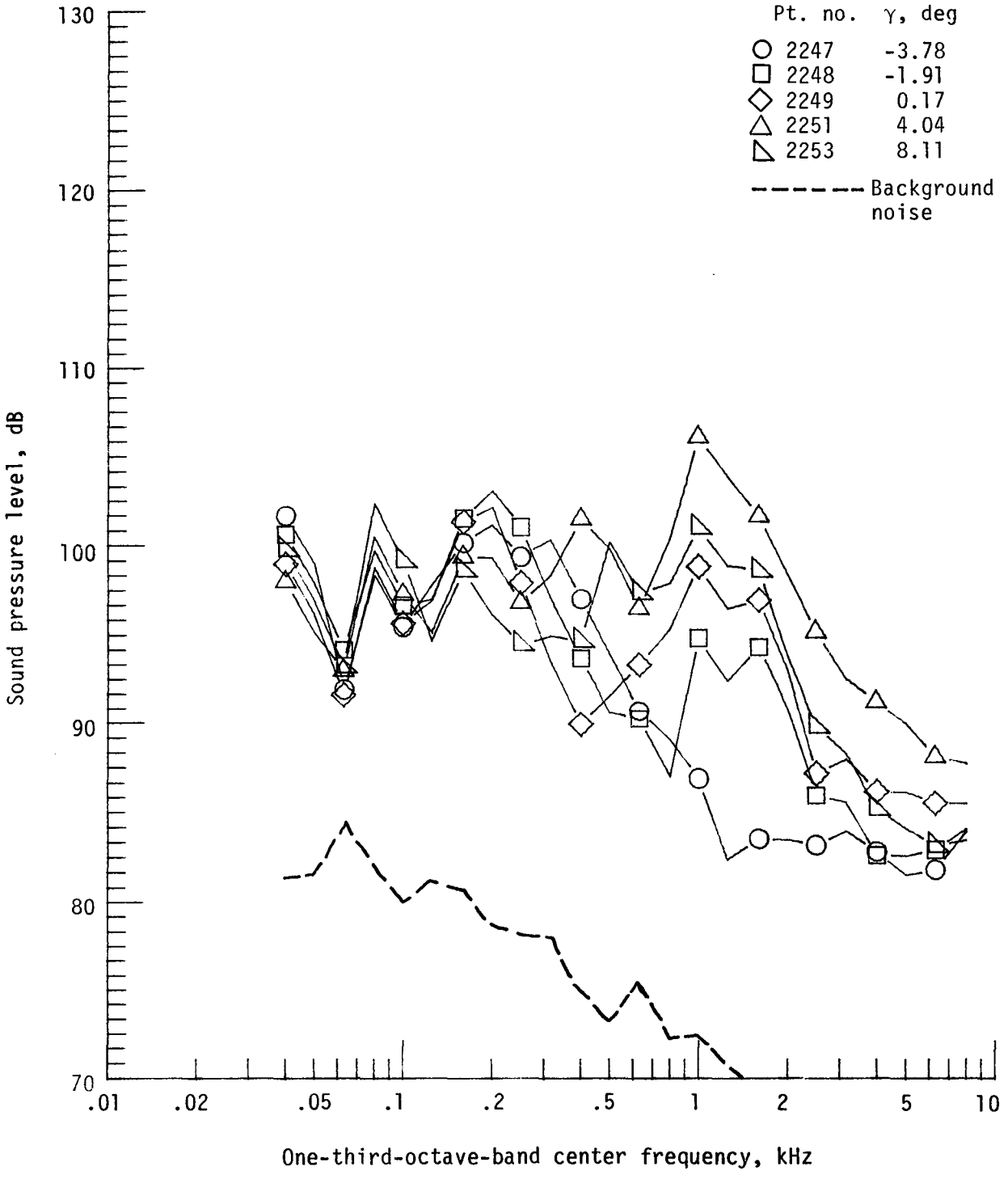

(g) One-third-octave spectra, microphone 7.

Figure 8. - Continued.

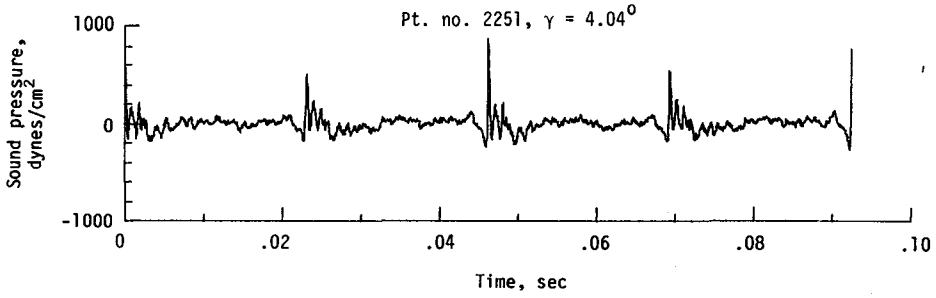

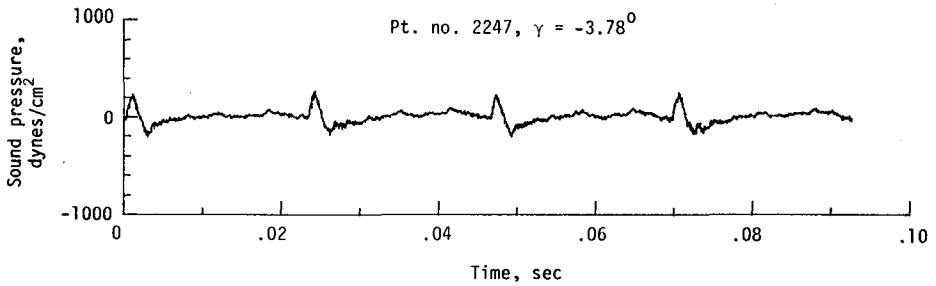

(h) Pressure-time histories; microphone 7.

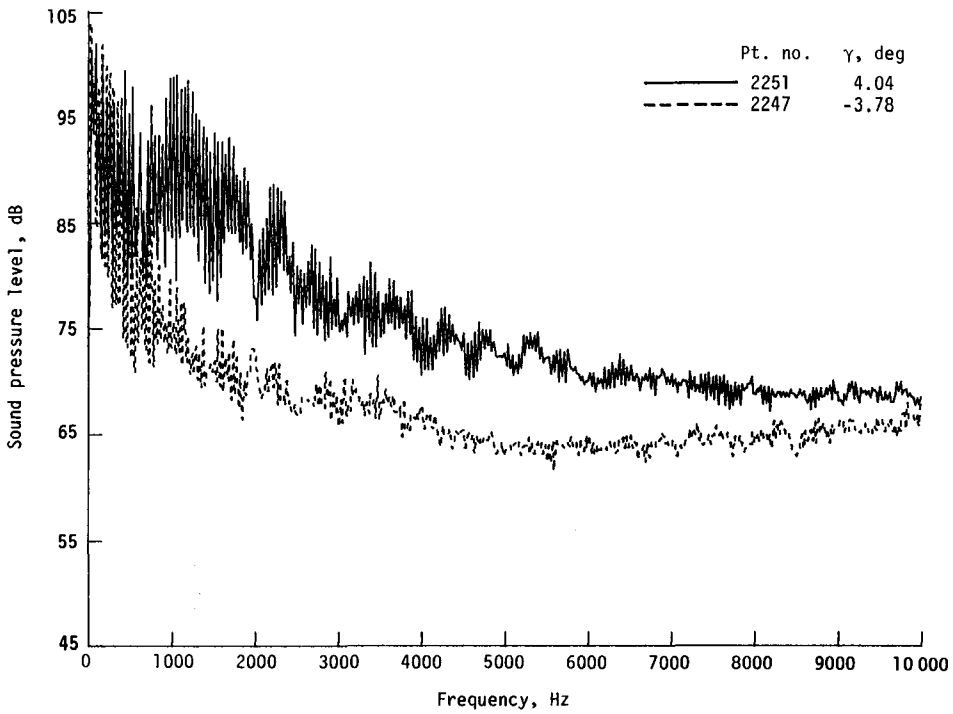

(i) Narrowband analysis; microphone 7.

Figure 8. - Continued.

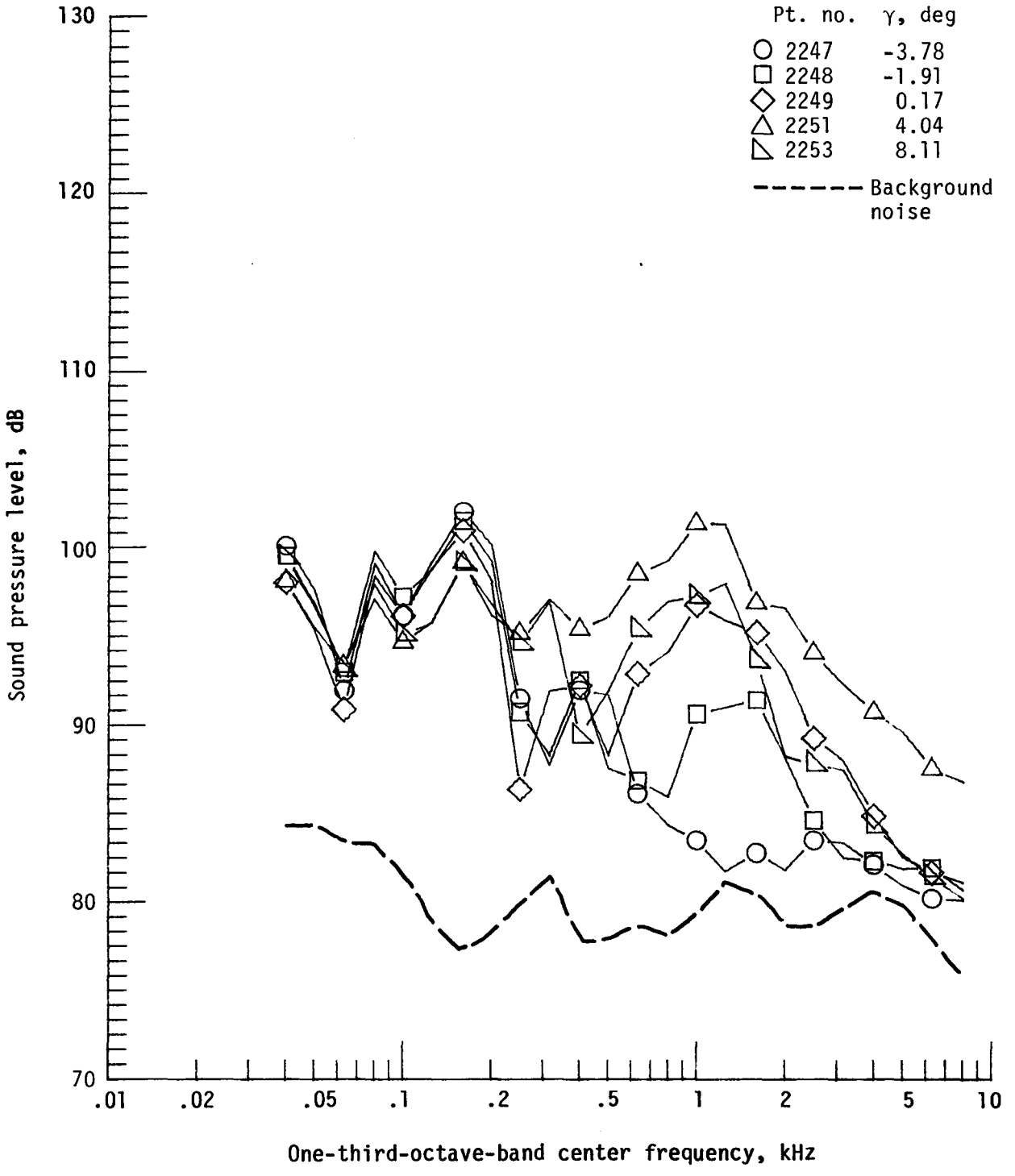

(j) One-third-octave spectra, microphone 8.

Figure 8. - Continued.

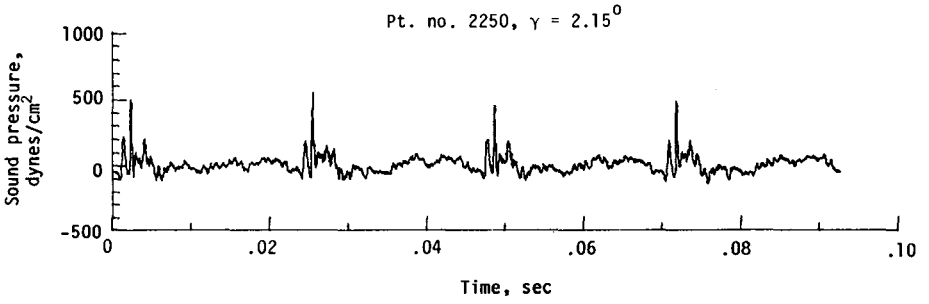

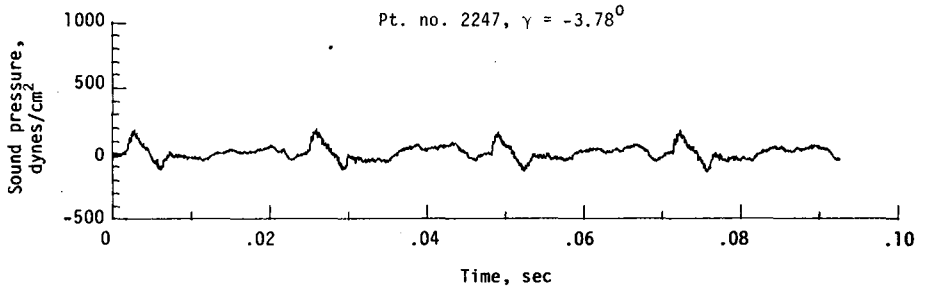

(k) Pressure-time histories; microphone 8.

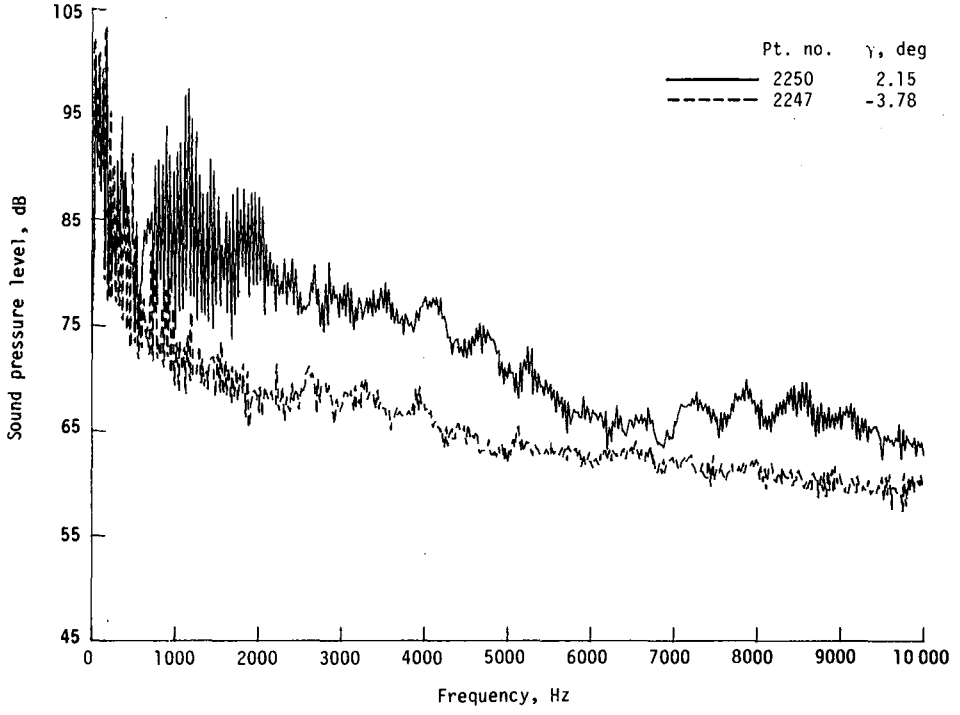

(l) Narrowband analysis; microphone 8.

Figure 8. - Concluded.

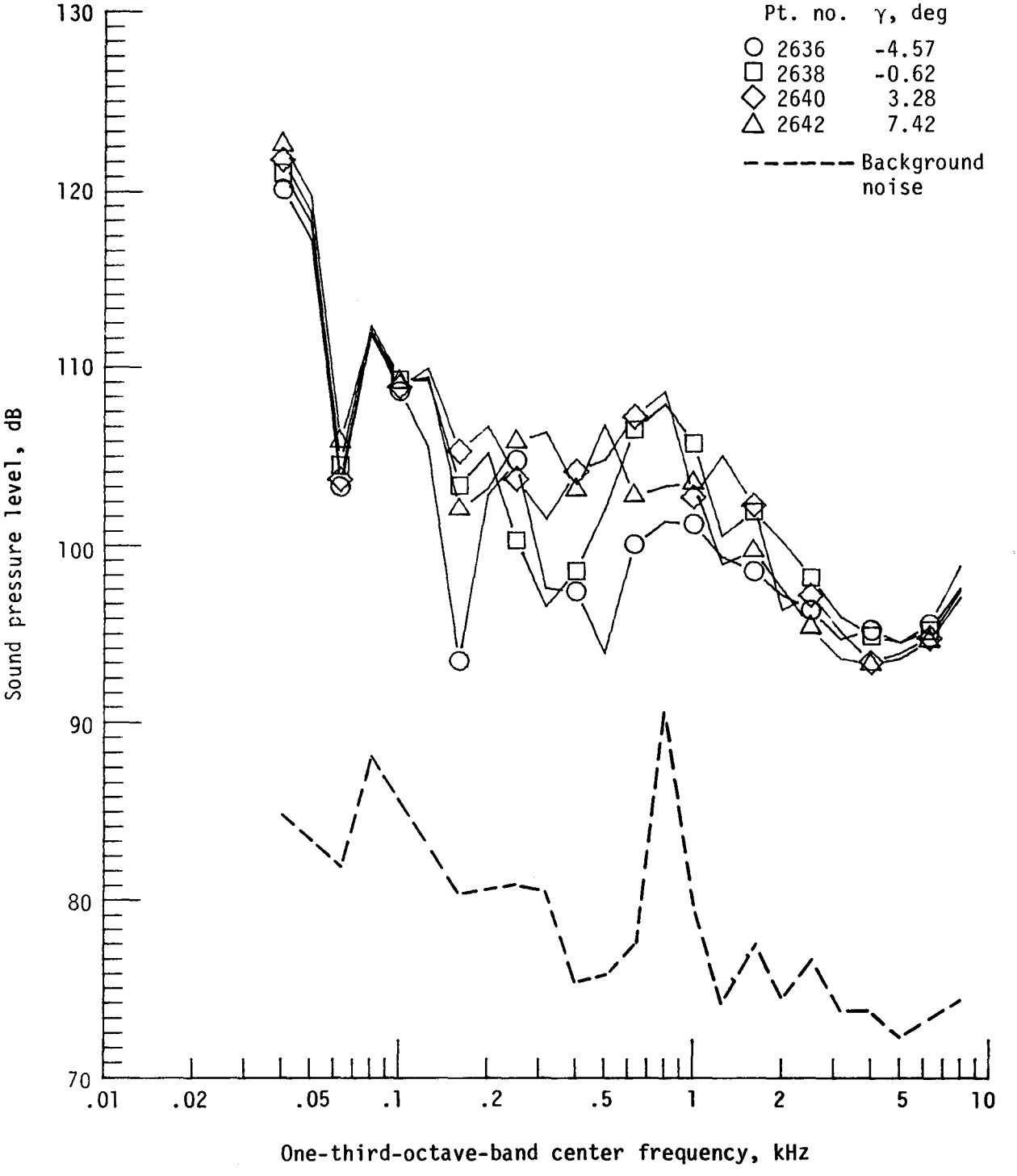

(a) One-third-octave spectra, microphone 2.

Figure 9. - Effect of descent angle variation on noise generated by helicopter model with advanced rotor system, run 211. V_∞ = 49.9 knots, C_T = .0036.

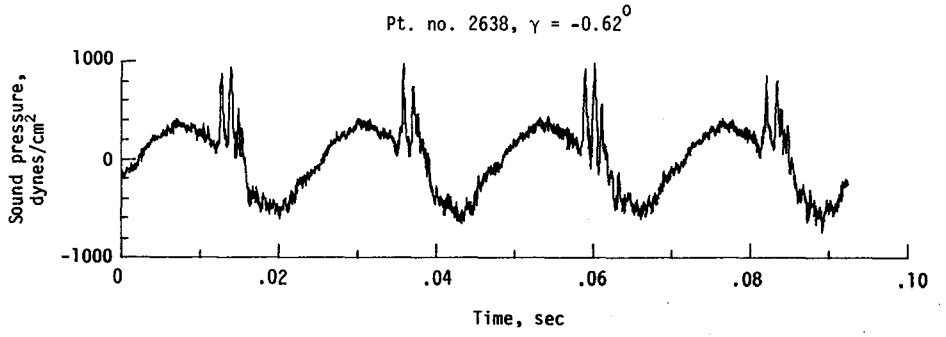

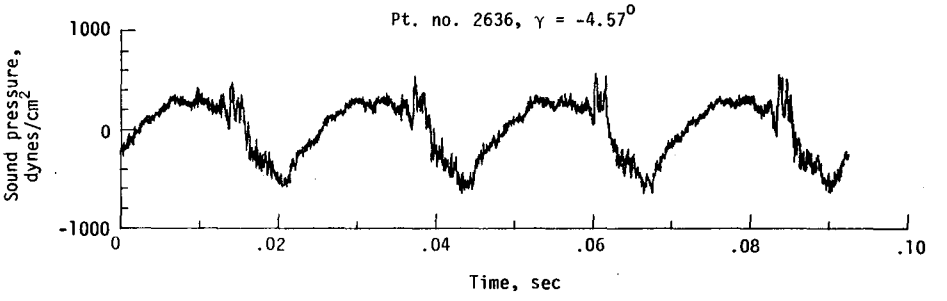

(b) Pressure-time histories; microphone 2.

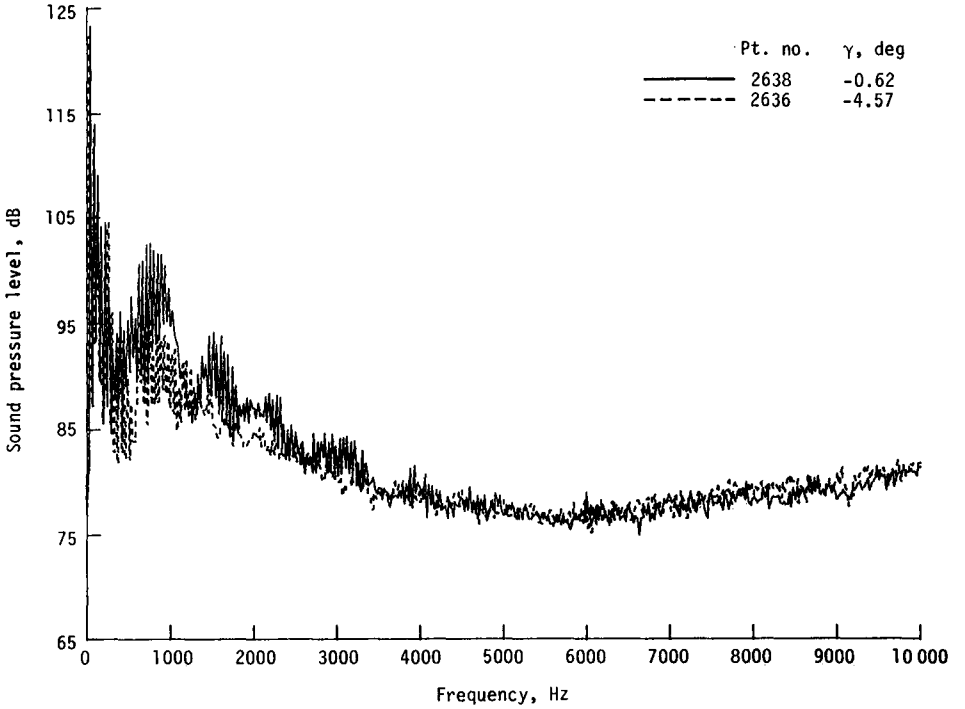

(c) Narrowband analysis; microphone 2.

Figure 9. - Continued.

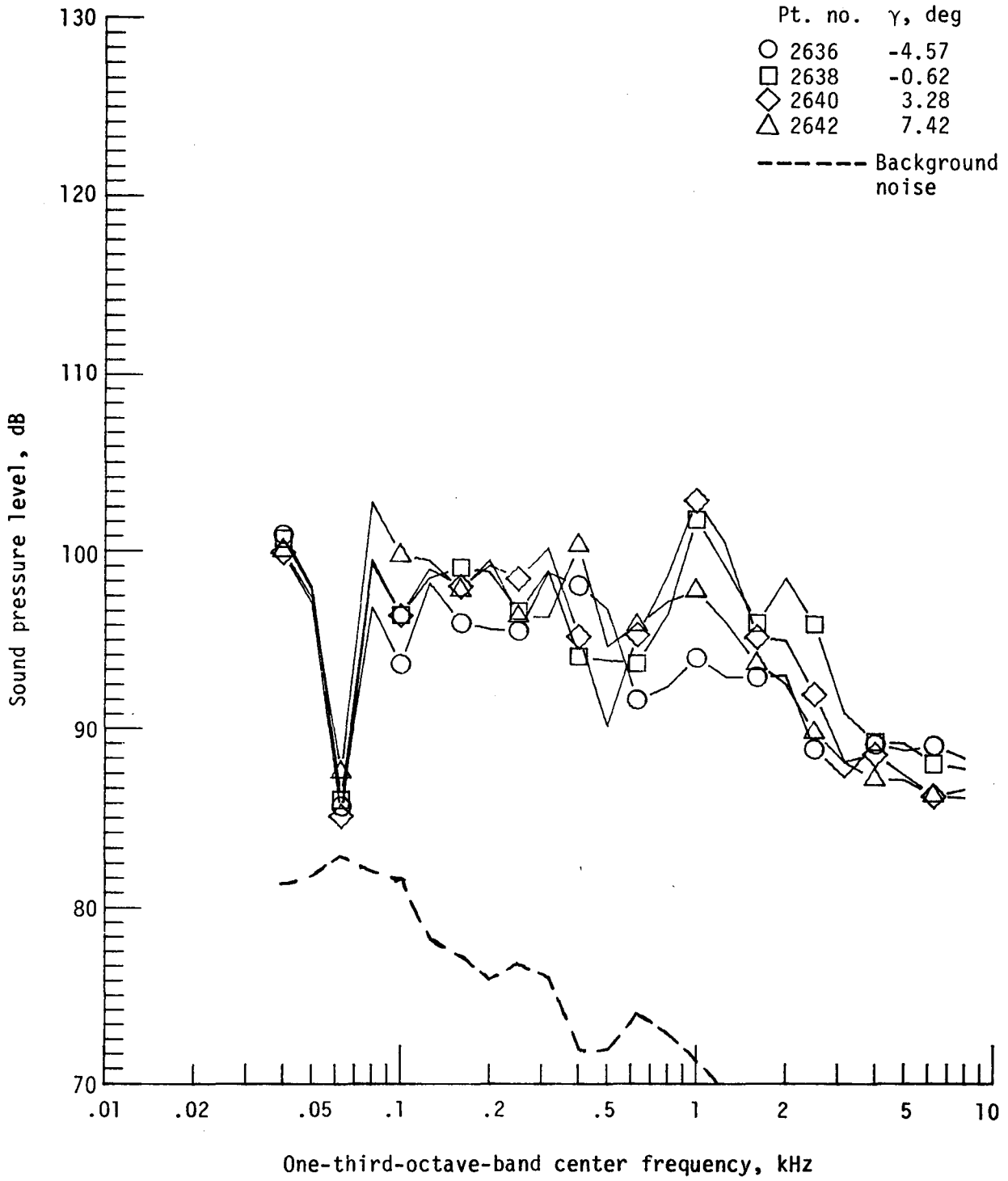

(c) Narrowband analysis; microphone 2.

Figure 9. - Continued.

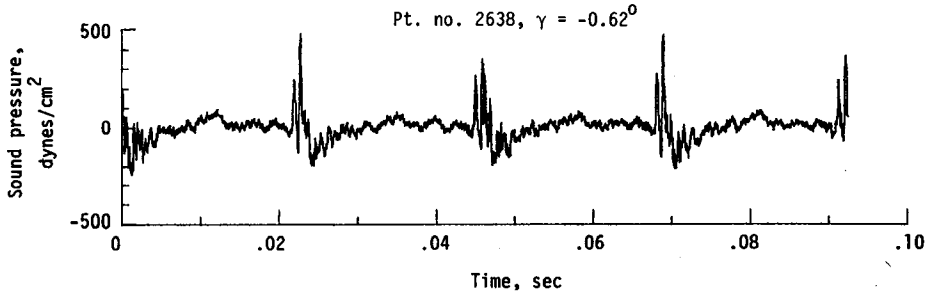

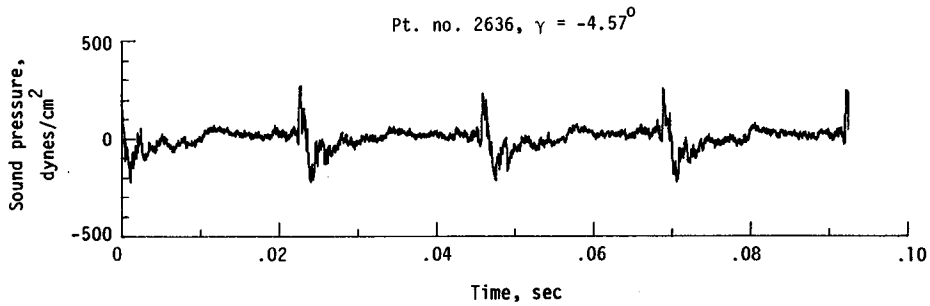

(e) Pressure-time histories; microphone 6.

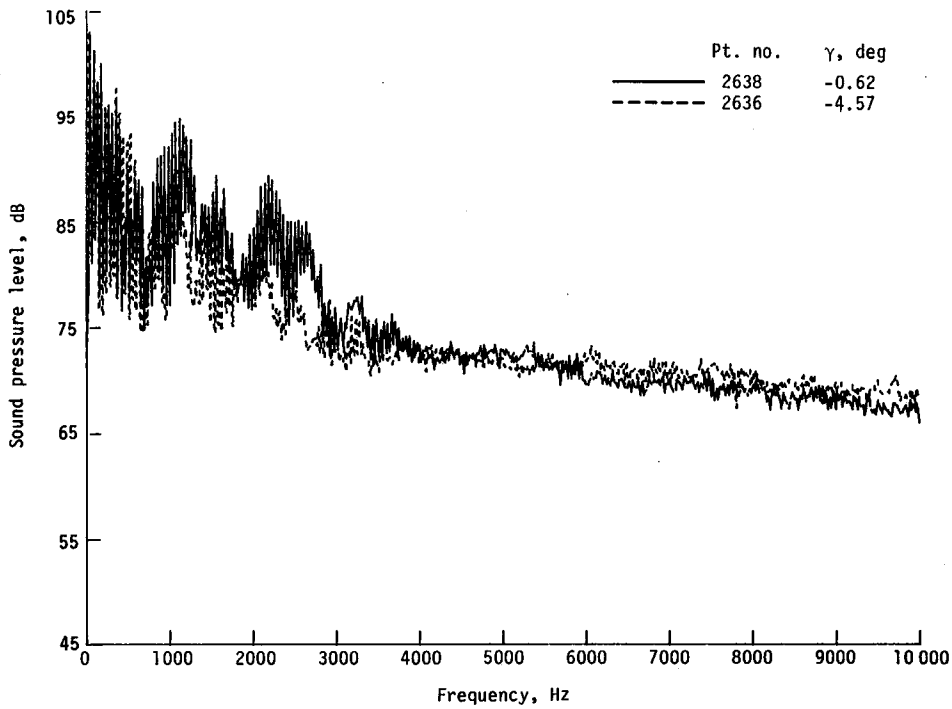

(f) Narrowband analysis; microphone 6.

Figure 9. - Continued.

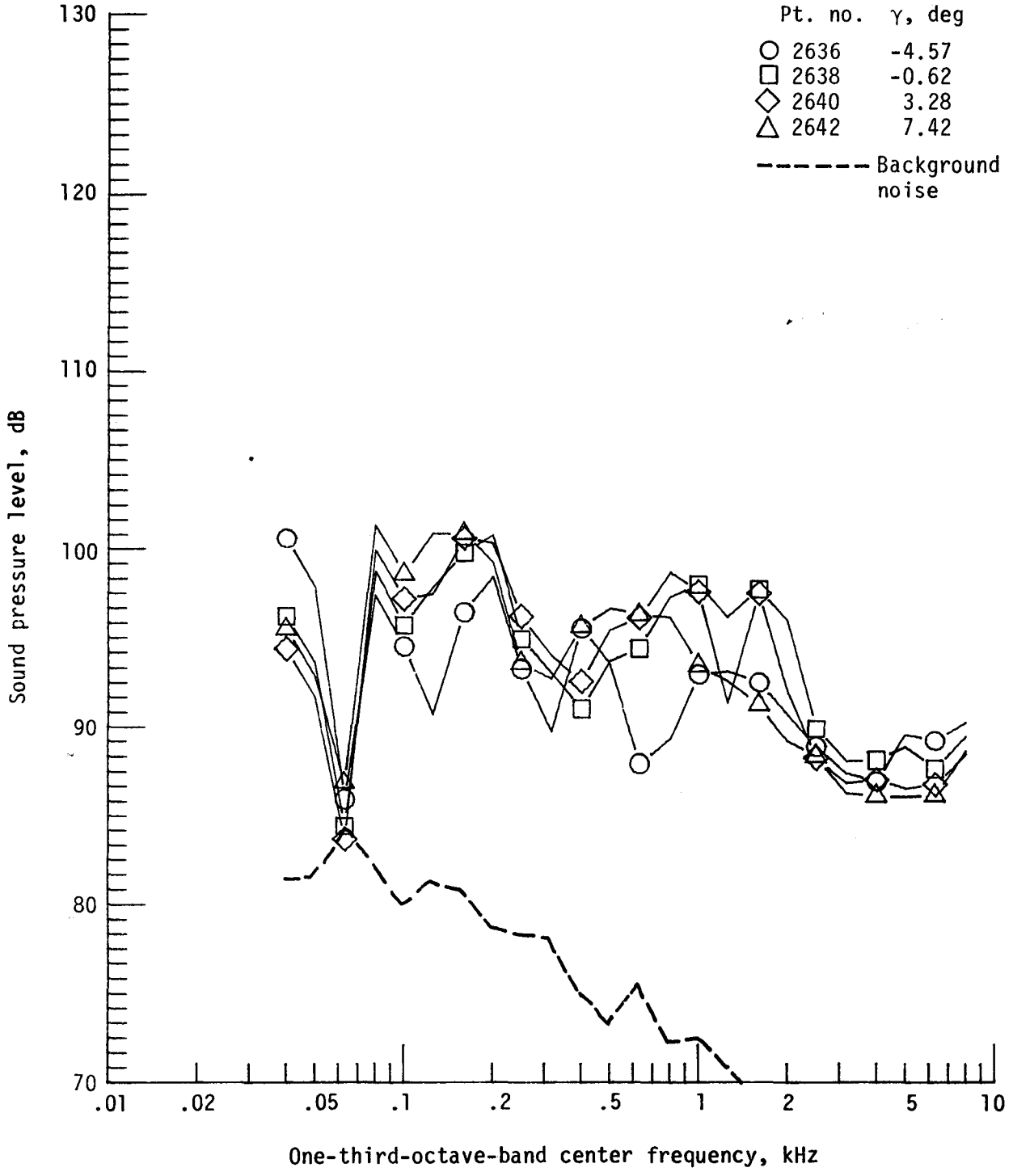

(g) One-third-octave spectra, microphone 7.

Figure 9. - Continued.

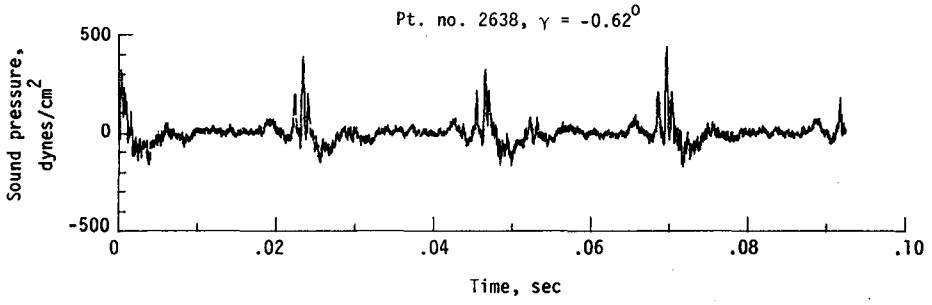

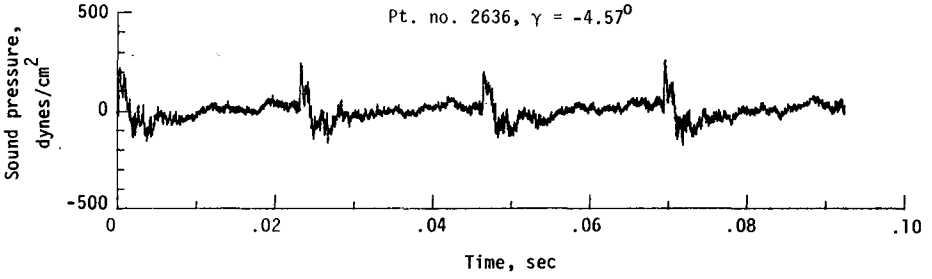

(h) Pressure-time histories; microphone 7.

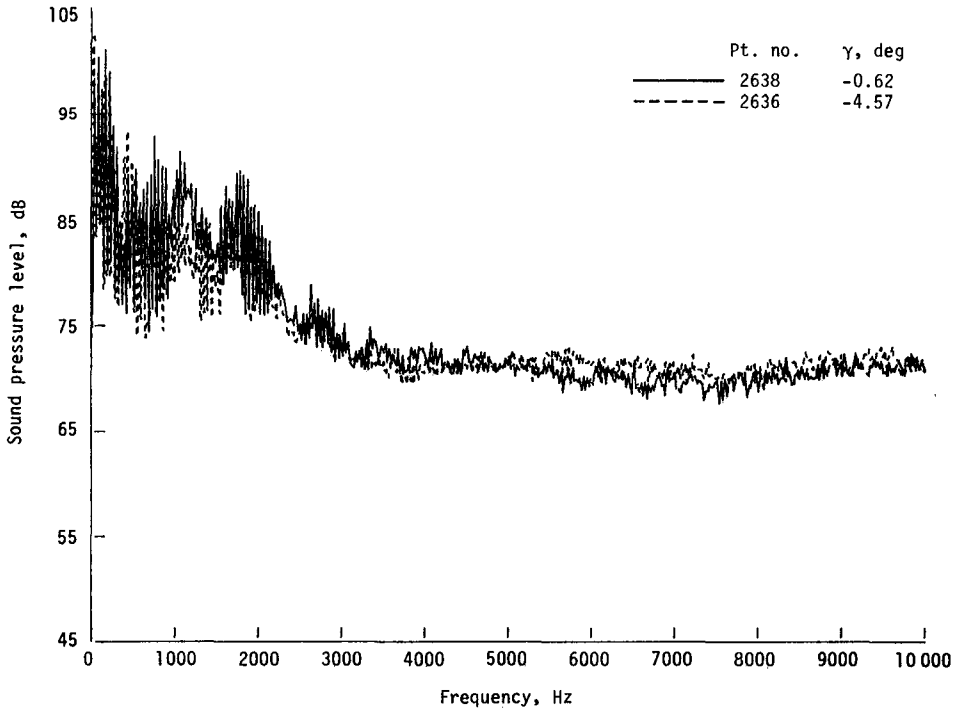

(i) Narrowband analysis; microphone 7.
Figure 9. - Continued.

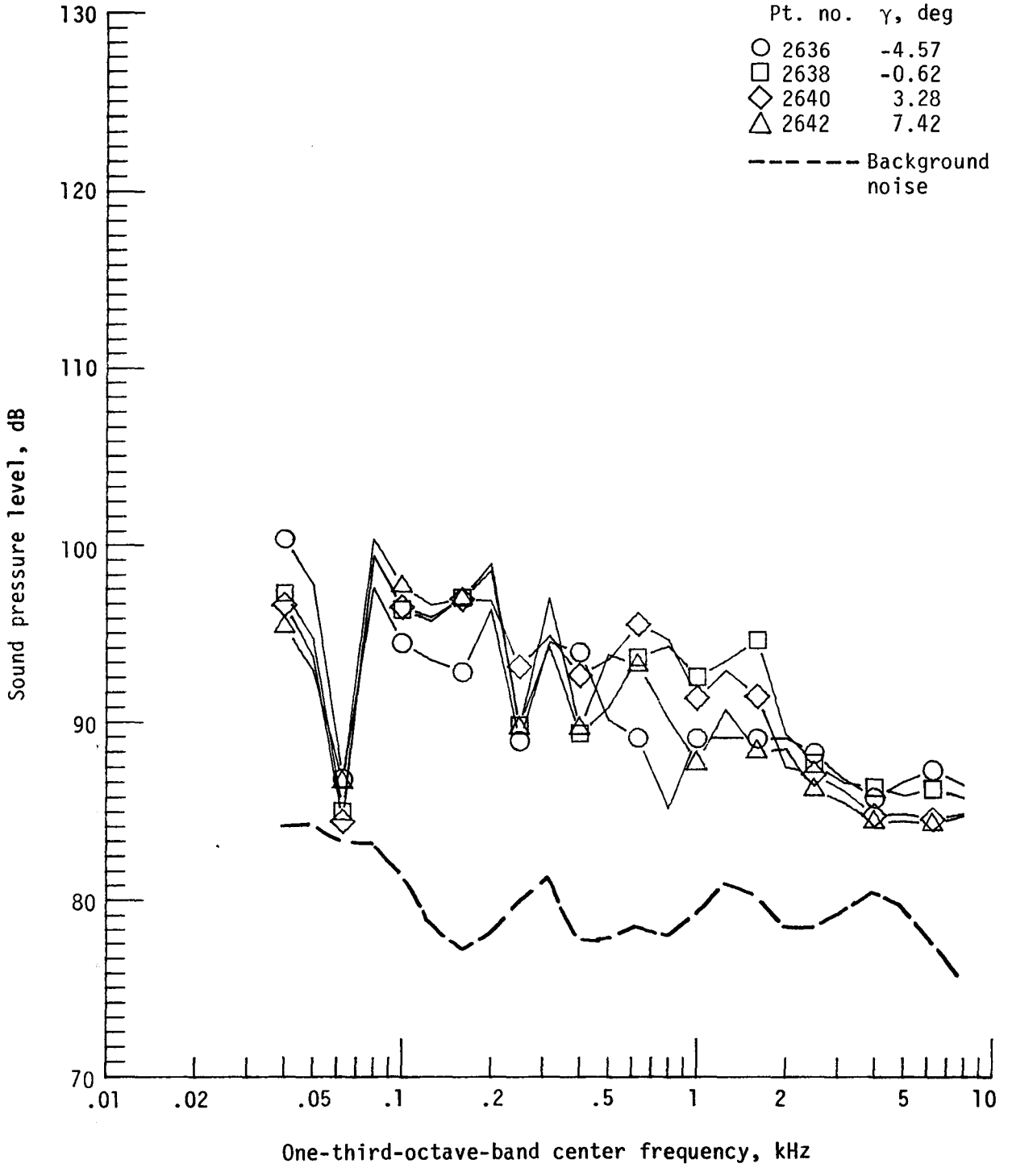

(j) One-third-octave spectra, microphone 8.

Figure 9. - Continued.

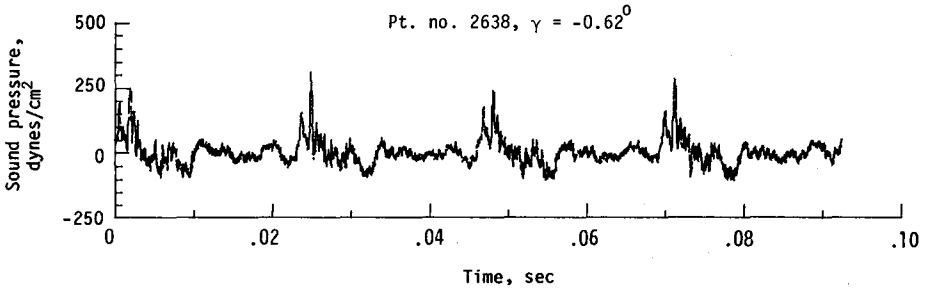

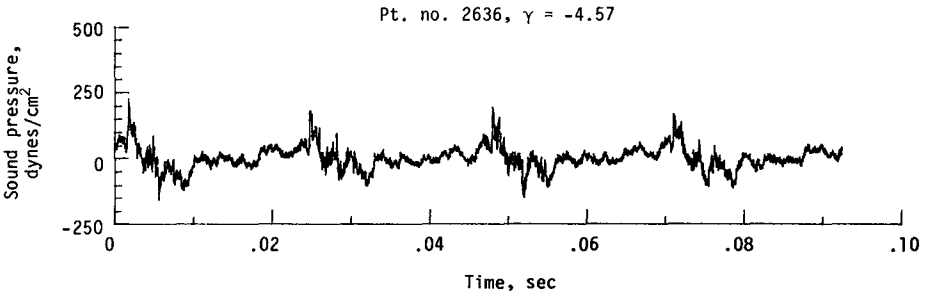

(k) Pressure-time histories; microphone 8.

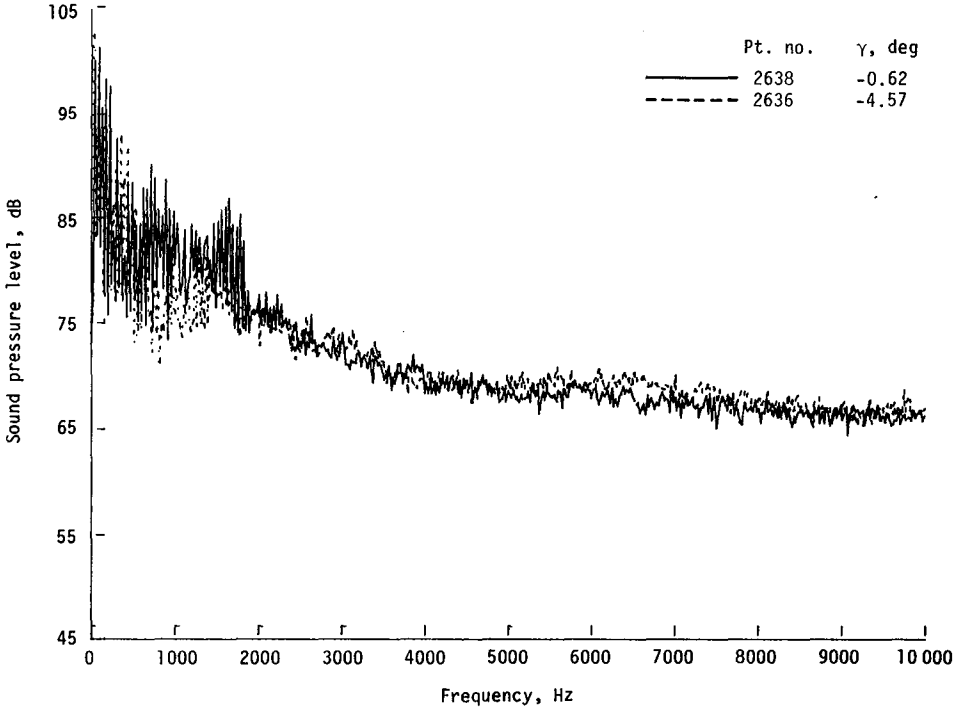

(l) Narrowband analysis; microphone 8.

Figure 9. - Concluded.

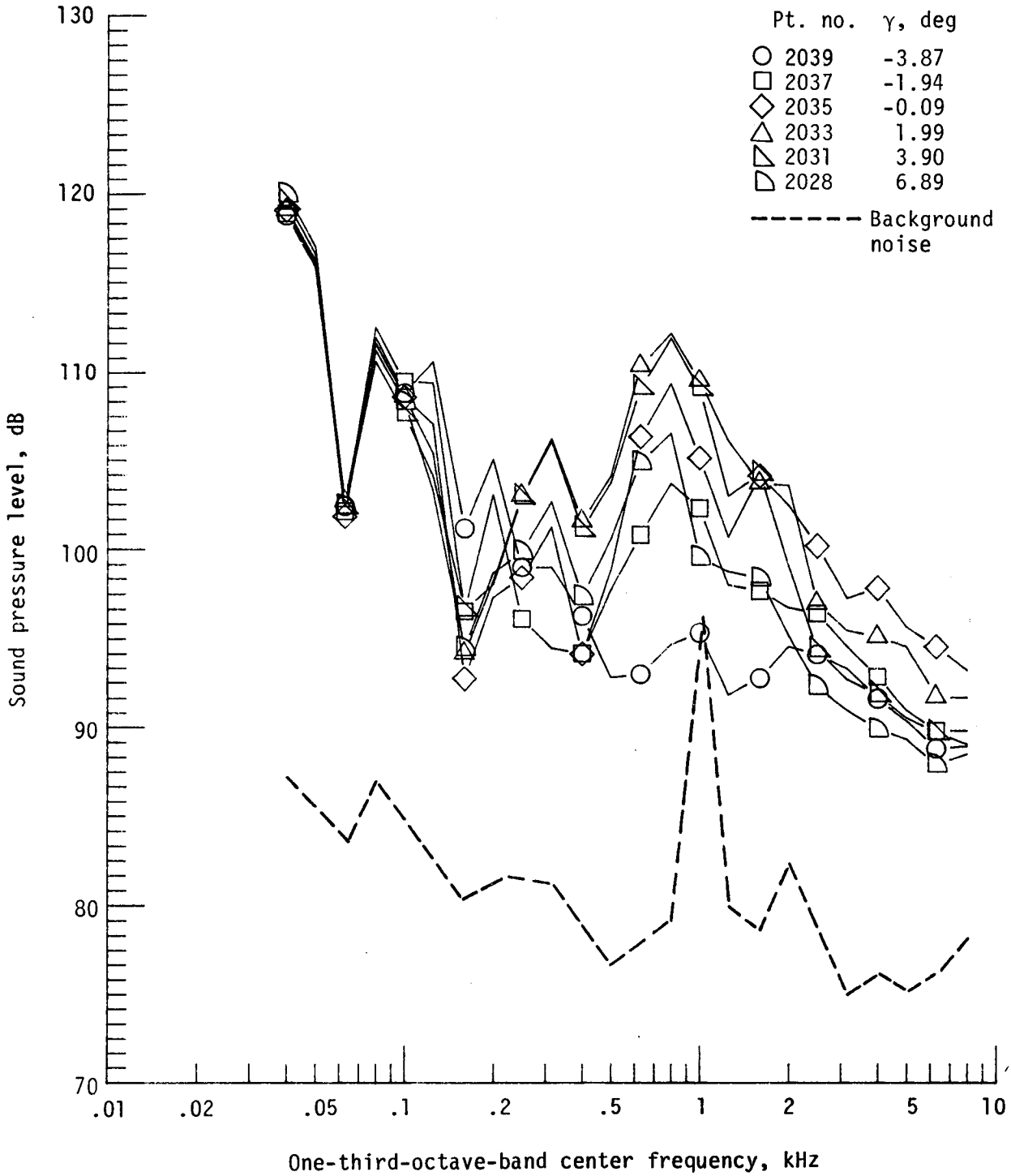

(a) One-third-octave spectra, microphone 2.

Figure 10. - Effect of descent angle variation on noise generated by helicopter model with standard rotor system, run 155; V_∞ = 55.3 knots, C_T = .0032.

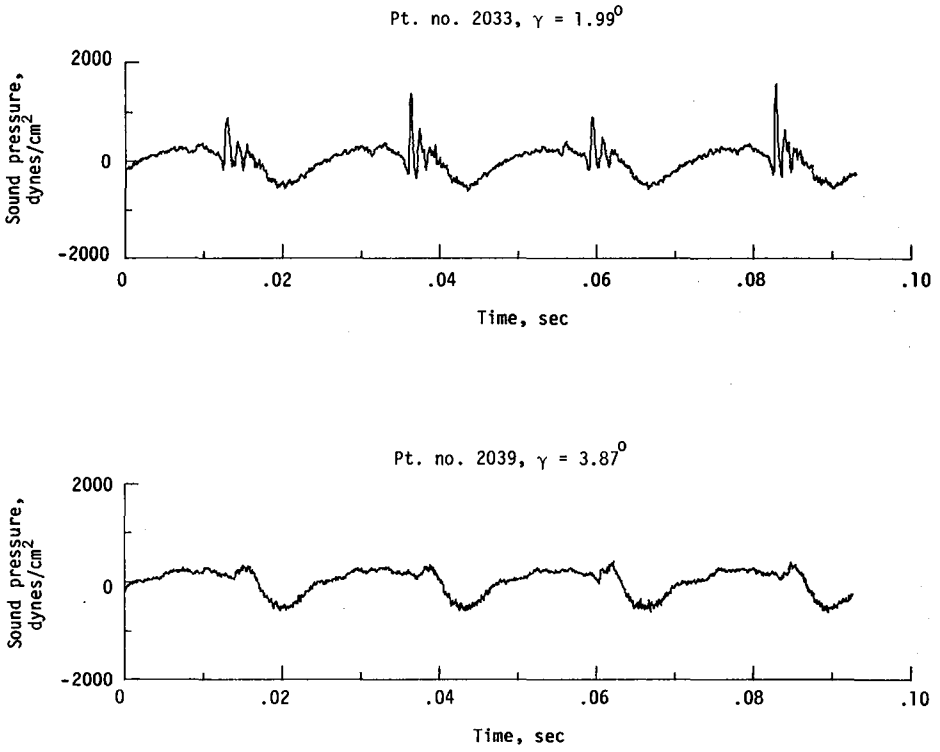

(b) Pressure-time histories; microphone 2.

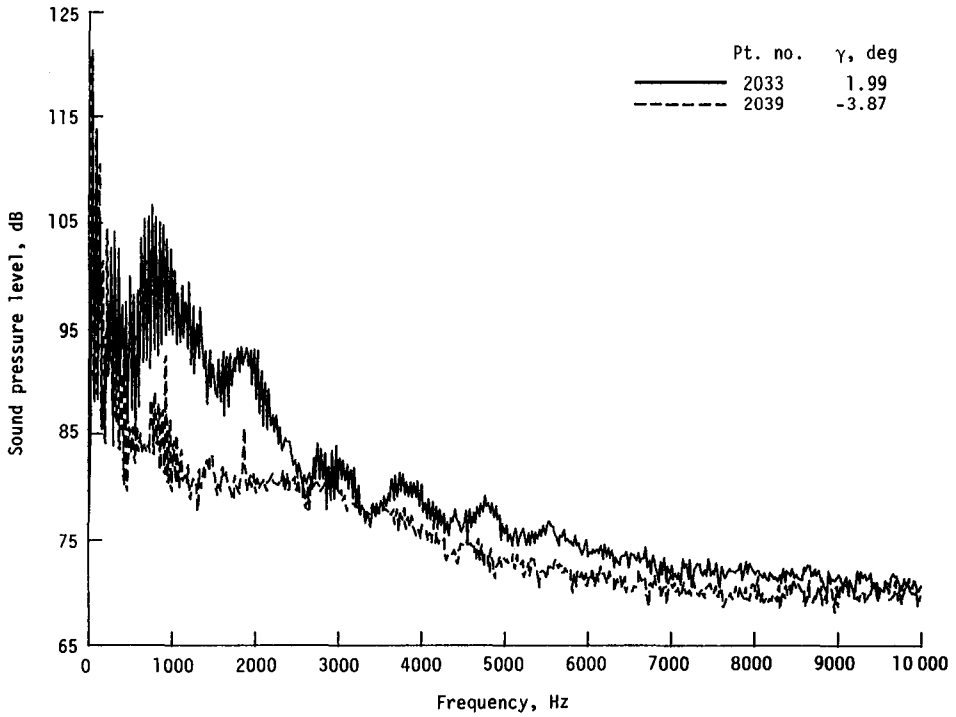

(c) Narrowband analysis; microphone 2.
Figure 10. - Continued.

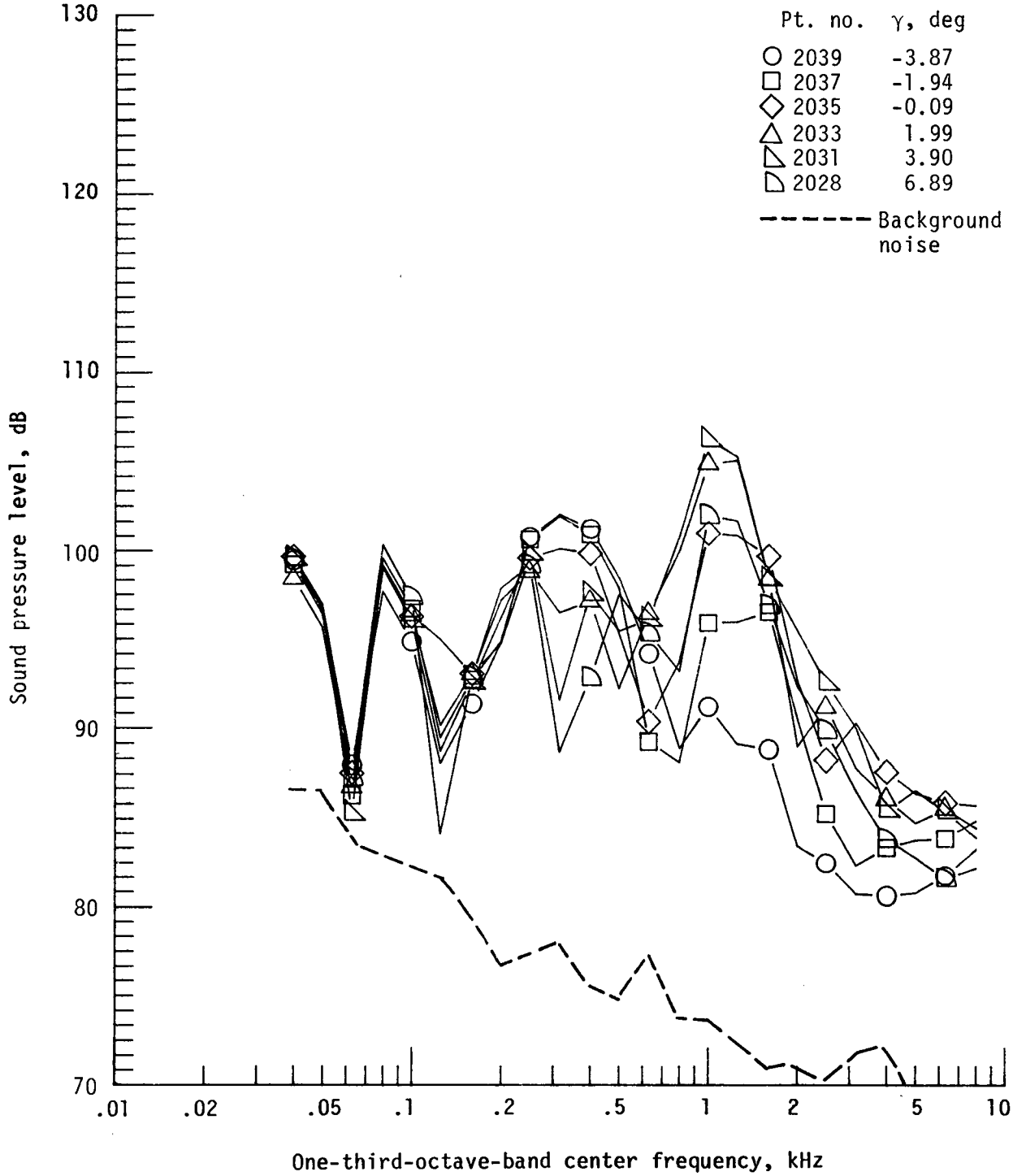

(d) One-third-octave spectra, microphone 6.

Figure 10. - Continued.

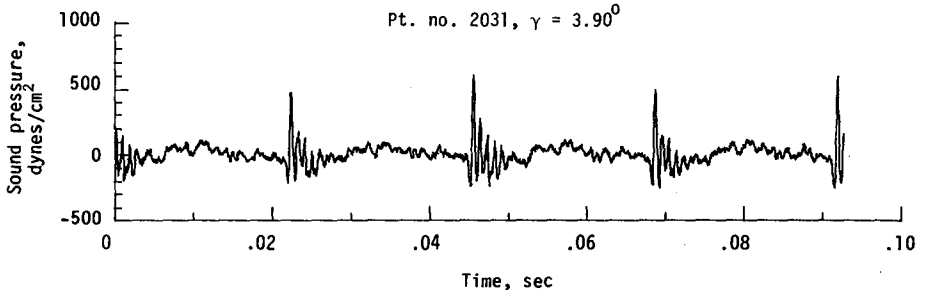

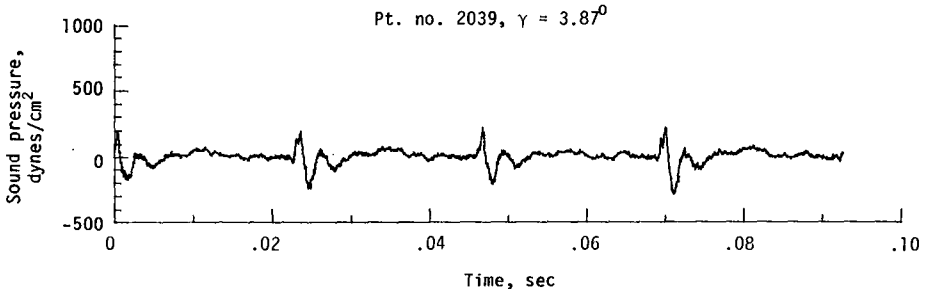

(e) Pressure-time histories; microphone 6.

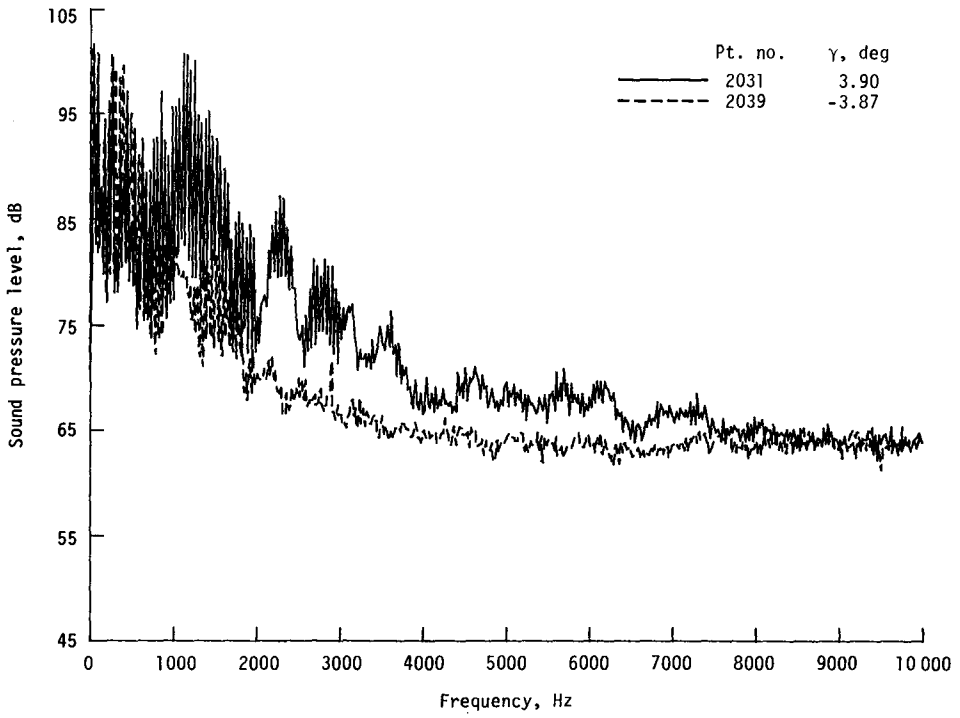

(f) Narrowband analysis; microphone 6.

Figure 10. - Continued.

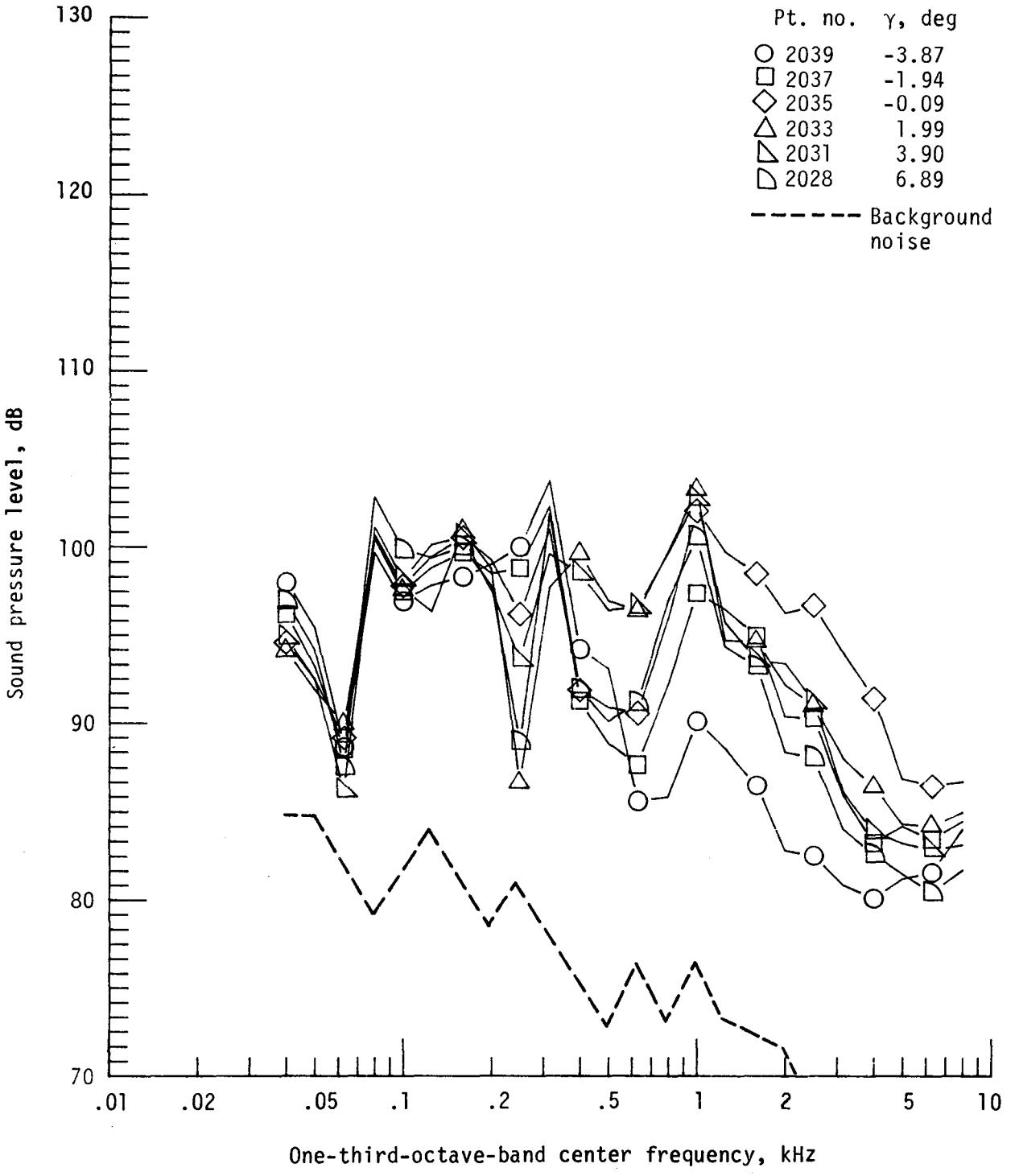

(g) One-third-octave spectra, microphone 7.

Figure 10. - Continued.

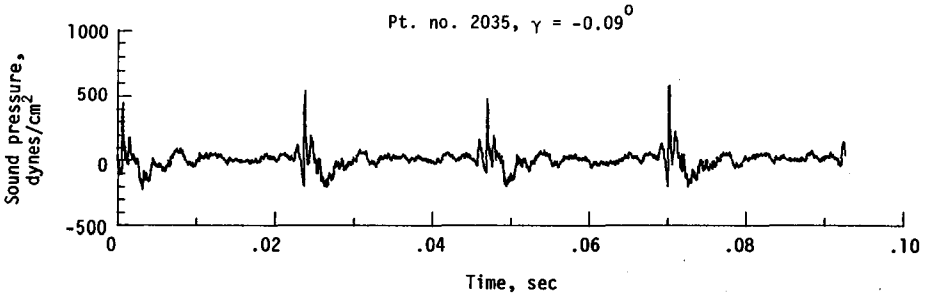

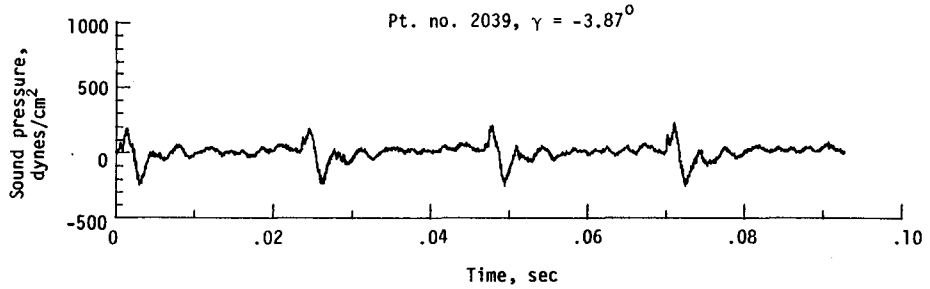

(h) Pressure-time histories; microphone 7.

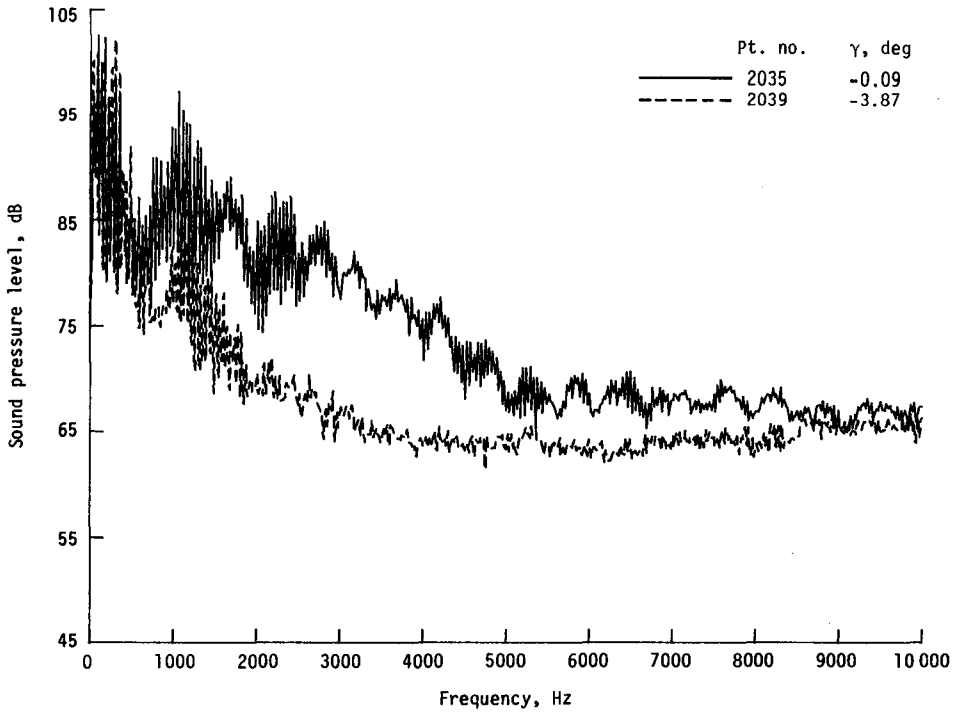

(i) Narrowband analysis; microphone 7.

Figure 10. - Continued.

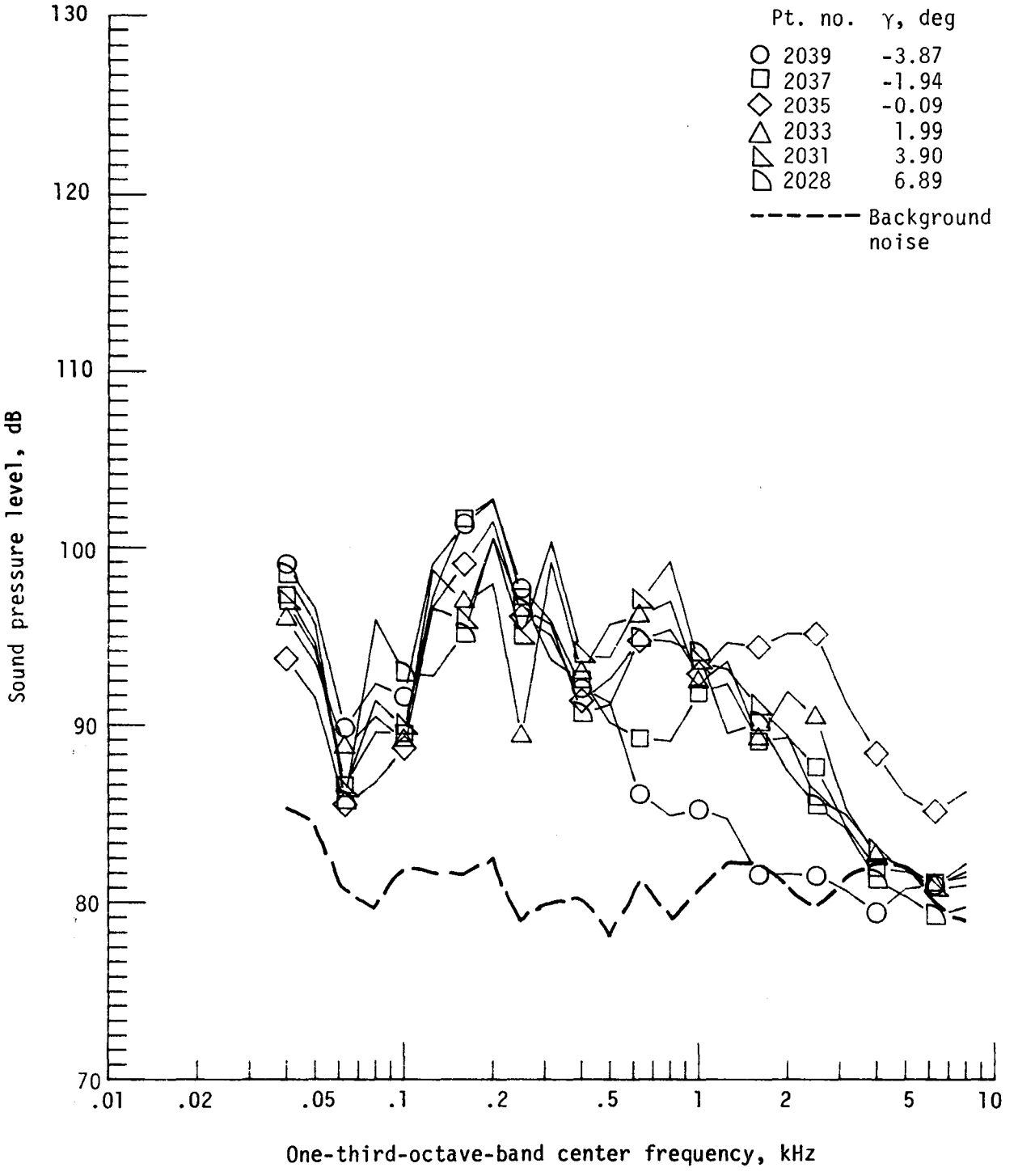

(j) One-third-octave spectra, microphone 8.

Figure 10. - Continued.

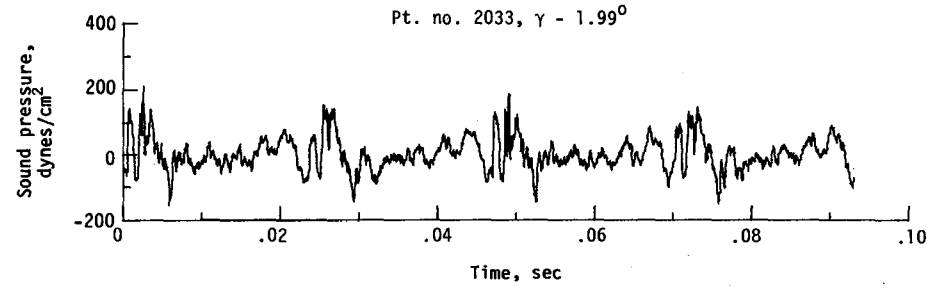

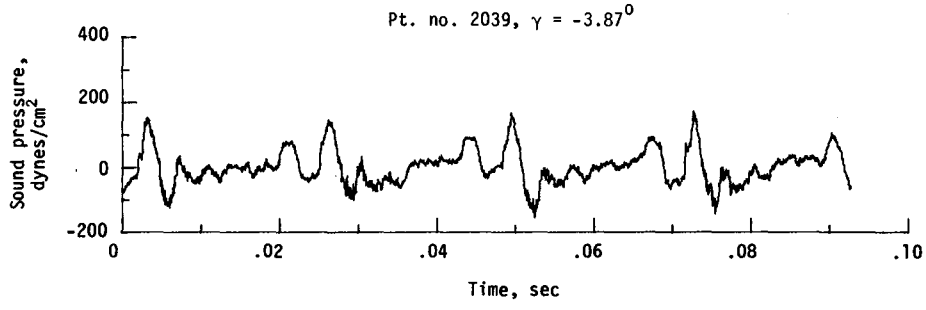

(k) Pressure-time histories; microphone 8.

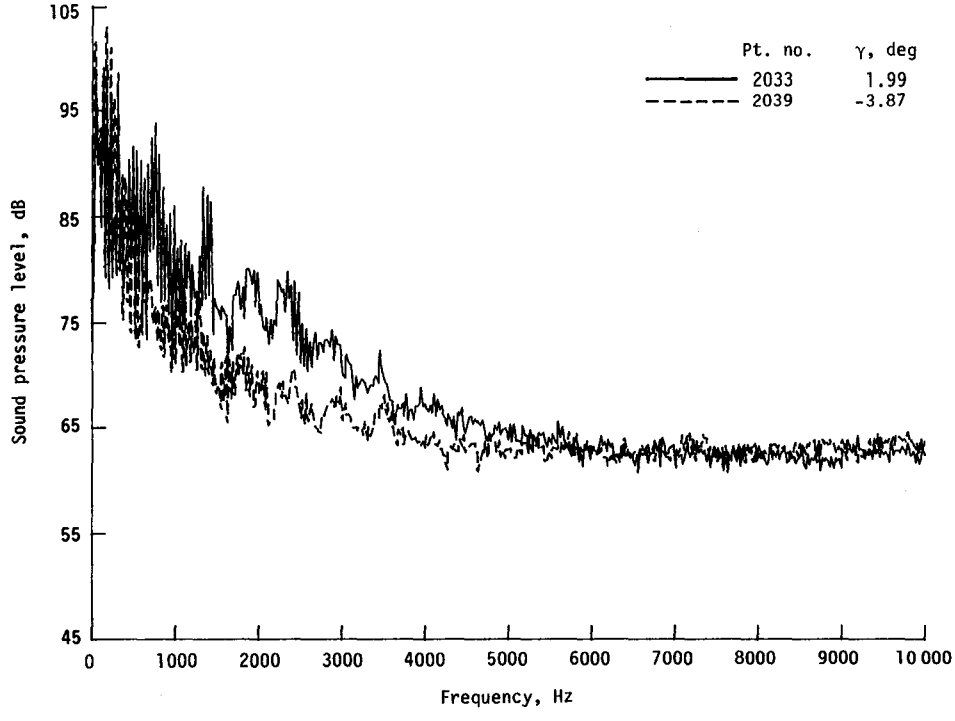

(l) Narrowband analysis; microphone 8.

Figure 10. - Concluded.

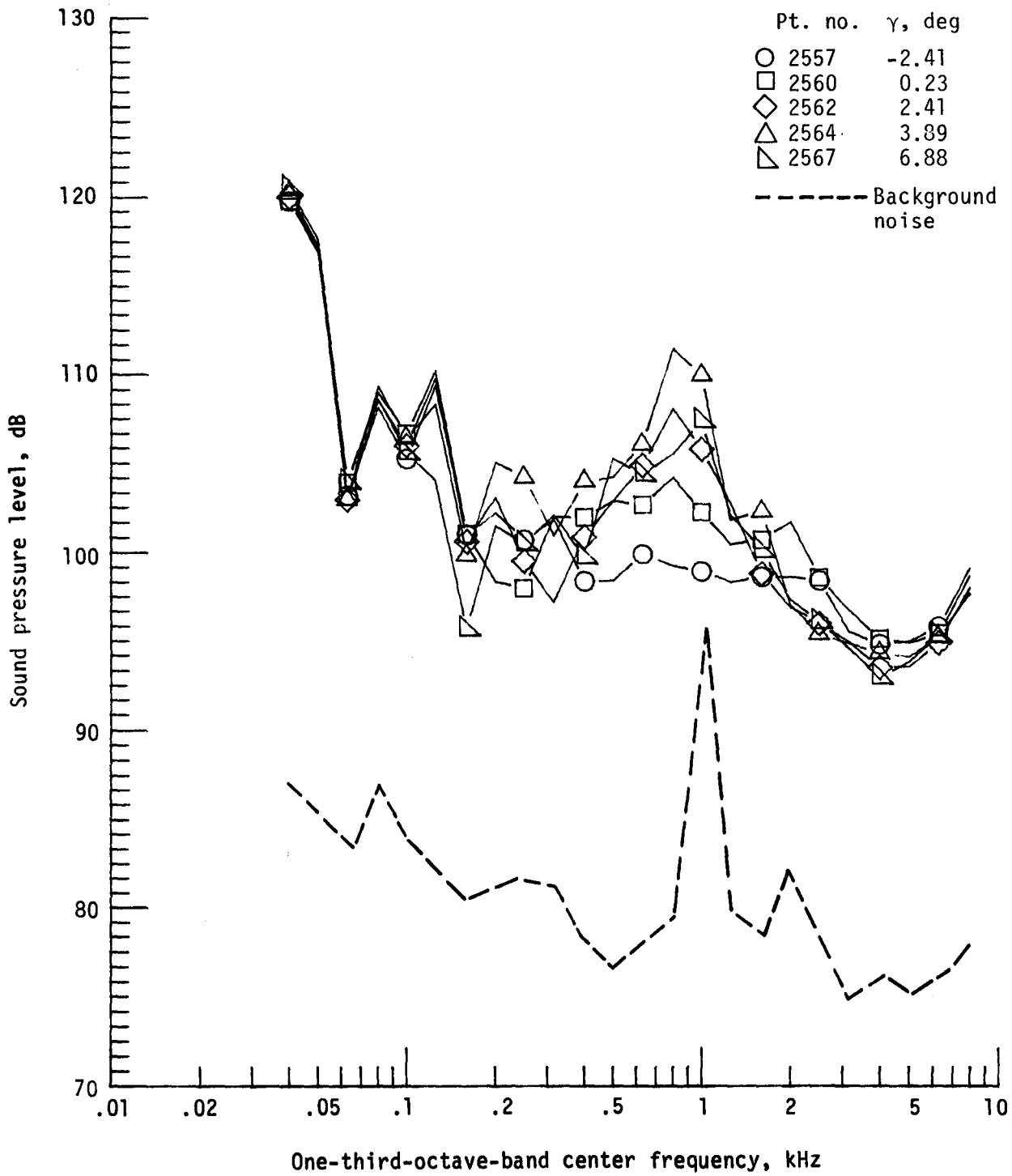

(a) One-third-octave spectra, microphone 2.

Figure 11. - Effect of descent angle variation on noise generated by helicopter model with advanced rotor system, run 199. V_∞ = 55.6 knots, C_T = .0031.

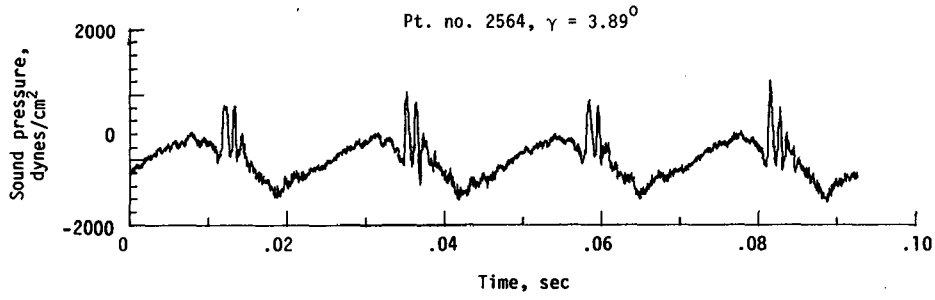

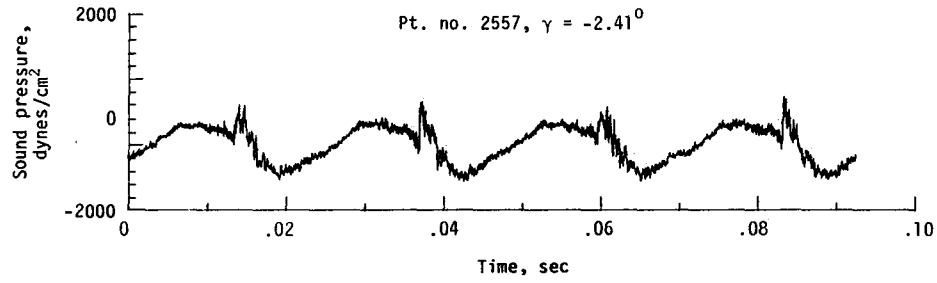

(b) Pressure-time histories; microphone 2.

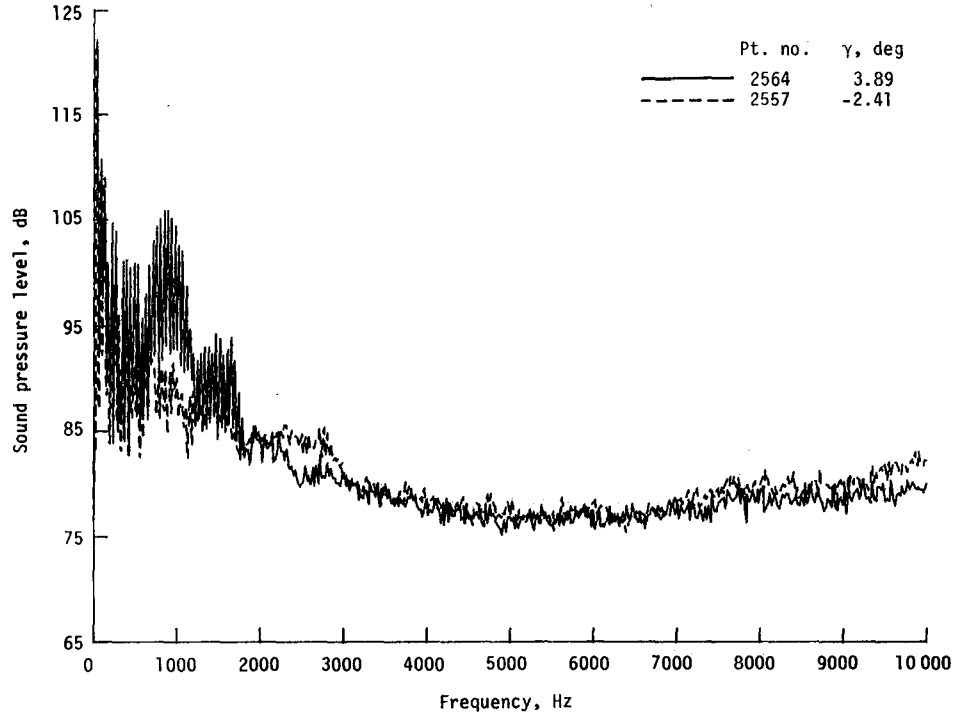

(c) Narrowband analysis; microphone 2.

Figure 11. - Continued.

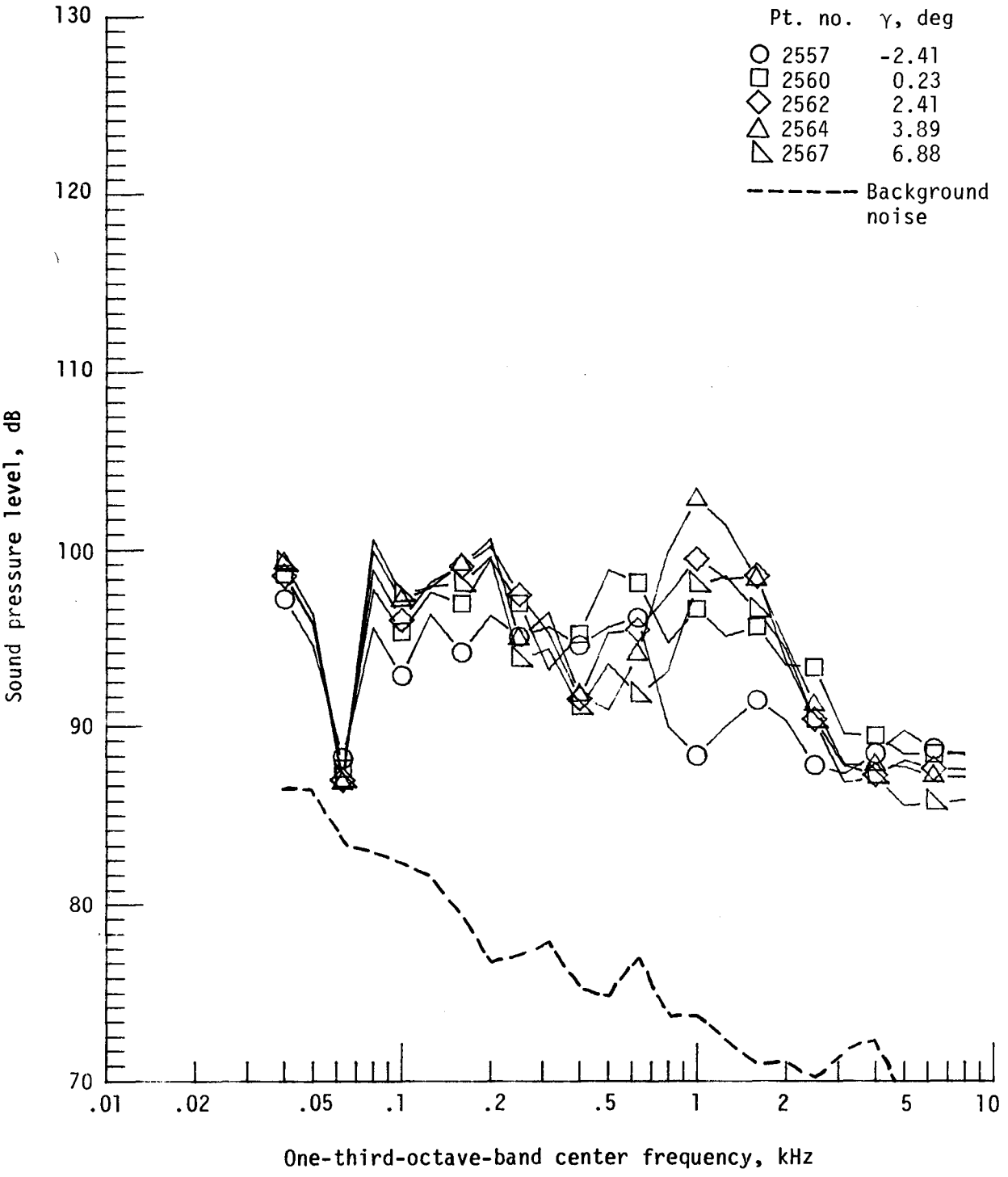

(d) One-third-octave spectra, microphone 6.

Figure 11. - Continued.

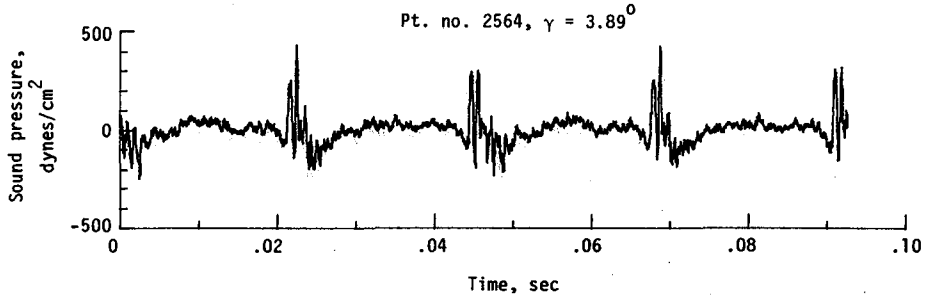

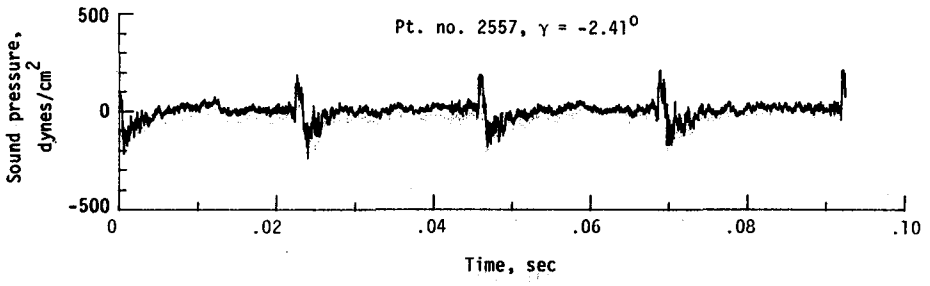

(e) Pressure-time histories; microphone 6.

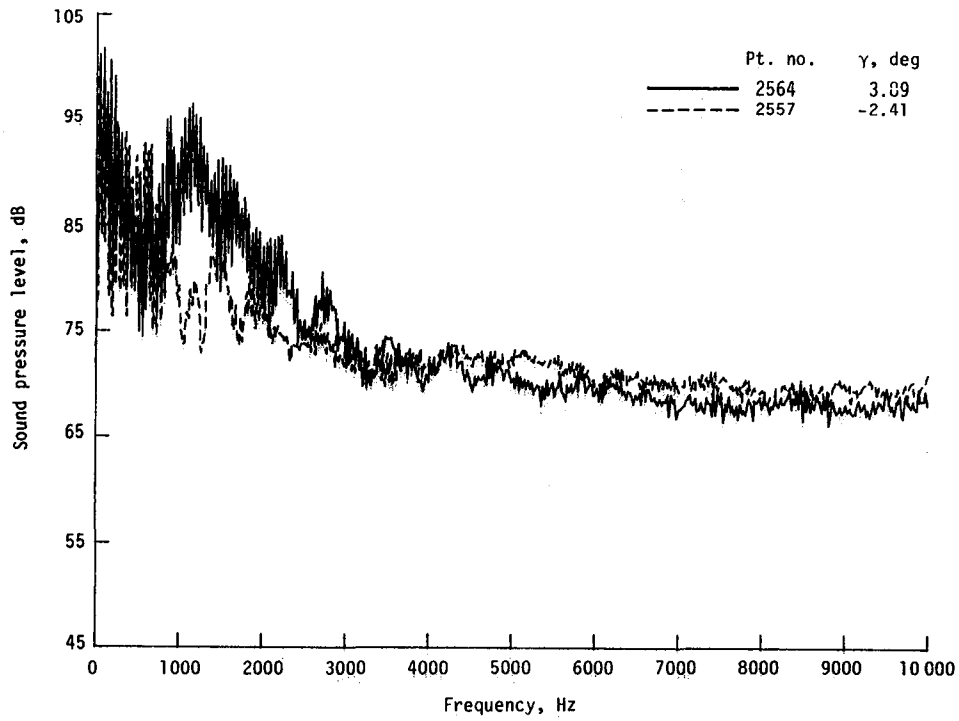

(f) Narrowband analysis; microphone 6.
Figure 11. - Continued.

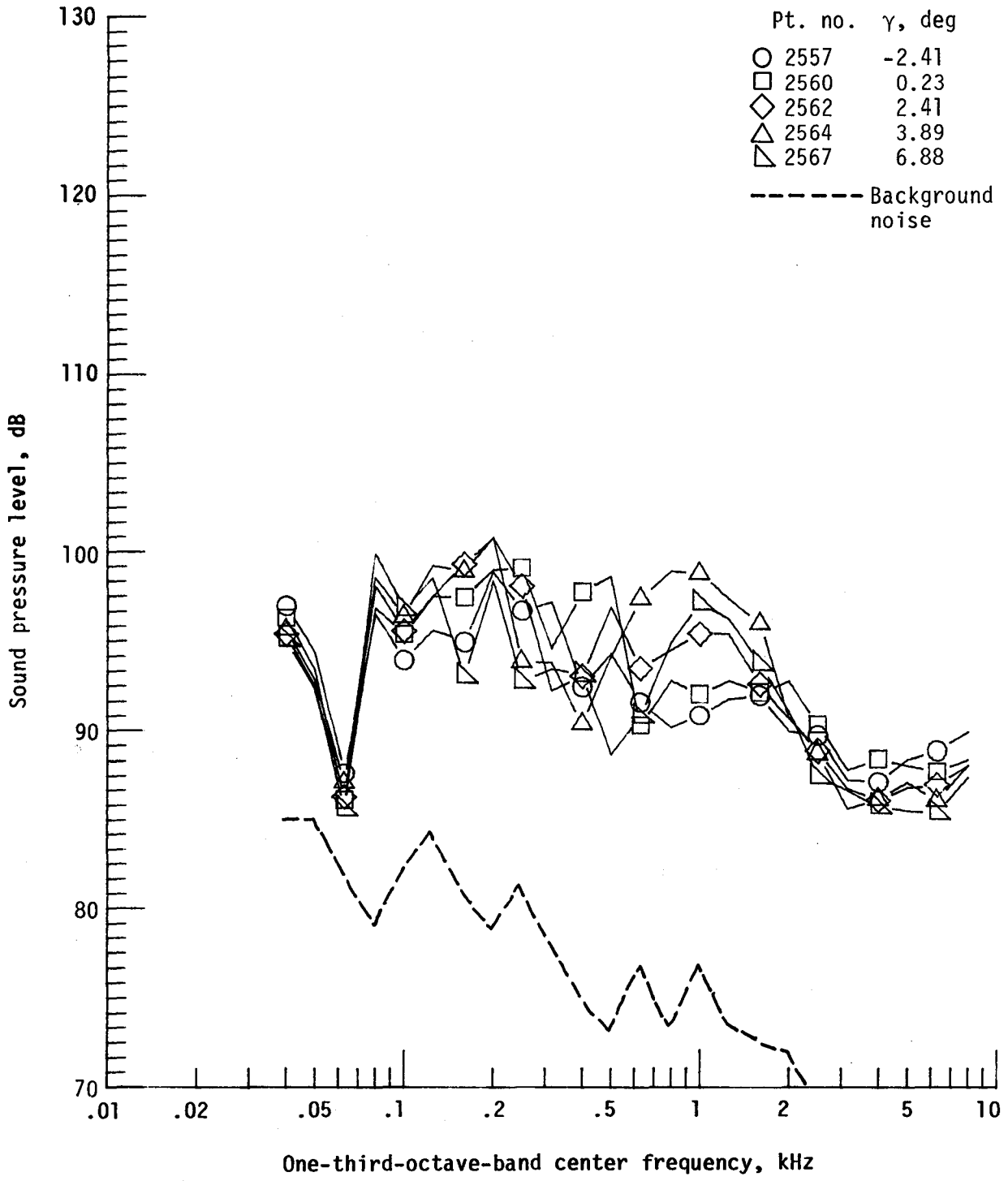

(g) One-third-octave spectra, microphone 7.

Figure 11. - Continued.

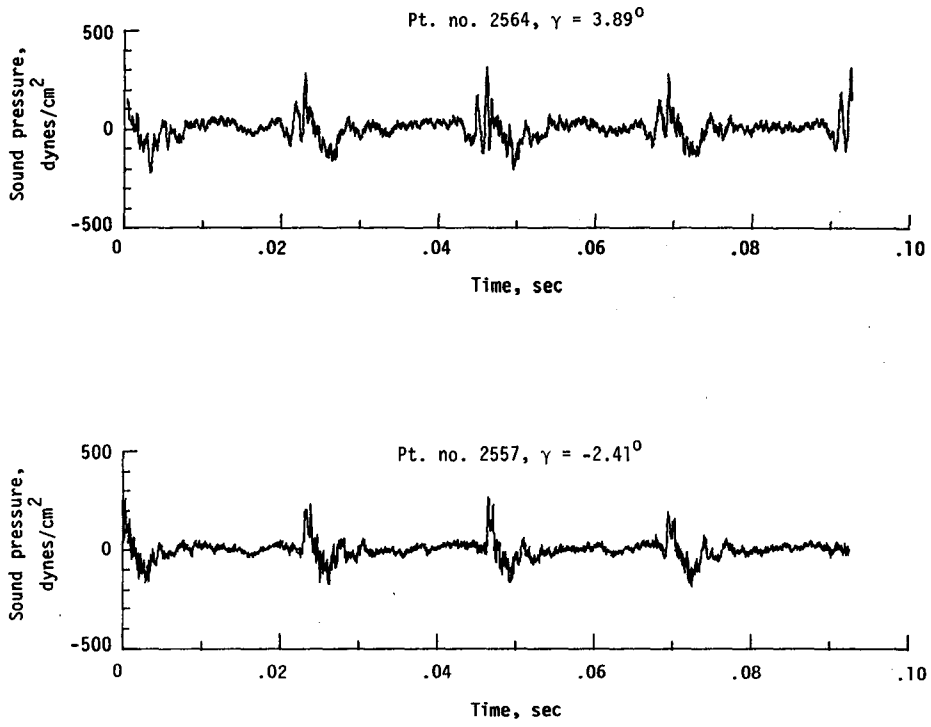

(h) Pressure-time histories; microphone 7.

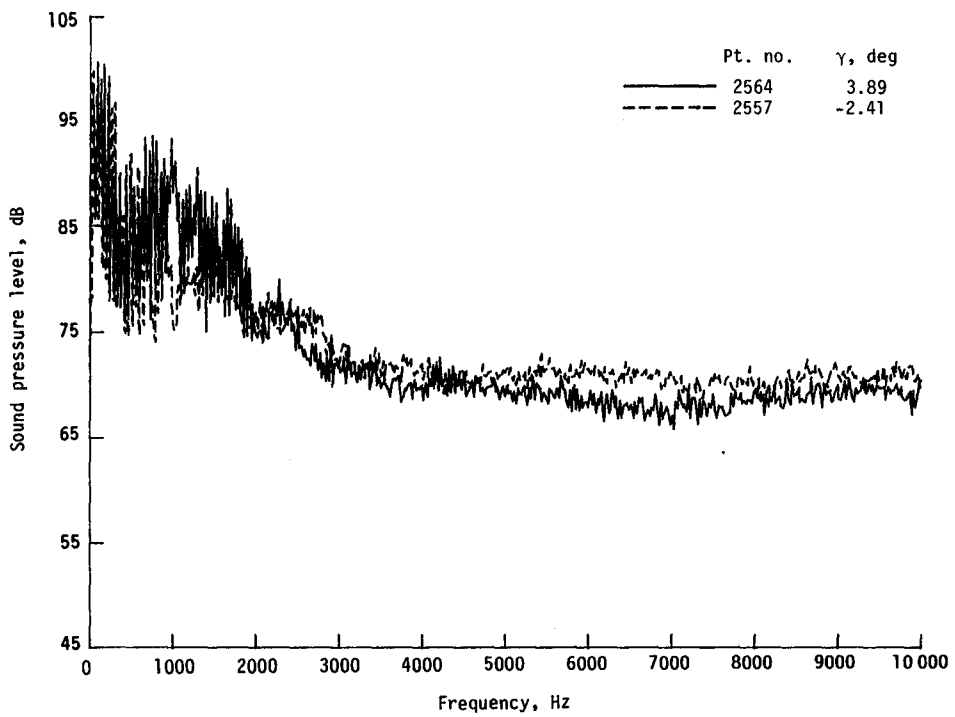

(i) Narrowband analysis; microphone 7.

Figure 11. - Continued.

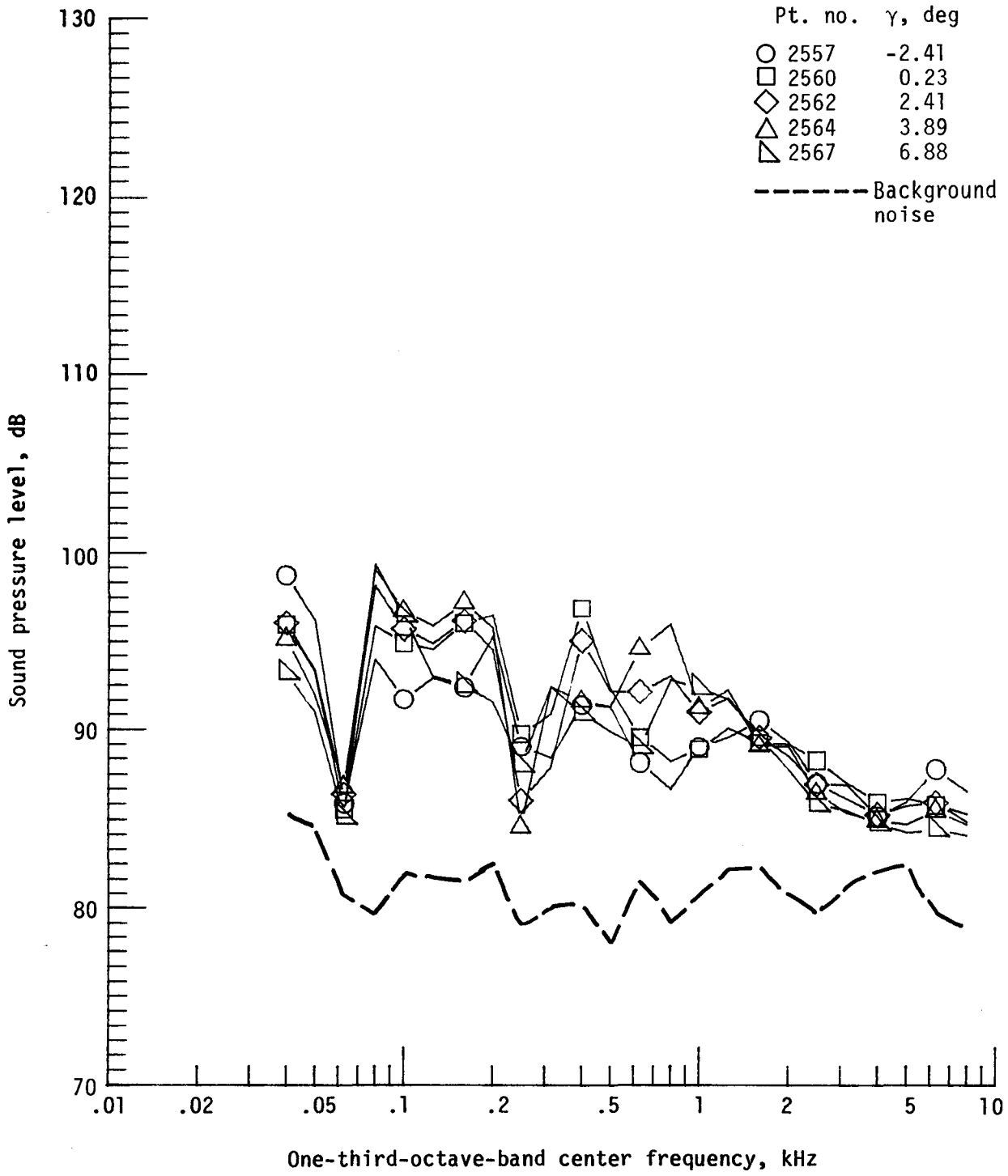

(j) One-third-octave spectra, microphone 8.

Figure 11. - Continued.

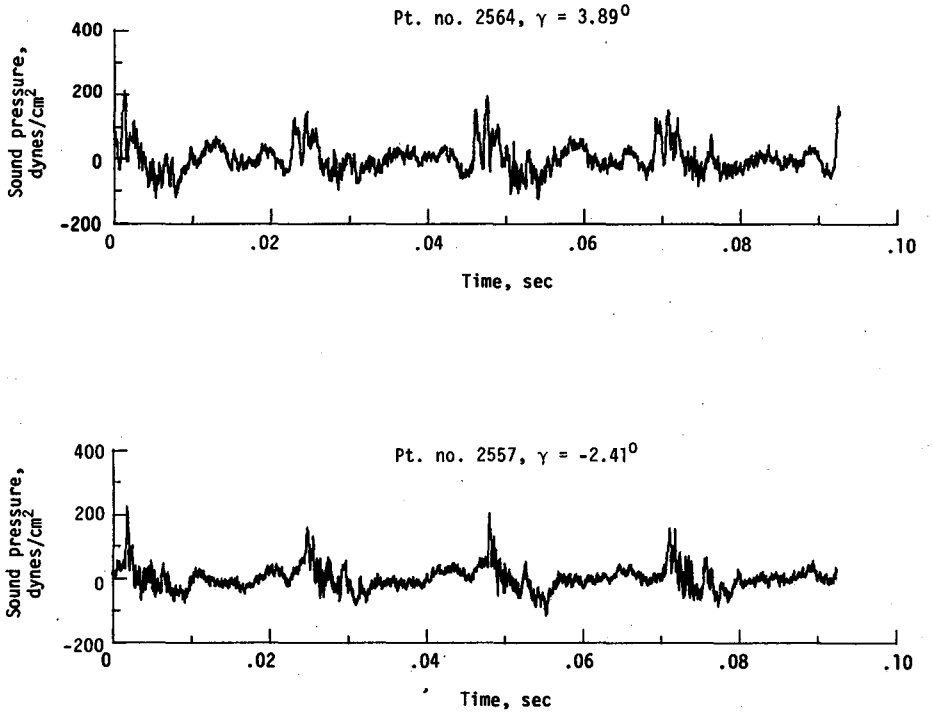

(k) Pressure-time histories; microphone 8.

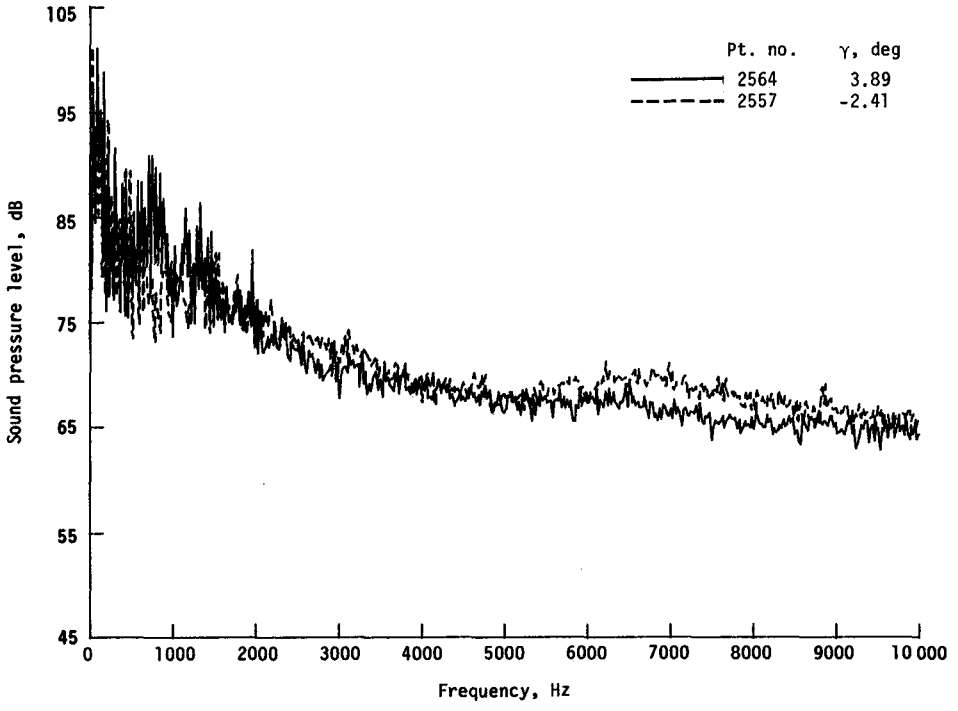

(l) Narrowband analysis; microphone 8.

Figure 11. - Concluded.

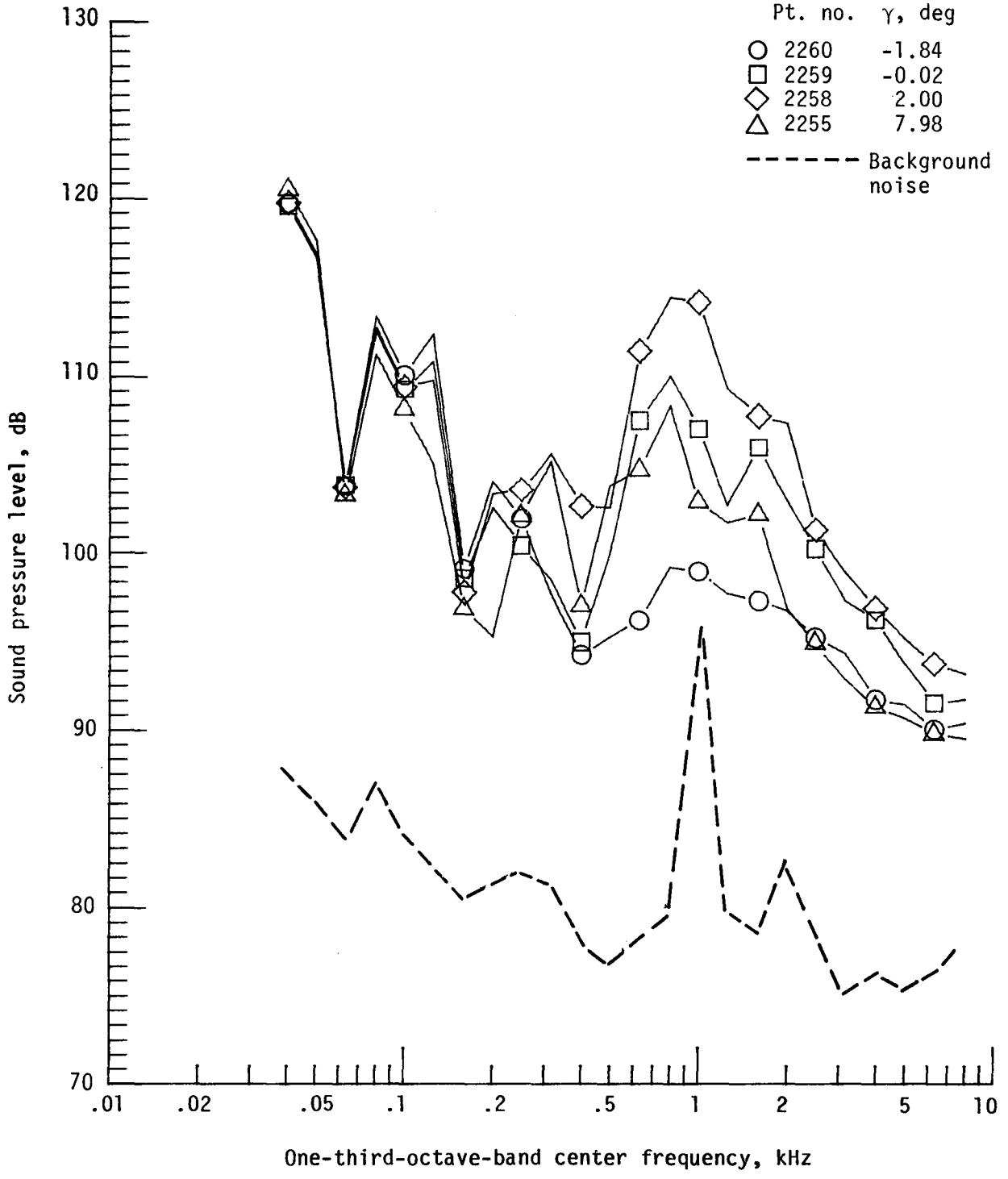

(a) One-third-octave spectra, microphone 2.

Figure 12. - Effect of descent angle variation on noise generated by helicopter model with standard rotor system, run 180; V_∞ = 55.6 knots, C_T = .0036.

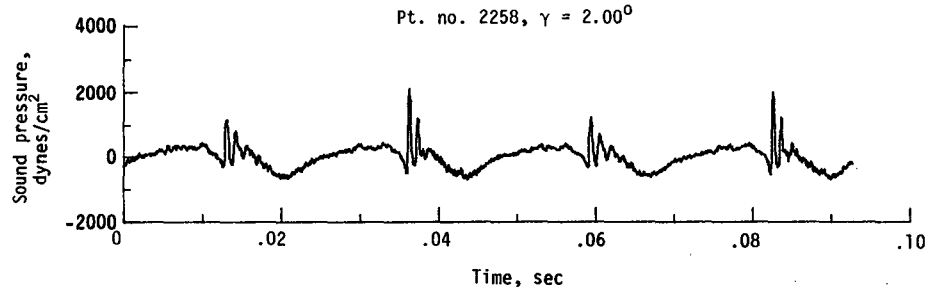

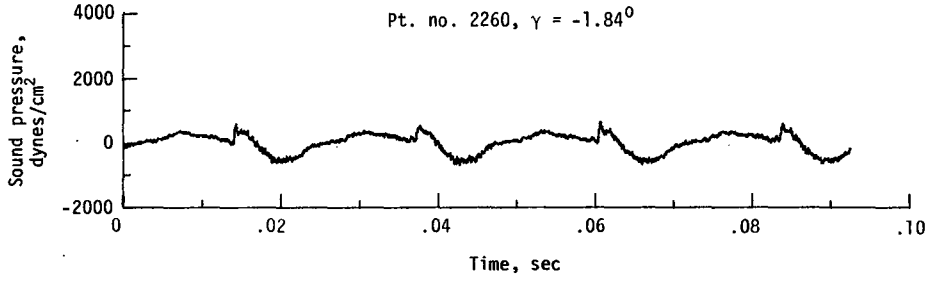

(b) Pressure-time histories; microphone 2.

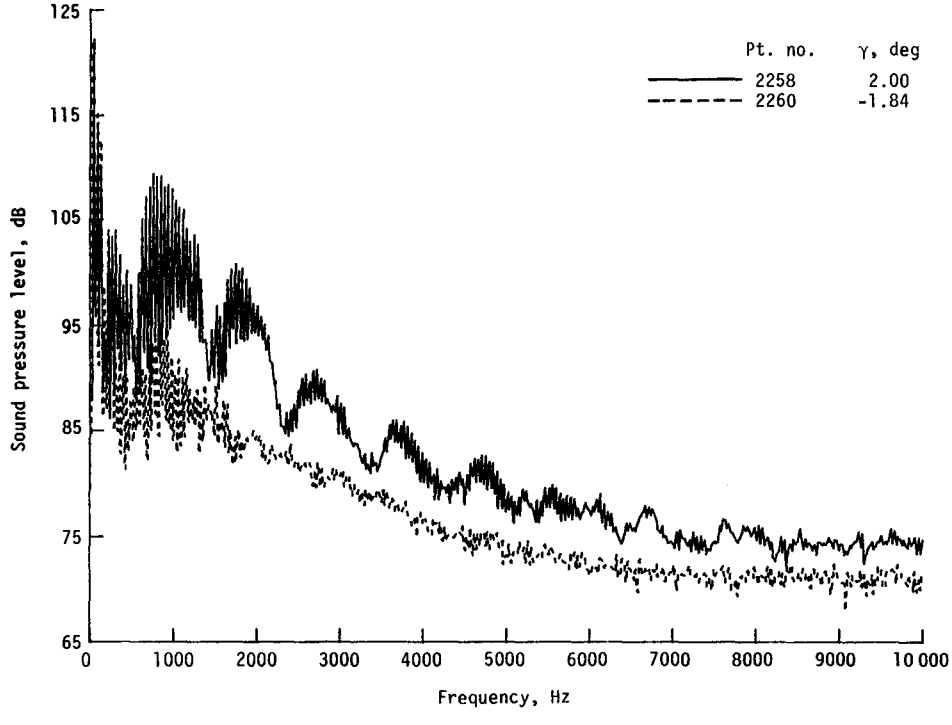

(c) Narrowband analysis; microphone 2.
Figure 12. - Continued.

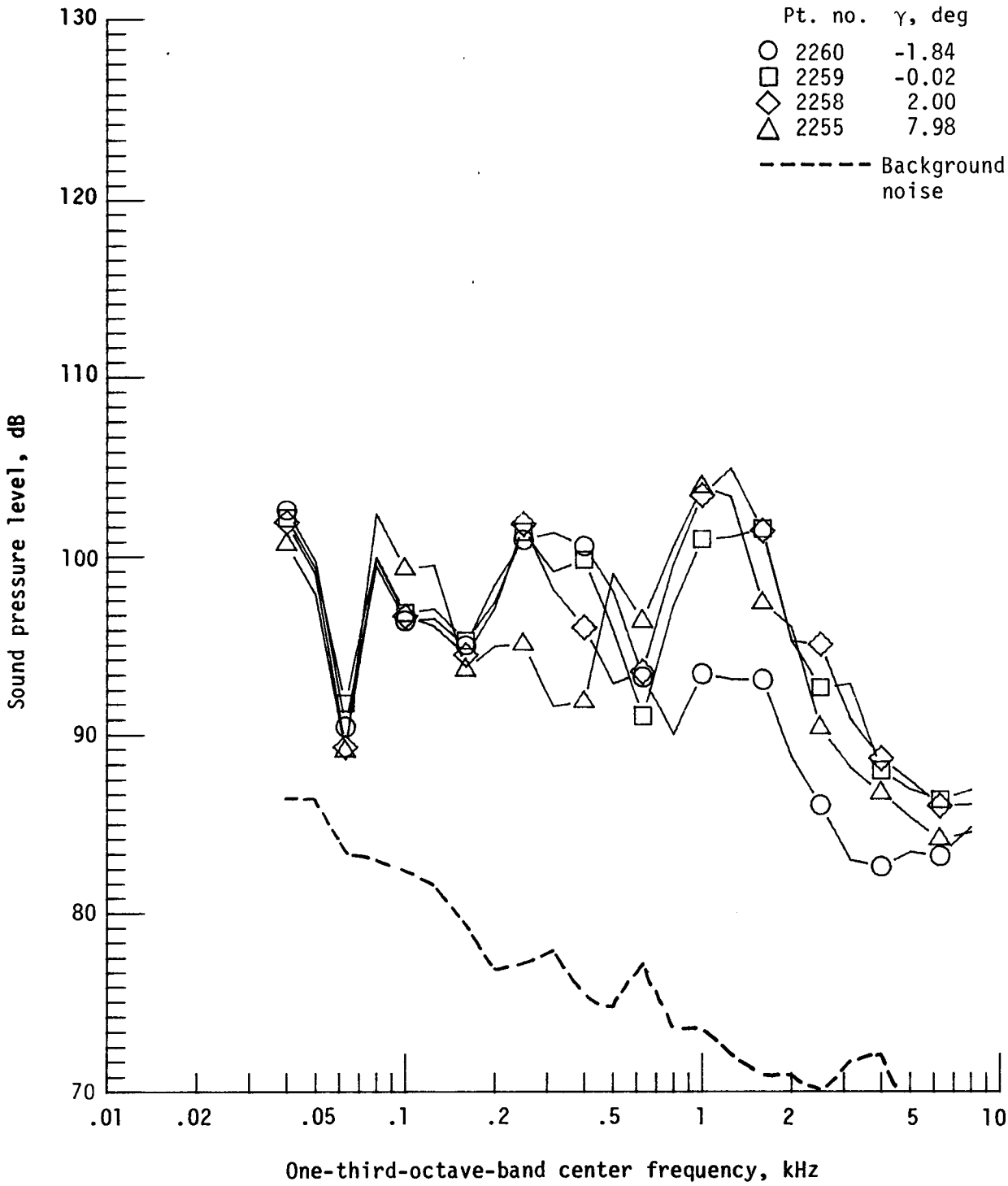

(d) One-third-octave spectra, microphone 6.

Figure 12. - Continued.

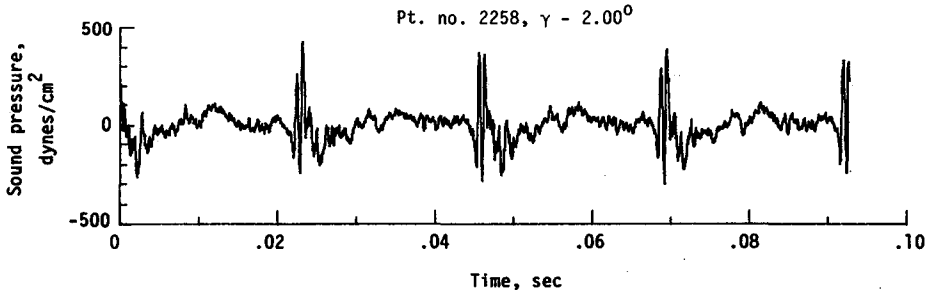

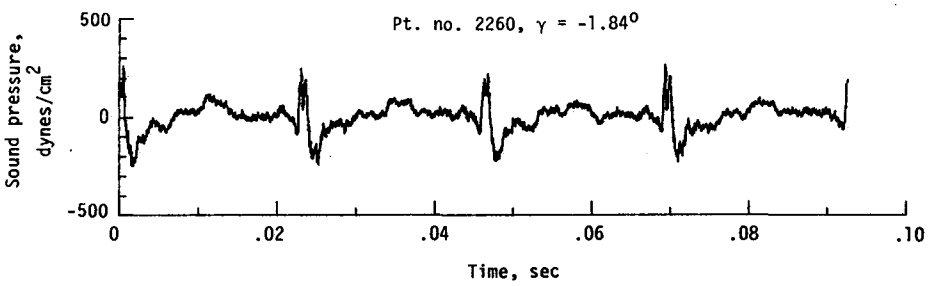

(e) Pressure-time histories; microphone 6.

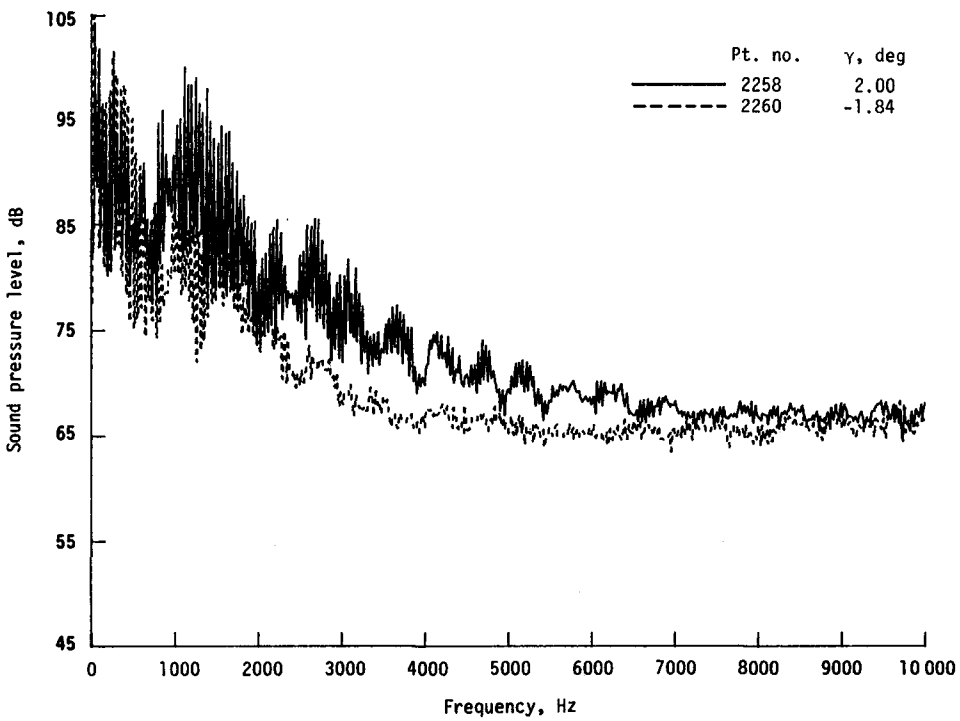

(f) Narrowband analysis; microphone 6.
Figure 12. - Continued.

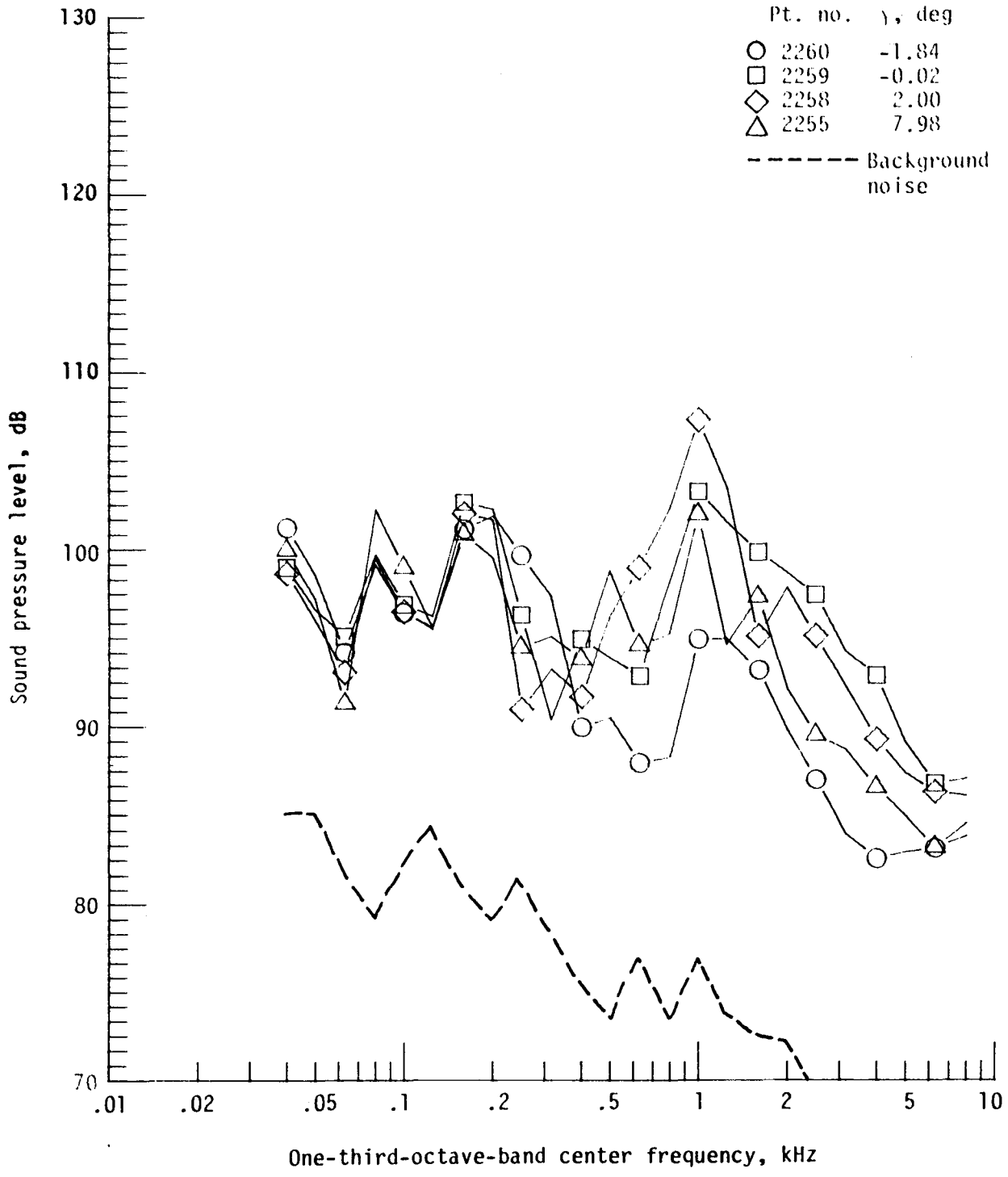

(g) One-third-octave spectra, microphone 7.

Figure 12. - Continued.

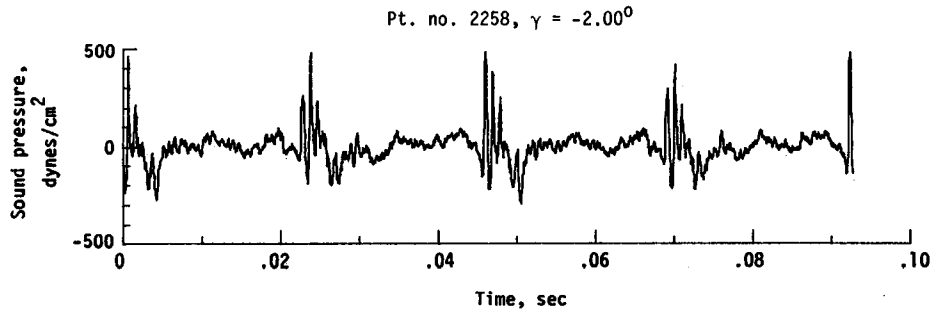

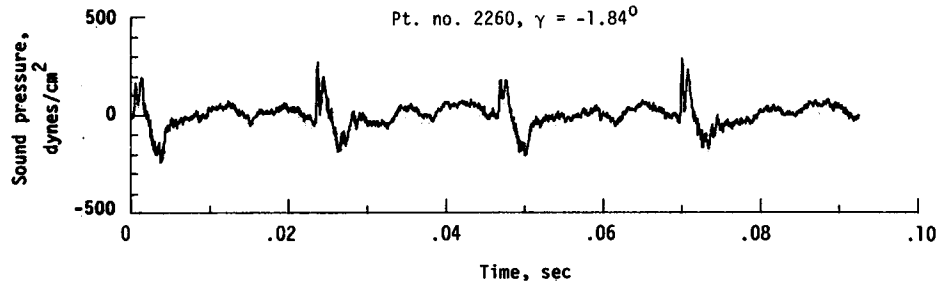

(h) Pressure-time histories; microphone 7.

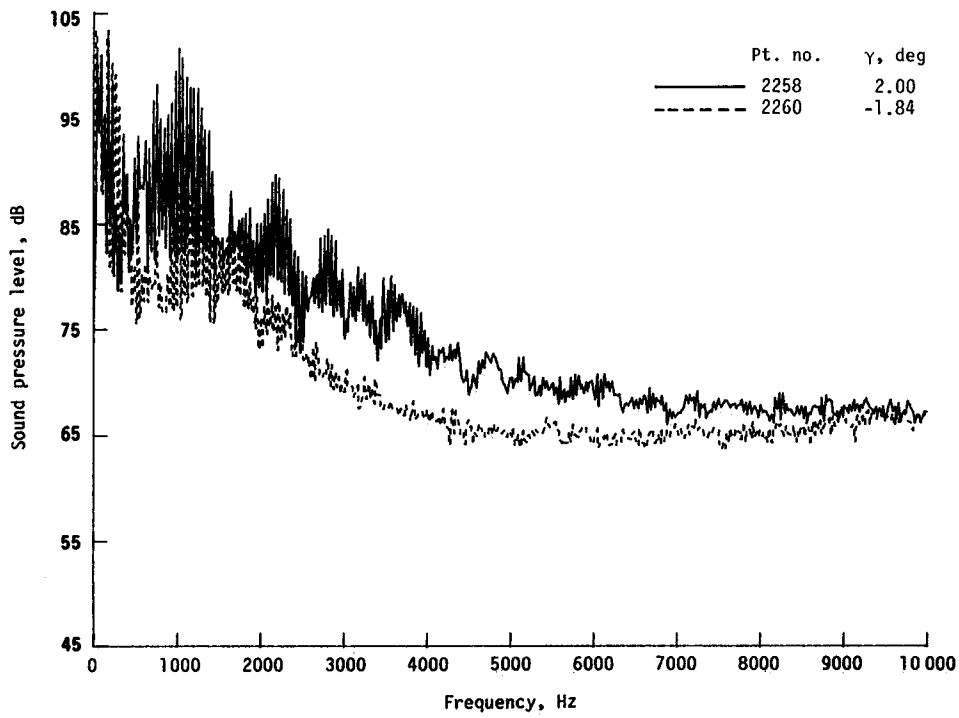

(i) Narrowband analysis; microphone 7.

Figure 12. - Continued.

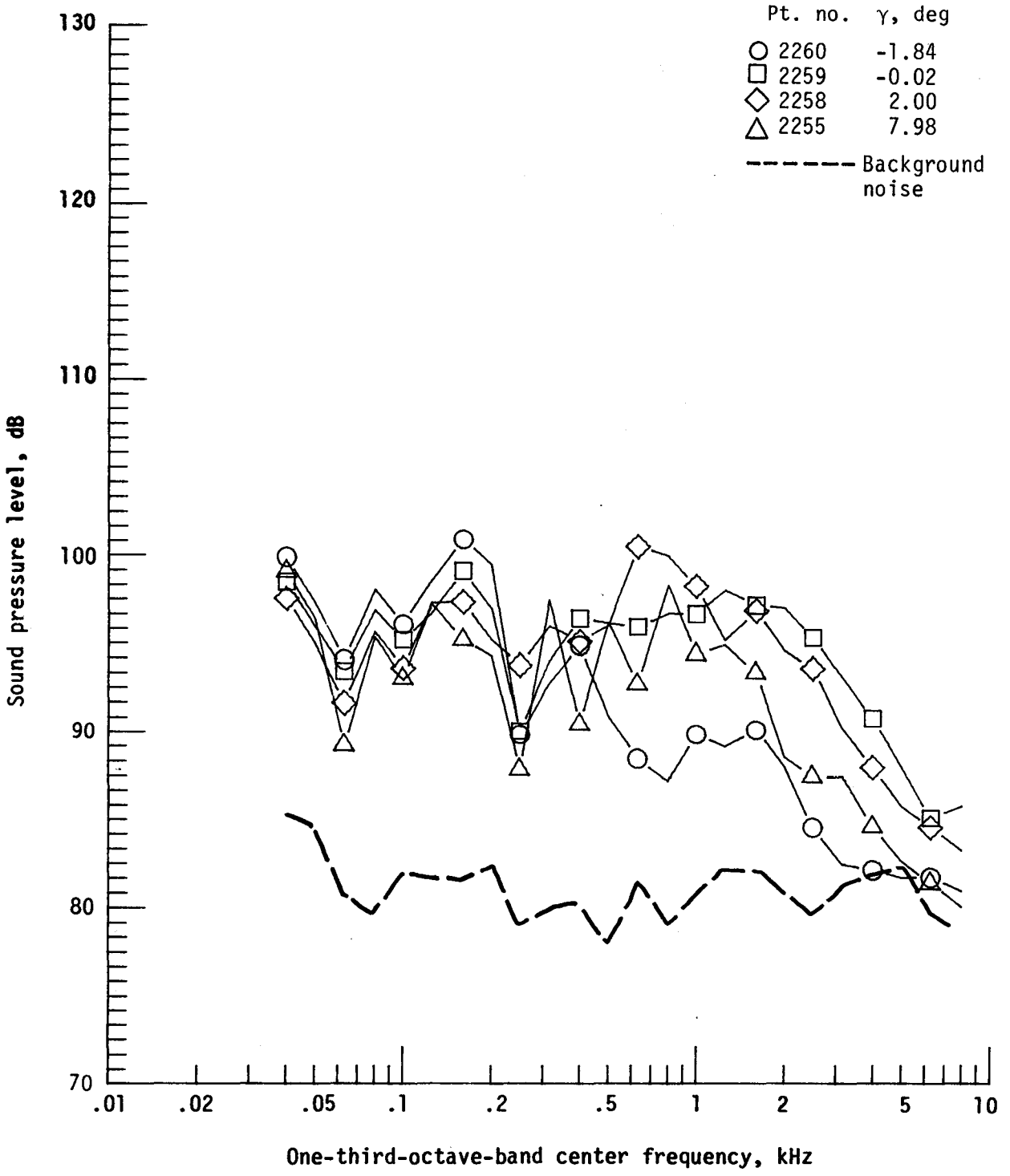

(j) One-third-octave spectra, microphone 8.

Figure 12. - Continued.

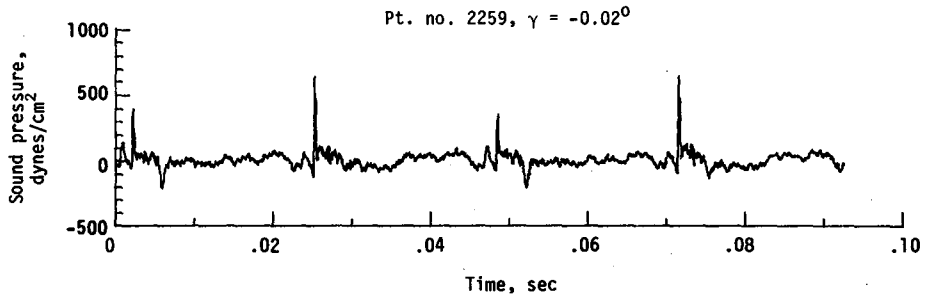

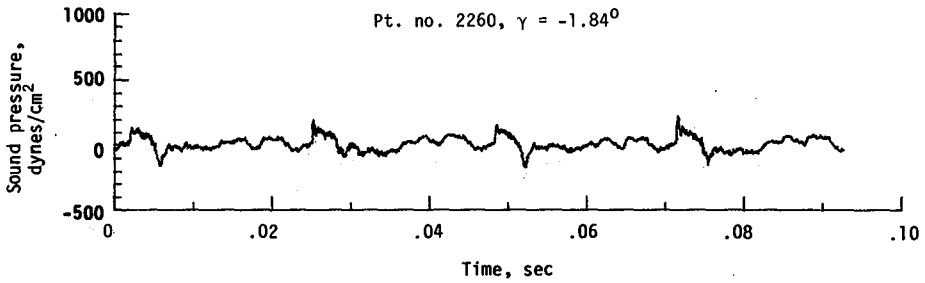

(k) Pressure-time histories; microphone 8.

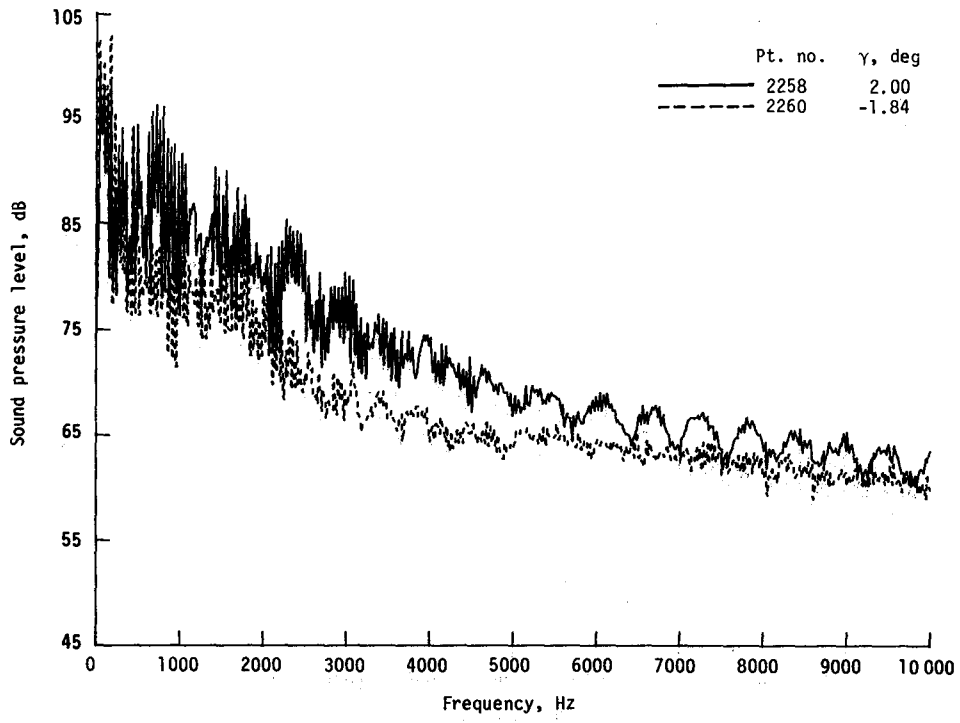

(l) Narrowband analysis; microphone 8.
Figure 12. - Concluded.

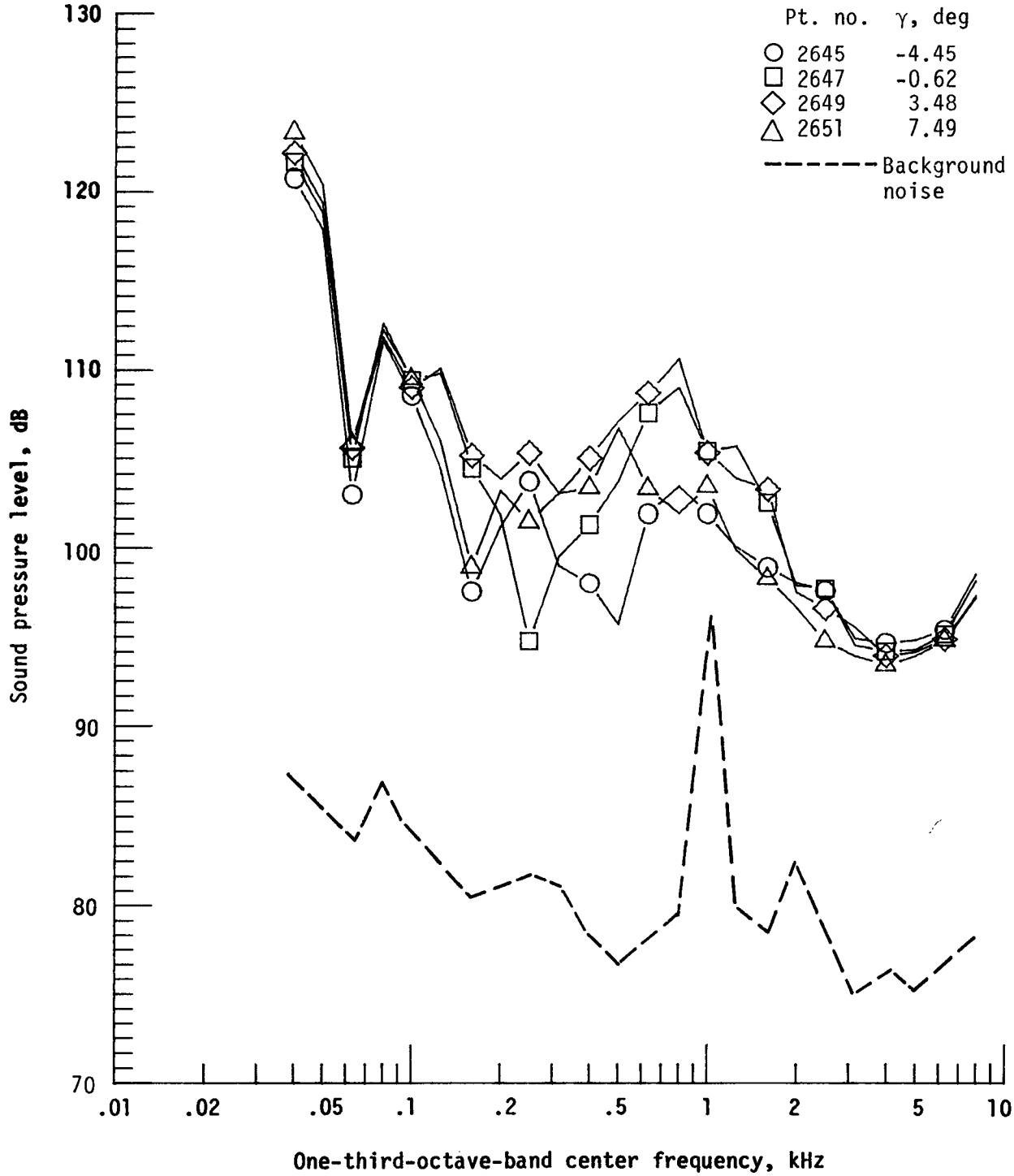

(a) One-third-octave spectra, microphone 2.

Figure 13. - Effect of descent angle variation on noise generated by helicopter model with advanced rotor system, run 212. V_∞ = 55.5 knots, C_T = .0036.

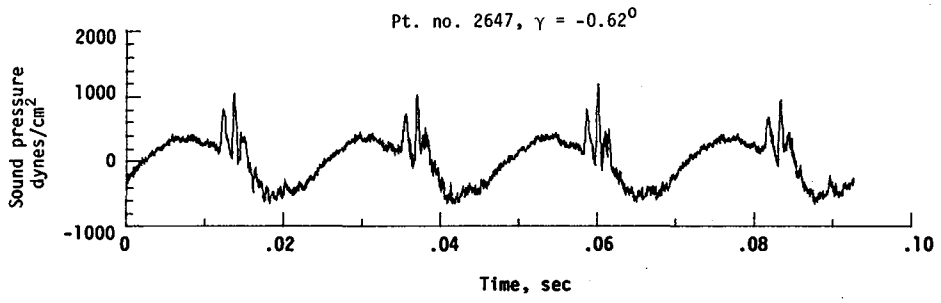

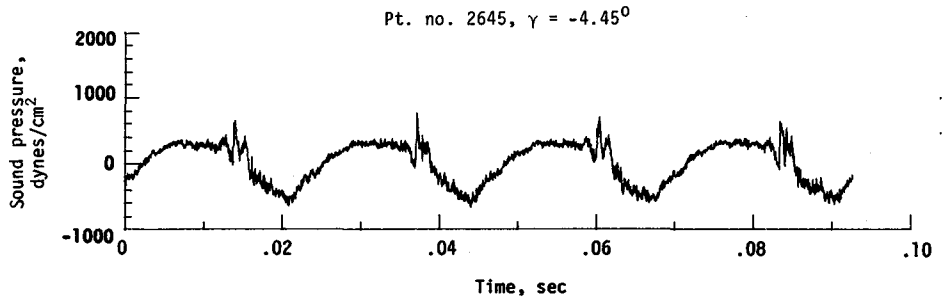

(b) Pressure-time histories; microphone 2.

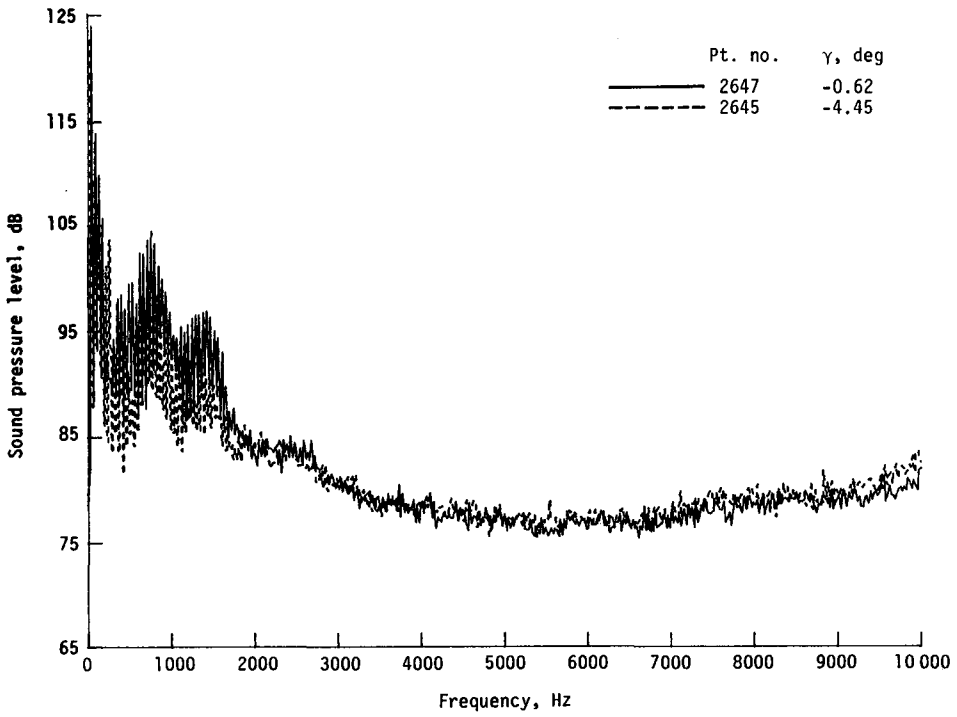

(c) Narrowband analysis; microphone 2.
Figure 13. - Continued.

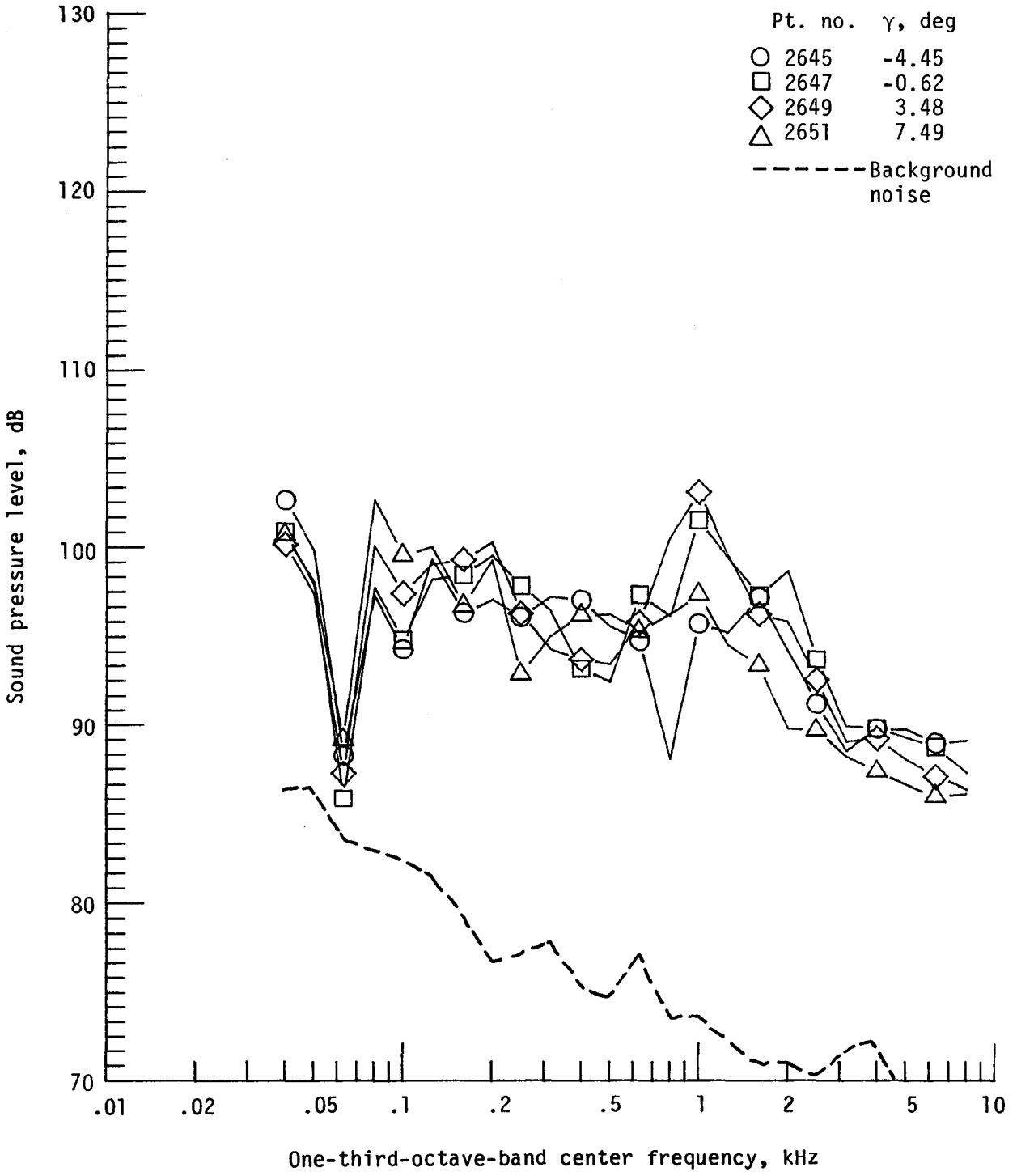

(d) One-third-octave spectra, microphone 6.

Figure 13. - Continued.

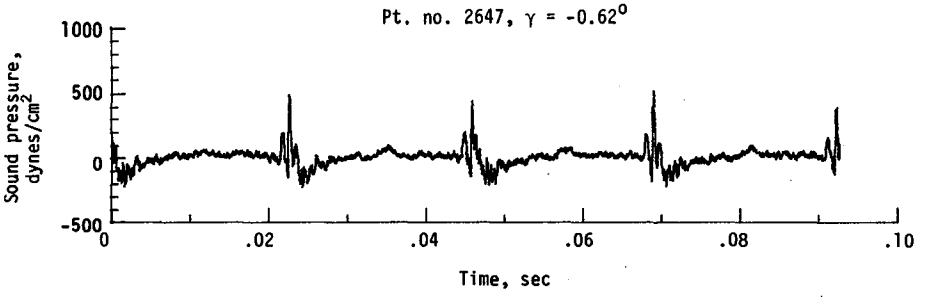

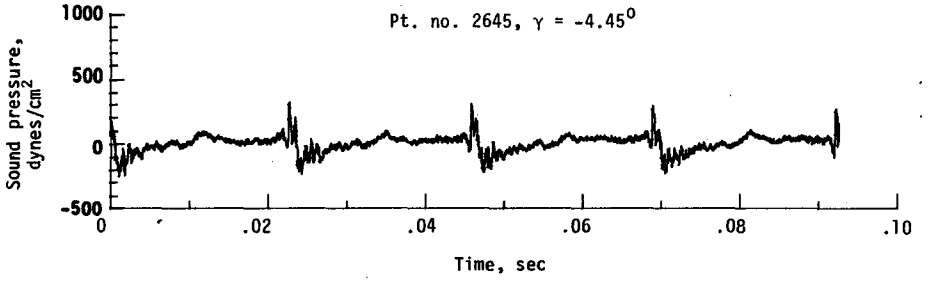

(e) Pressure-time histories; microphone 6.

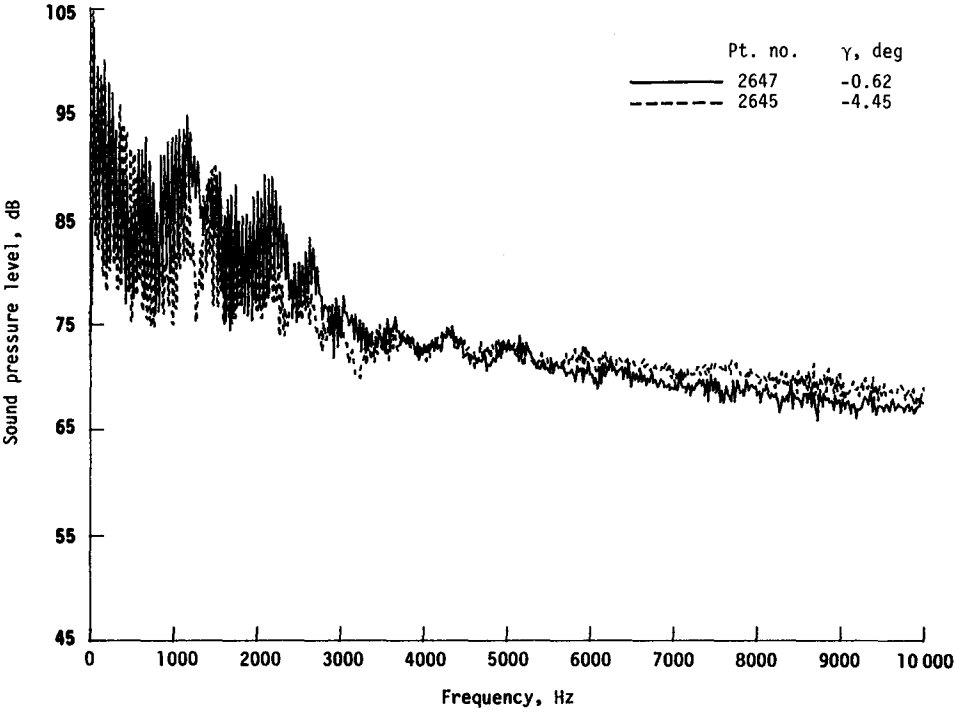

(f) Narrowband analysis; microphone 6.

Figure 13. - Continued.

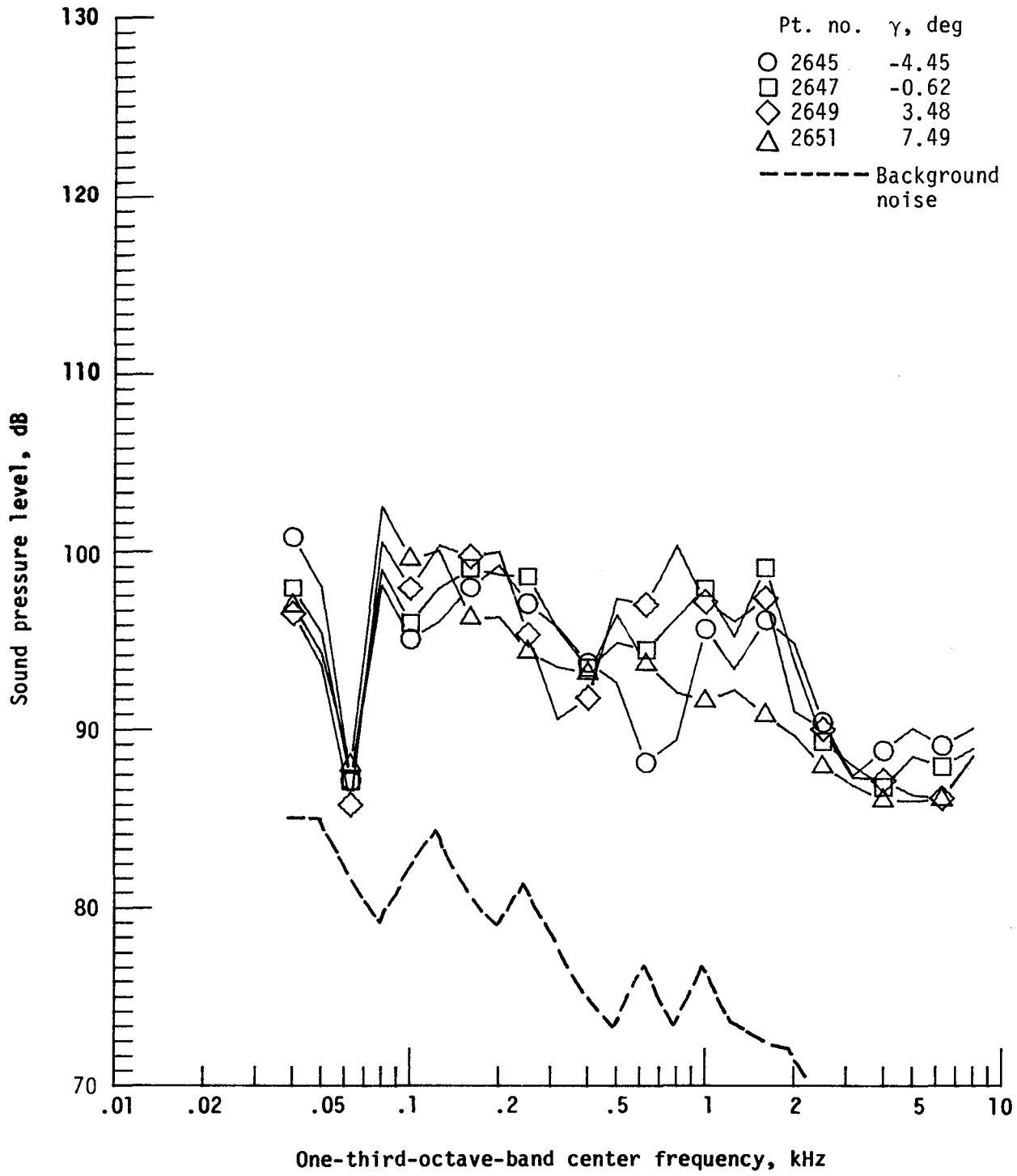

(g) One-third-octave spectra, microphone 7.

Figure 13. - Continued.

This Page Intentionally Left Blank

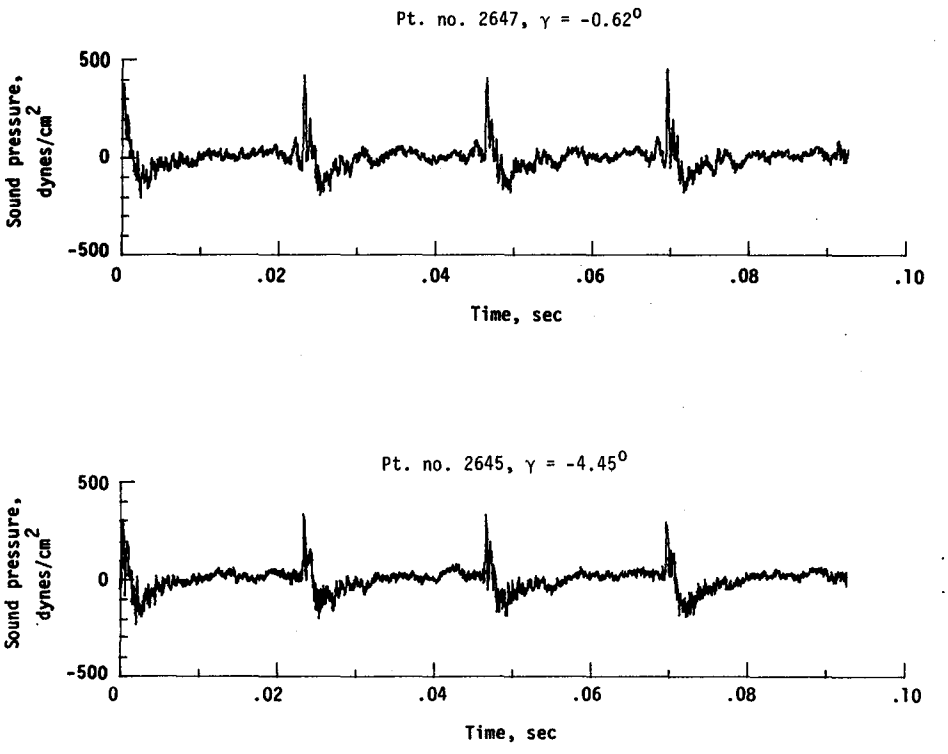

(h) Pressure-time histories; microphone 7.

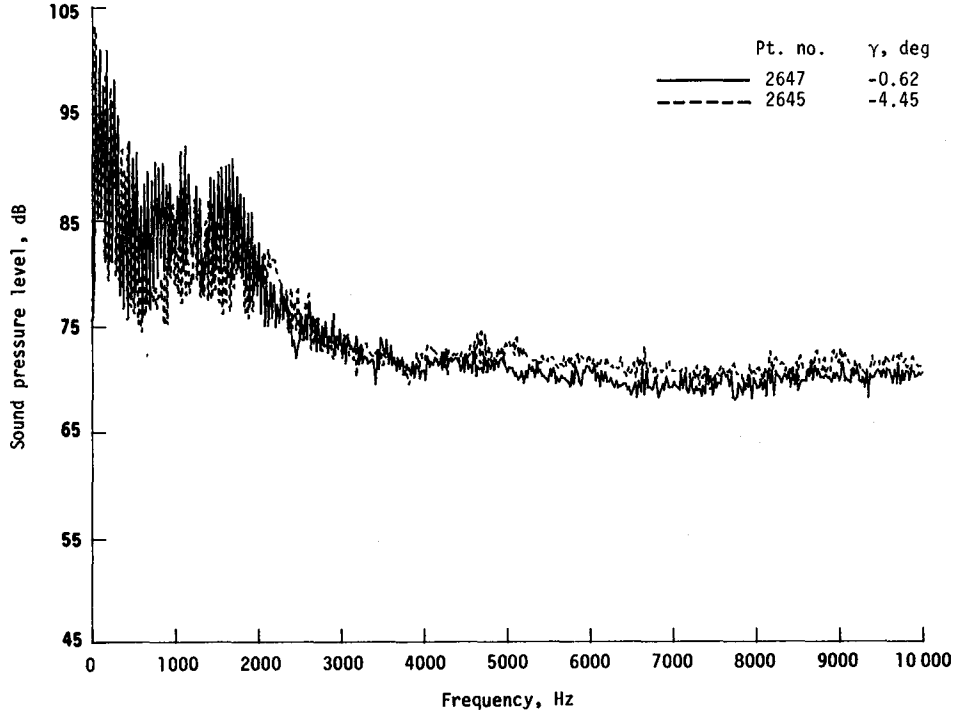

(i) Narrowband analysis; microphone 7.
Figure 13. - Continued.

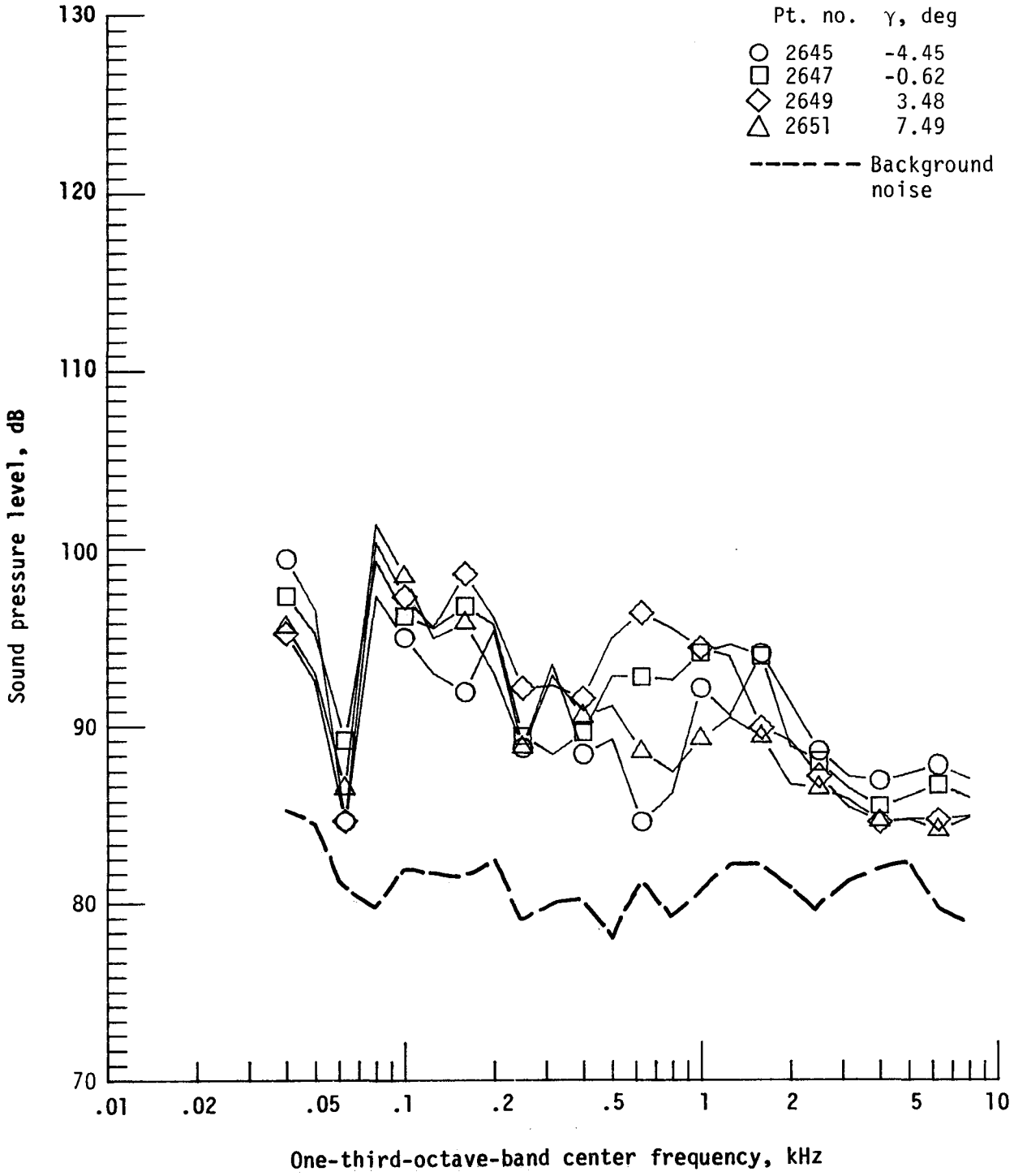

(j) One-third-octave spectra, microphone 8.

Figure 13. - Continued.

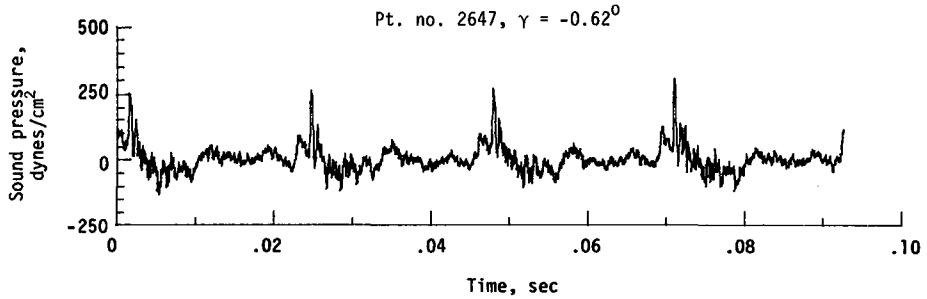

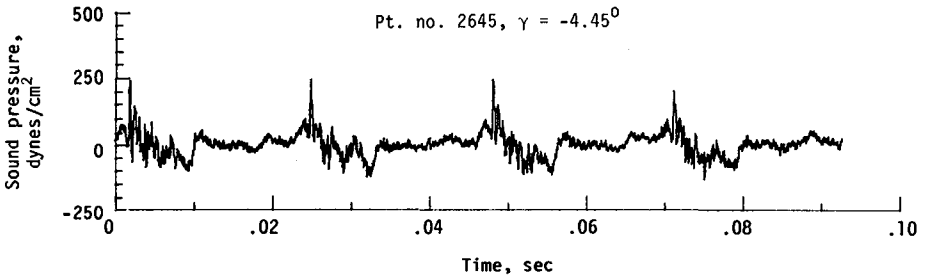

(k) Pressure-time histories; microphone 8.

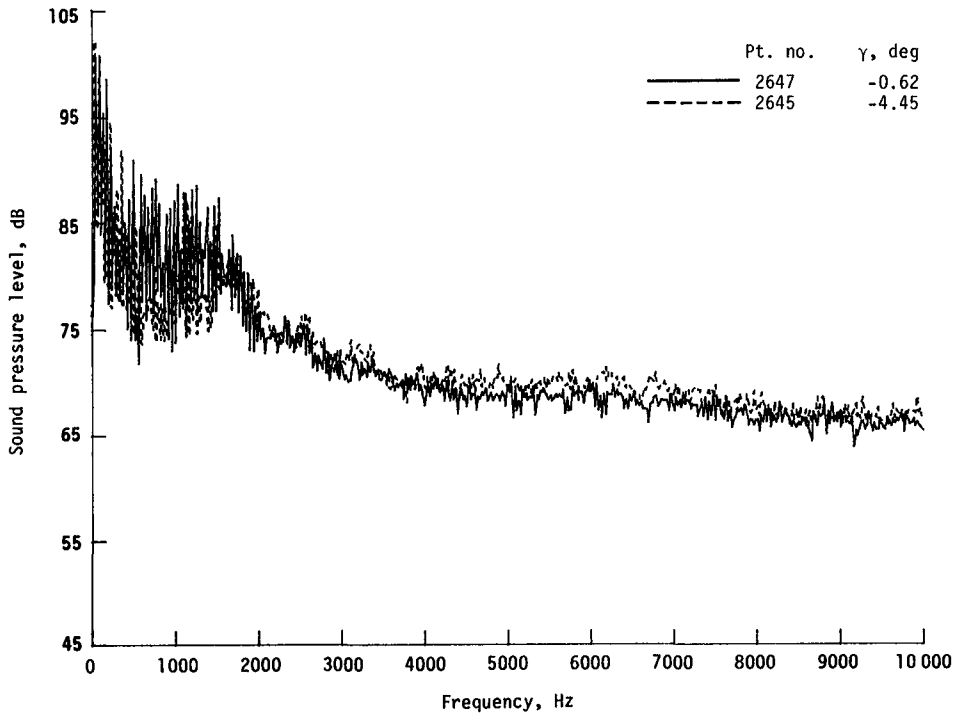

(l) Narrowband analysis; microphone 8.

Figure 13. - Concluded.

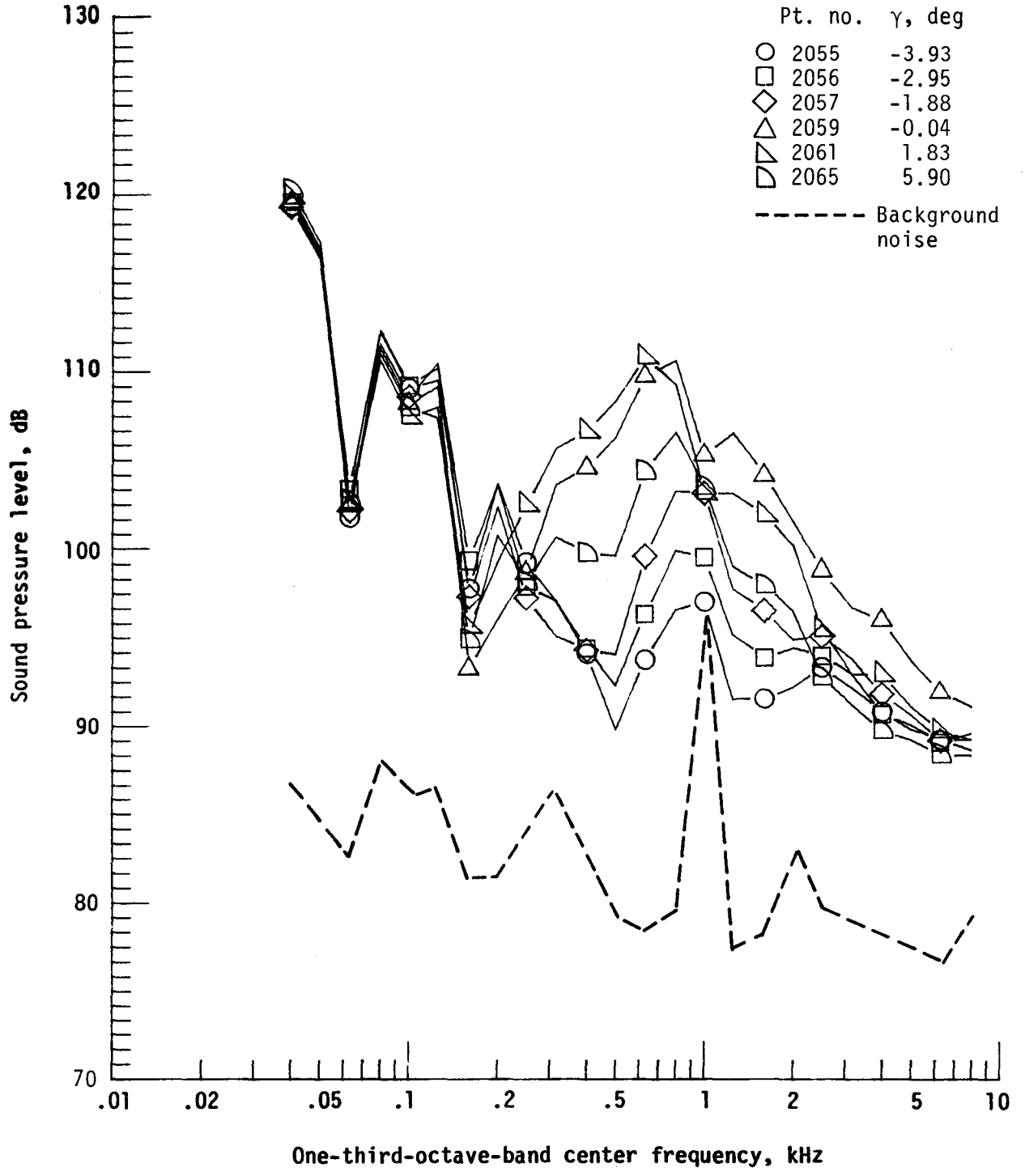

(a) One-third-octave spectra, microphone 2.

Figure 14. - Effect of descent angle variation on noise generated by helicopter model with standard rotor system, run 158. V_∞ = 60.2 knots, C_T = .0032.

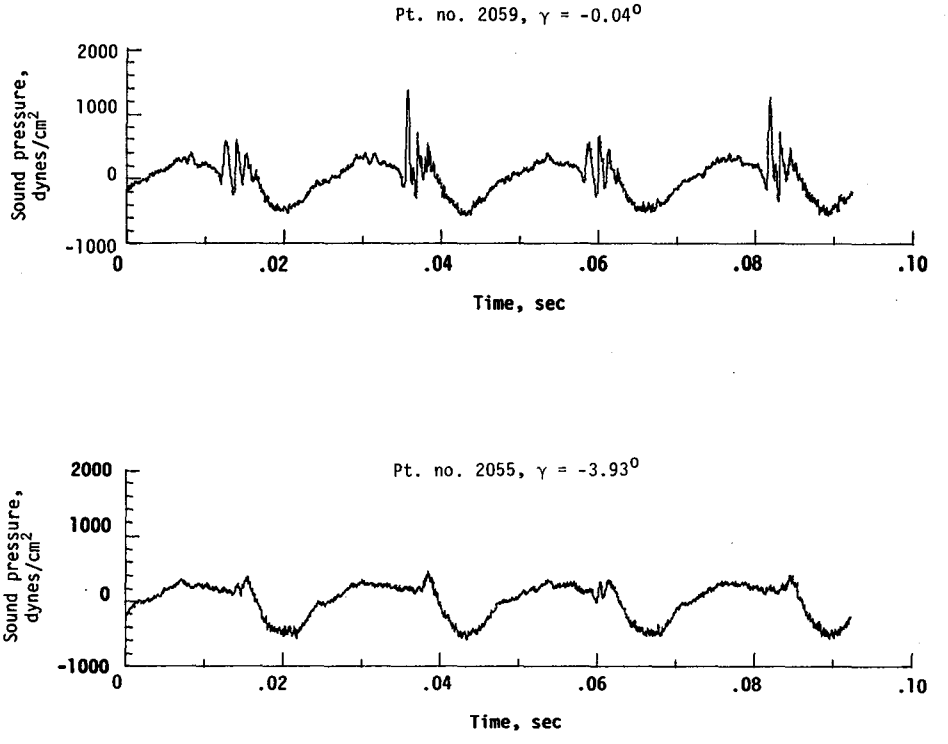

(b) Pressure-time histories; microphone 2.

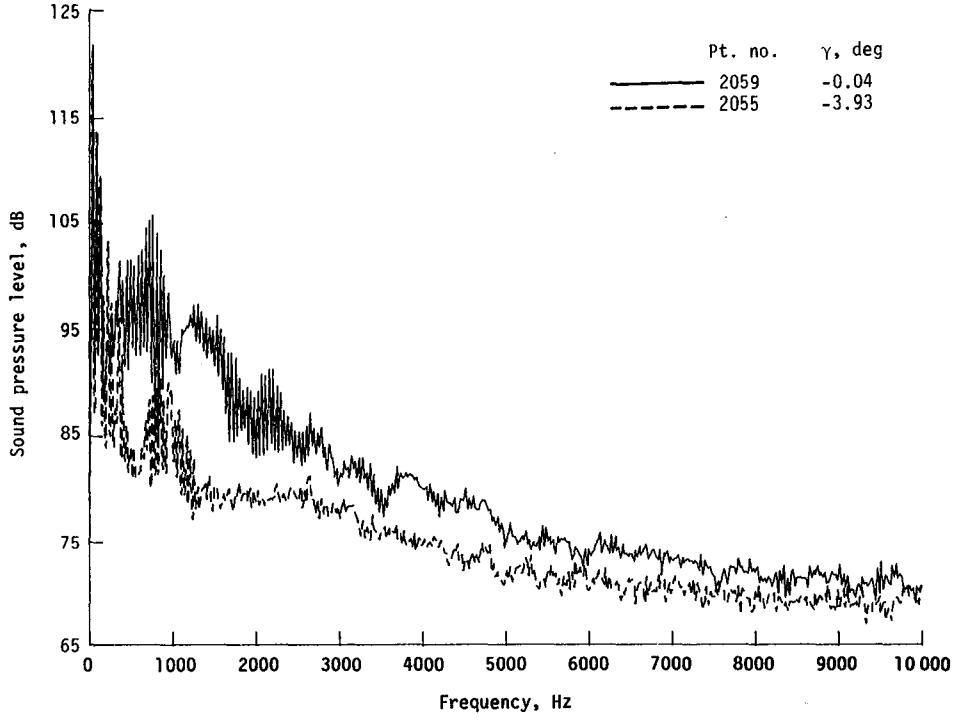

(c) Narrowband analysis; microphone 2.
Figure 14. - Continued.

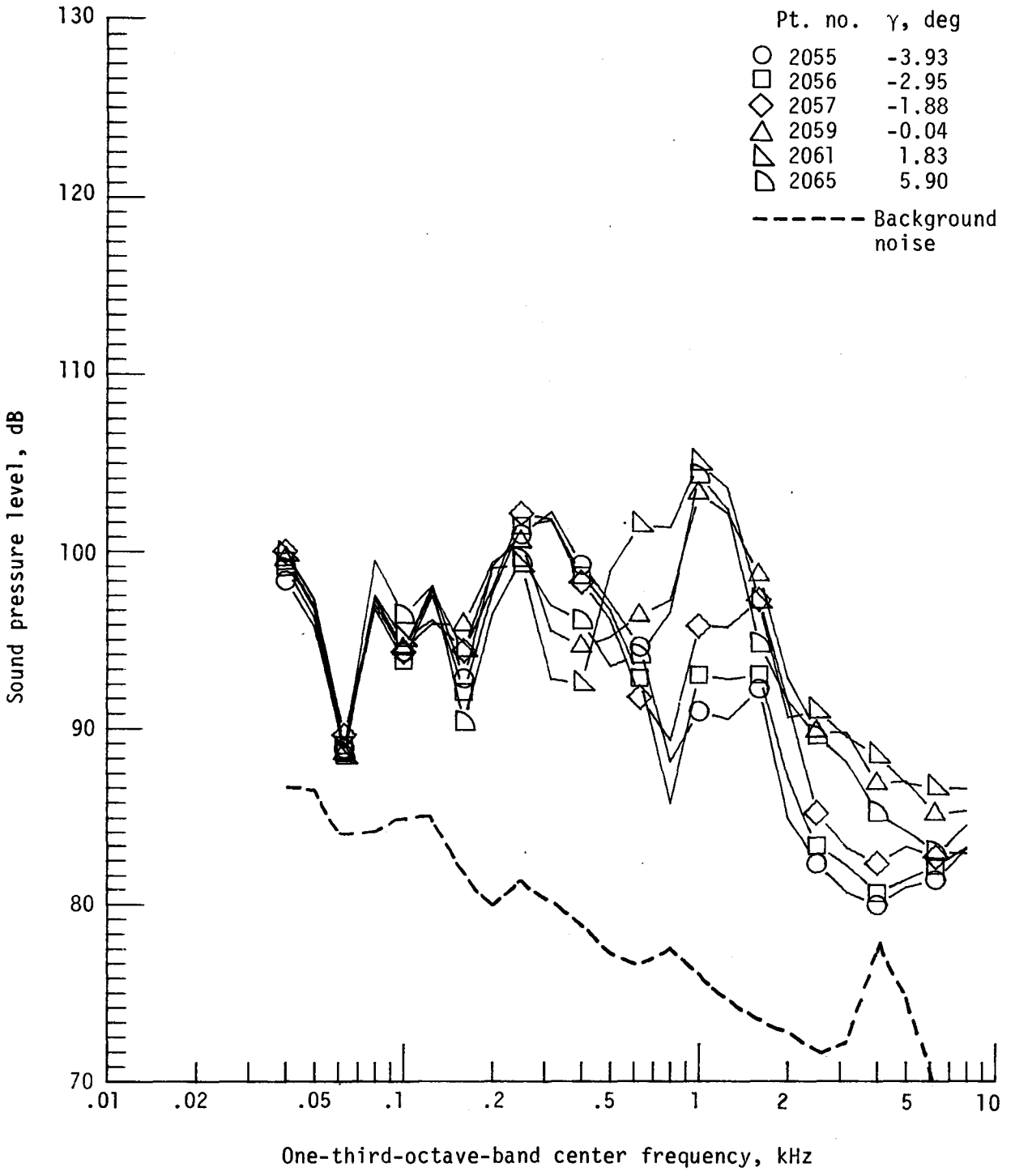

(d) One-third-octave spectra, microphone 6.

Figure 14. - Continued.

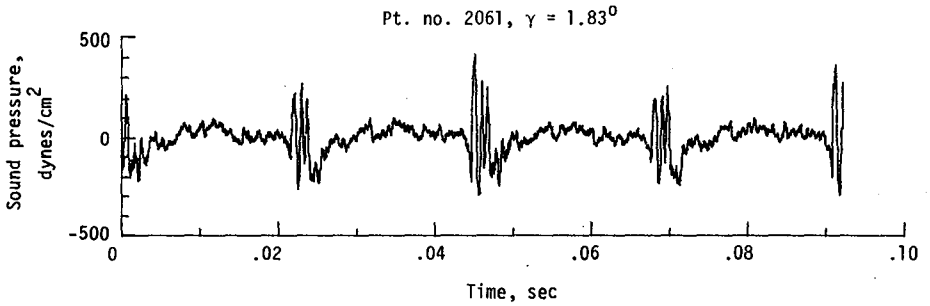

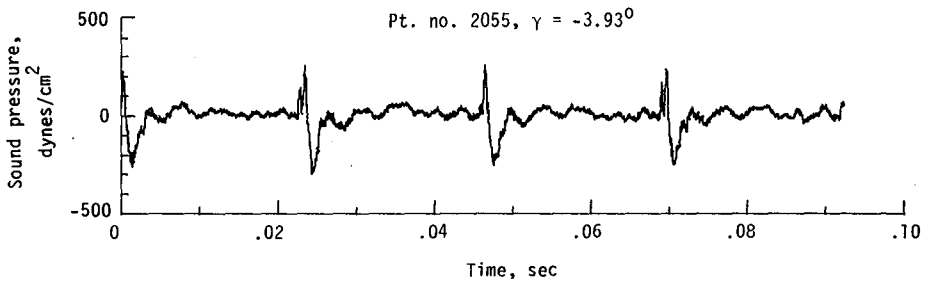

(e) Pressure-time histories; microphone 6.

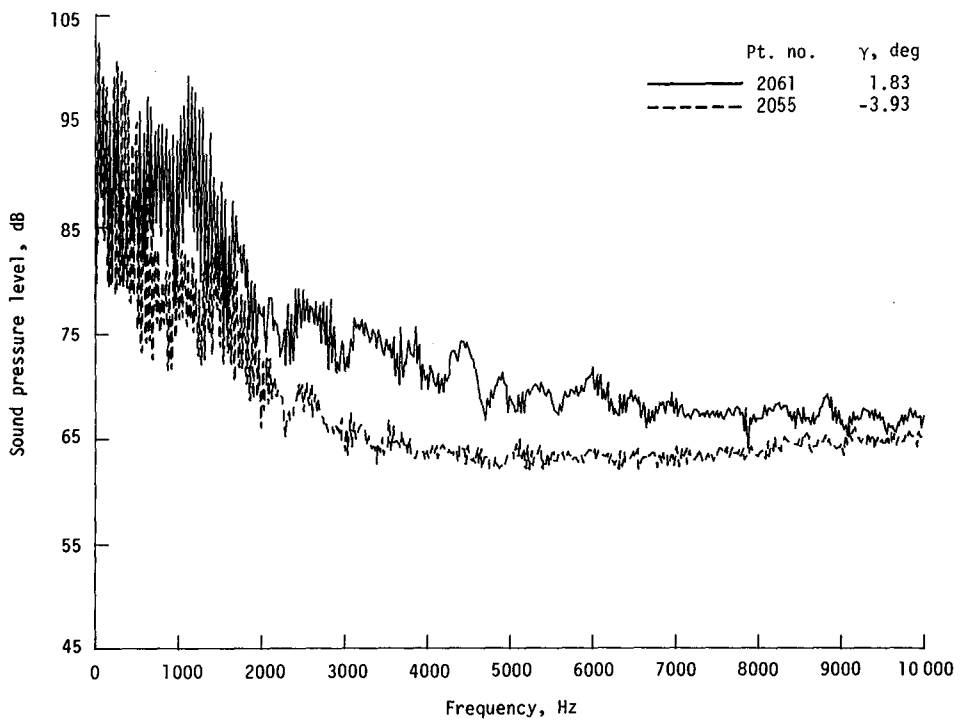

(f) Narrowband analysis; microphone 6.
Figure 14. - Continued.

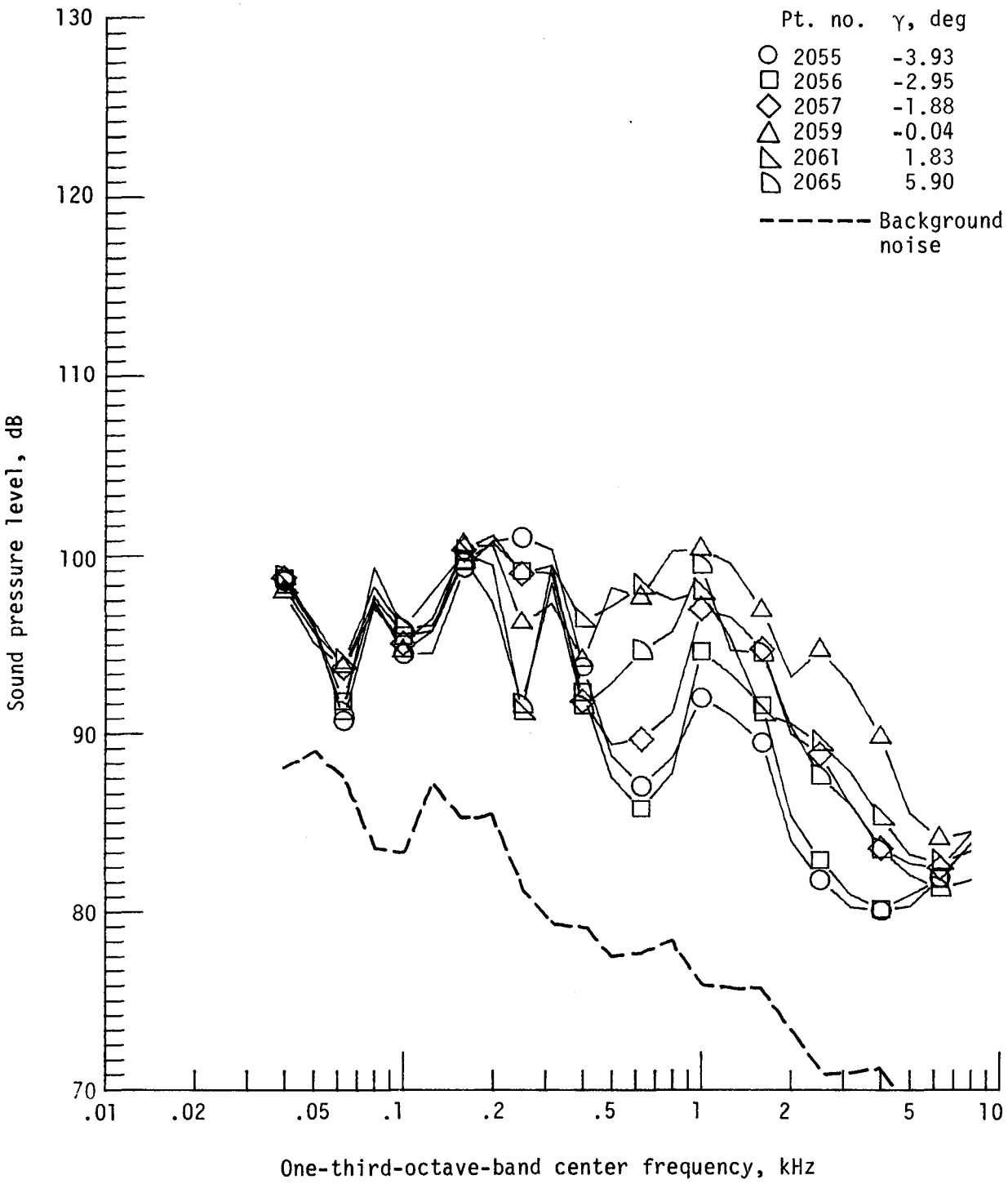

(g) One-third-octave spectra, microphone 7.

Figure 14. - Continued.

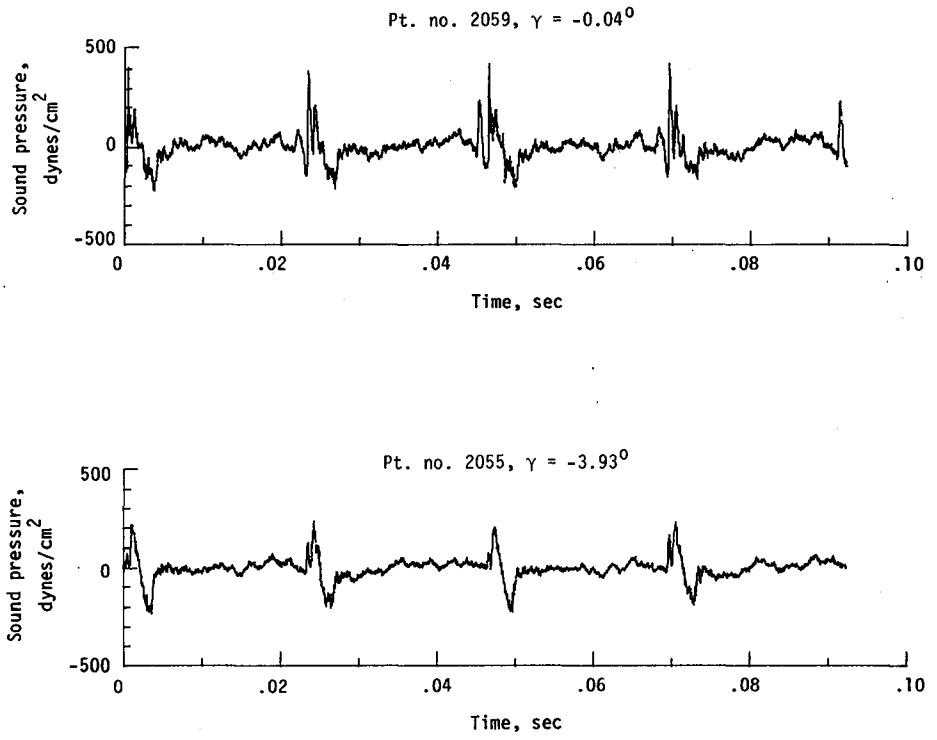

(h) Pressure-time histories; microphone 7.

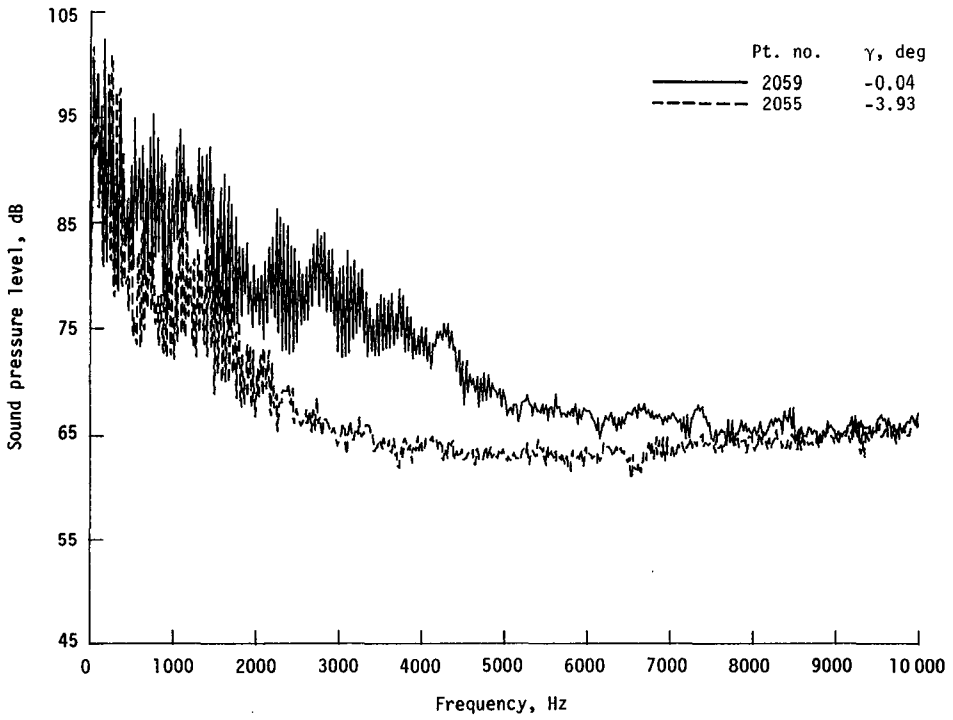

(i) Narrowband analysis; microphone 7.

Figure 14. - Continued.

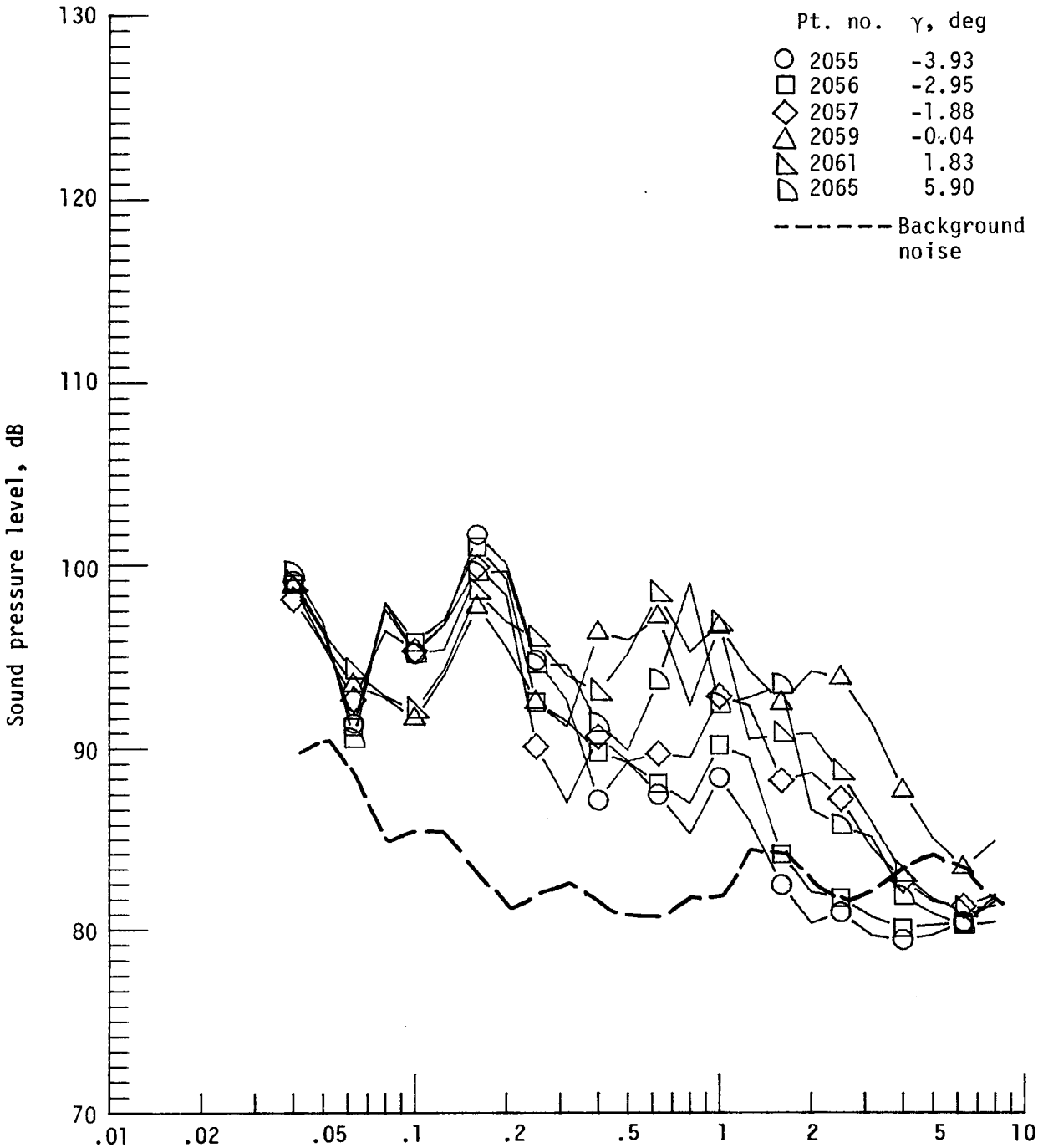

(j) One-third-octave spectra, microphone 8.

Figure 14. - Continued.

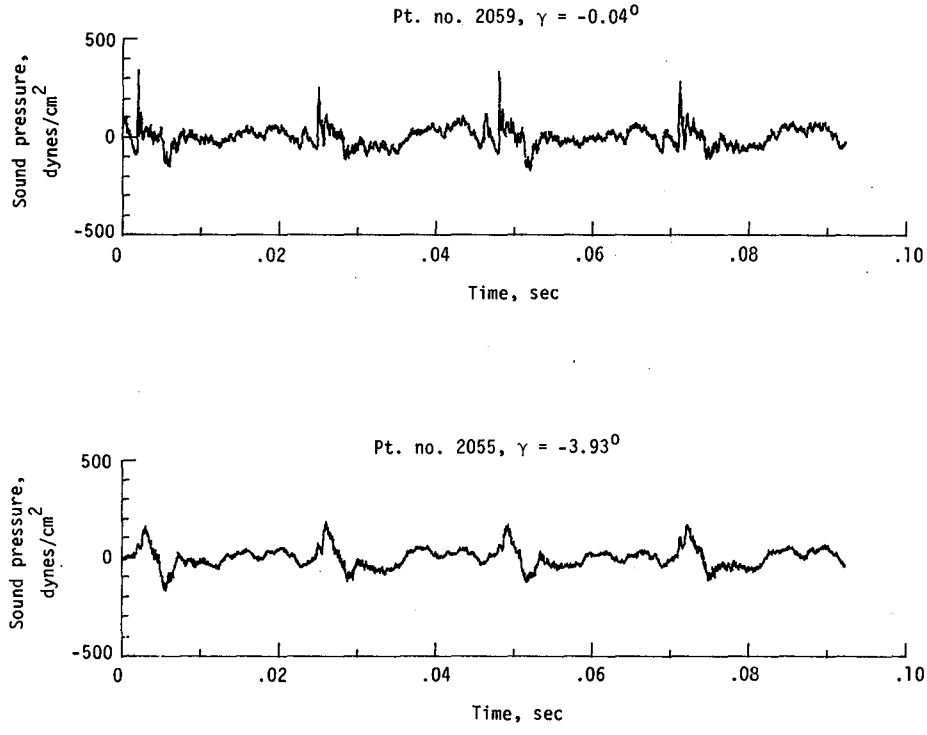

(k) Pressure-time histories; microphone 8.

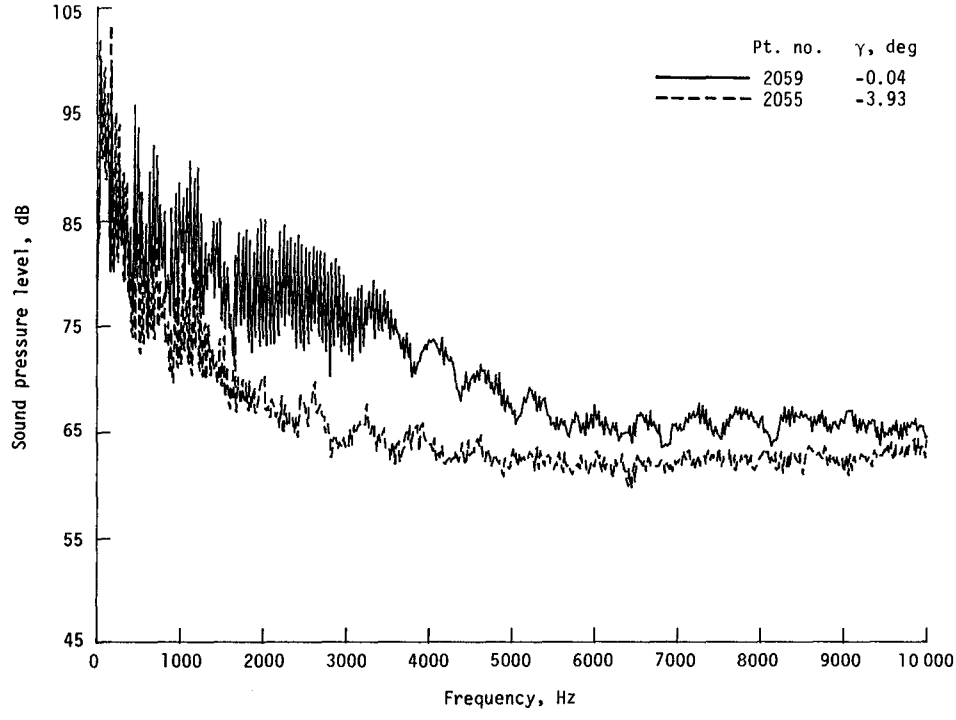

(l) Narrowband analysis; microphone 8.
Figure 14. - Concluded.

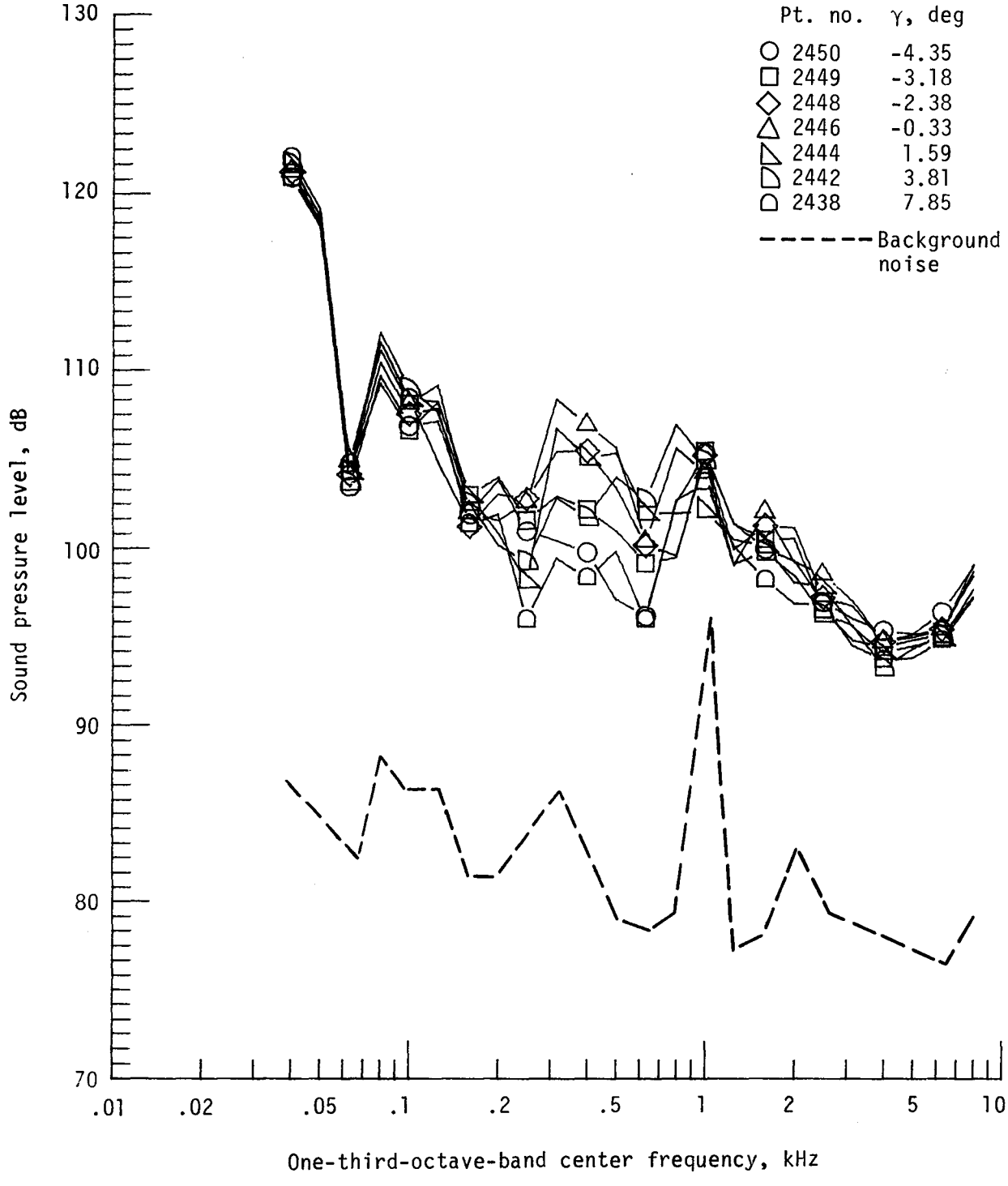

(a) One-third-octave spectra, microphone 2.

Figure 15. - Effect of descent angle variation on noise generated by helicopter model with advanced rotor system, run 194. V_∞ = 60.3 knots, C_T = .0031.

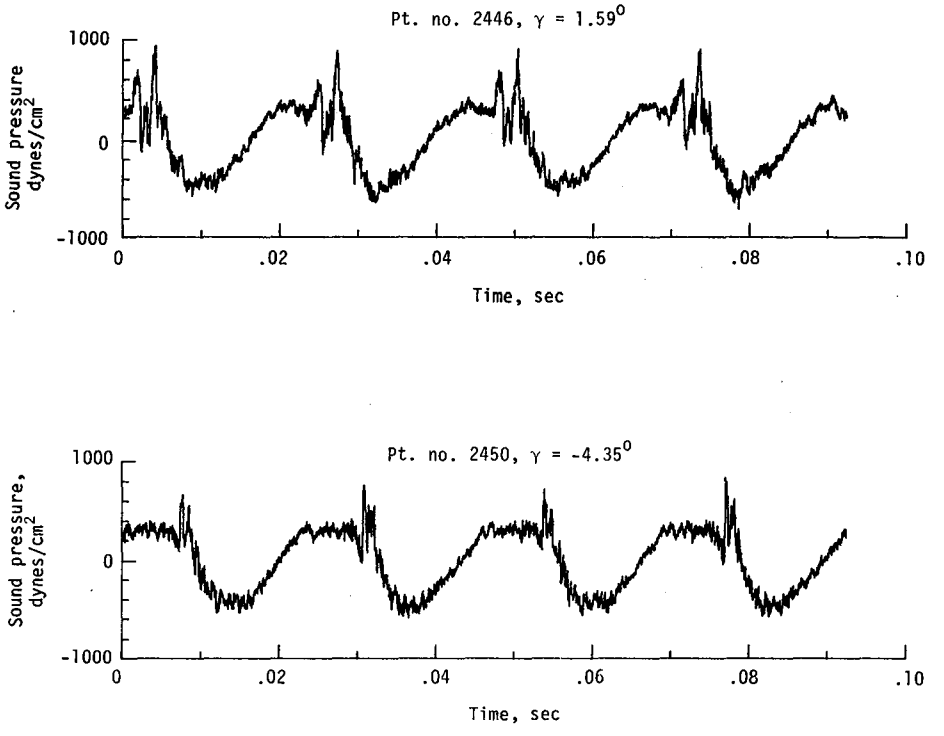

(b) Pressure-time histories; microphone 2.

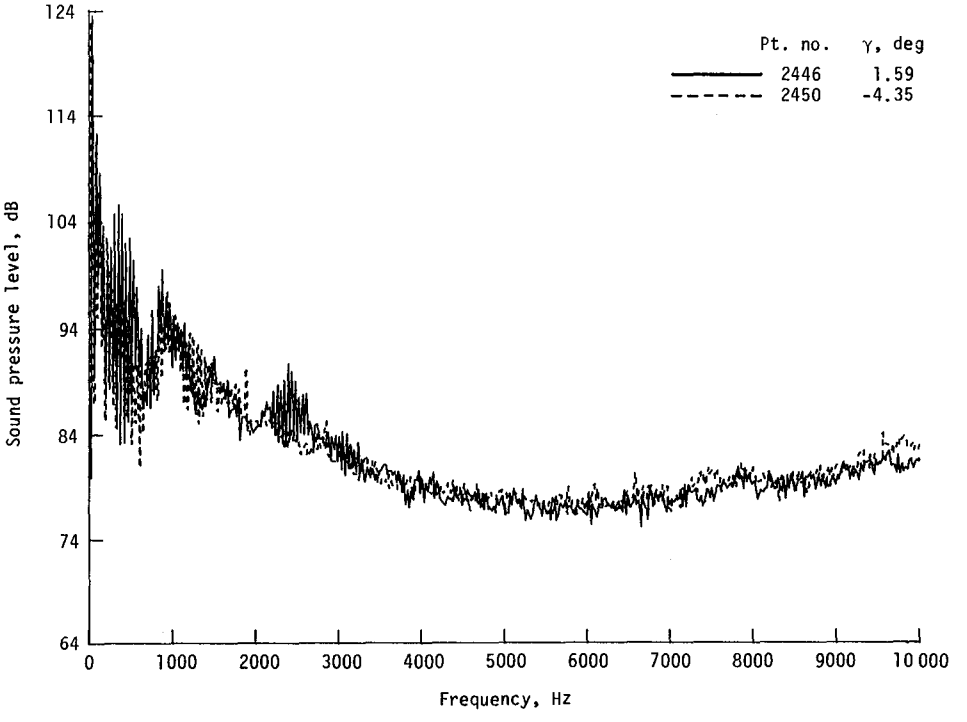

(c) Narrowband analysis; microphone 2.
Figure 15. - Continued.

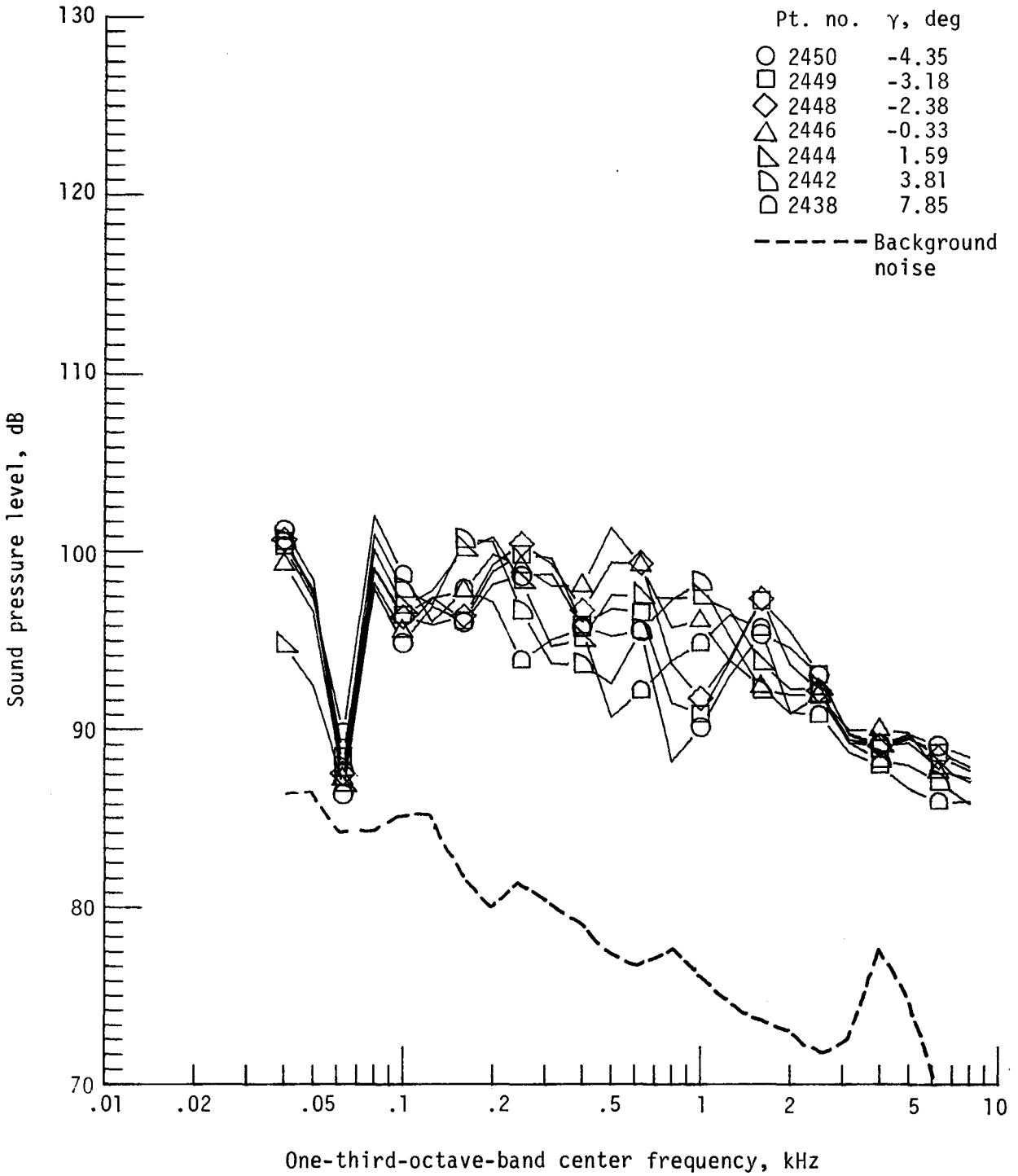

(d) One-third-octave spectra, microphone 6.

Figure 15. - Continued.

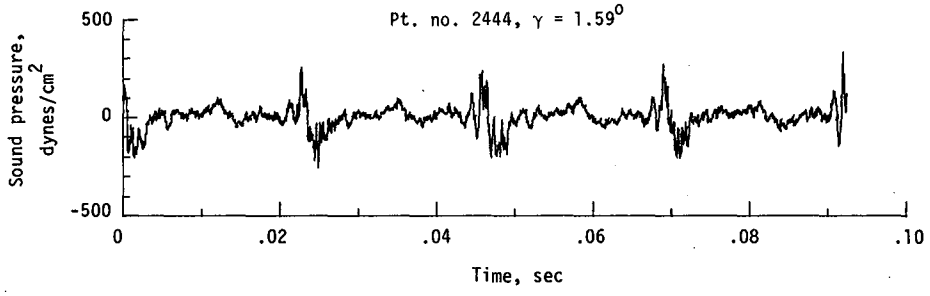

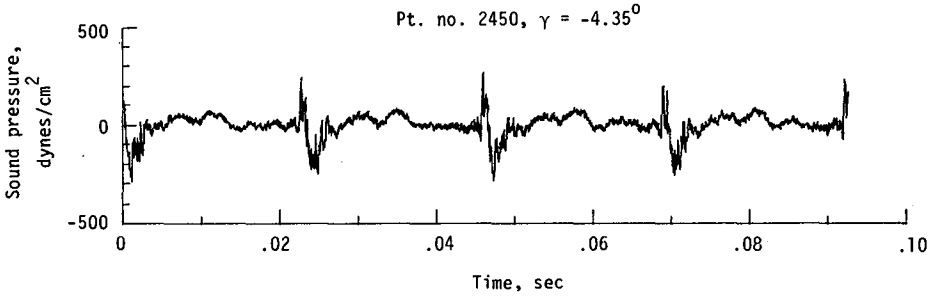

(e) Pressure-time histories; microphone 6.

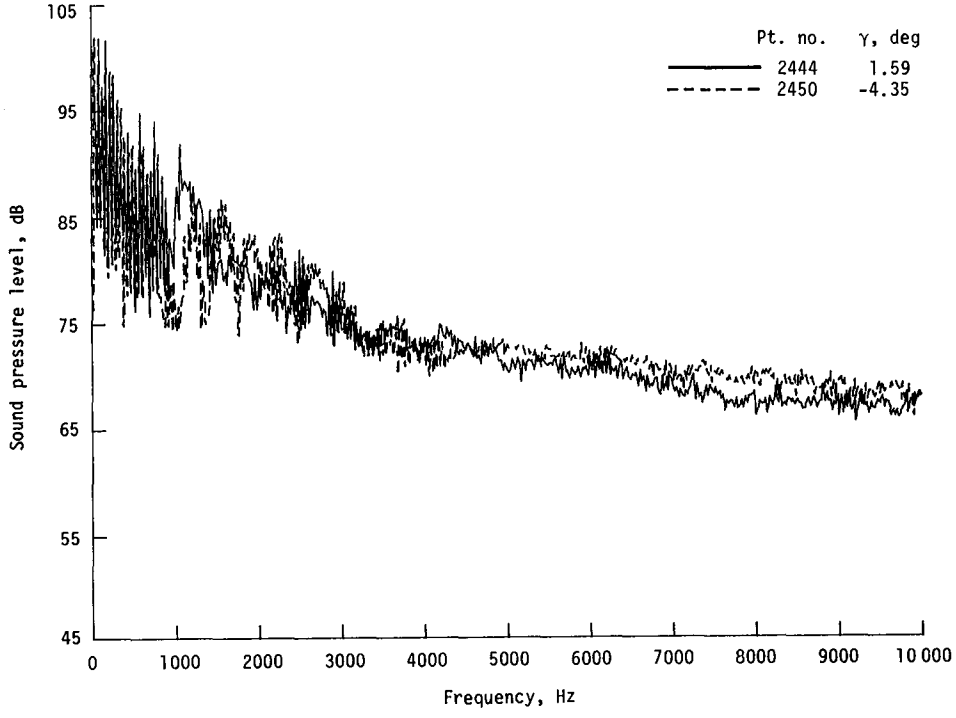

(f) Narrowband analysis; microphone 6.
Figure 15. - Continued.

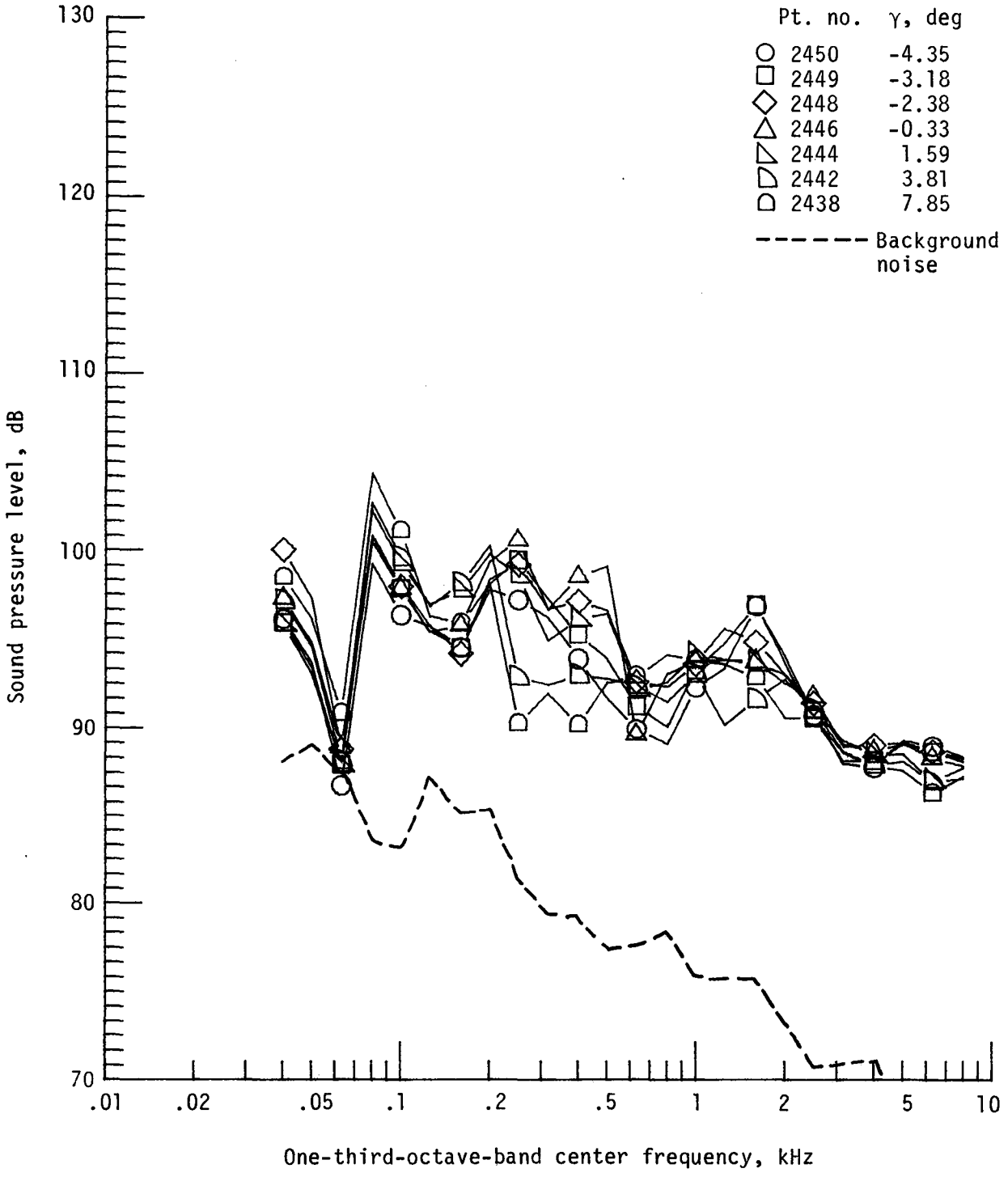

(g) One-third-octave spectra, microphone 7.

Figure 15. - Continued.

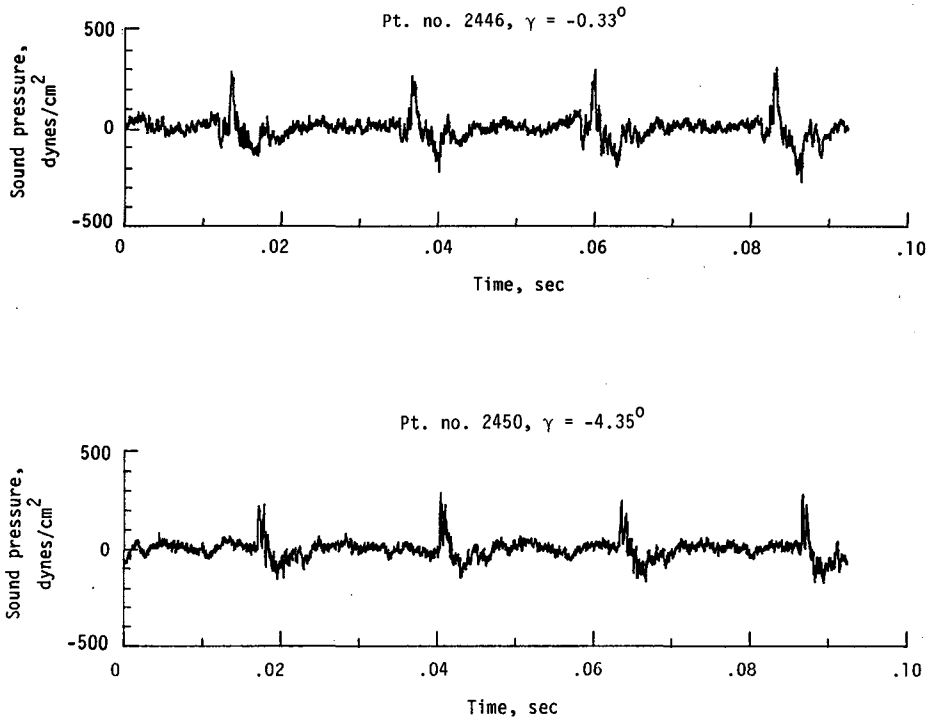

(h) Pressure-time histories; microphone 7.

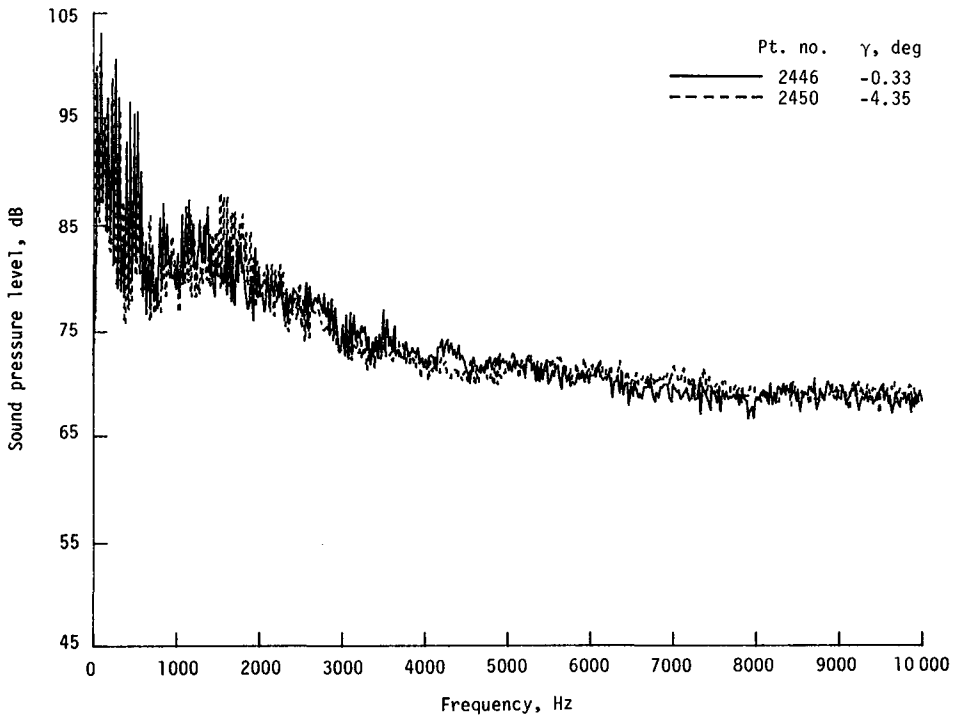

(i) Narrowband analysis; microphone 7.
Figure 15. - Continued.

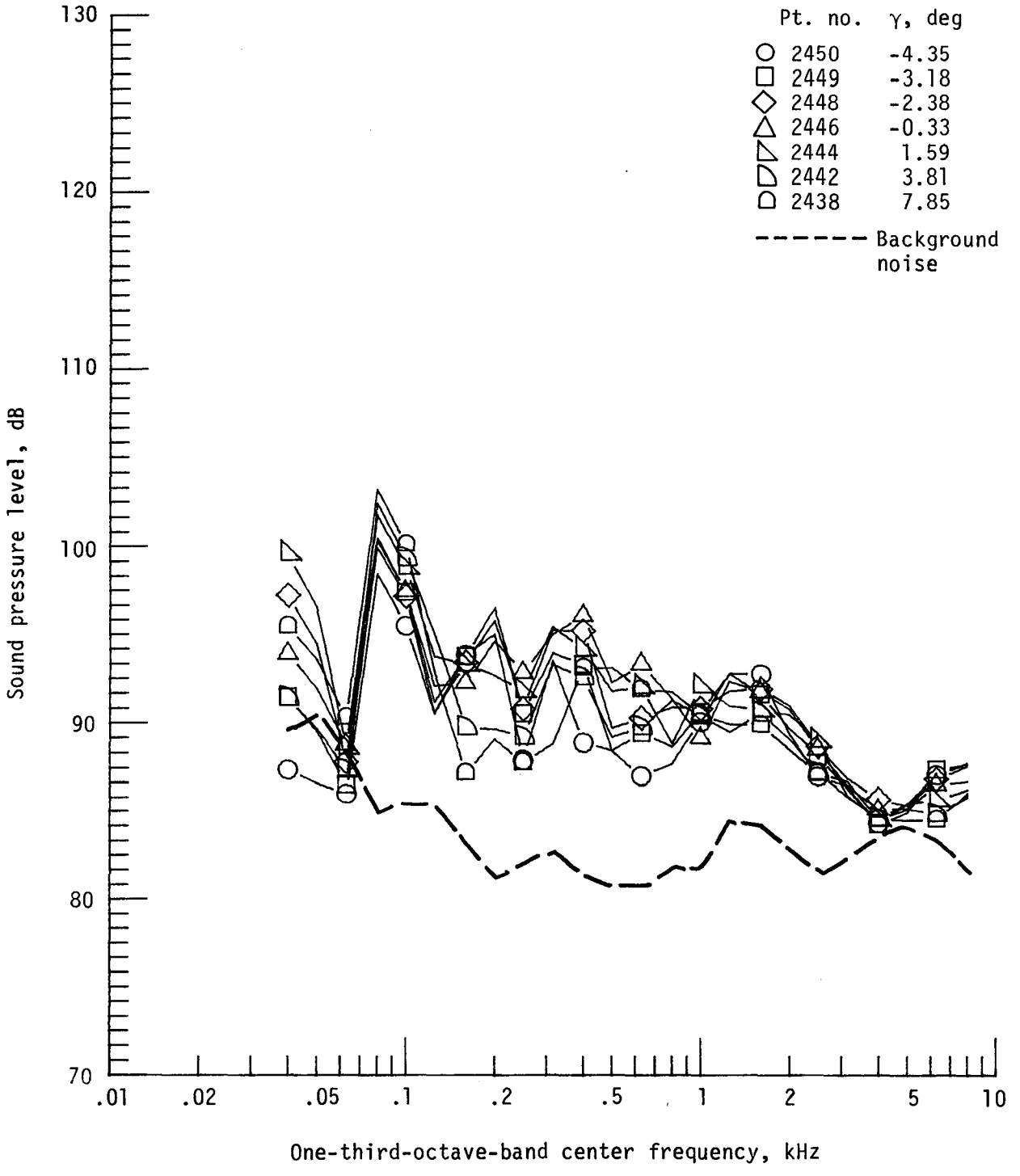

(j) One-third-octave spectra, microphone 8.

Figure 15. - Continued.

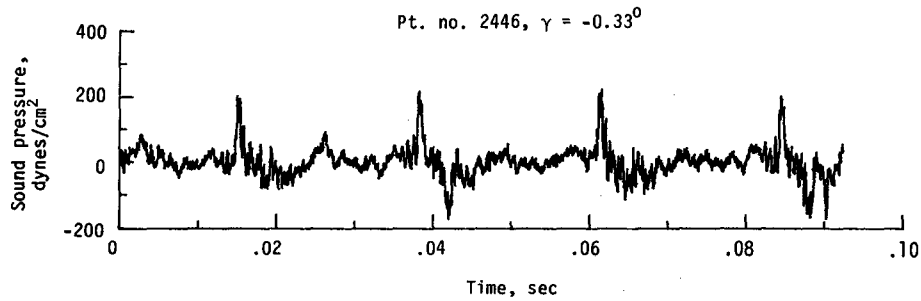

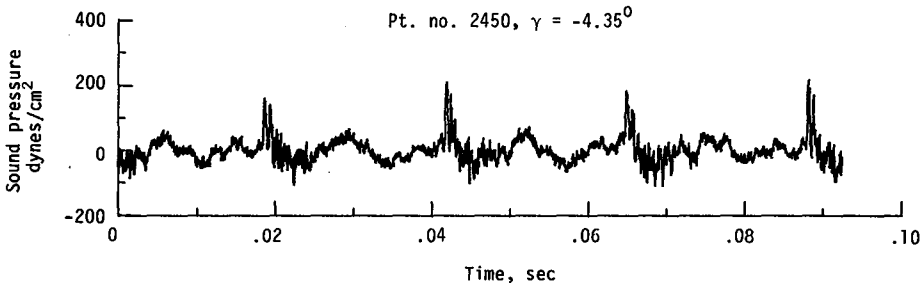

(k) Pressure-time histories; microphone 8.

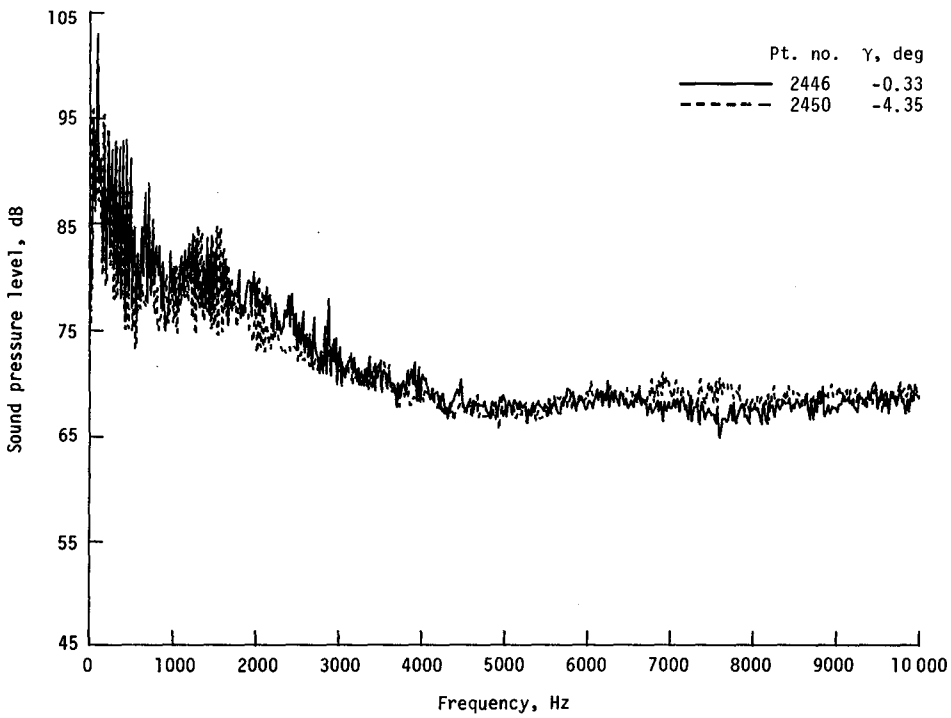

(l) Narrowband analysis; microphone 8.

Figure 15. - Concluded.

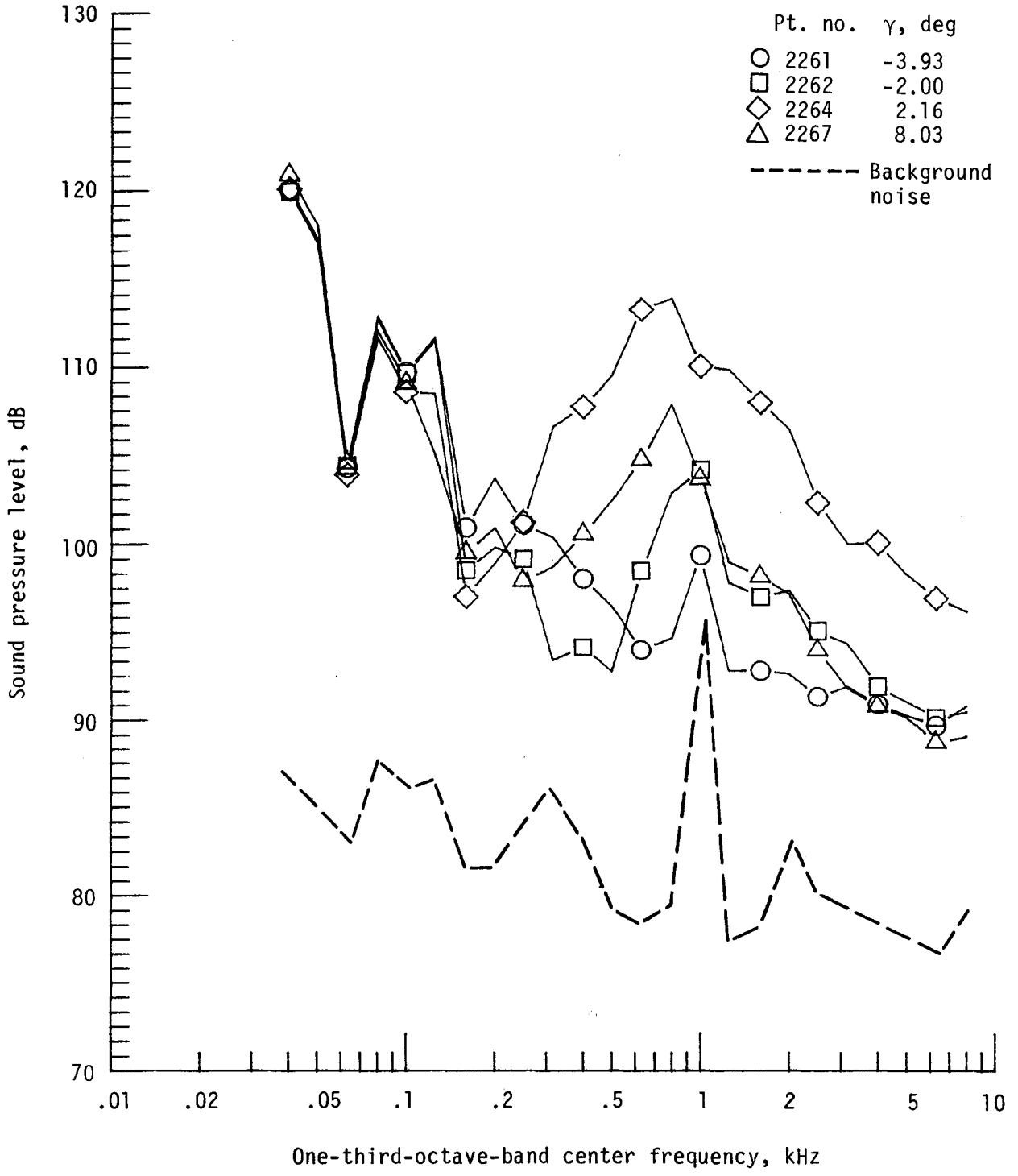

(a) One-third-octave spectra, microphone 2.

Figure 16. - Effect of descent angle variation on noise generated by helicopter model with standard rotor system, run 181; V_∞ = 59.9 knots, C_T = .0036.

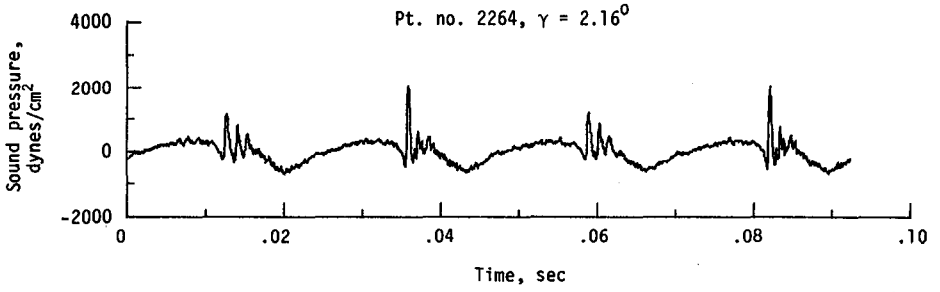

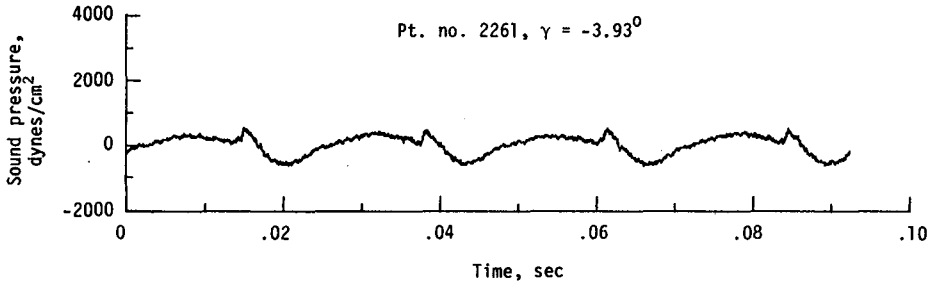

(b) Pressure-time histories; microphone 2.

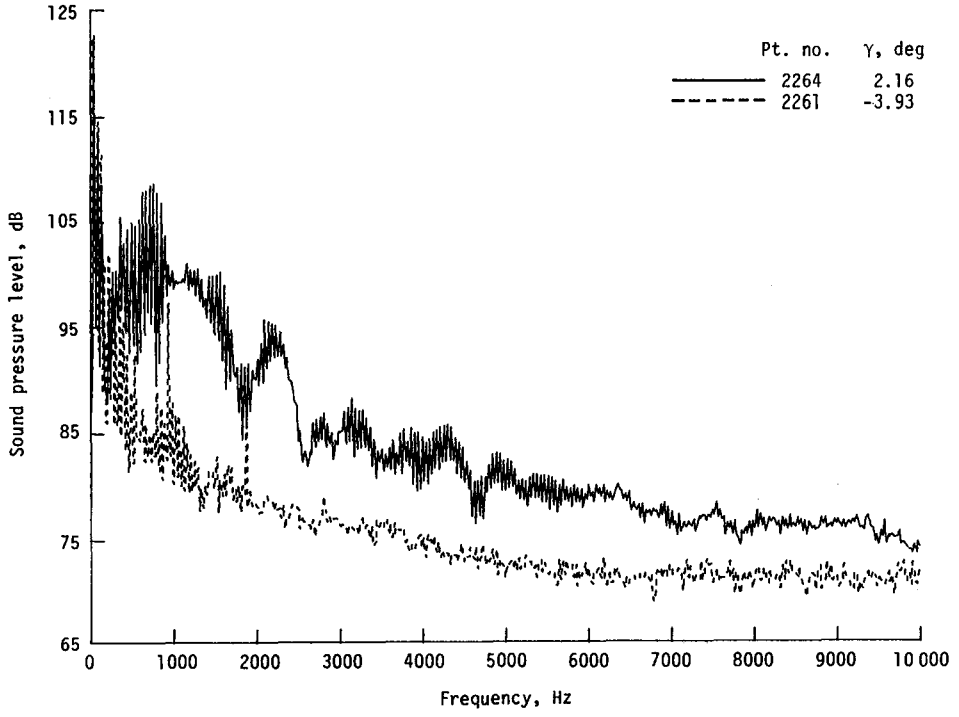

(c) Narrowband analysis; microphone 2.
Figure 16. - Continued.

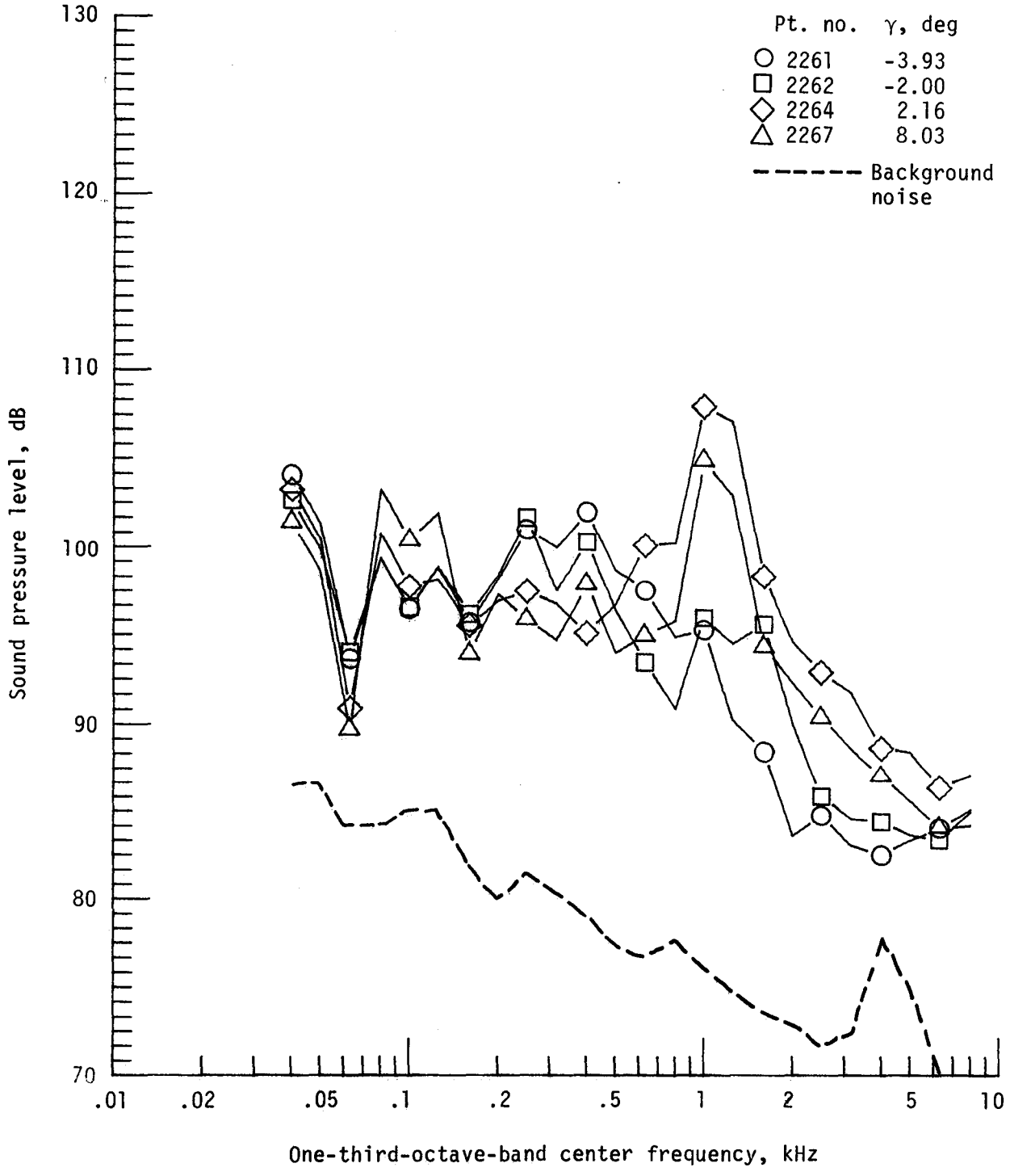

(d) One-third-octave spectra, microphone 6.

Figure 16. - Continued.

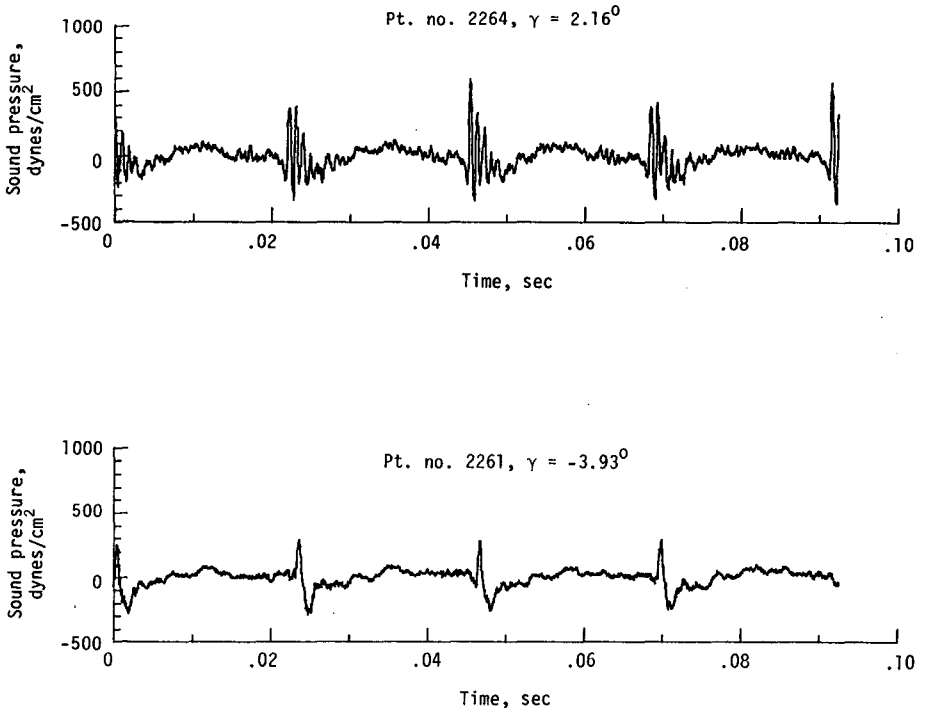

(e) Pressure-time histories; microphone 6.

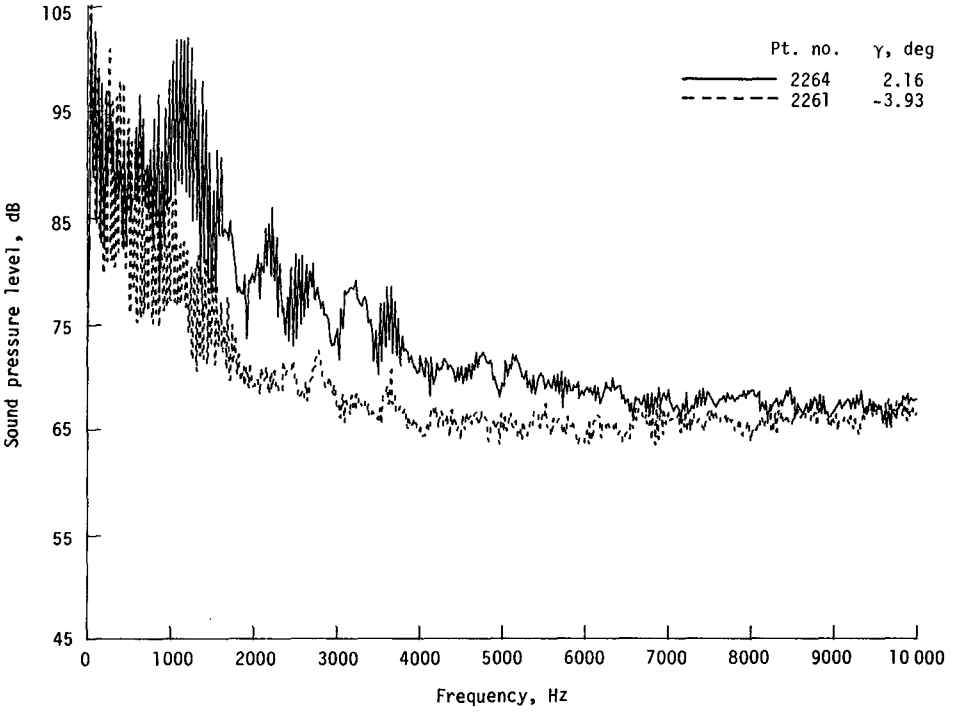

(f) Narrowband analysis; microphone 6.
Figure 16. - Continued.

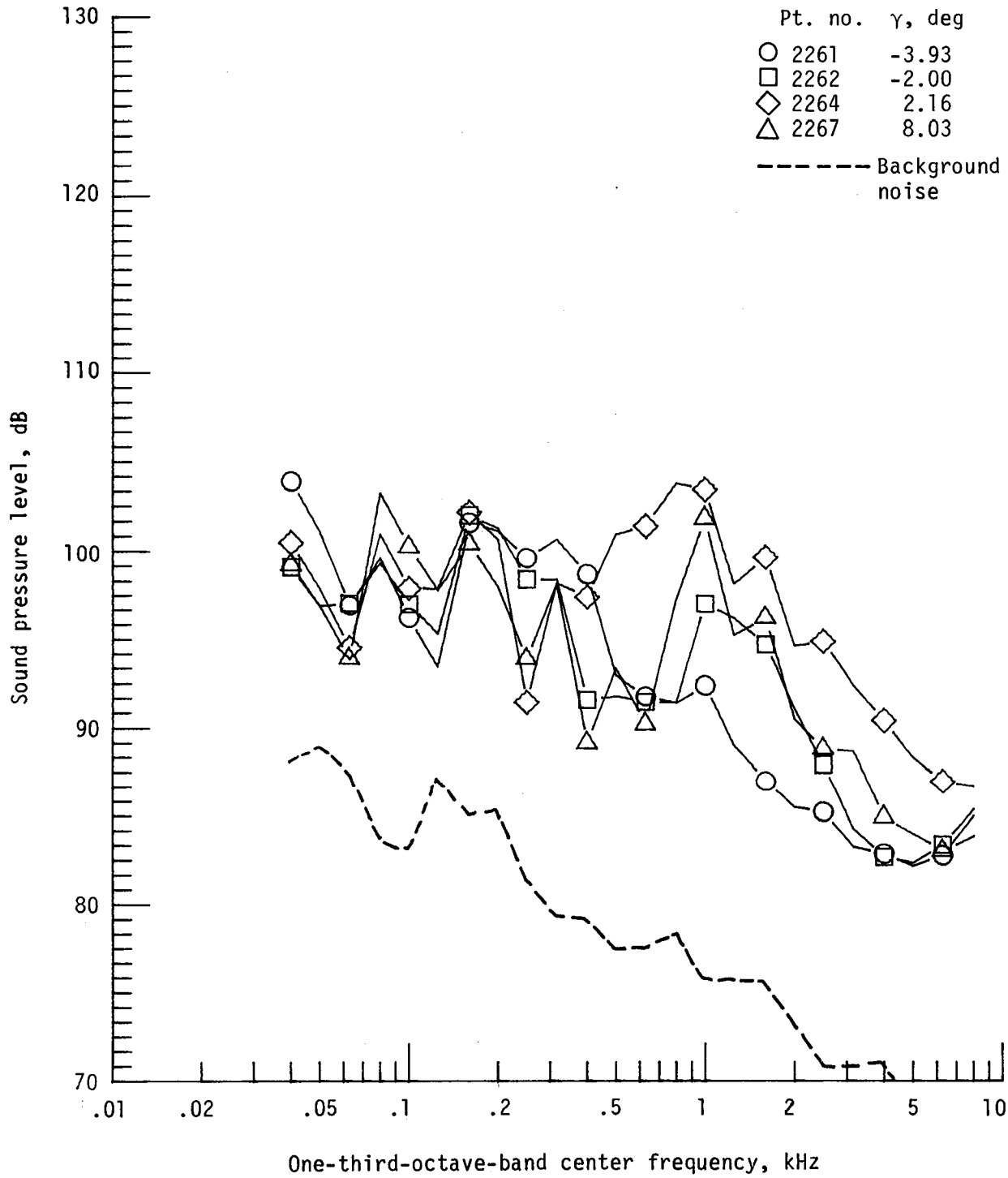

(g) One-third-octave spectra, microphone 7.

Figure 16. - Continued.

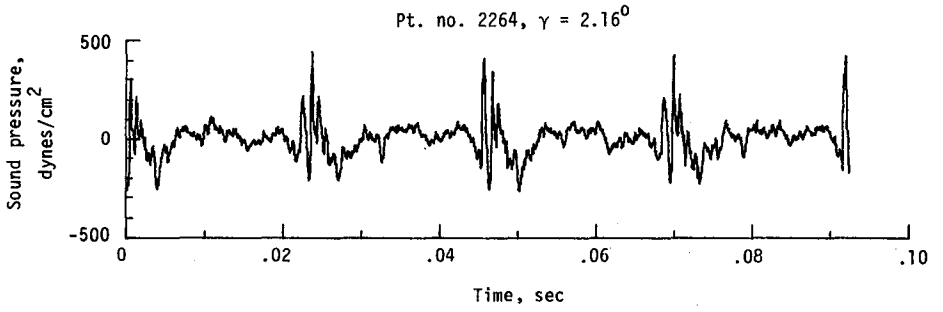

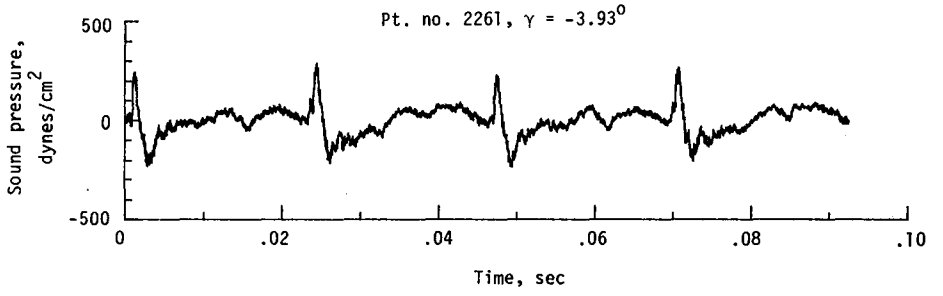

(h) Pressure-time histories; microphone 7.

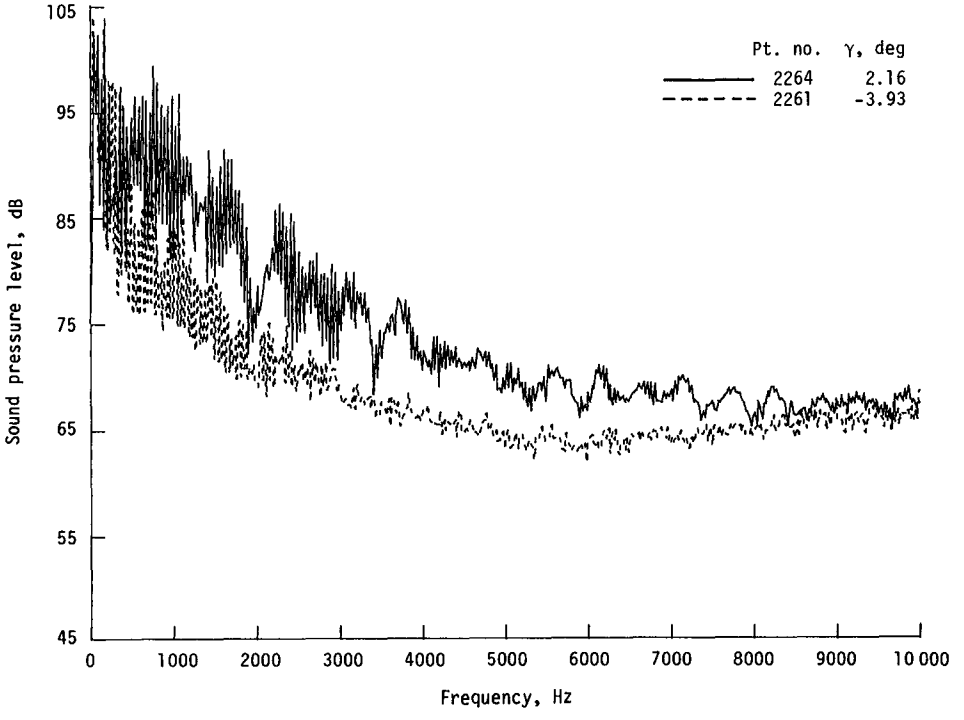

(i) Narrowband analysis; microphone 7.

Figure 16. - Continued.

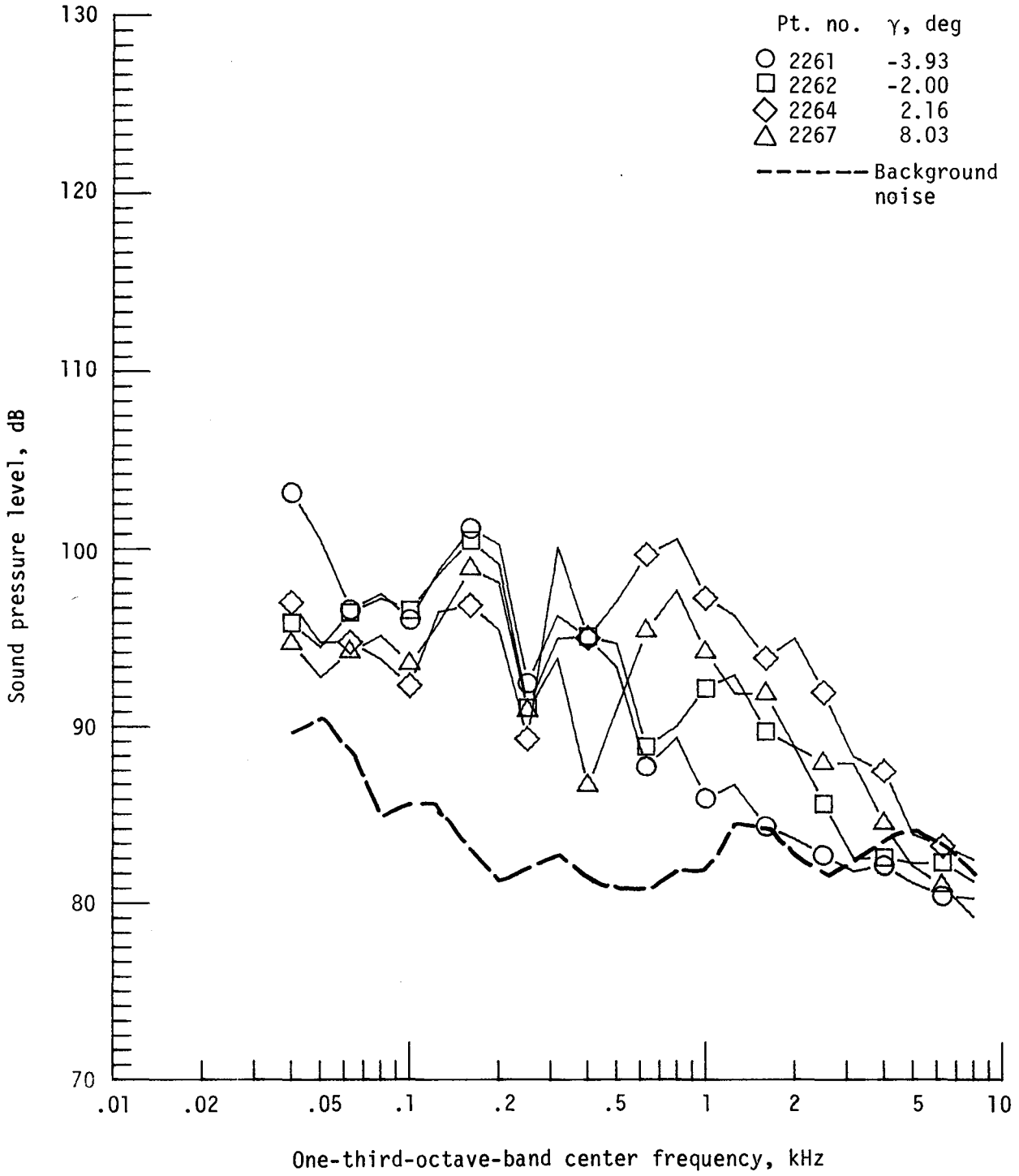

(j) One-third-octave spectra, microphone 8.

Figure 16. - Continued.

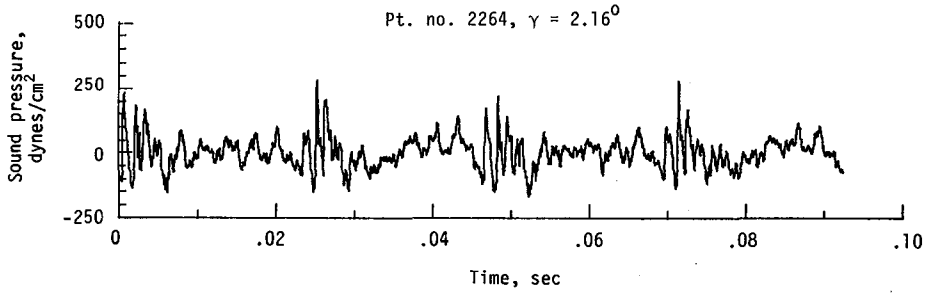

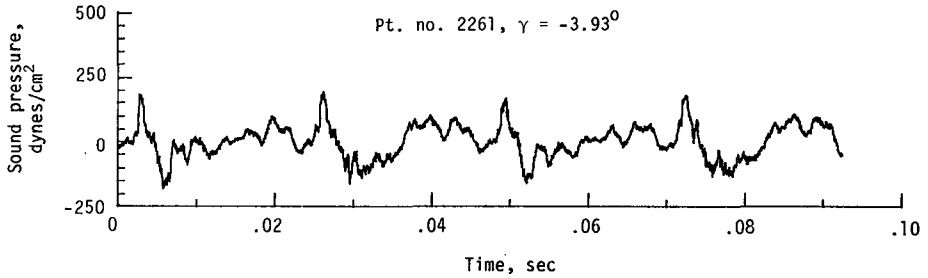

(k) Pressure-time histories; microphone 8.

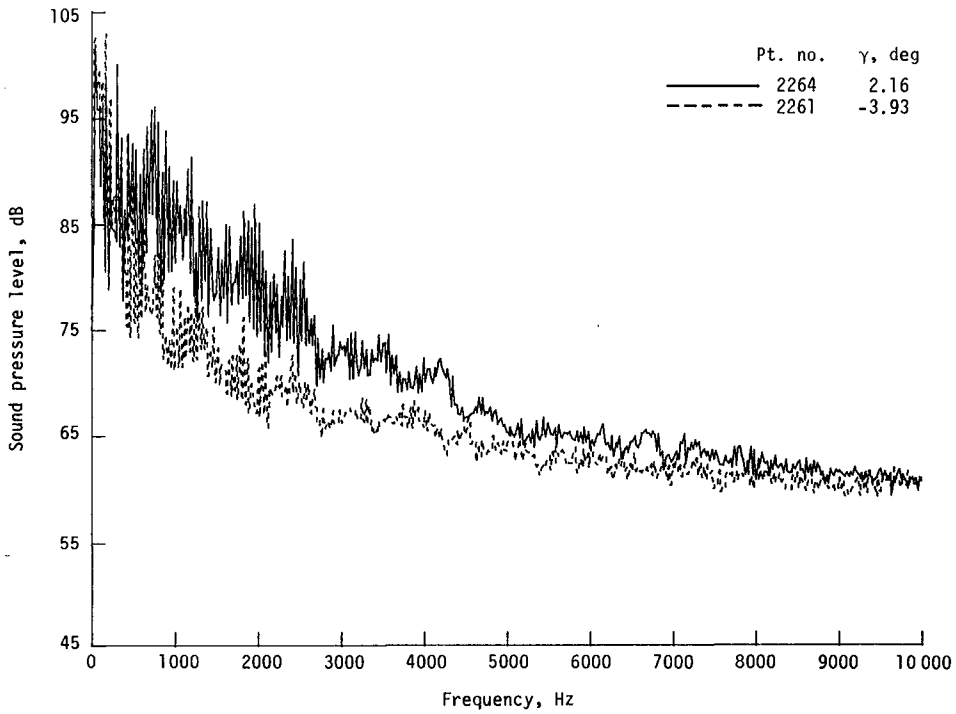

(l) Narrowband analysis; microphone 8.
Figure 16. - Concluded.

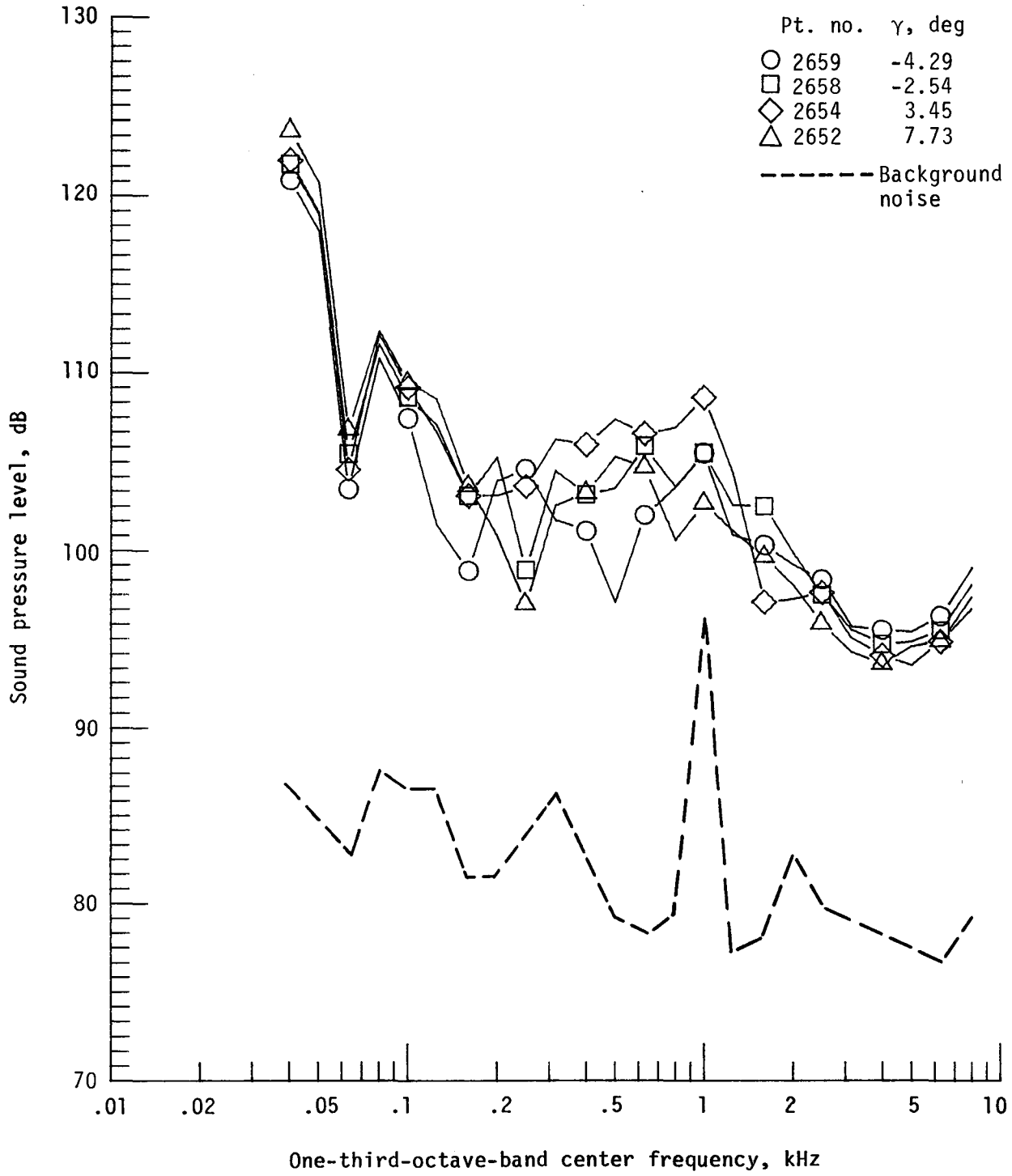

(a) One-third-octave spectra, microphone 2.

Figure 17. - Effect of descent angle variation on noise generated by helicopter model with advanced rotor system, run 213. V_∞ = 60.8 knots, C_T = .0036.

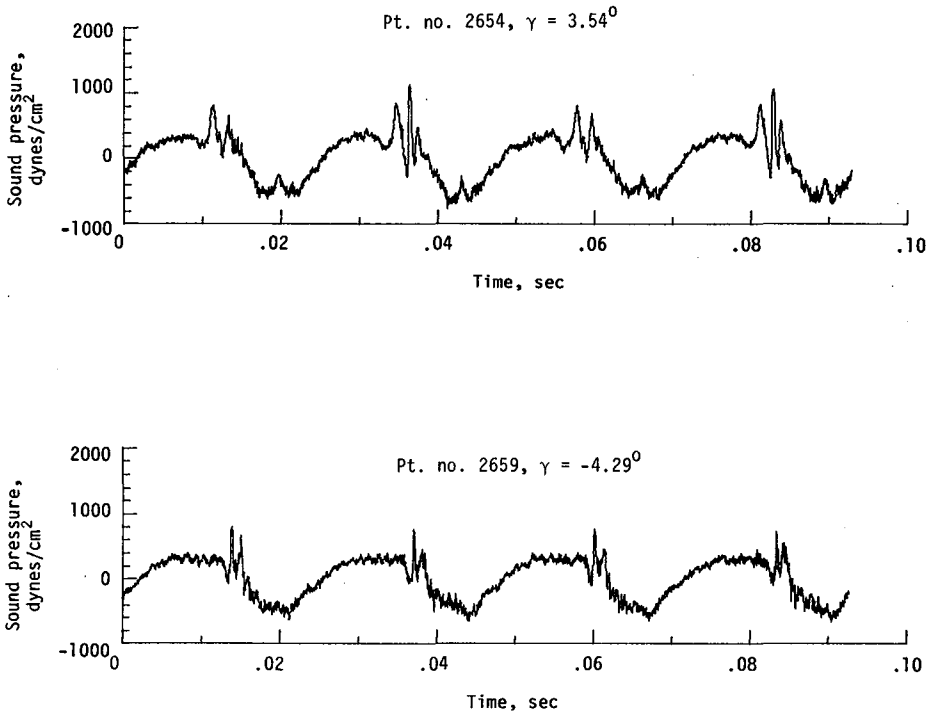

(b) Pressure-time histories; microphone 2.

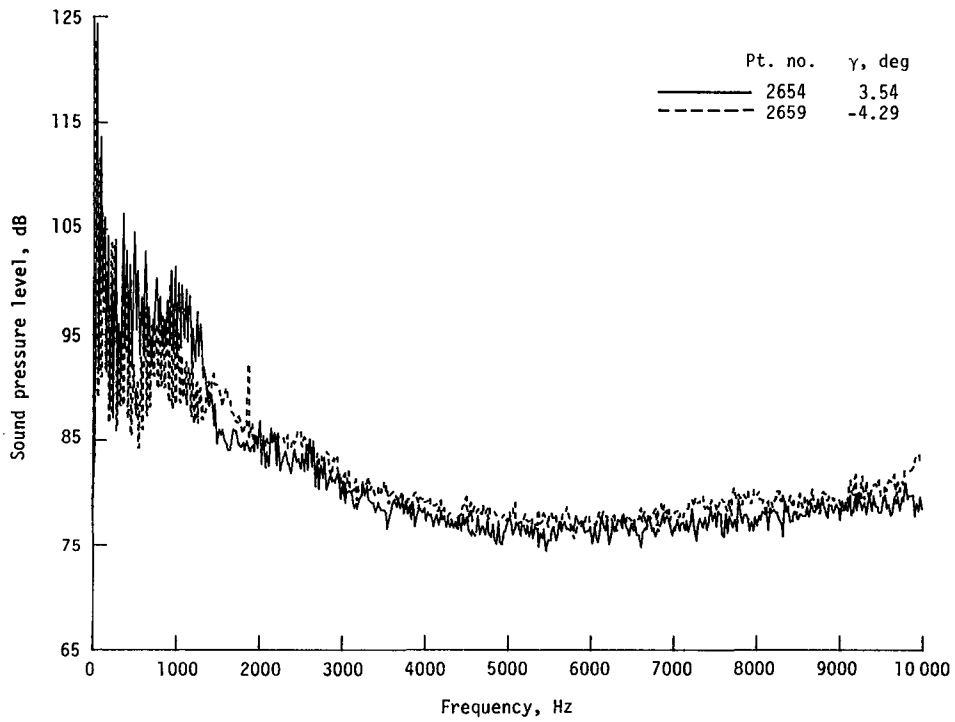

(c) Narrowband analysis; microphone 2.
Figure 17. - Continued.

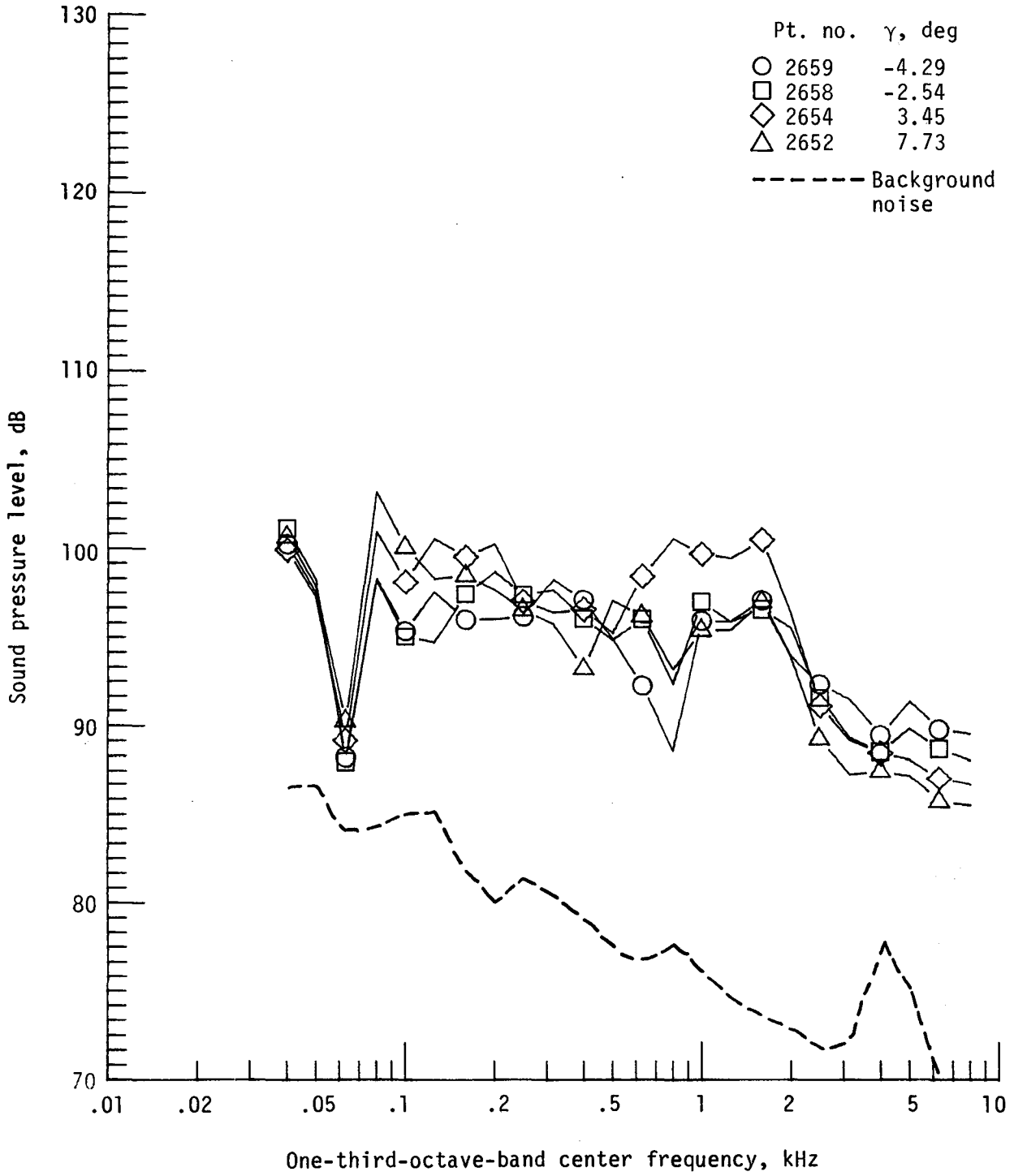

(d) One-third-octave spectra, microphone 6.

Figure 17. - Continued.

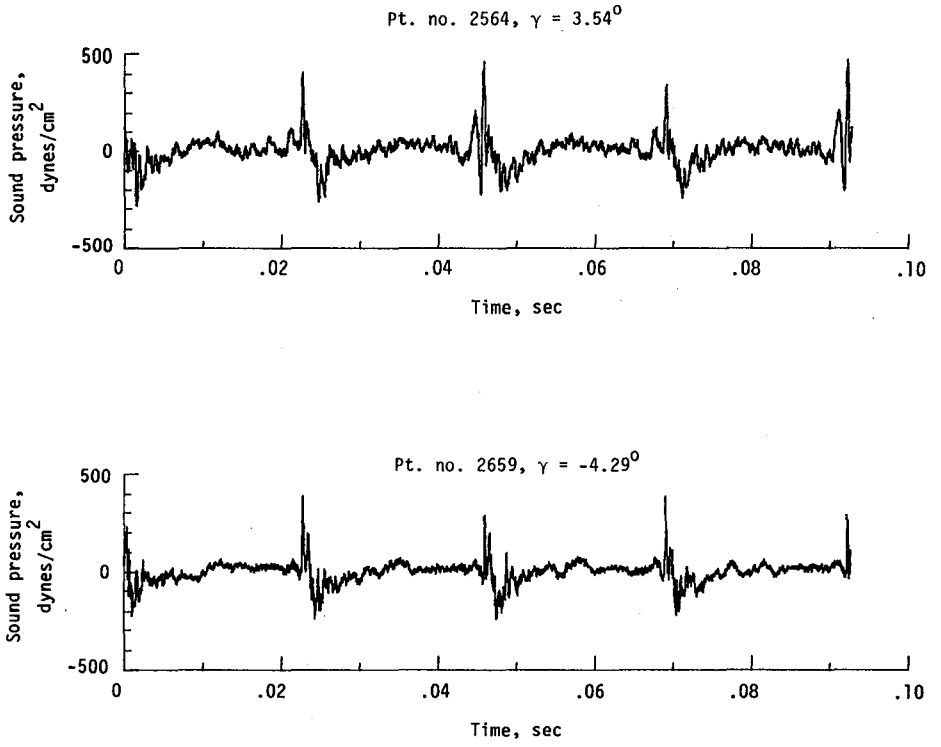

(e) Pressure-time histories; microphone 6.

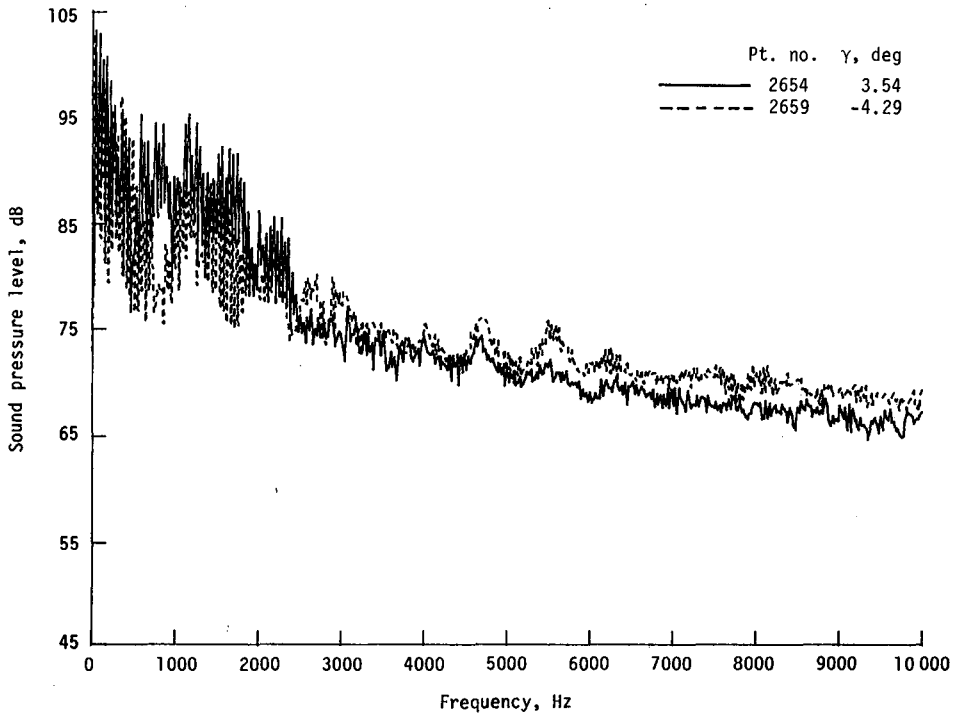

(f) Narrowband analysis; microphone 6.
Figure 17. - Continued.

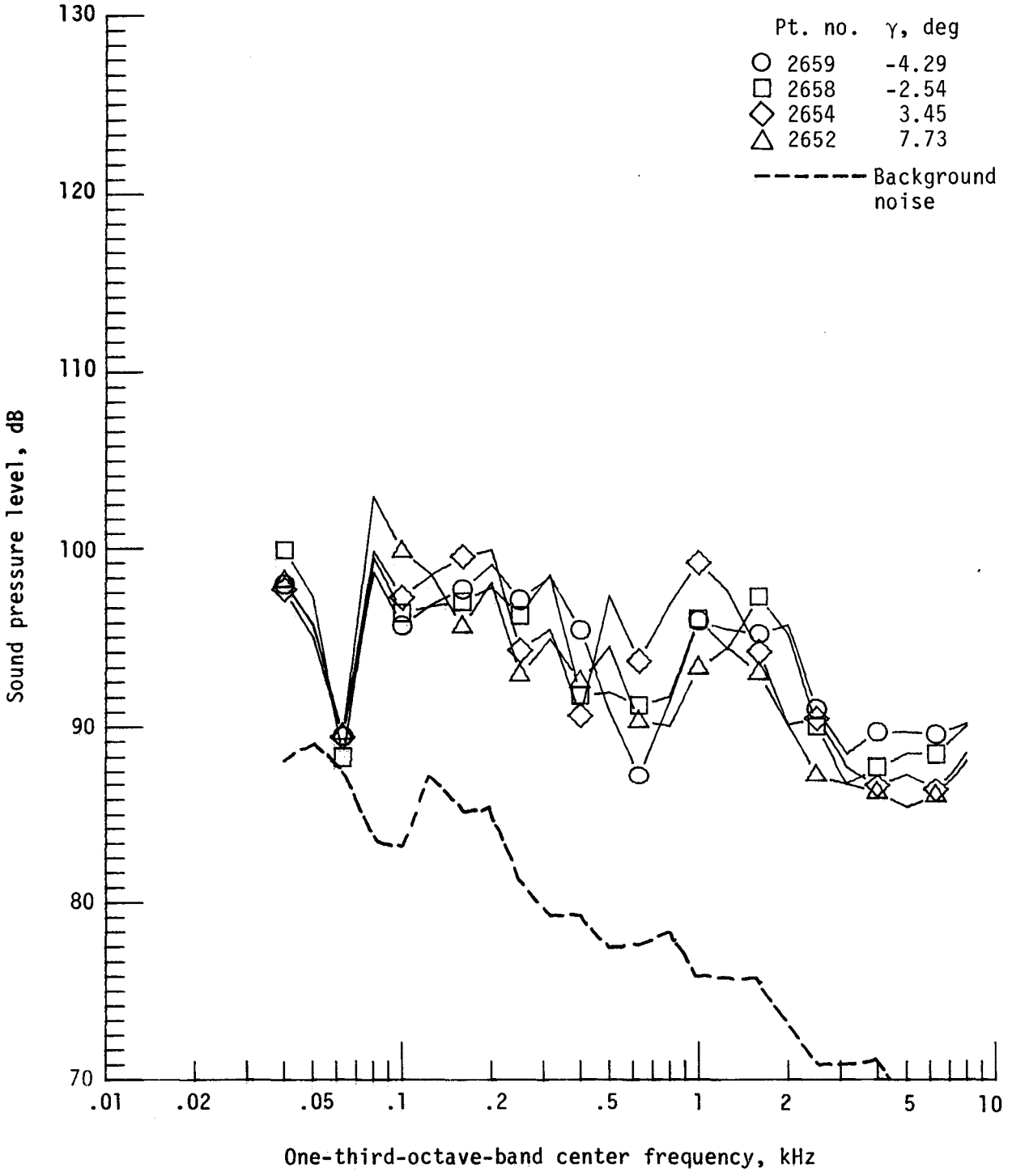

(g) One-third-octave spectra, microphone 7.

Figure 17. - Continued.

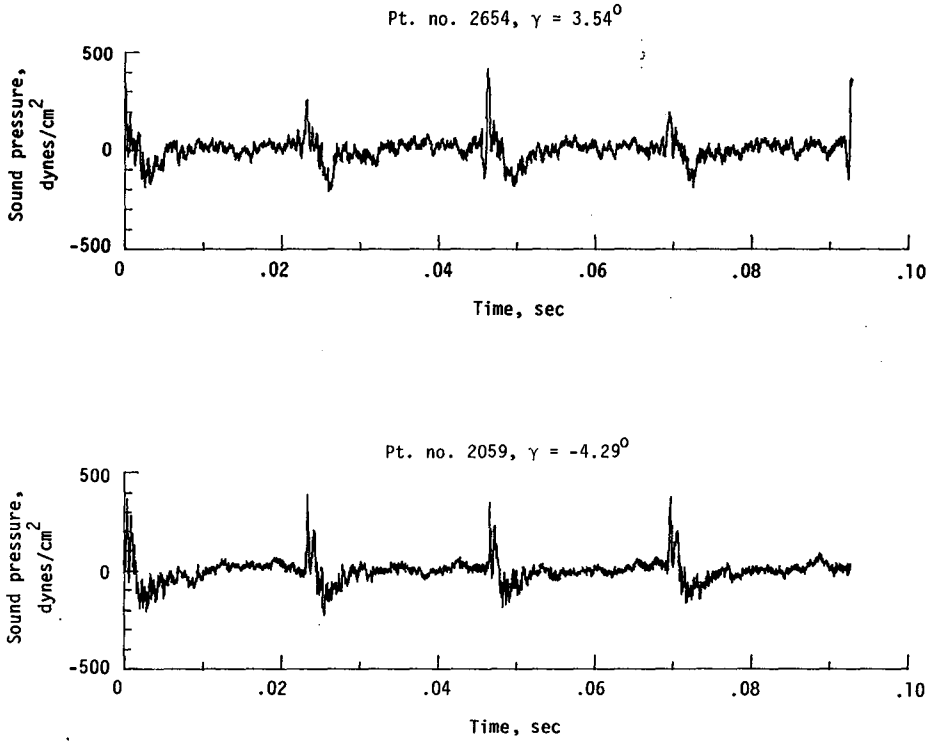

(h) Pressure-time histories; microphone 7.

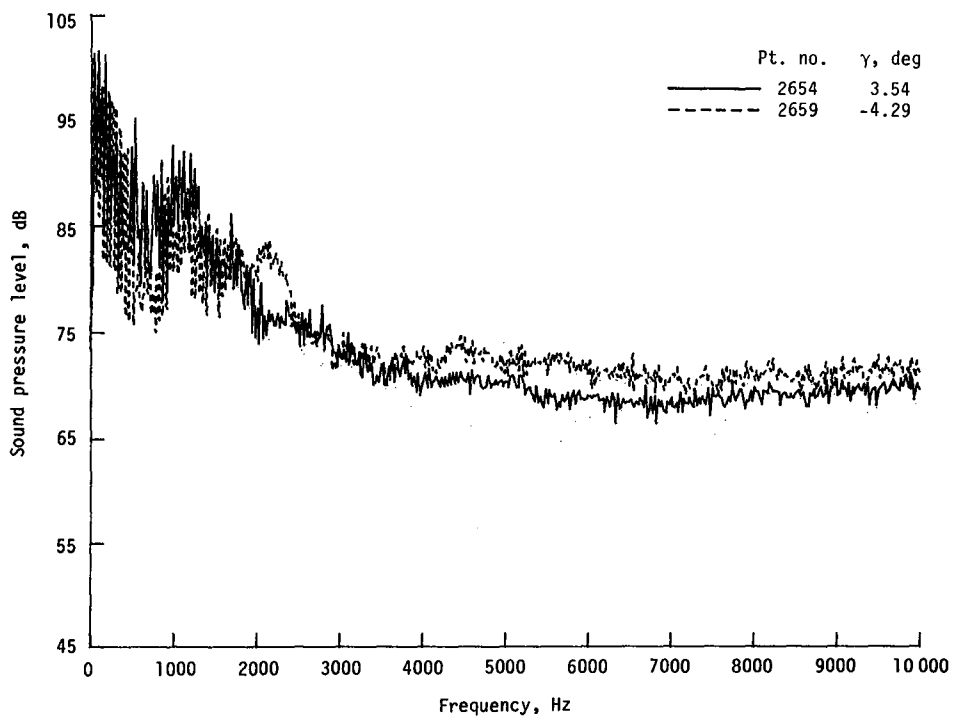

(i) Narrowband analysis; microphone 7.

Figure 17. - Continued.

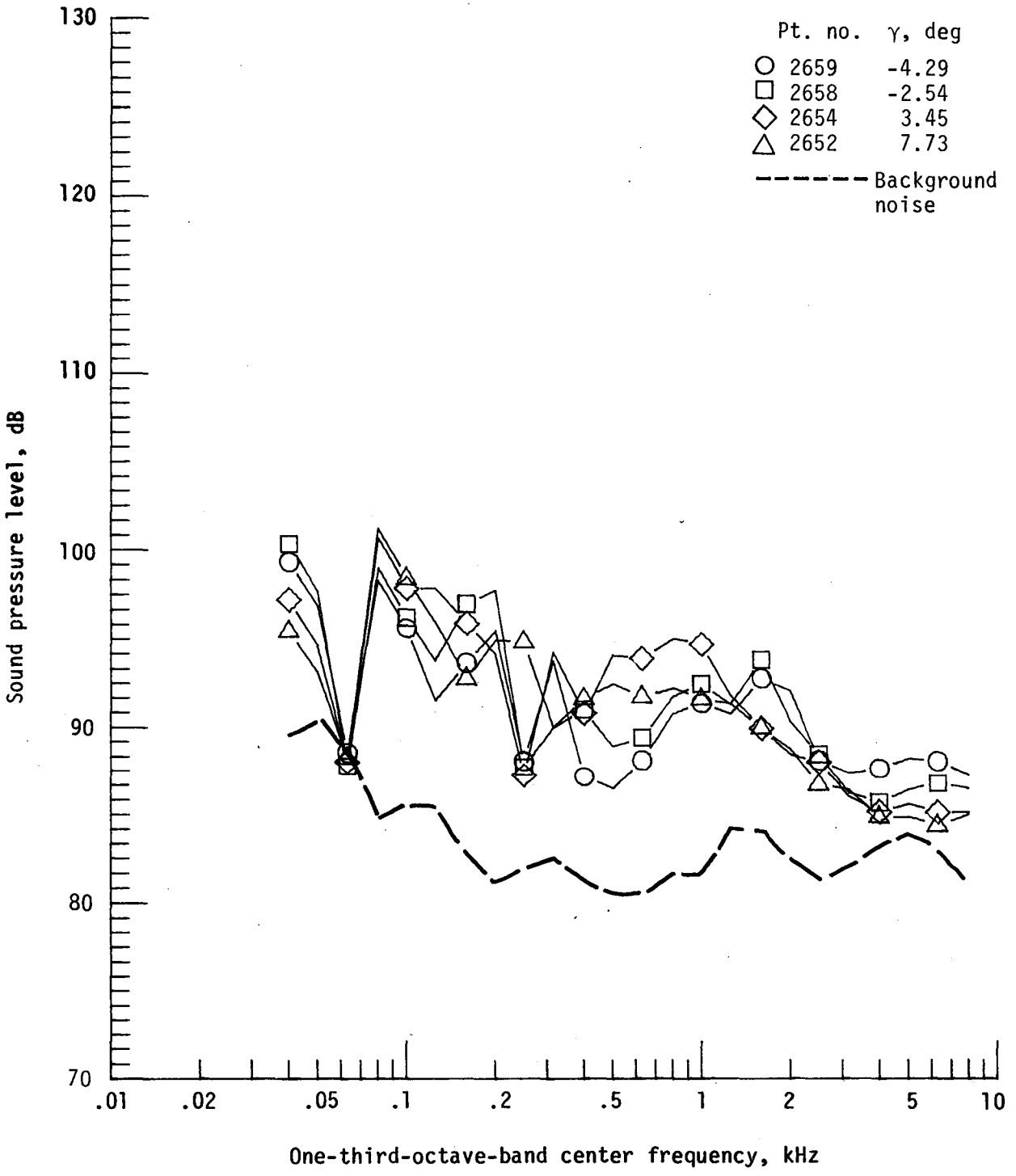

(j) One-third-octave spectra, microphone 8.

Figure 17. - Continued.

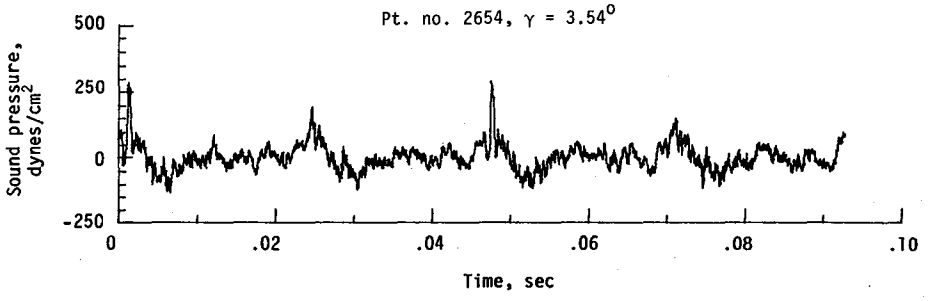

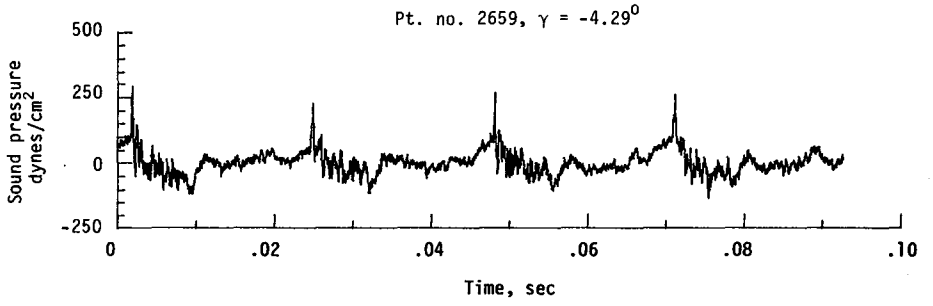

(k) Pressure-time histories; microphone 8.

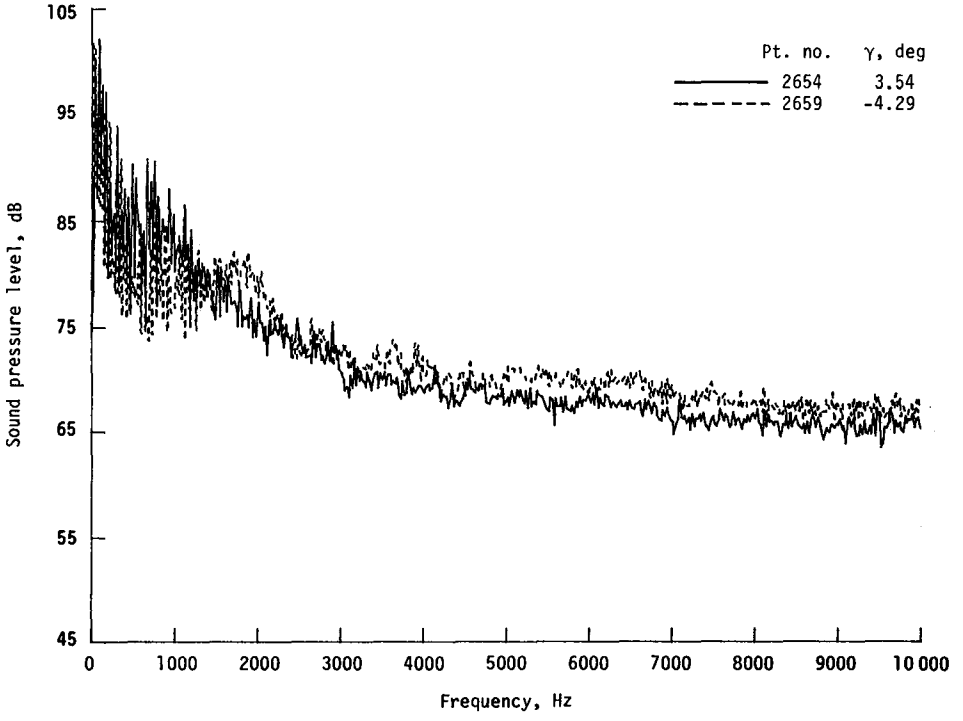

(l) Narrowband analysis; microphone 8.
Figure 17. - Concluded.

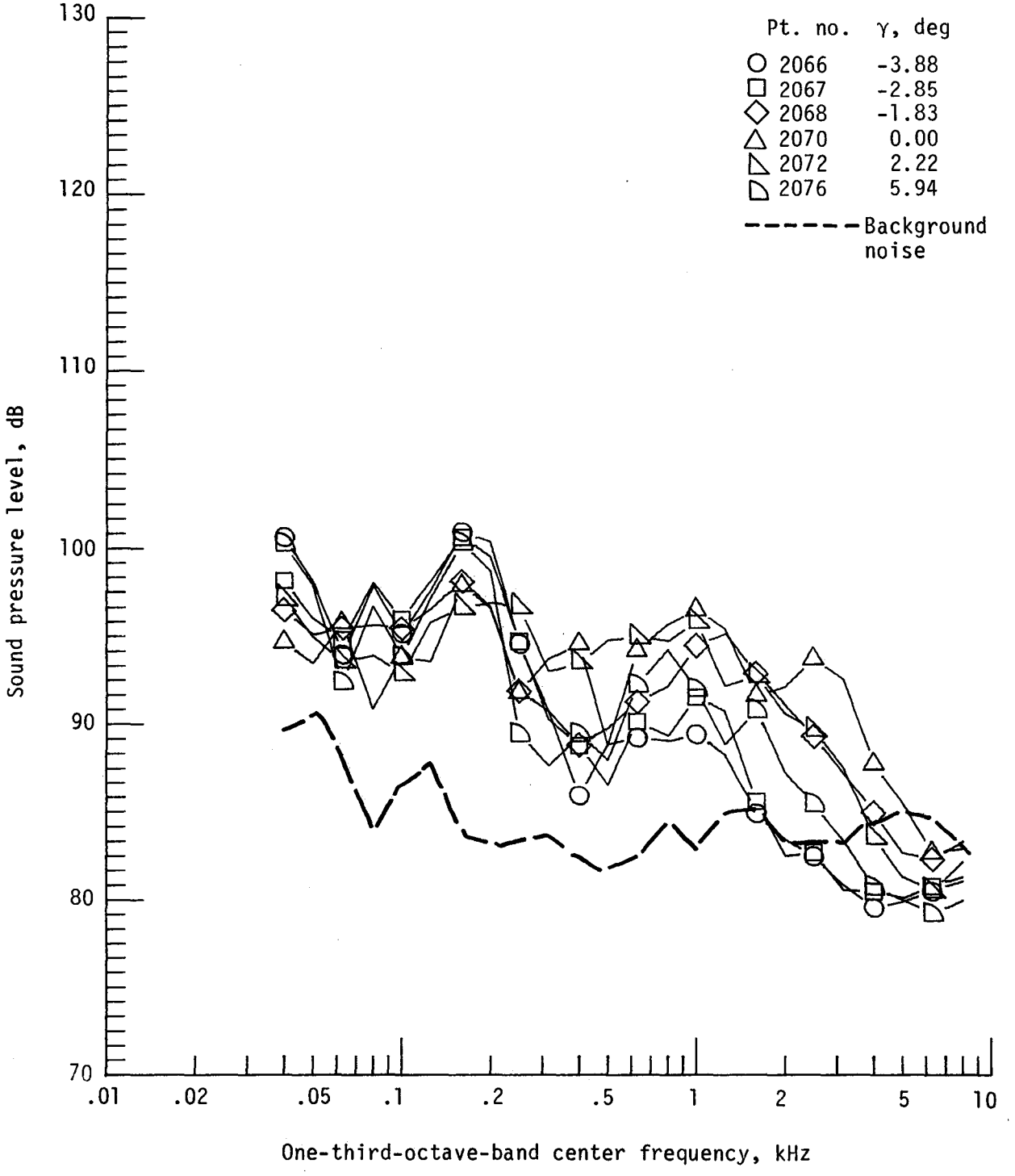

(a) One-third-octave spectra, microphone 2.

Figure 18. - Effect of descent angle variation on noise generated by helicopter model with standard rotor system, run 159. V_∞ = 65.2 knots, C_T = .0032.

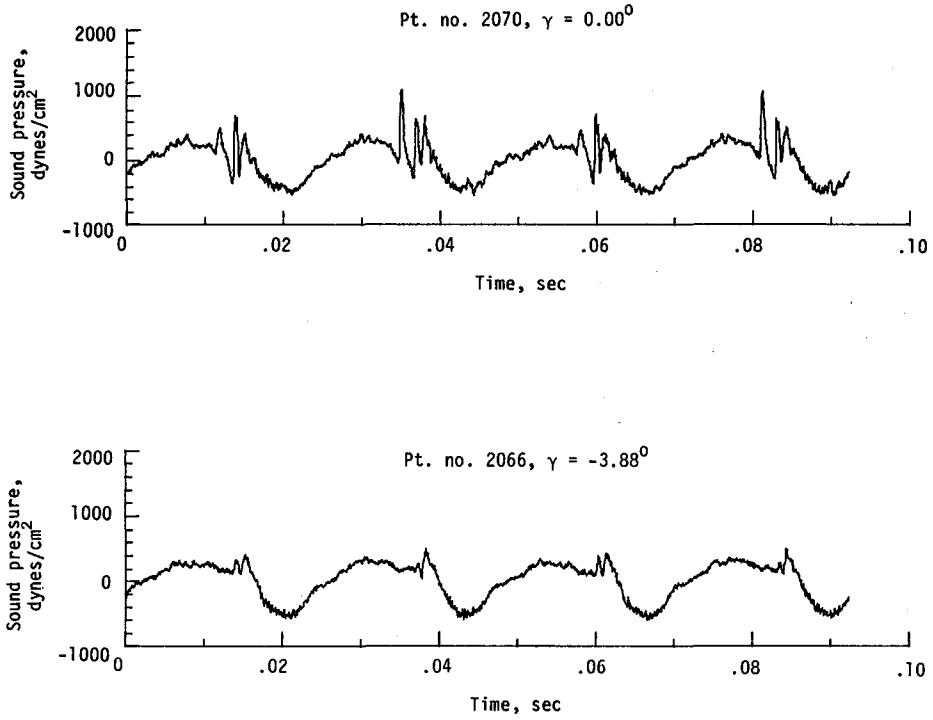

(b) Pressure-time histories; microphone 2.

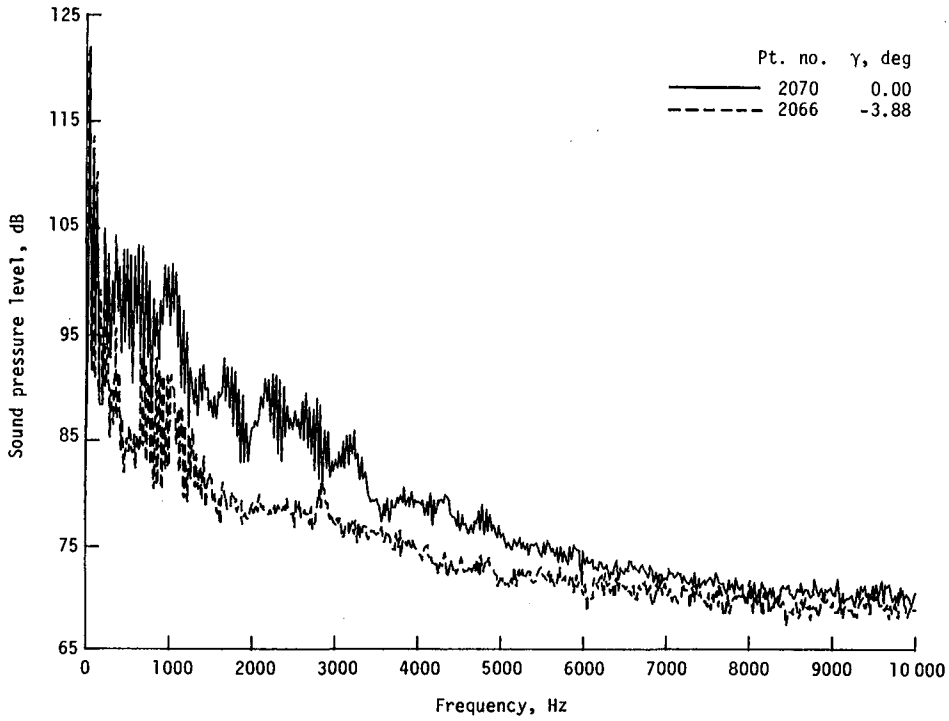

(c) Narrowband analysis; microphone 2.
Figure 18. - Continued.

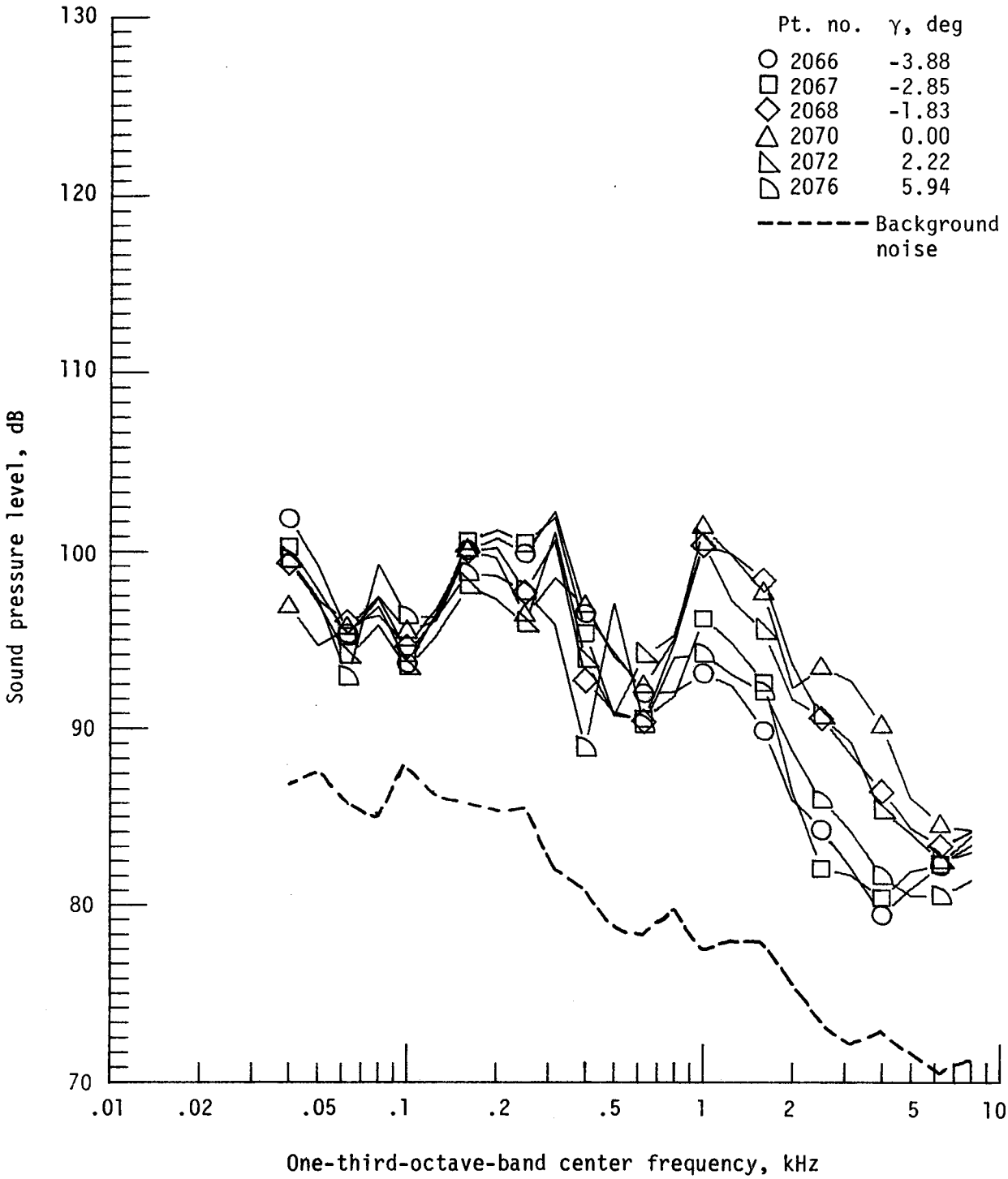

(d) One-third-octave spectra, microphone 6.

Figure 18. - Continued.

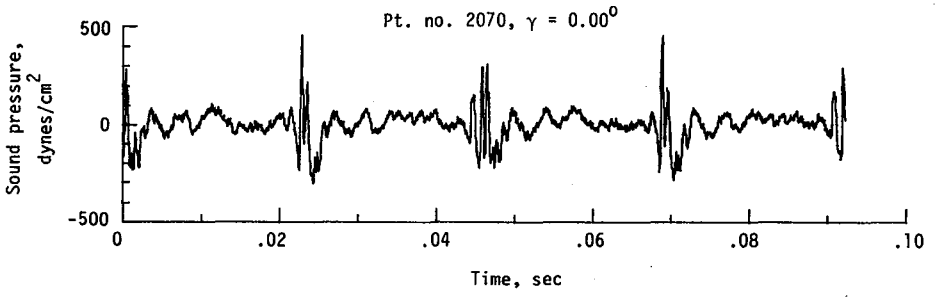

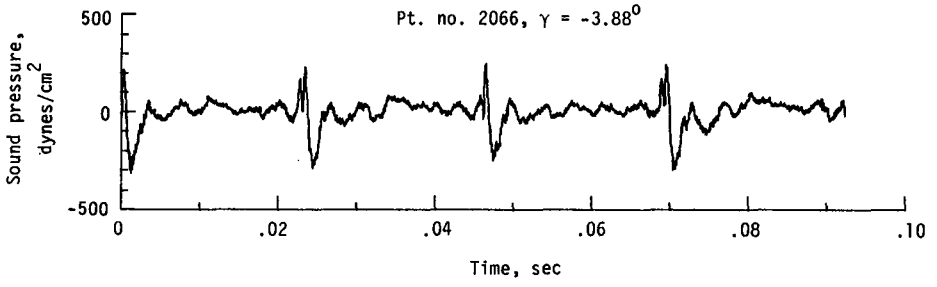

(e) Pressure-time histories; microphone 6.

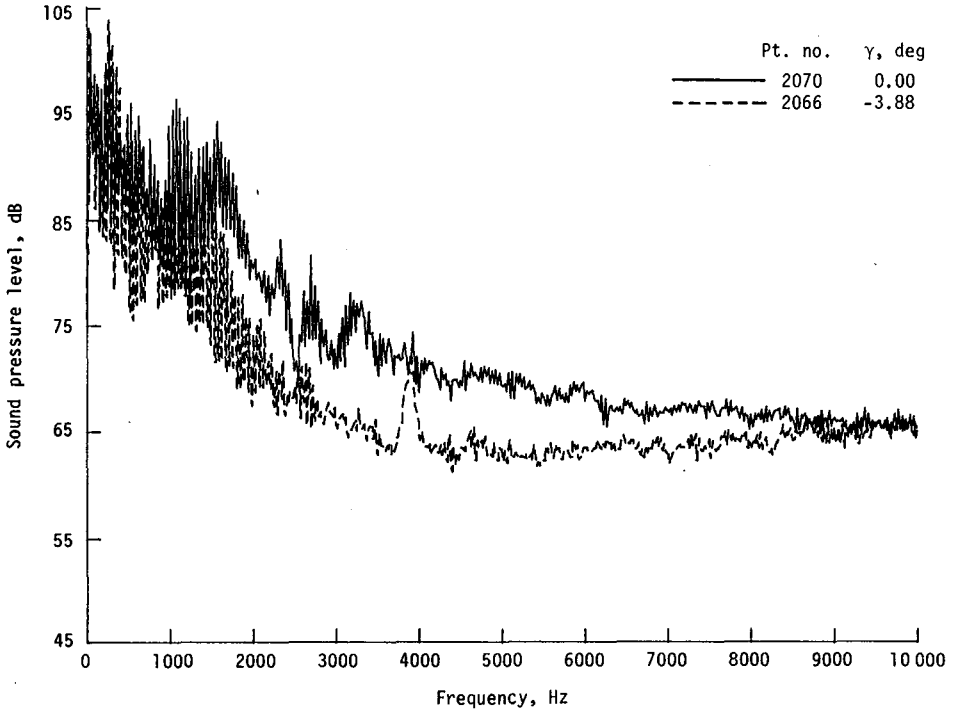

(f) Narrowband analysis; microphone 6.
Figure 18. - Continued.

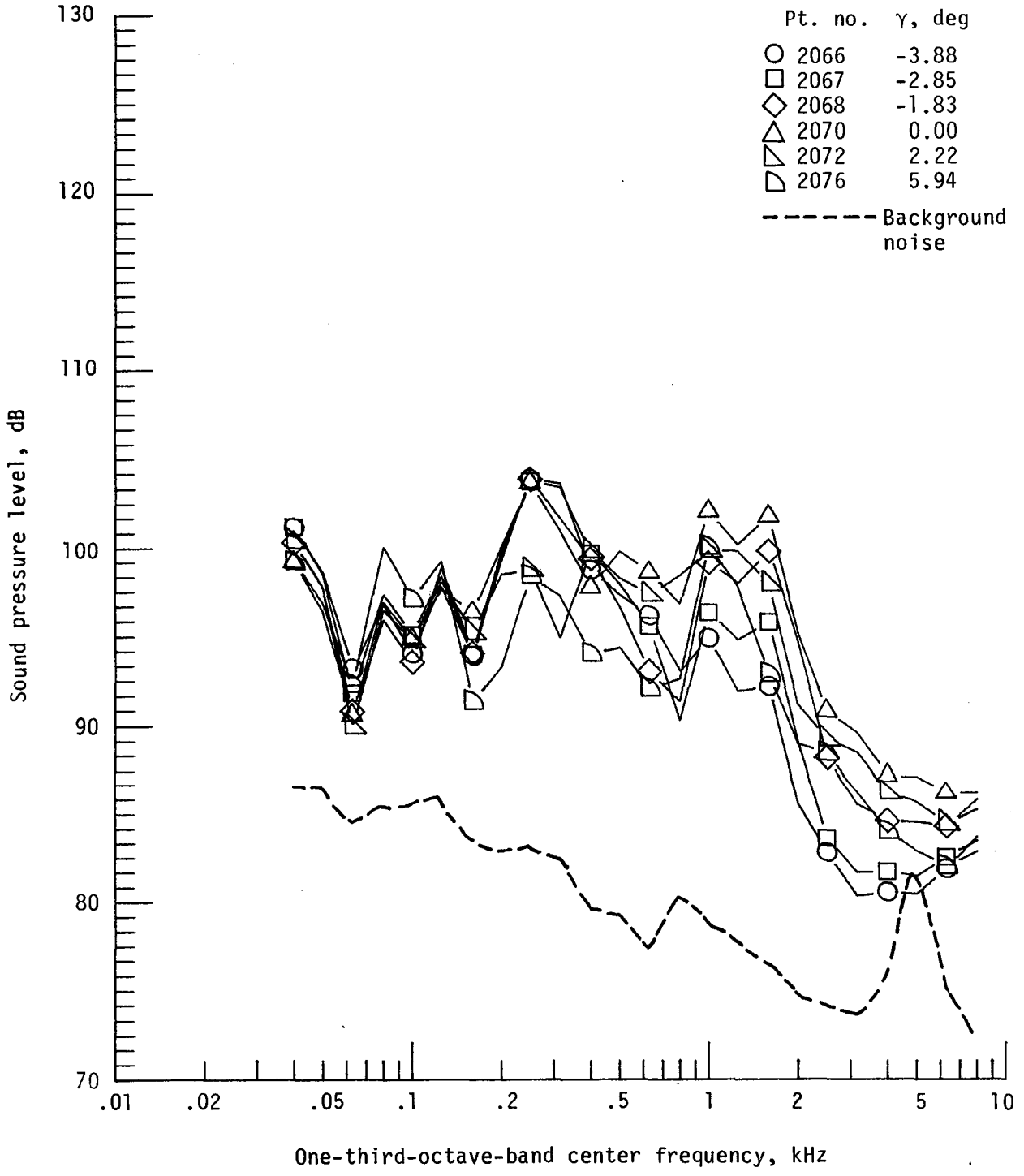

(g) One-third-octave spectra, microphone 7.

Figure 18. - Continued.

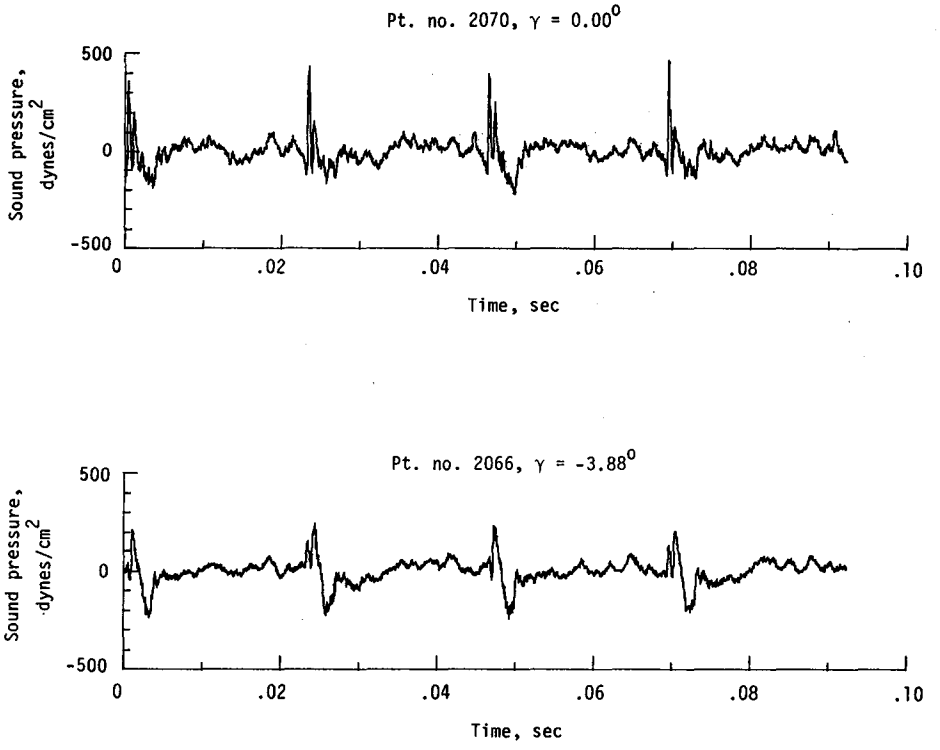

(h) Pressure-time histories; microphone 7.

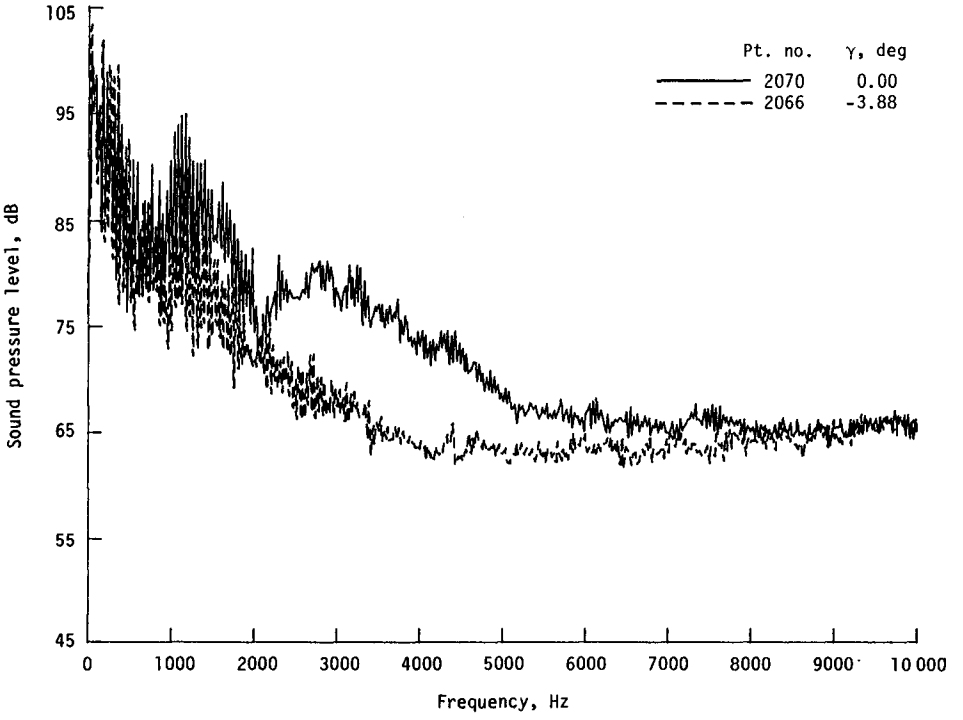

(i) Narrowband analysis; microphone 7.
Figure 18. - Continued.

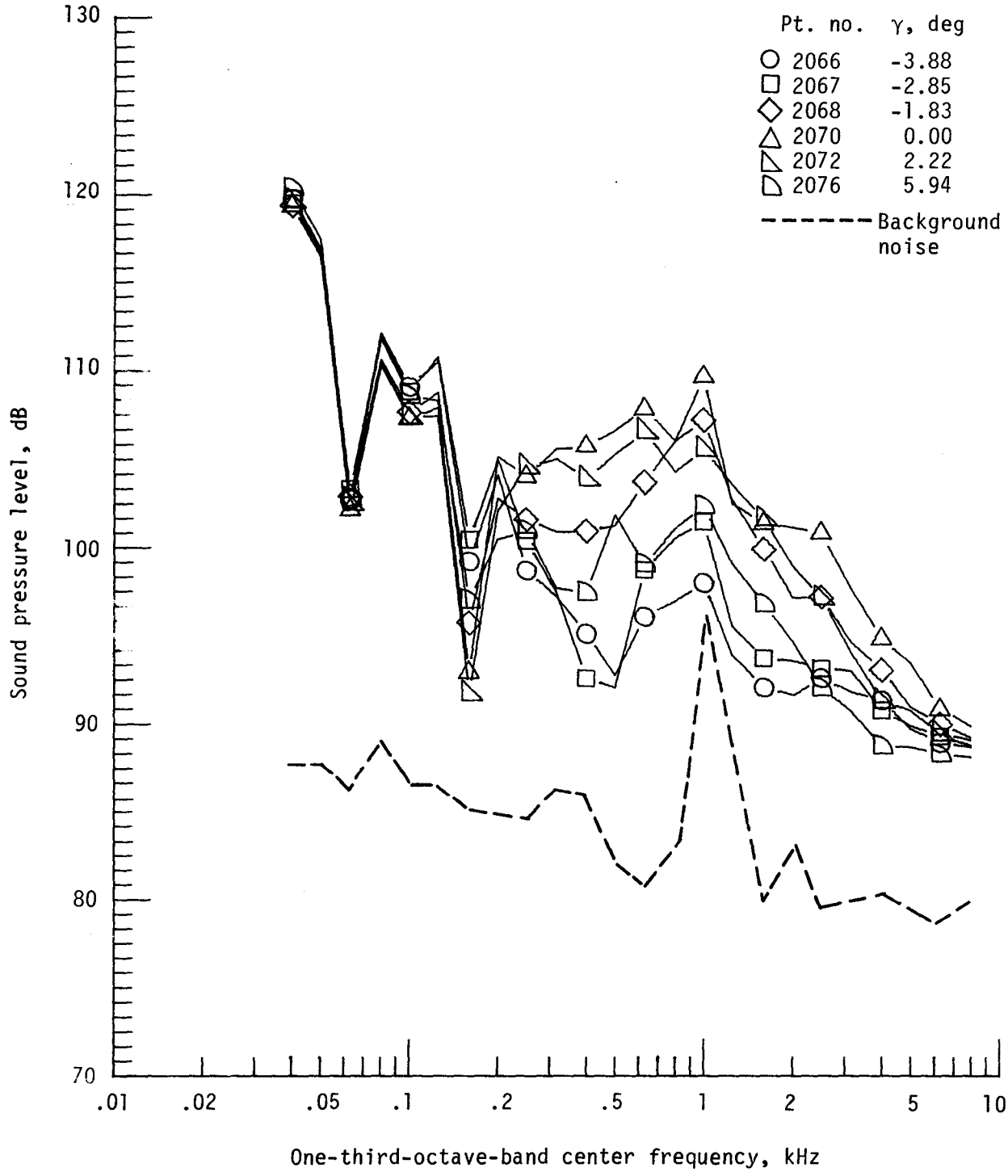

(j) One-third-octave spectra, microphone 8.

Figure 18. - Continued.

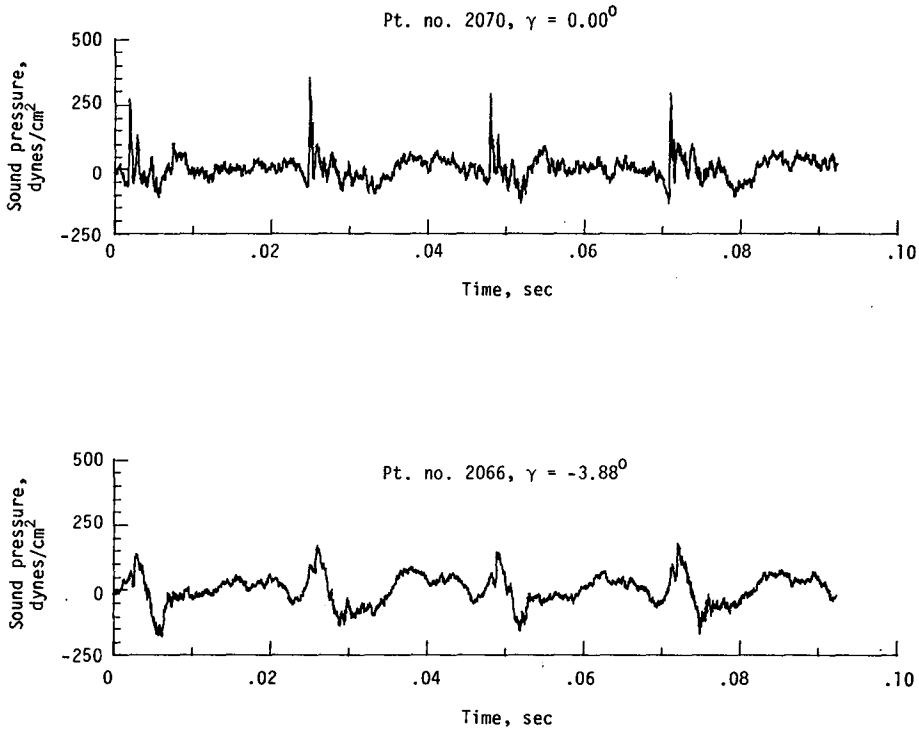

(k) Pressure-time histories; microphone 8.

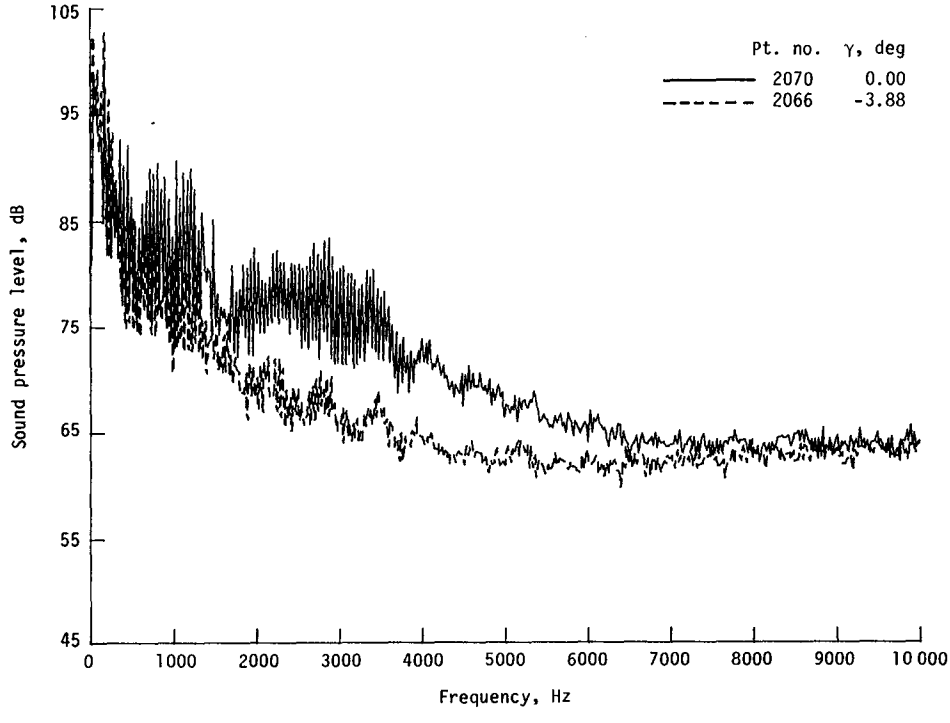

(l) Narrowband analysis; microphone 8.
Figure 18. - Concluded.

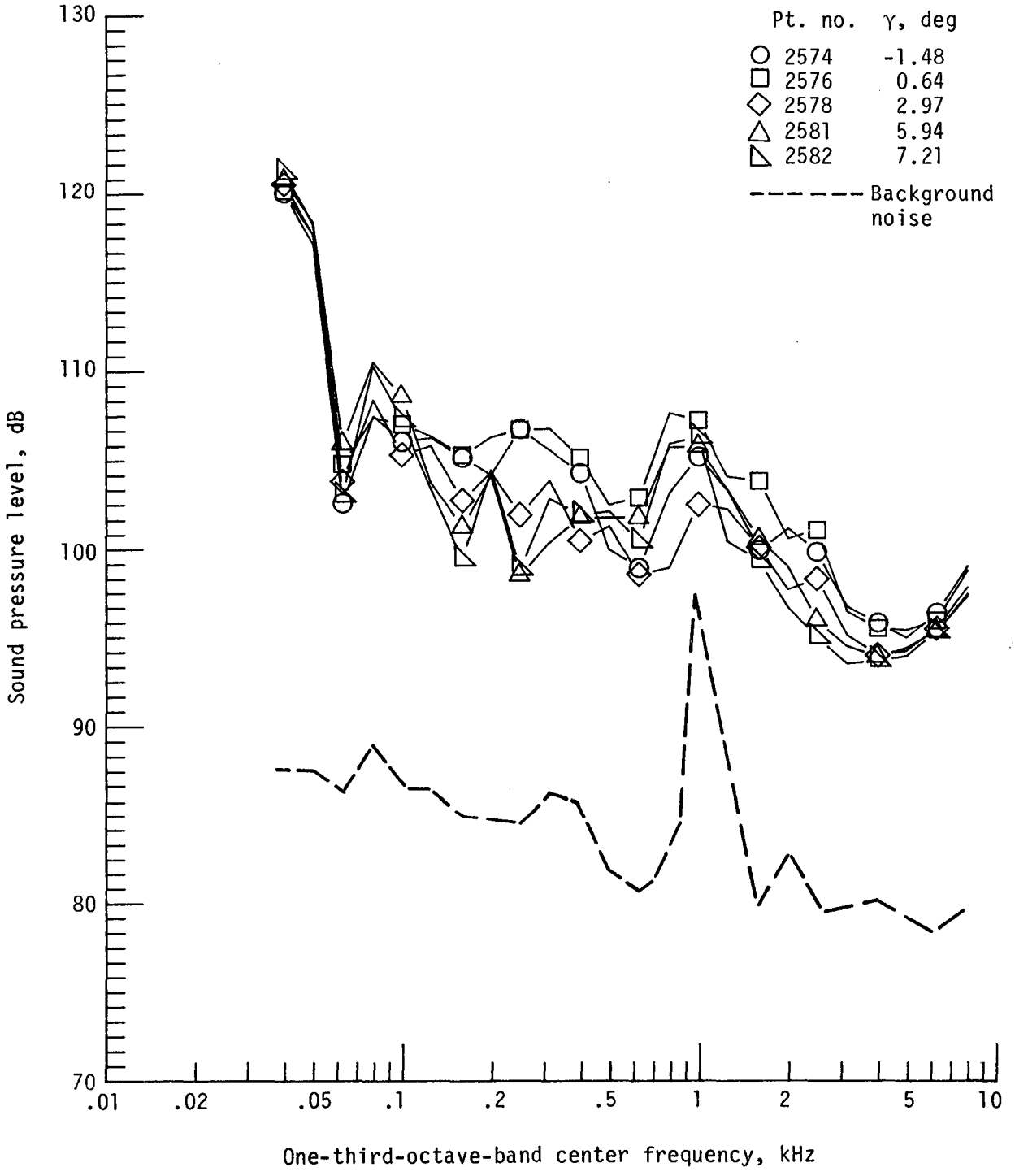

(a) One-third-octave spectra, microphone 2.

Figure 19. - Effect of descent angle variation on noise generated by helicopter model with advanced rotor system; run 200. V_∞ = 65.4 knots, C_T = .0031.

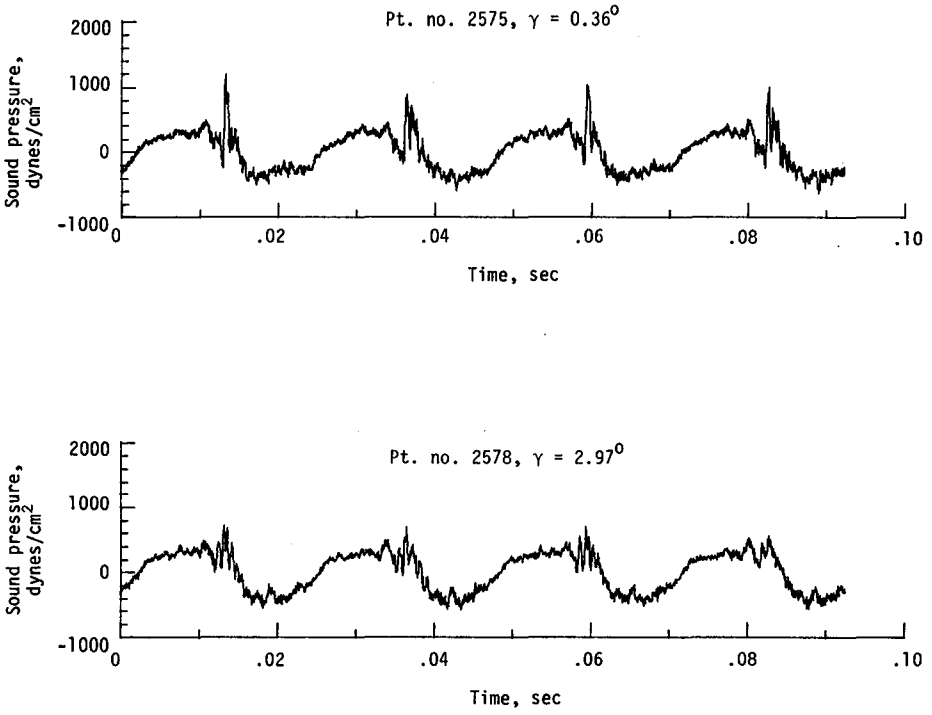

(b) Pressure-time histories; microphone 2.

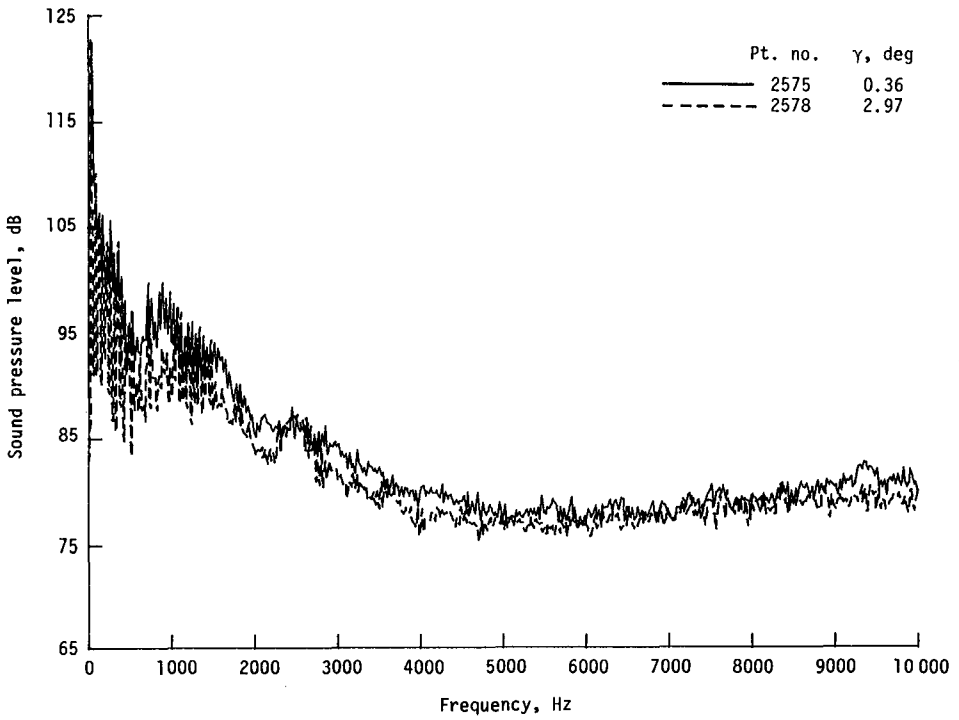

(c) Narrowband analysis; microphone 2.
Figure 19. - Continued.

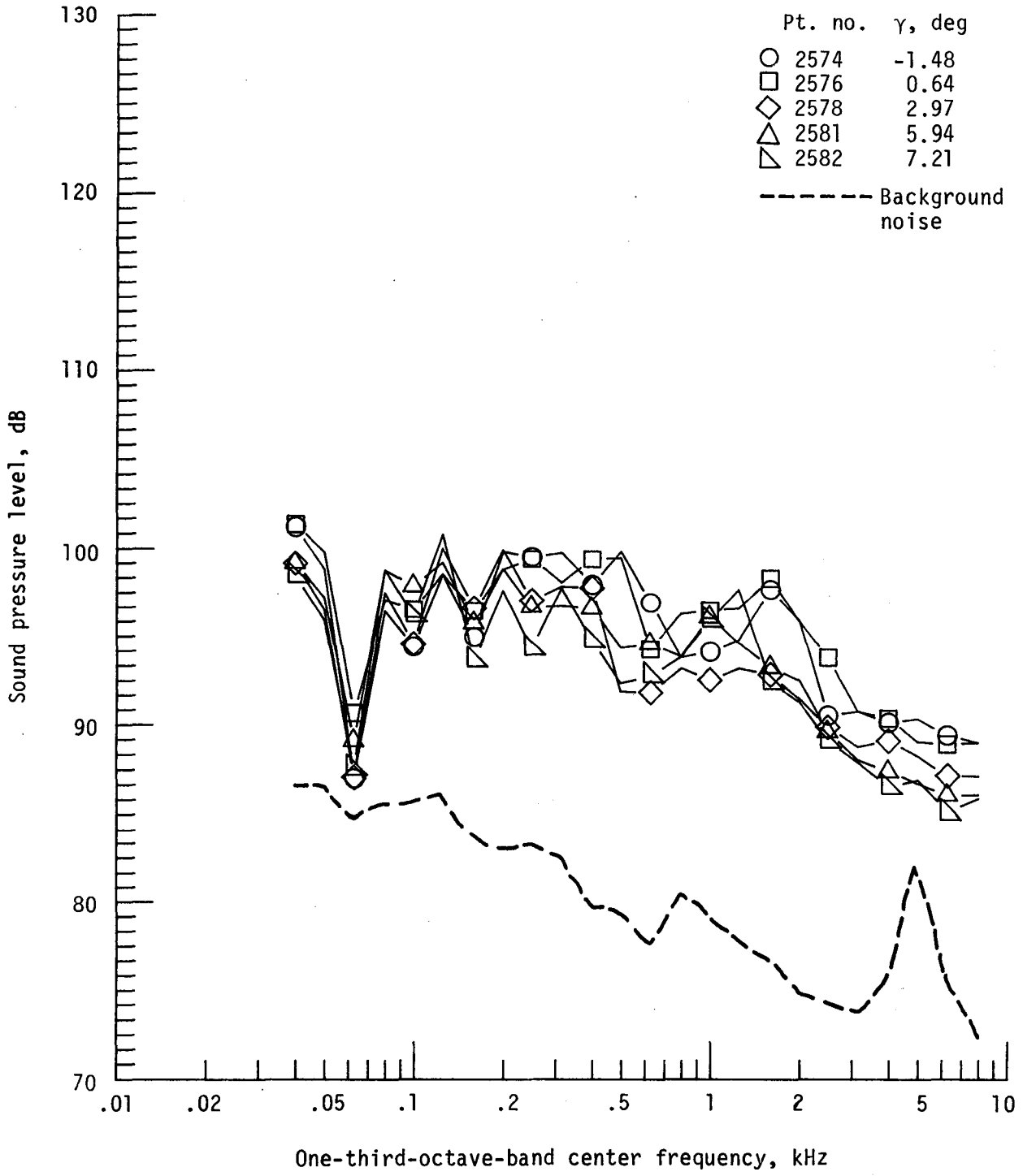

(d) One-third-octave spectra, microphone 6.

Figure 19. - Continued.

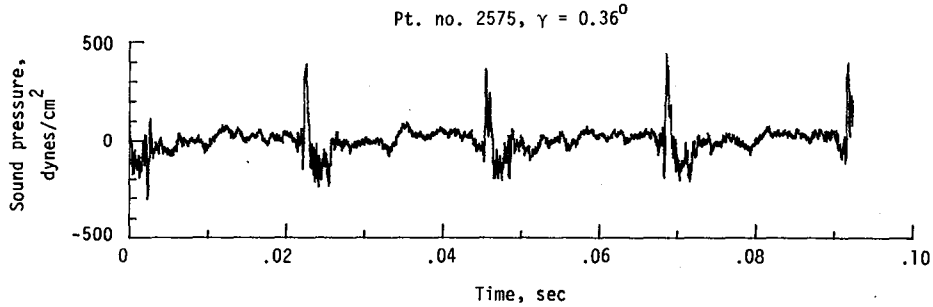

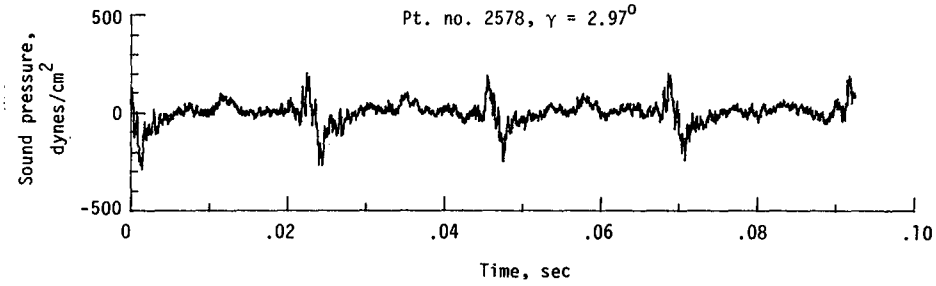

(e) Pressure-time histories; microphone 6.

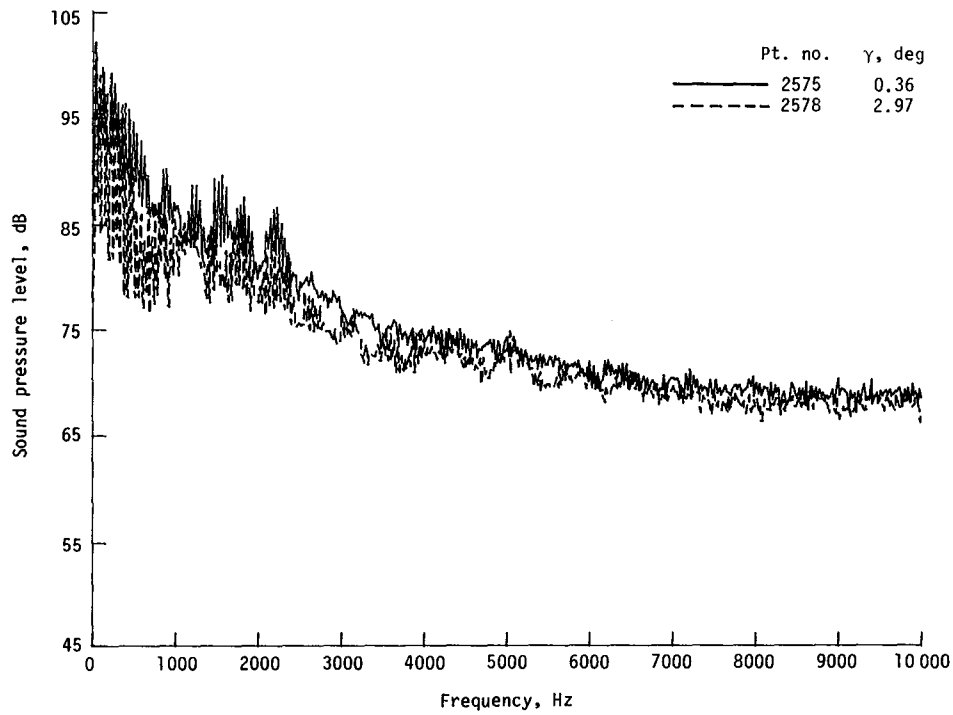

(f) Narrowband analysis; microphone 6.

Figure 19. - Continued.

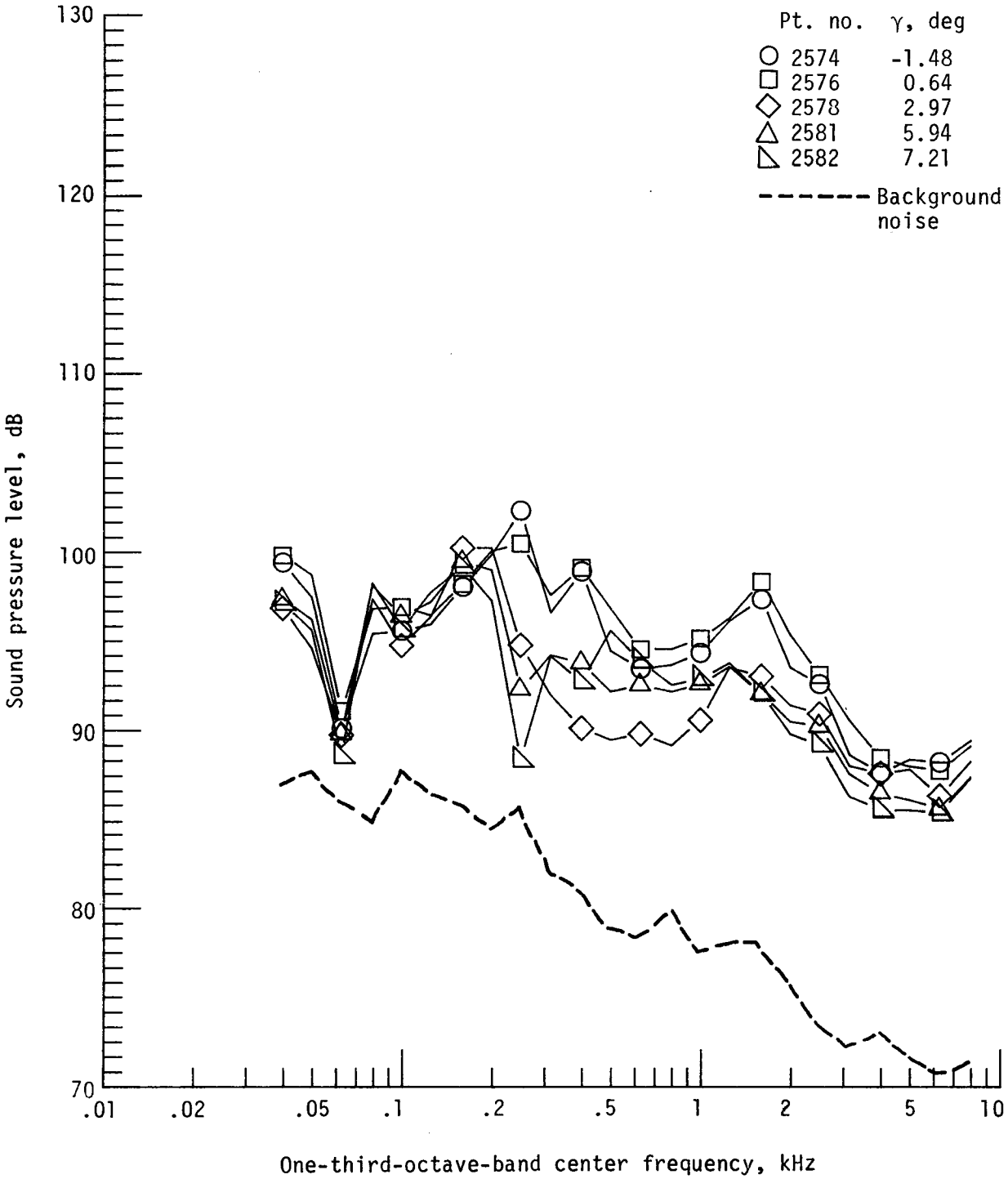

(g) One-third-octave spectra, microphone 7.

Figure 19. - Continued.

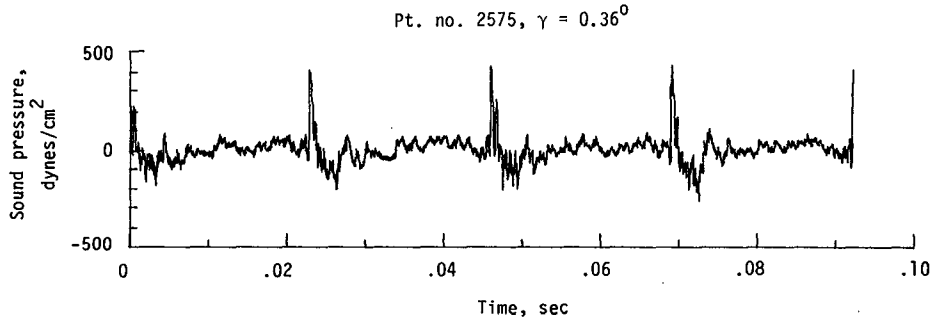

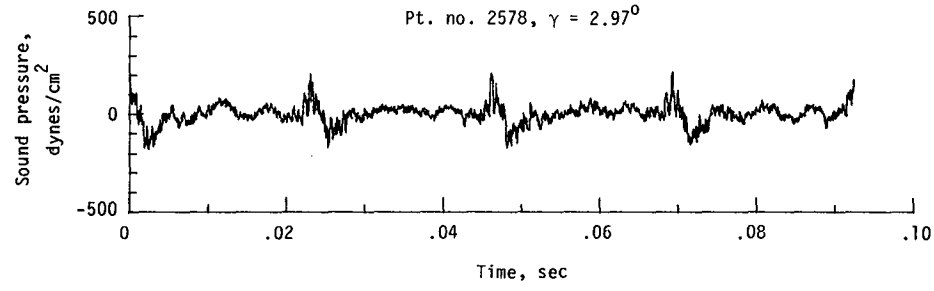

(h) Pressure-time histories; microphone 7.

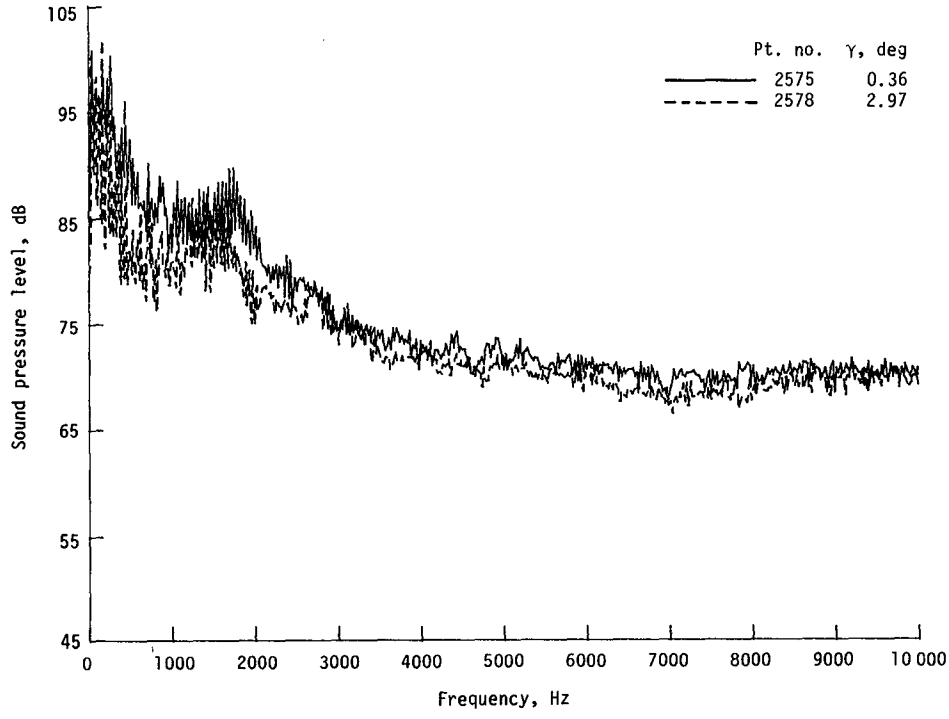

(i) Narrowband analysis; microphone 7.
Figure 19. - Continued.

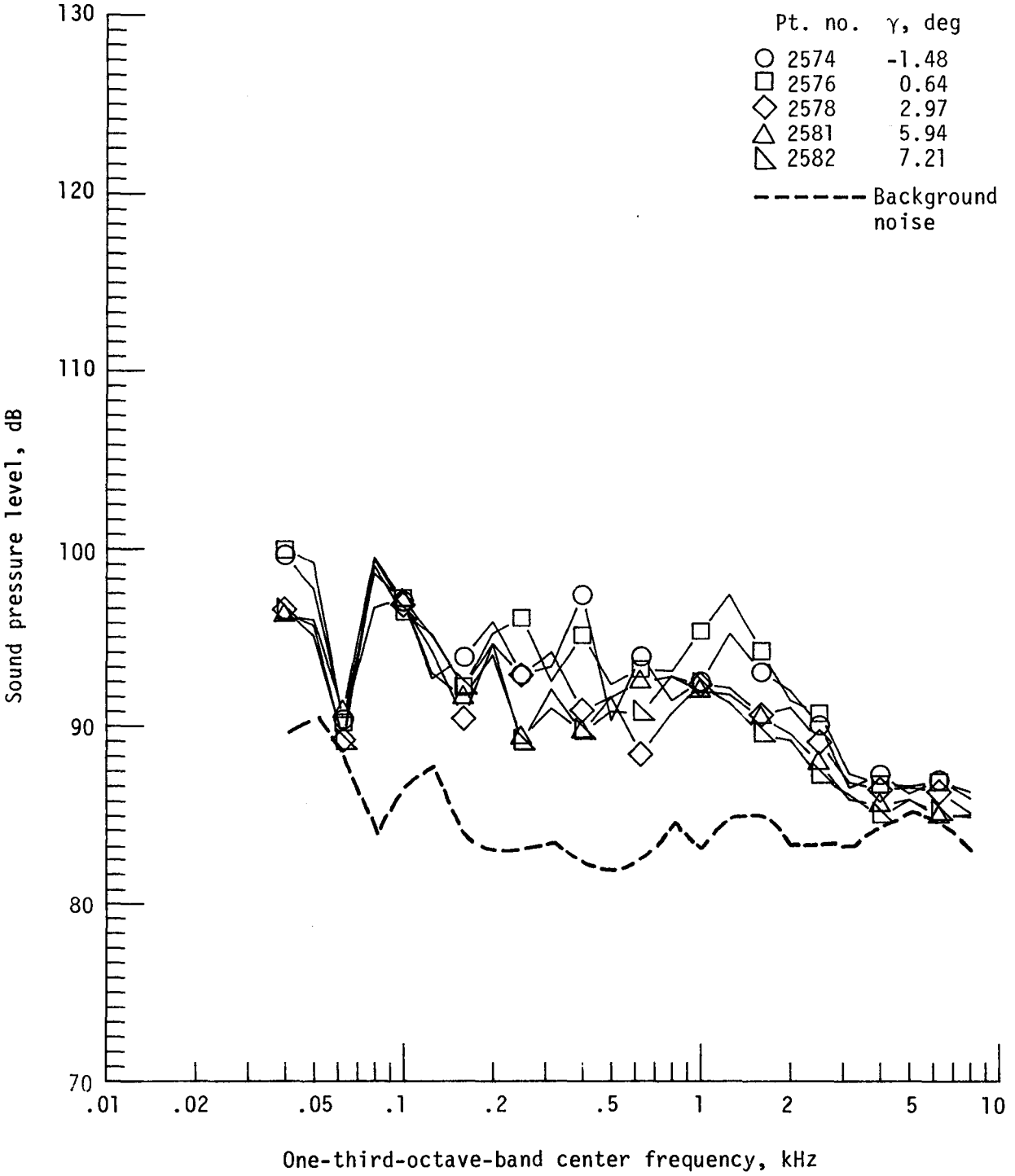

(j) One-third-octave spectra, microphone 8.

Figure 19. - Continued.

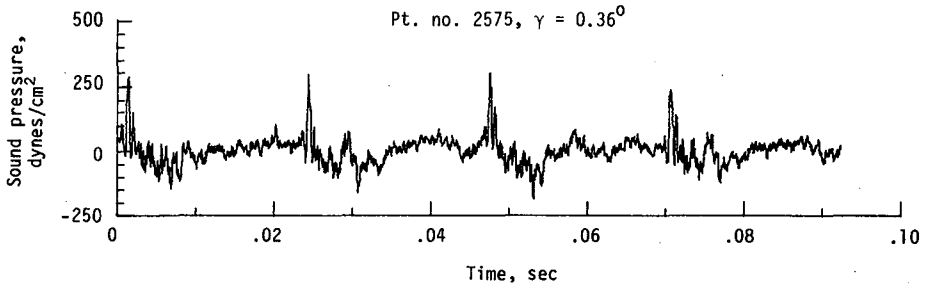

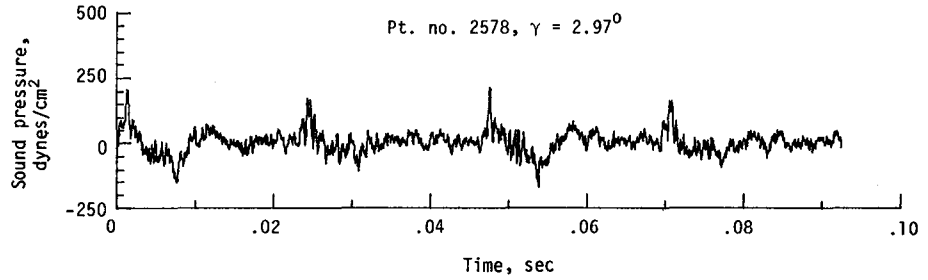

(k) Pressure-time histories; microphone 8.

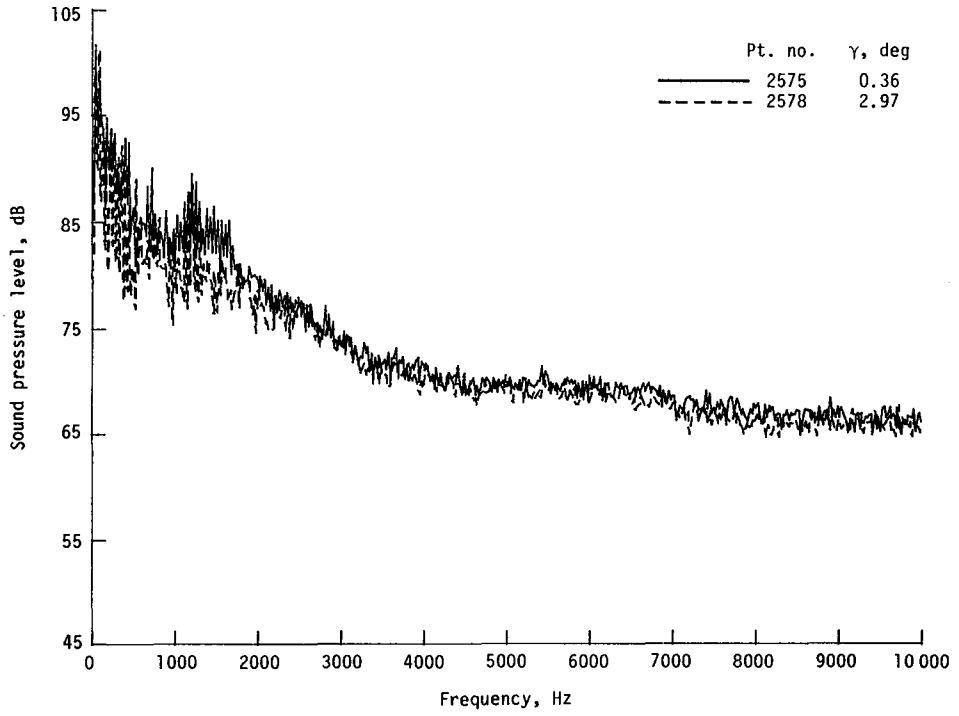

(l) Narrowband analysis; microphone 8.

Figure 19. - Concluded.

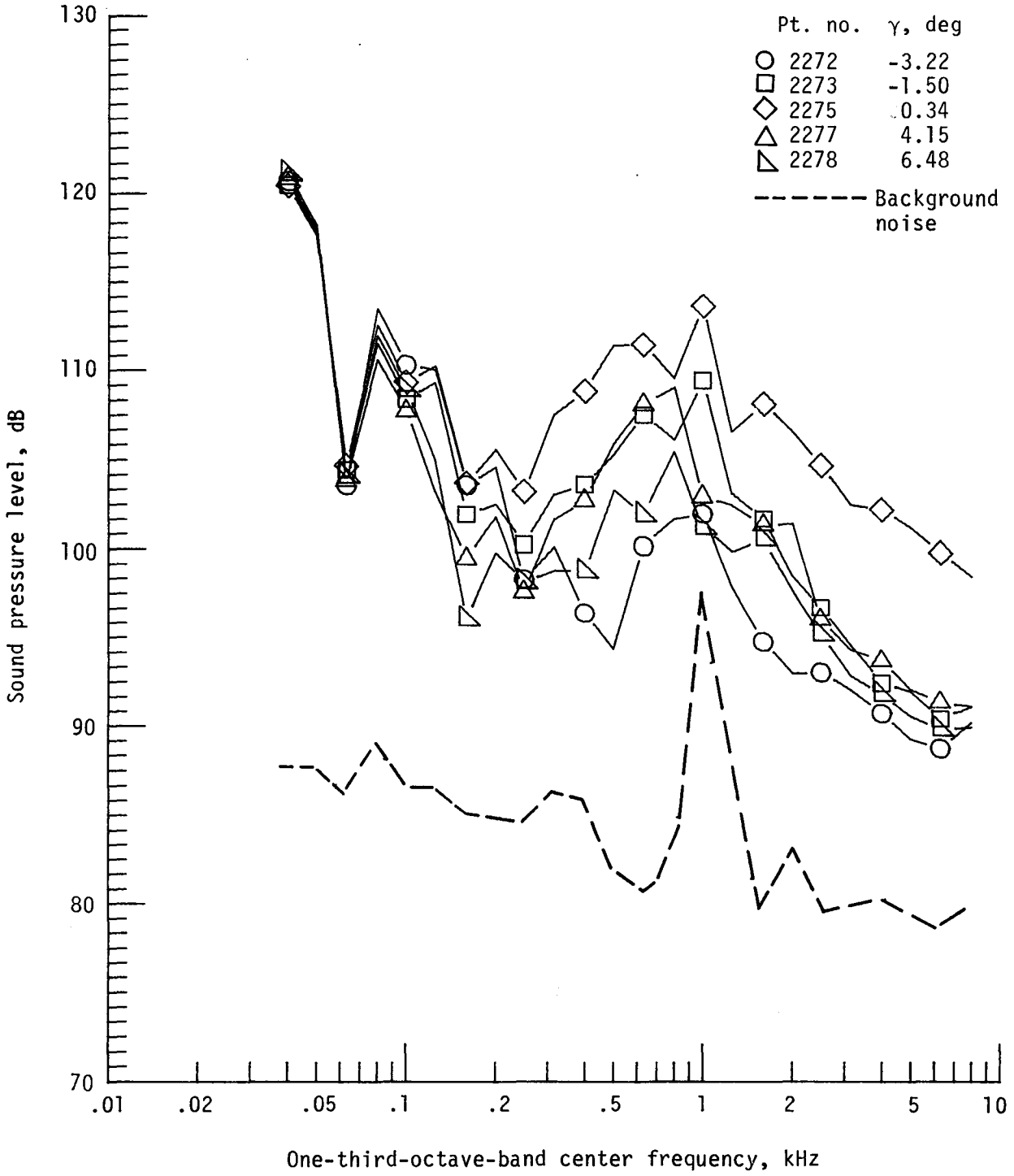

(a) One-third-octave spectra, microphone 2.

Figure 20. - Effect of descent angle variation on noise generated by helicopter model with standard rotor system, run 182; V_∞ = 65.0 knots, C_T = .0036.

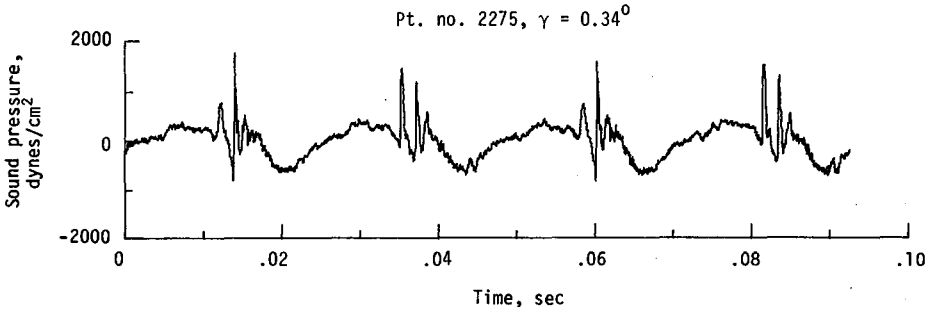

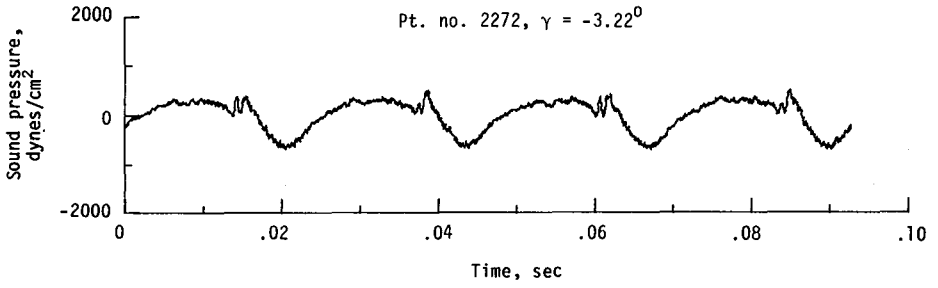

(b) Pressure-time histories; microphone 2.

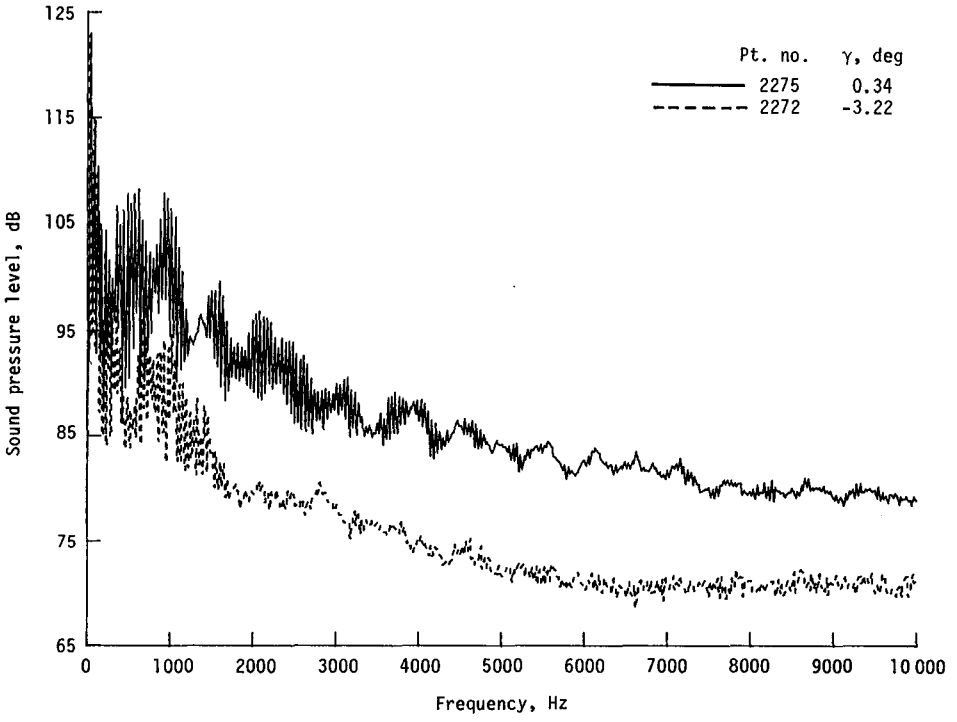

(c) Narrowband analysis; microphone 2.
Figure 20. - Continued.

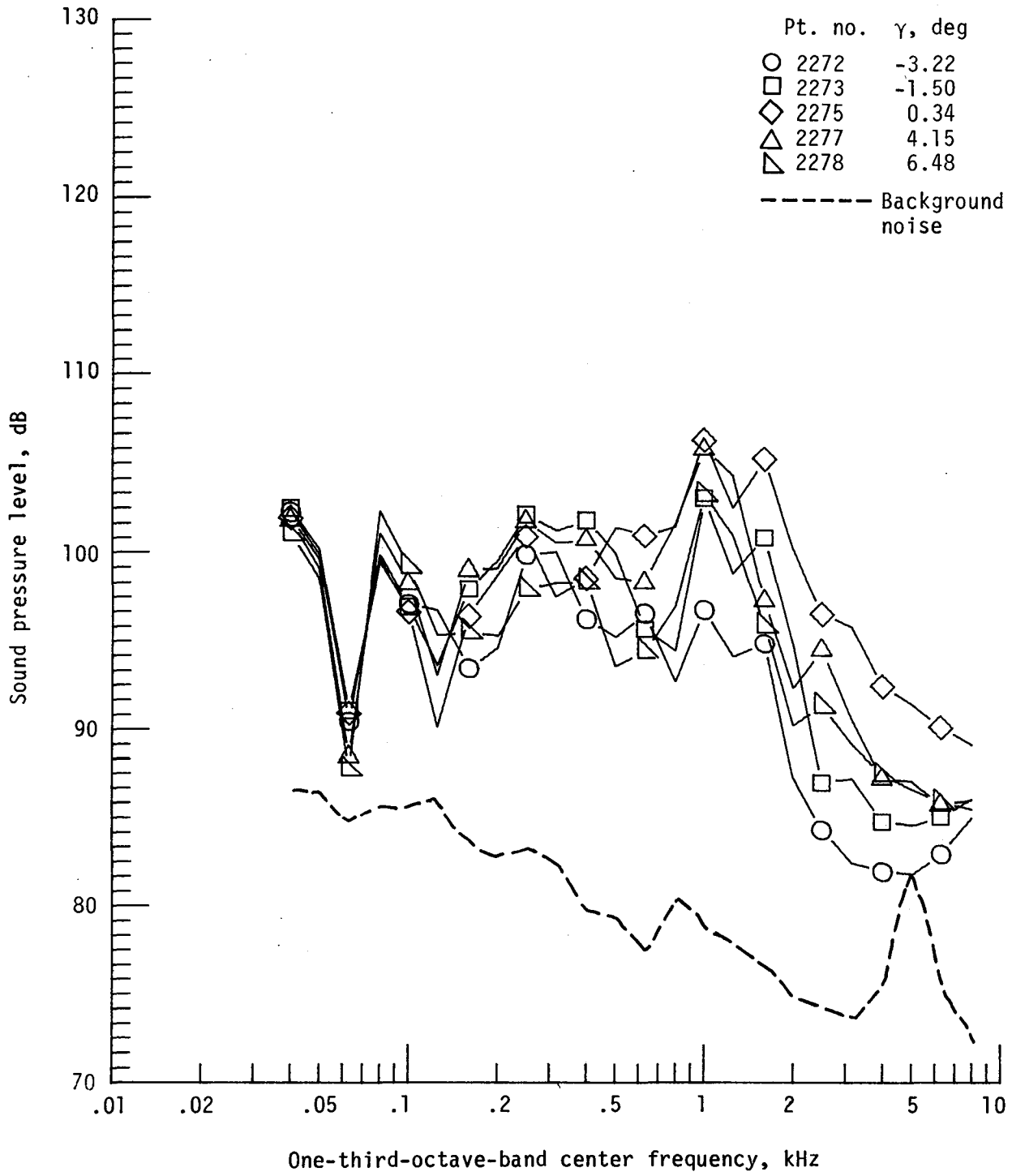

(d) One-third-octave spectra, microphone 6.

Figure 20. - Continued.

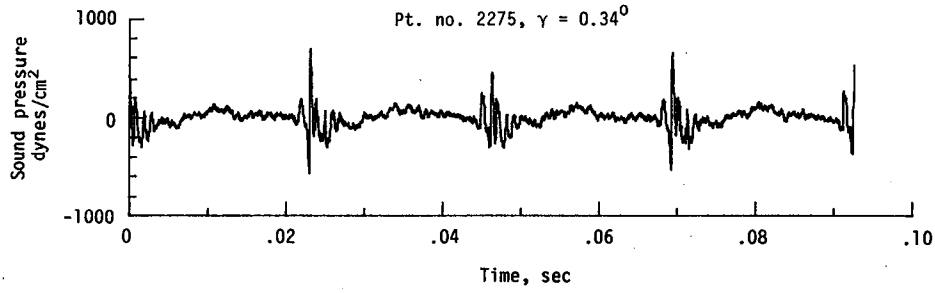

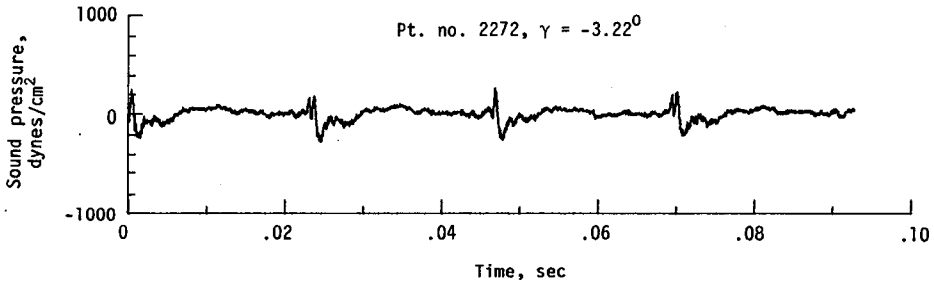

(e) Pressure-time histories; microphone 6.

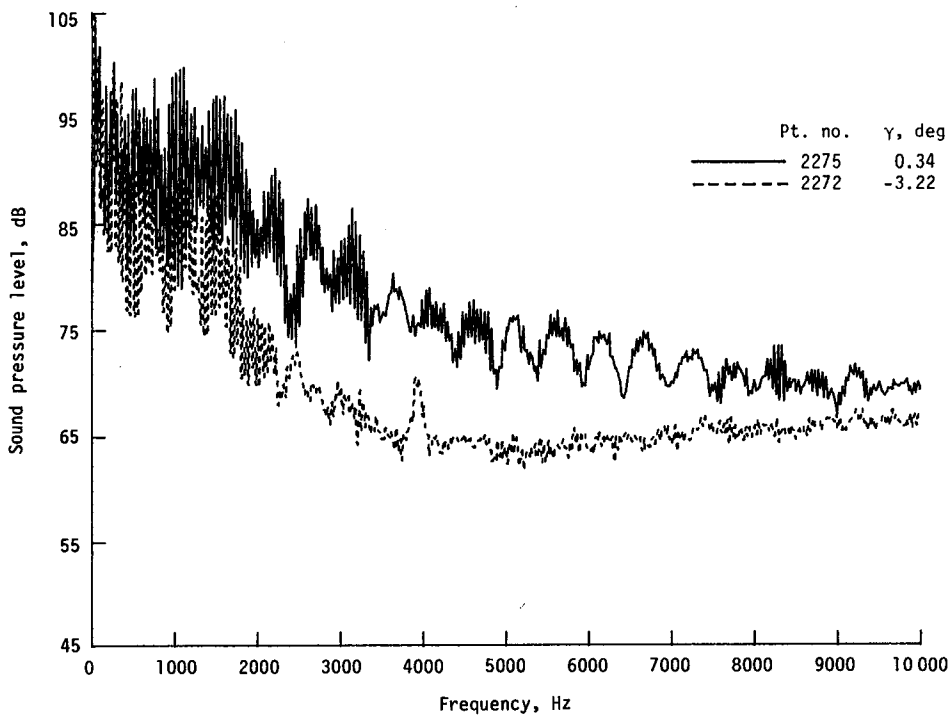

(f) Narrowband analysis; microphone 6.
Figure 20. - Continued.

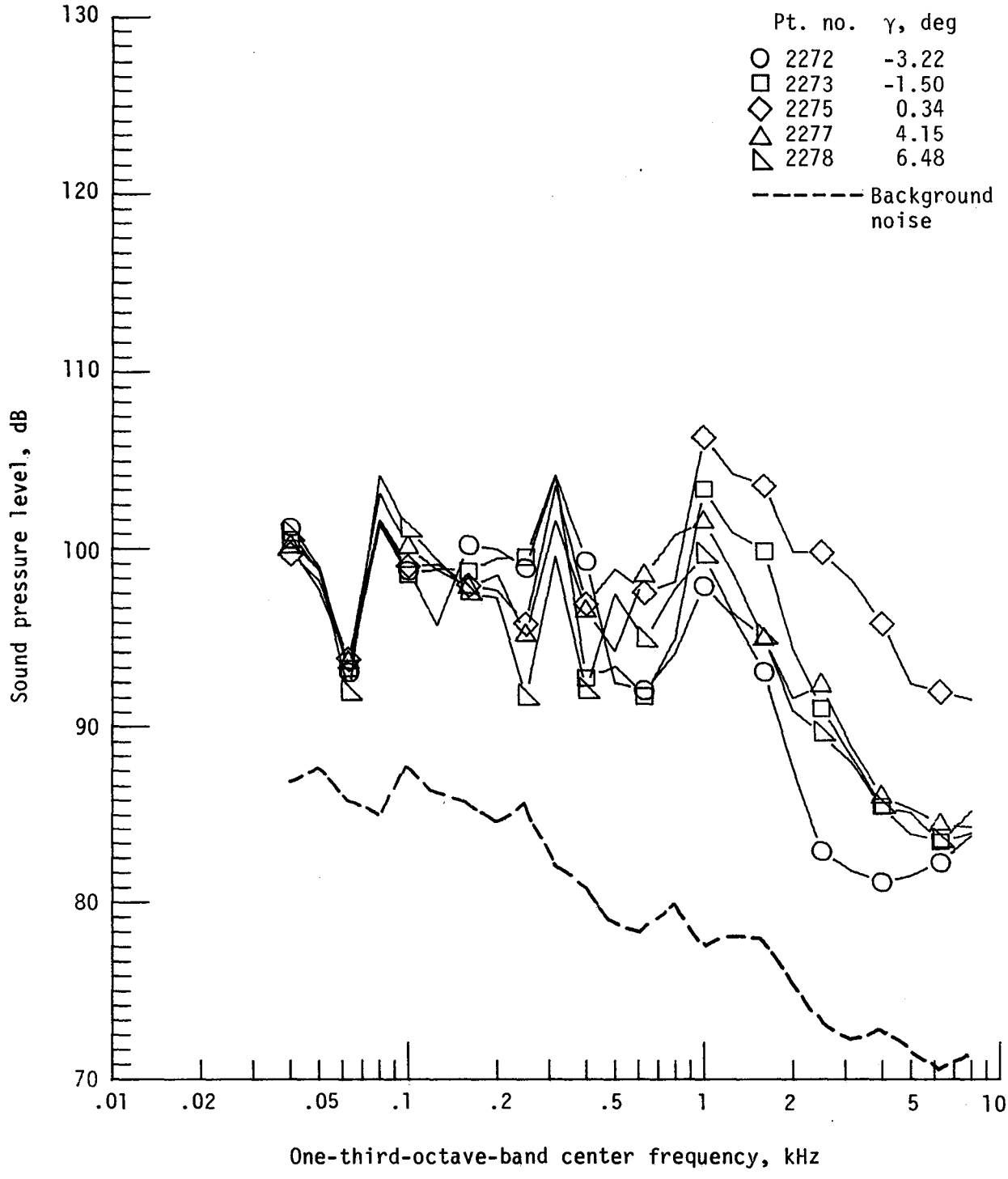

(g) One-third-octave spectra, microphone 7.

Figure 20. - Continued.

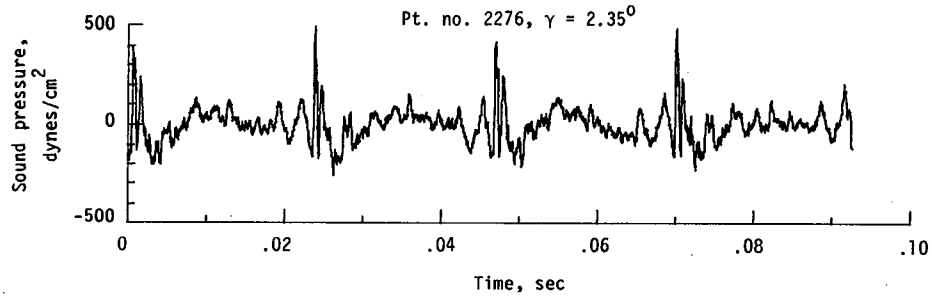

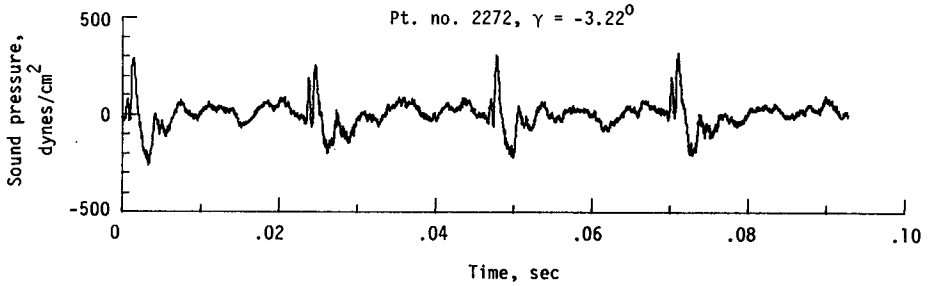

(h) Pressure-time histories; microphone 7.

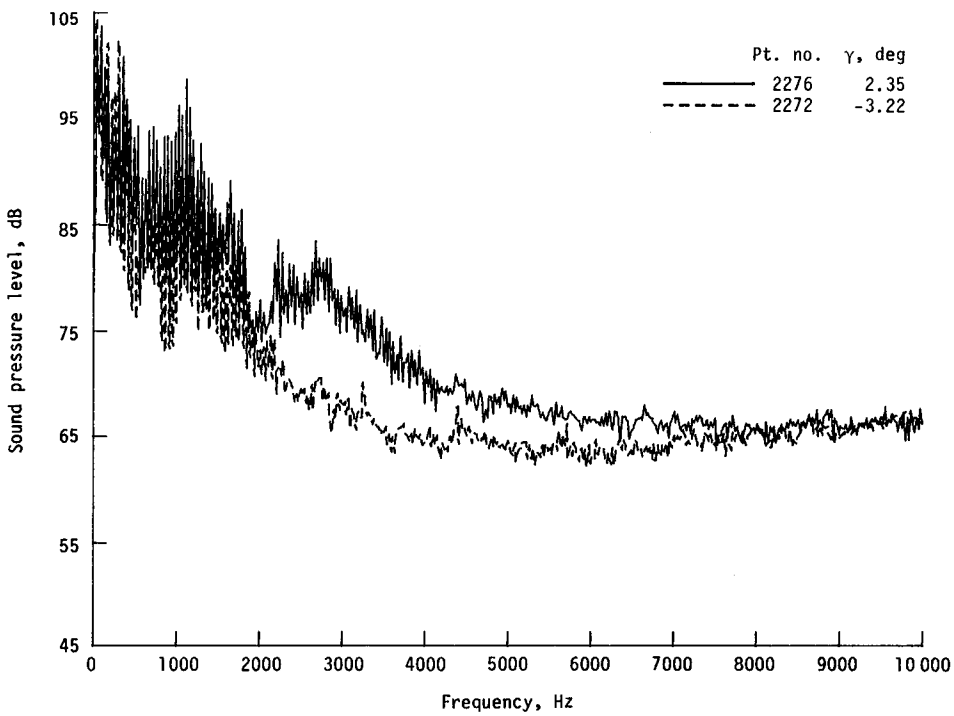

(i) Narrowband analysis; microphone 7.
Figure 20. - Continued.

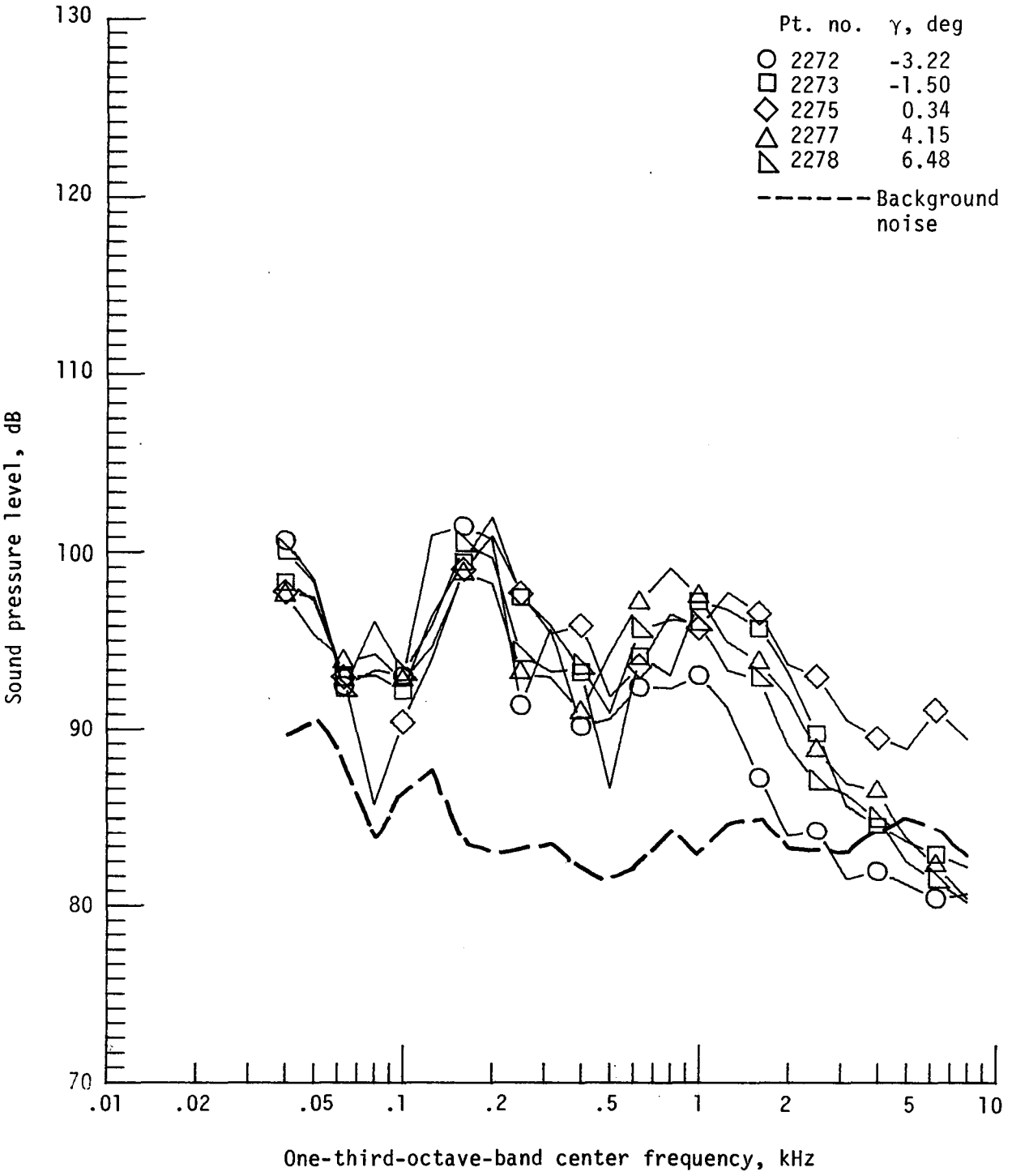

(j) One-third-octave spectra, microphone 8.

Figure 20. - Continued.

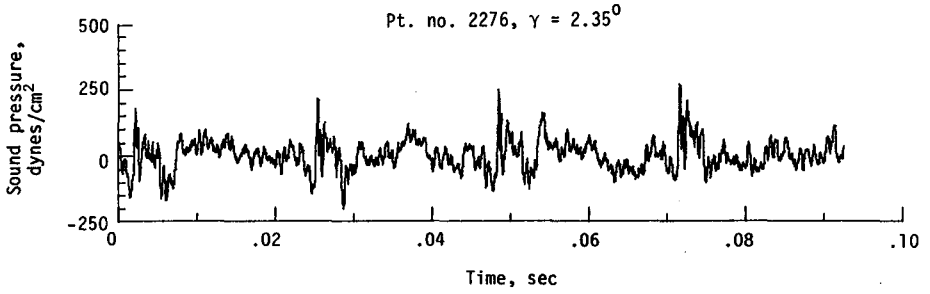

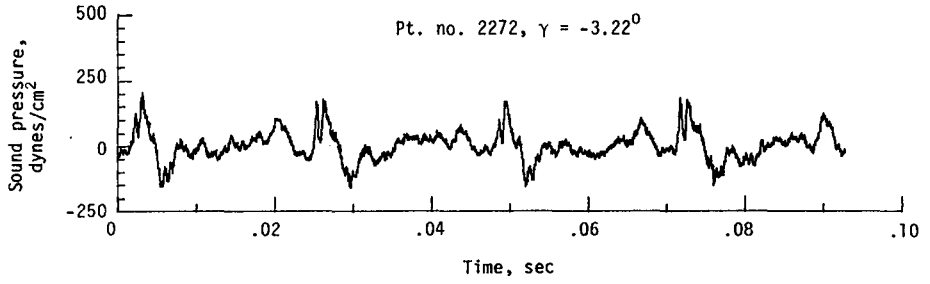

(k) Pressure-time histories; microphone 8.

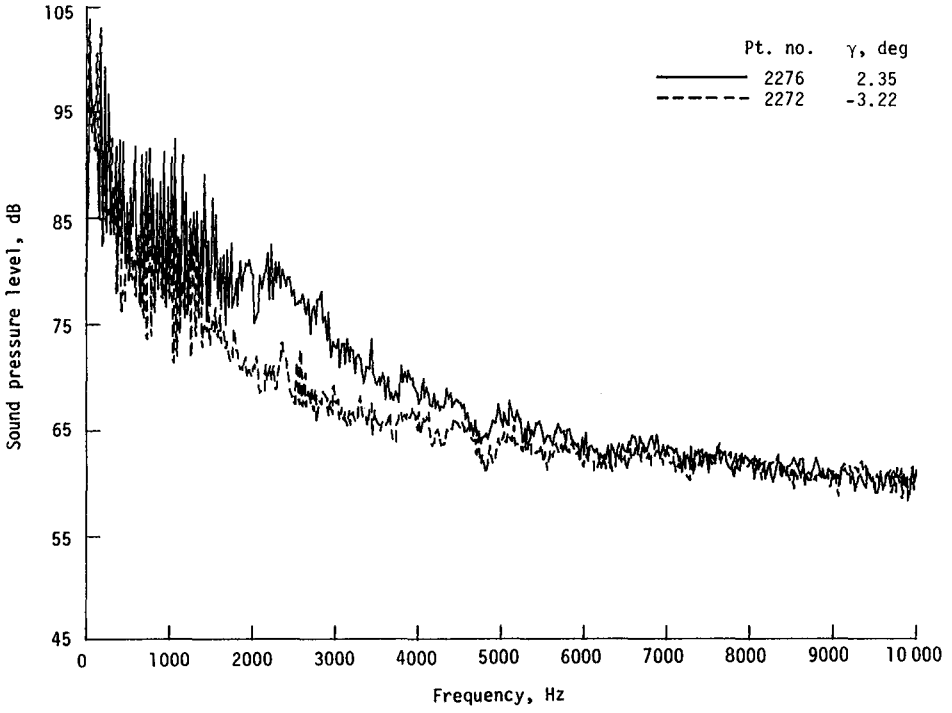

(l) Narrowband analysis; microphone 8.

Figure 20. - Concluded.

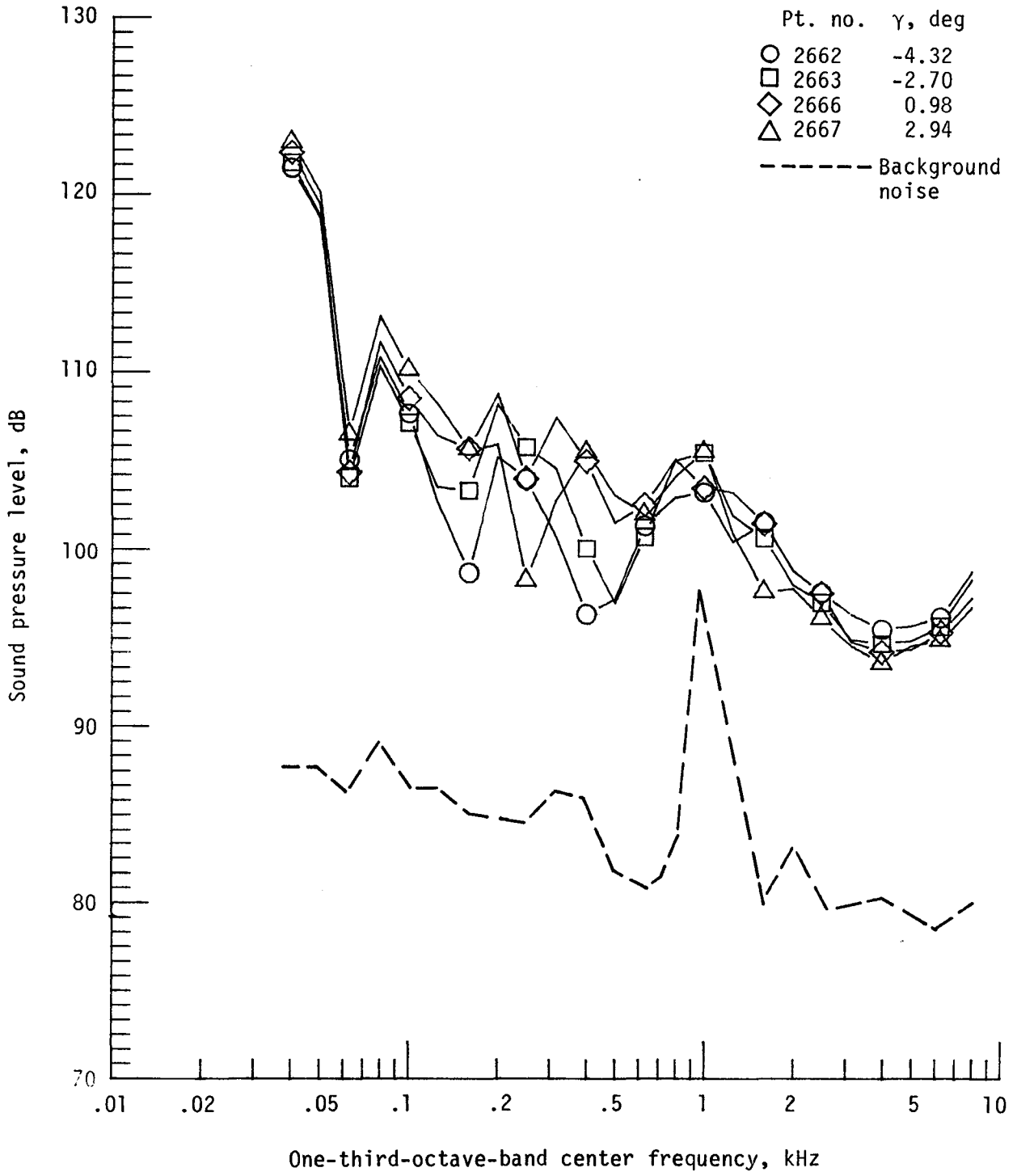

(a) One-third-octave spectra, microphone 2.

Figure 21. - Effect of descent angle variation on noise generated by helicopter model with advanced rotor system, run 214. V_∞ = 65.2 knots, C_T = .0036.

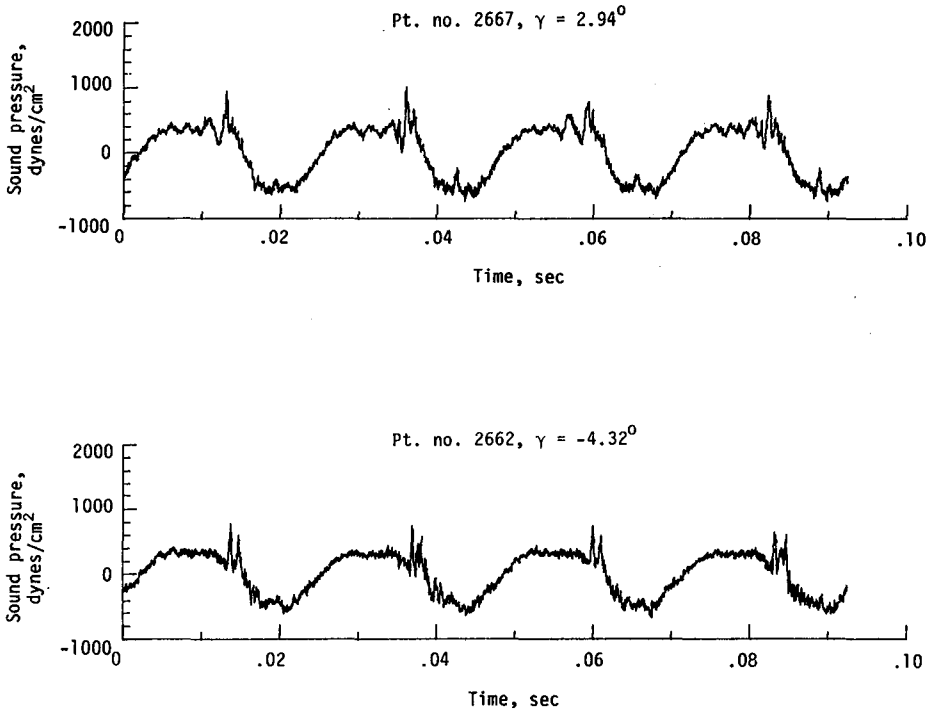

(b) Pressure-time histories; microphone 2.

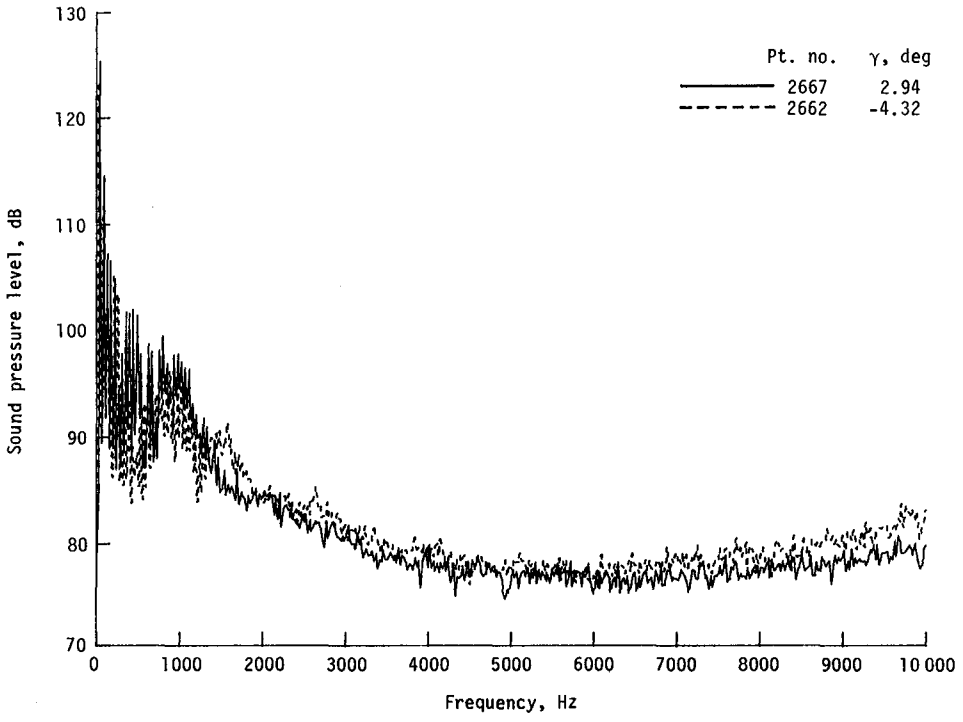

(c) Narrowband analysis; microphone 2.

Figure 21. - Continued.

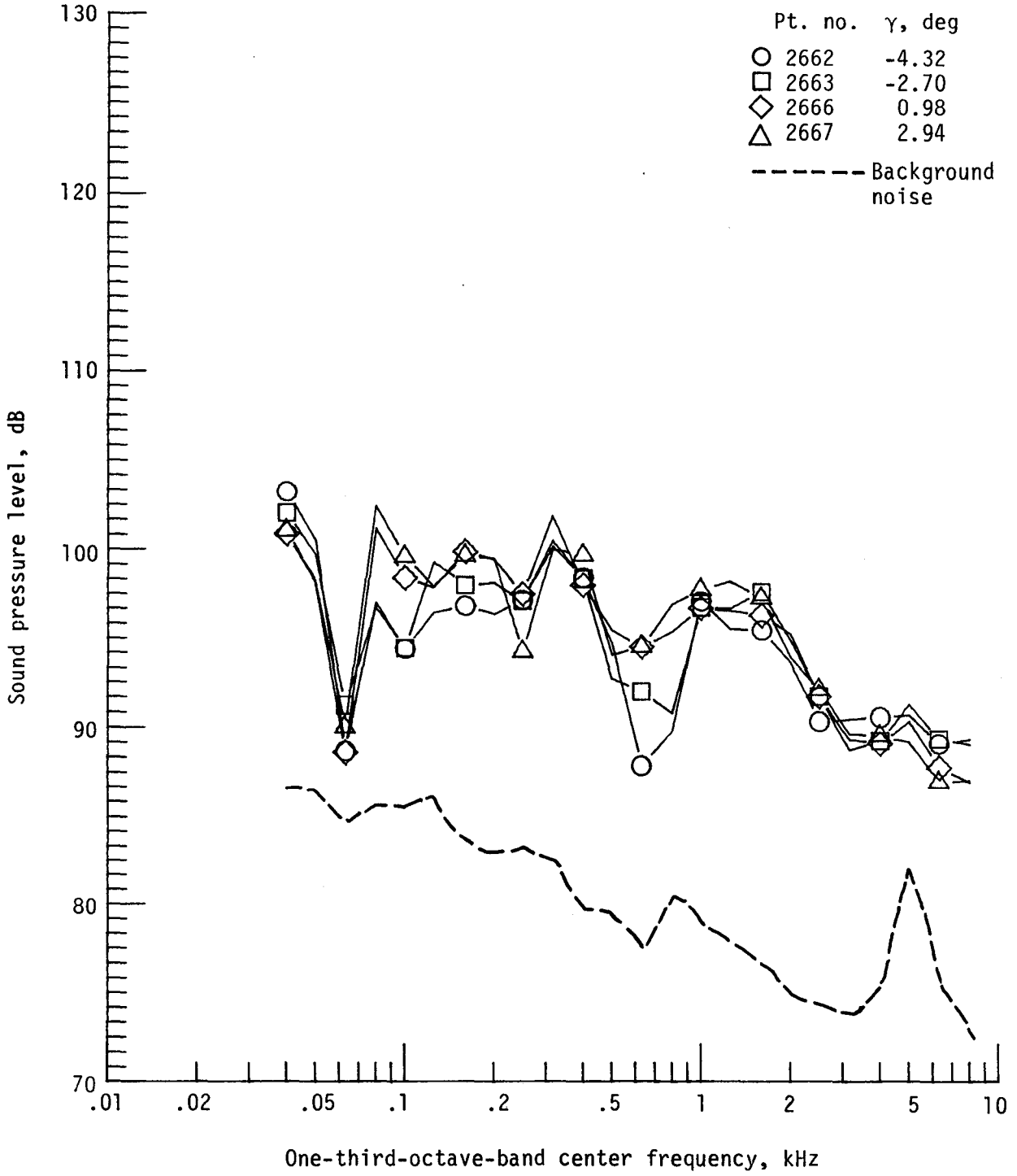

(d) One-third-octave spectra, microphone 6.

Figure 21. - Continued.

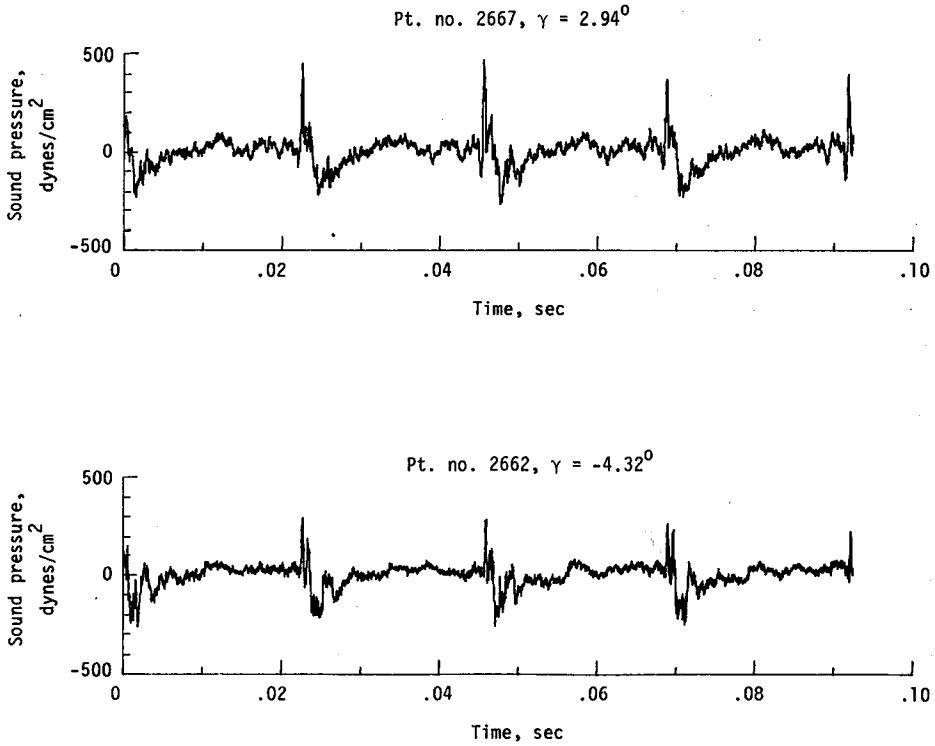

(e) Pressure-time histories; microphone 6.

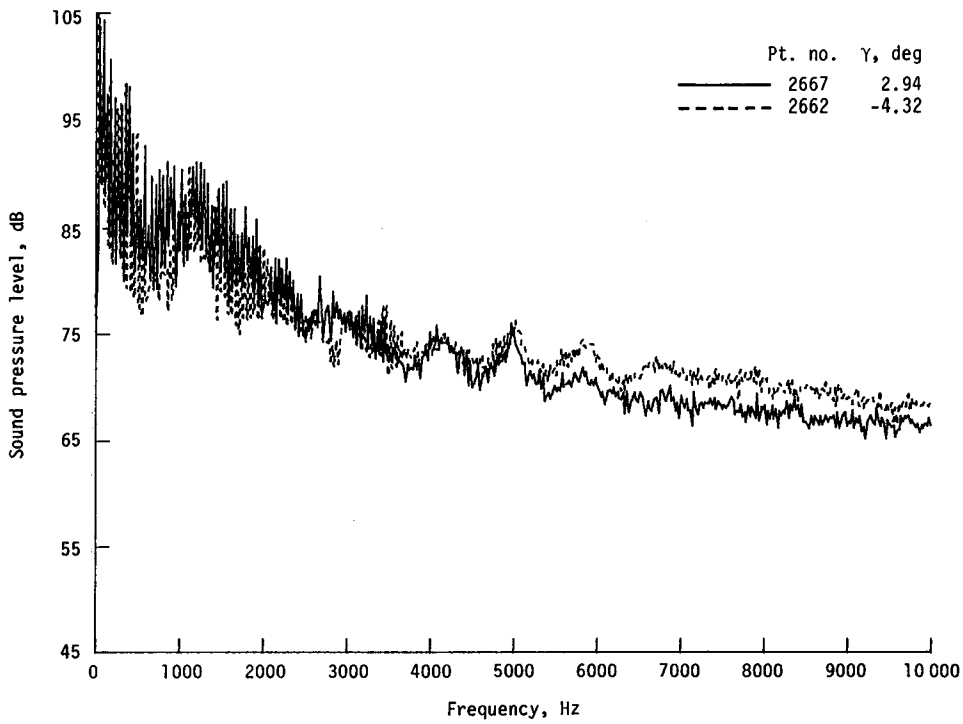

(f) Narrowband analysis; microphone 6.

Figure 21. - Continued.

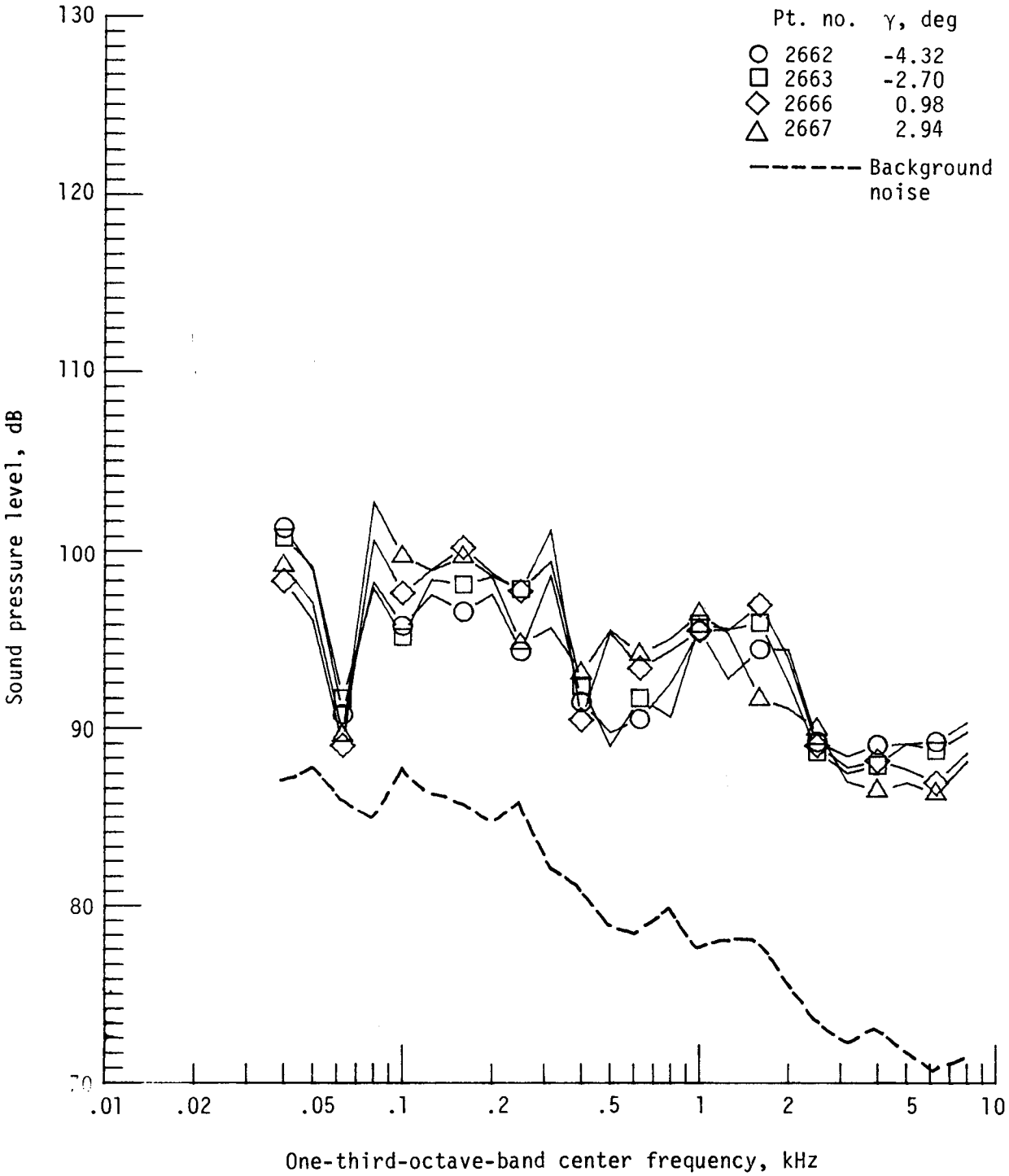

(g) One-third-octave spectra, microphone 7.

Figure 21. - Continued.

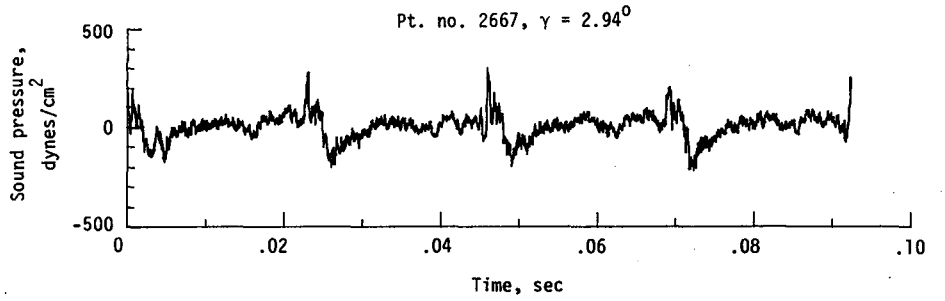

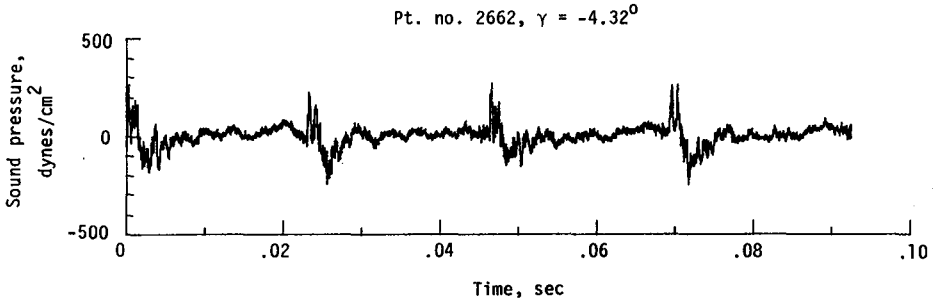

(h) Pressure-time histories; microphone 7.

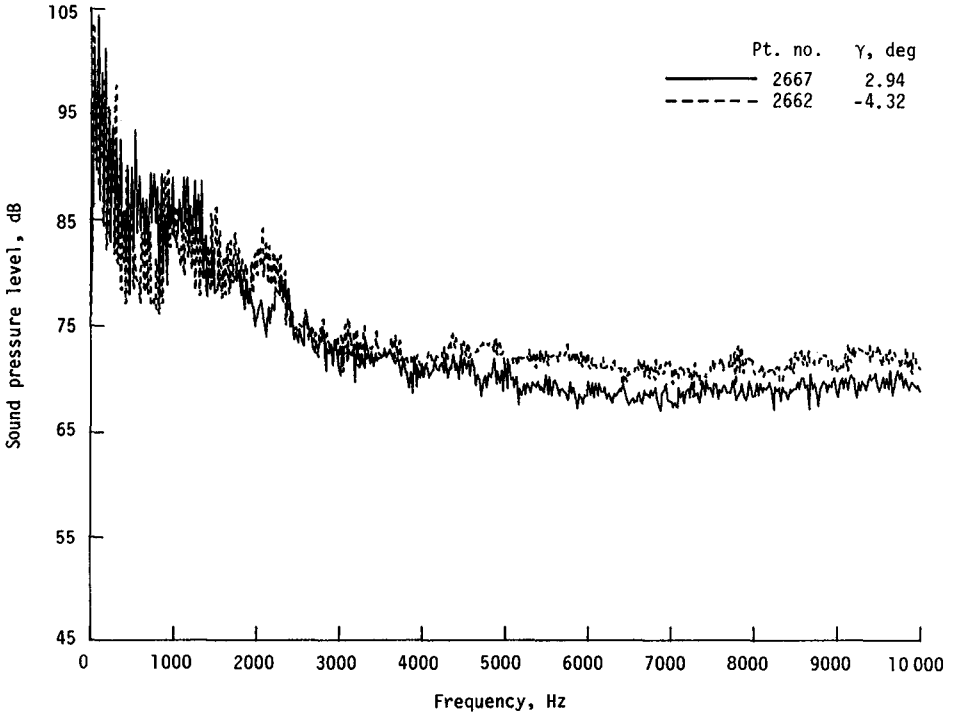

(i) Narrowband analysis; microphone 7.

Figure 21. - Continued.

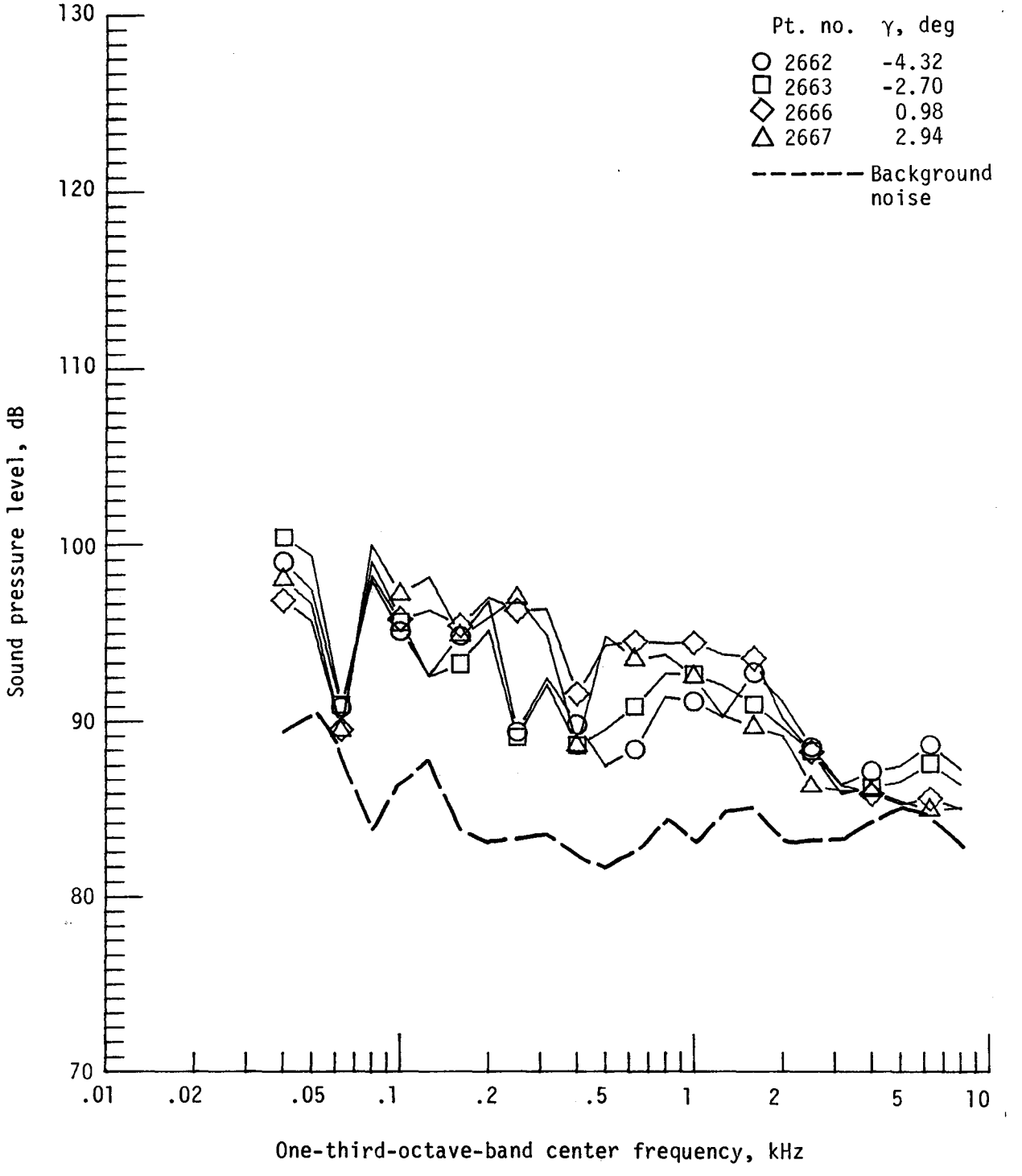

(j) One-third-octave spectra, microphone 8.

Figure 21. - Continued.

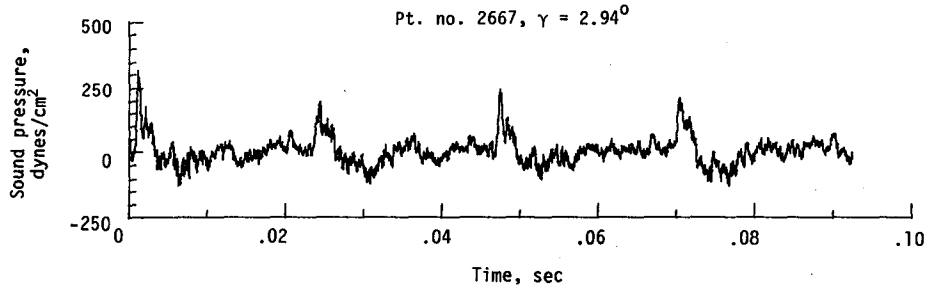

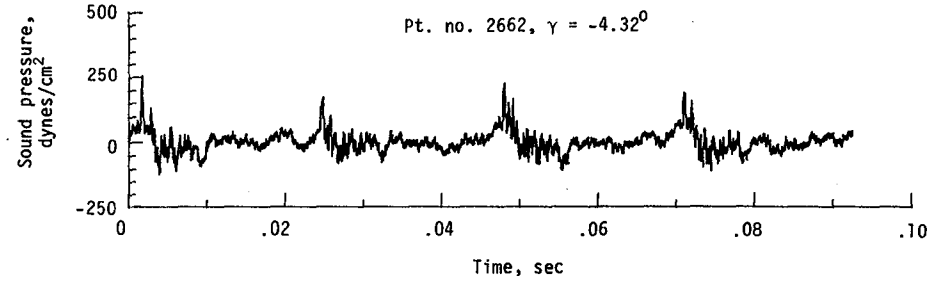

(k) Pressure-time histories; microphone 8.

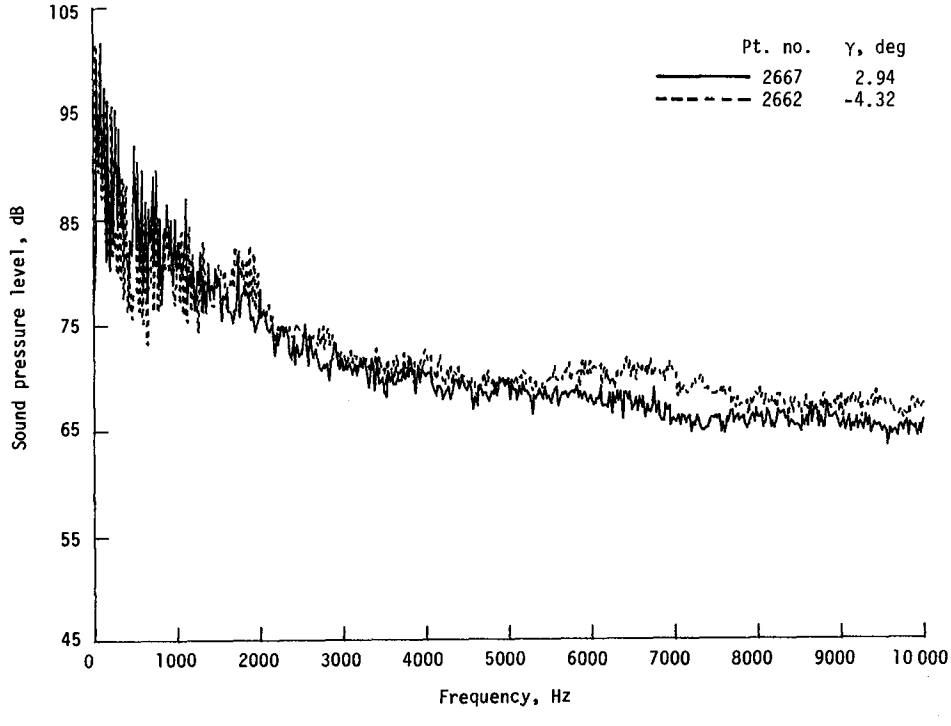

(l) Narrowband analysis; microphone 8.

Figure 21. - Concluded.

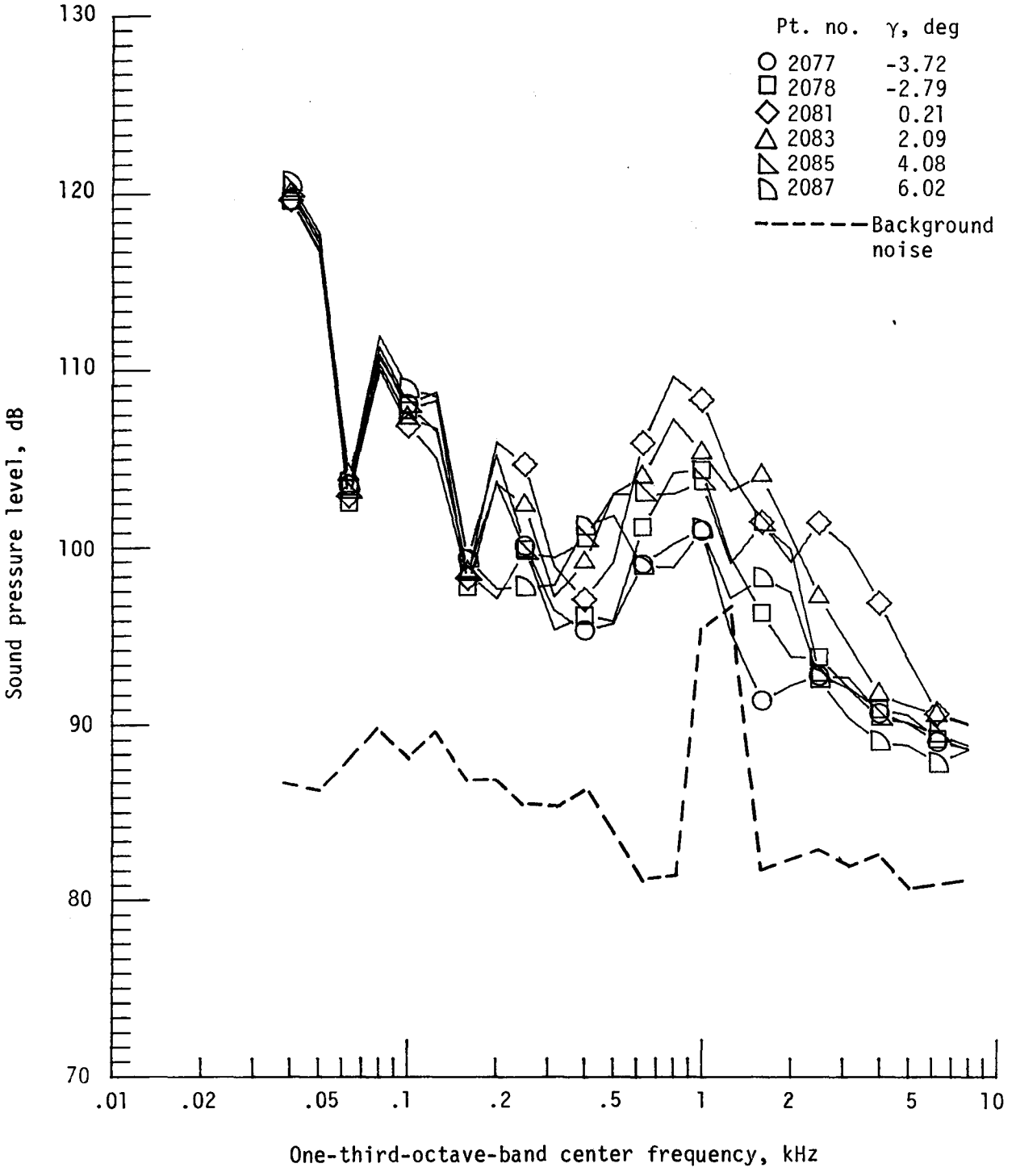

(a) One-third-octave spectra, microphone 2.

Figure 22. - Effect of descent angle variation on noise generated by helicopter model with standard rotor system, run 160. V_∞ = 70.2 knots, C_T = .0032.

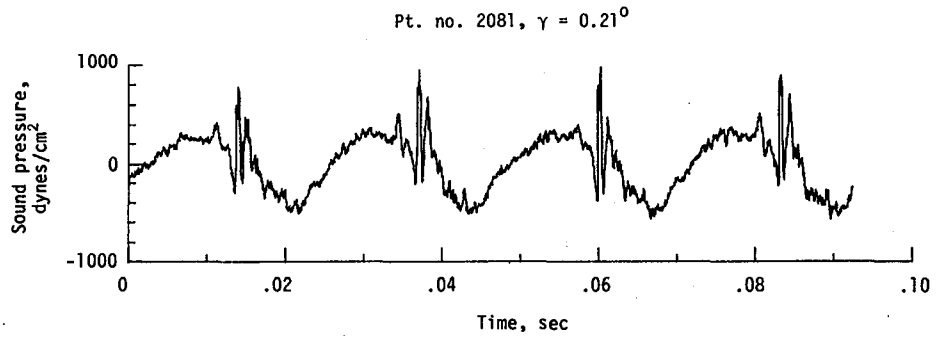

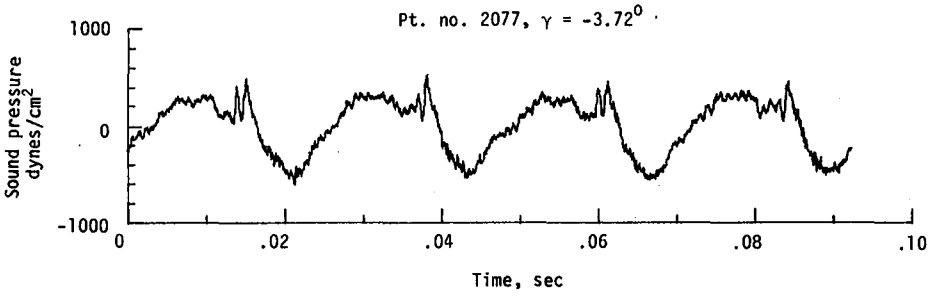

(b) Pressure-time histories; microphone 2.

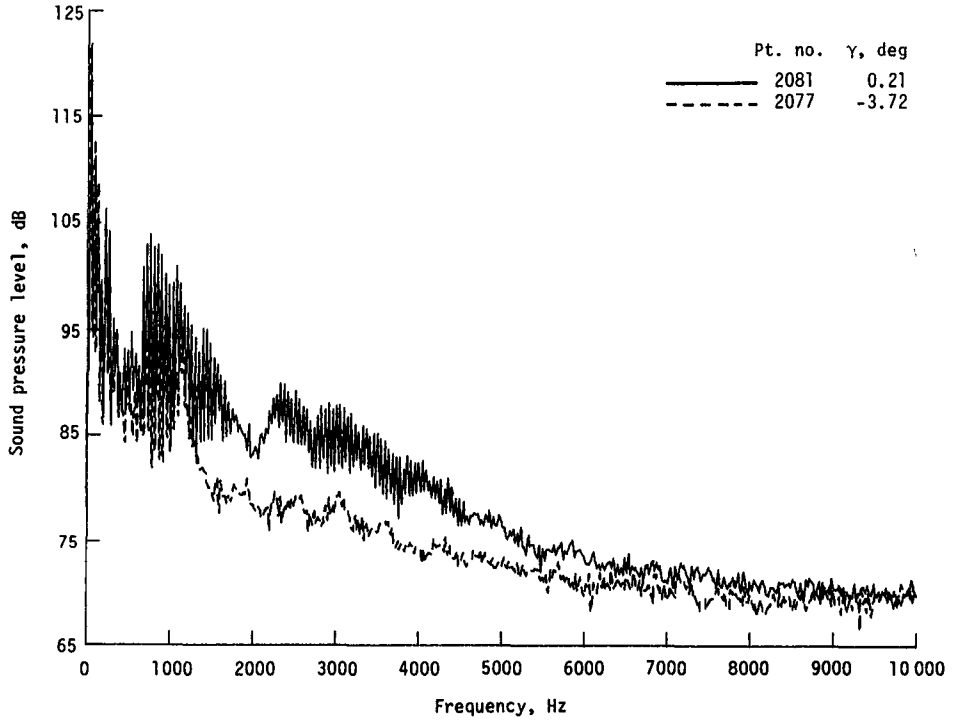

(c) Narrowband analysis; microphone 2.
Figure 22. - Continued.

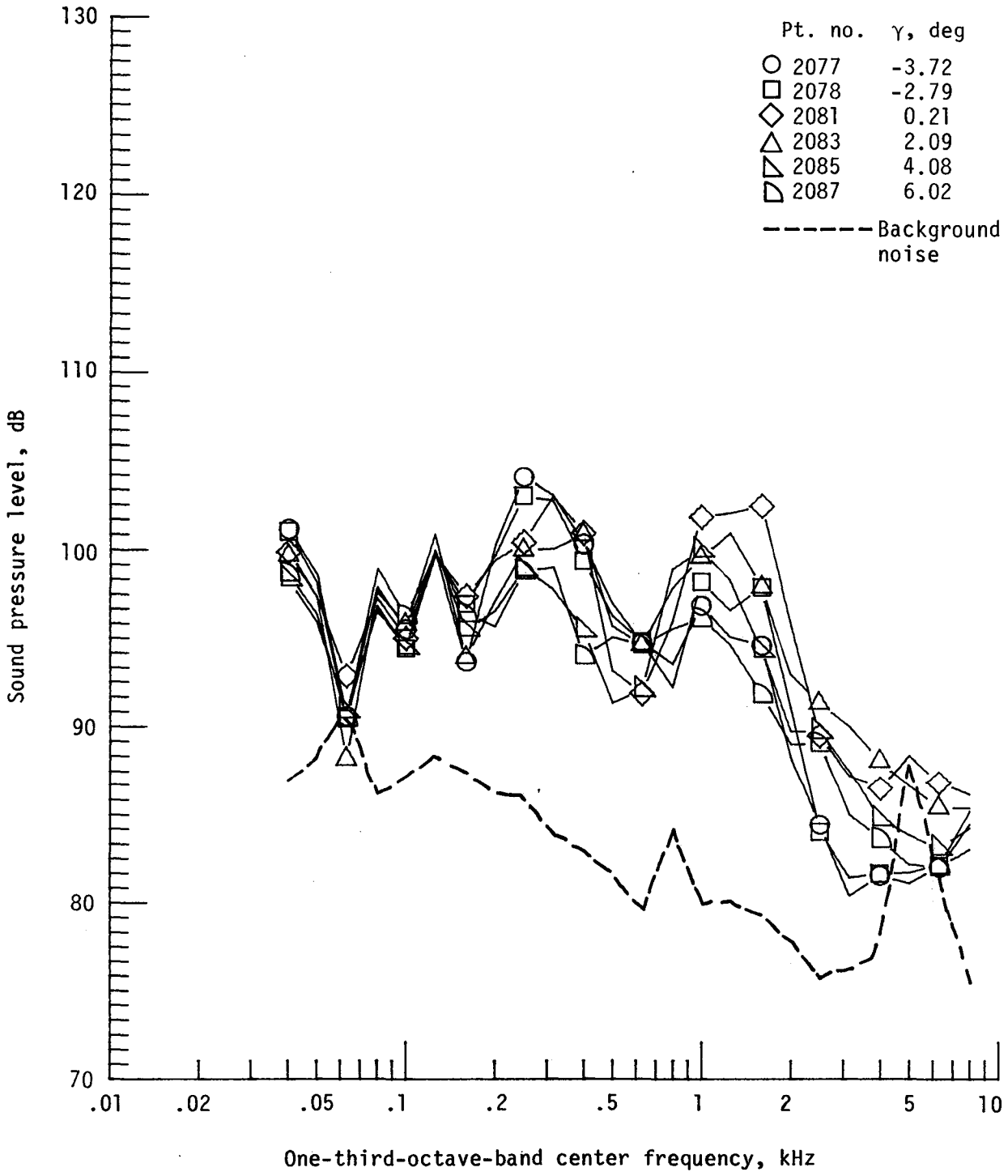

(d) One-third-octave spectra, microphone 6.

Figure 22. - Continued.

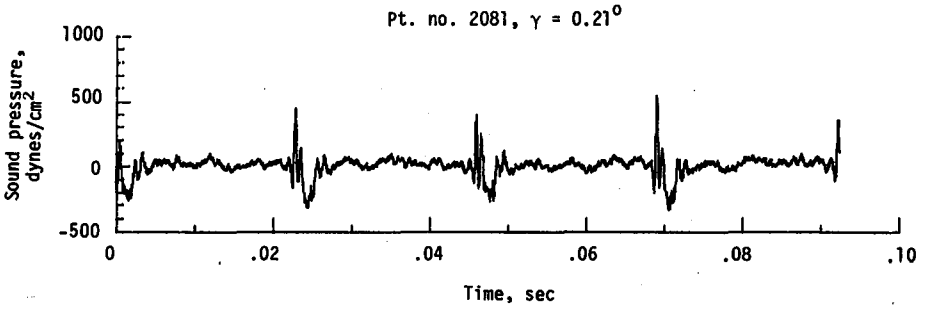

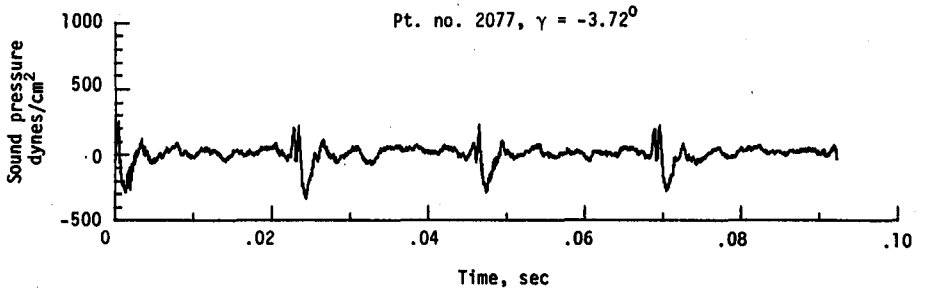

(e) Pressure-time histories; microphone 6.

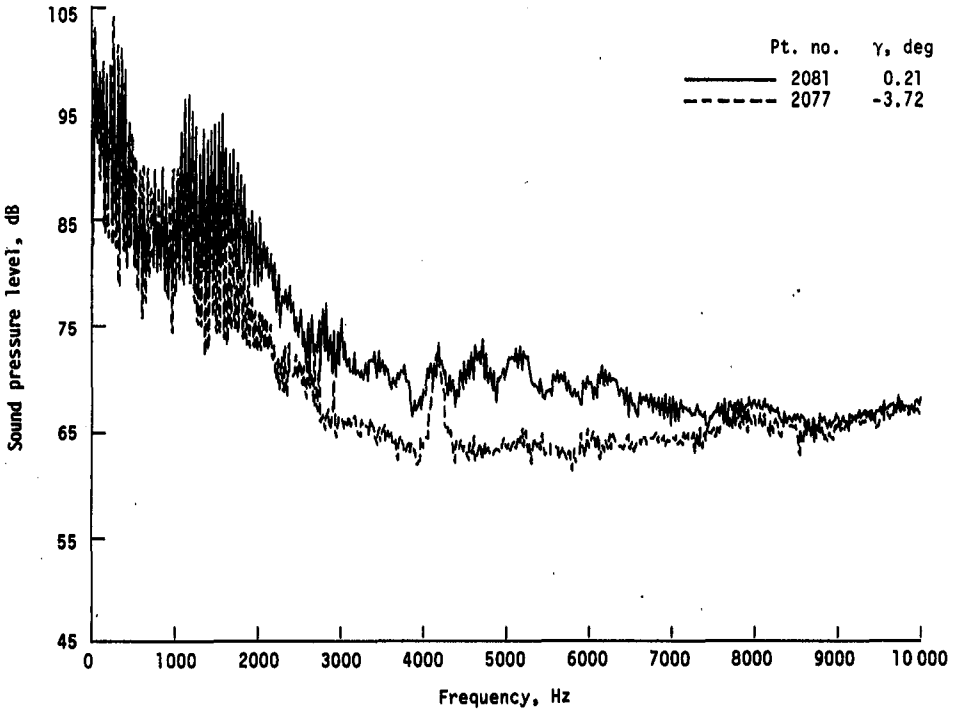

(f) Narrowband analysis; microphone 6.
Figure 22. - Continued.

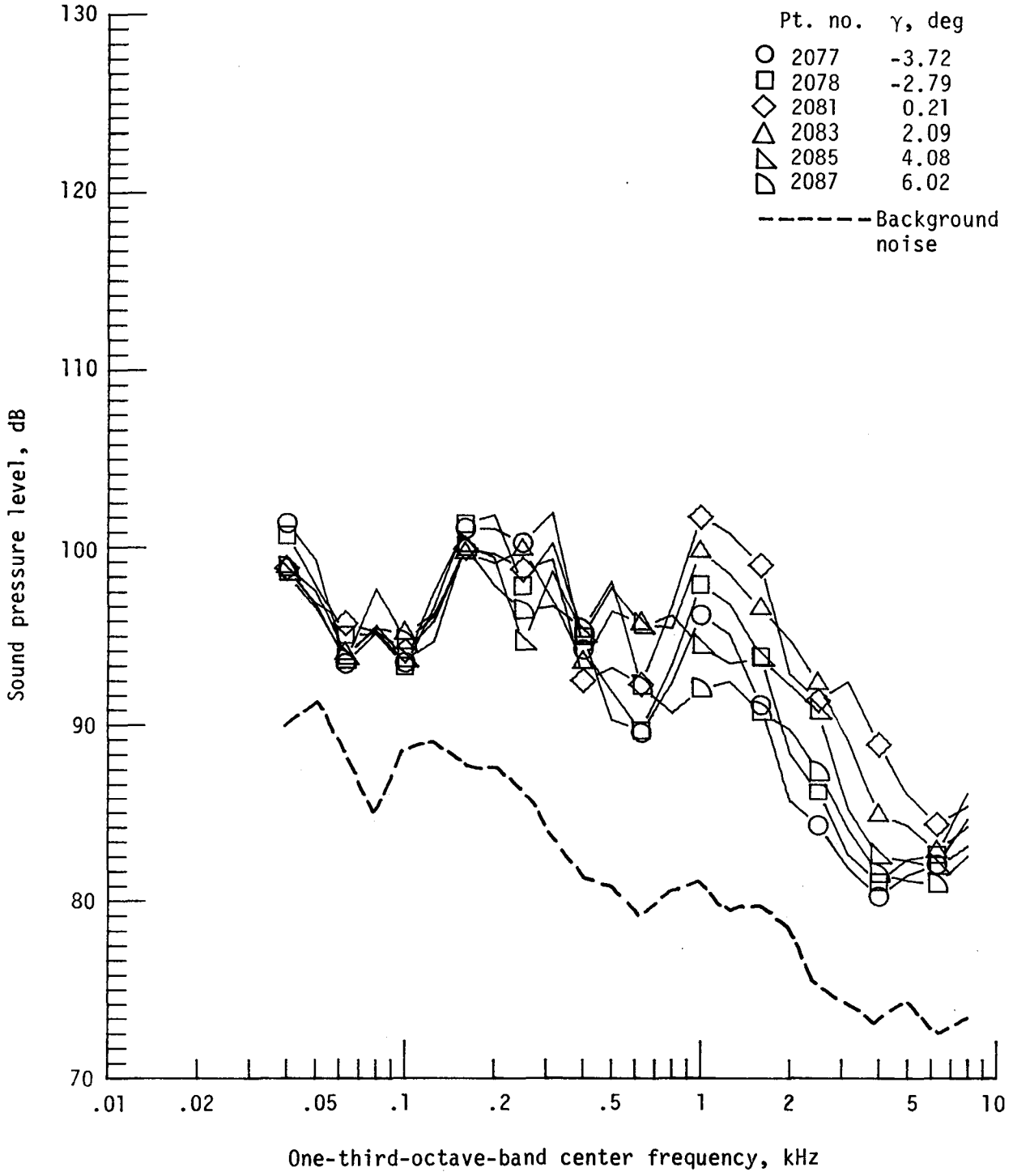

(g) One-third-octave spectra, microphone 7.

Figure 22. - Continued.

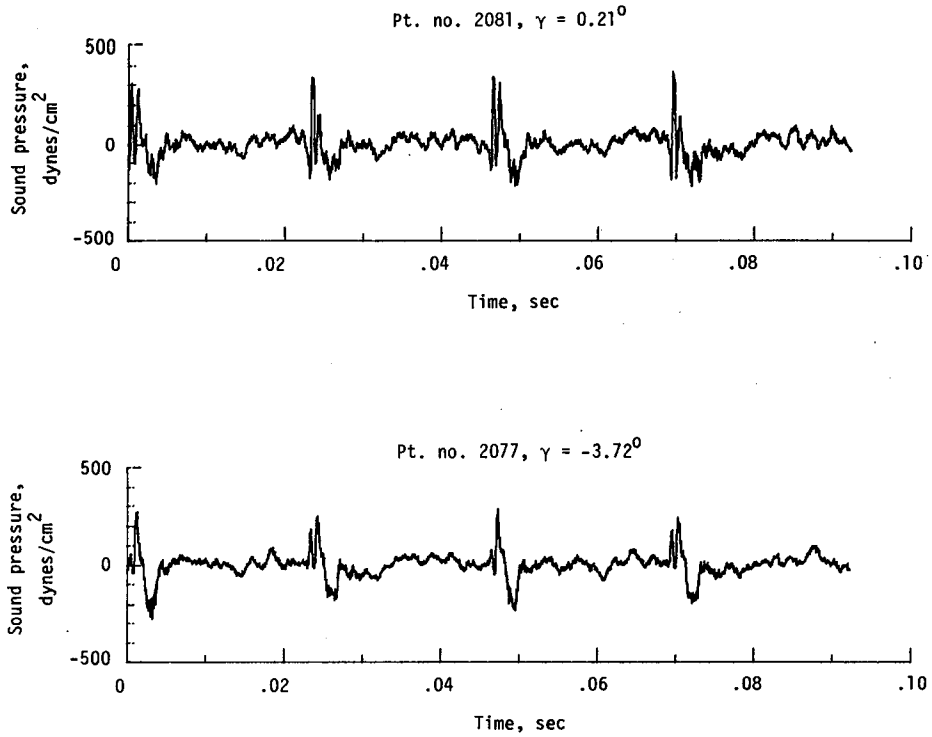

(h) Pressure-time histories; microphone 7.

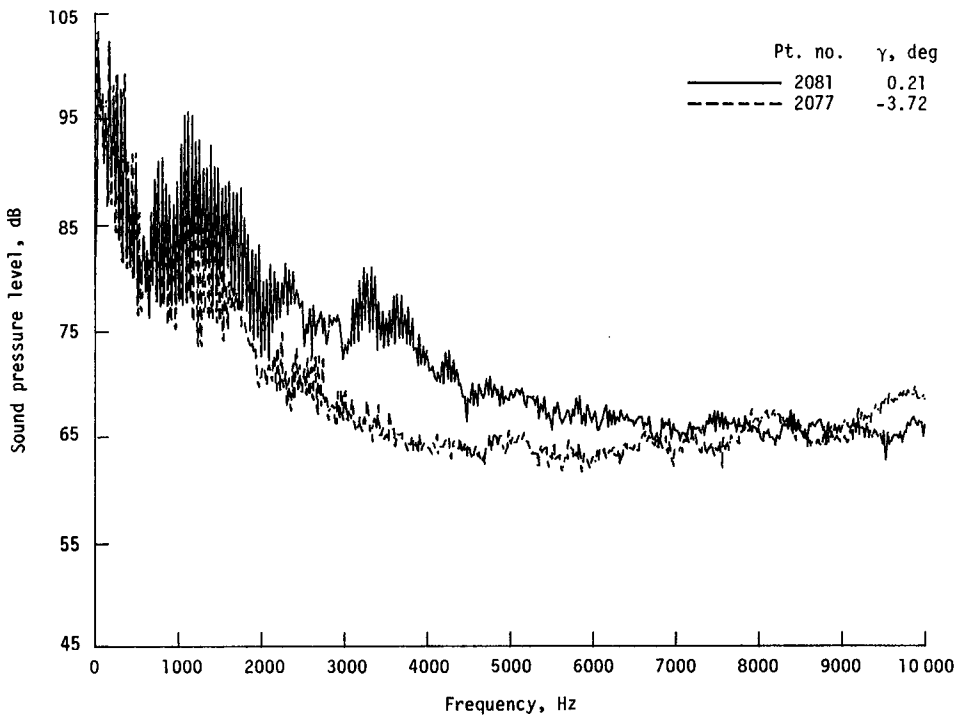

(i) Narrowband analysis; microphone 7.

Figure 22. - Continued.

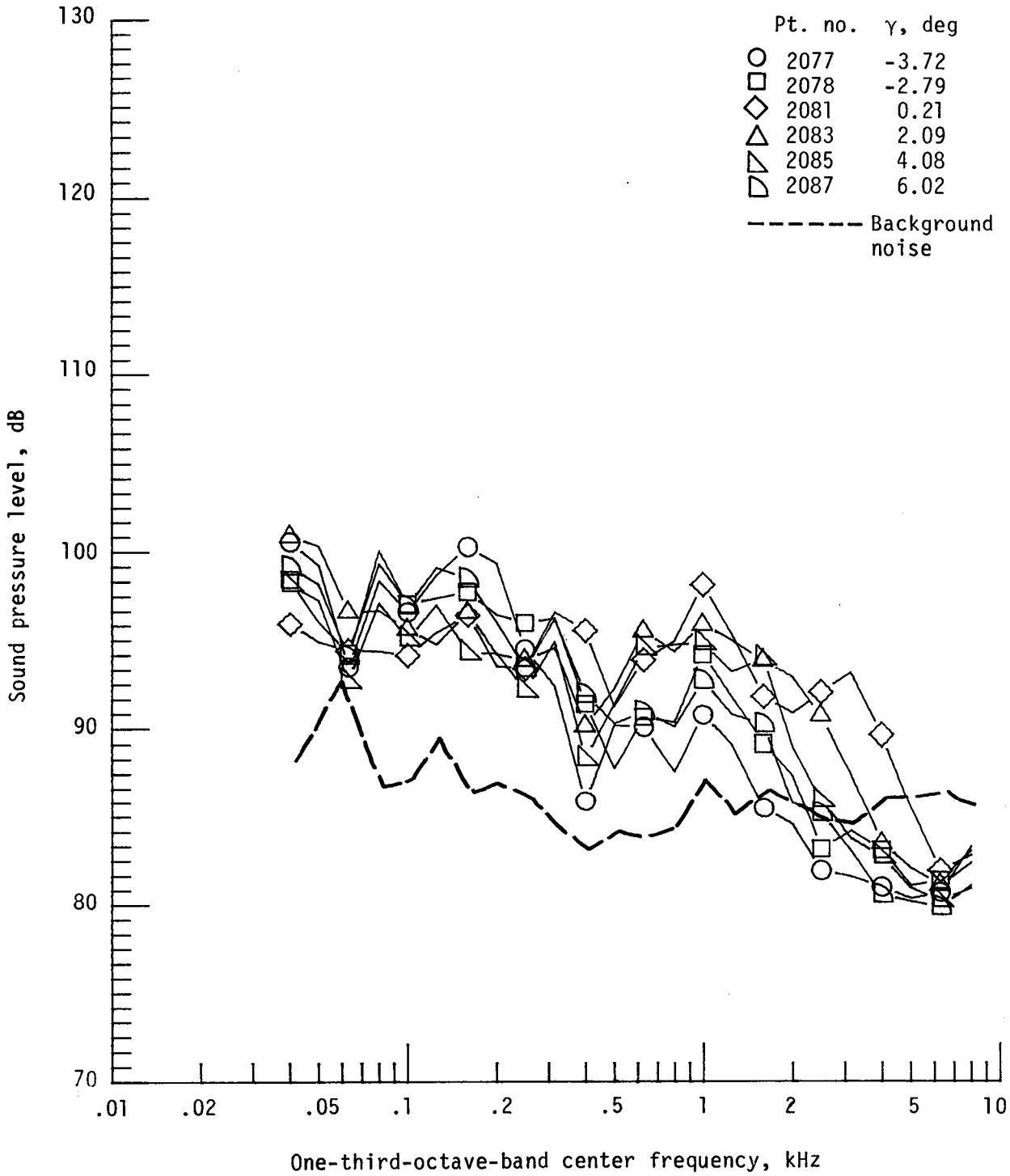

(j) One-third-octave spectra, microphone 8.

Figure 22. - Continued.

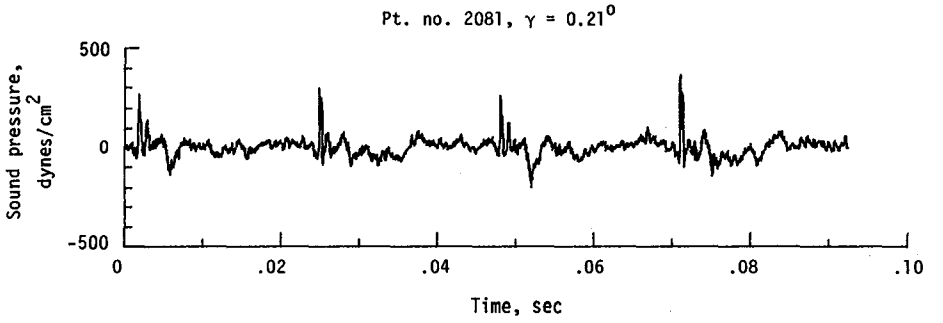

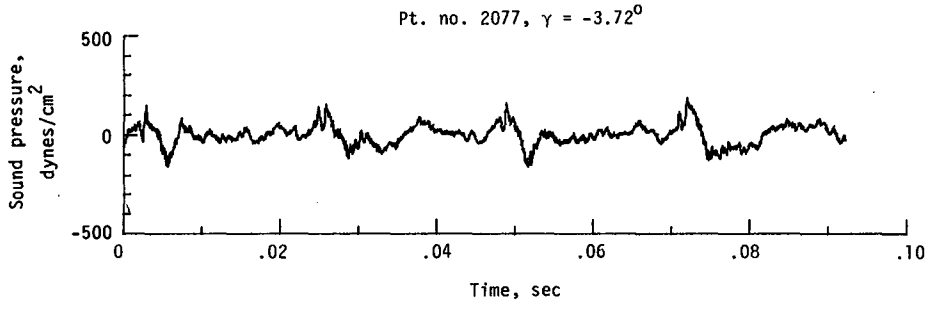

(k) Pressure-time histories; microphone 8.

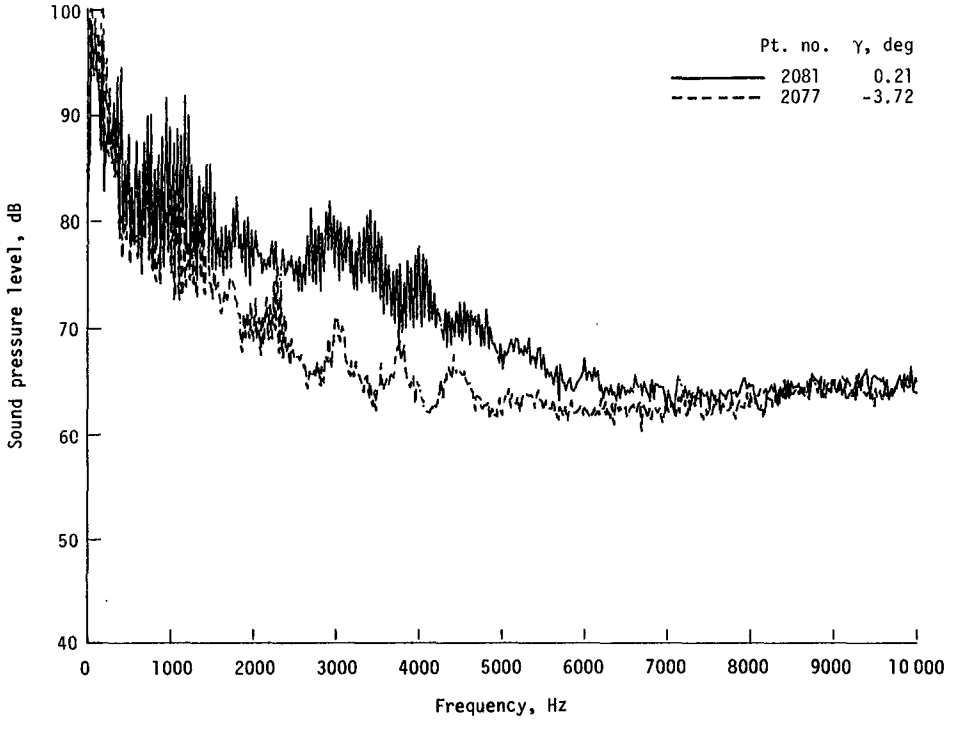

(l) Narrowband analysis; microphone 8.
Figure 22. - Concluded.

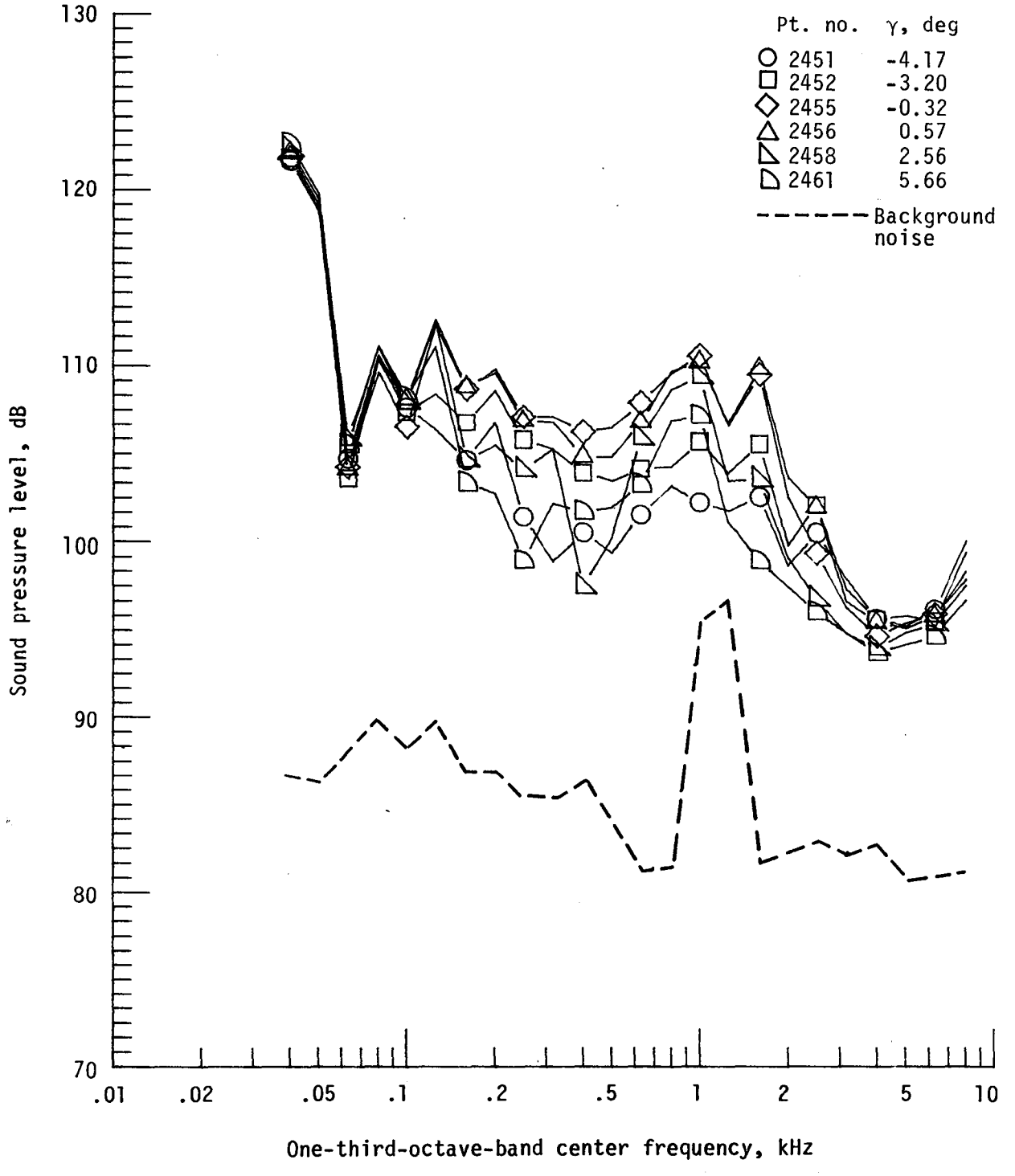

(a) One-third-octave spectra, microphone 2.

Figure 23. - Effect of descent angle variation on noise generated by helicopter model with advanced rotor system, run 195. V_∞ = 70.3 knots, C_T = .0031.

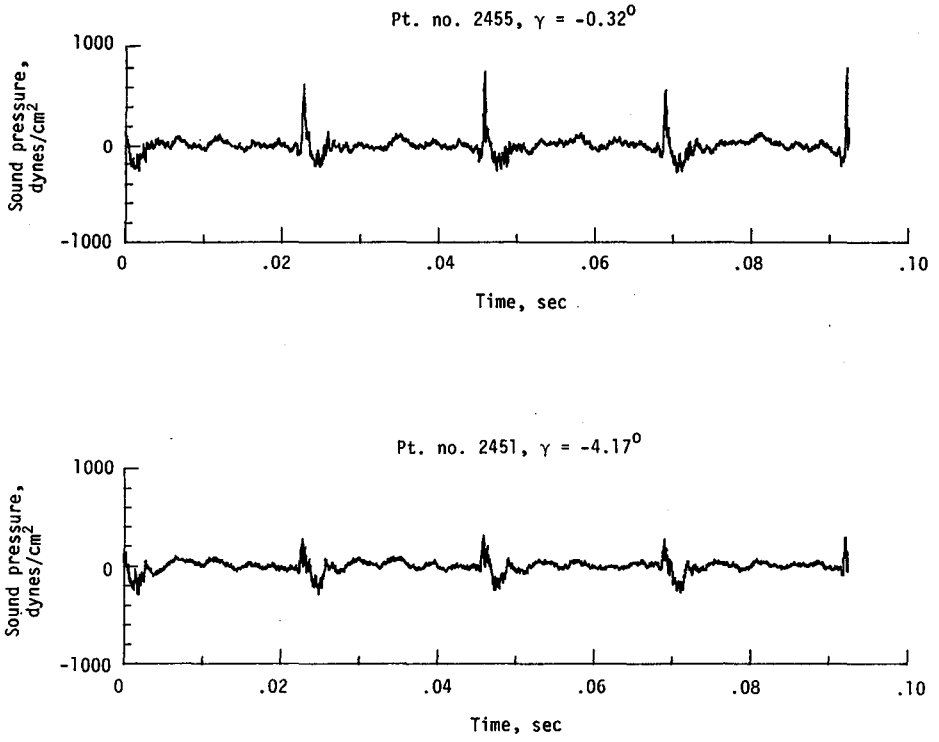

(b) Pressure-time histories; microphone 2.

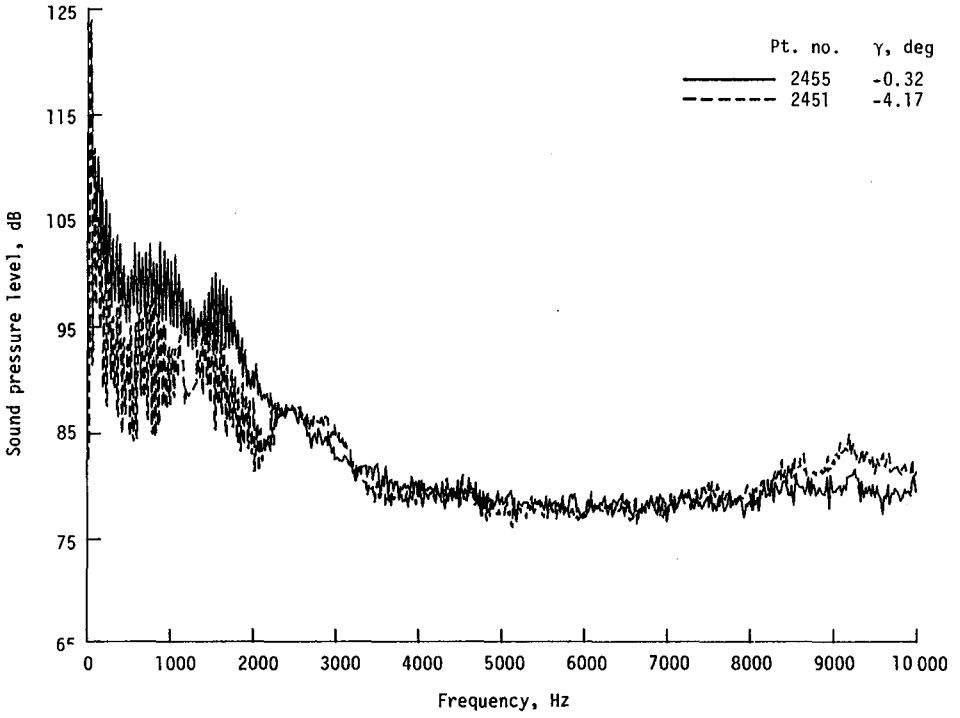

(c) Narrowband analysis; microphone 2.
Figure 23. - Continued.

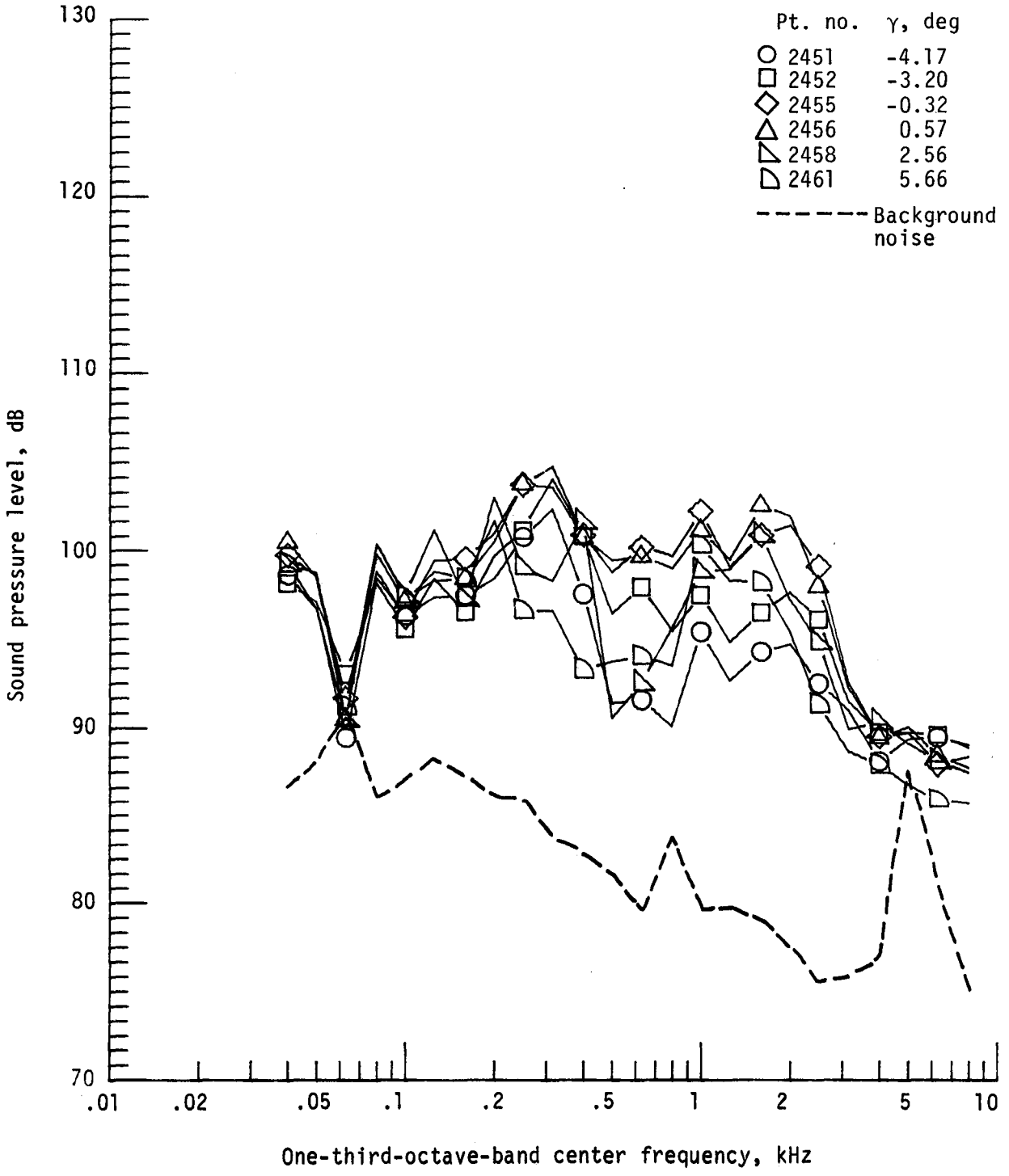

(d) One-third-octave spectra, microphone 6.

Figure 23. - Continued.

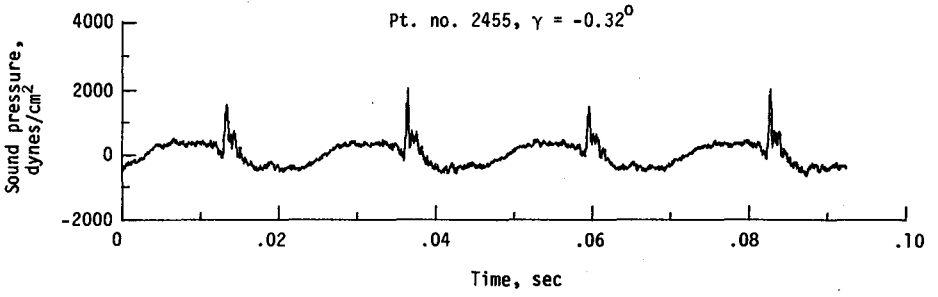

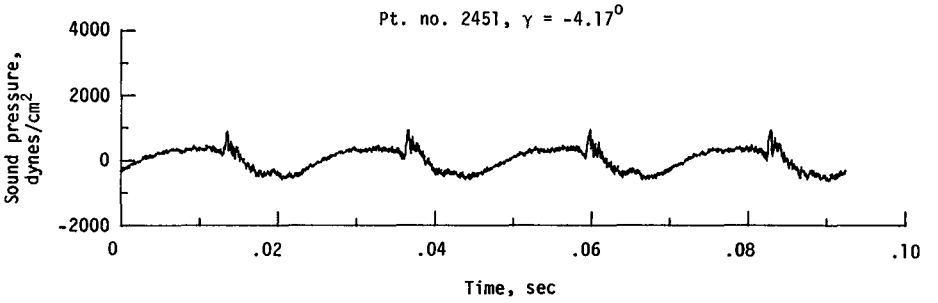

(e) Pressure-time histories; microphone 6.

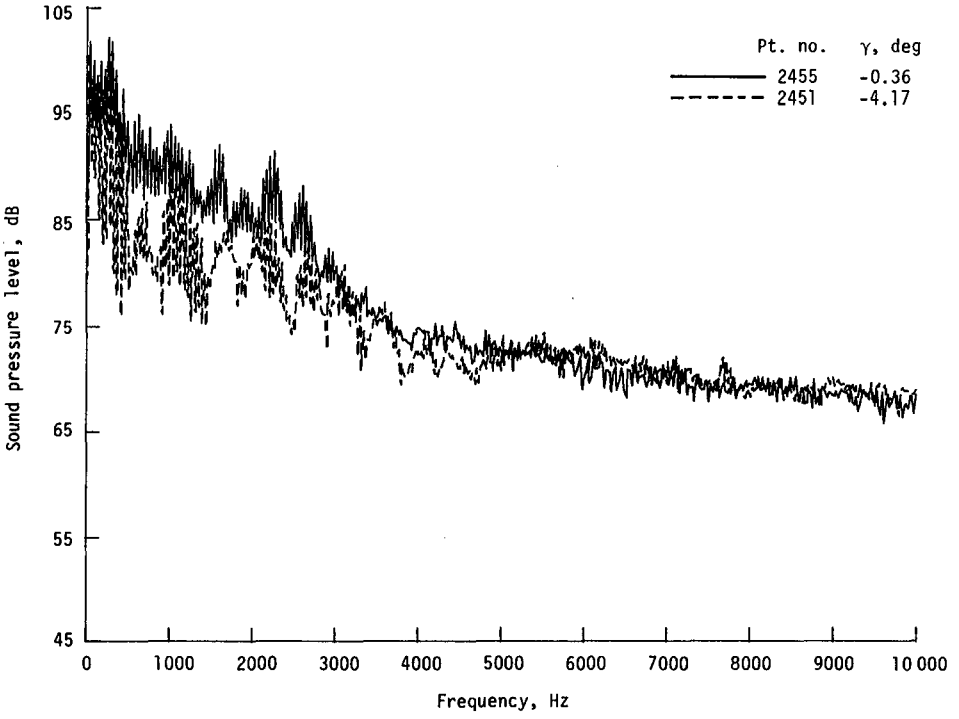

(f) Narrowband analysis; microphone 6.
Figure 23. - Continued.

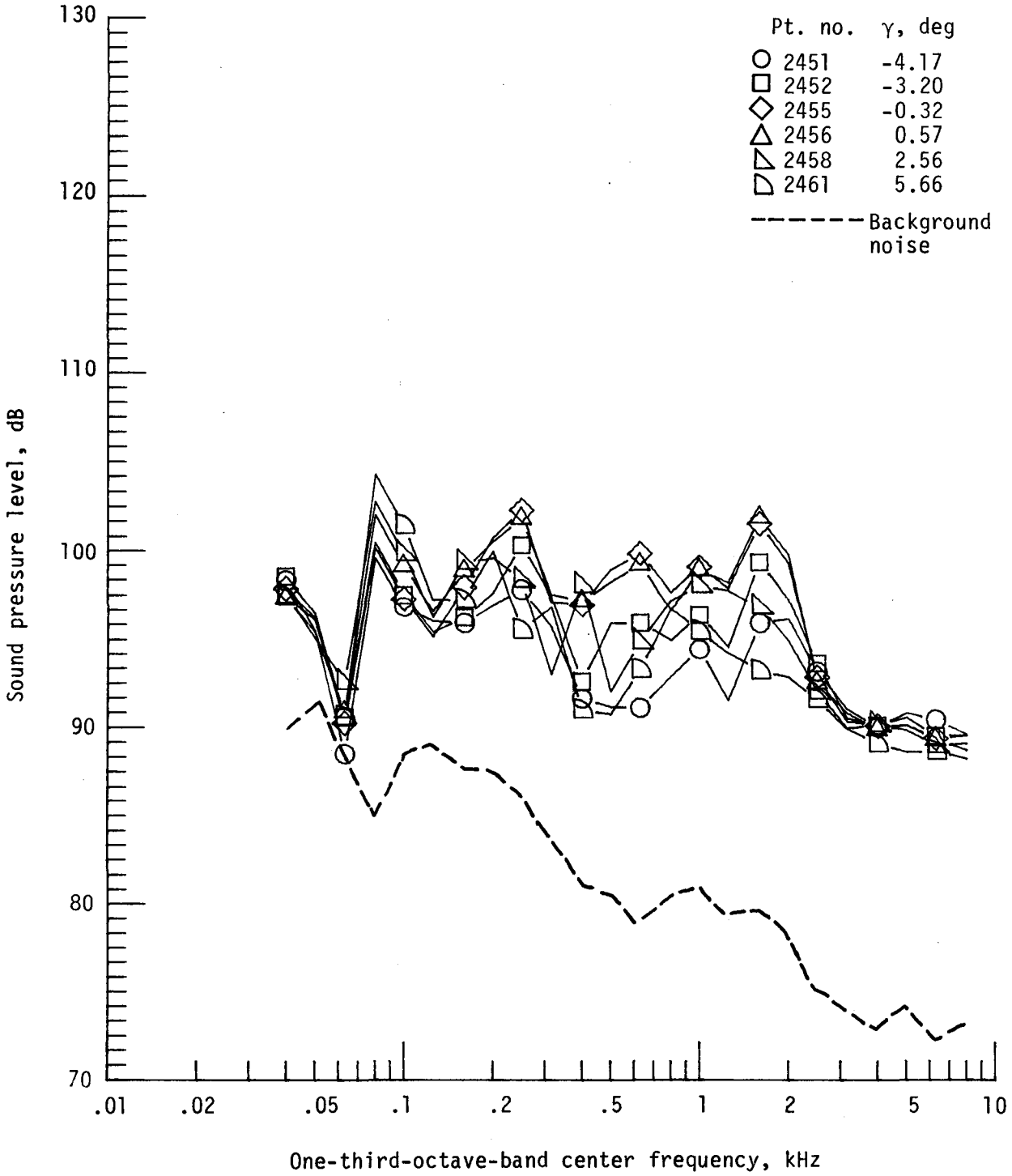

(g) One-third-octave spectra, microphone 7.

Figure 23. - Continued.

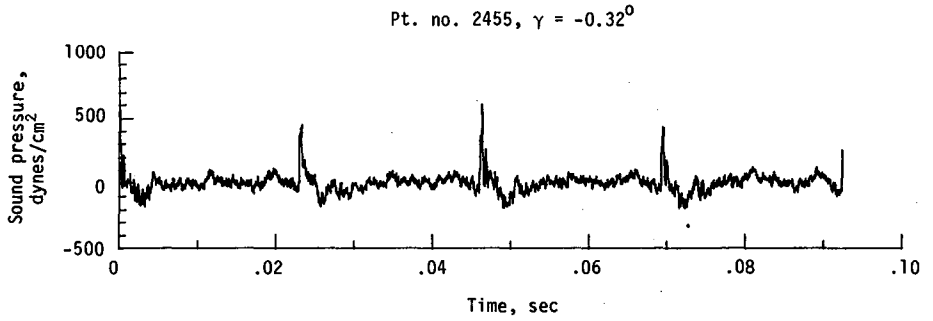

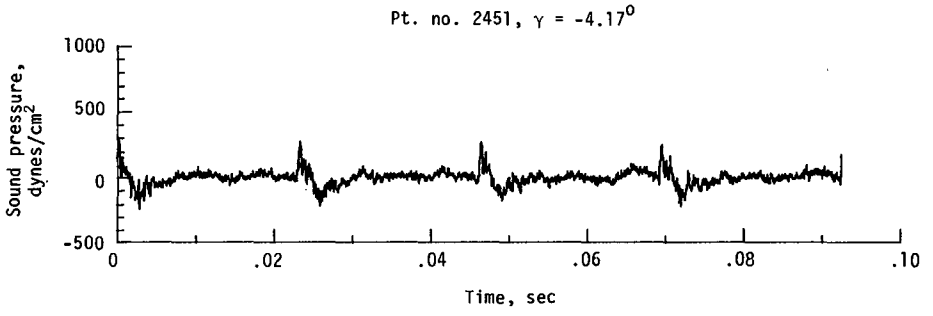

(h) Pressure-time histories; microphone 7.

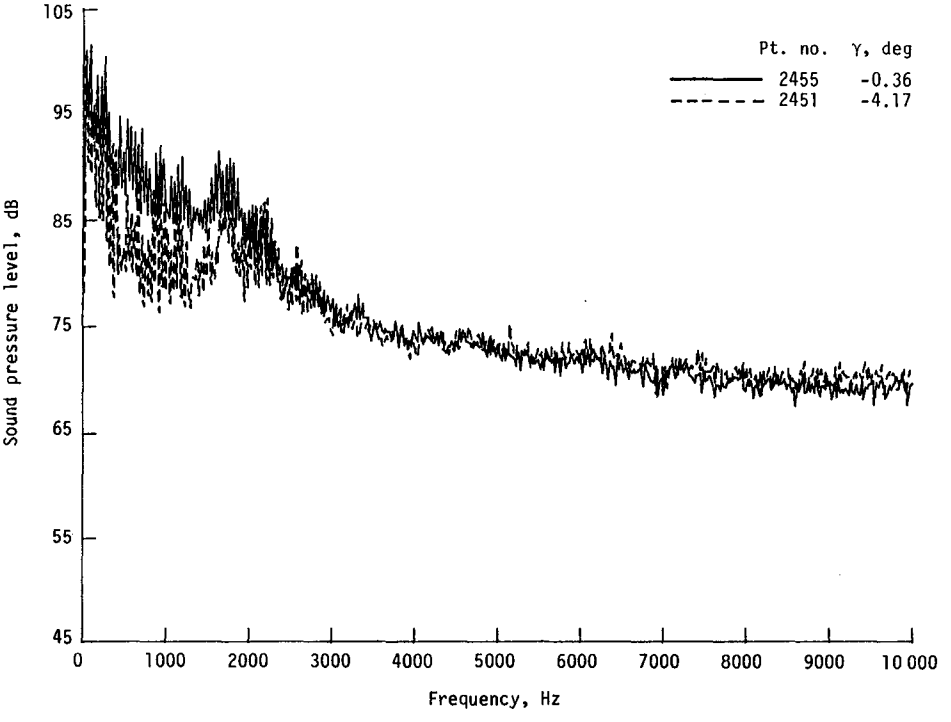

(i) Narrowband analysis; microphone 7.
Figure 23. - Continued.

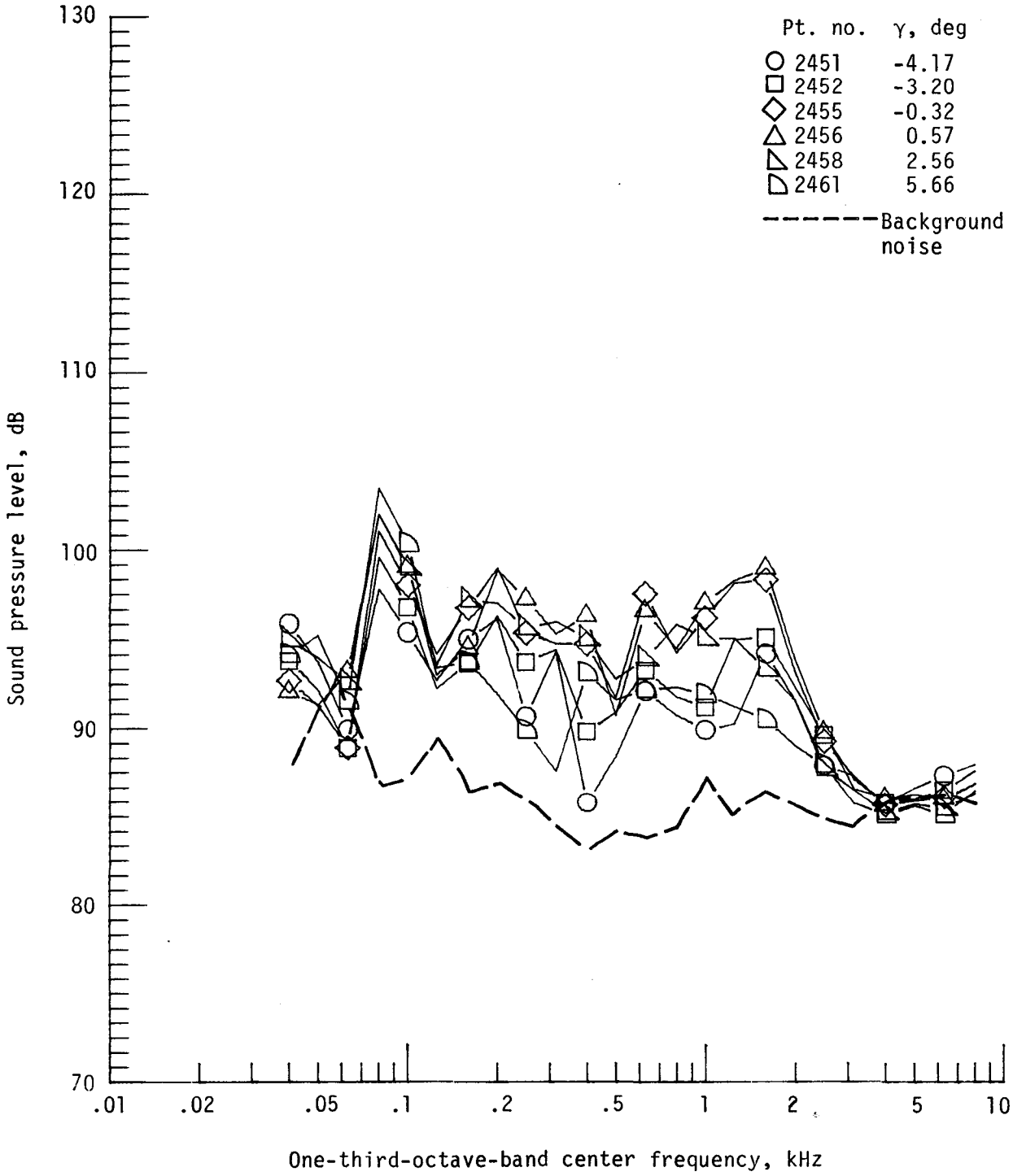

(j) One-third-octave spectra, microphone 8.

Figure 23. - Continued.

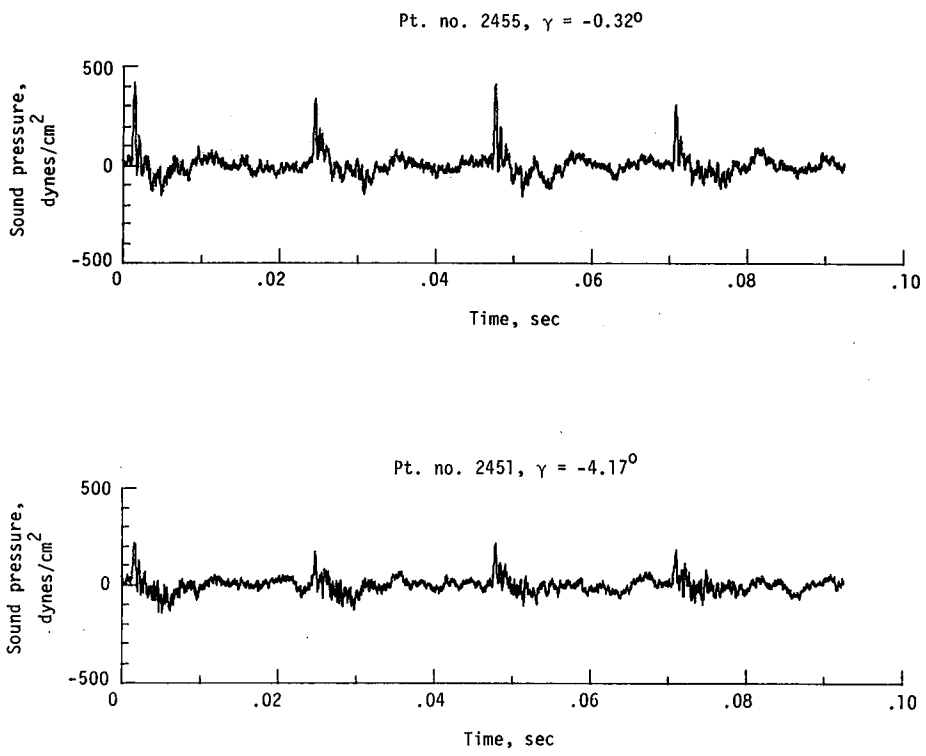

(k) Pressure-time histories; microphone 8.

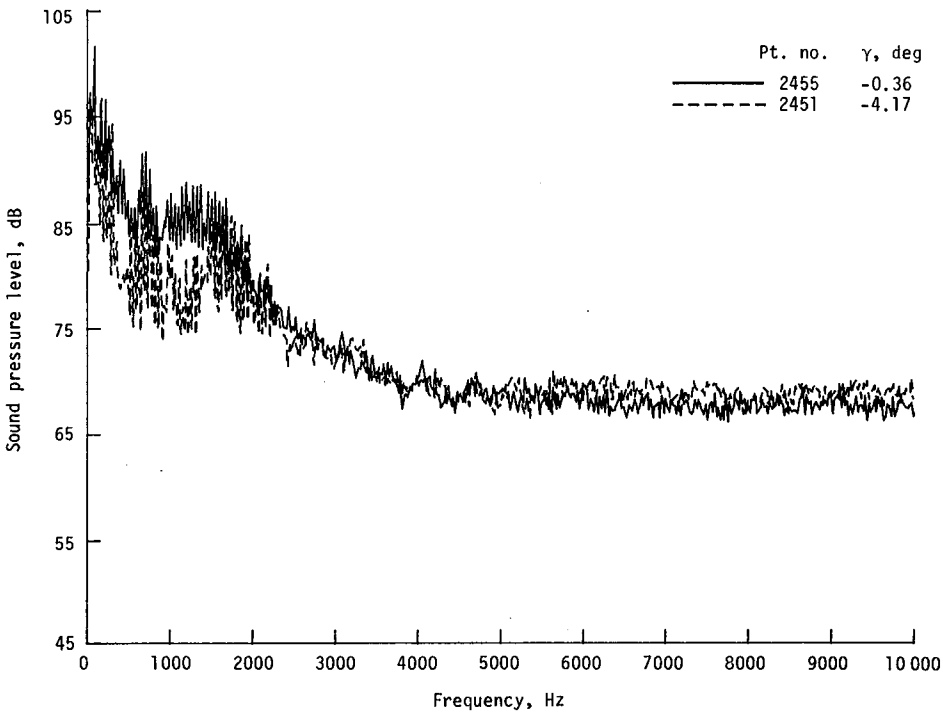

(l) Narrowband analysis; microphone 8.
Figure 23. - Concluded.

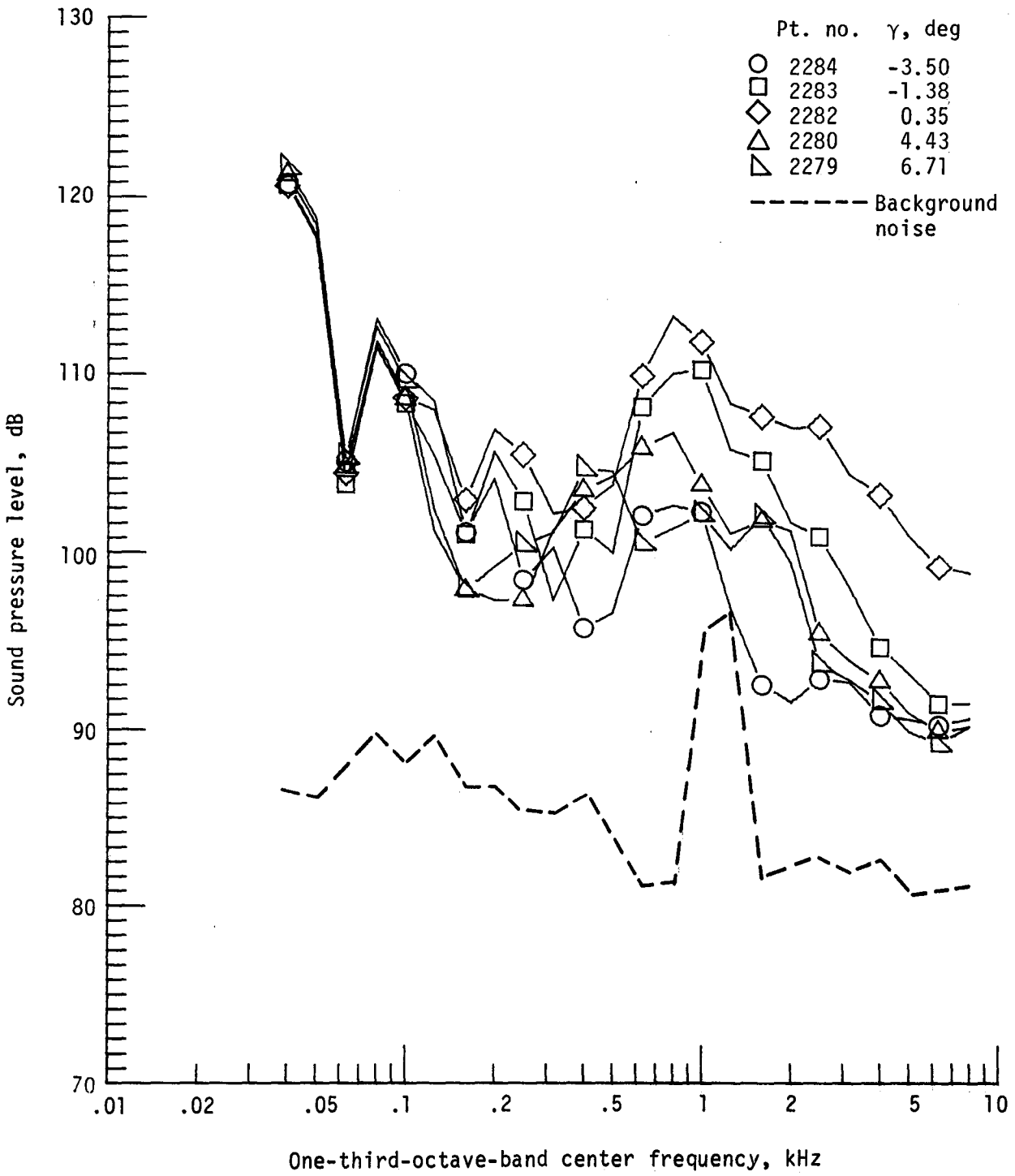

(a) One-third-octave spectra, microphone 2.

Figure 24. - Effect of descent angle variation on noise generated by helicopter model with standard rotor system, run 183; V_∞ = 70.4 knots, C_T = .0036.

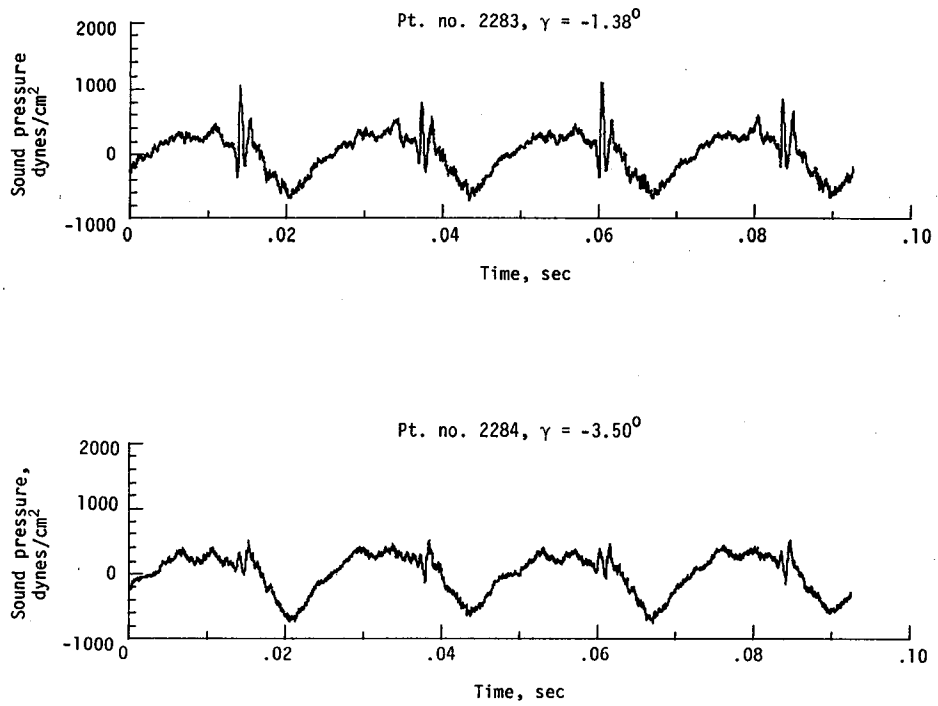

(b) Pressure-time histories; microphone 2.

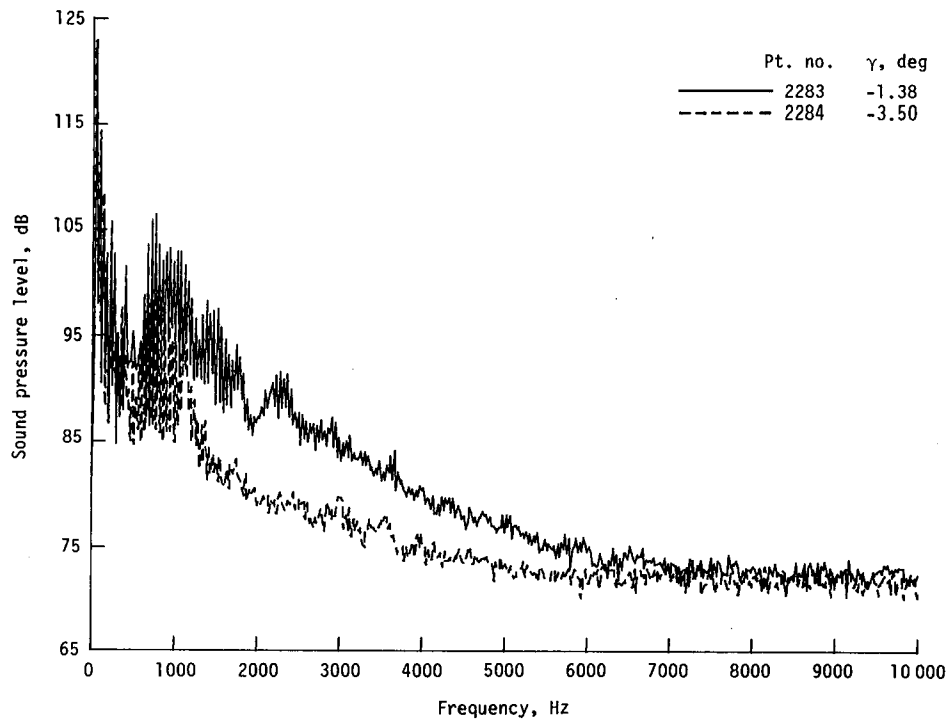

(c) Narrowband analysis; microphone 2.

Figure 24. - Continued.

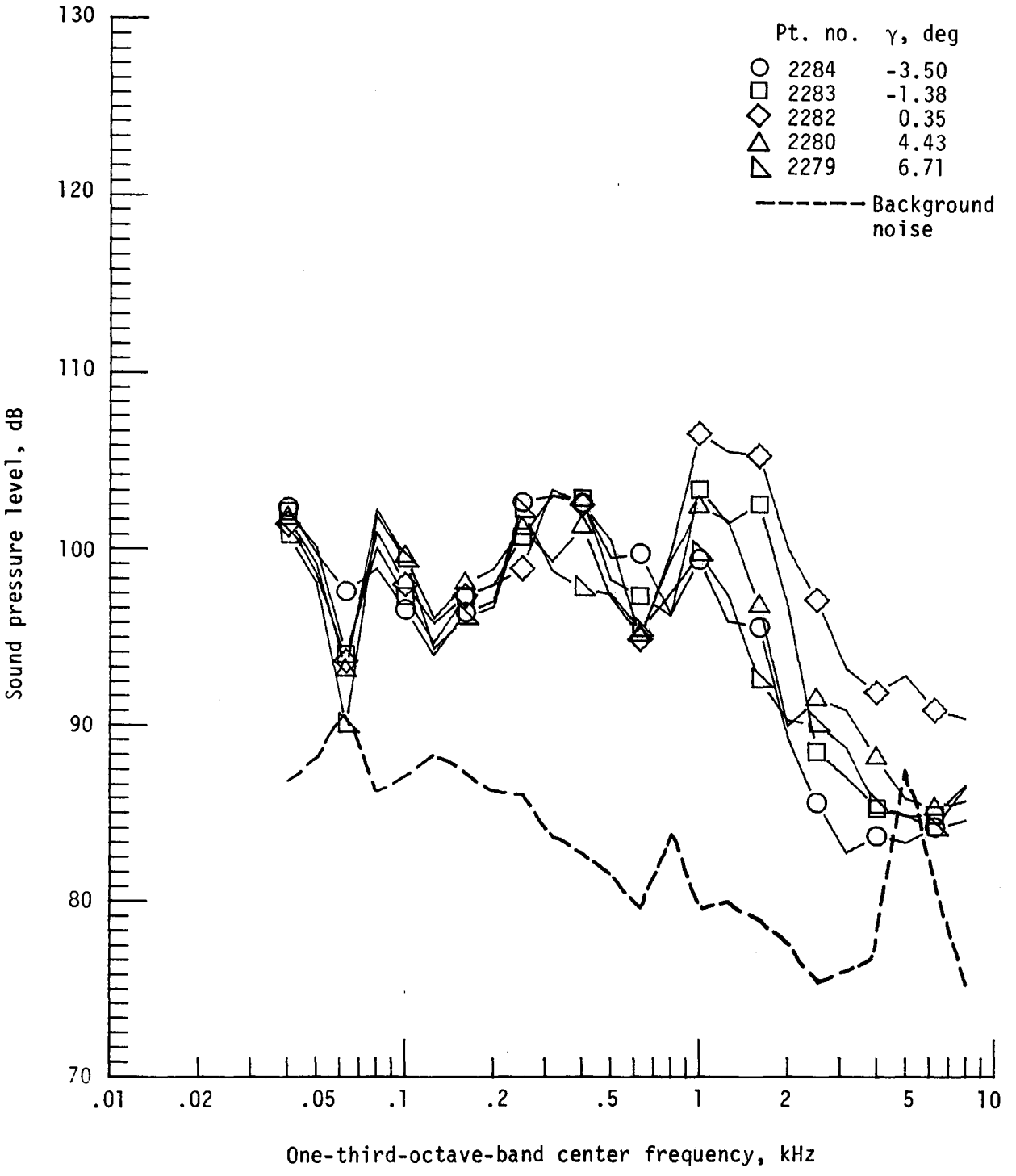

(d) One-third-octave spectra, microphone 6.

Figure 24. - Continued.

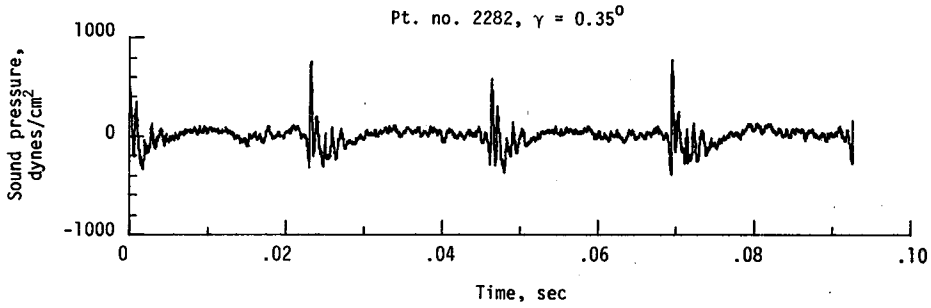

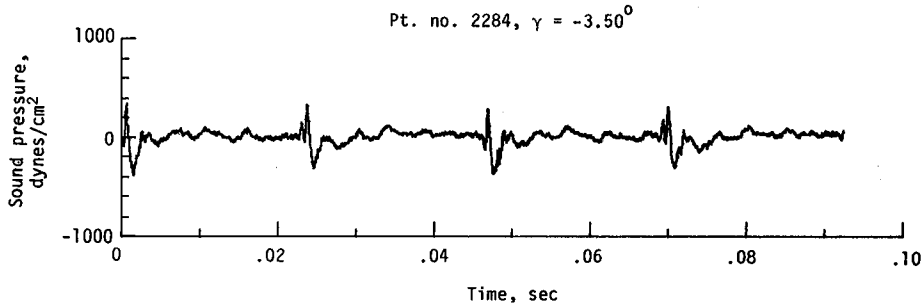

(e) Pressure-time histories; microphone 6.

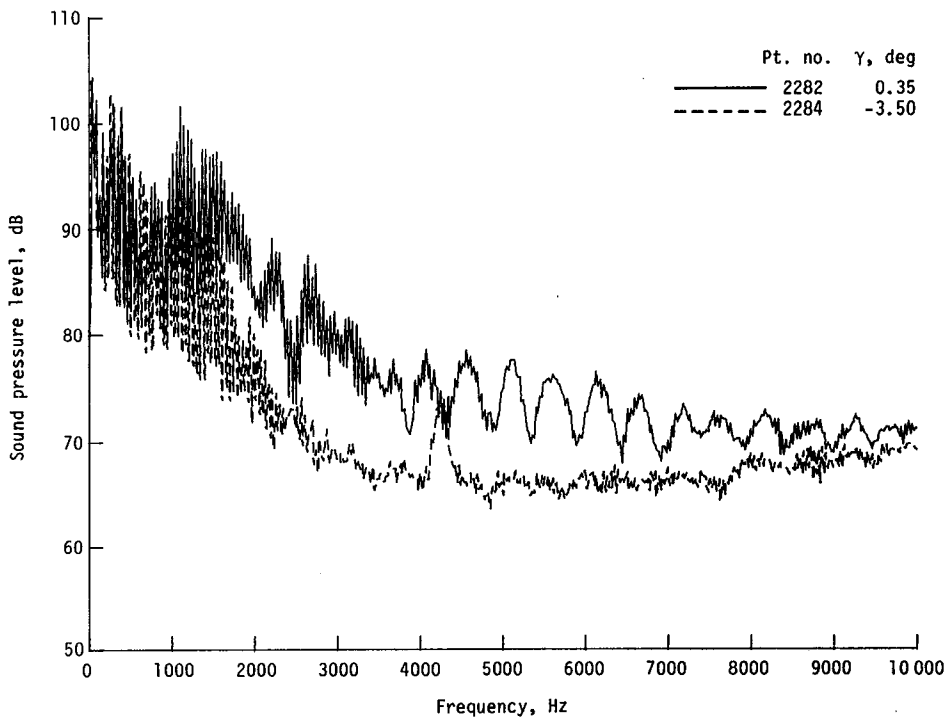

(f) Narrowband analysis; microphone 6.
Figure 24. - Continued.

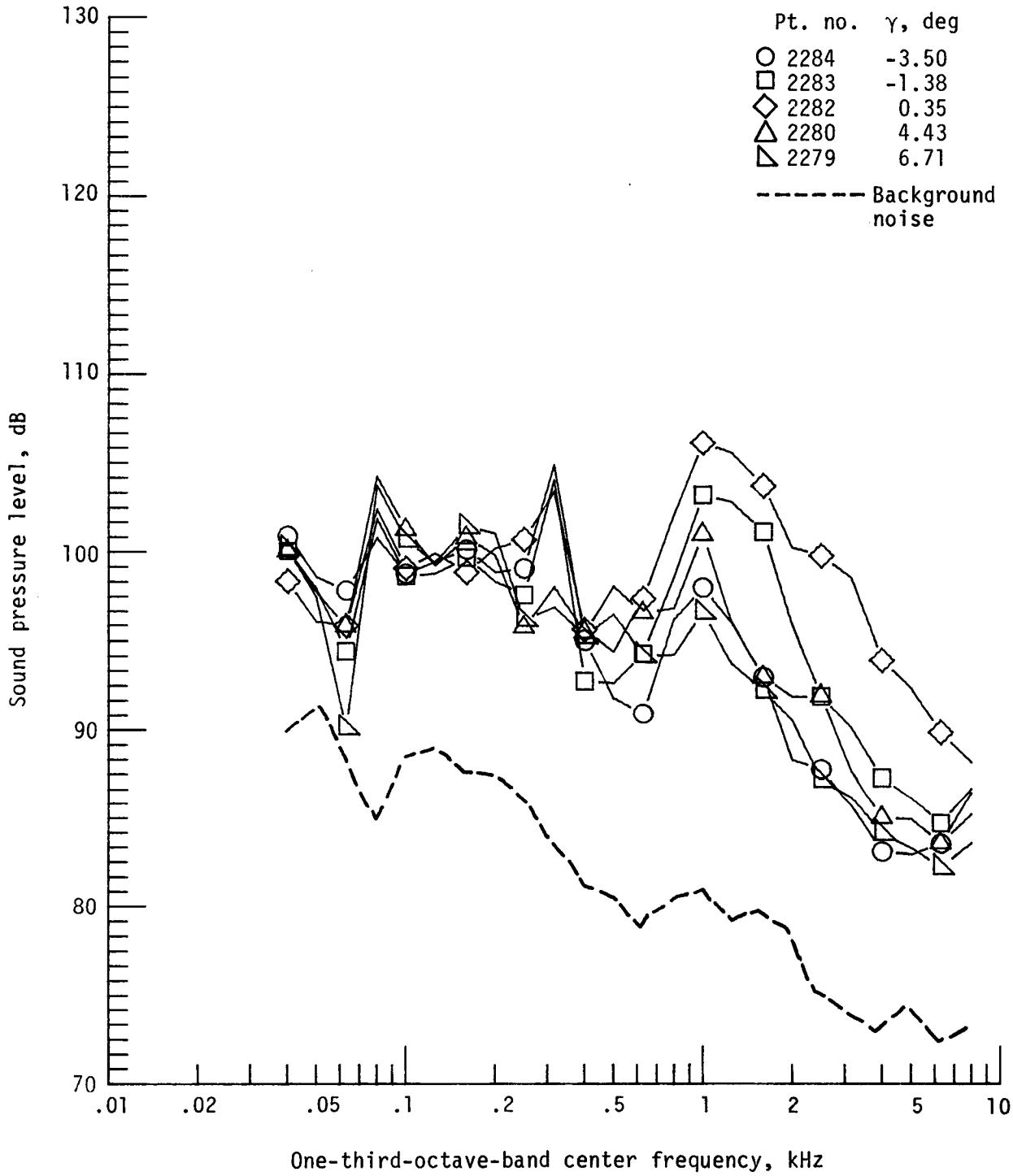

(g) One-third-octave spectra, microphone 7.

Figure 24. - Continued.

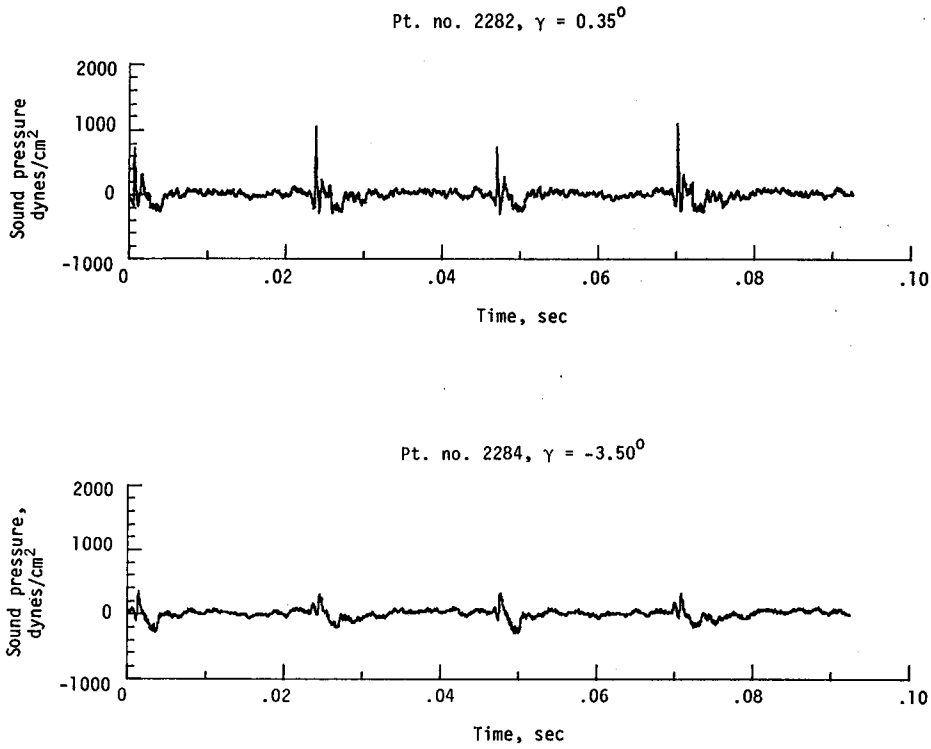

(h) Pressure-time histories; microphone 7.

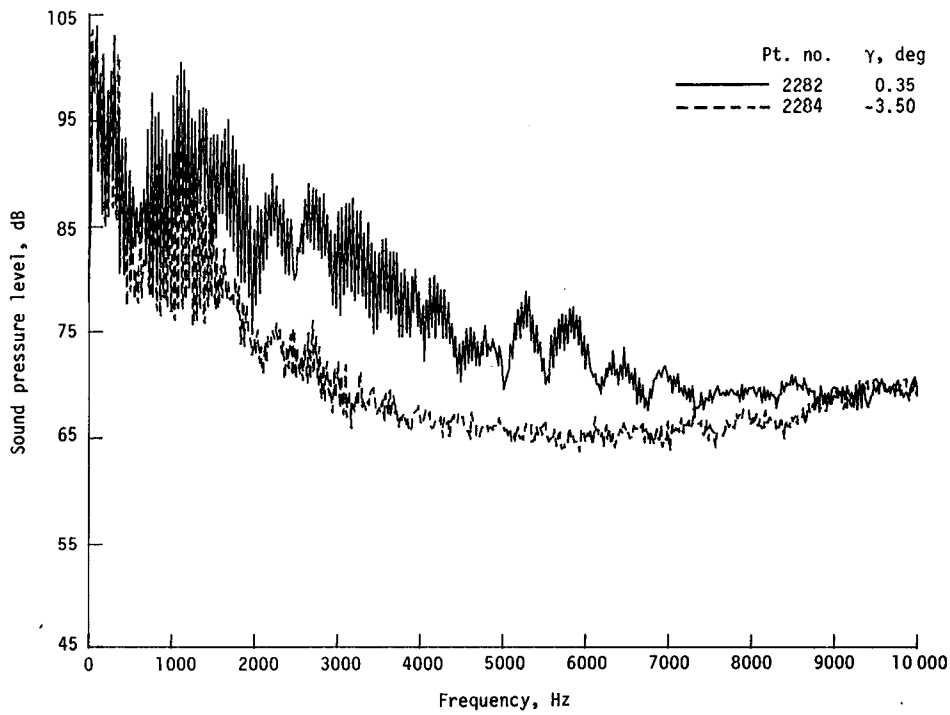

(i) Narrowband analysis; microphone 7.

Figure 24. - Concluded.

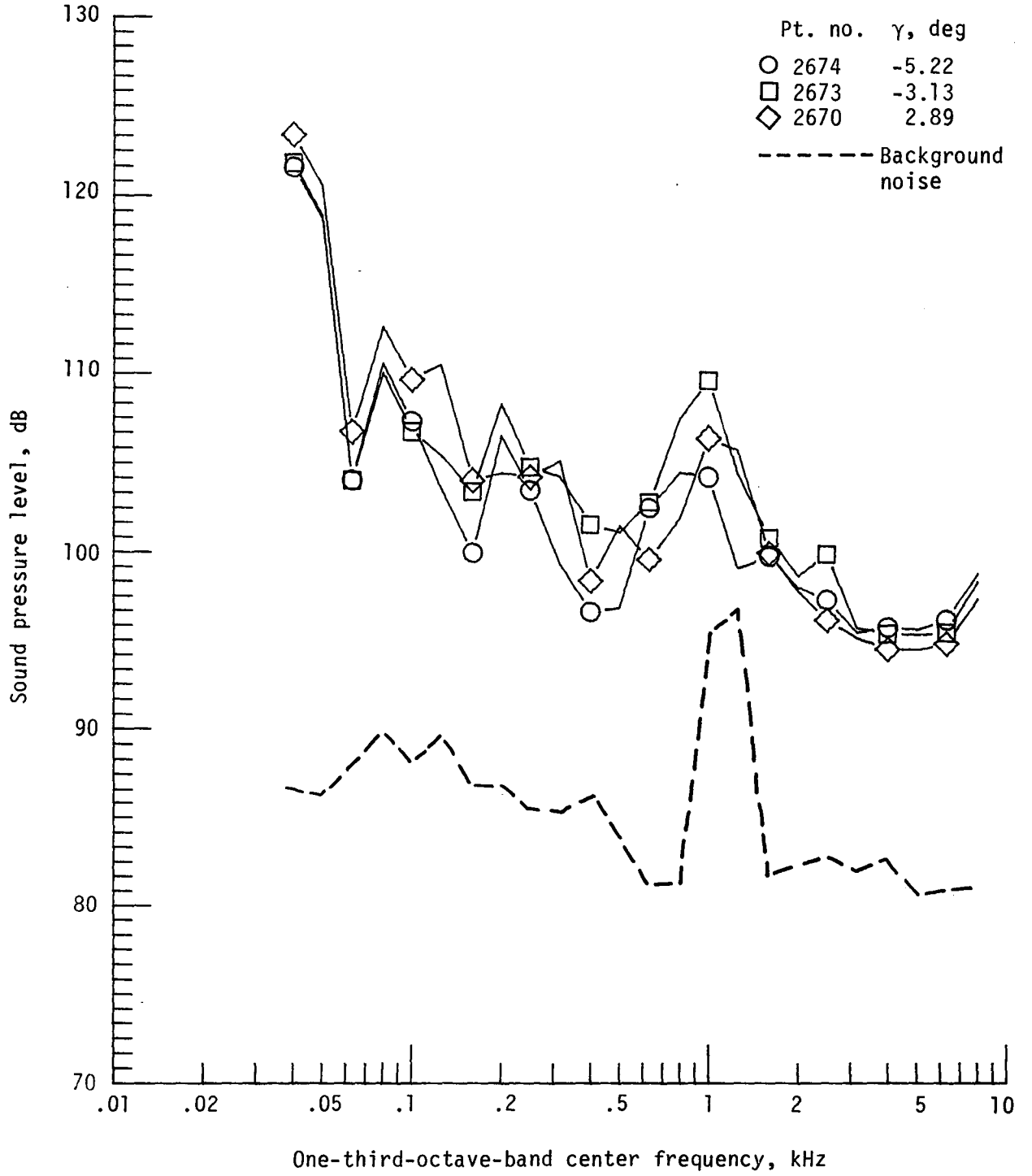

(a) One-third-octave spectra, microphone 2.

Figure 25. - Effect of descent angle variation on noise generated by helicopter model with advanced rotor system, run 215. V_∞ = 70.6 knots, C_T = .0036.

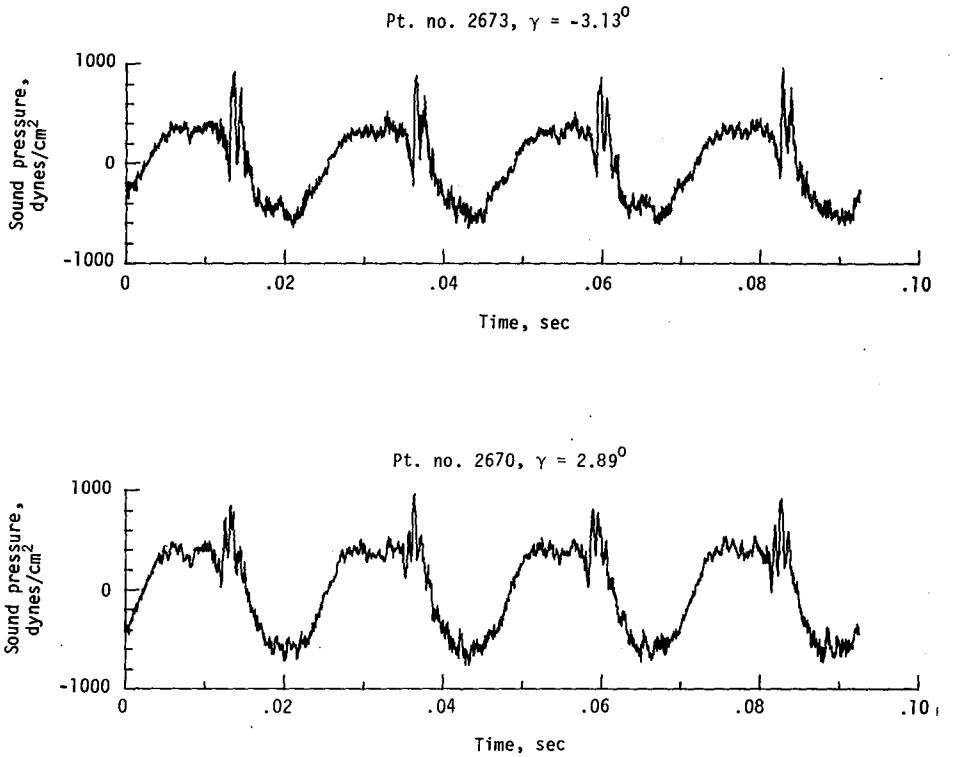

(b) Pressure-time histories; microphone 2.

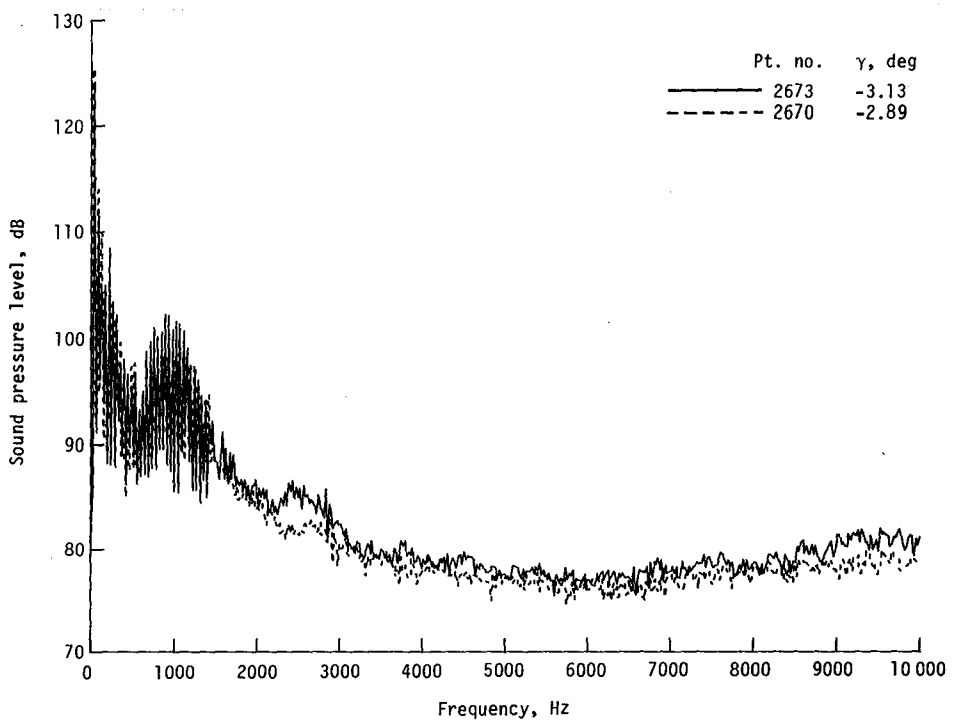

(c) Narrowband analysis; microphone 2.
Figure 25. - Continued.

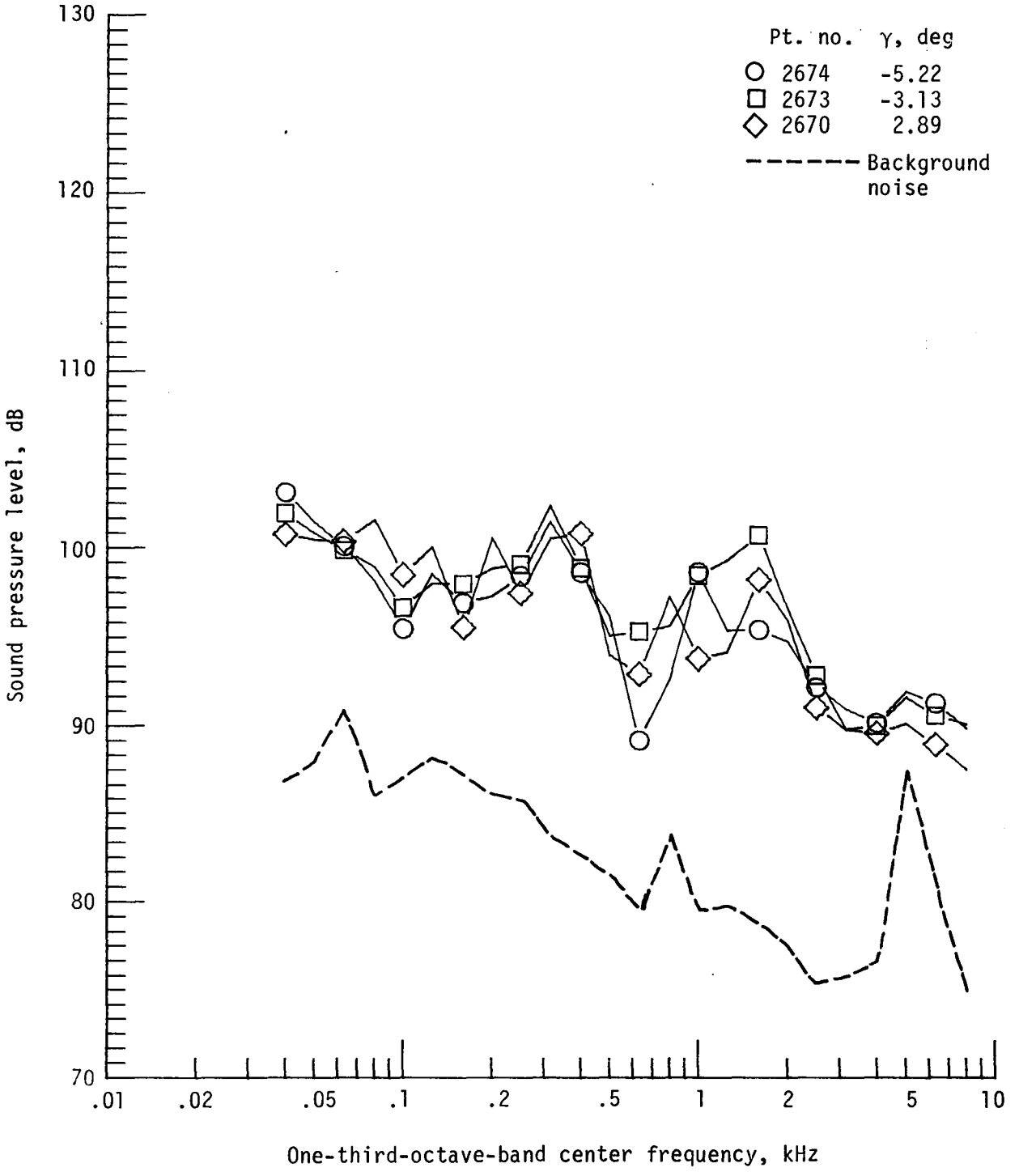

(d) One-third-octave spectra, microphone 6.

Figure 25. - Continued.

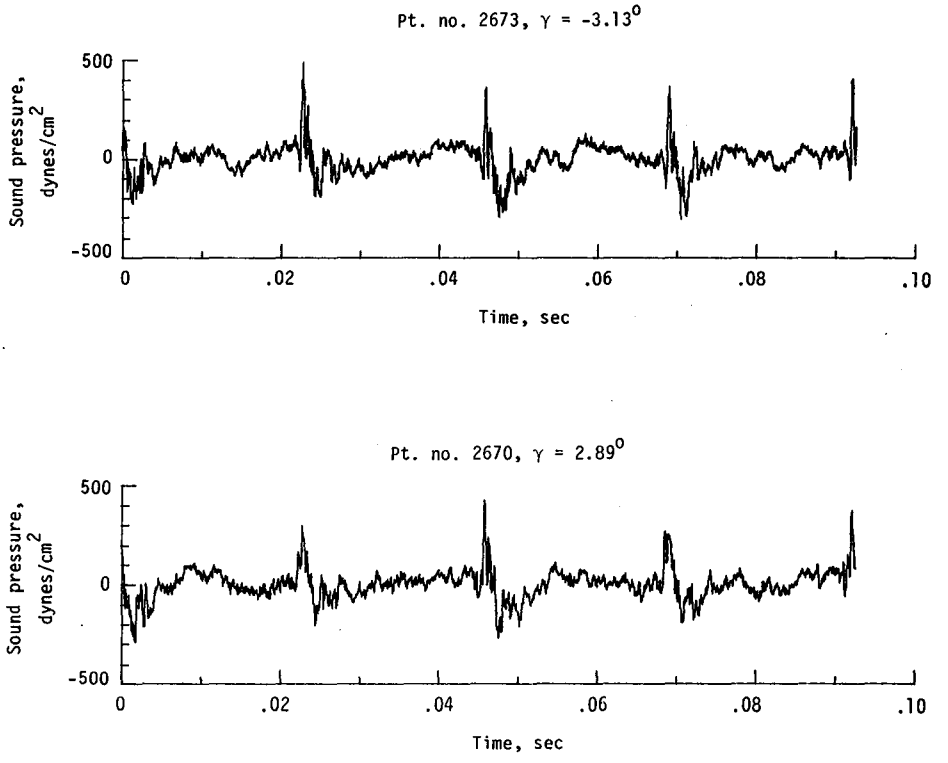

(e) Pressure-time histories; microphone 6.

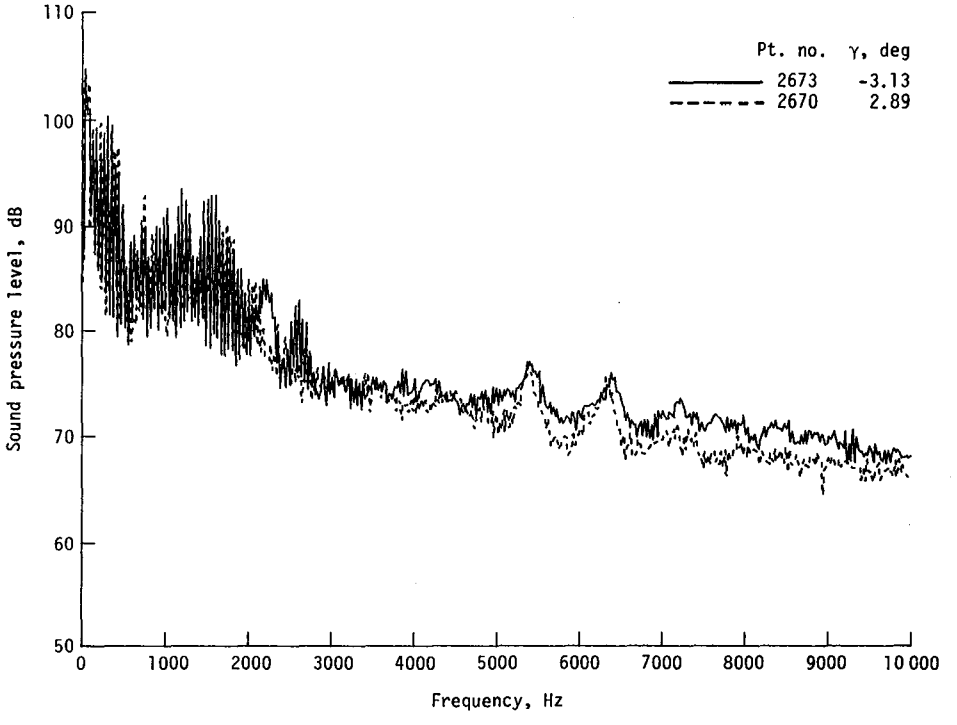

(f) Narrowband analysis; microphone 6.

Figure 25. - Continued.

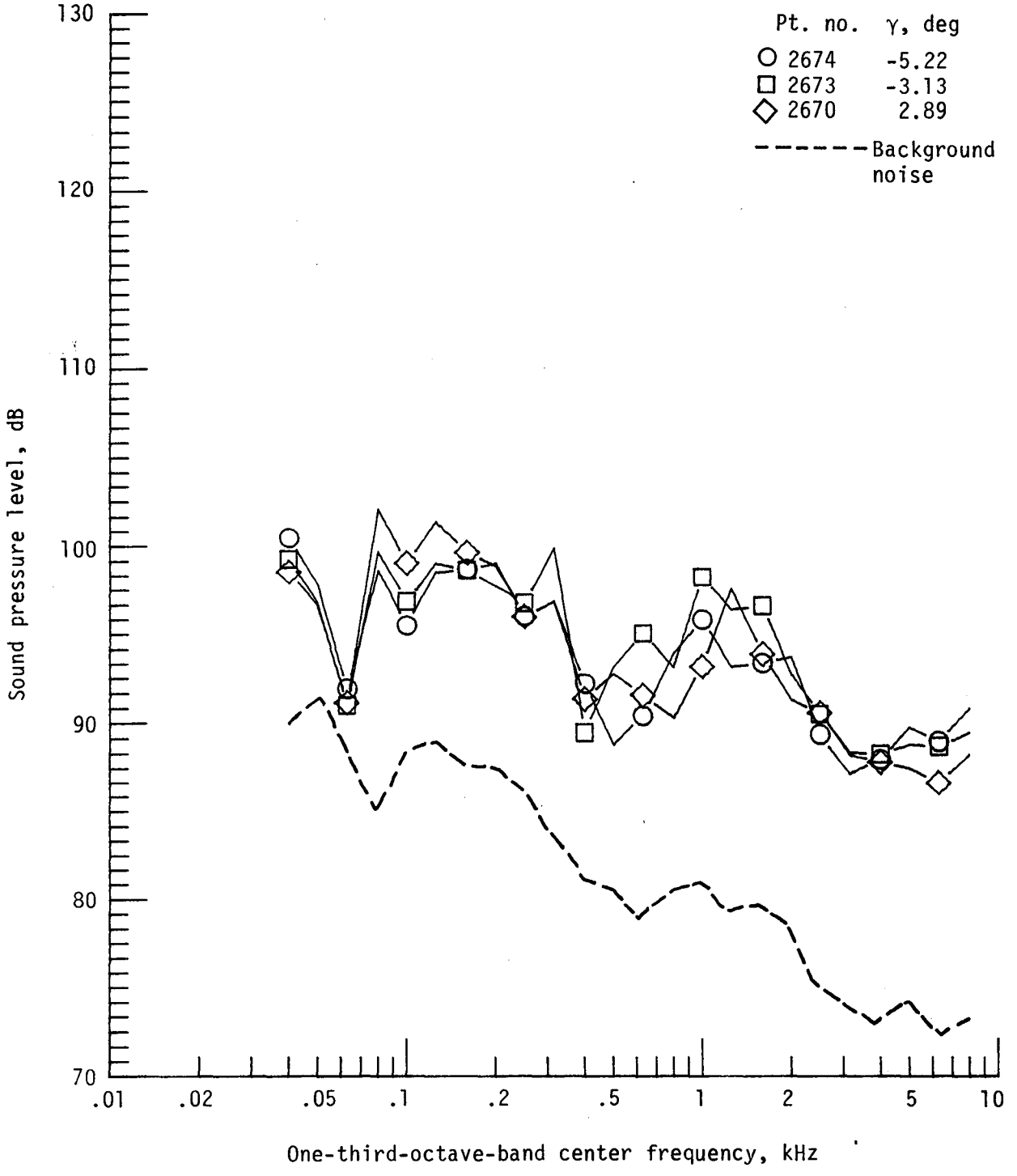

(g) One-third-octave spectra, microphone 7.

Figure 25. - Continued.

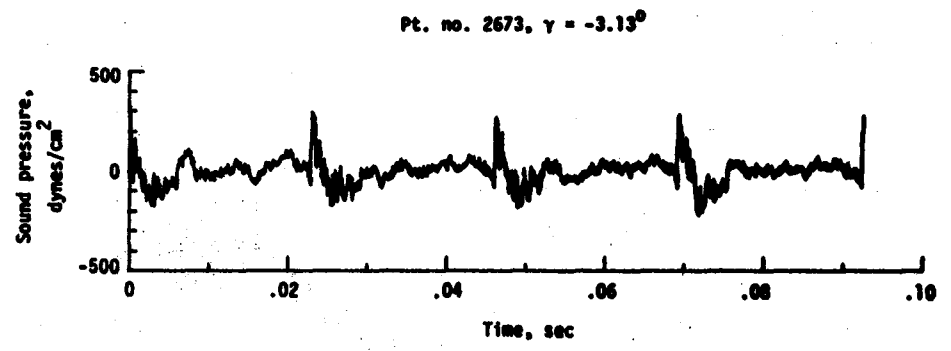

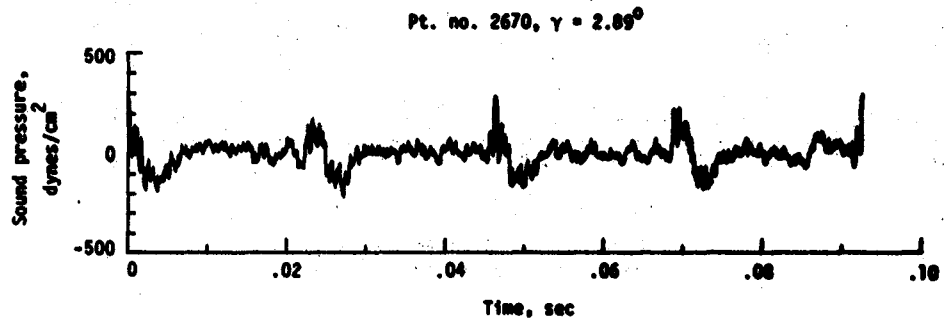

(h) Pressure-time histories; microphone 7.

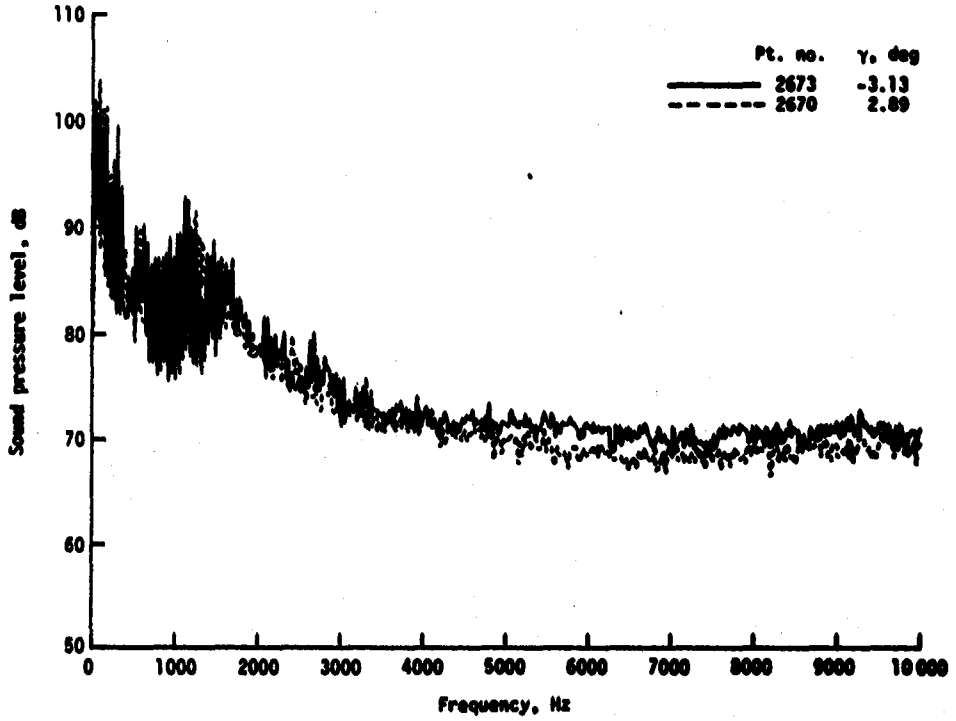

(i) Narrowband analysis; microphone 7.

Figure 25. - Continued.

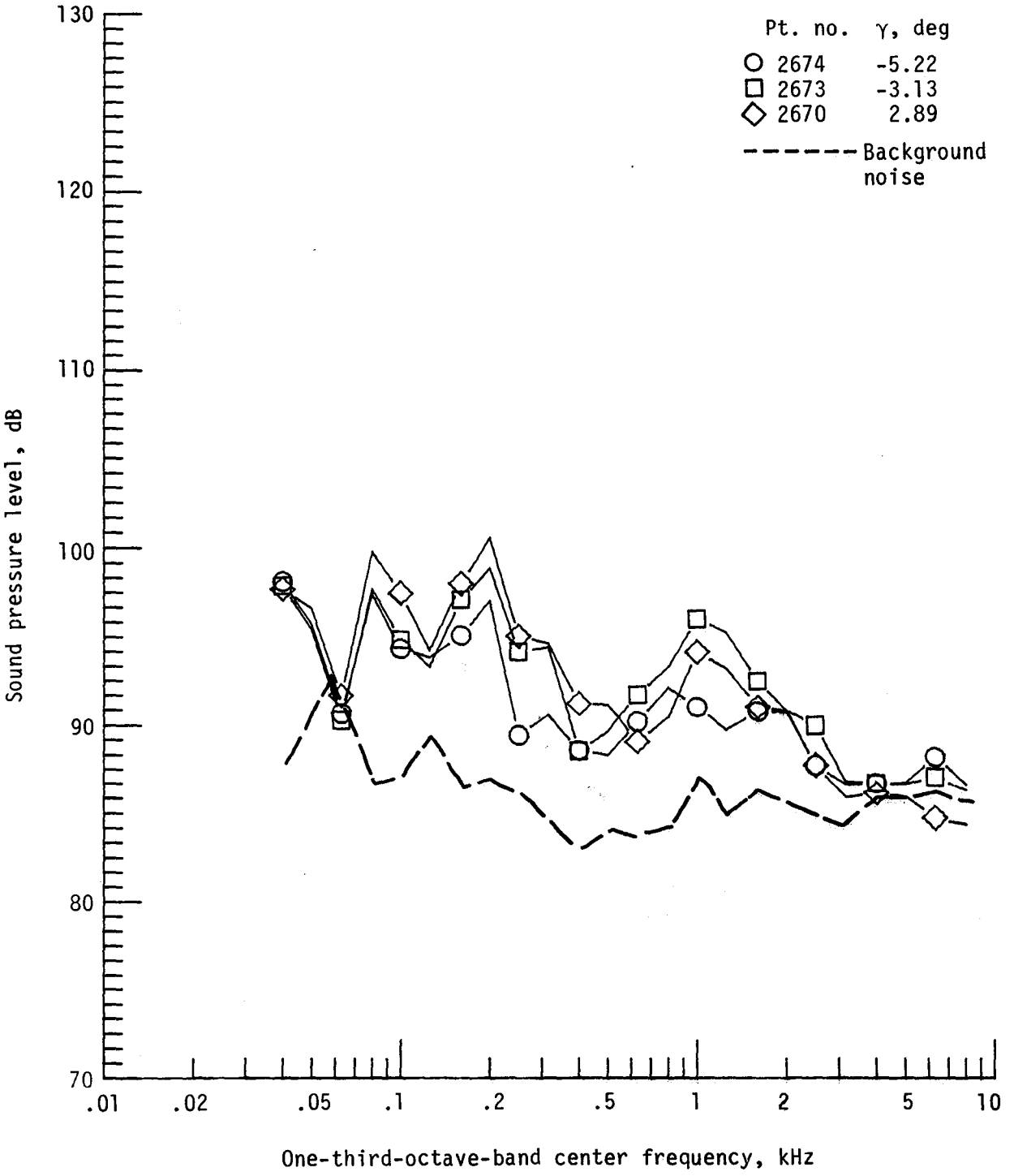

(j) One-third-octave spectra, microphone 8.

Figure 25. - Continued.

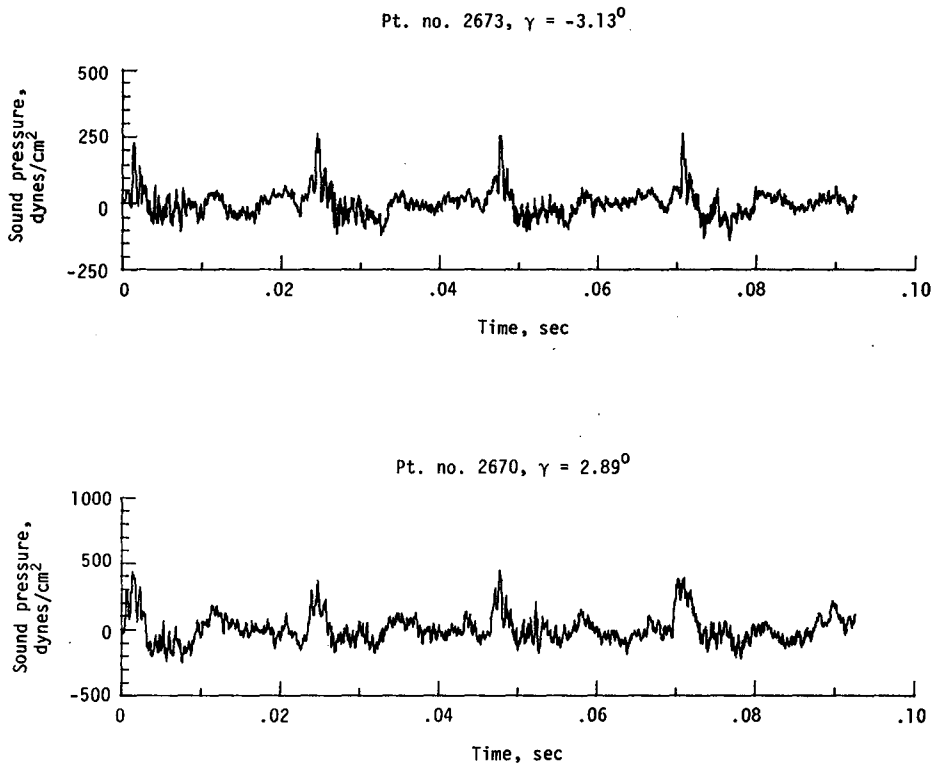

(k) Pressure-time histories; microphone 8.

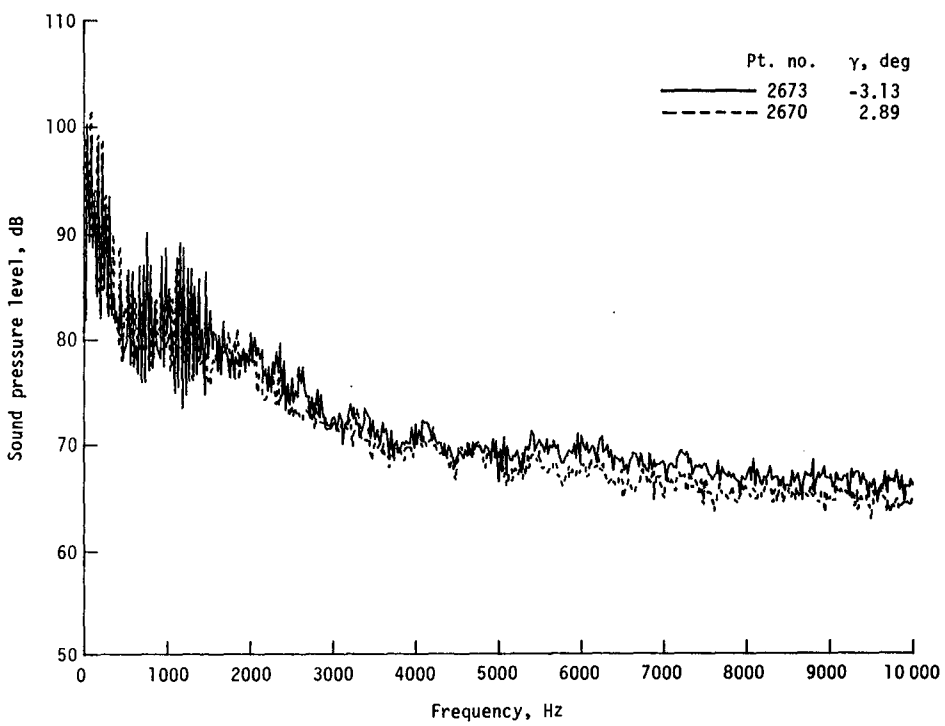

(l) Narrowband analysis; microphone 8.
Figure 25. - Concluded.

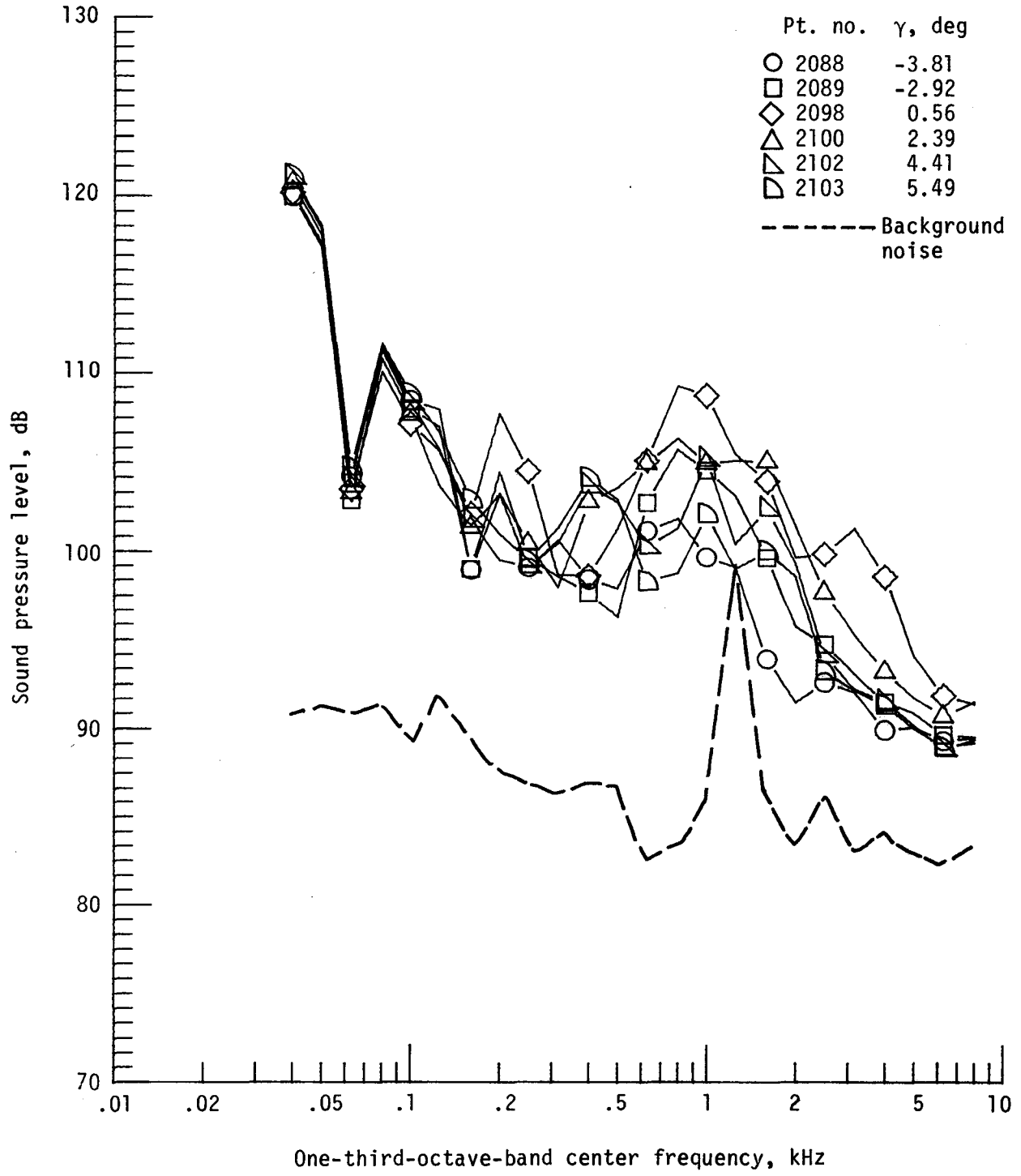

(a) One-third-octave spectra, microphone 2.

Figure 26. - Effect of descent angle variation on noise generated by helicopter model with standard rotor system, run 162. V_∞ = 75.0 knots, C_T = .0032.

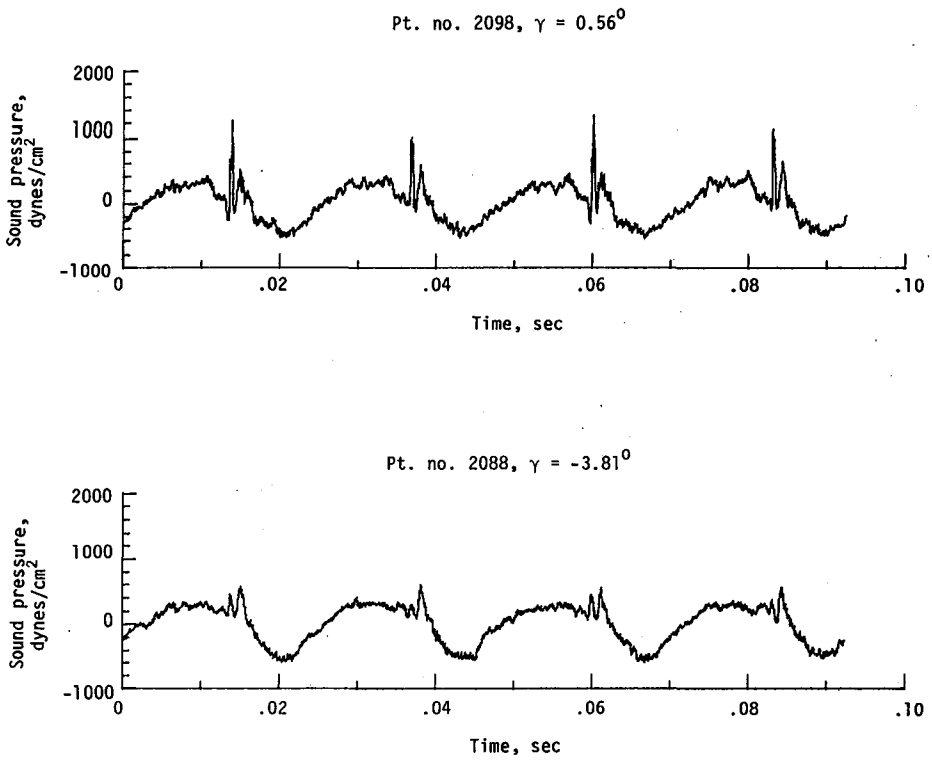

(b) Pressure-time histories; microphone 2.

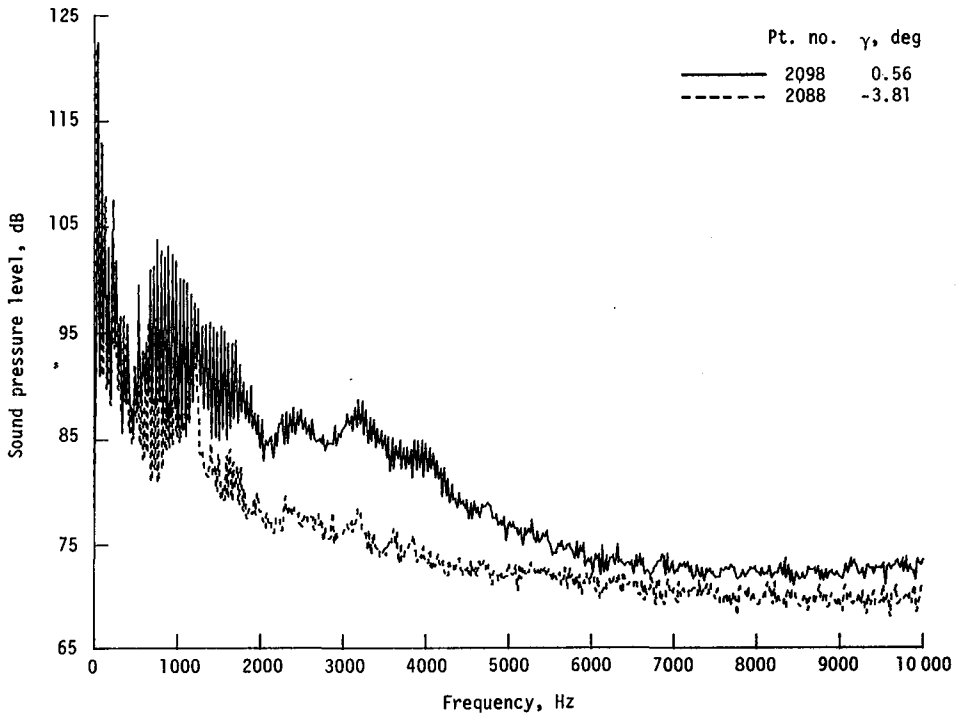

(c) Narrowband analysis; microphone 2.
Figure 26. - Continued.

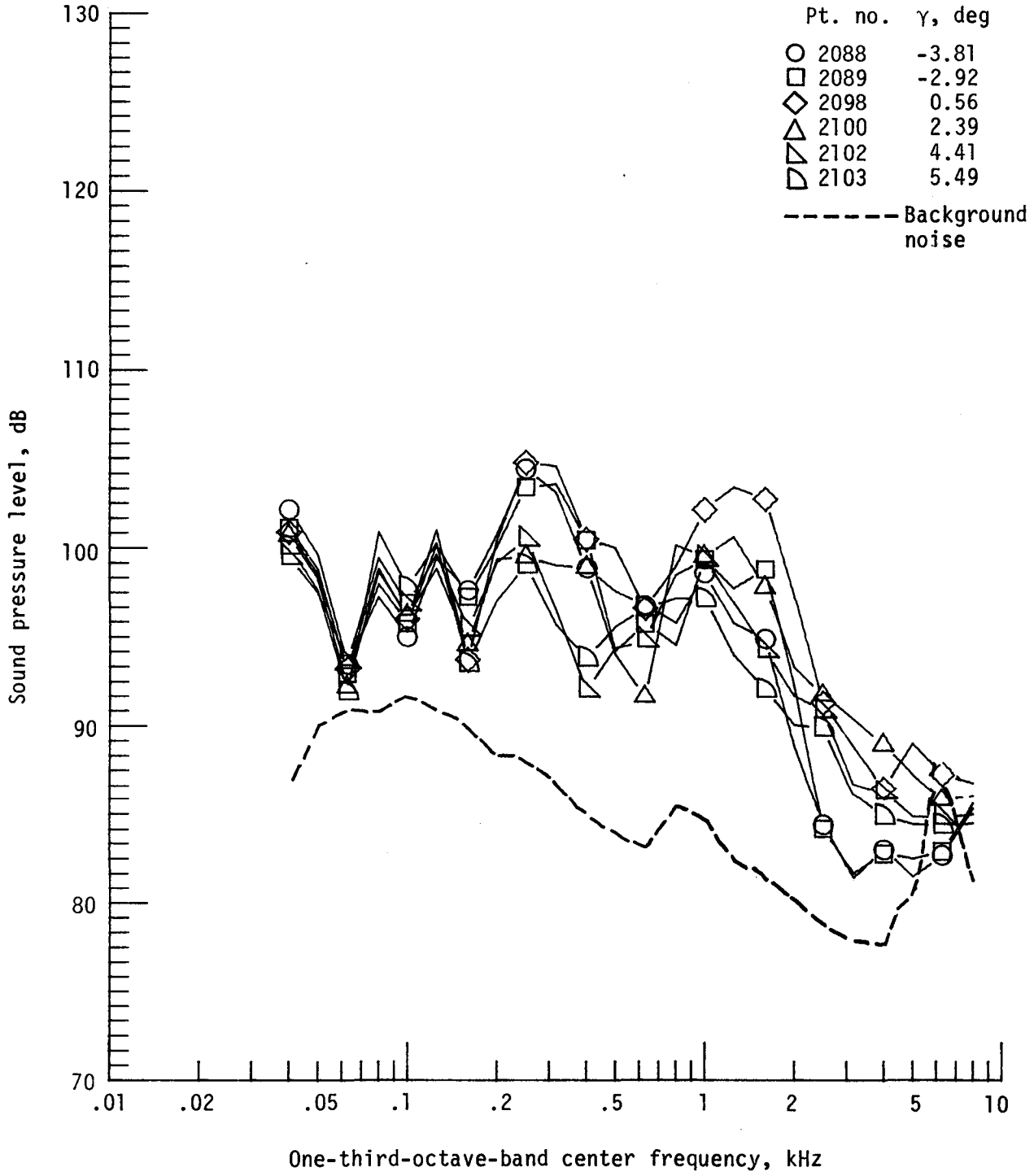

(d) One-third-octave spectra, microphone 6.

Figure 26. - Continued.

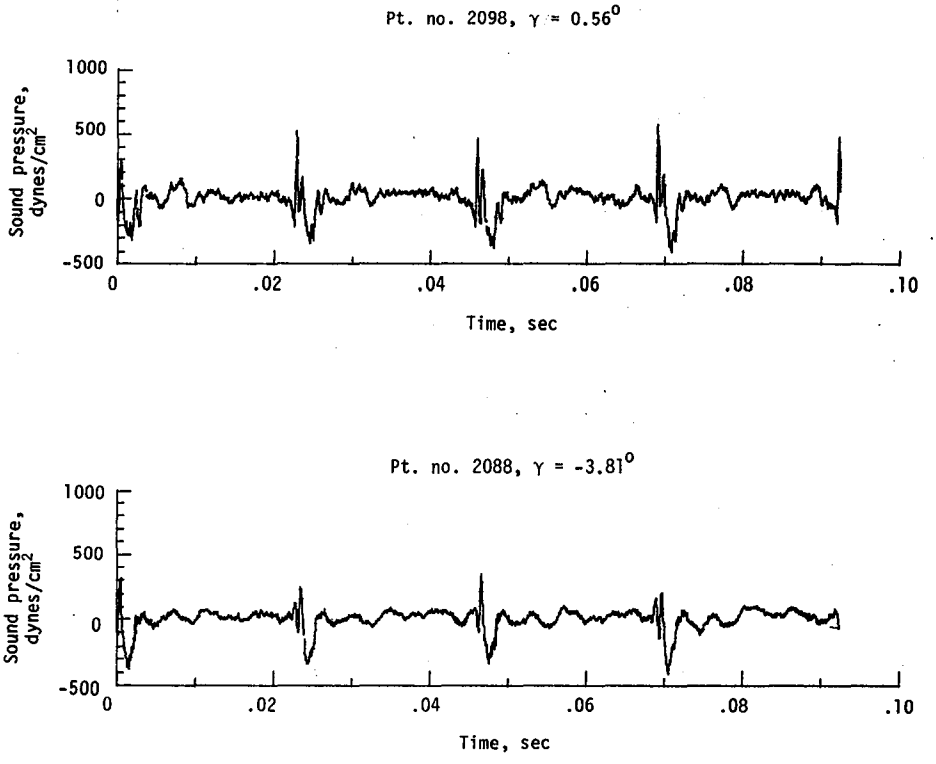

(e) Pressure-time histories; microphone 6.

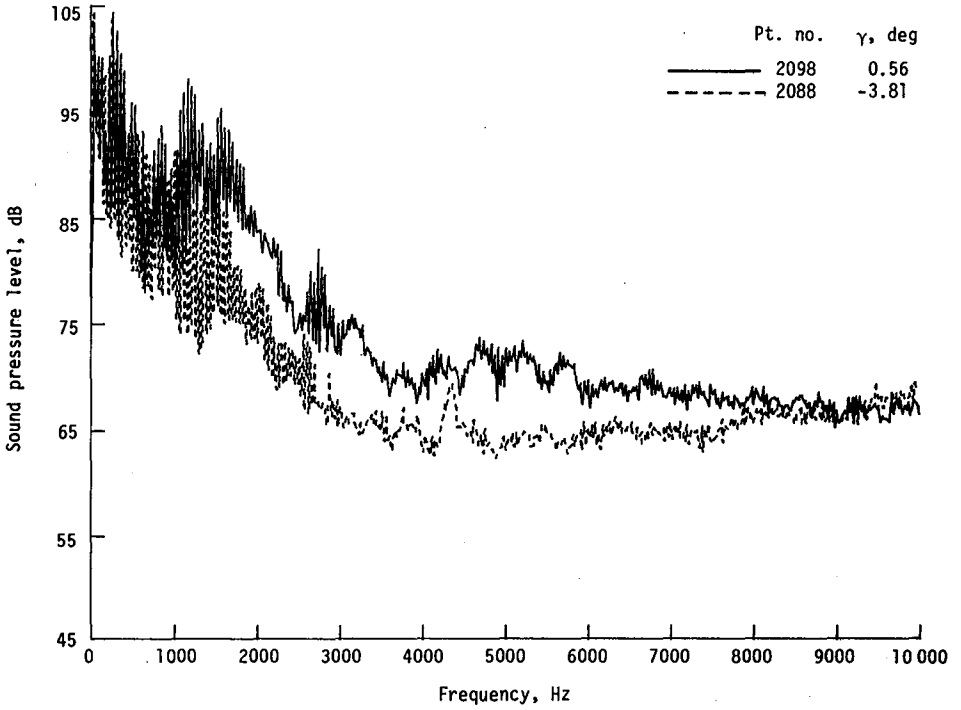

(f) Narrowband analysis; microphone 6.
Figure 26. - Continued.

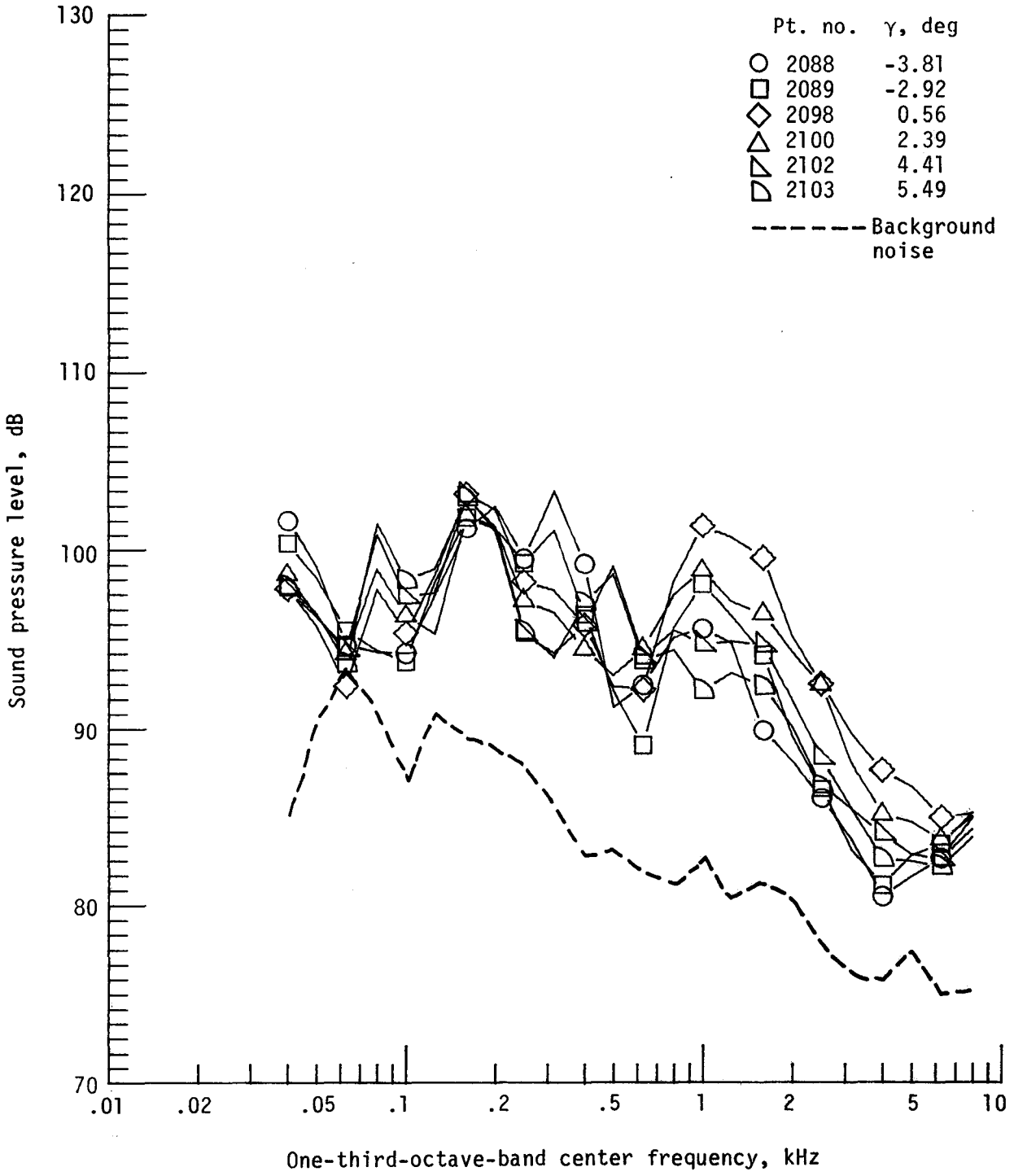

(g) One-third-octave spectra, microphone 7.

Figure 26 - Continued.

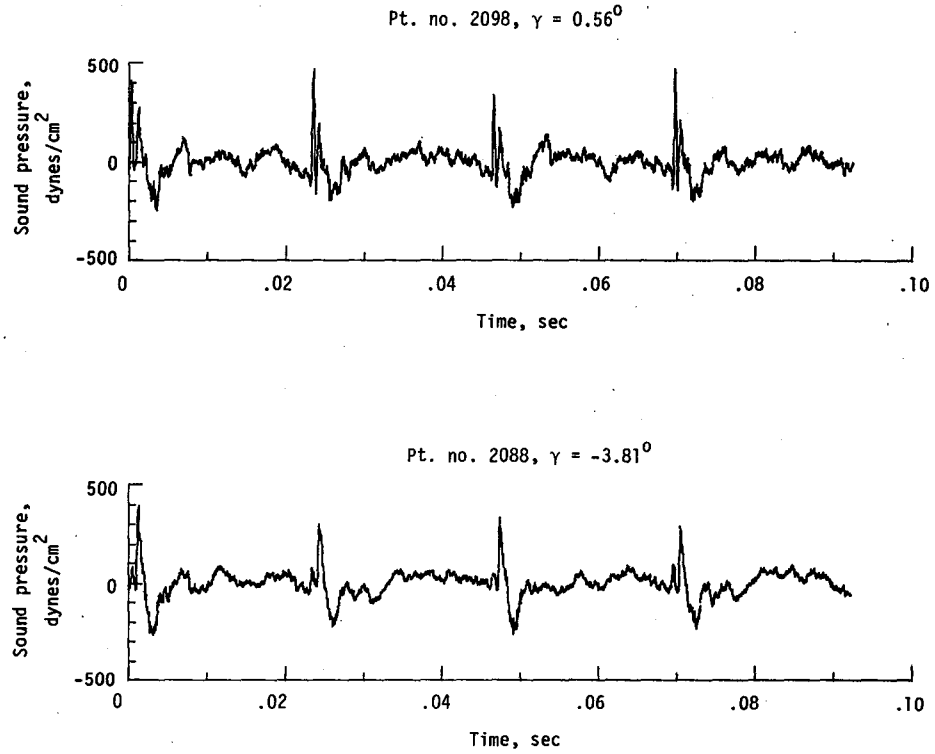

(h) Pressure-time histories; microphone 7.

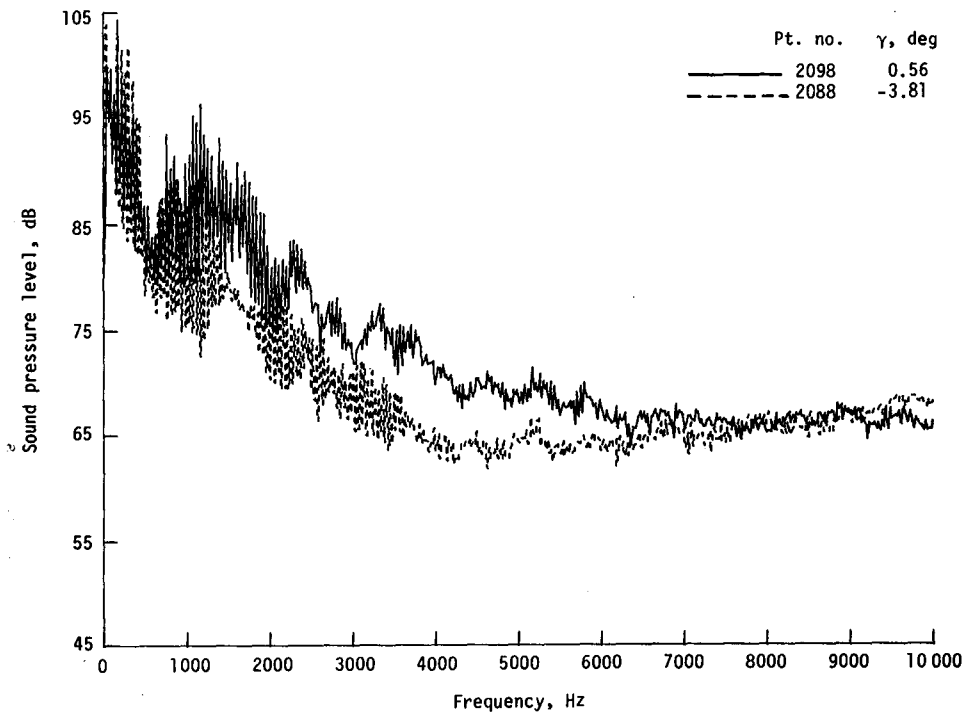

(i) Narrowband analysis; microphone 7.
Figure 26. - Continued.

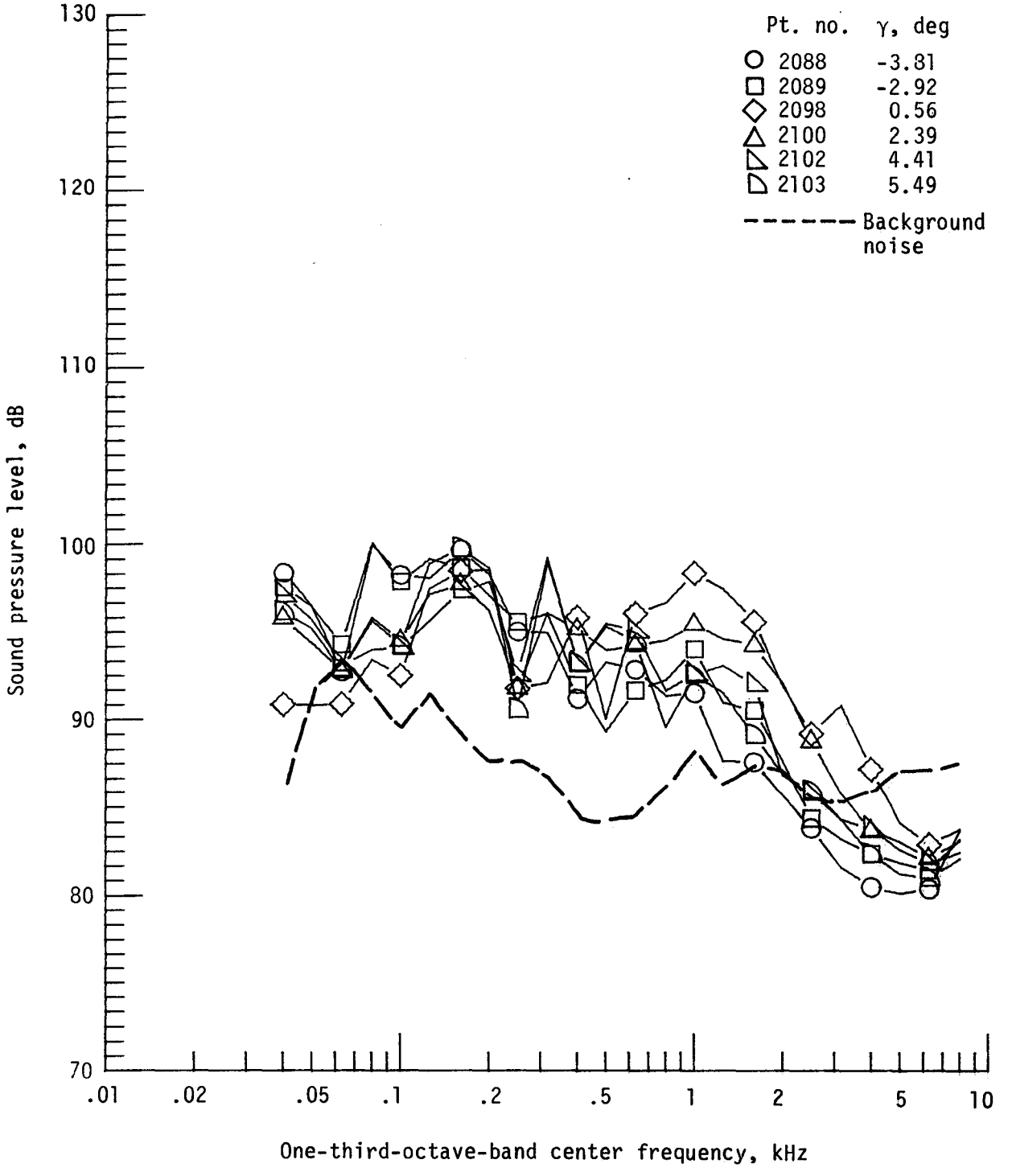

(j) One-third-octave spectra, microphone 8.

Figure 26. - Continued.

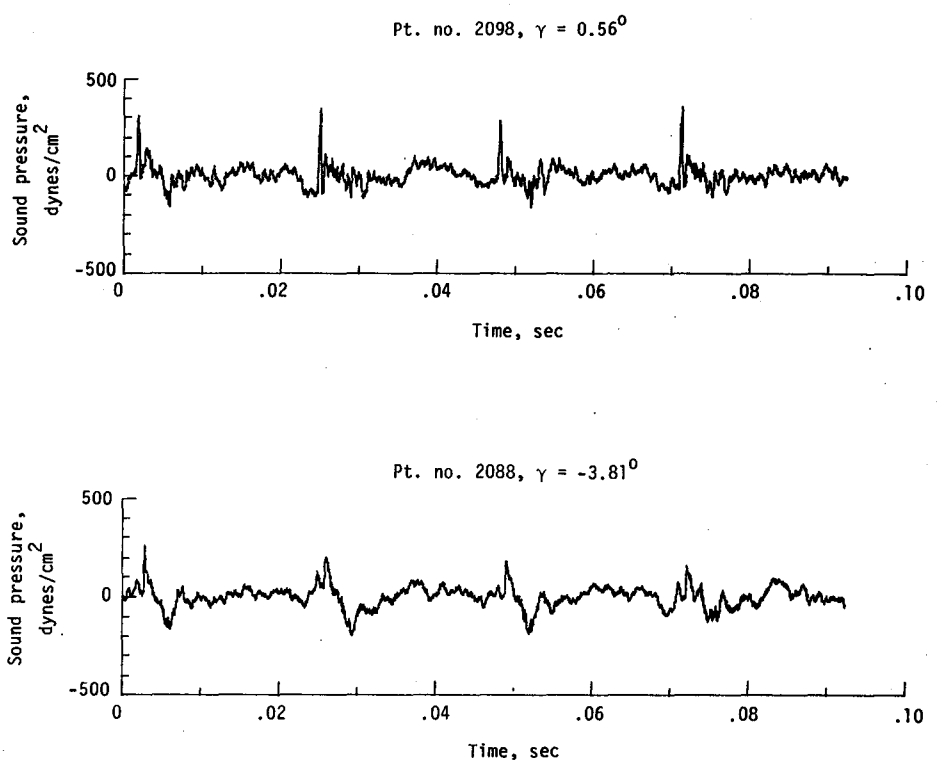

(k) Pressure-time histories; microphone 8.

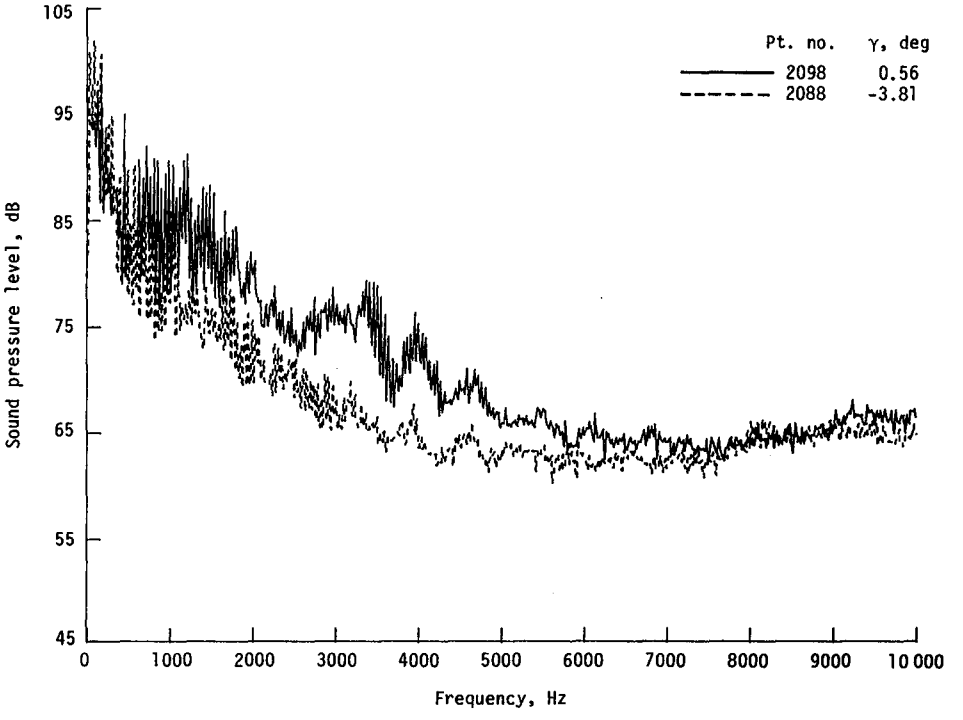

(l) Narrowband analysis; microphone 8.
Figure 26. - Concluded.

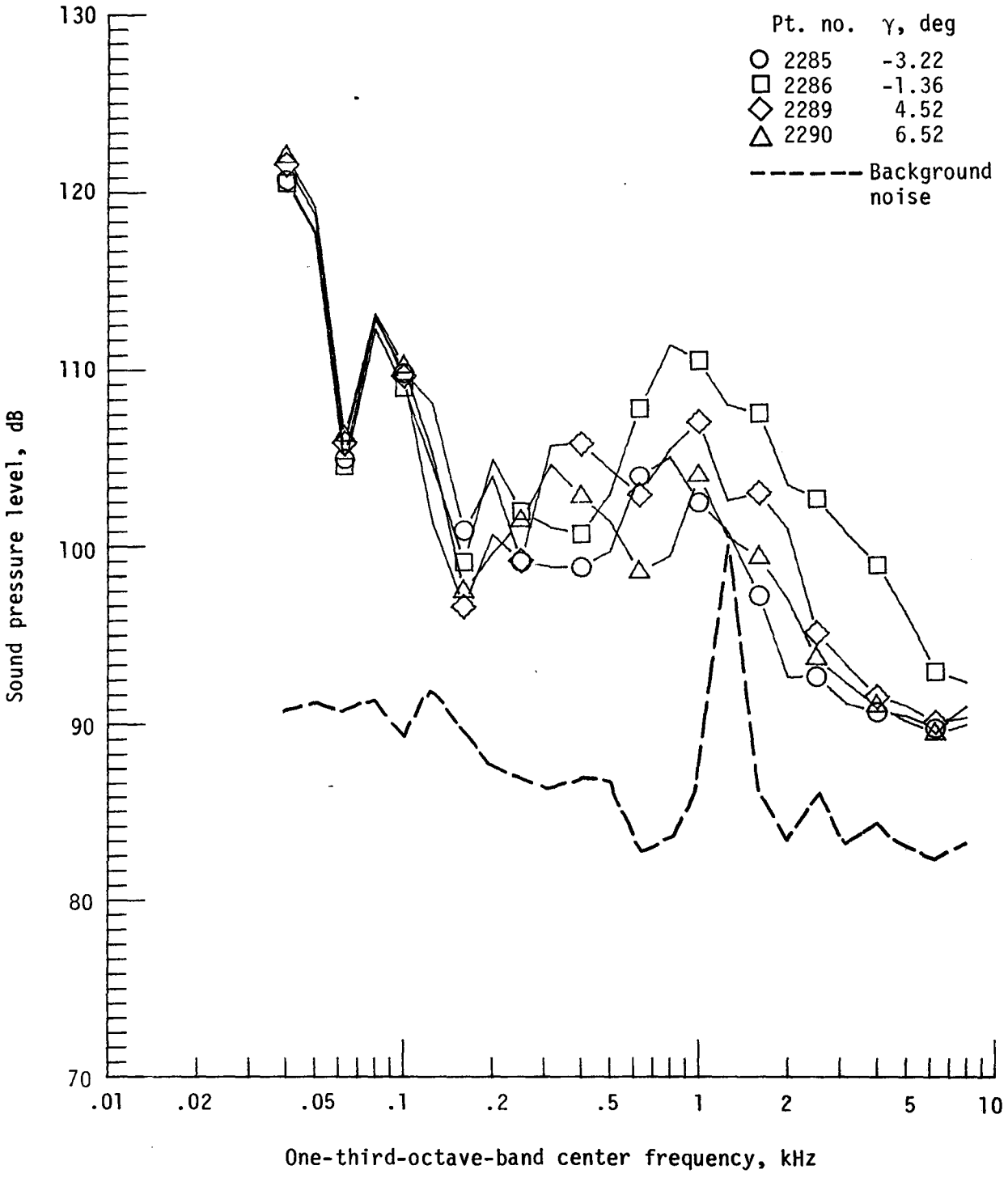

(a) One-third-octave spectra, microphone 2.

Figure 27. - Effect of descent angle variation on noise generated by helicopter model with standard rotor system, run 184. V_∞ = 74.8 knots, C_T = .0036.

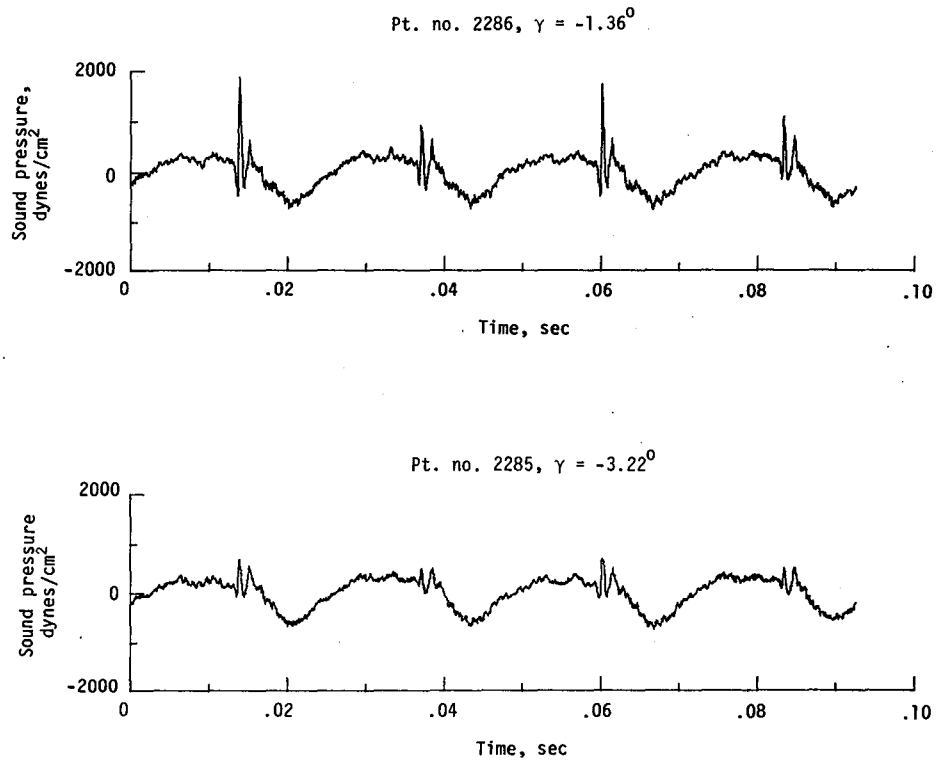

(b) Pressure-time histories; microphone 2.

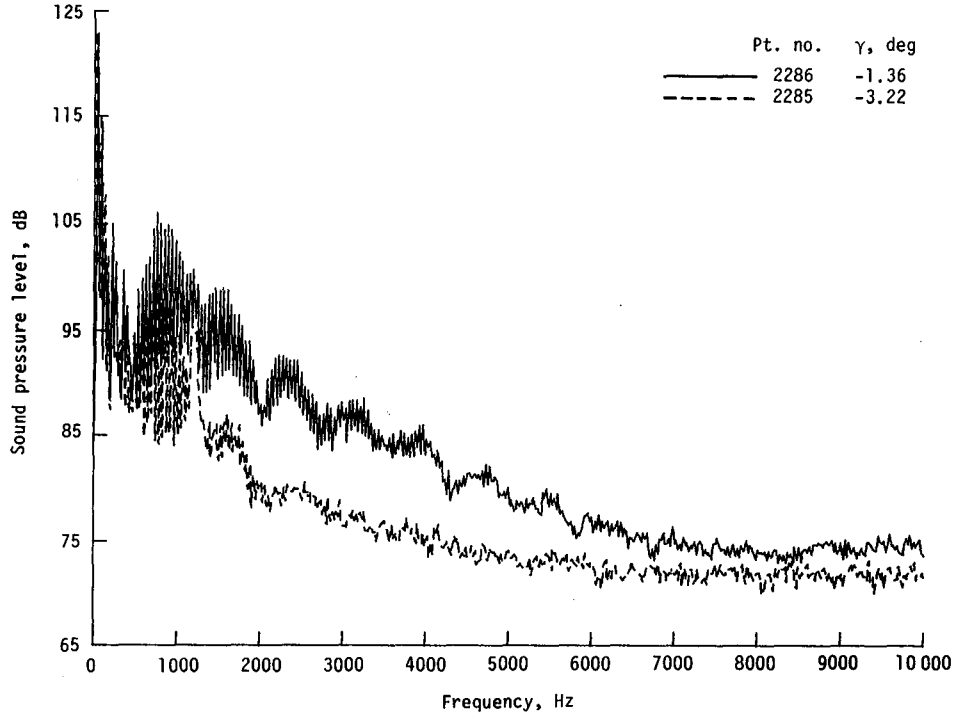

(c) Narrowband analysis; microphone 2.

Figure 27. - Continued.

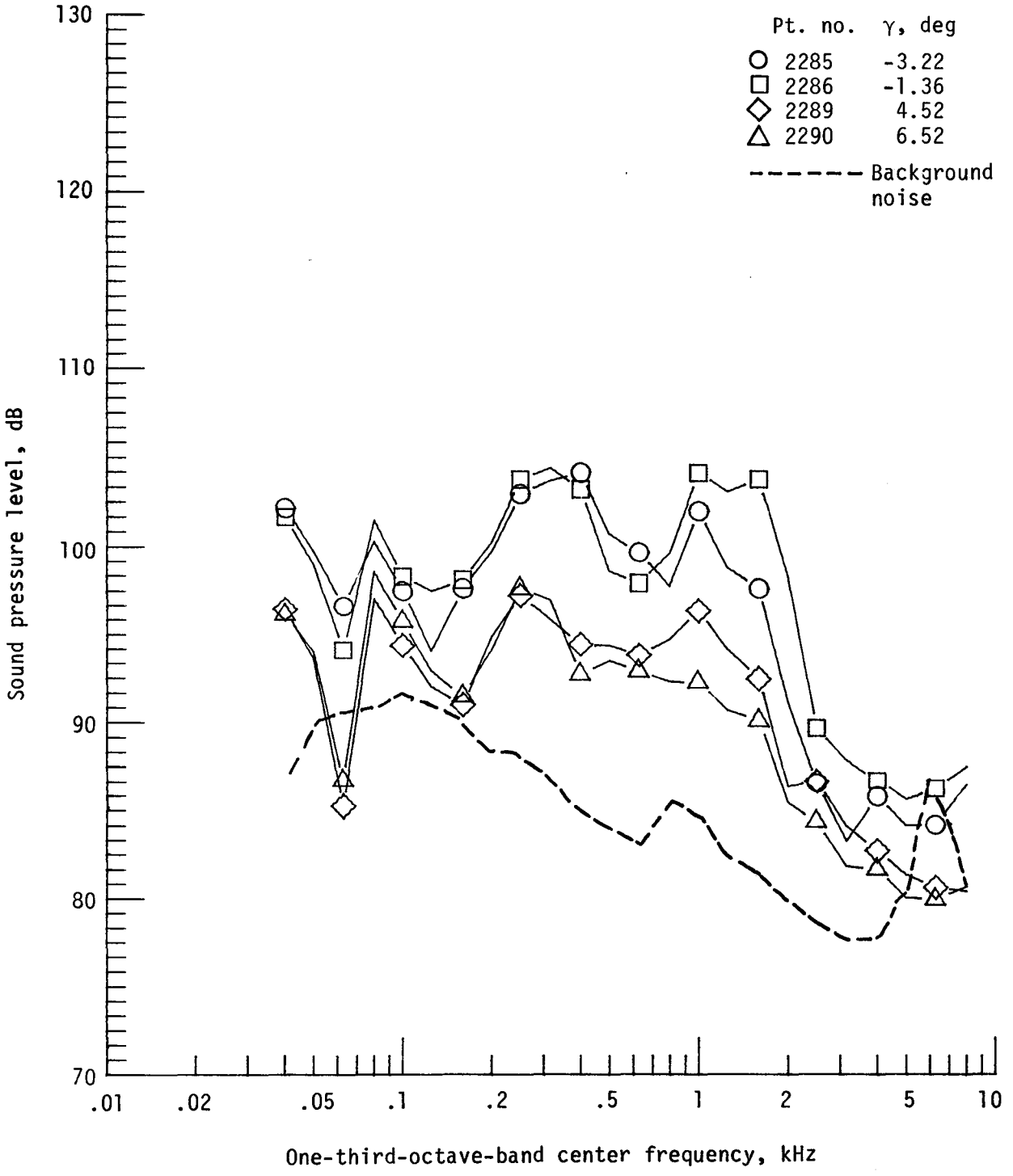

(d) One-third-octave spectra, microphone 6.

Figure 27. - Continued.

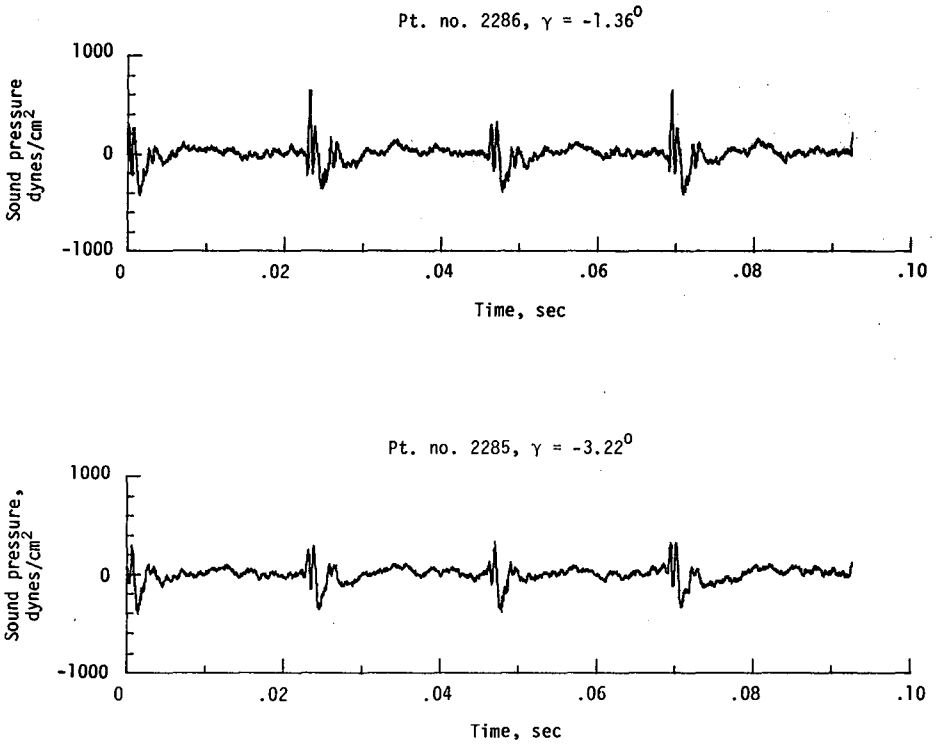

(e) Pressure-time histories; microphone 6.

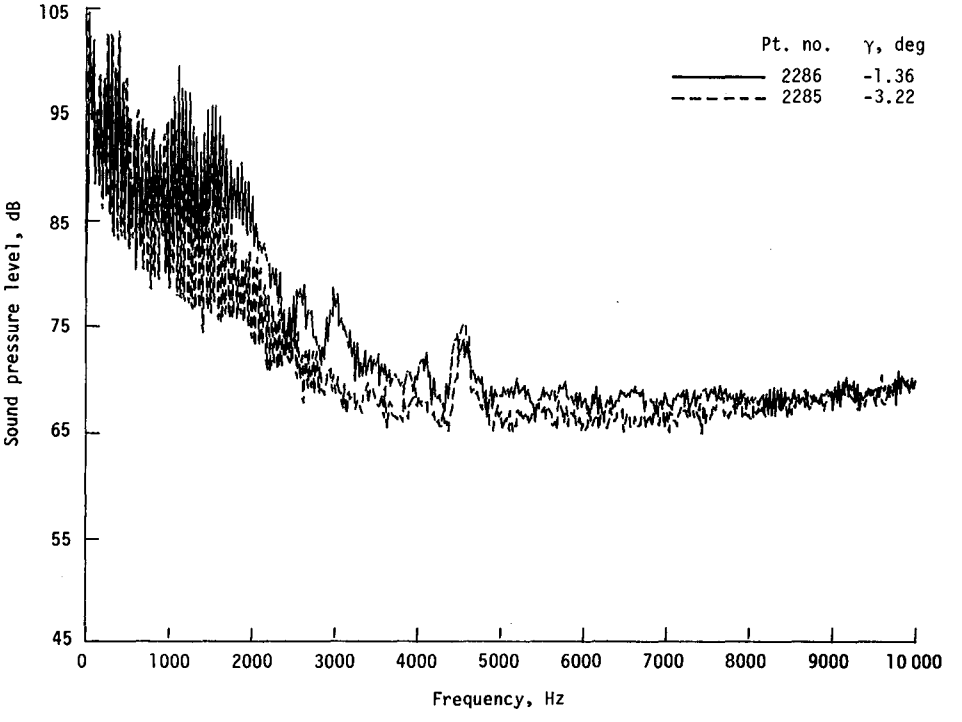

(f) Narrowband analysis; microphone 6.
Figure 27. - Continued.

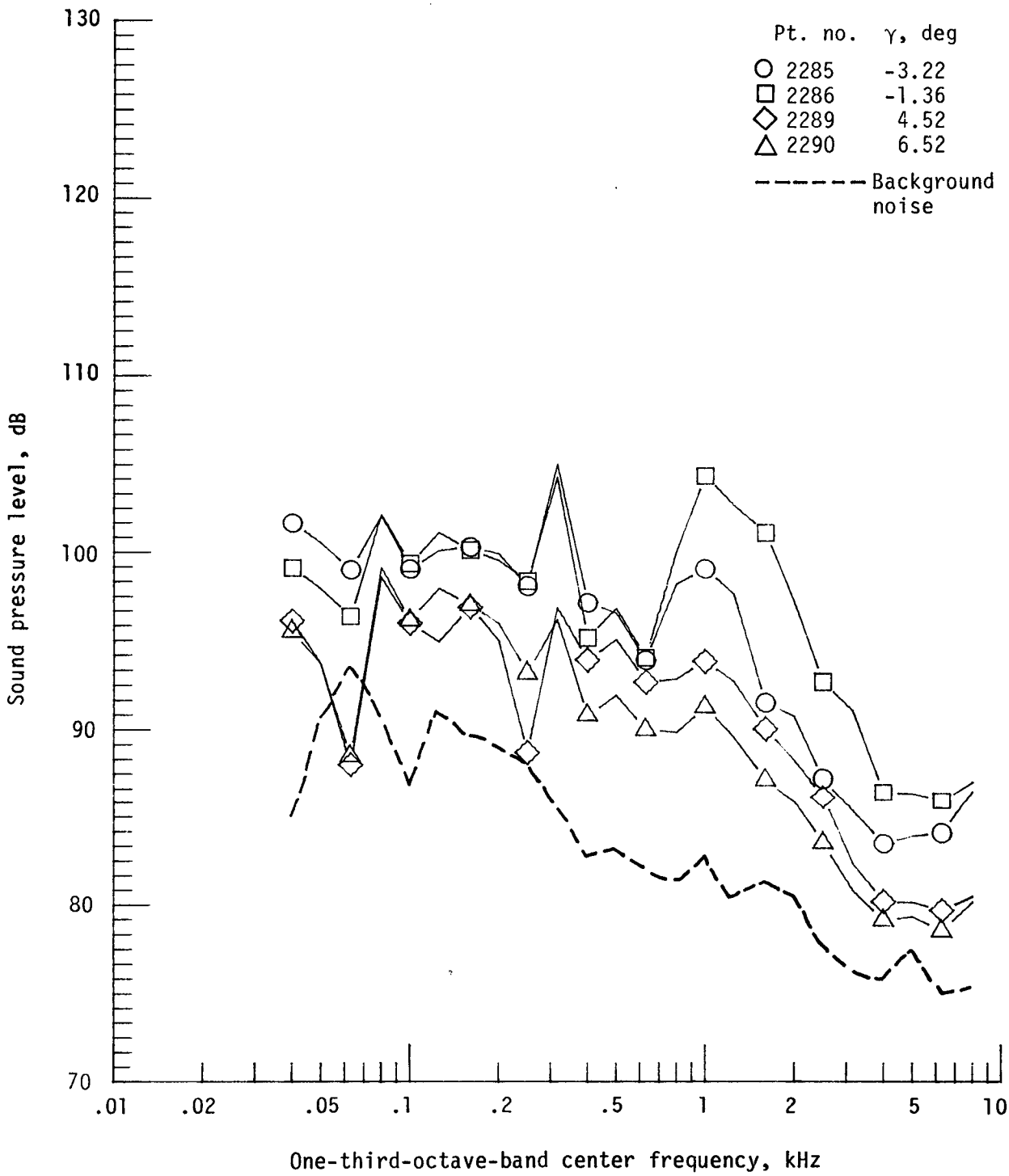

(g) One-third-octave spectra, microphone 7.

Figure 27. - Continued.

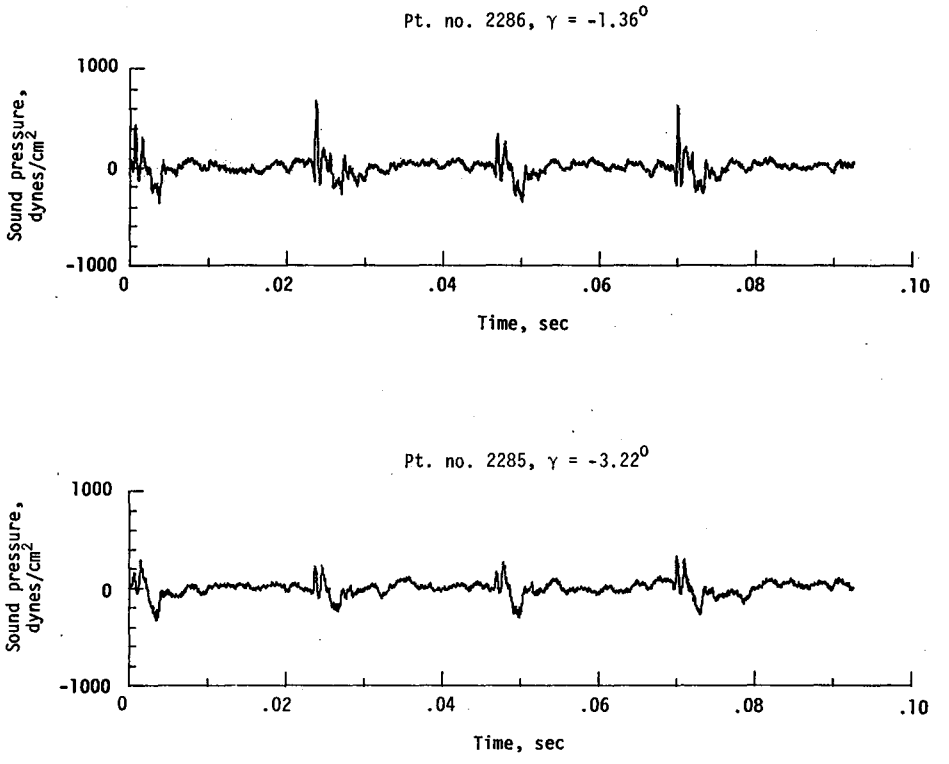

(h) Pressure-time histories; microphone 7.

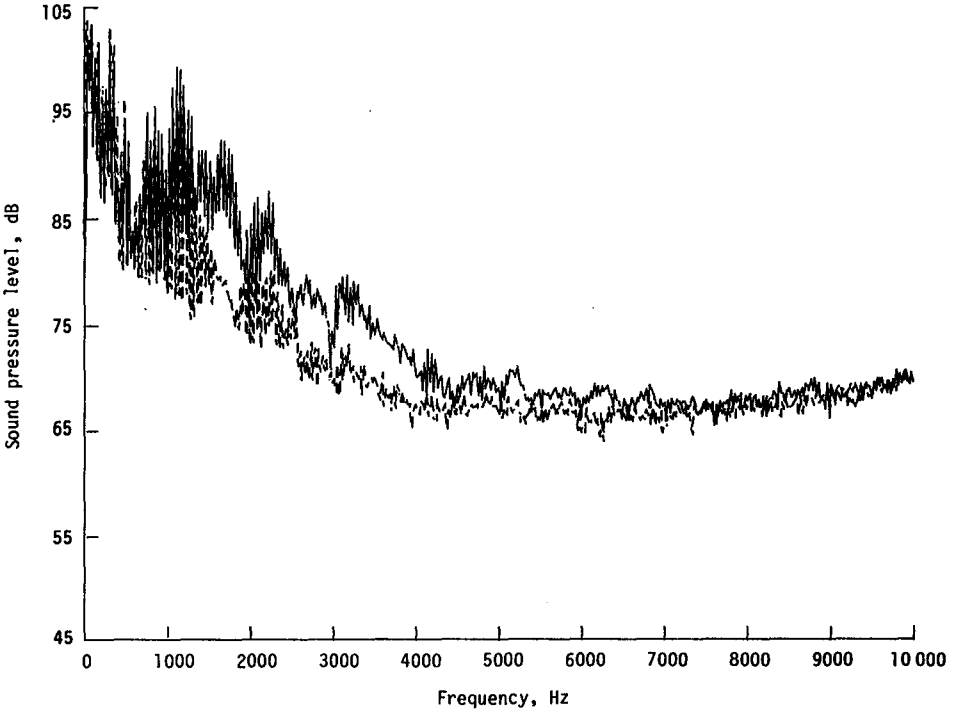

(i) Narrowband analysis; microphone 7.

Figure 27. - Continued.

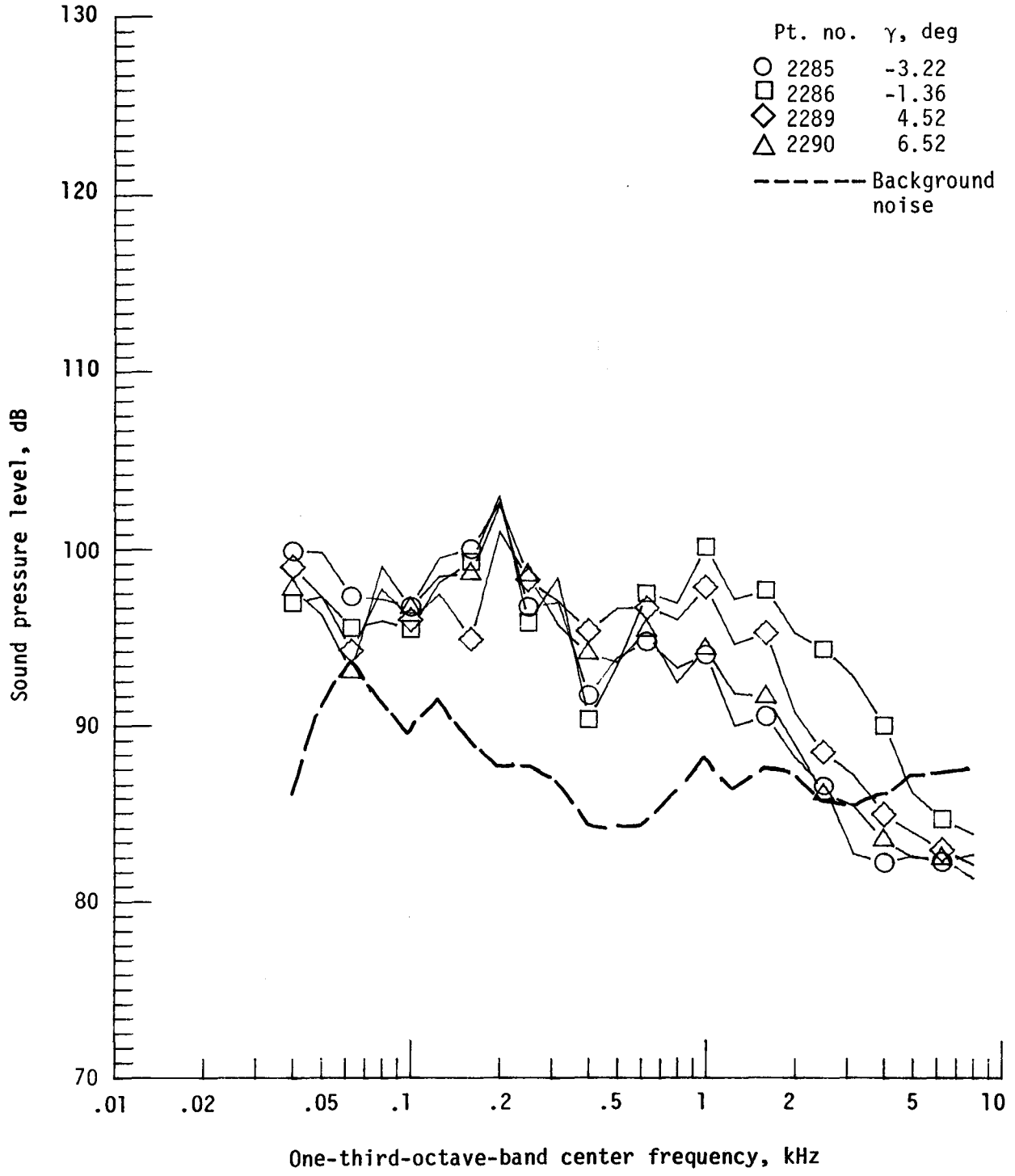

(j) One-third-octave spectra, microphone 8.

Figure 27. - Continued.

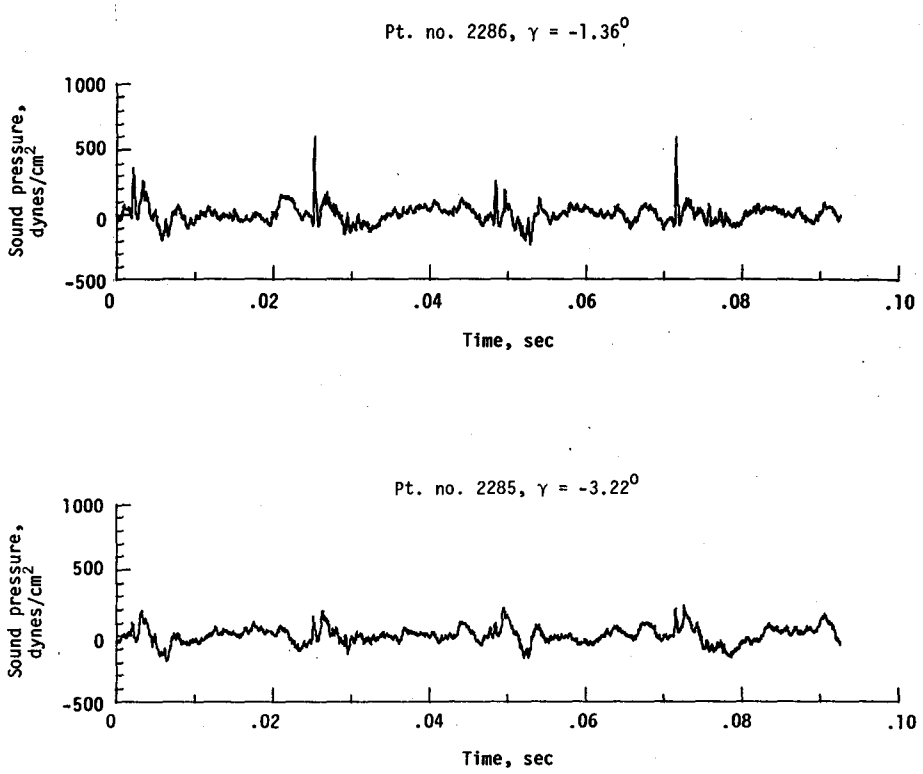

(k) Pressure-time histories; microphone 8.

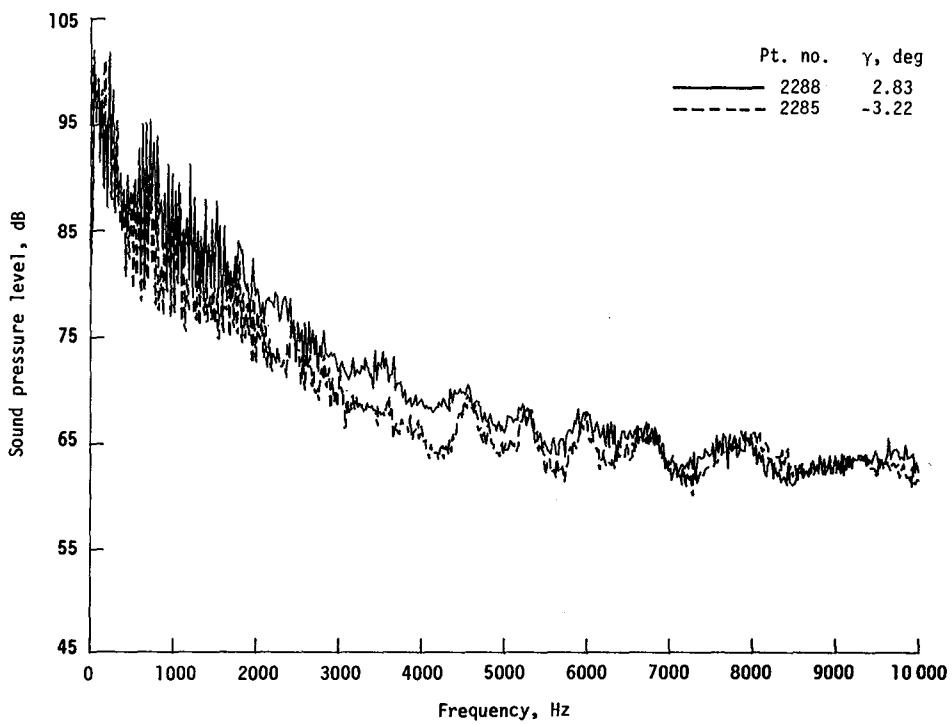

(l) Narrowband analysis; microphone 8.
Figure 27. - Concluded.

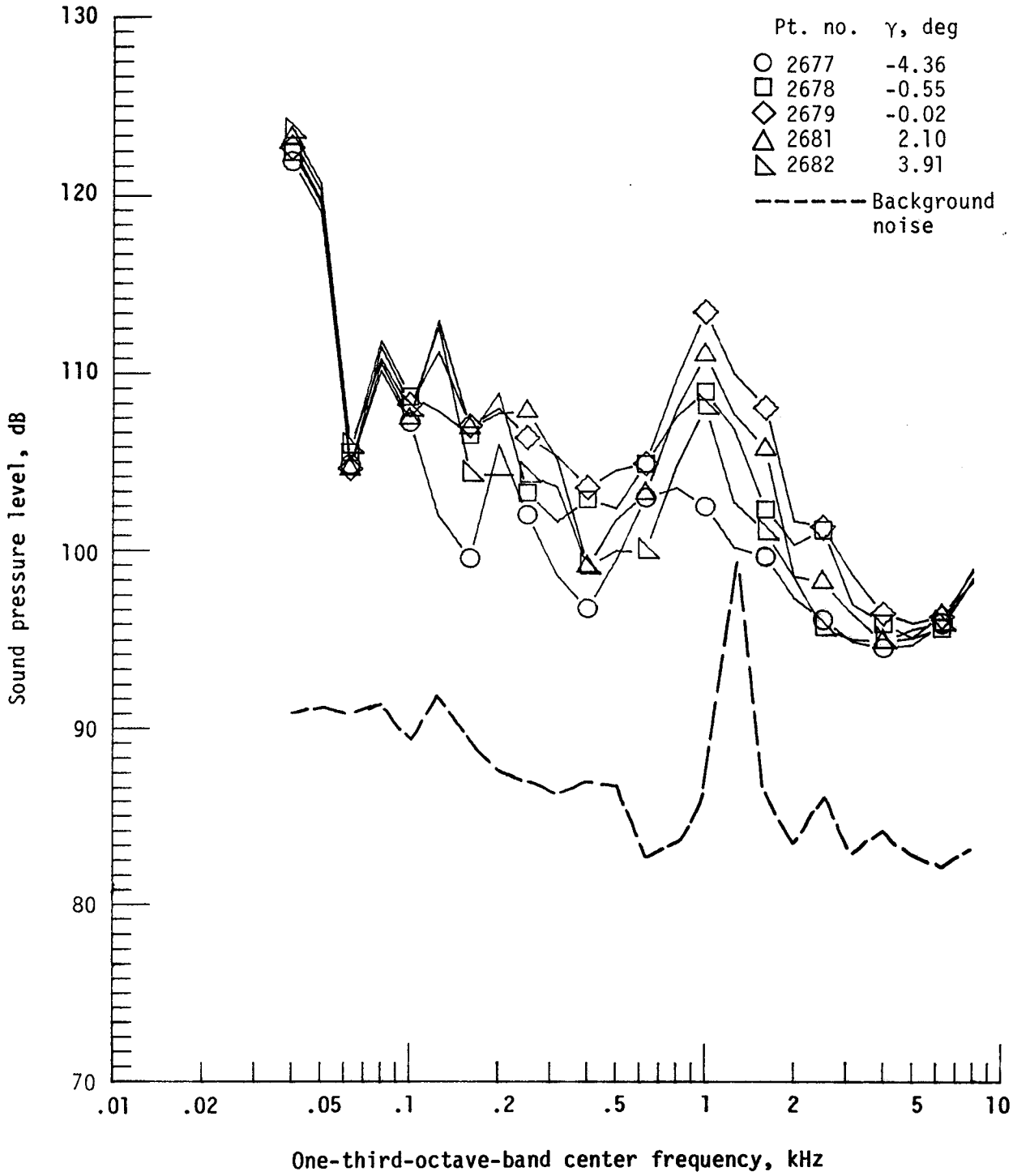

(a) One-third-octave spectra, microphone 2.

Figure 28. - Effect of descent angle variation on noise generated by helicopter model with advanced rotor system, run 216. V_∞ = 75.0 knots, C_T = .0036.

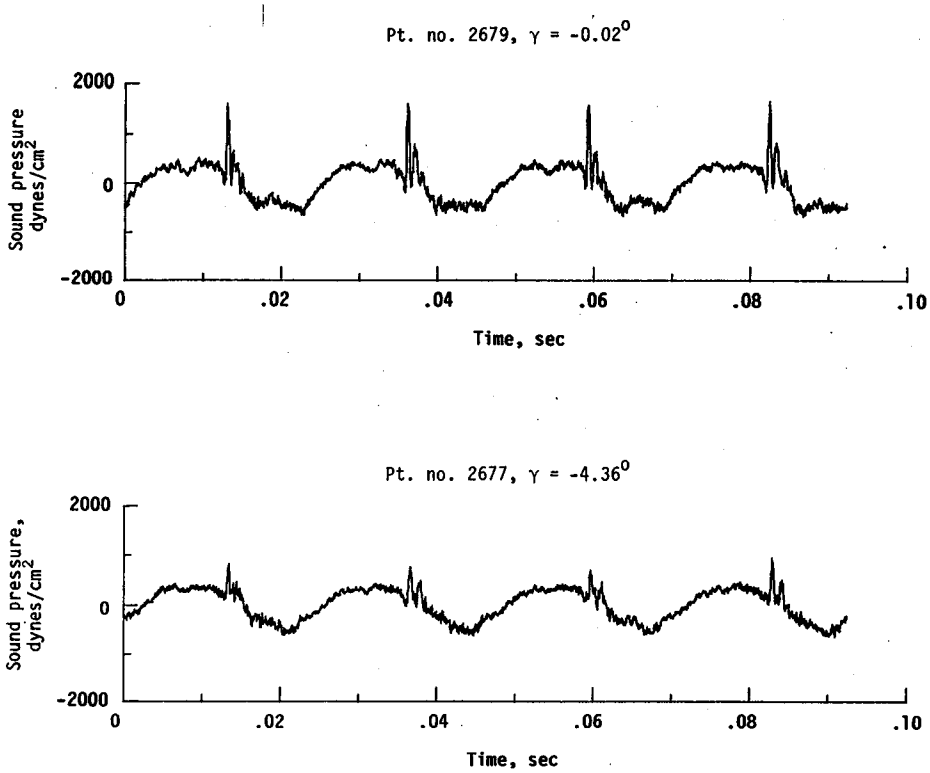

(b) Pressure-time histories; microphone 2.

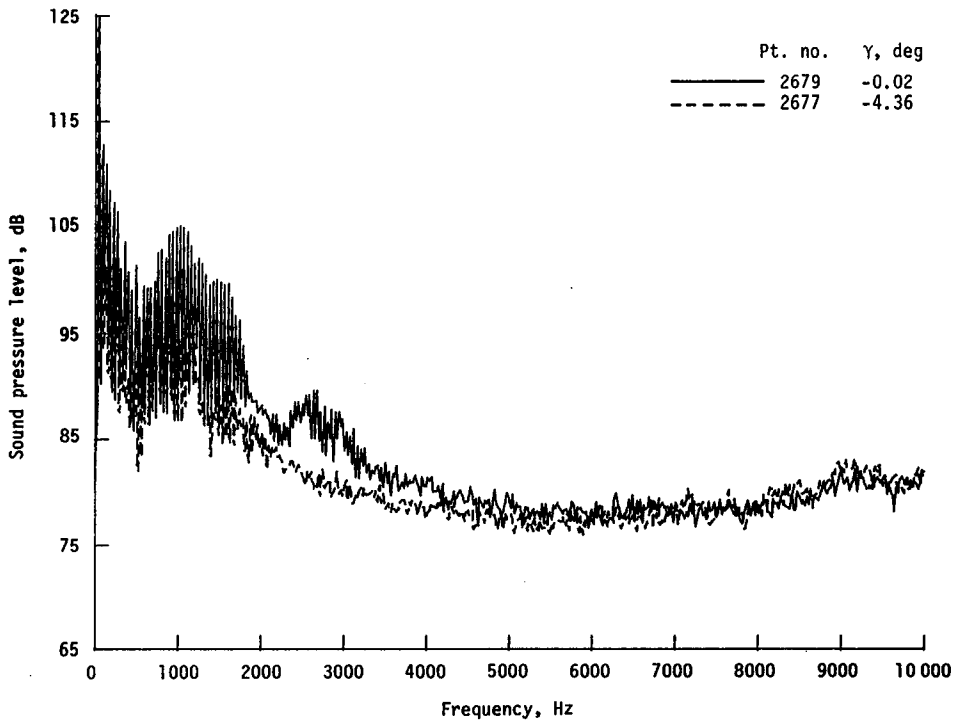

(c) Narrowband analysis; microphone 2.
Figure 28. - Continued.

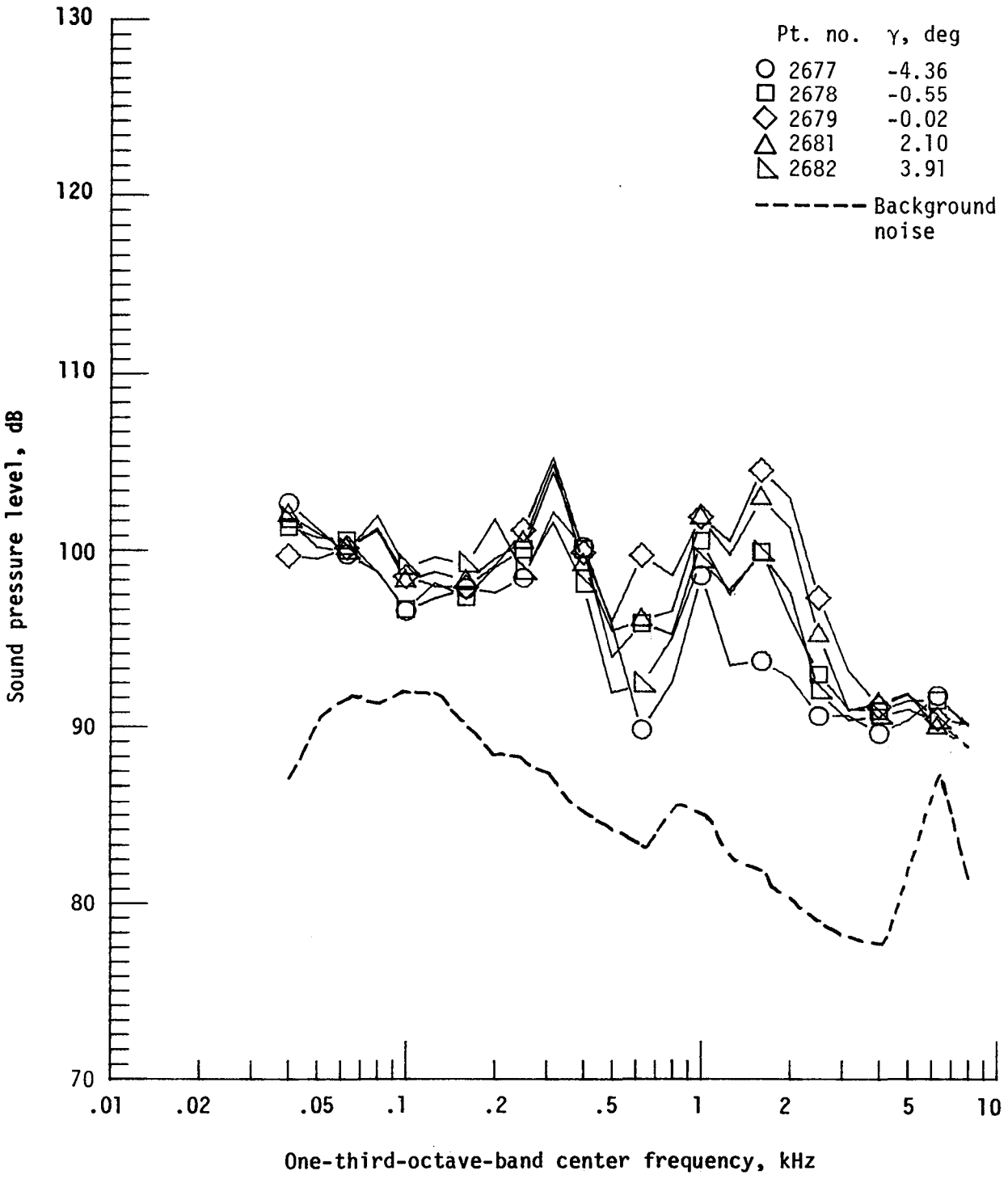

(d) One-third-octave spectra, microphone 6.

Figure 28. - Continued.

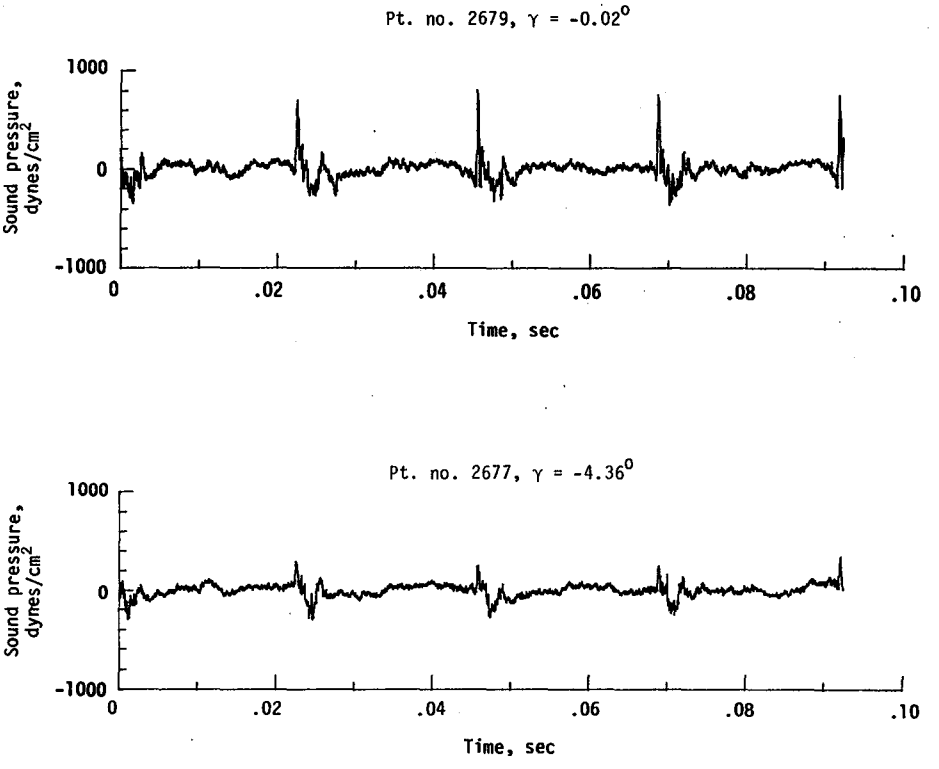

(e) Pressure-time histories; microphone 6.

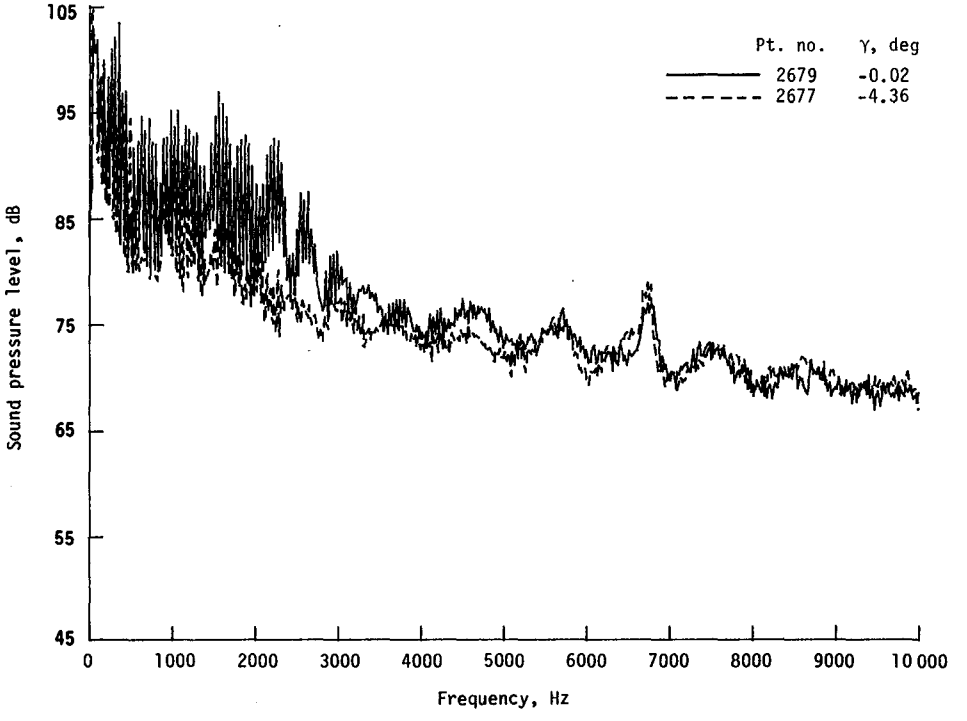

(f) Narrowband analysis; microphone 6.
Figure 28. - Continued.

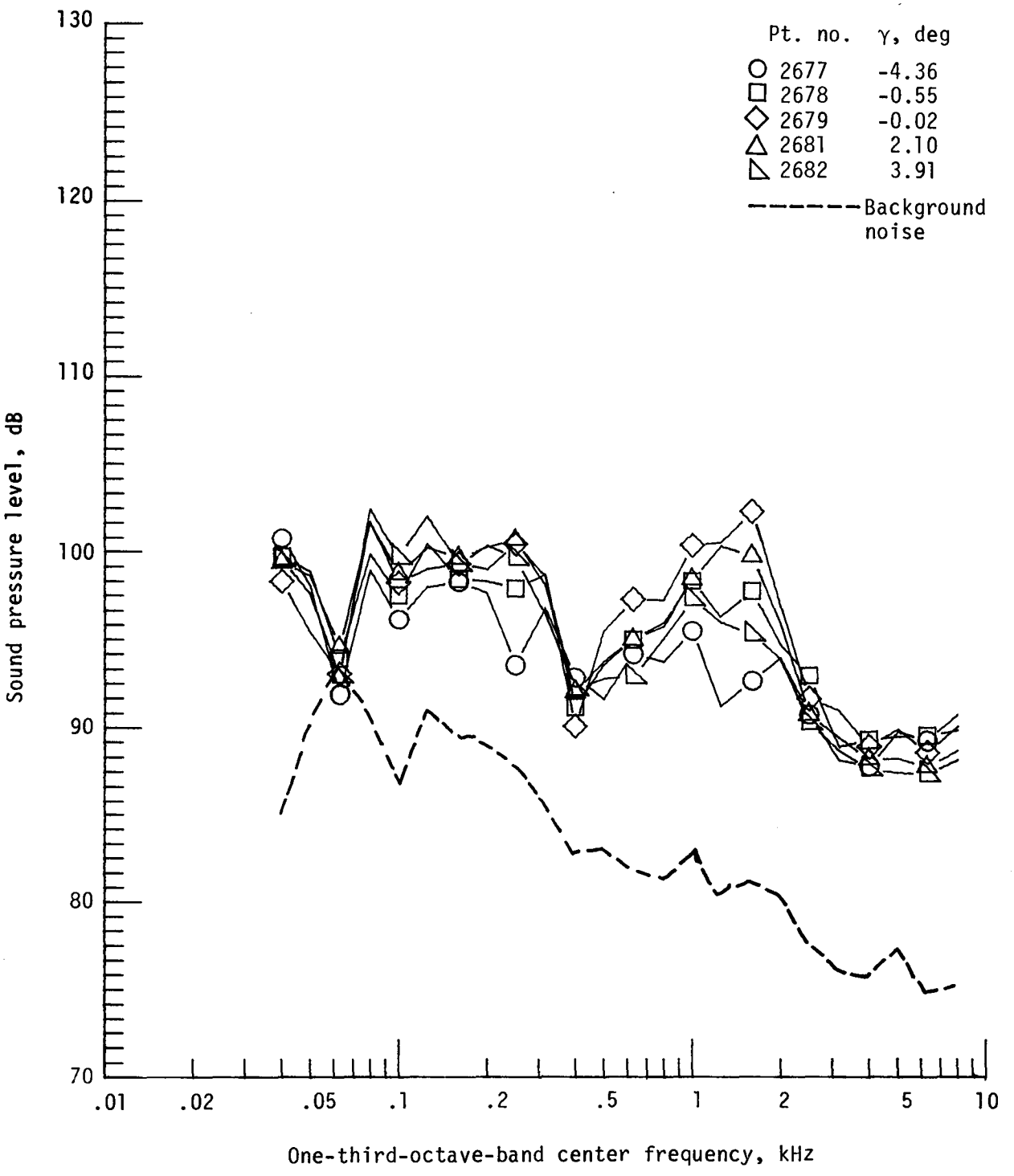

(g) One-third-octave spectra, microphone 7.

Figure 28. - Continued.

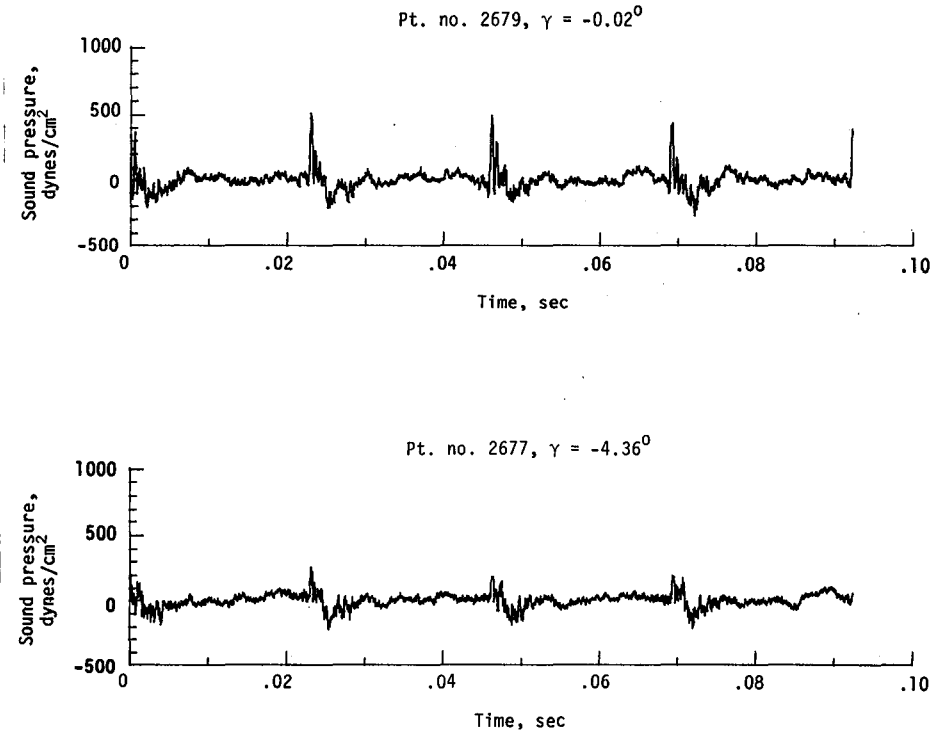

(h) Pressure-time histories; microphone 7.

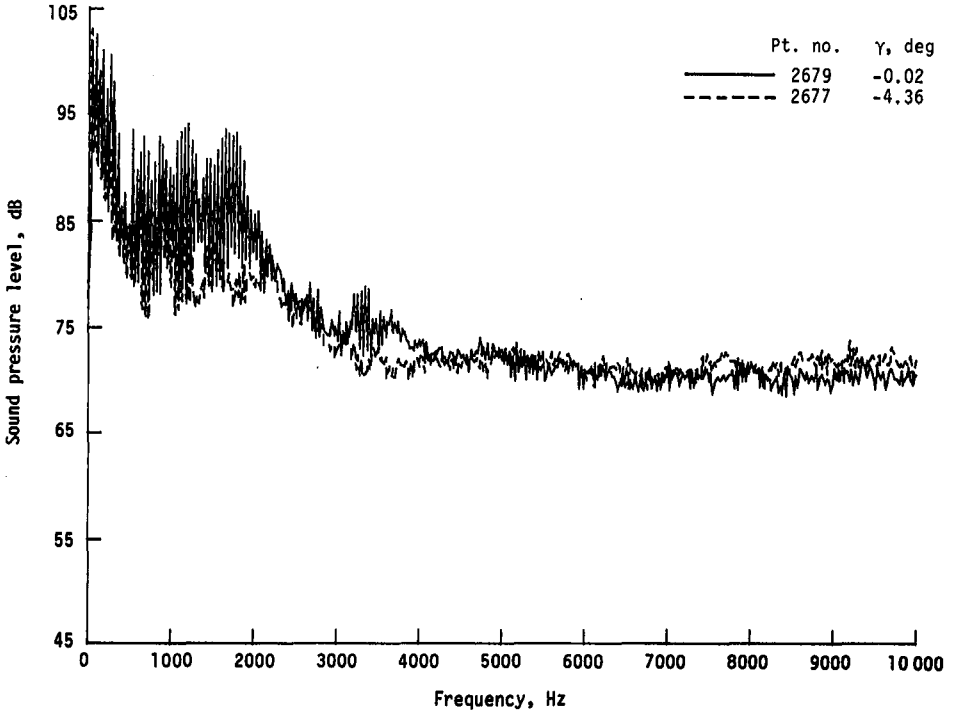

(i) Narrowband analysis; microphone 7.
Figure 28. - Continued.

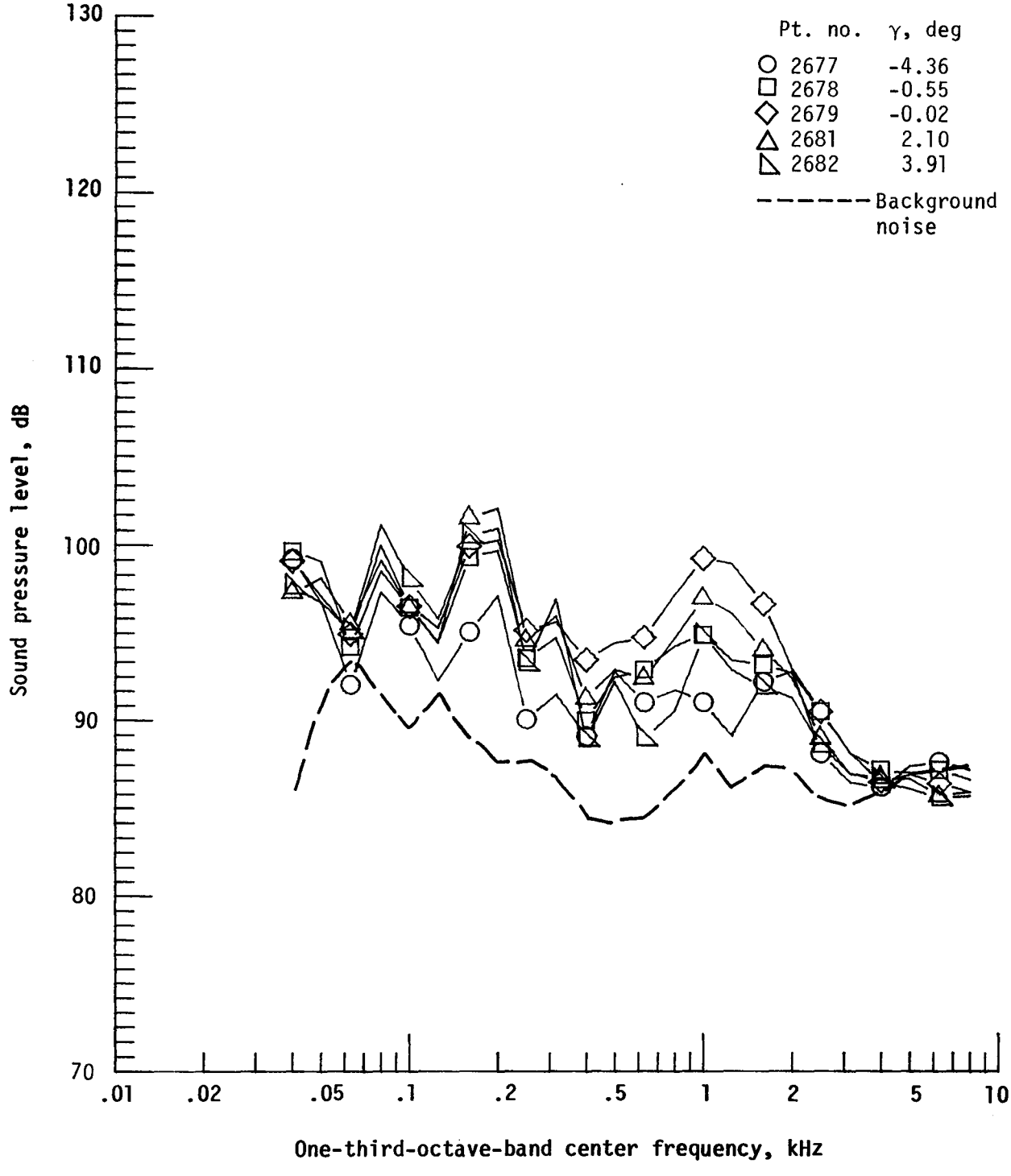

(j) One-third-octave spectra, microphone 8.

Figure 28. - Continued.

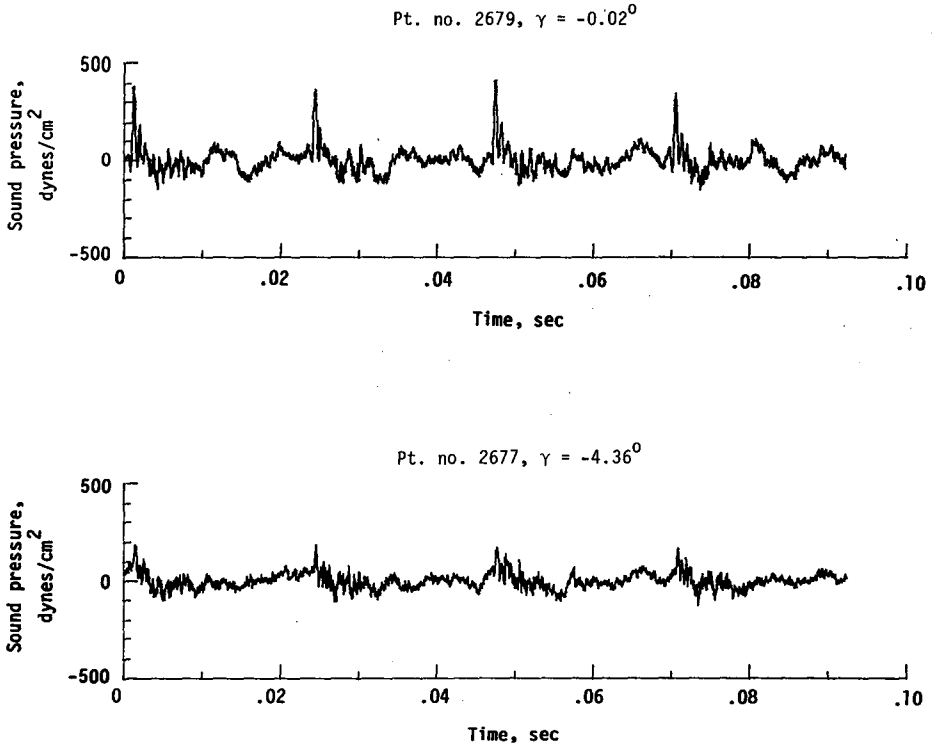

(k) Pressure-time histories; microphone 8.

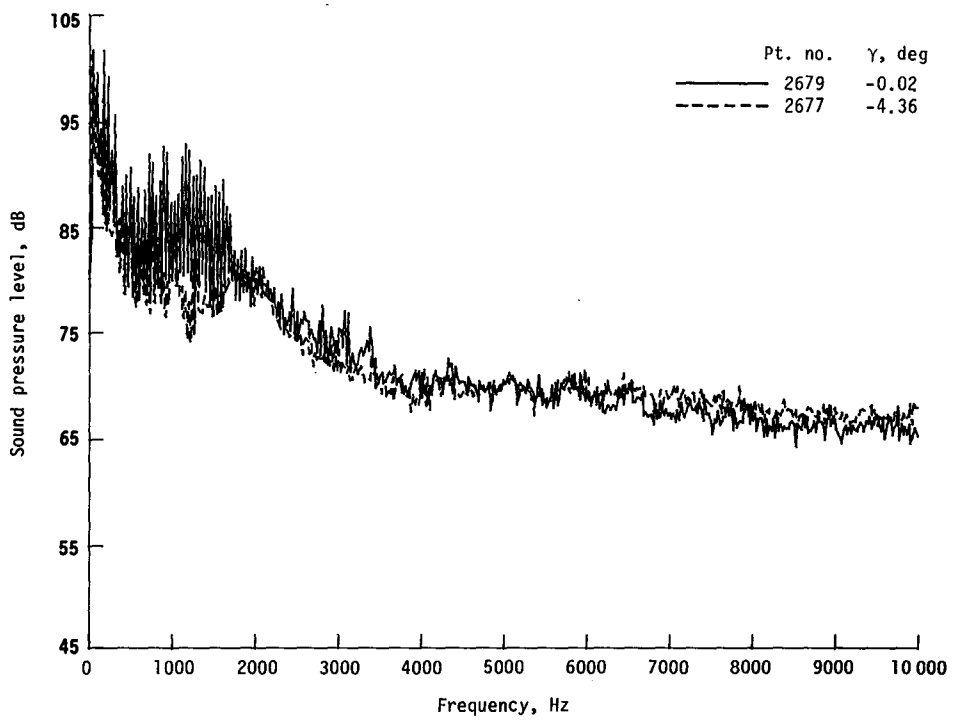

(l) Narrowband analysis; microphone 8.
Figure 28. - Concluded.

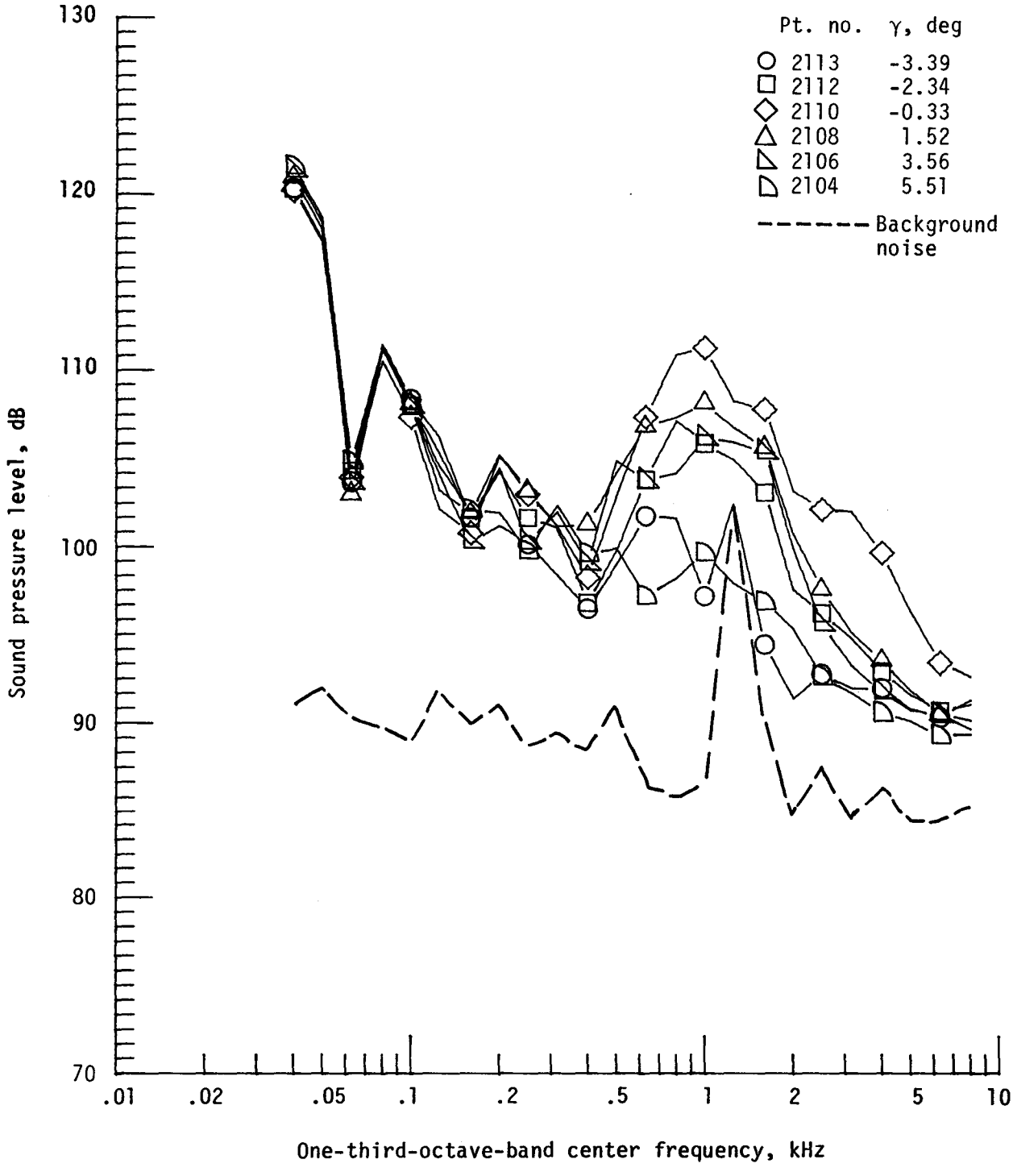

(a) One-third-octave spectra, microphone 2.

Figure 29. - Effect of descent angle variation on noise generated by helicopter model with standard rotor system, run 163. V_∞ = 80.2 knots, C_T = .0032.

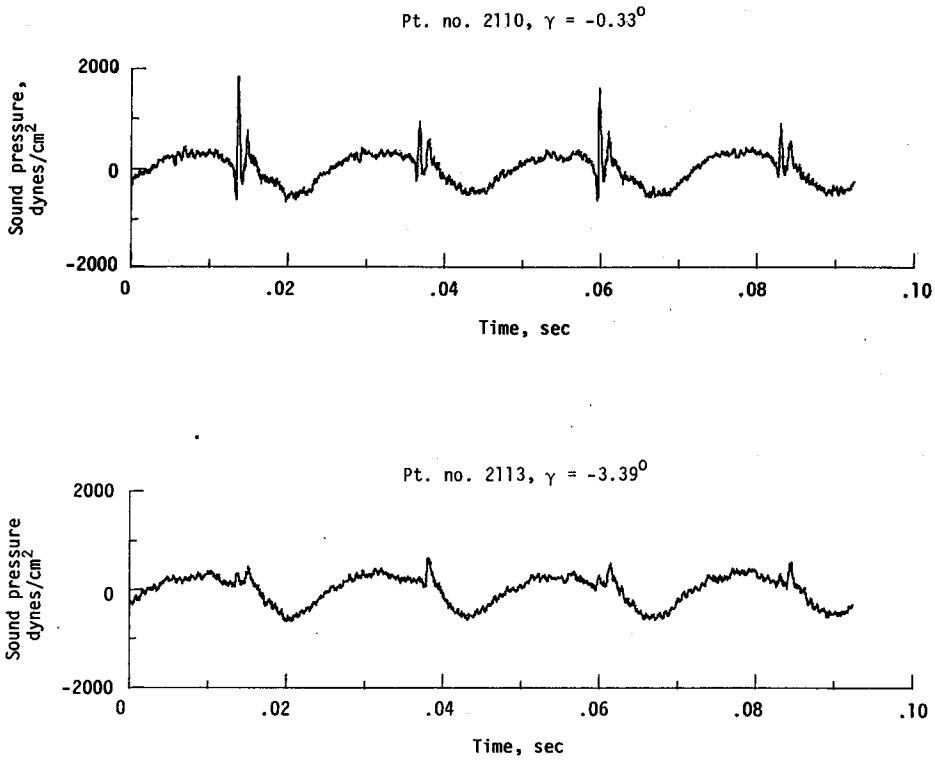

(b) Pressure-time histories; microphone 2.

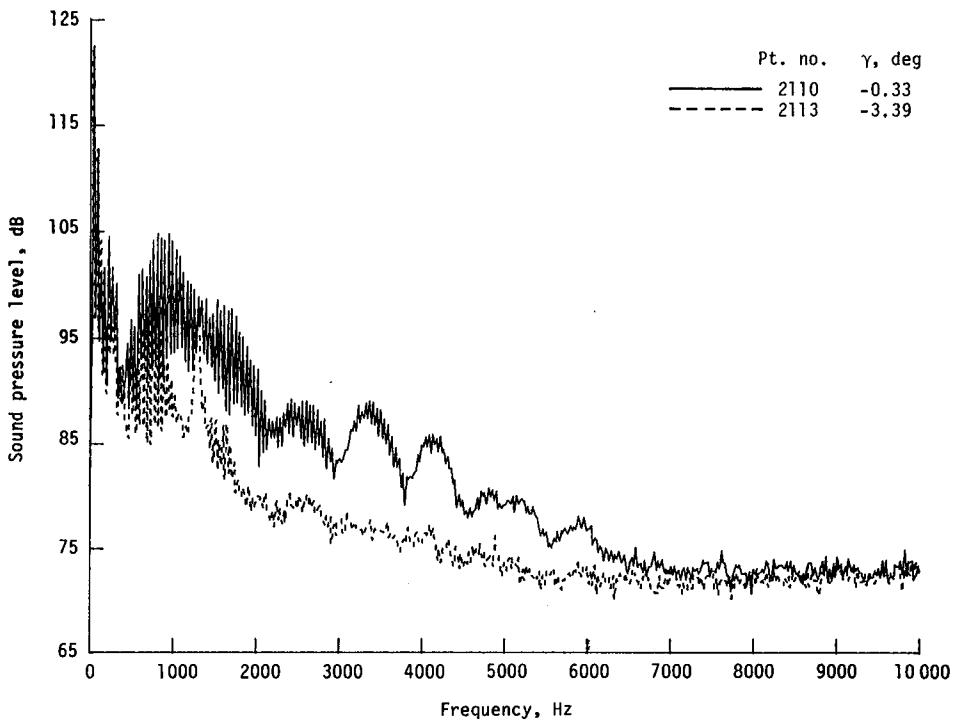

(c) Narrowband analysis; microphone 2.
Figure 29. - Continued.

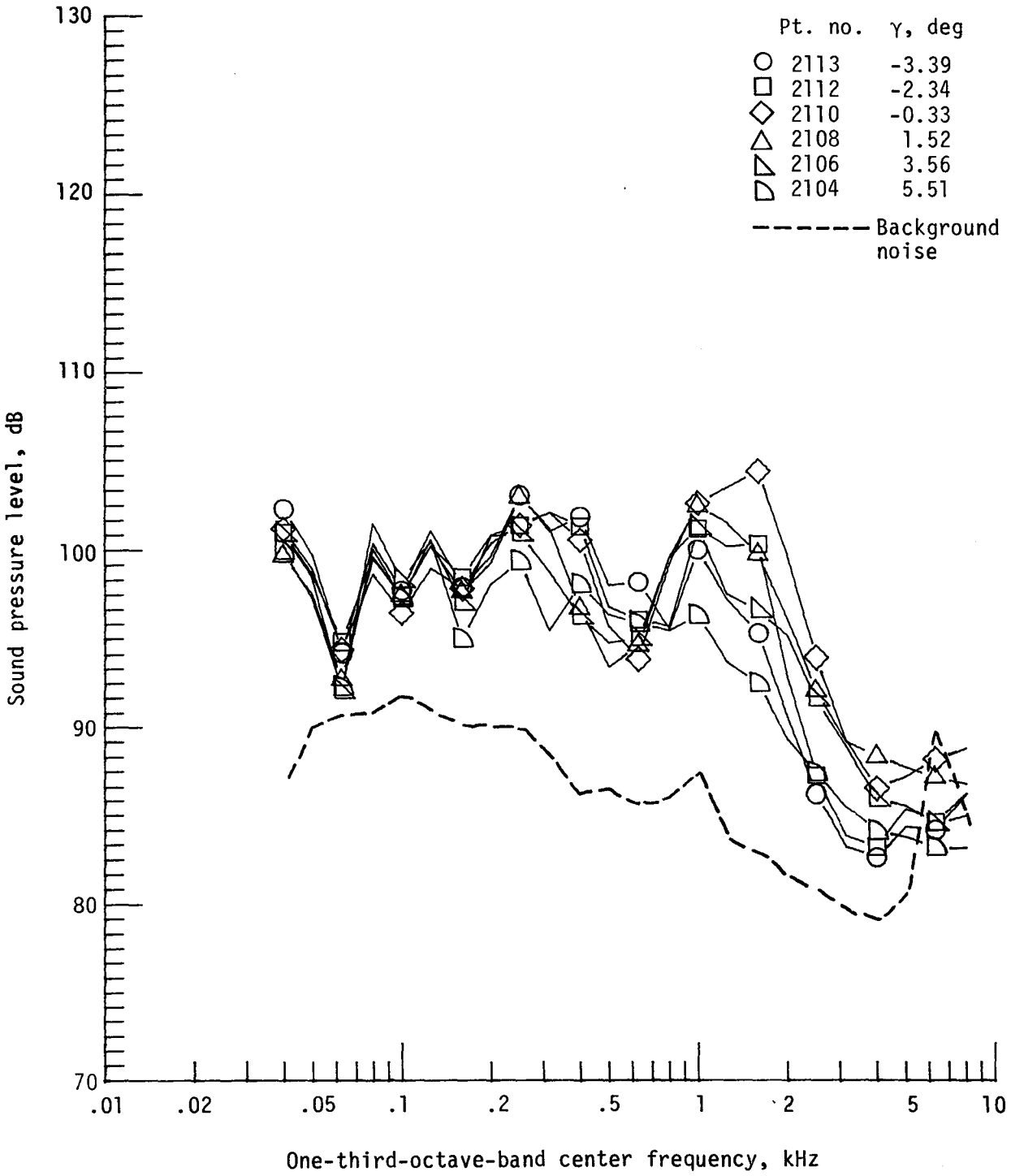

(d) One-third-octave spectra, microphone 6.

Figure 29. - Continued.

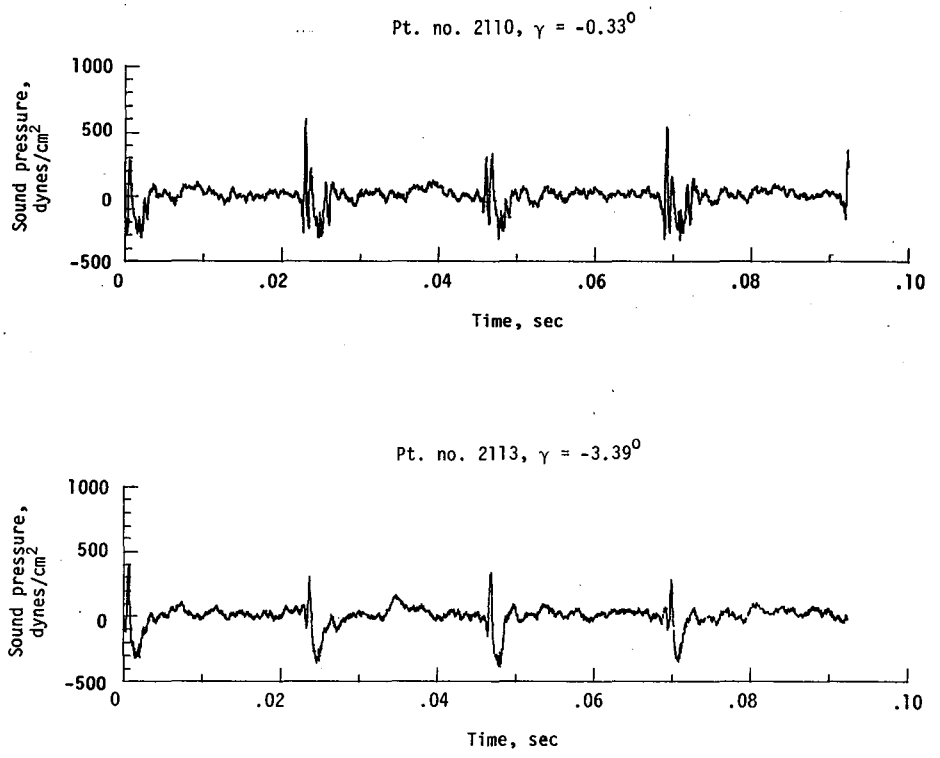

(e) Pressure-time histories; microphone 6.

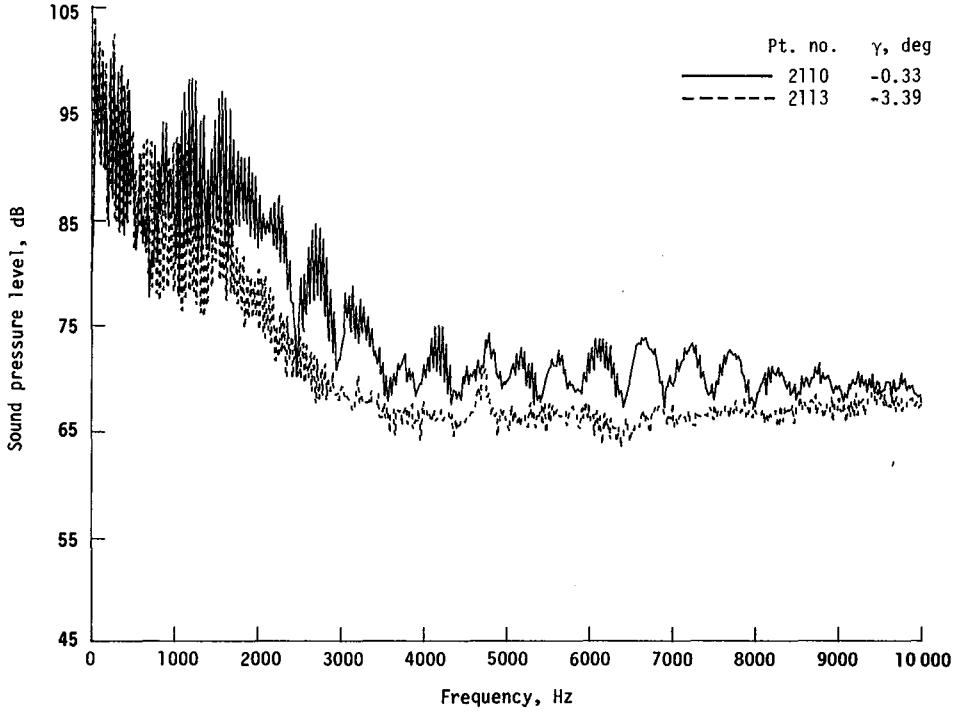

(f) Narrowband analysis; microphone 6.
Figure 29. - Continued.

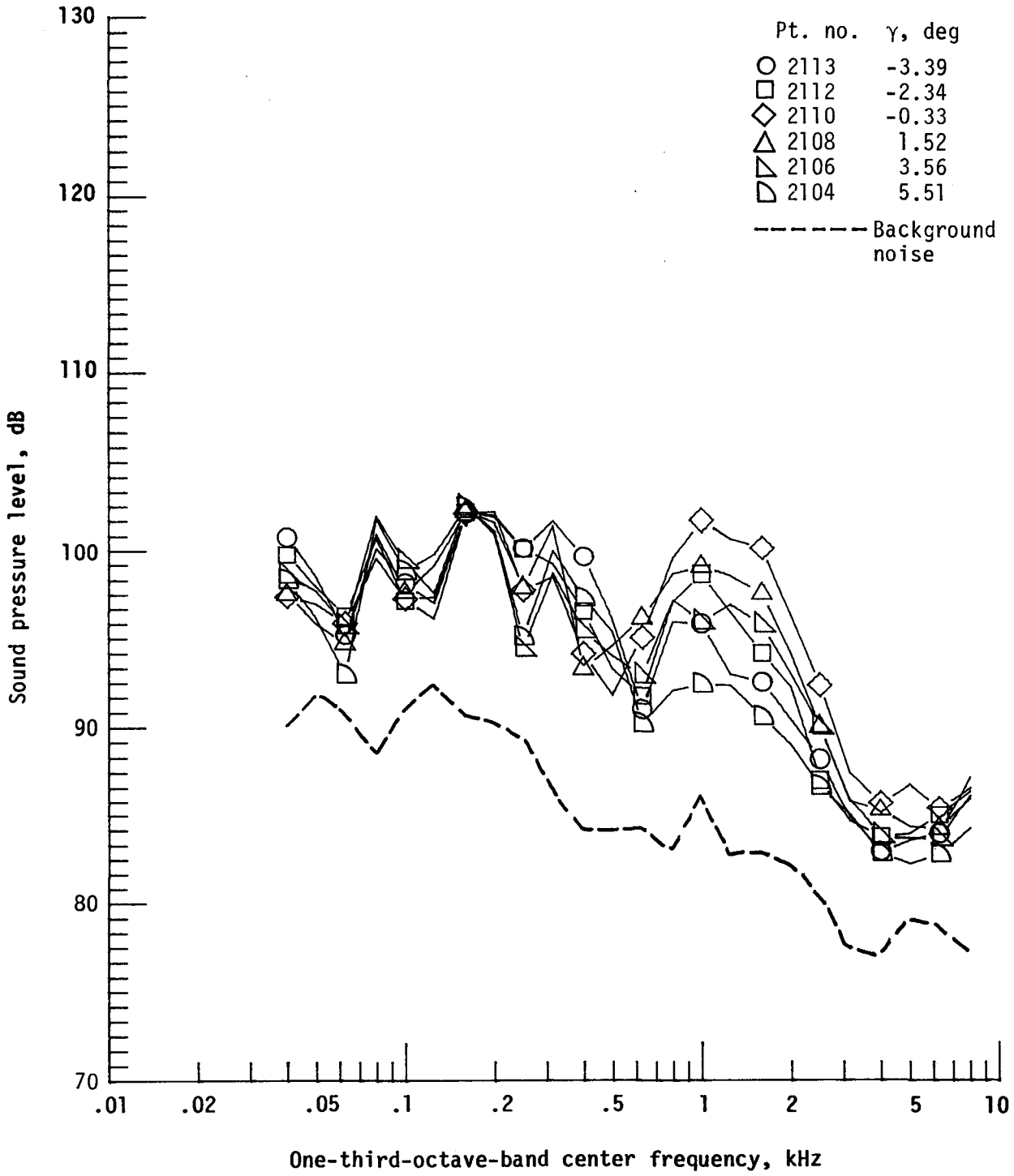

(g) One-third-octave spectra, microphone 7.

Figure 29. - Continued.

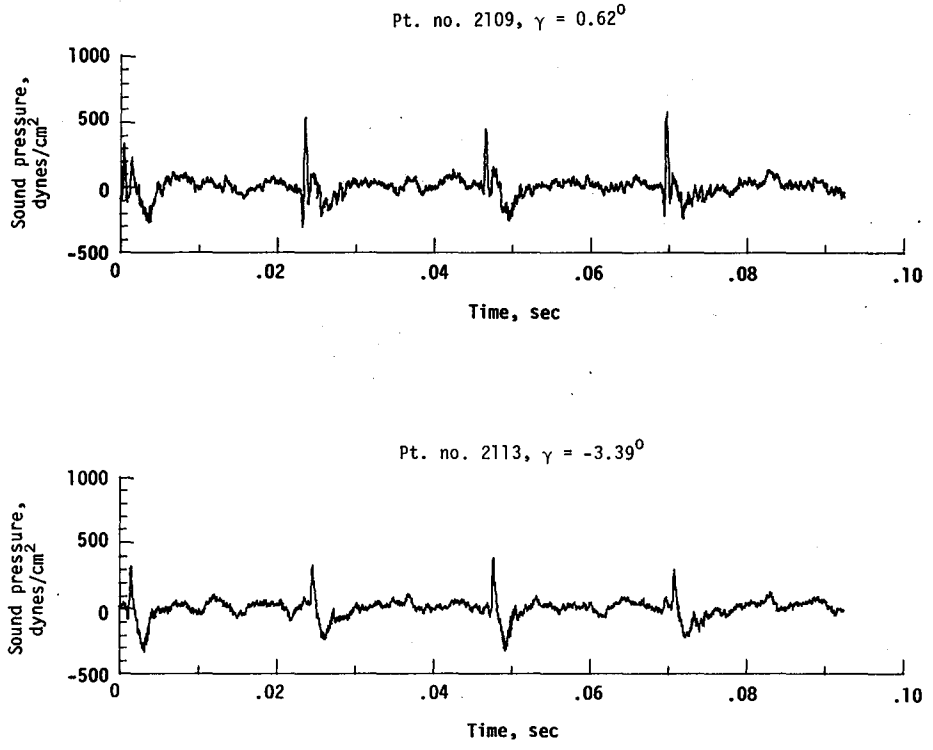

(h) Pressure-time histories; microphone 7.

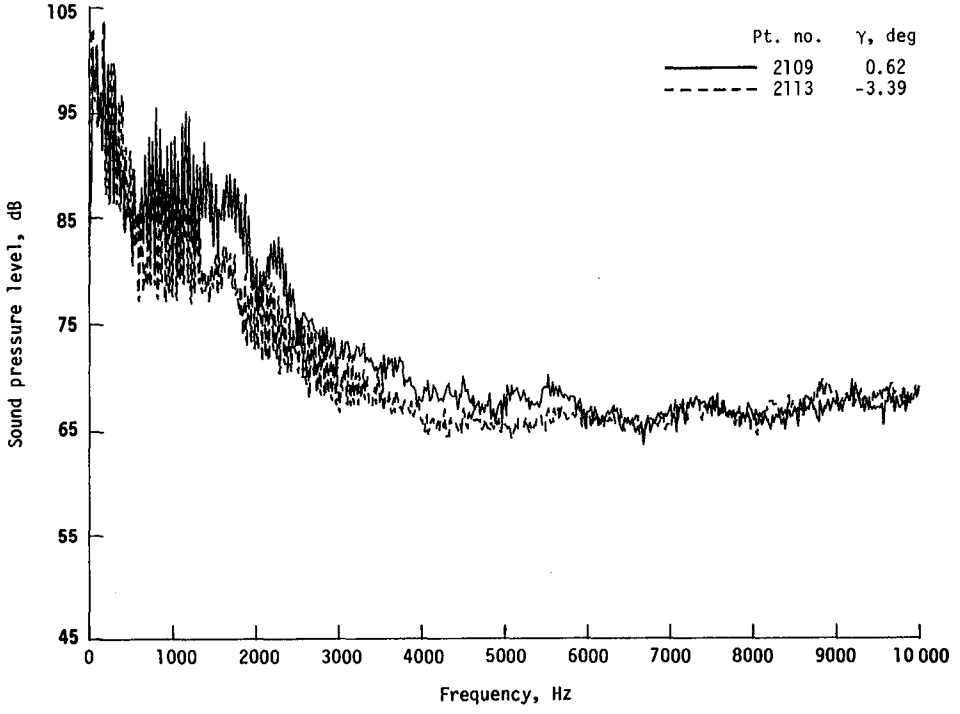

(i) Narrowband analysis; microphone 7.
Figure 29. - Continued.

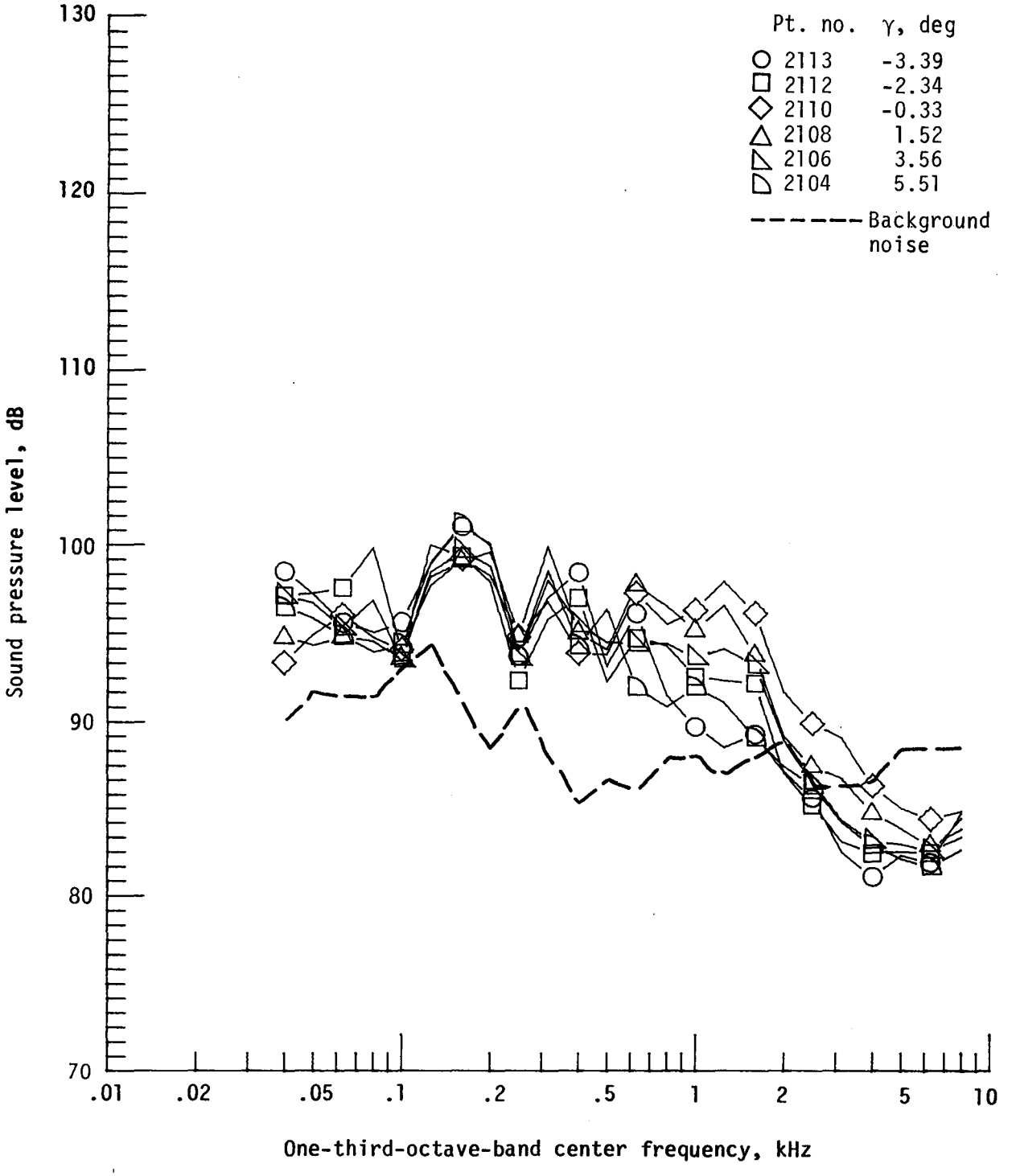

(j) One-third-octave spectra, microphone 8.

Figure 29. - Continued.

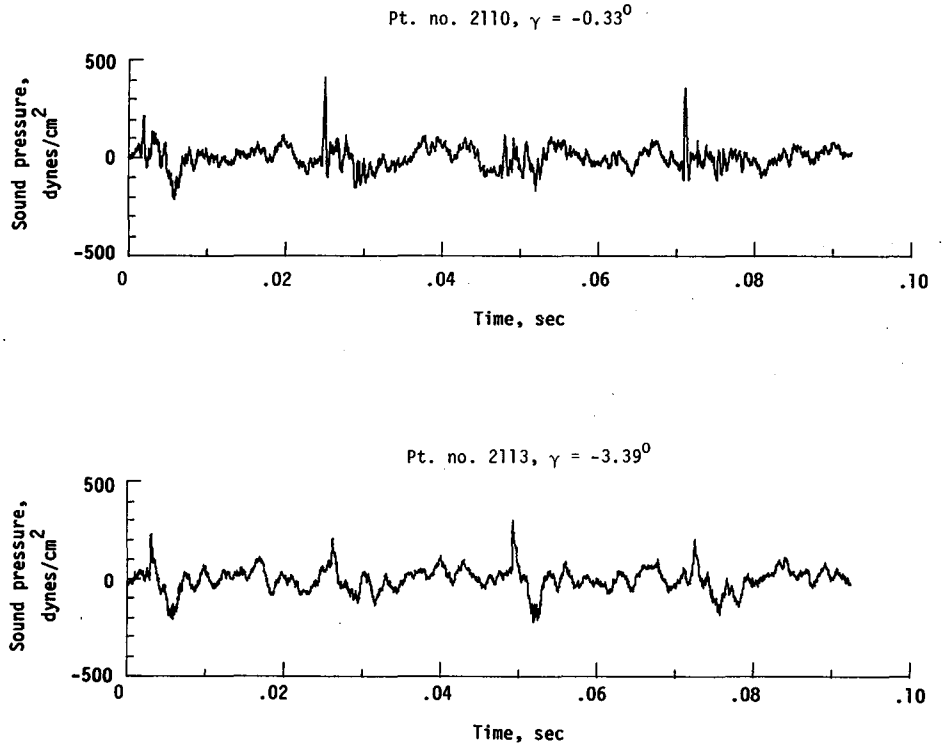

(k) Pressure-time histories; microphone 8.

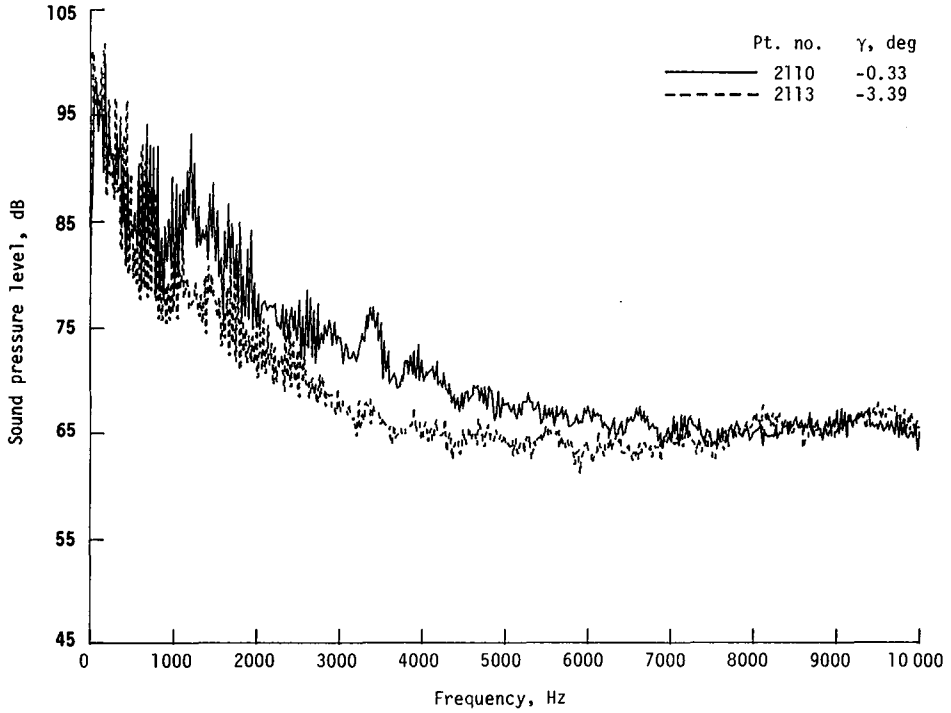

(l) Narrowband analysis; microphone 8.
Figure 29. - Concluded.

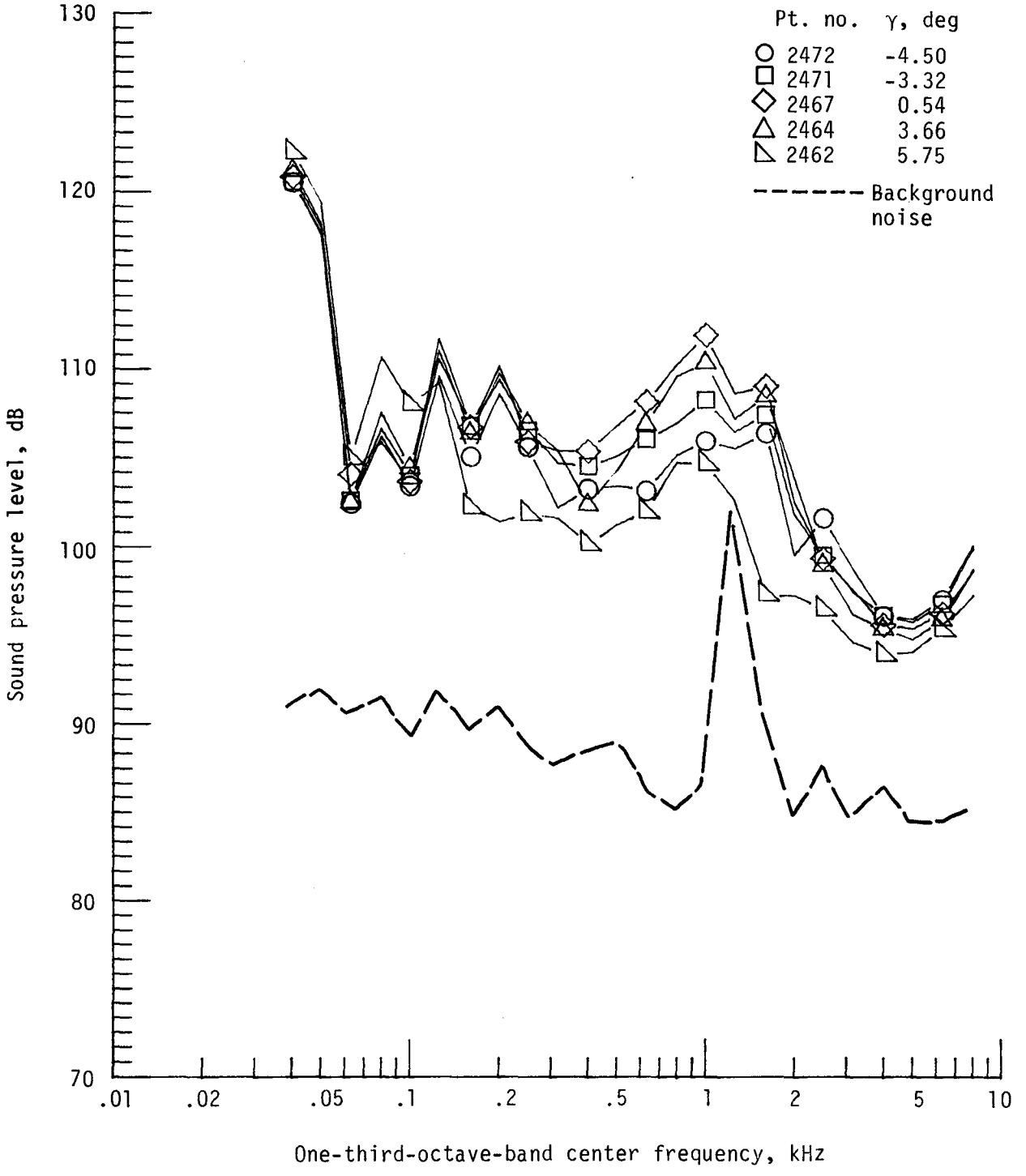

(a) One-third-octave spectra, microphone 2.

Figure 30. - Effect of descent angle variation on noise generated by helicopter model with advanced rotor system, run 196. V_∞ = 80.4 knots, C_T = .0031.

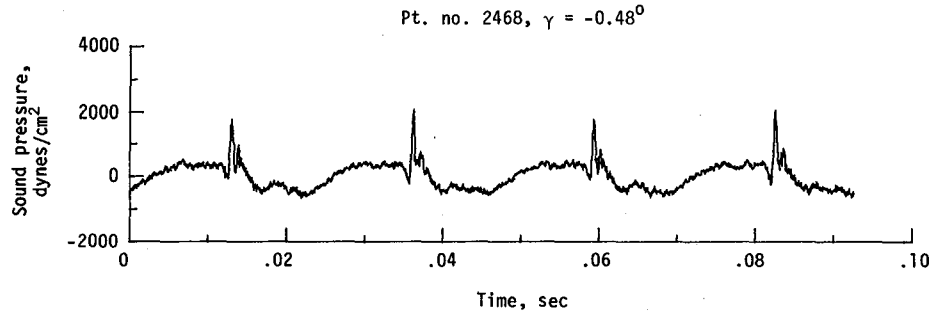

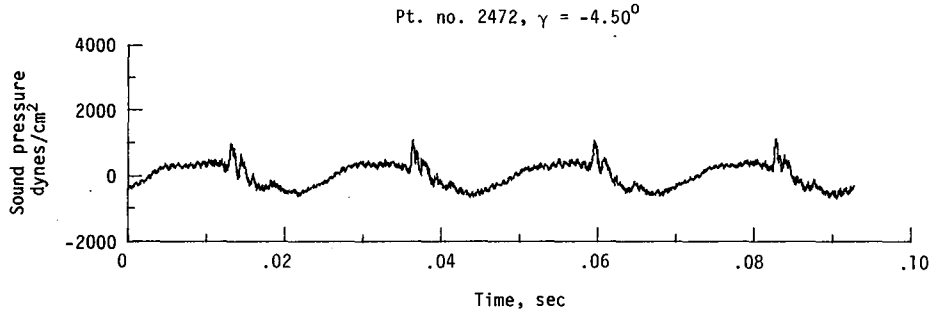

(b) Pressure-time histories; microphone 2.

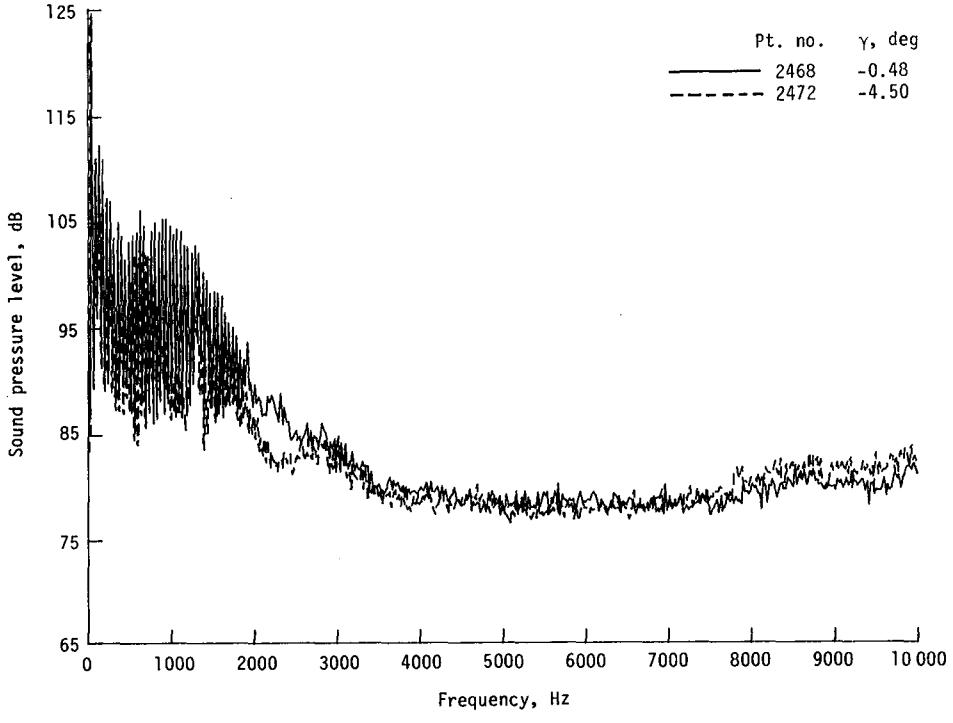

(c) Narrowband analysis; microphone 2.
Figure 30. - Continued.

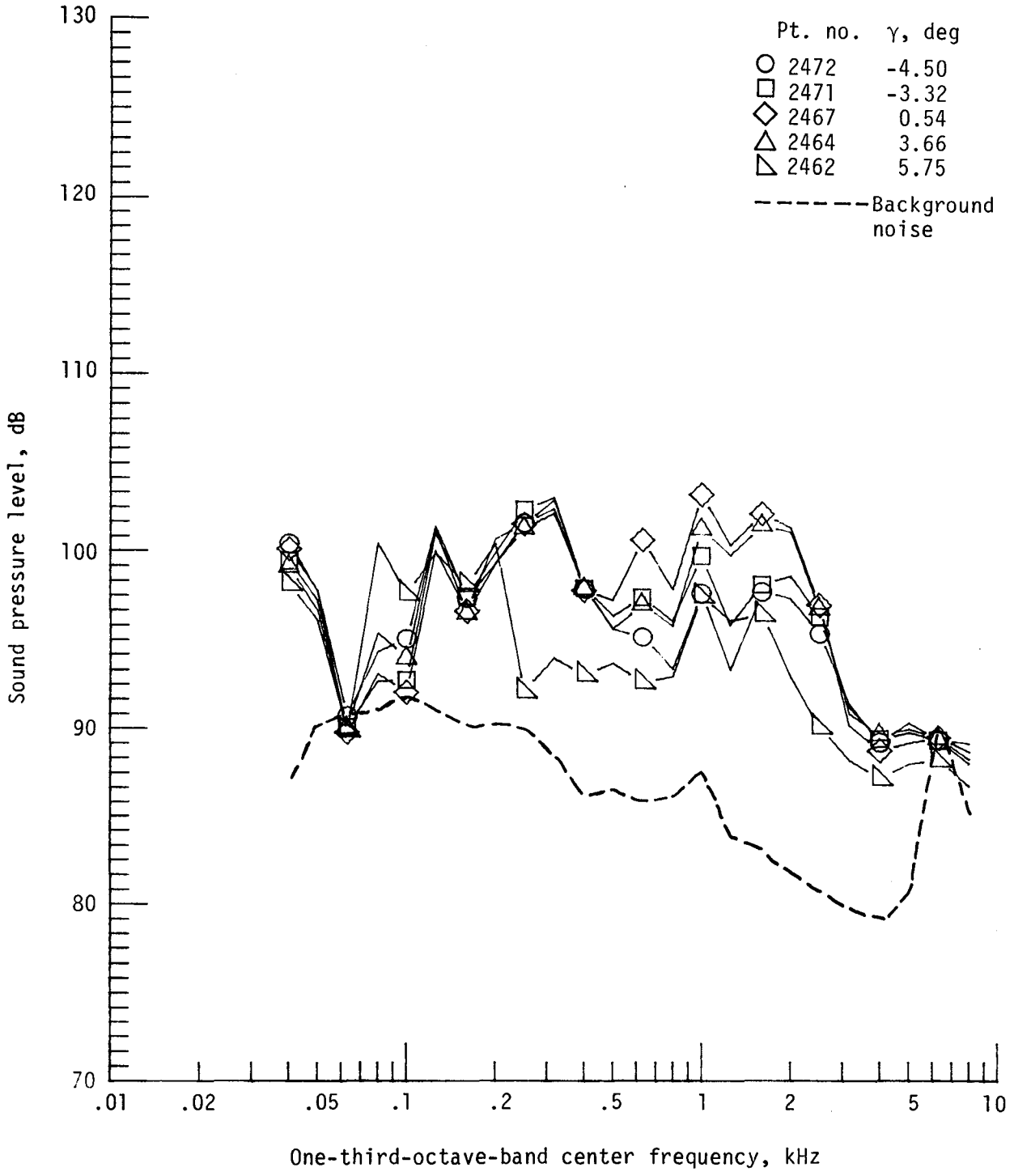

(d) One-third-octave spectra, microphone 6.

Figure 30. - Continued.

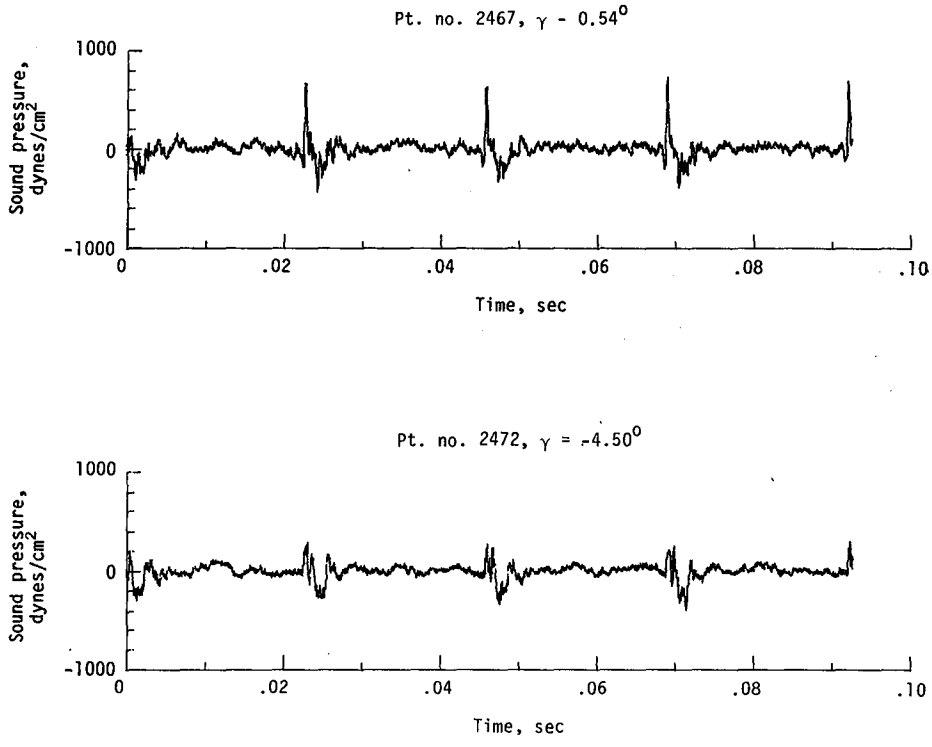

(e) Pressure-time histories; microphone 6.

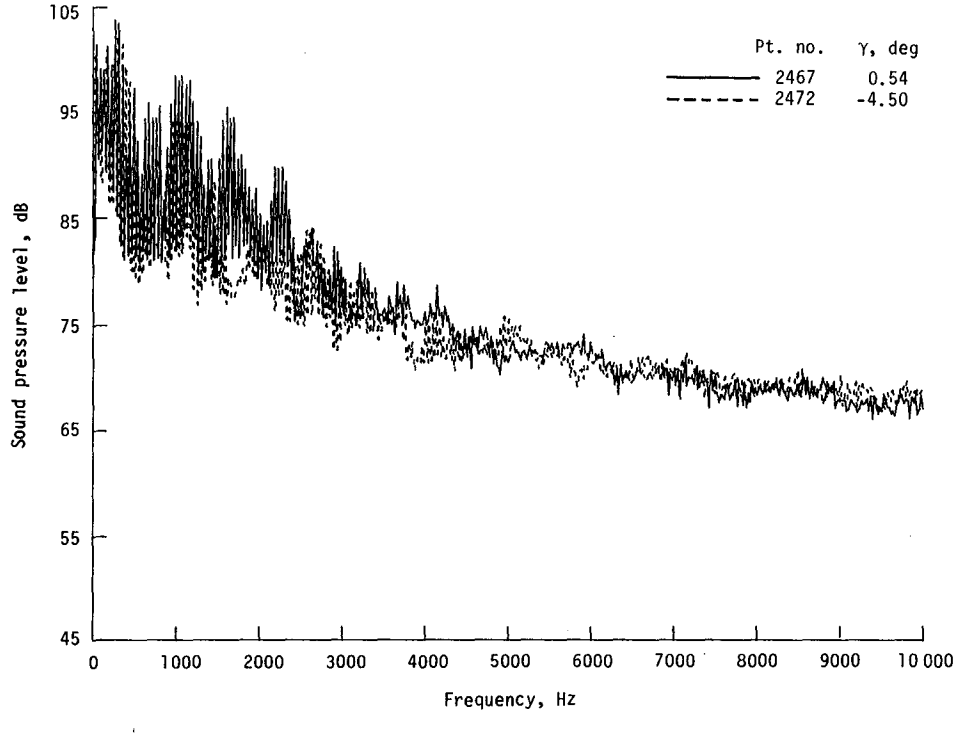

(f) Narrowband analysis; microphone 6.

Figure 30. - Continued.

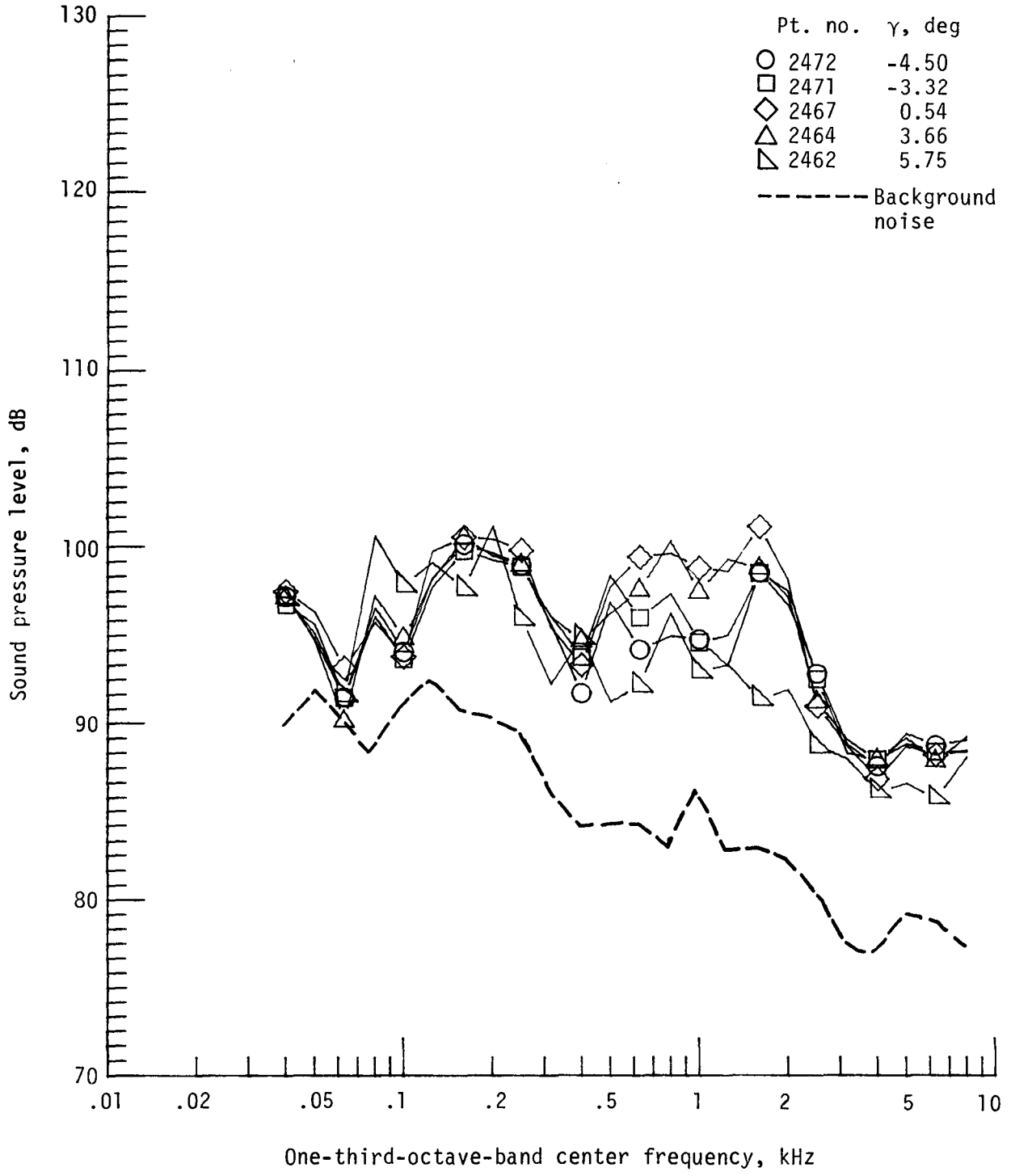

(g) One-third-octave spectra, microphone 7.

Figure 30. - Continued.

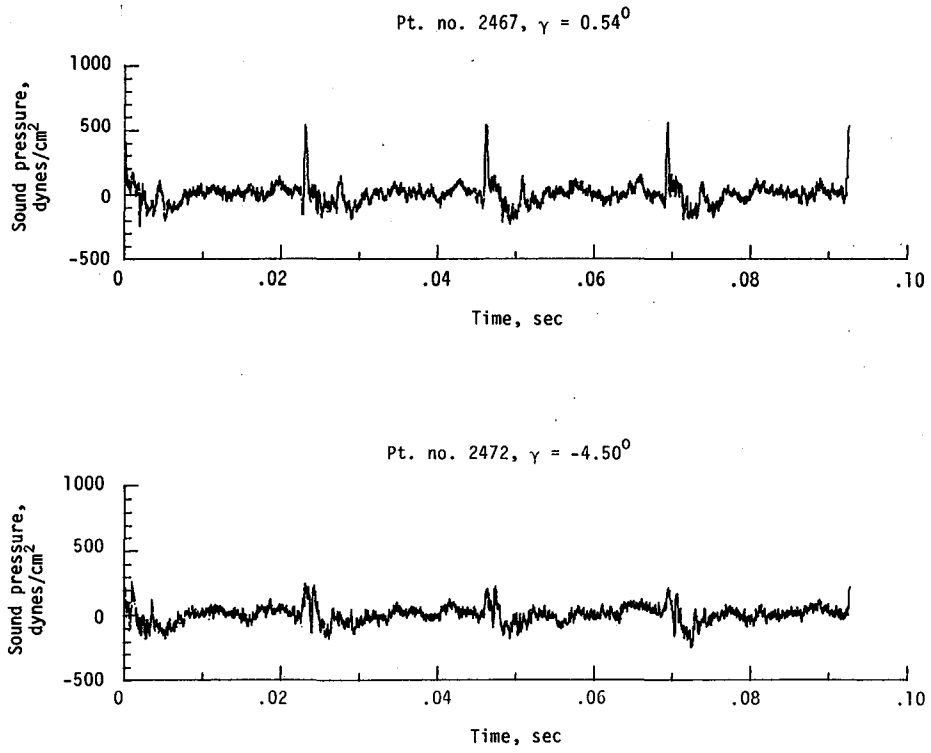

(h) Pressure-time histories; microphone 7.

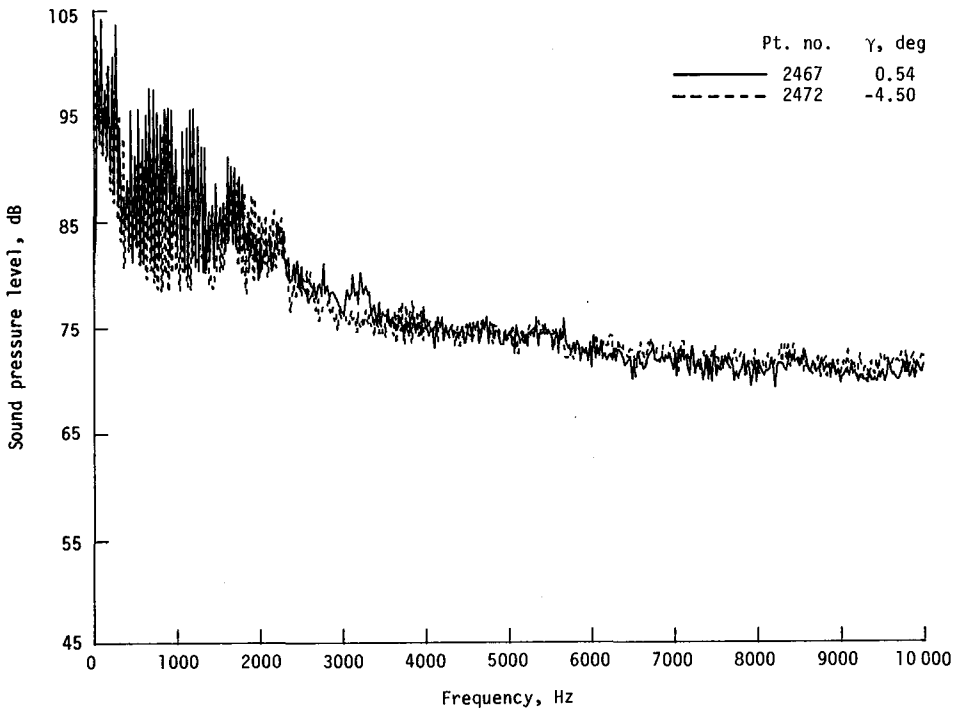

(i) Narrowband analysis; microphone 7.
Figure 30. - Continued.

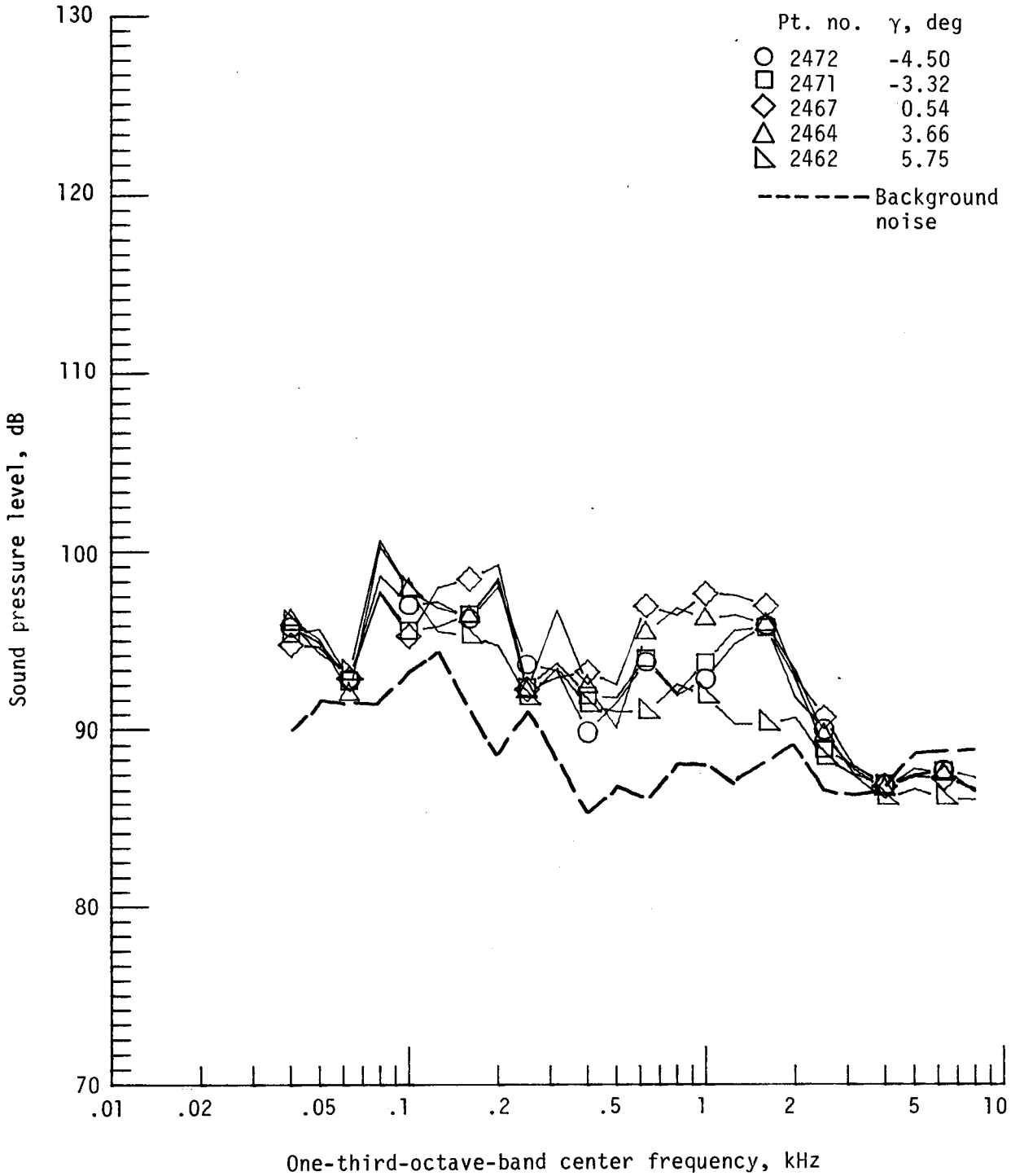

(j) One-third-octave spectra, microphone 8.

Figure 30. - Continued.

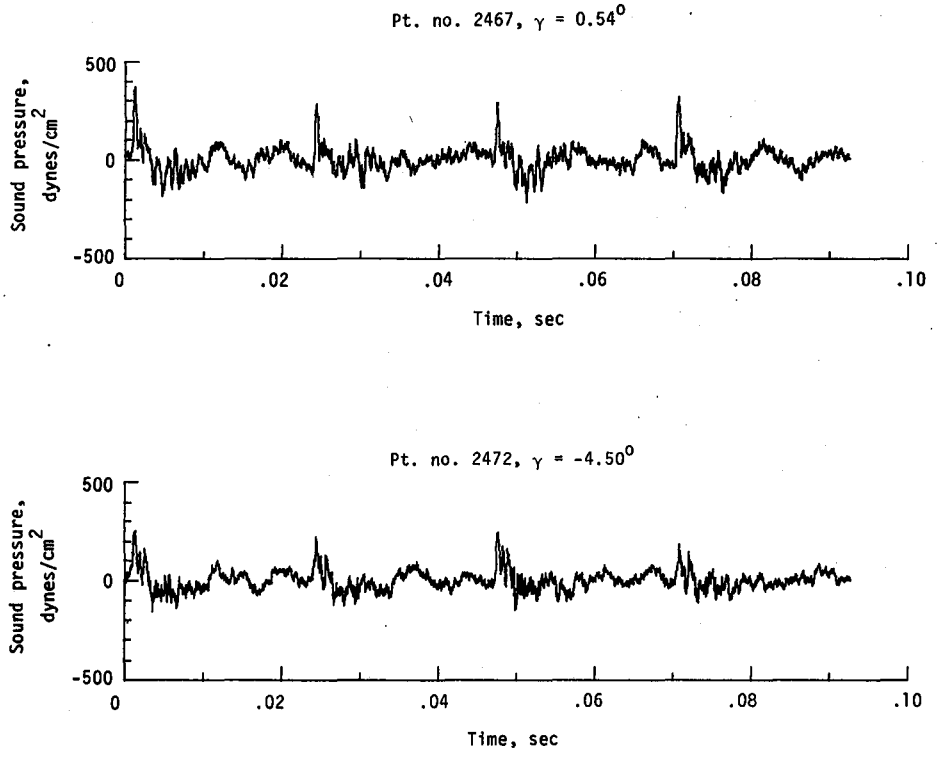

(k) Pressure-time histories; microphone 8.

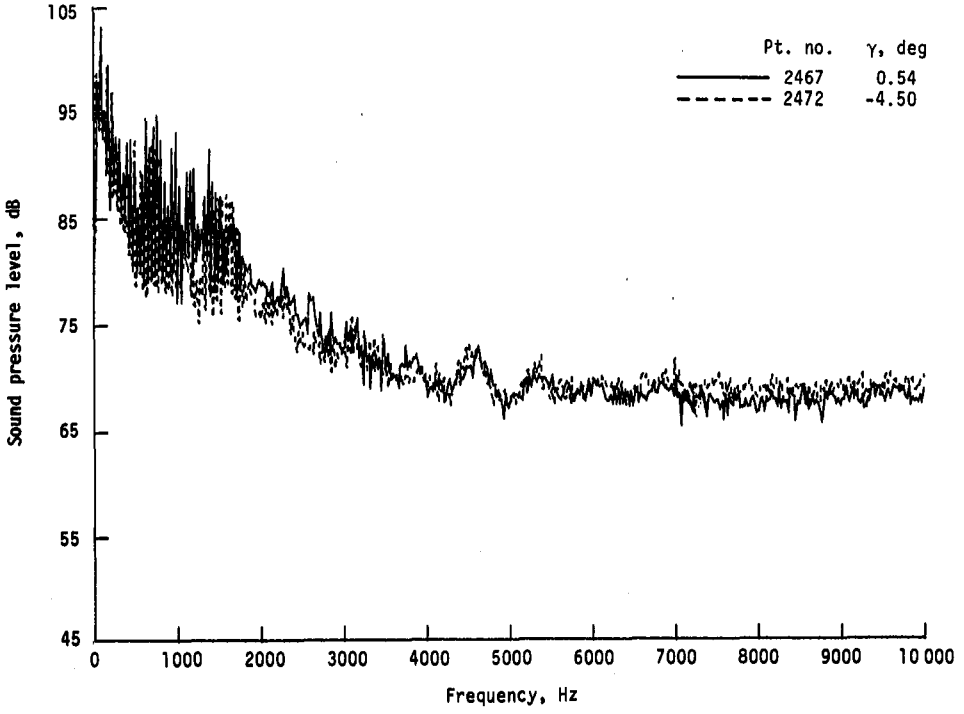

(l) Narrowband analysis; microphone 8.
Figure 30. - Concluded.

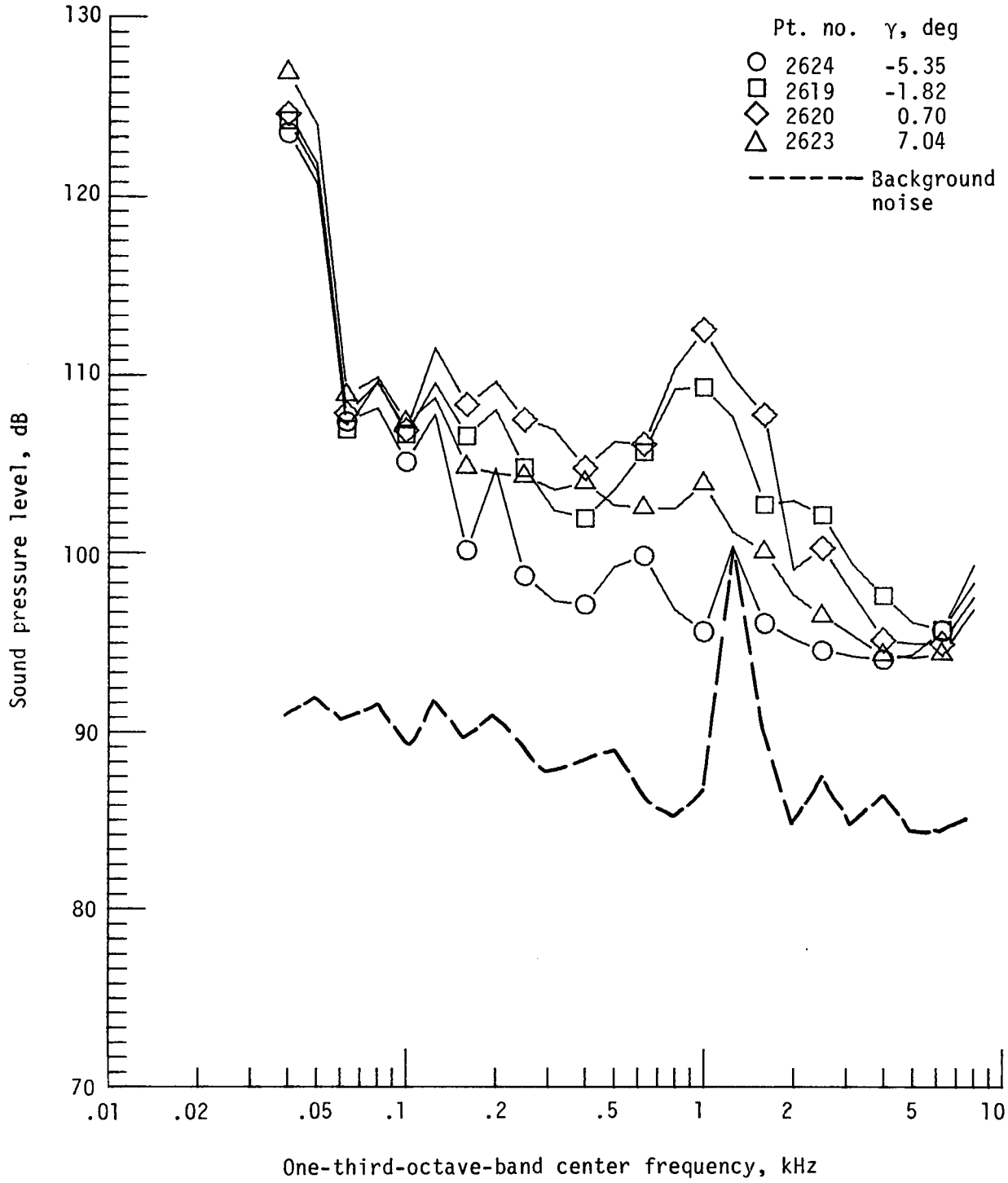

(a) One-third-octave spectra, microphone 2.

Figure 31. - Effect of descent angle variation on noise generated by helicopter model with advanced rotor system, run 217. V_∞ = 80.3 knots, C_T .0036.

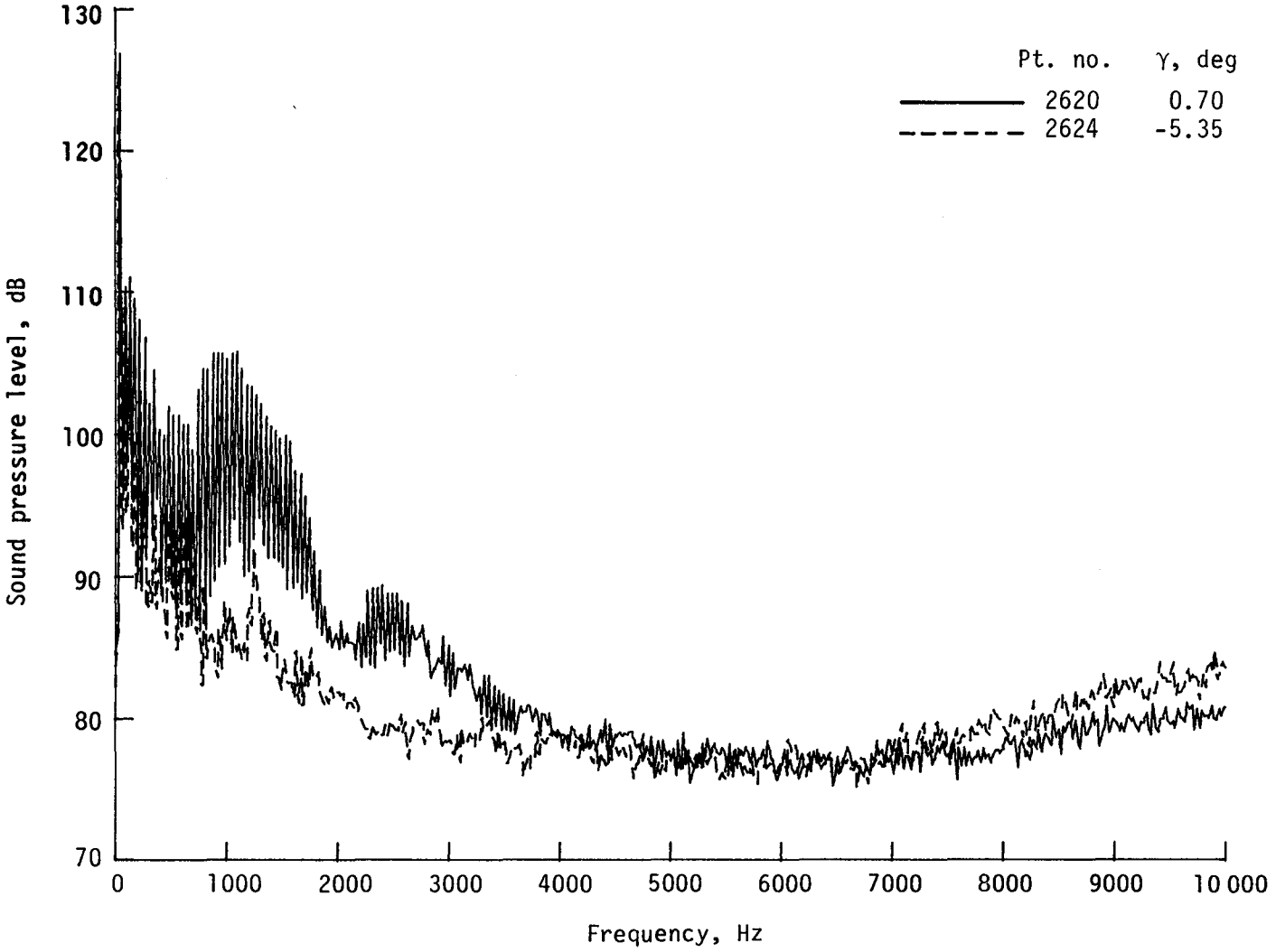

(b) Narrowband analysis; microphone 2.
Figure 31. - Continued.

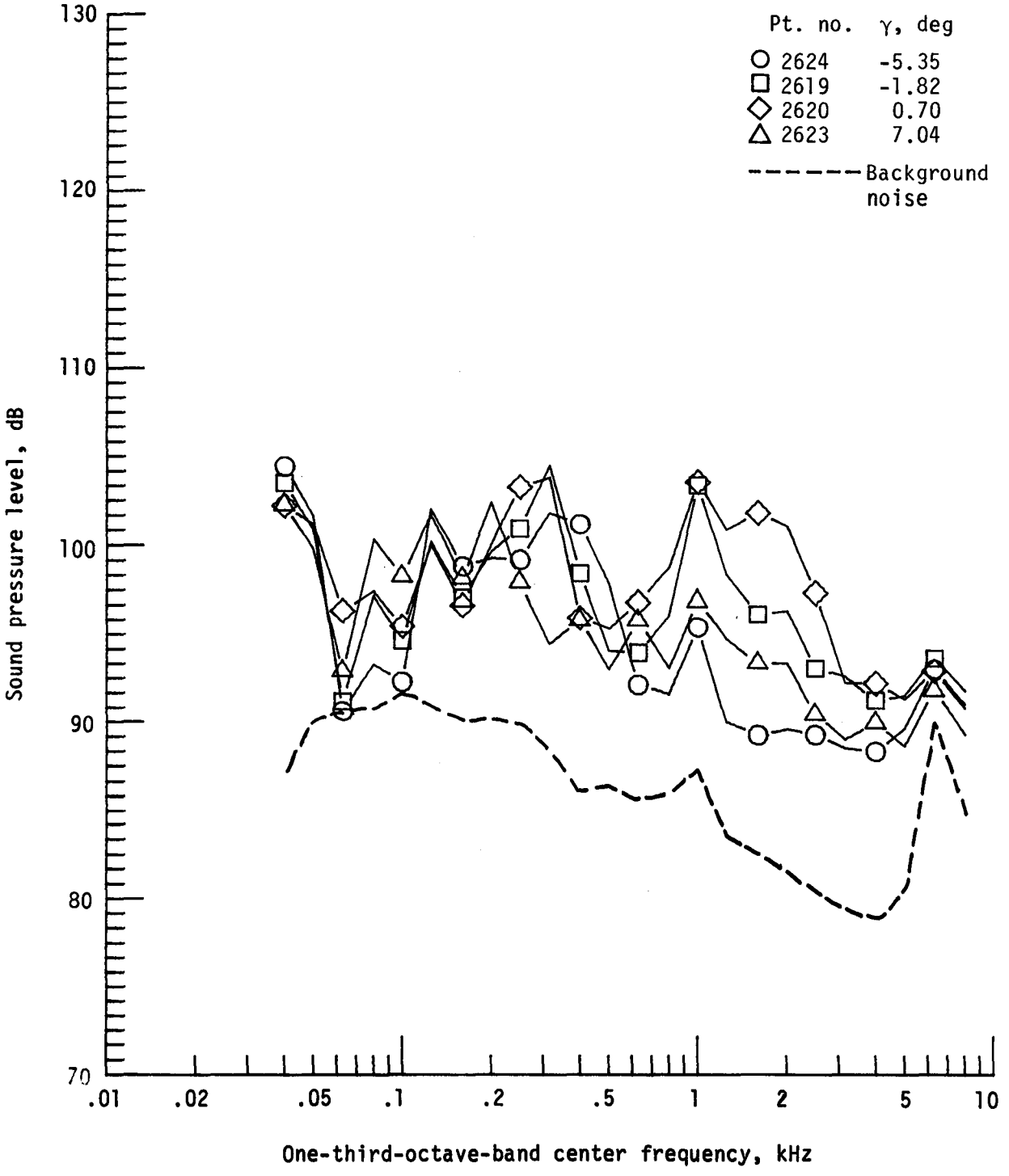

(c) One-third-octave spectra, microphone 6.

Figure 31. - Continued.

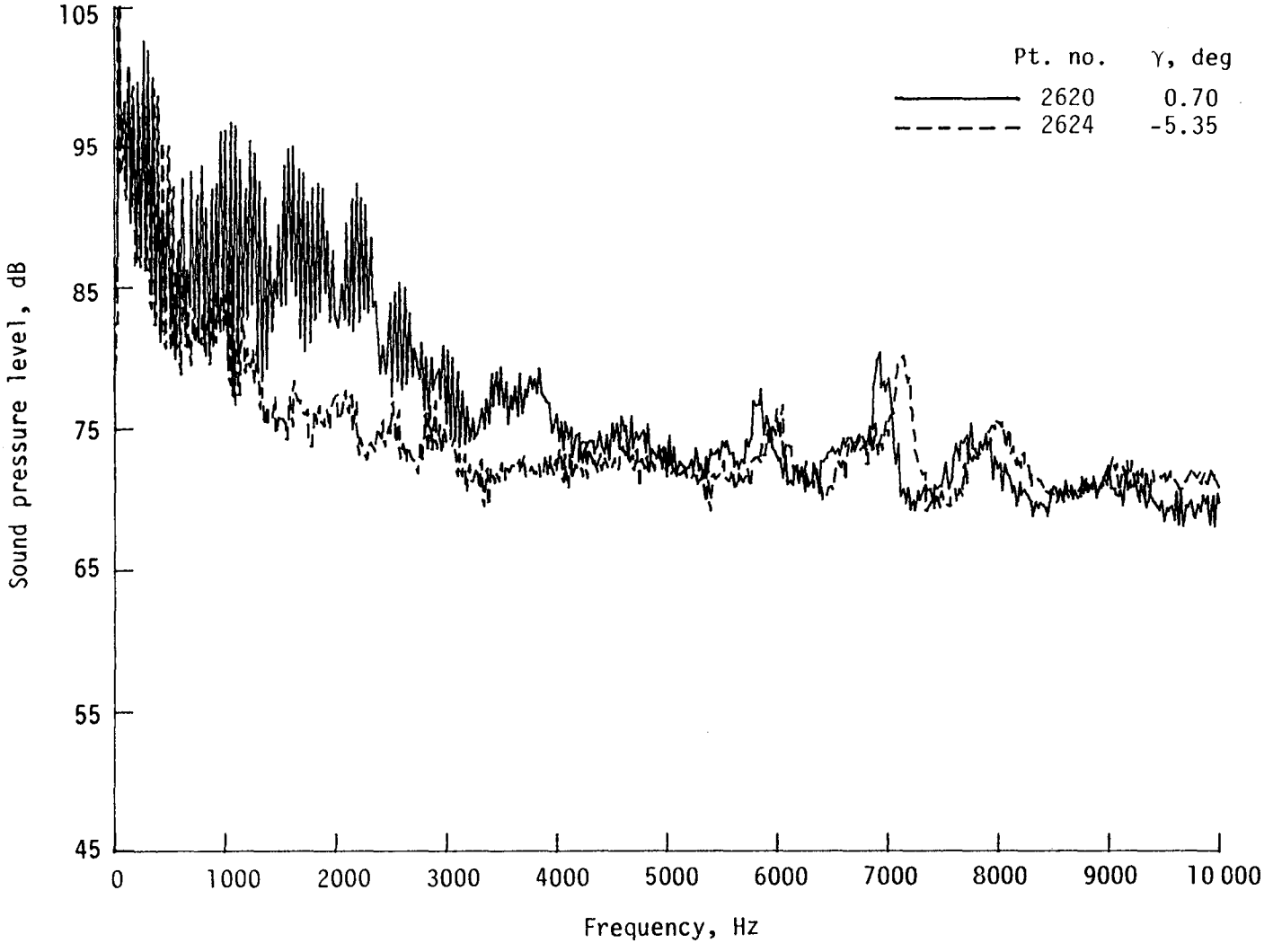

(d) Narrowband analysis; microphone 6.
Figure 31. - Continued.

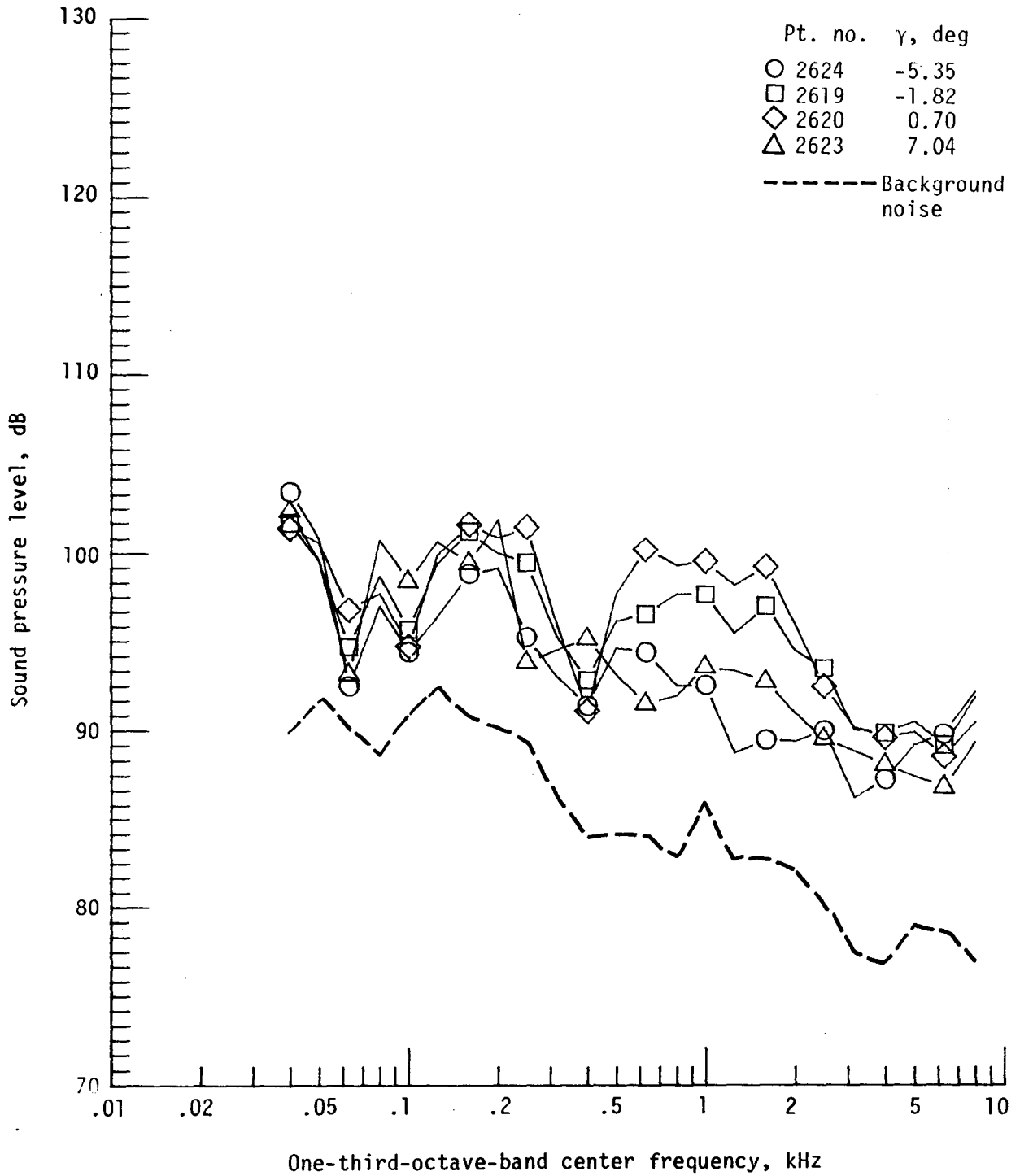

(e) One-third-octave spectra; microphone 7.

Figure 31. - Continued.

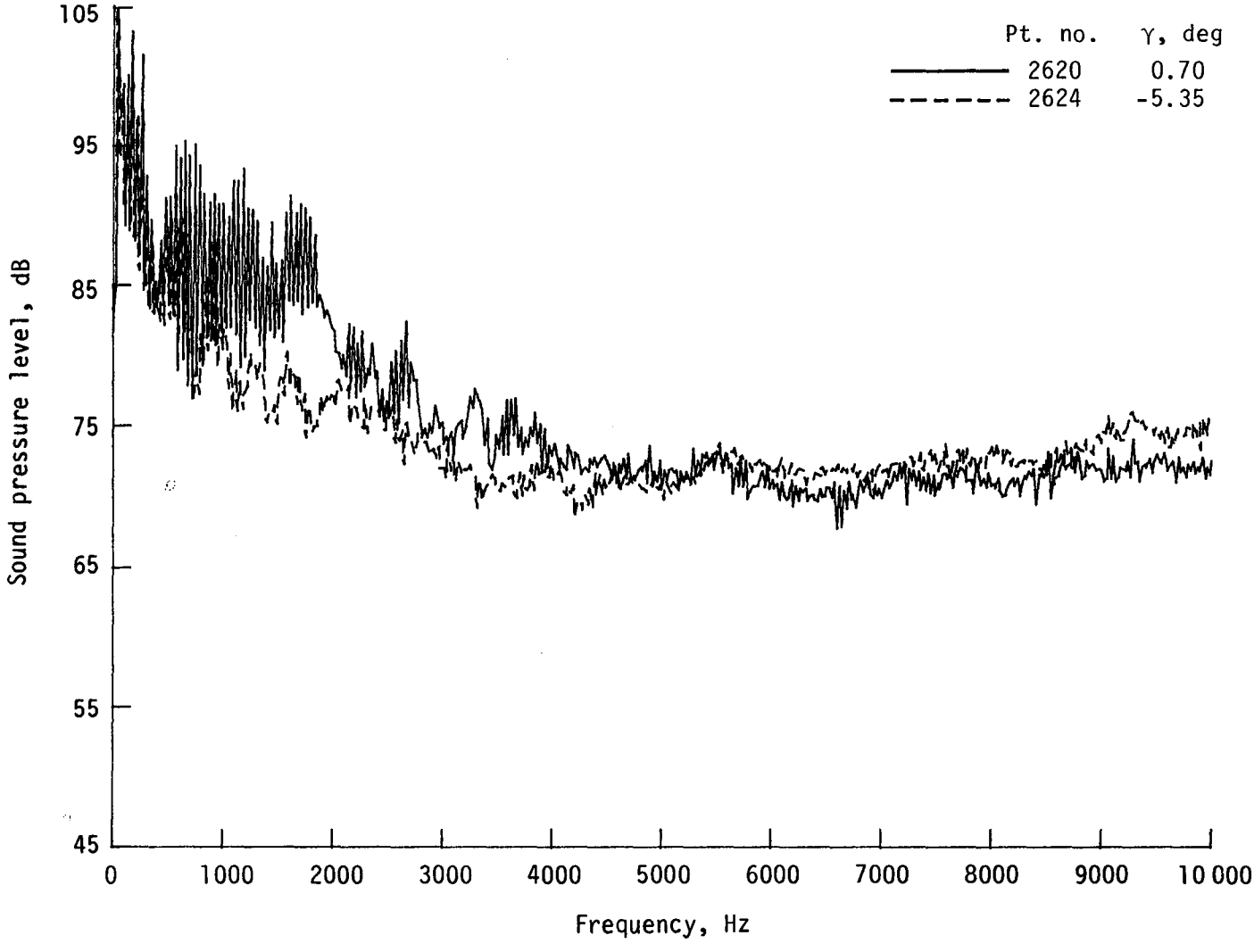

(f) Narrowband analysis; microphone 7.
Figure 31. - Continued.

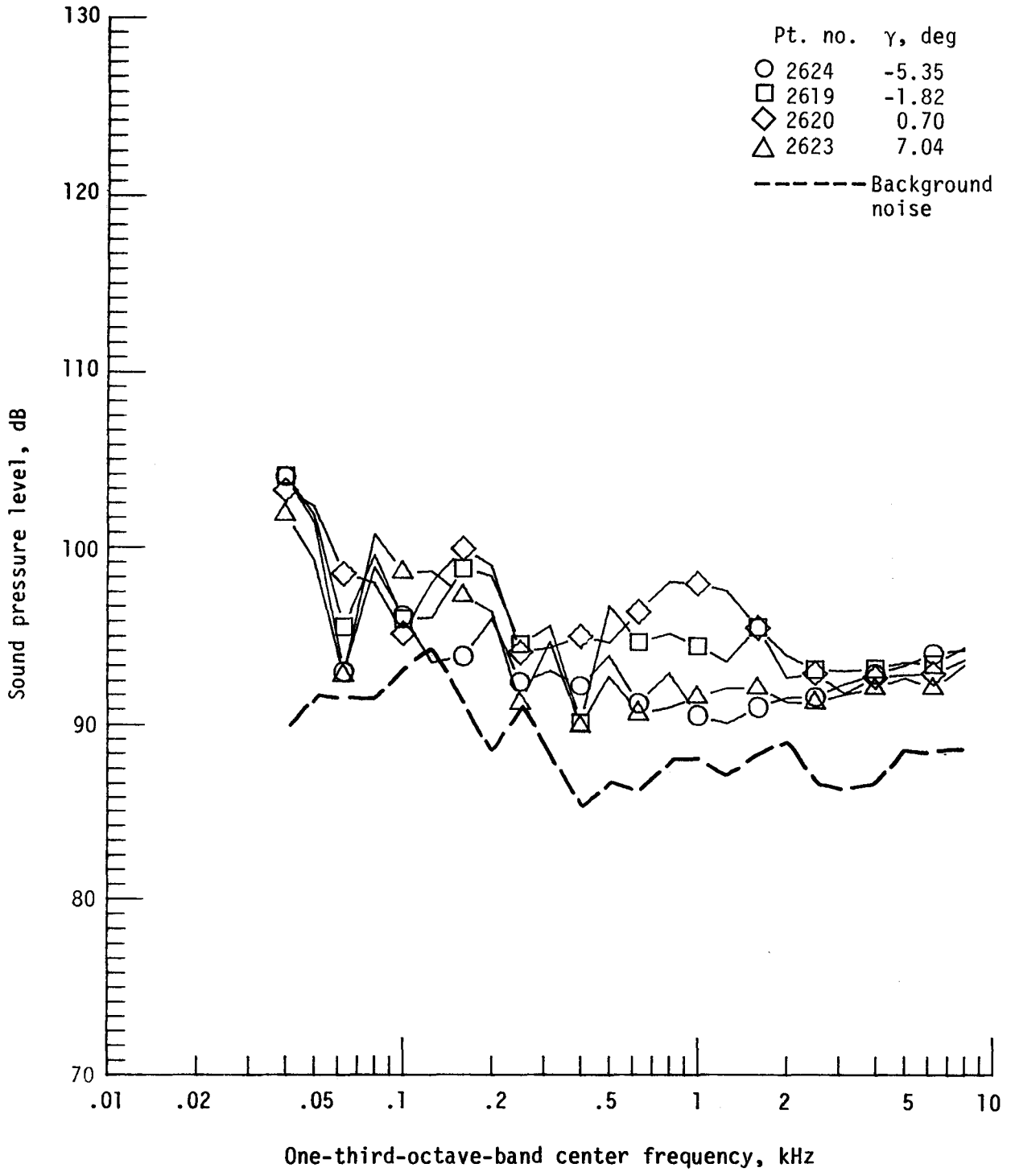

(g) One-third-octave spectra; microphone 8.

Figure 31. - Continued.

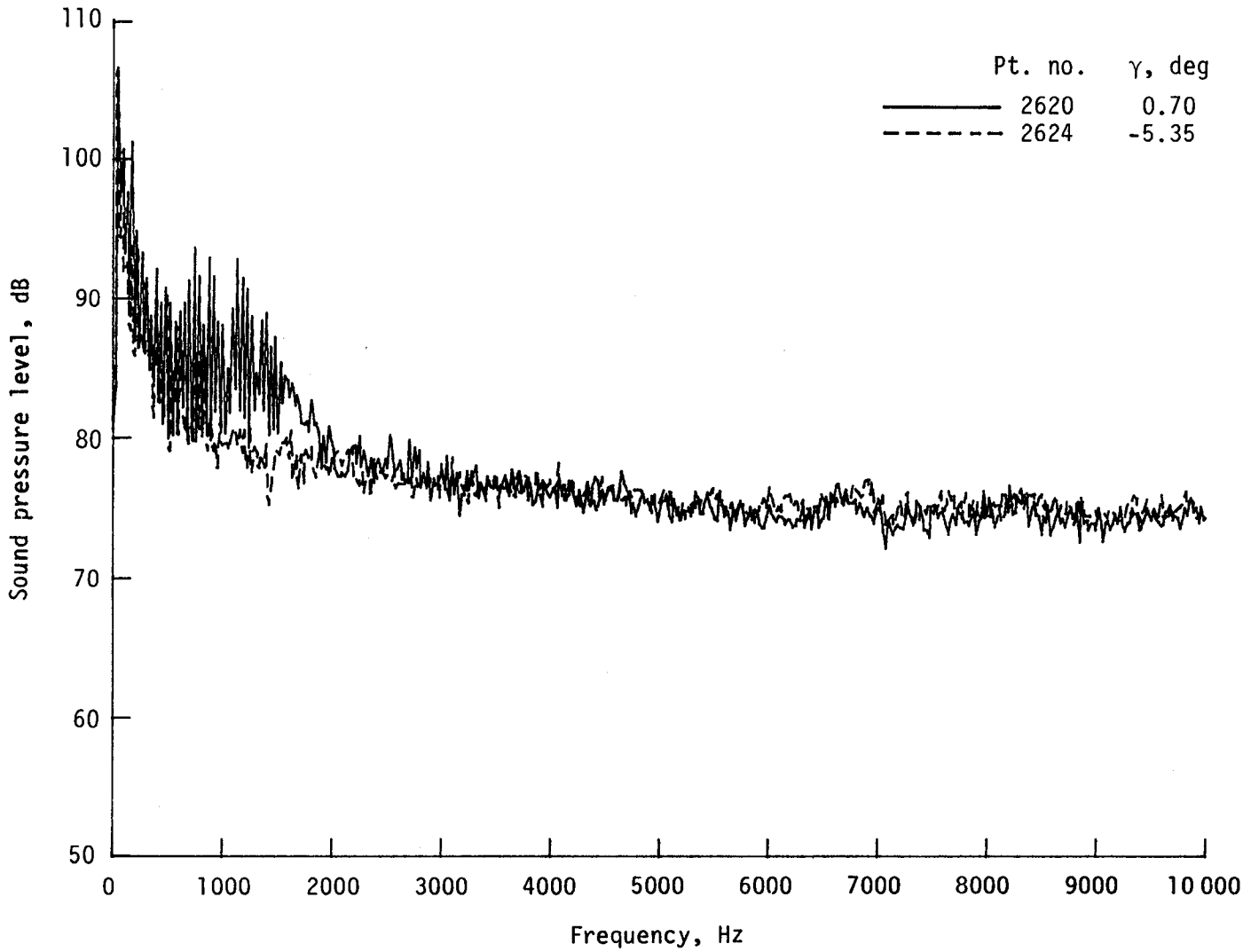

(h) Narrowband analysis; microphone 8.
Figure 31. - Concluded.

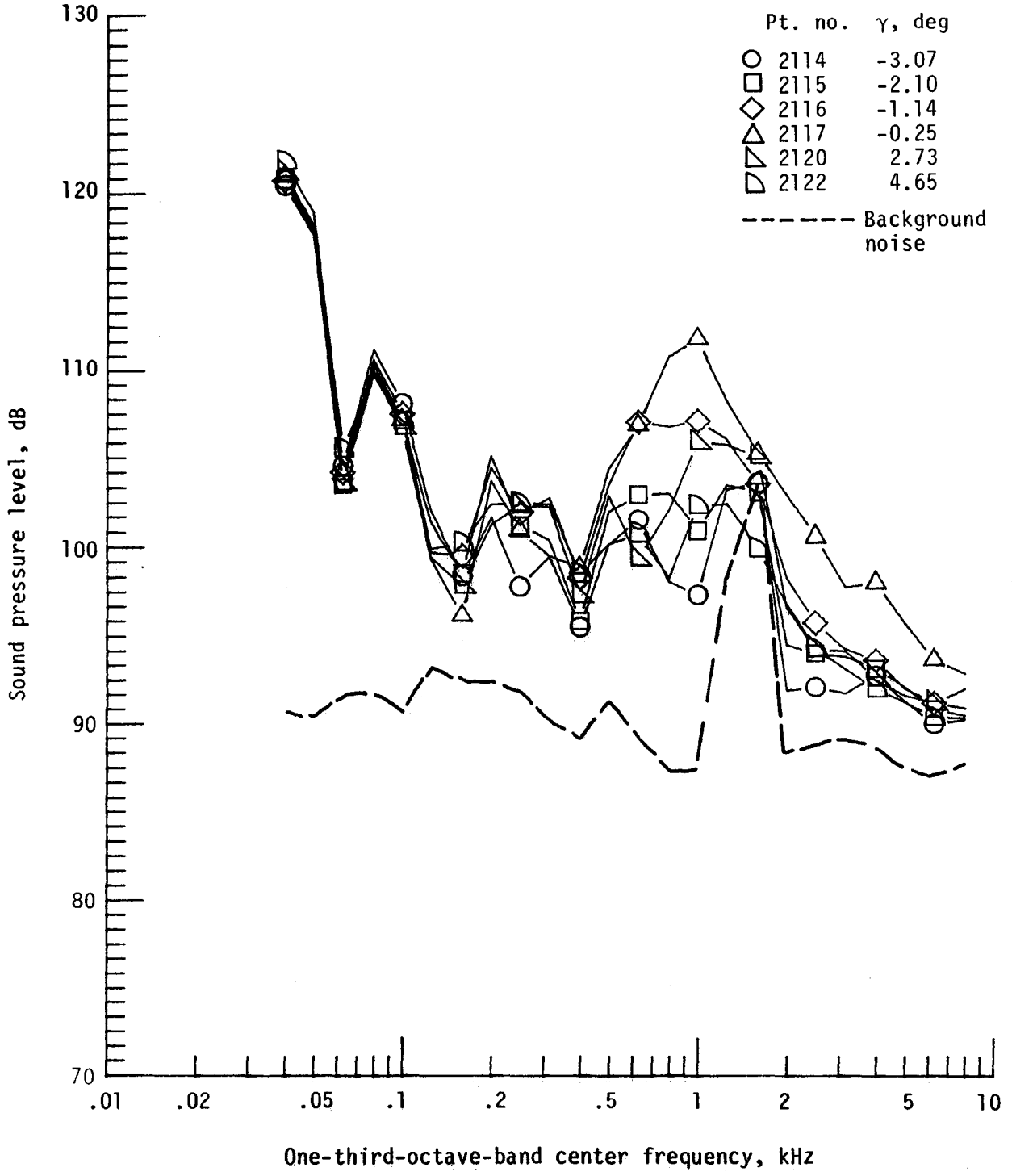

(a) One-third-octave spectra, microphone 2.

Figure 32. - Effect of descent angle variation on noise generated by helicopter model with standard rotor system, run 164. V_∞ = 90.1 knots, C_T .0032.

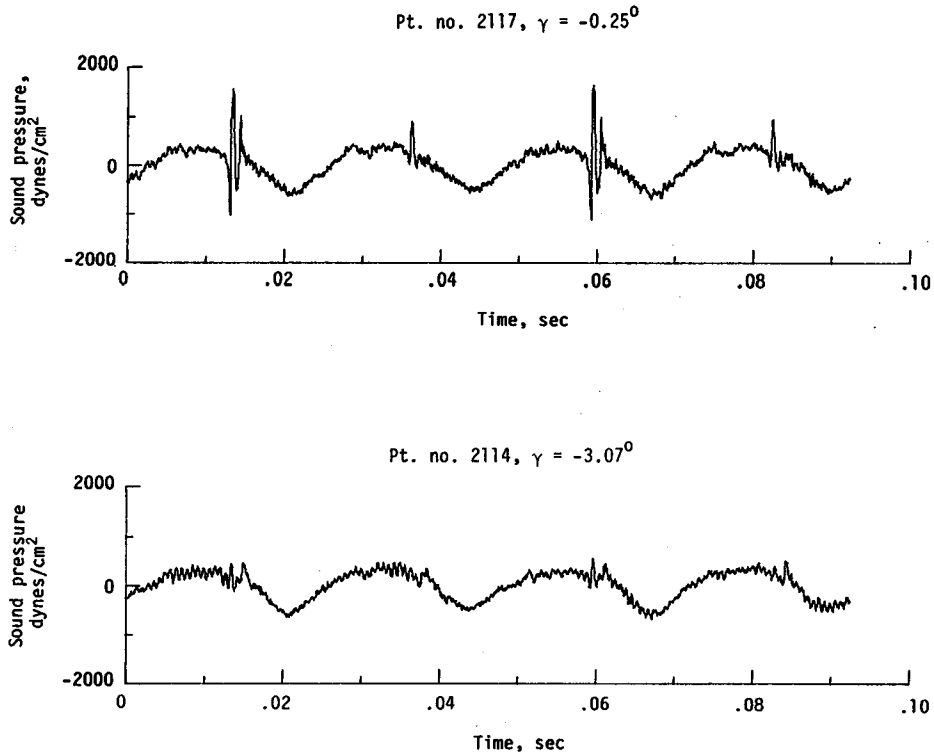

(b) Pressure-time histories; microphone 2.

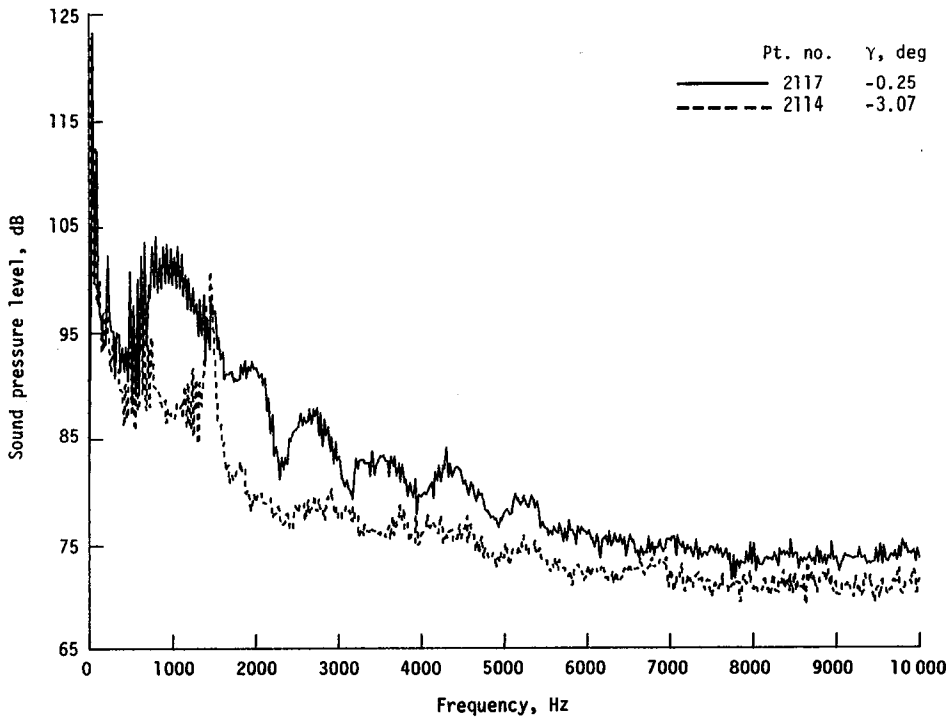

(c) Narrowband analysis; microphone 2.
Figure 32. - Continued.

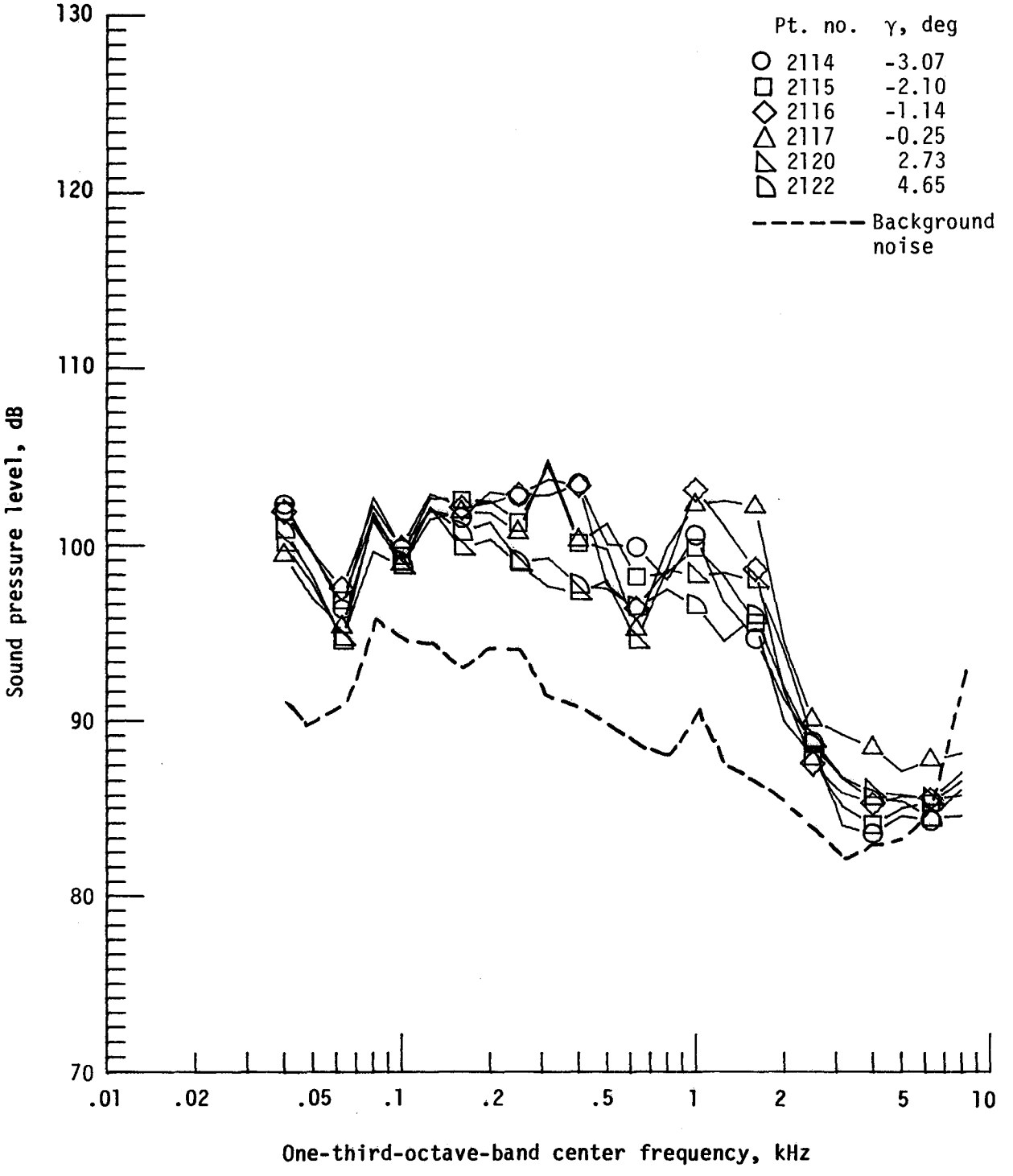

(d) One-third-octave spectra, microphone 6.

Figure 32. - Continued.

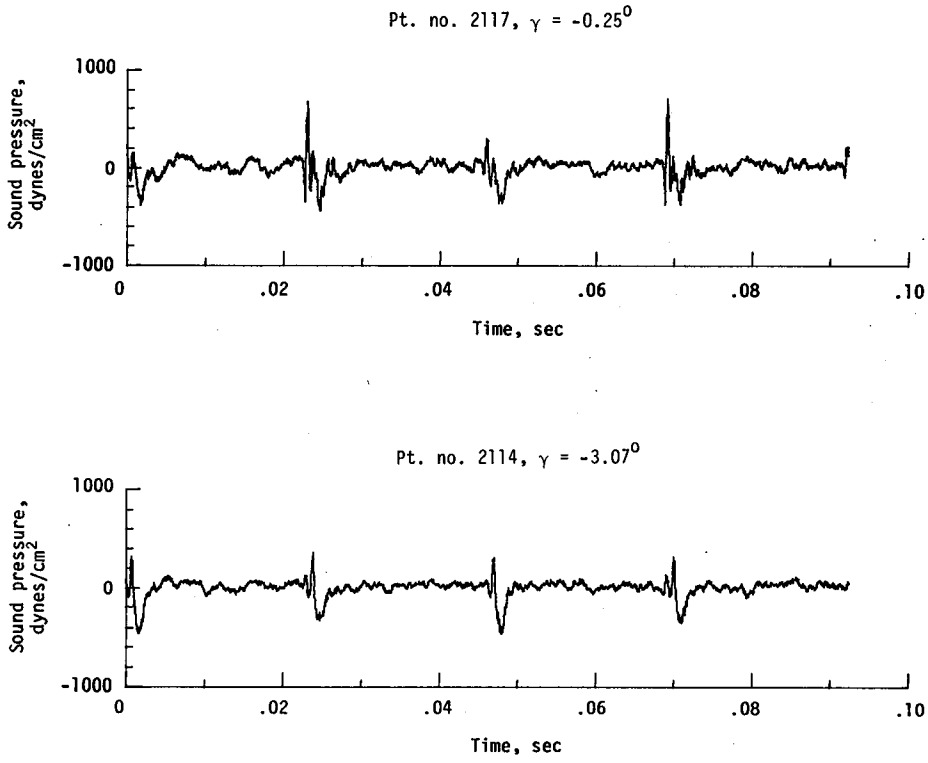

(e) Pressure-time histories; microphone 6.

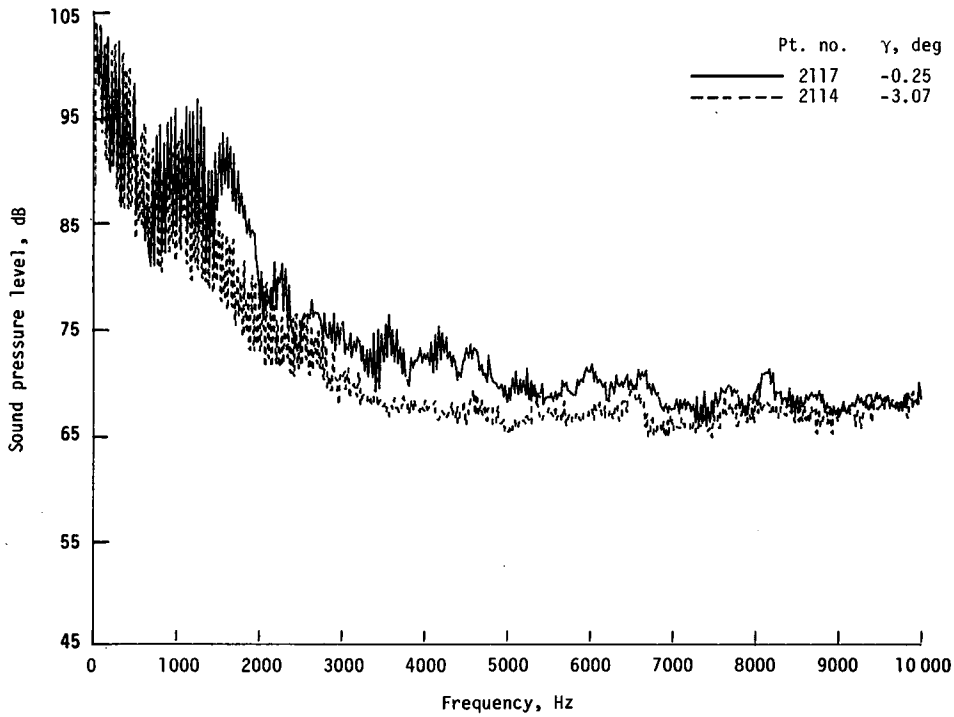

(f) Narrowband analysis; microphone 6.
Figure 32. - Continued.

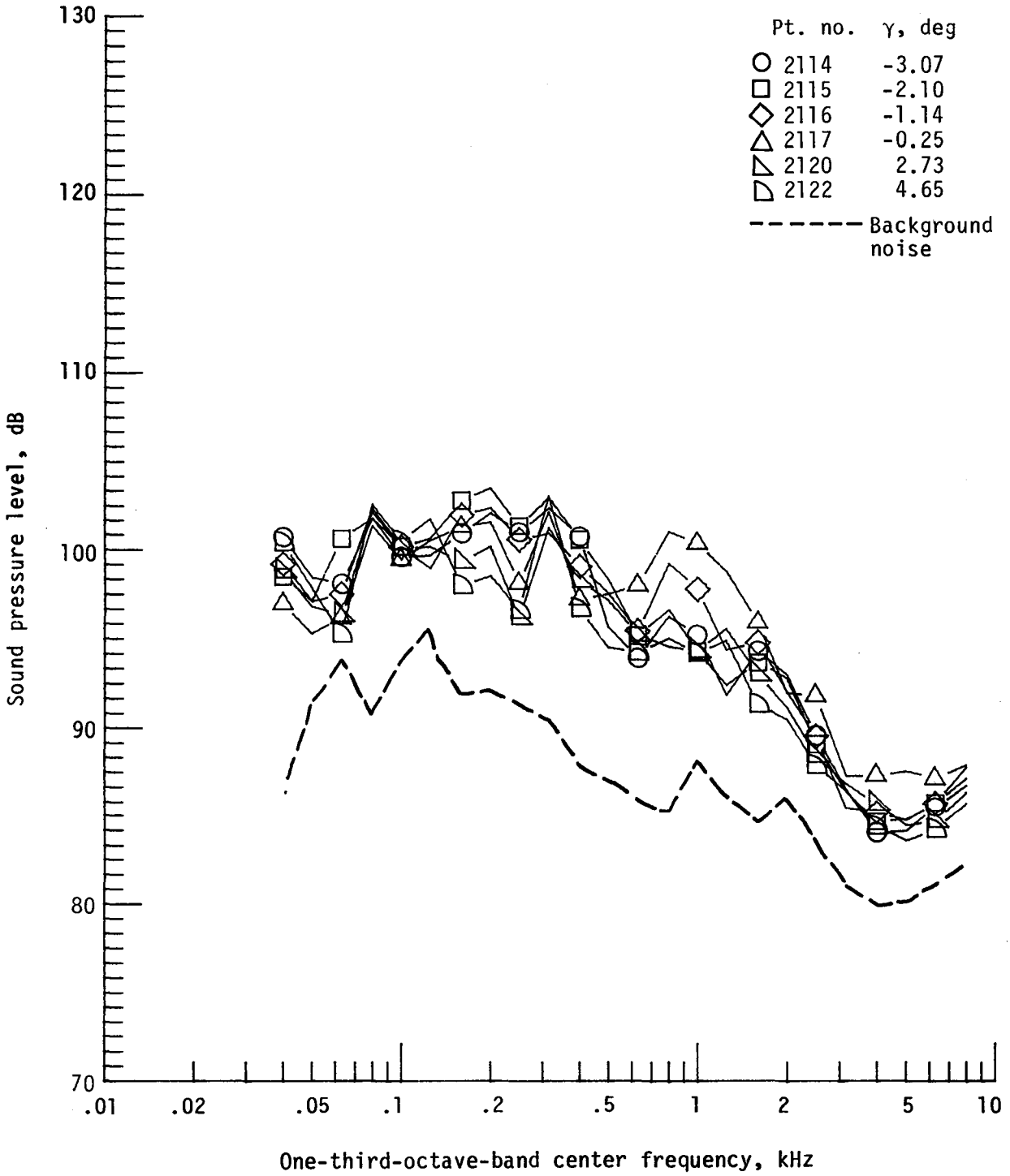

(g) One-third-octave spectra, microphone 7.

Figure 32. - Continued.

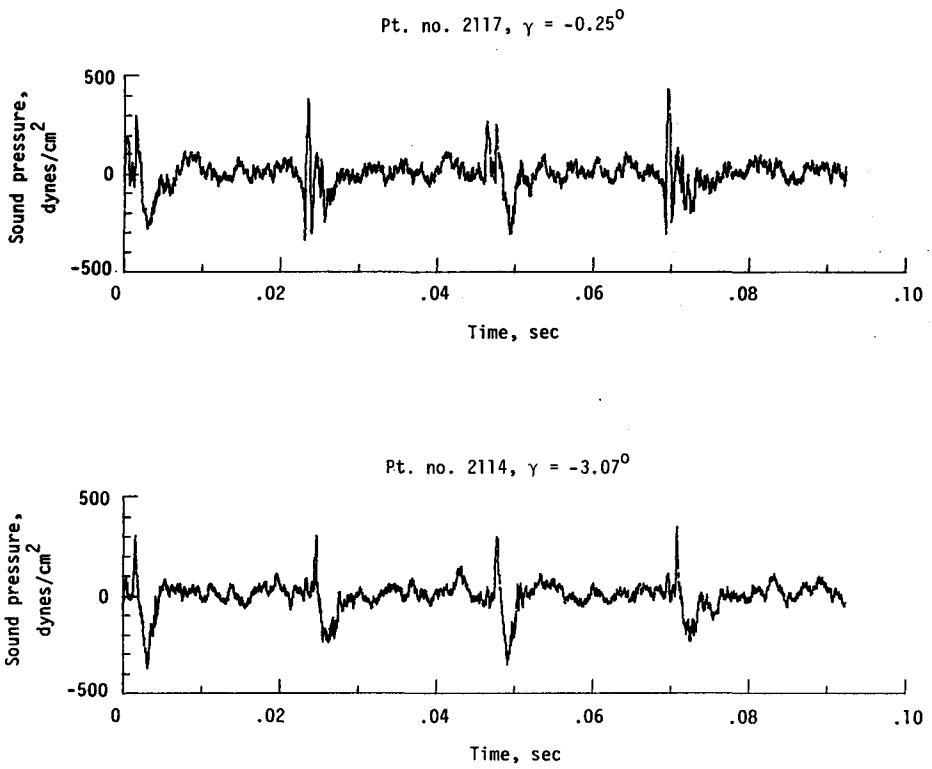

(h) Pressure-time histories; microphone 7.

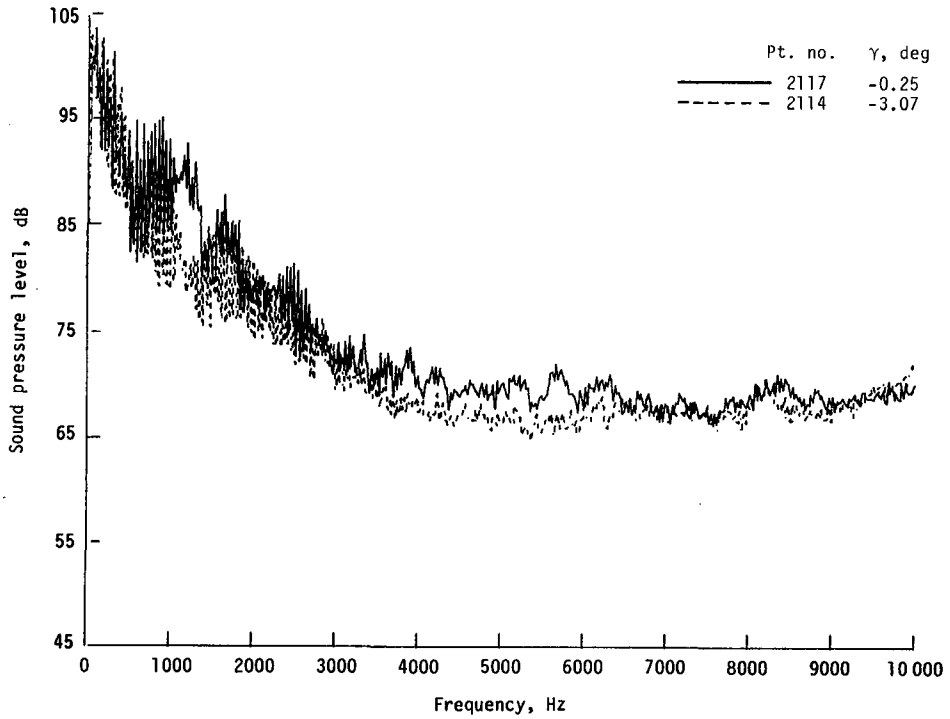

(i) Narrowband analysis; microphone 7.
Figure 32. - Continued.

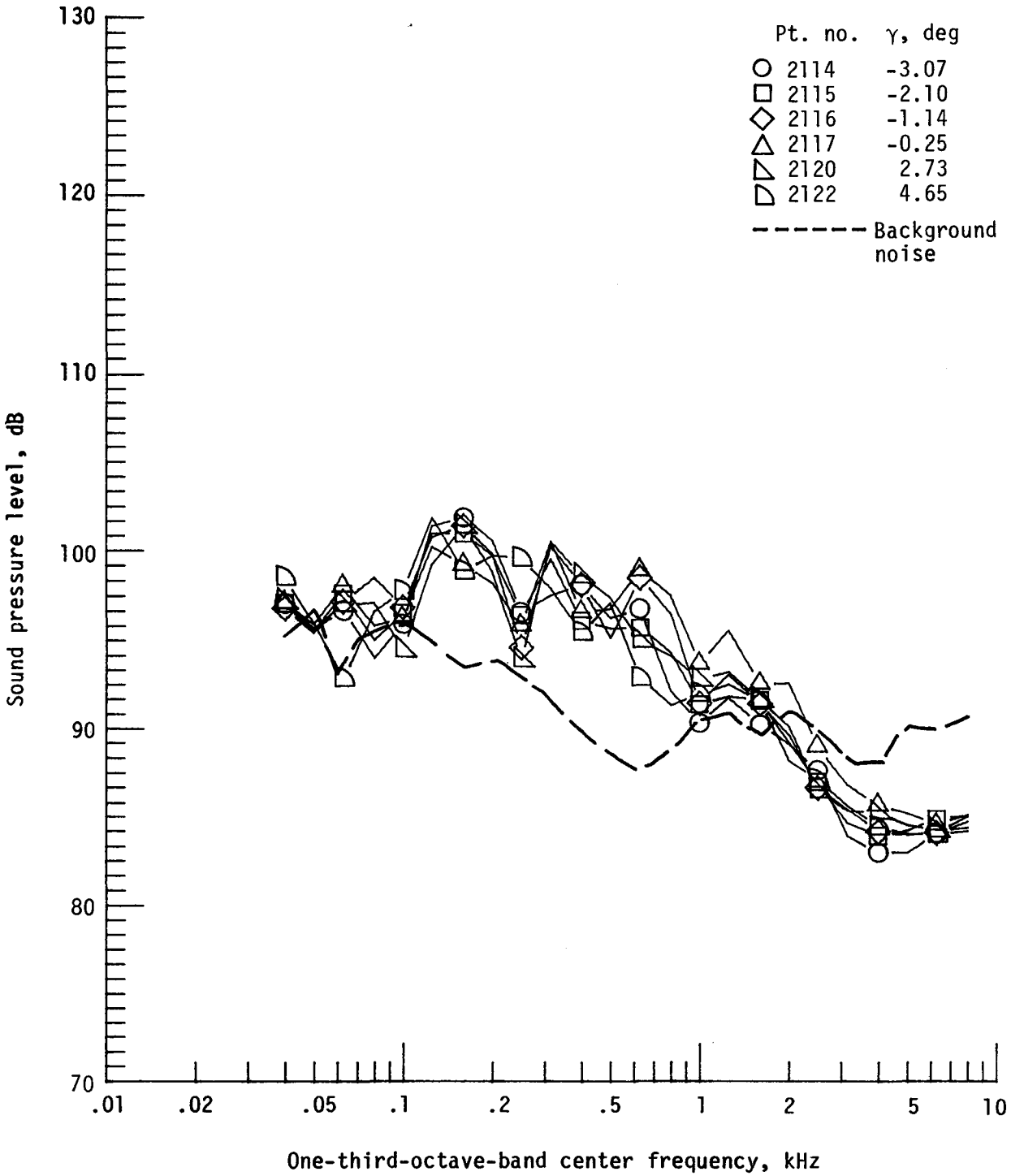

(j) One-third-octave spectra, microphone 8.

Figure 32. - Continued.

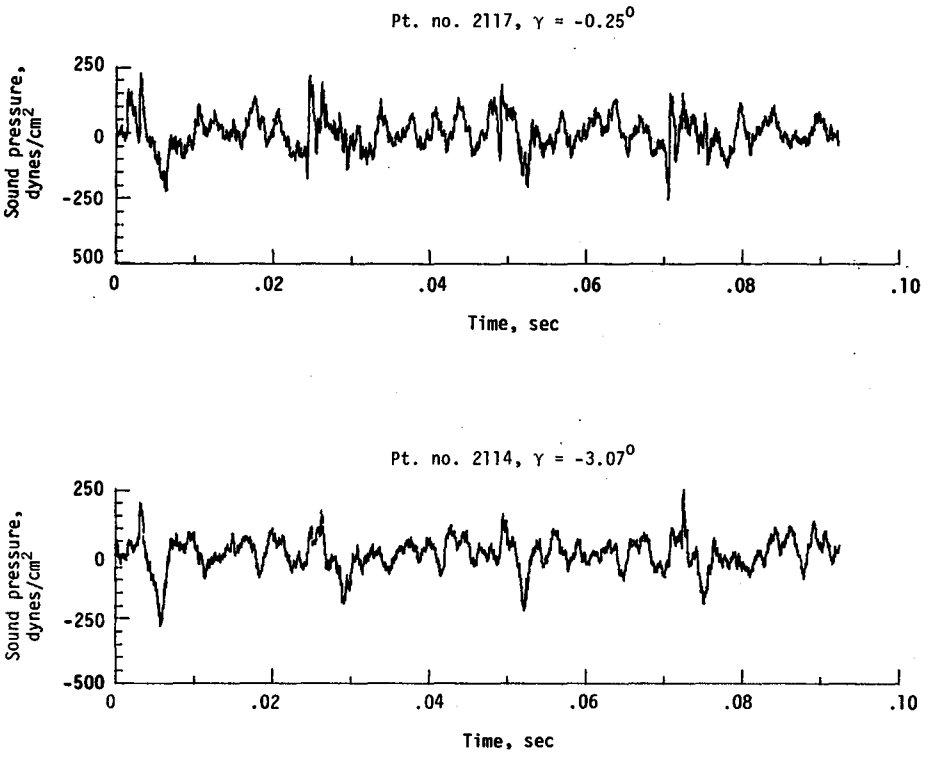

(k) Pressure-time histories; microphone 8.

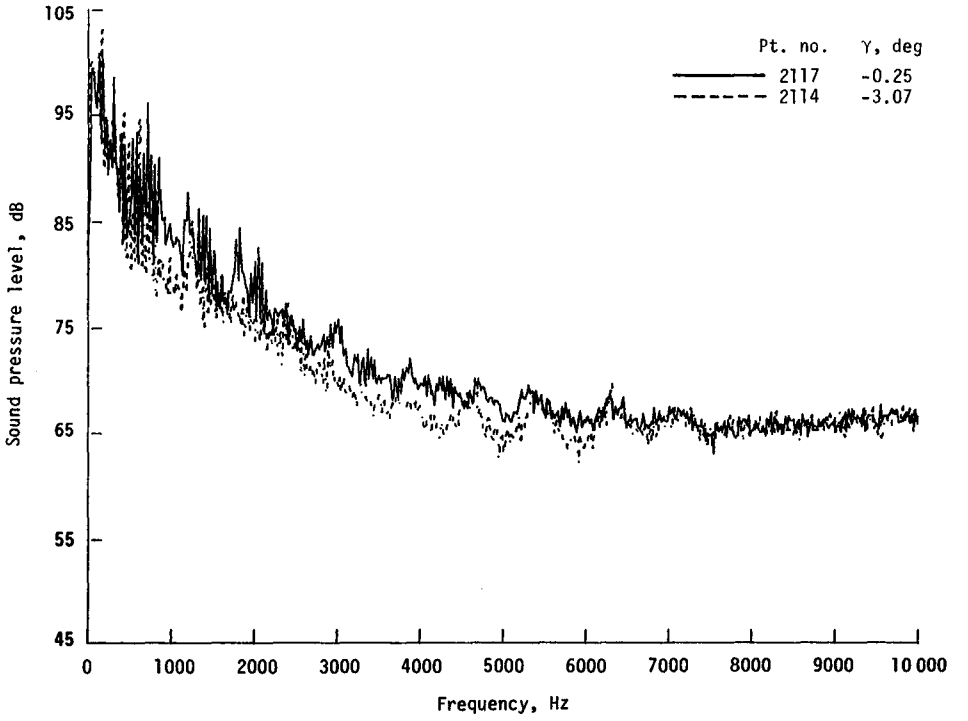

(l) Narrowband analysis; microphone 8.

Figure 32. - Concluded.

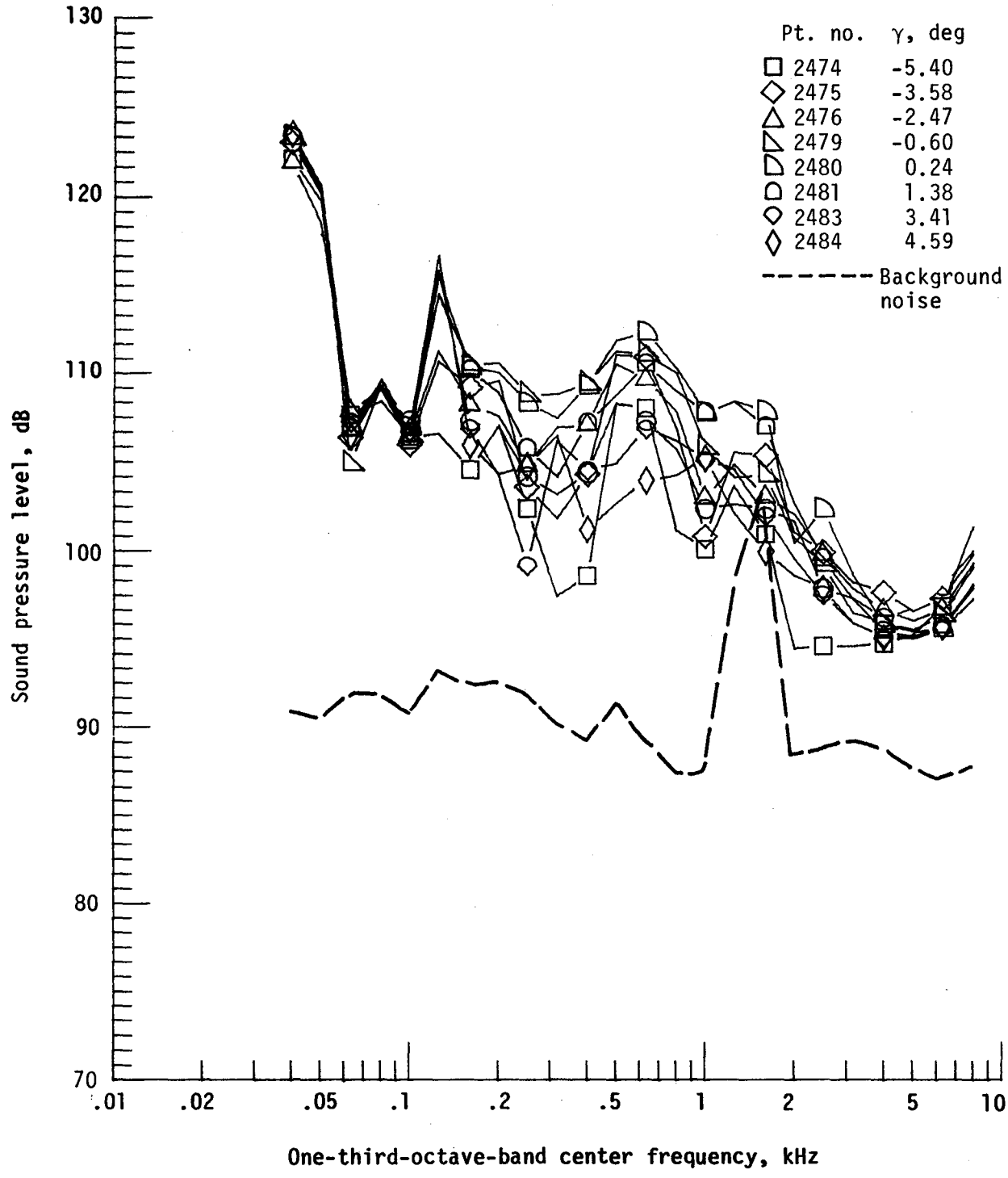

(a) One-third-octave spectra, microphone 2.

Figure 33. - Effect of descent angle variation on noise generated by helicopter model with advanced rotor system, run 197. V_∞ = 90.4 knots, C_T .0031.

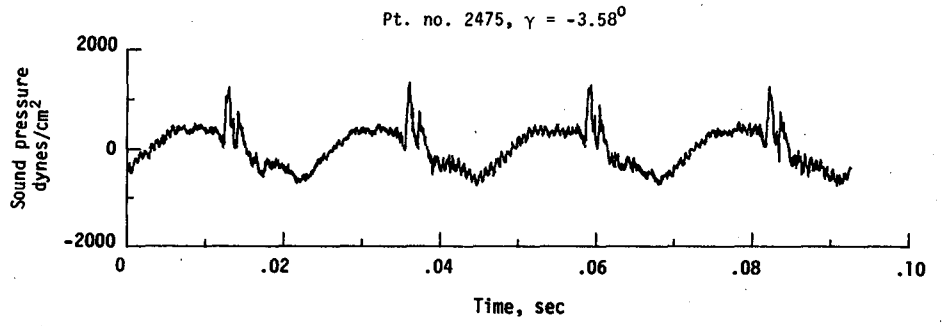

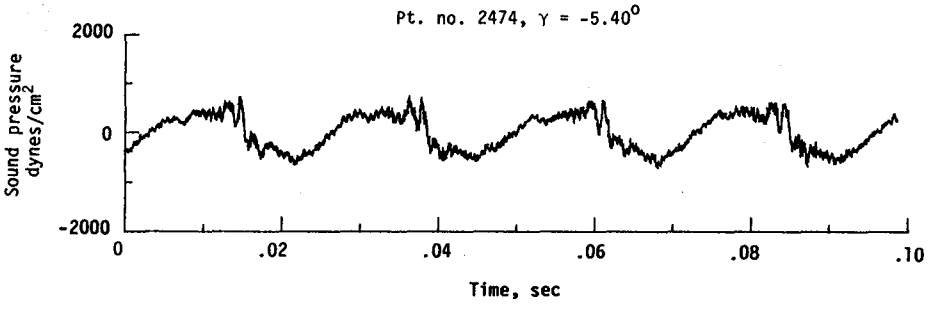

(b) Pressure-time histories; microphone 2.

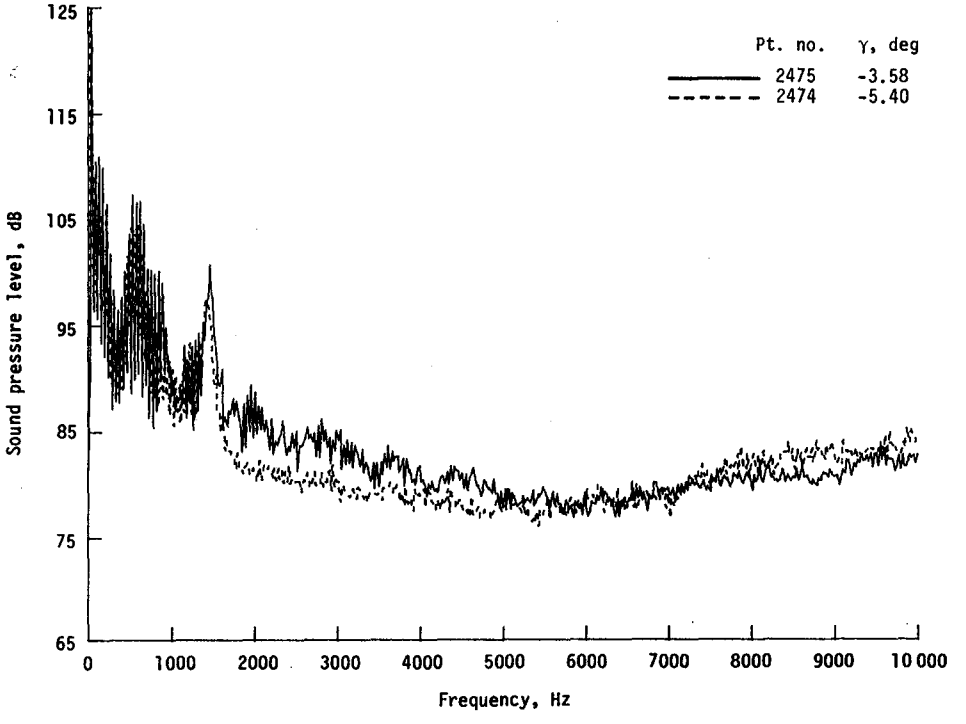

(c) Narrowband analysis; microphone 2.
Figure 33. - Continued.

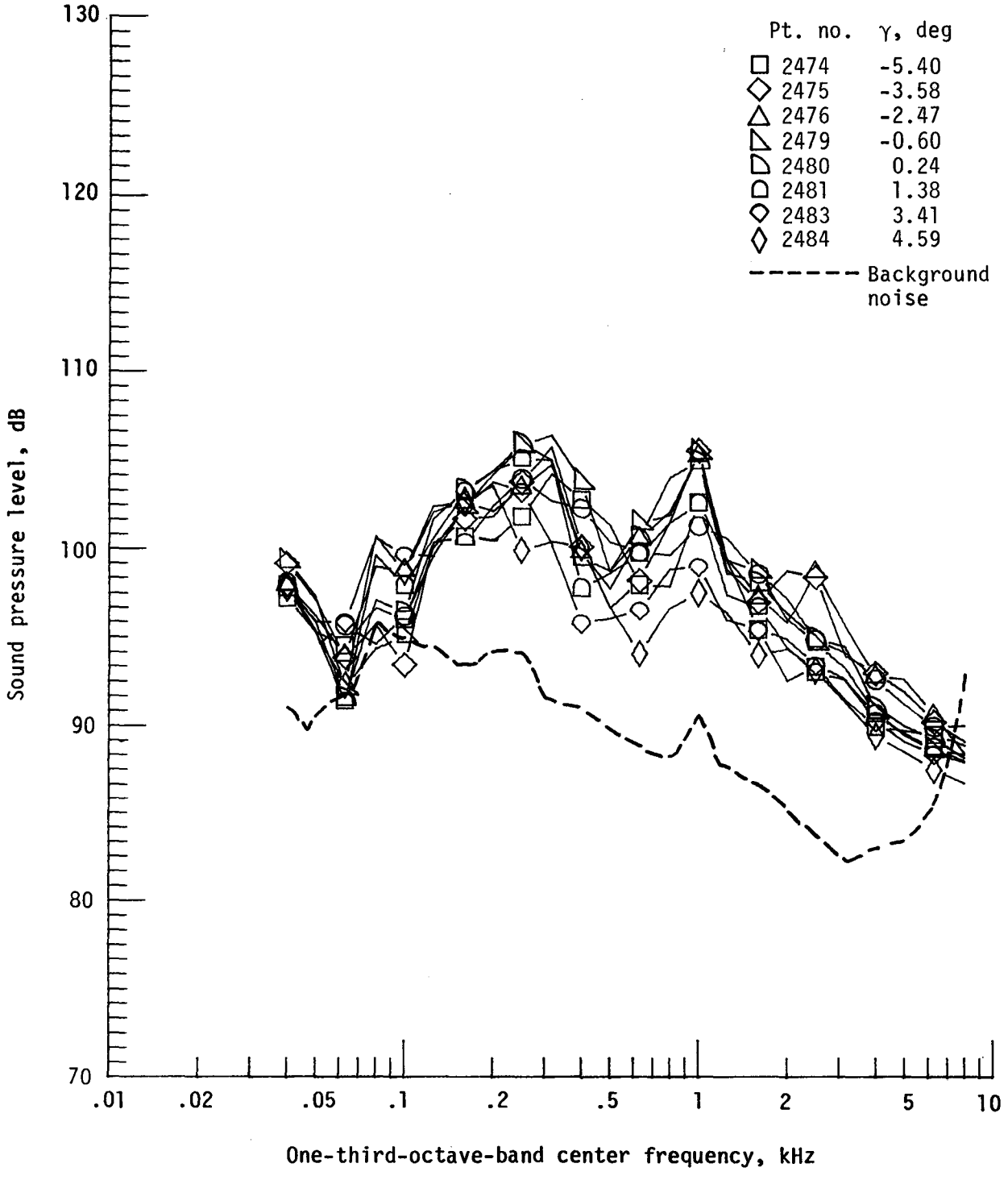

(d) One-third-octave spectra, microphone 6.

Figure 33. - Continued.

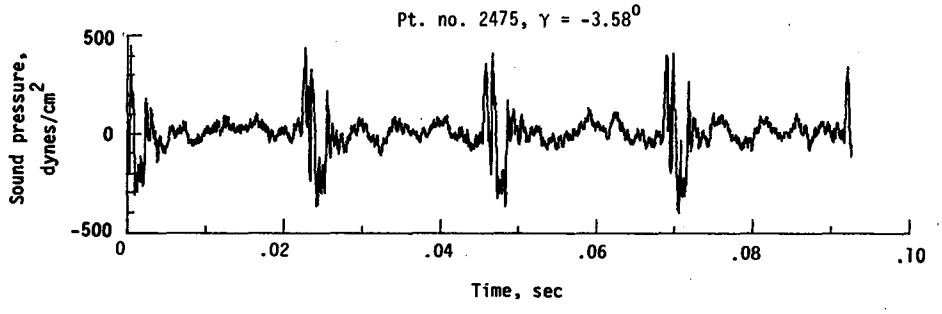

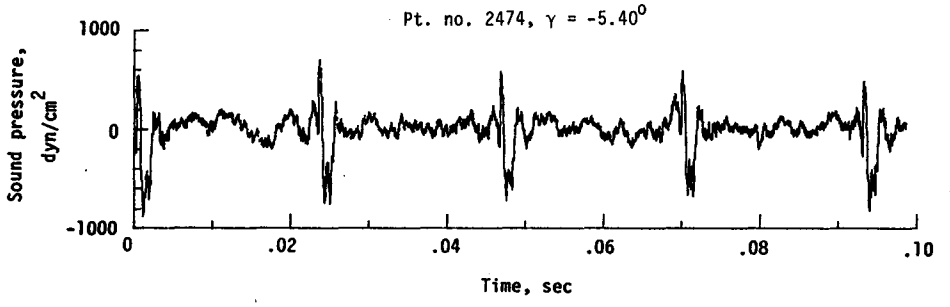

(e) Pressure-time histories; microphone 6.

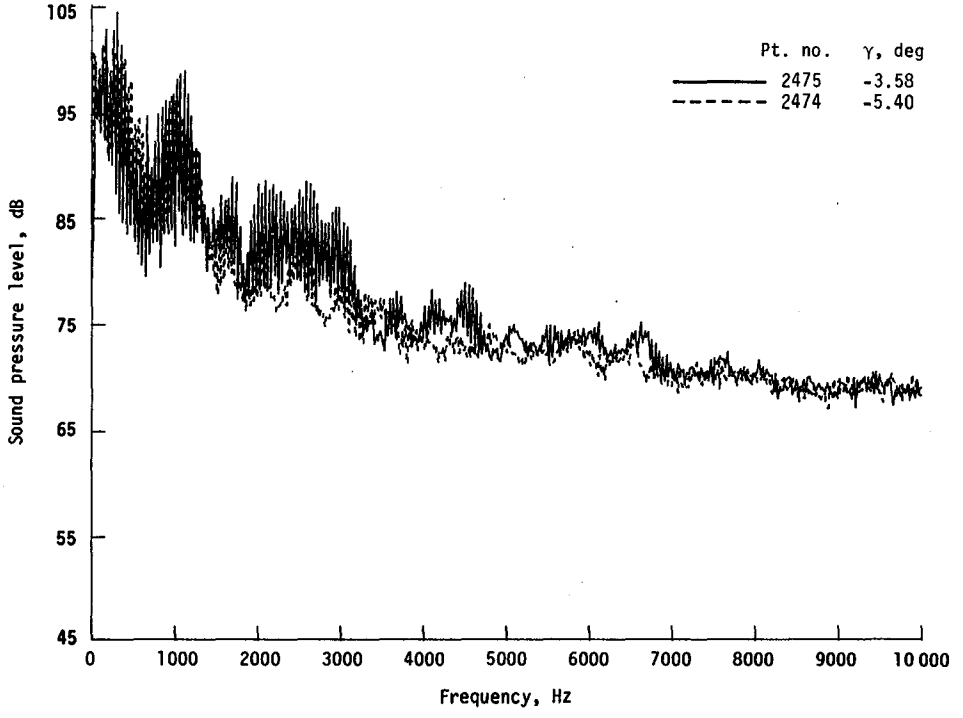

(f) Narrowband analysis; microphone 6.
Figure 33. - Continued.

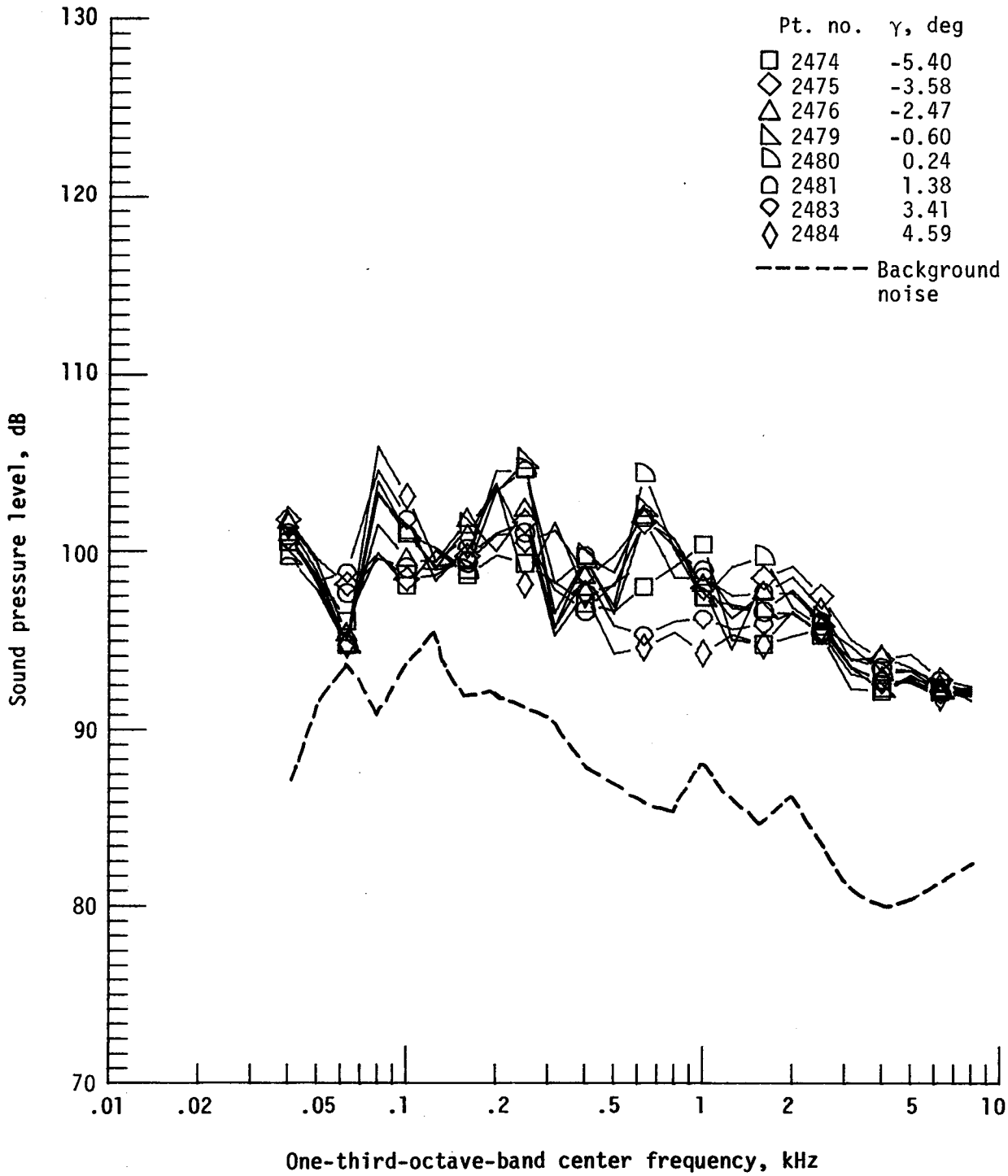

(g) One-third-octave spectra, microphone 7.

Figure 33. - Continued.

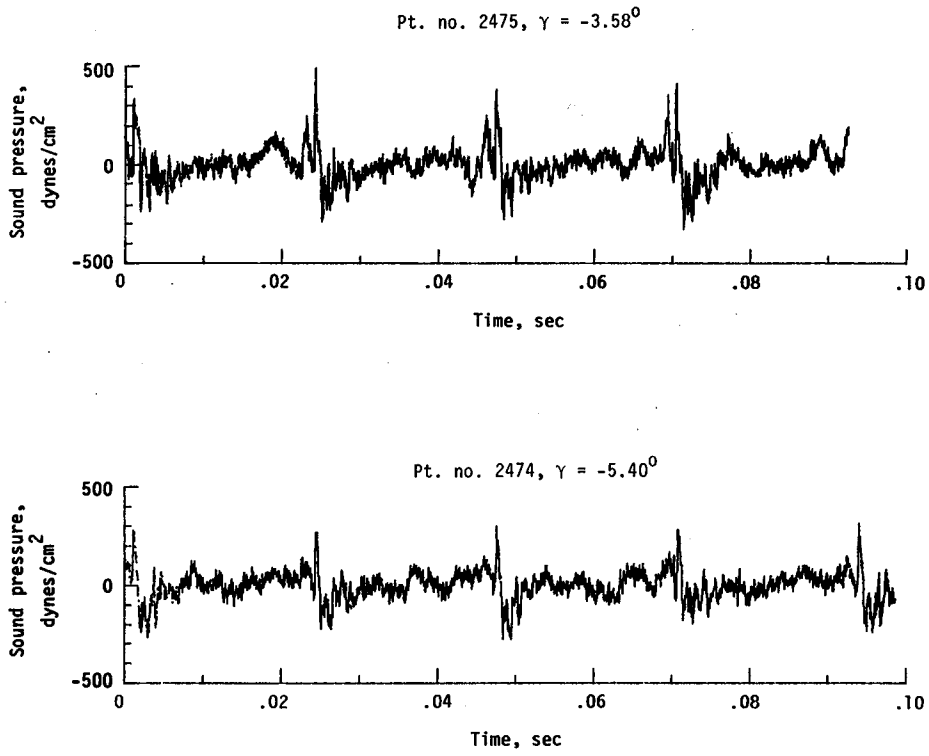

(h) Pressure-time histories; microphone 7.

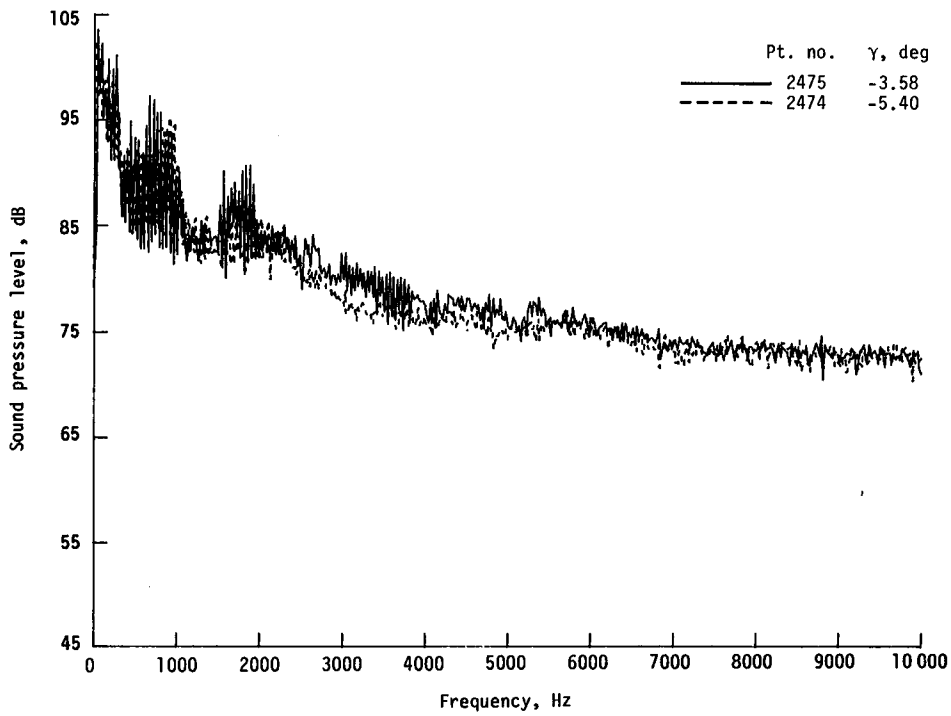

(i) Narrowband analysis; microphone 7.
Figure 33. - Continued.

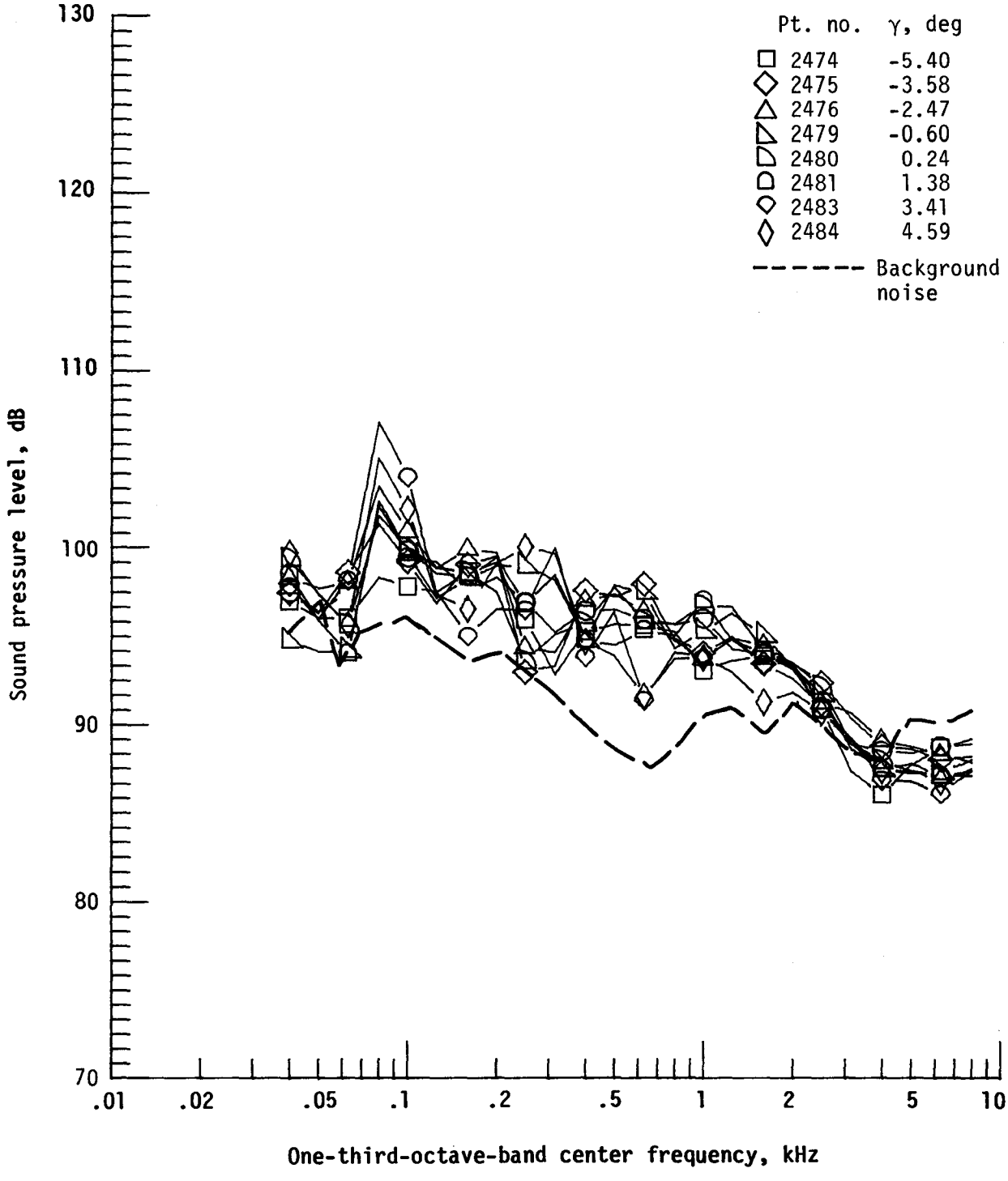

(j) One-third-octave spectra, microphone 8.

Figure 33. - Continued.

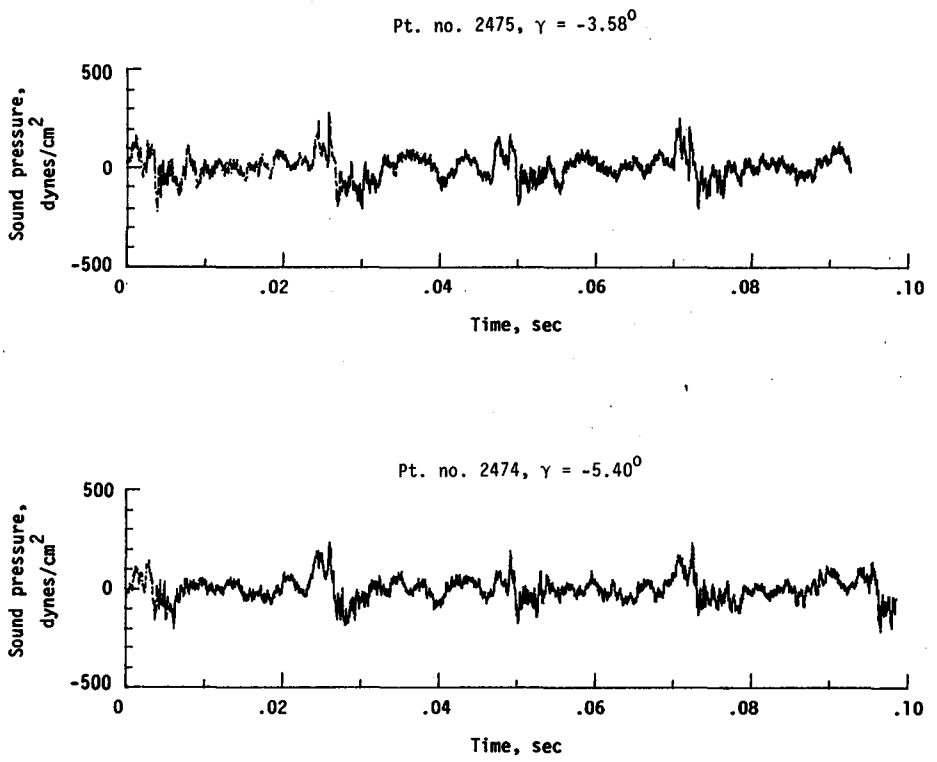

(k) Pressure-time histories; microphone 8.

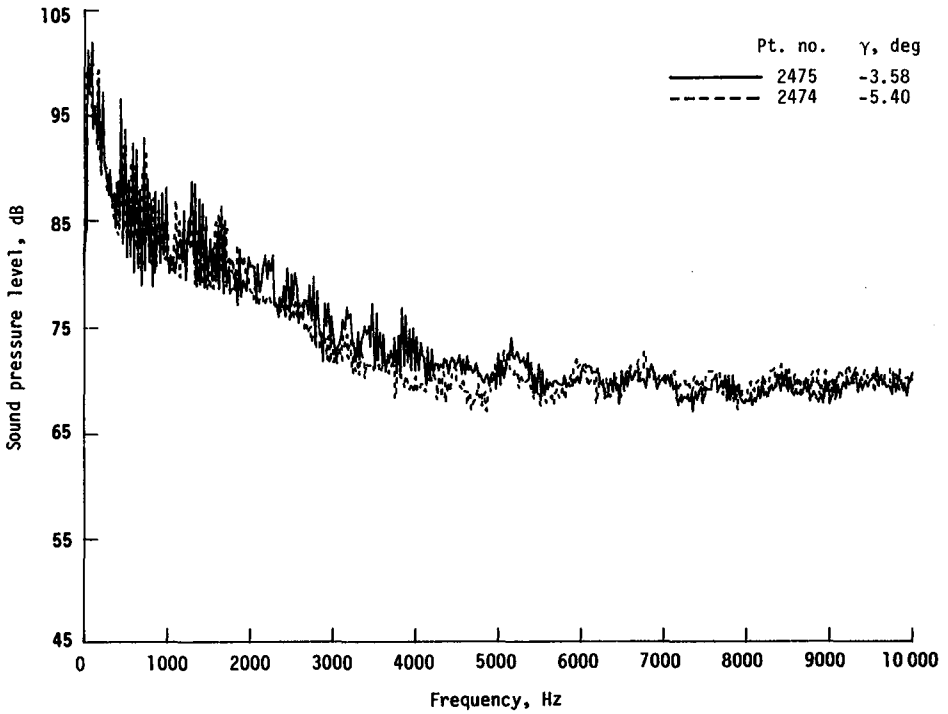

(l) Narrowband analysis; microphone 8.
Figure 33. - Concluded.

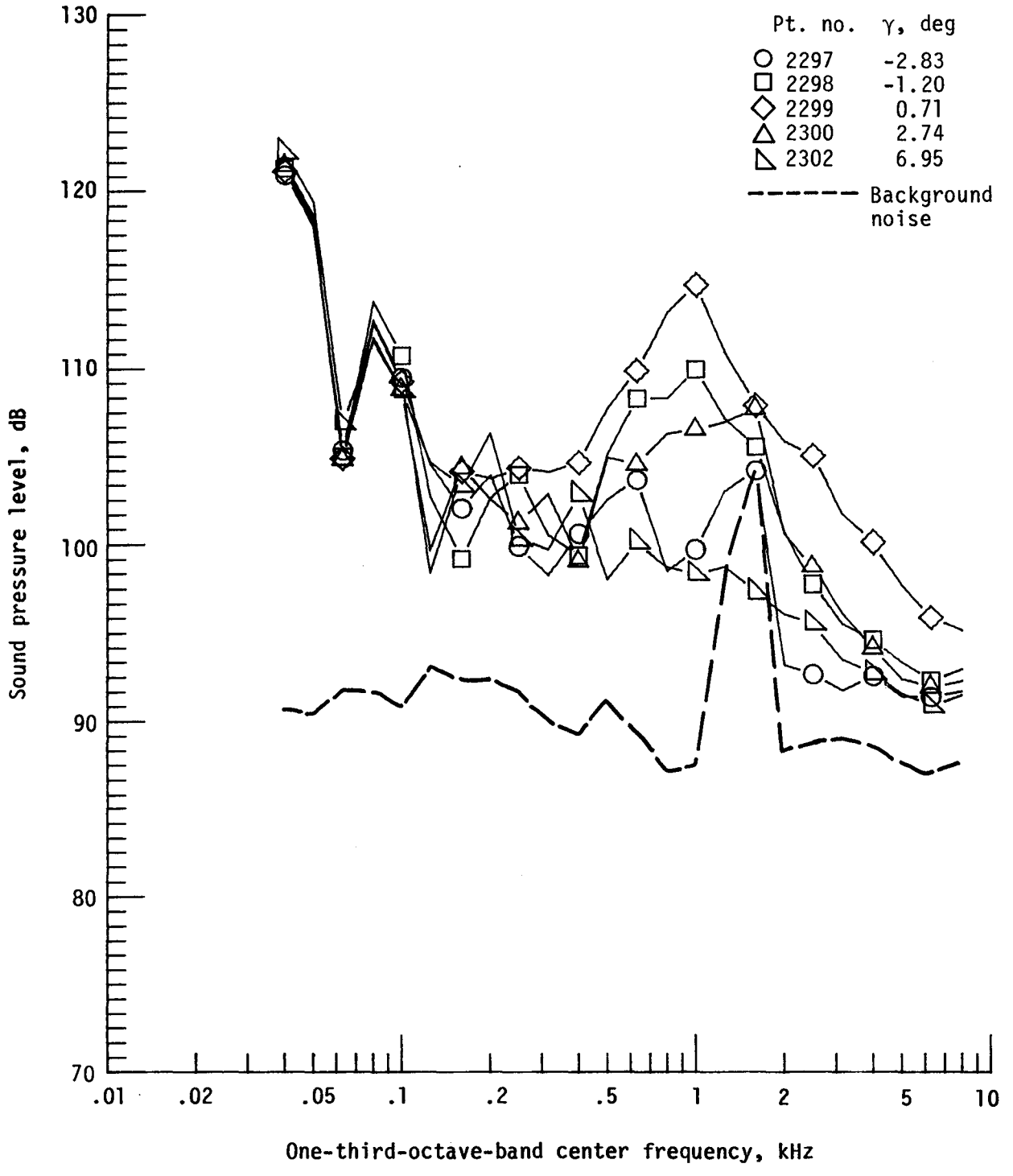

(a) One-third-octave spectra, microphone 2.

Figure 34. - Effect of descent angle variation on noise generated by helicopter model with standard rotor system, run 186. V_∞ = 90.3 knots, C_T .0036.

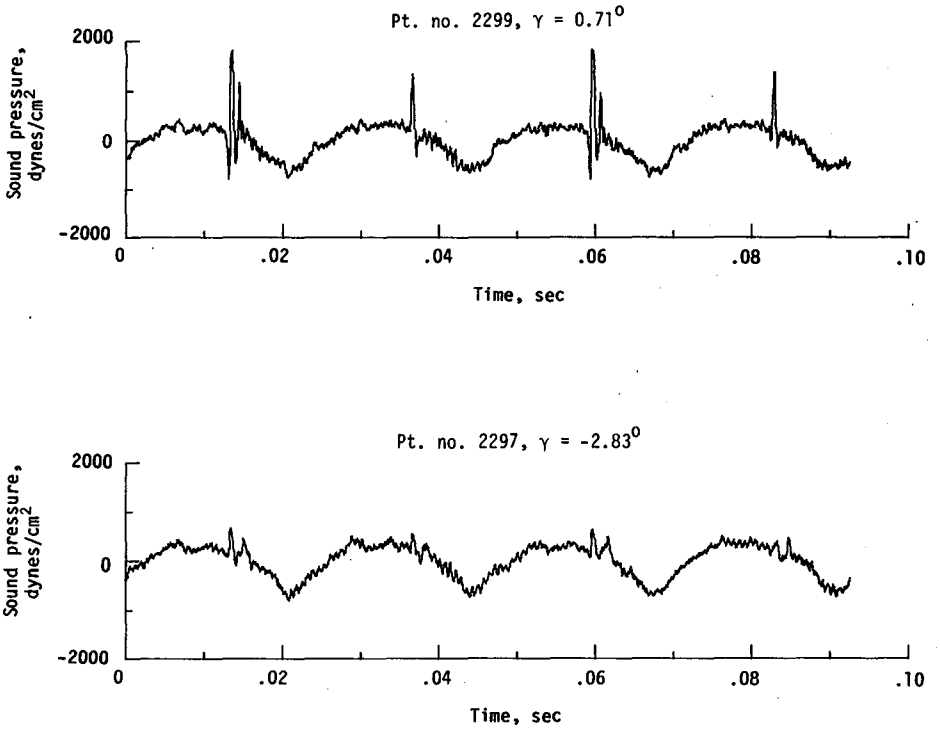

(b) Pressure-time histories; microphone 2.

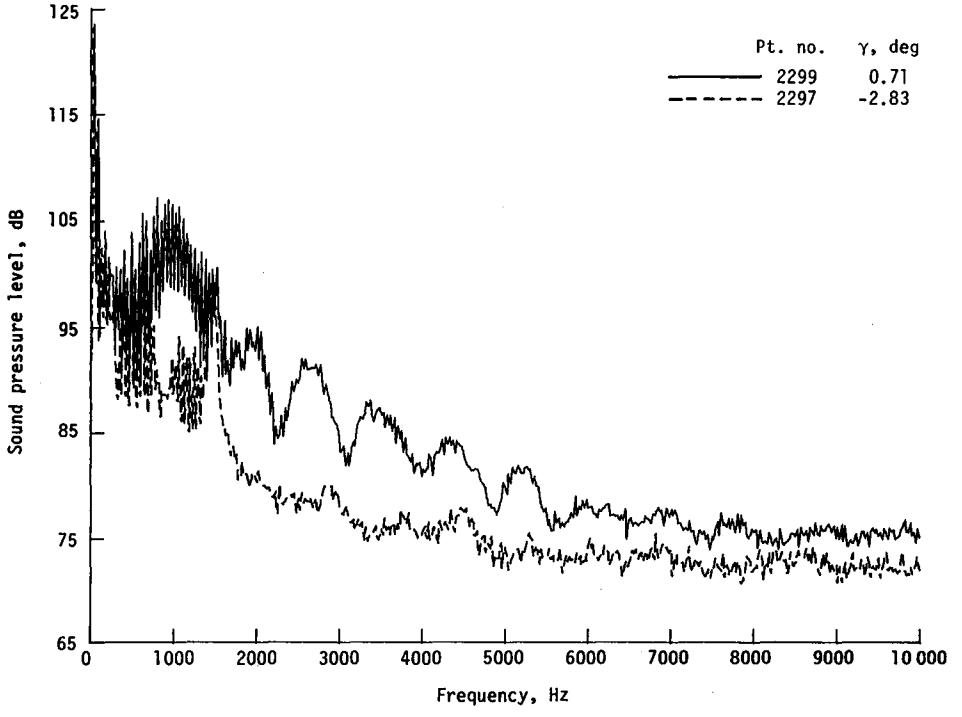

(c) Narrowband analysis; microphone 2.
Figure 34. - Continued.

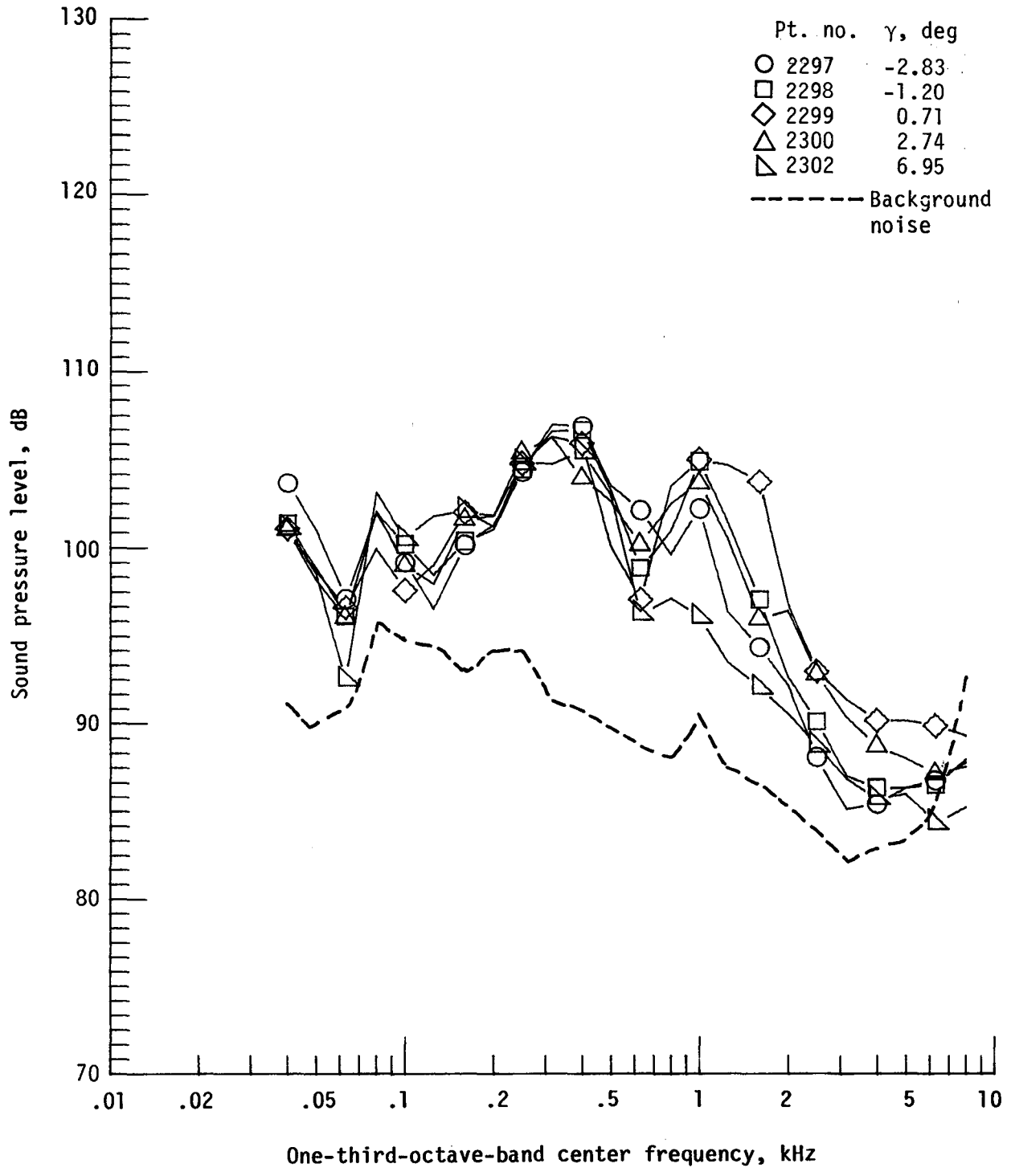

(d) One-third-octave spectra, microphone 6.

Figure 34. - Continued.

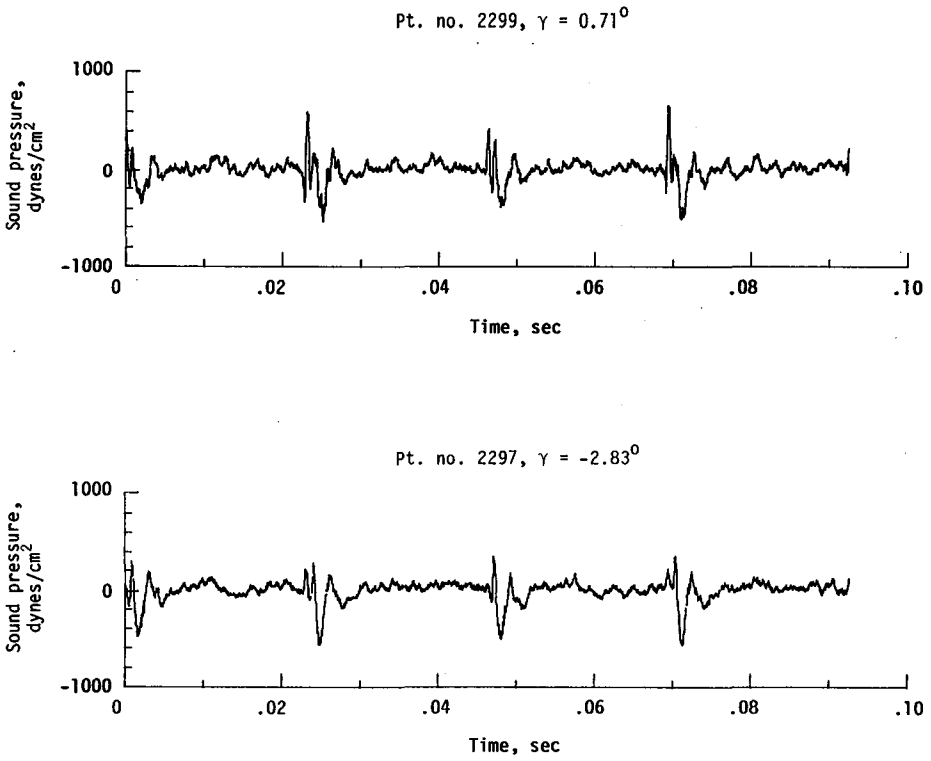

(e) Pressure-time histories; microphone 6.

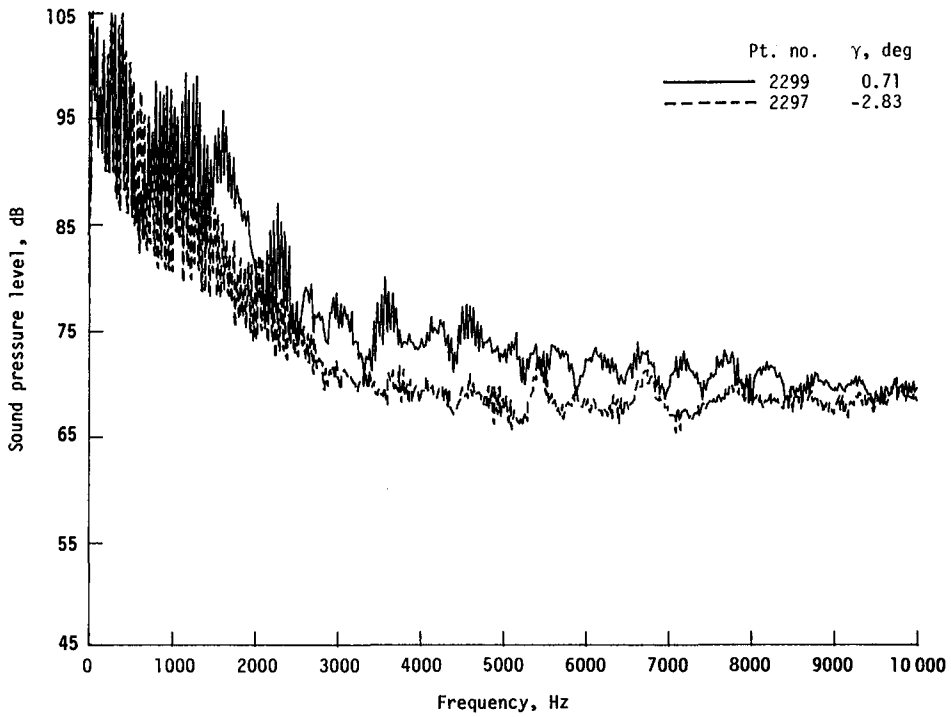

(f) Narrowband analysis; microphone 6.
Figure 34. - Continued.

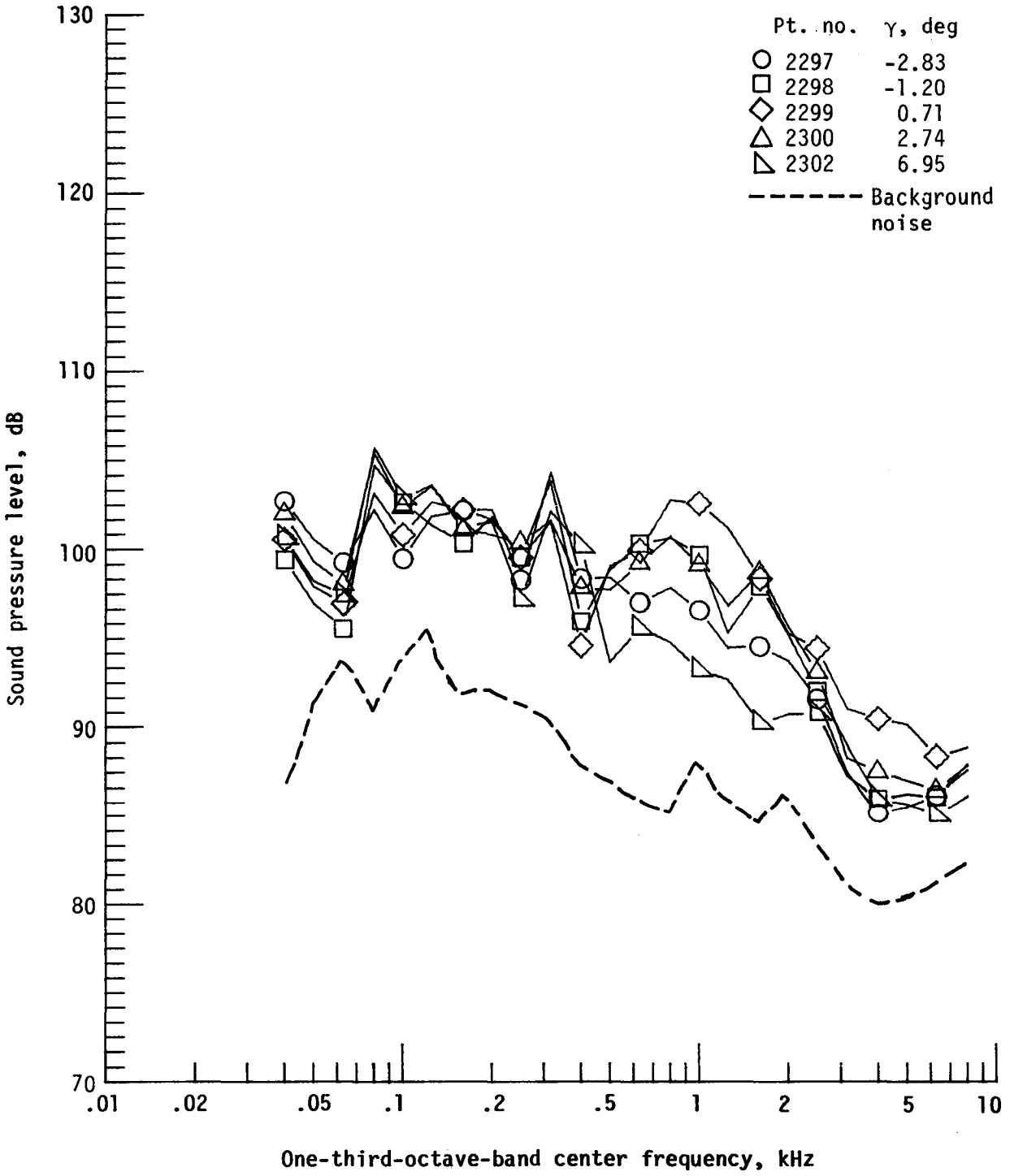

(g) One-third-octave spectra, microphone 7.

Figure 34. - Continued.

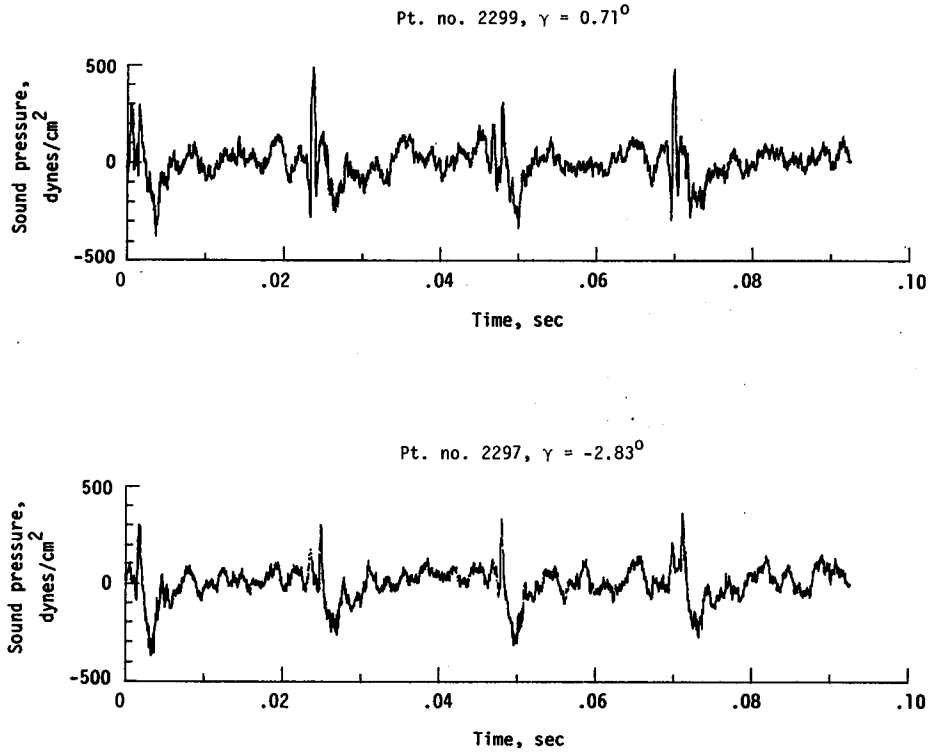

(h) Pressure-time histories; microphone 7.

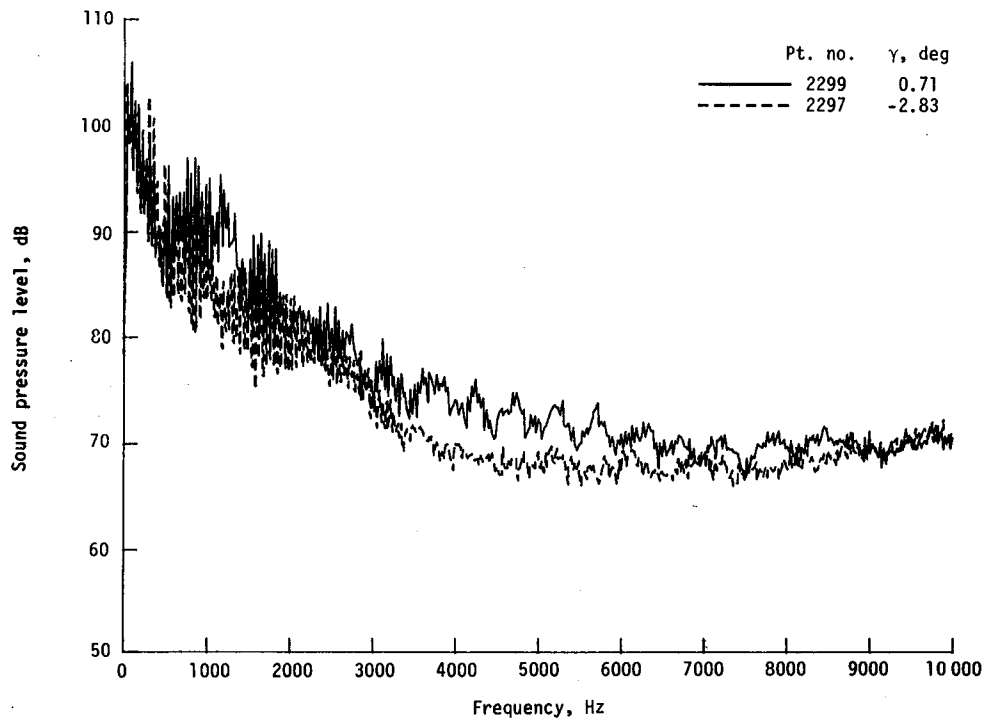

(i) Narrowband analysis; microphone 7.
Figure 34. - Continued.

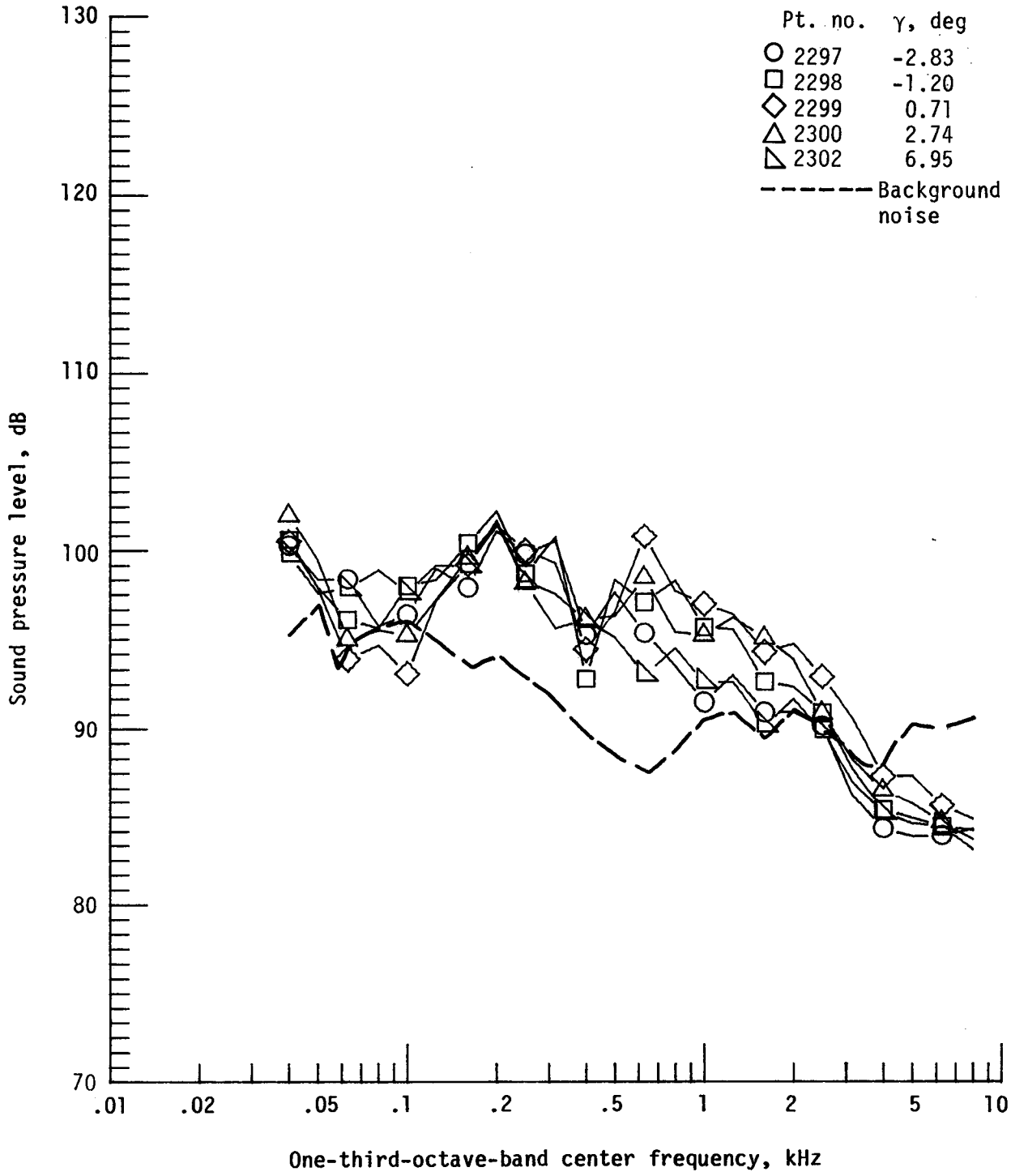

(j) One-third-octave spectra, microphone 8.

Figure 34. - Continued.

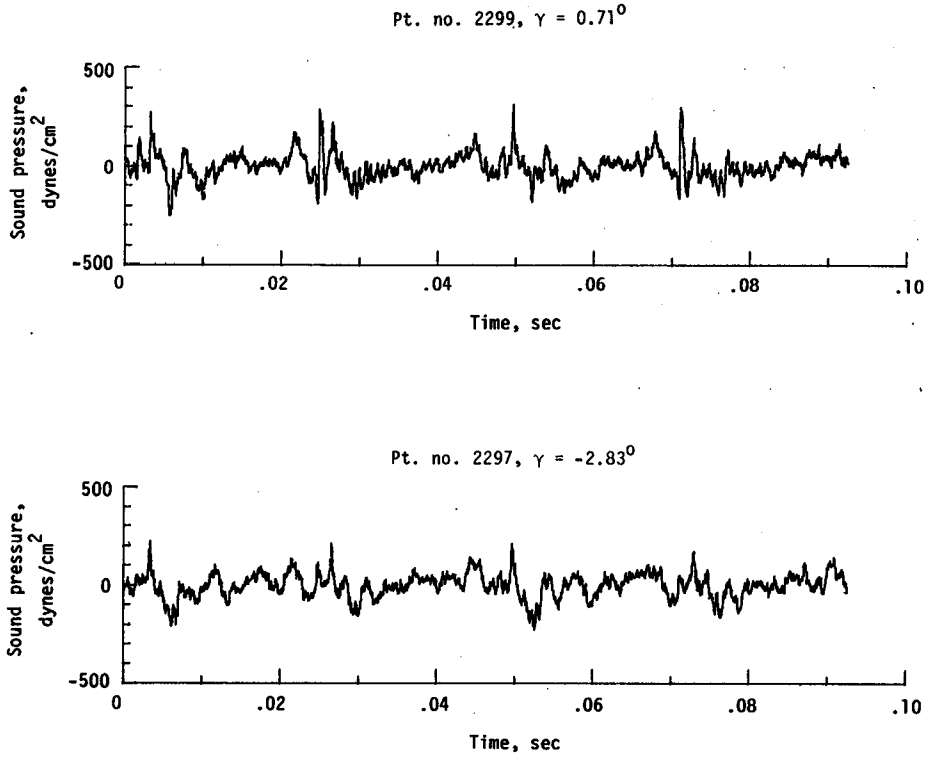

(k) Pressure-time histories; microphone 8.

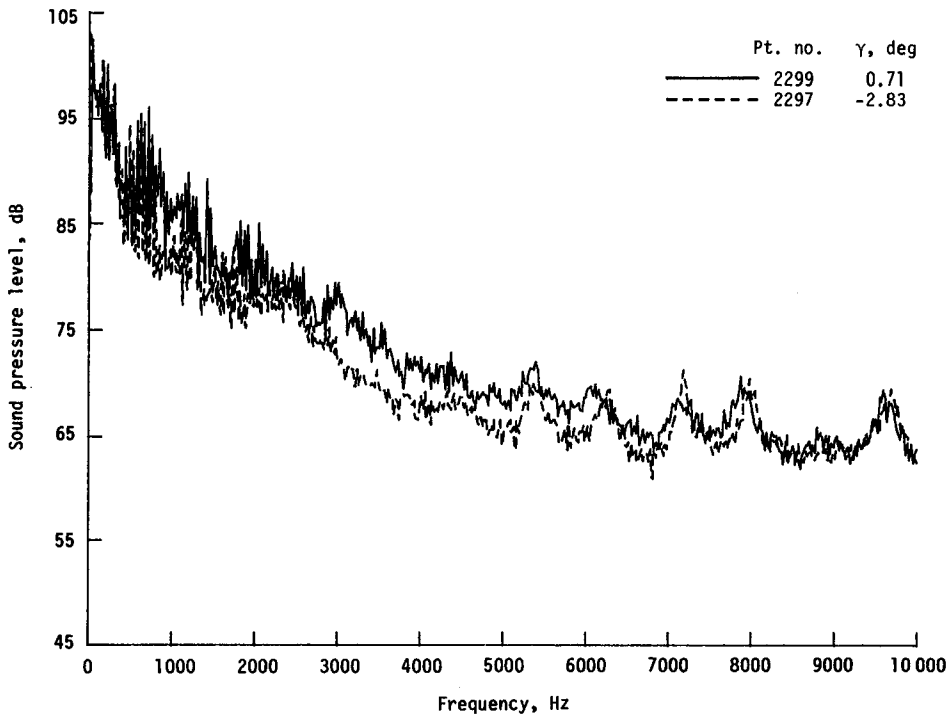

(l) Narrowband analysis; microphone 8.
Figure 34. - Concluded.

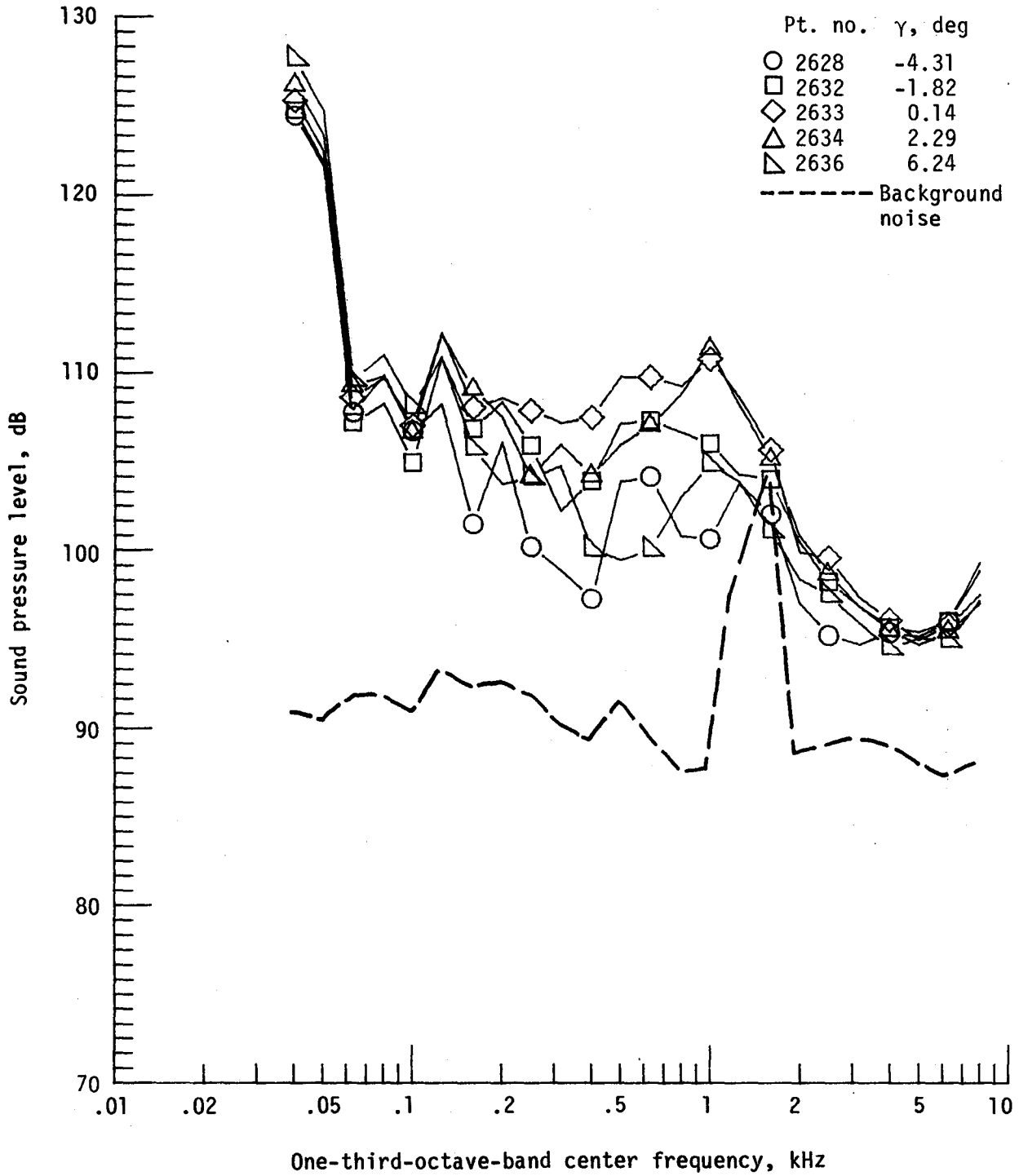

(a) One-third-octave spectra, microphone 2.

Figure 35. - Effect of descent angle variation on noise generated by helicopter model with advanced rotor system, run 218 and 219. V_∞ = 90.3 knots, C_T .0036.

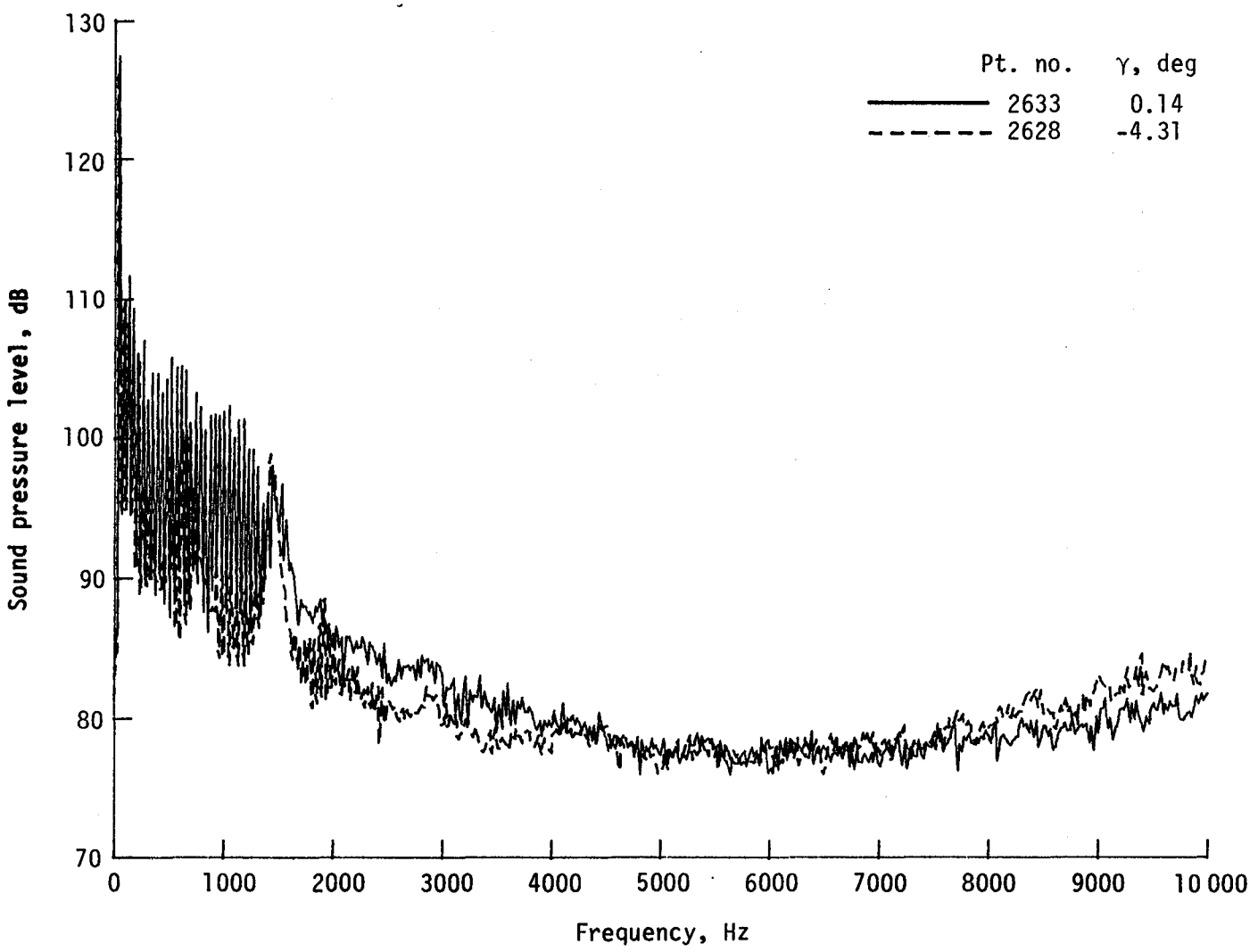

(b) Narrowband analysis; microphone 2.
Figure 35. - Continued.

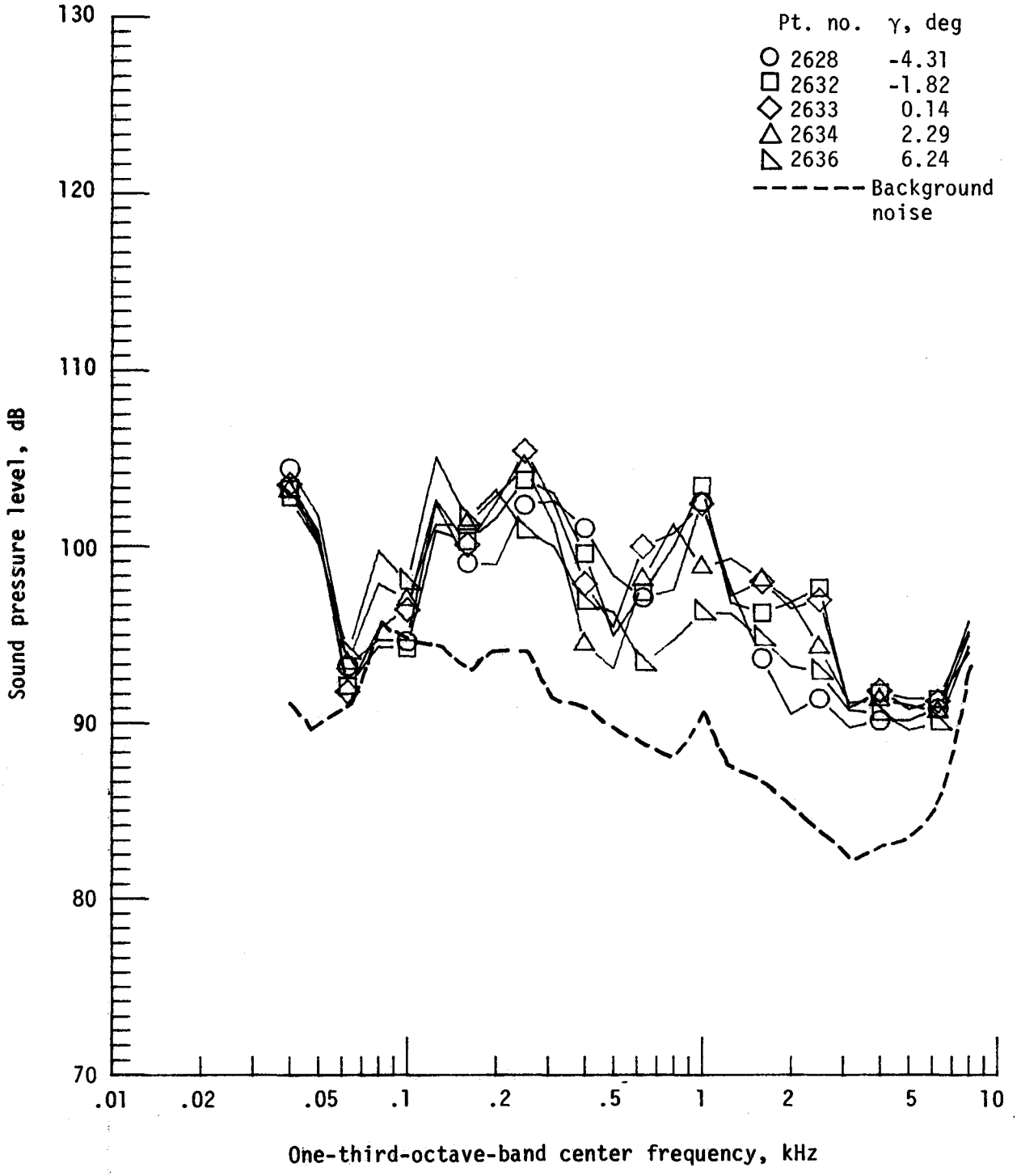

(c) One-third-octave spectra, microphone 6.

Figure 35. - Continued.

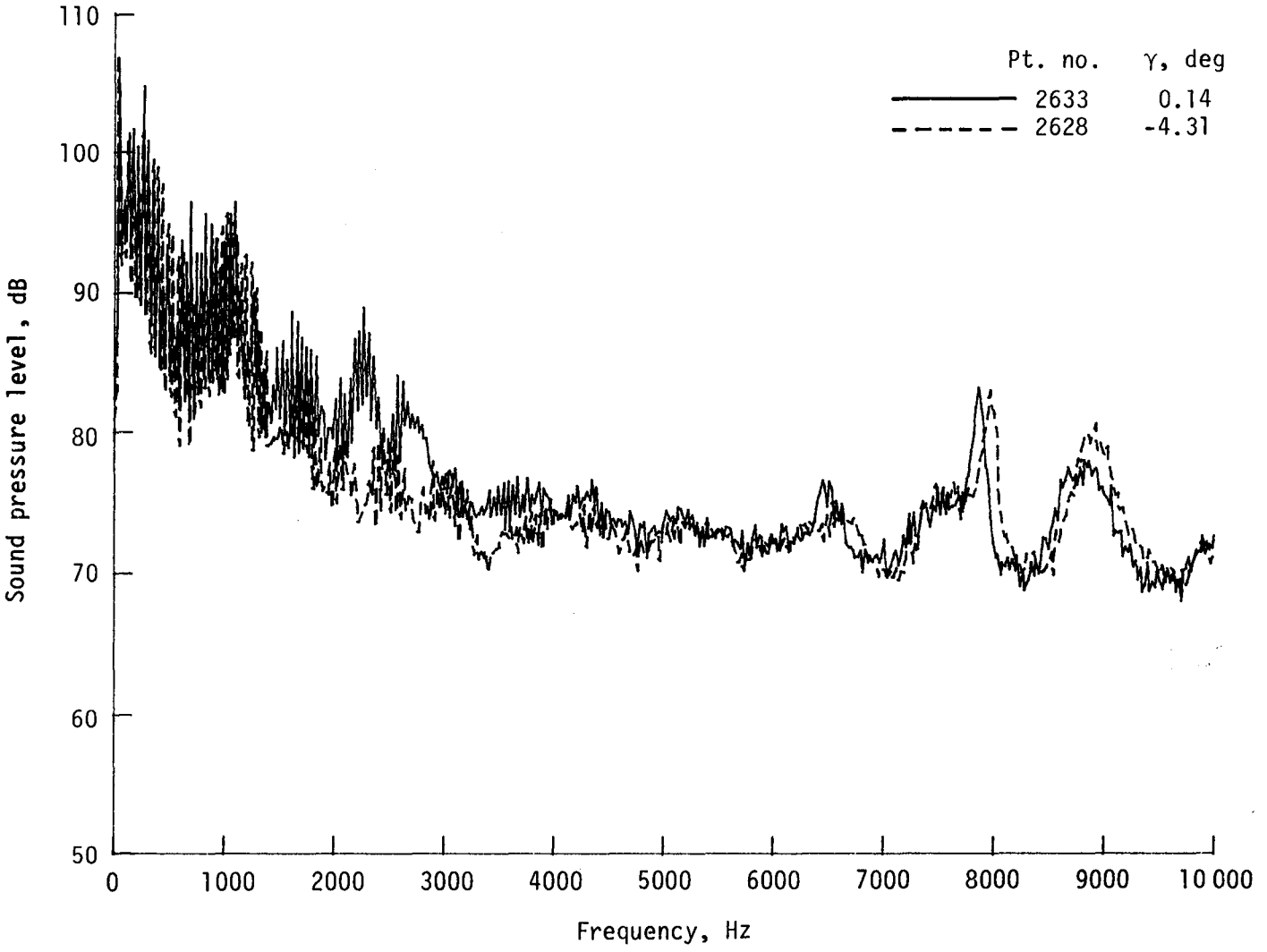

(d) Narrowband analysis; microphone 6.
Figure 35. - Continued.

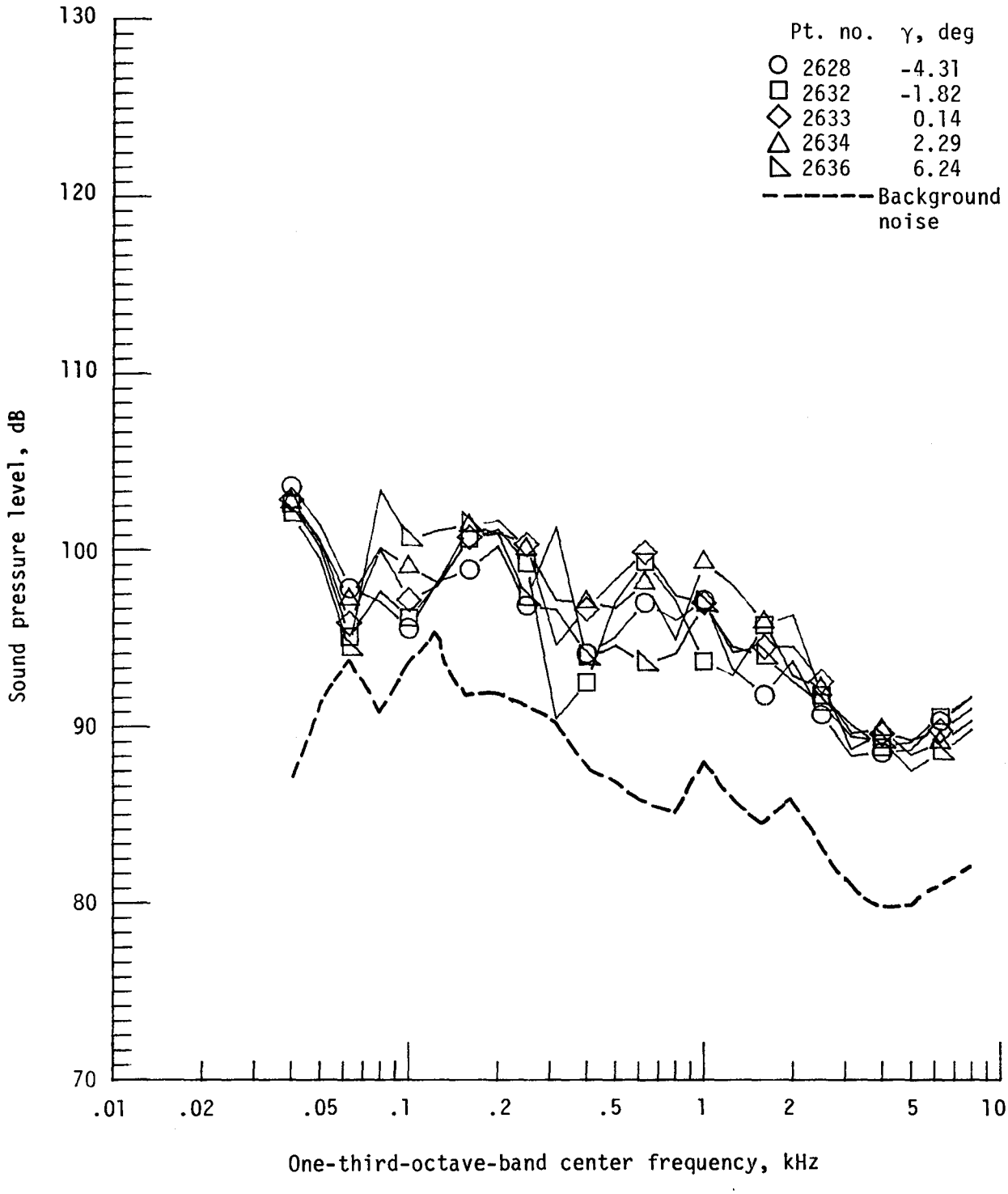

(e) One-third-octave spectra; microphone 7.

Figure 35. - Continued.

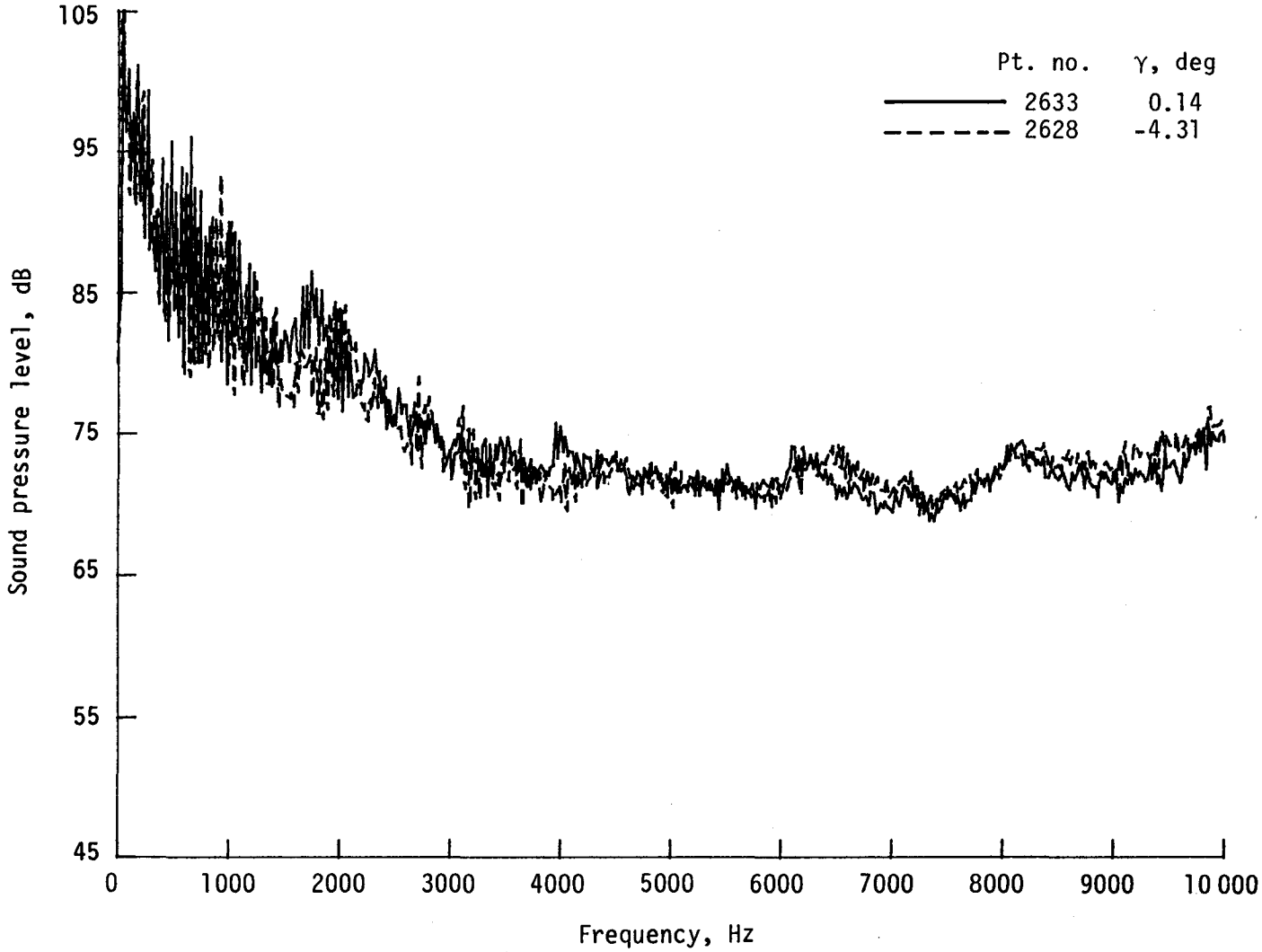

(f) Narrowband analysis; microphone 7.
Figure 35. - Continued.

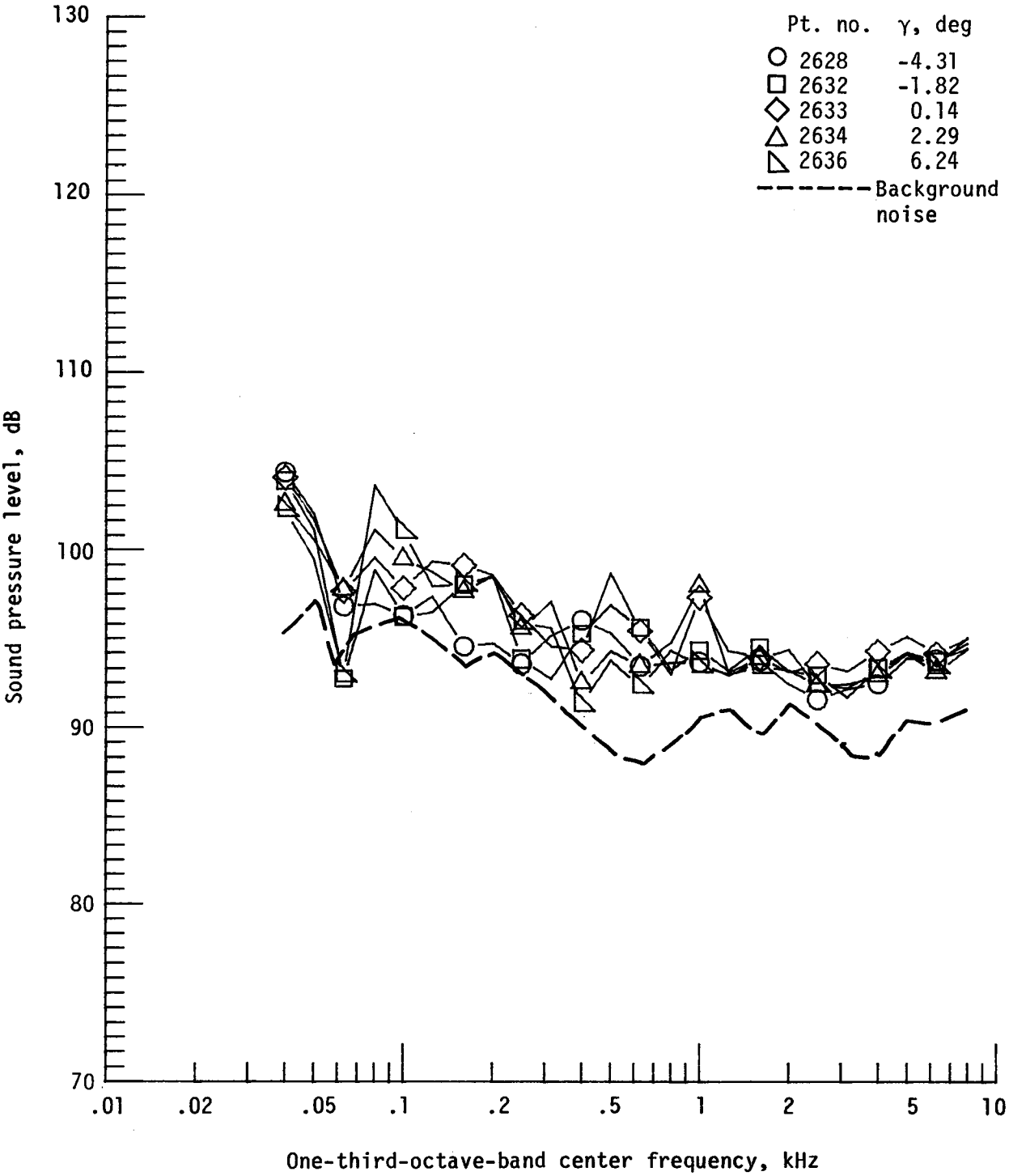

(g) One-third-octave spectra; microphone 8.

Figure 35. - Continued.

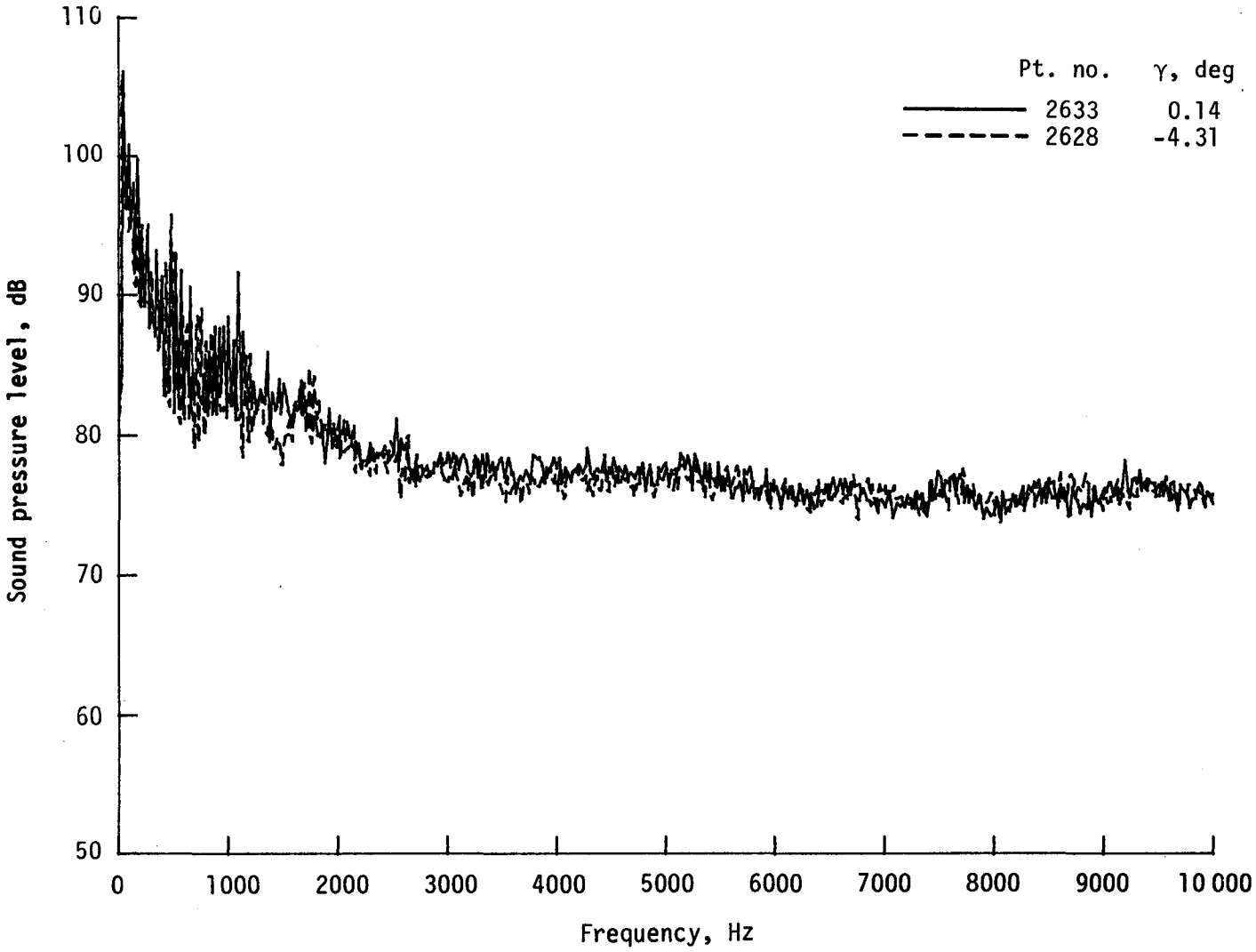

(h) Narrowband analysis; microphone 8.

Figure 35. - Concluded.

1. Report No. NASA TM-84653 AVSCOM TM 83-B-1	2. Government Accession No.	3. Recipient's Catalog No.

4. Title and Subtitle EXPERIMENTAL BLADE VORTEX INTERACTION NOISE CHARACTERISTICS OF A UTILITY HELICOPTER AT 1/4 SCALE	5. Report Date January 1984 6. Performing Organization Code 532-06-13-03
7. Author(s) David A. Conner and Danny R. Hoad	8. Performing Organization Report No. 10. Work Unit No.
9. Performing Organization Name and Address Structures Laboratory USAAVSCOM Research and Technology Laboratories NASA Langley Research Center Hampton, VA 23665	11. Contract or Grant No. 13. Type of Report and Period Covered Technical Memorandum
12. Sponsoring Agency Name and Address National Aeronautics and Space Administration Washington, DC 20546; and U.S. Army Aviation Systems Command, St. Louis, MO 63166	14. Sponsoring Agency Code

15. Supplementary Notes

David A. Conner and Danny R. Hoad: Structures Laboratory, USAAVSCOM Research and Technology Laboratories.

16. Abstract

An experimental investigation of the blade-vortex interaction impulsive noise characteristics of an advanced main rotor system for the UH-1 helicopter has been conducted. Models of both the advanced main rotor system and the standard or "baseline" UH-1 main rotor system were tested at one-quarter scale in the Langley 4- by 7-Meter (V/STOL) Tunnel using the General Rotor Model System (GRMS). Tests were conducted over a range of descent angles which bracketed the blade-vortex interaction phenomenon for a range of simulated forward speeds. The tunnel was operated in the open-throat configuration with acoustic treatment to improve the semi-anechoic characteristics of the test chamber. This investigation provided detailed acoustical data for these two rotor systems operating at similar flight conditions. These data are presented without analysis or discussion.

17. Key Words (Suggested by Author(s)) Helicopter noise Rotor acoustics Blade-vortex interaction impulsive noise Advanced rotor system UH-1H helicopter Wind-tunnel test	18. Distribution Statement Unclassified - Unlimited Subject Category 71

19. Security Classif. (of this report)	20. Security Classif. (of this page)	21. No. of Pages	22. Price*
Unclassified	Unclassified	273	A12

* For sale by the National Technical Information Service, Springfield, Virginia 22161